Development of phenolic concrete mixes and structural behaviour of phenolic concrete components

Shariatmadari, Ali Akbar

Development of Phenolic Concrete Mixes and Structural Behaviour of Phenolic Concrete Components

by

Ali Akbar Shariatmadari

A Thesis submitted in partial fulfilment of the requirements for the degree of Doctor of Philosophy

School of Engineering and Computer Science

The University of Durham

1991

Declaration

The work contained in this thesis has not been submitted elsewhere for any other degree or qualification and unless otherwise referenced it is the author's own work.

To my wife Mahin, and my daughters Ida and Ilar

Abstract

This work relates to the development of a method of preparing a filled phenolic resin, for use particularly, but not exclusively, in building materials. The method includes mixing filler and micro-filler, a catalyst, resin and a hetrocyclic alcohol (i.e. furfuryl alcohol) at a stable temperature, compacting the mixture and allowing the mixture to set and cure. The condition for setting may be with heat and pressure, with heat and/or pressure, or at ambient temperature and pressure.

To design a particular grading from the various numbers of filler components available, a computer program was produced permiting up to 14 components of known grading to be combined into the closest possible approximation to a defined target grading. This was compared to the grading obtained using a combination of trial and error and graphical procedures.

In developing the Phenolic Concrete mixes, initially, the cold set resol phenolic systems were used which resulted in products with low strength as a result of insufficient bond development between the inert granular or powder like materials (fillers) and the resin. Consequently, modified resins were developed which resulted in the production of high strength Phenolic Concrete systems. The determination of the Phenolic Concrete properties was used in describing the indicative inter-relation between the mix constituents, mix proportioning, and criteria of both strength and economy. In addition, Phenolic Concrete mixes were designed with optimization of the mix matrix resin in developing highly fillable media and defining its macro-properties affecting the strength of the end product. Its material properties as a function of its microstructure was investigated using fracture mechanics. The maximum mix ratio devised was 9:1 weight by weight of filler to resin. Maximum compressive cylinder strength obtained was 88.3 N/mm^2 and maximum disc tensile strength was 8.85 N/mm^2 with maximum flexural strength being 30.5 N/mm^2. The unit weights ranged from 2.08 to 2.28 g/cm^3, modulus of elasticity ranged from 14.64×10^9 to 19.6×10^9 N/m^2 and flexural modulus ranged from 17.4×10^9 to 32.4×10^9 N/m^2. Maximum fracture toughness obtained was 2.12 $N/m^{3/2}$, and maximum fracture energy was 220.7 J/m^2.

The development, construction techniques and properties of various phenolic resin concretes were investigated and described. Using the modified resin systems and the techniques developed here, filled phenolic resin concrete was produced cheaply without sacrificing strength and stiffness. The use of wet or dry fibre glass laminates as primary reinforcement resulted in exceptionally strong composite systems. Alternatively, or in addition, the filled phenolic resin systems were combined with further reinforcing materials such as profiled high yield steel bars. These were then used in manufacturing box beams, bridge deck panels, (and subsequently, access floor tiles). The technique by which these components were constructed proved to be reliable and repeatable. The structural behaviour of these Phenolic Concrete components was studied and proved to be predictable applying elastic theory and ultimate load analysis.

Table of Contents

List of Figures

List of Tables

List of Plates

Nomenclature

A Area

A_p Effective cross sectional area of Phenolic Concrete

A_s Area of steel bars

a Maximum moment lever arm, defect size, distance

B Width

B_{di} Bending stiffness at applied moment level M_i

B_p Tensile force exerted on the encased steel bar surface (developed bond stress)

C Constant

C_c Deflection constant relating to centre position

C_l Deflection constant relating to loading position

D Bar diameter, thickness, depth

D_{max} Maximum particle size

D_n Sieve size

D_s Steel bar centriod from compression face

d Diameter, thickness

dA Element of area

E Young's modulus

E_c Compressive modulus

E_f Flexural modulus

E_s Steel modulus

E_t Tensile modulus

E_p Phenolic concrete modulus

E_{Fg} Flexural modulus relating to the specimens reinforced with the laminated fibre glass mats

E_{Tg} Tensile modulus relating to the specimens reinforced with the laminated fibre glass mats

E_t Tensile modulus

F_{C1} Extreme compression face stress

F_{T1} Extreme tension face stress

F_C Effective total compressive force due to compression zone

F_T Effective total tensile force due to tension zone

F_s Effective total tensile force due to the internal steels

f_{ct} Phenolic Concrete tensile strength relating to Brizilian disc test

G_{IC} Fracture energy

H Height

I Second moment of area

I_E Effective second moment of area of a section

I_C Effective second moment of area of the compression zone

I_e Effective second moment of area

$I_{U.C.}$ Second moment of area of transformed uncracked section

I_s Second moment of area of steel

I_p Second moment of area of Phenolic Concrete

I_t Second moment of area of tension zone

I_{tp} Total second moment of area of whole section

k Curvature

K_{IC} Fracture toughness

L Length, span, etc

m Modular ratio

m_s Dry mass of solid

m_{ws} Mass of solid immersed in water

M_o Couple

M Applied moment

M_U Sustained ultimate moment

M_{UR} Moment of resisatance

M_i Applied moment at level i

P Applied load

P_n Percentage weight of filler passing sieve size D_n

P_{max} Maximum load to cause failure (fracture)

R Radius of curvature

s Distance

T, t Thickness

V_s Water volume occupied by solids

W Applied load

W_c Load relating to cracking

W/y Slope of load-deflection curve (elastic region)

Y Distance from neutral axis

$\bar{Y}$ Distance of compression face from neutral axis

$\bar{Y}_p$ Distance from neutral axis to centriod of the Phenolic Concrete

$\bar{Y}_s$ Distance from neutral axis to centriod of steel

Y_{bs} Neutral axis distance from extreme tension face of steel bars

Y_{ts} Neutral axis distance from extreme compression face of steel bars

Y_{bp} Neutral axis distance from extreme tension face of Phenolic Concrete

Y_{tp} Neutral axis distance from extreme compression face of Phenolic Concrete

$Y_{U.C.}$ Position of neutral axis from compression face of the uncracked section

y_c Deflection at centre position

y_l Deflection at loading position

Z_{bs} Tension steel section modulus

Z_{ts} Compression steel section modulus

Z_{bp} Tension Phenolic Concrete section modulus

Z_{tp} Compression Phenolic Concrete section modulus

α Tension zone coefficient

ϵ_x Normal strains

ϵ_s Steel strain

ϵ_p Phenolic Concrete strain

ϵ_{ys} Steel yield strain

ϵ_{Fp} Phenolic Concrete strain at failure

ϵ_{ubp} Phenolic Concrete tension face strain at ultimate failure load

ϵ_{2ts} Steel strain at the end of elastic range

ϵ_{2bp} Phenolic Concrete tensile strain at the end of elastic range

ϵ_{uts} Compression steel strain at the ultimate sustained load

ϵ_c Strains over the height of compression zone

ϵ_t Strains over the height of tension zone

θ Angle of rotation

ν Possion's ratio

ρ_b Bulk density

σ_t Tensile strength

σ_f Flexural strength

σ_{fu} Ultimate flexural strength

σ_{tu} Ultimate tensile strength

σ_{xs} Normal stresses relating to the steel

σ_{xf} Normal stresses relating to the Phenolic Concrete

σ_{bs} Tension steel stress

σ_{ts} Compression steel stress

σ_{bp} Tension Phenolic Concrete stress

σ_{tp} Compression Phenolic Concrete stress

ϕ Curvature

ϕ_i Curvature at applied moment level M_i

ψ Dimensionless factor

Acknowledgements

This research was carried out in the School of Engineering and Computer Sience at the University of Durham. The author wishes to express his sincere thanks to Dr. G.M. Parton for his kind and generous guidance, constant help, encouragement and supervision during the research work and preparation of this thesis. The auther also thanks Dr. T.V. Parry for his valuable guidance in parts of the research work. Thanks are also due to the technical staff, in particular Mr. T. Brown, Mr. B. Scurr, Mr. S. Richardson, Mr. B. McEleavey and Mr. A. Swann, in the Concrete Laboratory for their help in construction and the experimental work.

The author further thanks Mr. D. Dyke and Mr. T. York of Fordath Chemicals of BIS and Dr. J. Hunter and Mr. K. Forsdyke of BP Chemicals in Applied Phenolic Division, for their generous supply of material, technical information and also continuous support in the course of the research work. Thanks are also due to BP Chemicals, Applied Phenolic Division, and their technical staff for providing the facilities and the use of their Laboratories at Sully.

Chapter One

1. Introduction to Polymers in Concrete

1.1. Introduction

There has been an increasing interest and need in improving the strength, toughness, ductility, and durability of the conventional cement-based concrete. In achieving such requirements various techniques have been adopted in improving the properties of the ordinary concrete, and with introducing polymers in concrete technology, as an alternative, has led to the use of silicious materials with polymers. This has resulted in devising systems as replacements to cement based concrete that can exhibit a superior cost-property balance. Although successful developments have been reported in applied research work on various polymer concrete systems, much work is still required in combining the science, technology, design, and economy involved in understanding design, and material selection.

Polymer concrete systems are new in the construction industry. They are included in the discussion of structural concrete[1] in view of their potential as structural materials for future. They differ from the conventional structural concrete only in using a polymer as the cementing or impregnating agent.

The continued search for lightweight durable materials has resulted in the use of polymers today in virtually all types of industry products. There are several useful thermosetting polymers that can be cast into moulds in much the same way that concrete is placed. Epoxy, phenolic, amino, polyester, polyurethane, and acrylic are all in this category of polymers. So far epoxies and polyesters have been particularly versatile in that various types of filler may be blended into the polymers to adjust

their physical properties. Not only are there broad classification of resin products, but even within each resin class, a bewildering number of products are presented to the engineer. Selection of suitable products for structural purposes by the engineer cannot easily be made on a chemical basis and it is essential to specify the application as far as possible in terms of requirements, performance and use in the environmental condition.

1.2. Polymers in Concrete

1.2.1. Polymer Concrete Materials

Polymer concrete materials have been introduced to the conservative technological world over the past 40 years. Major interest in polymers in concrete developed in middle 1960s[2] which led to numerous work to be reported in this field world wide. The American Concrete Institute formed the "Polymers in Concrete" Committee 548[3] in early 1970s. By the late 1970s, several International Symposa and Congresses were held on the general topics[4,5,6] from the papers published worldwide, which covered an extraordinarily wide range of research work and applications. Since then the International Congress on Polymers in Concrete has moved round the world[7–10].

A comprehensive review of the state-of-the-art has been reported[11,12,13] with highlights of the principal areas of applications and research works. Increasing interest in polymers, in general, has resulted in more research work being reported[14–18] on the uses, properties and applications of the Polymers in Concrete.

There are three basic types of polymer concrete systems[1–3,11] available to the concrete technology. The polymer portland cement concrete (PPCC), the polymer

impregnated concrete (PIC), and the polymer concrete (PC) which is the scope of present research work.

1.2.2. Polymer Portland Cement Concrete

PPCC, which is also referred to as Polymer Cement Concrete (PCC), is obtained by mixing a monomer, prepolymer, or dispersed polymer to a fresh portland cement concrete mixture. The polymer can be either in a liquid, powdery or dispersed phase forming an in situ polymer network during curing of the concrete. PPCC has similar process technology for conventional portland cement concrete. The most common applications have been in mortars, bridge deck overlays, prefabricated brick panels, flooring and patching compounds. The monomers such as styrene and vinyl derivatives, prepolymers such as polyester-styrene and epoxies have been widely used in PPCC systems. The most successful and favoured polymer used in these systems is the incorporation of a polymeric latex in which, the physical proccess of film formation is required rather than the chemical polymerization. The latex type PPCCs exhibit[2] excellent bonding to steel reinforcement and to old concrete, good ductility, resistance to penetration by water and salt, good shock and abrasion resistance, and excellent durability to freezing and thawing.

1.2.3. Polymer Impregnated Concrete

PIC is one in which, the previousely formed concrete has been impregnated with a low viscosity monomer and is consequently polymerized in situ. In PIC the impregnated polymer affords further properties to the characteristics of the original concrete. It has been shown[2] that the PIC system has superior structural and durability properties than the concrete from which it was produced. Fully or partialy impregnated components have been used. The former provides enhanced structural

and durability properties, with the latter improving only the durability properties. The cost limitation determines the impregnation process to a great deal, as the process is complex and monomer costs high if more than a surface impregnation is required. However, the gain in service life is believed to offset the high cost, or in which no other material or process appears to be more suitable. PIC has long been considered as a potential material where properties such as high strength and stiffness, or resistance to corrosion of concrete or reinforcing steel are important. In PIC components, much emphasis has been given to acrylic monomer systems since they have generaly led to superior properties in the composite. They are in liquid phase with high surface tensions, low viscosities, good wetting properties, relatively low costs, and high reactivities. Epoxies, vinyl and other viscous monomers have also been used though the rate of impregnation is necessarily reduced. The most common applications have been in bridge deck and hydraulic structures[4,5,6].

1.2.4. Polymer Concrete

PC or resin concrete, is a composite material made of a monomer and aggregate. The polymerized monomer acts as the binder for the aggregate. Polymer materials constitute a better binder for concrete than cementitious materials. Improved performance characteristics are gained in the substitution, yielding lightweight, increased tensile and compressive strength (hence flexural strength), resistance to moisture and other elements. Just as there are various types of cements, there are many varieties of polymer binders. In fact, the choice is almost limitless with each particular binder (organic and inorganic) having its own particular characteristics.

PC systems have been widely used to repair portland cement concrete in pavements, bridges, and hydraulic structures and to produce precast components such

as building panels, flooring, insulations, drains, facing panels, and manholes. Of the three types of the polymer concrete systems, mentioned above, PC has atracted the most attention. Unlike the extended cure time of the portland cement concrete, polymer concrete (PC) can be hardened in a few hours (customarily over night) or in minutes by heat. Porosity is minimal because, unlike standard concrete, no water is evaporated.

The mechanical properties of PC are strongly influenced by the viscoelastic behaviour of the polymer and, to some extent, the properties of the aggregate. The response of most polymers used in PC is a function of time, temperature, and the molecular structure. Shrinkage can vary widely depending upon the polymer type and polymer loading. The PC properties may vary although similar resin, (i.e. made of the same monomer), can be produced from many types and gradation of aggregate under a wide range of environmental and working conditions.

1.3. Some developments with PC systems

In PC formation usually thermosetting resins such as epoxy, polyester, phenolic etc are used. Properties of the thermosetting resins depend upon the degree of polymerization achieved. Reference [19] has a comprehensive chapter on resin properties, measurements of resin properties, and use of resins in the form of plastics in structural models.

For field applications, either user-formulated PC systems or commercially available prepacked systems are used. Several mixing techniques can be used. For manufactured products, continuous processing has been used for years in Europe and is now being used in other countries to produce a wide variety of components.

Prusinski, is co-inventor and developer of PC industry. In his paper[20], he

presents a comprehensive study of commercial development in precast polymer concrete, and gives evidence of an over expanding market in future. He assesses and concludes that on a cubic foot basis, polymer concrete costs about seven times more than the cementitious variety. But the thin section permitted to be cast tends to equate the two materials if function alone is considered. Additionally, with the PC system, savings in structural steel as well as high insulation values can help realize major savings, especially in this "conservation of energy" conscious world.

A great attention has been paid[21] to furane resin concrete at the Institute of Theoretical and Applied Mechanics of the Czechoslovak Academy of Science. It has been shown[21,22] that in PC systems subject to a long time to either load or temperature, the mixture composition, the material curing, its age and other factors influence the relationship between stress, strain, temperature and time. The test results have shown that the creep of resin concretes under mechanical loading to be essentially greater than that of traditional building materials. In resin concrete, the deflections (or creep) are influenced by mixture composition and curing temperature. At higher filler loadings and at optimum curing temperature the deflection becomes a minimum and with increase or decrease in optimum curing temperature the deflections are greater. The shrinkage, tensile and flexural properties, and compressive strength of the PC systems are also influenced[21,22] by mixture composition and curing temperature in similar manner.

In Czechoslovakia during period of 1963-1964, large diameter sewer pipes were constructed using furane resin concrete[22]. It is reported that PC systems made from furane resin were relatively cheap and possessed equivalent mechanical properties and superior chemical resistance to all other type of resin concrete. The furane resin concrete pipes were used as self-supporting interior shuttering for the freshly

placed concrete mix forming the sewer pipes for waste waters. The furane PC pipes acted as core afforded effective and continuous protection aggainst the effect of aggressive waste water to the concrete of the sewer pipes.

References [21 & 23] include discussions on test results obtained from PC systems made from furane resin (furfurol-furfural named berol), polyester resin, phenol-formaldehyde resin and epoxy resin. The limit strains for these resin concretes are related to their mix composition and developed strengths. For all these resin concrete systems, from pull-out tests, a fully satisfying bond resistance has been stated. The long term observation (up to five years) of reinforcement inside the bodies of resin concrete has proved a minimum corrosion due to hardener acidity, with very good bonding in epoxy resin concrete systems. Doubt may arise about the bond values in polycondensate resin concretes. In the case of acidic catalysts, the long term influence on the reinforcement should be considered. Care should be given so hardener or catalyst used have not been overdosed, so that it cannot be in any case decisive for the life time of the structural element in question.

Burleson, et al.[24], have reported a comprehenssive investigation of the properties of polymer concrete with the polyester resin as binder. In these, the polymer concretes used were composed of a number of varying polyester-styrene-methyl methacrylate resin systems mixed with combinations of sand, gypsum, gravel, clay, and chopped glass fibres. His findings from various tests on relative test specimens were; Maximum compressive strength obtained was 145.6 N/mm^2 and maximum splitting tensile strength was 15.2 N/mm^2, unit weights ranged from 1970 to 2350 kg/m^3 and modulus of elasticity ranged from 10.1 to 22.8 kN/mm^2. Rapid curing at ambient temperatures was possible. The addition of a chlorendic anhydride improved polymerization at both ambient and elevated temperatures. In these PC

systems the aggregate particle size and distribution affected the strength and resin requirements. The polymer concretes investigated cost more than conventional concretes for equal volume of materials but compare well with conventional concretes on a cost-to-strength basis.

A systematic study[23] of the properties of PC systems have been carried out in a number of organizations in USSR. Furane, polyester, epoxy, MMA, and vinyl ester resin concretes have been used for wear-resistant facings of hydrotechnical structures[23,25] instead of the usual facings in metals, stones and other materials in Central Asia in 1959, and in USA in late 1970s. These various resin concretes have also been used in chemical and oil refining industry, for the protection of building structures and equipments against chemical corrosion.

The composition of PC may be varied[23] over wide limits depending upon many factors such as; purpose, kind of structure, method of placement, grading of aggregate, ambient temperature, requisite hardening time. The strength of PC is dependent[21–24,26] upon the resin type, resin loading, acid content, curing conditions, and mineral-petrographic characteristic of the aggregate. If catalyst dosage is too small, the polymerization is incomplete and this has a negative influence on the strength and other qualities of PC system. At the same time, over-dosing will lead to rapid "setting" of the mix, thus increasing the brittleness of the PC system and defecting its other characteristics. The optimum dosage of catalyst may vary depending upon the temperature of the ambient air.

According to professor N.A. Moshtshansky[2] of USSR, the greater the amount of catalyst introduced, the higher is the temperature of the mix and of the air, the less is the amount of aggregate in the PC and the coarser the aggregate is, the more intensive will be the hardening. Two methods of hardening may be used;

"cold" hardening, that is when PC is hardened at natural temperature, and "hot" hardening, that is when PC is subjected to short time dry warming up.

There exists[2,6] contradictory information concerning the change in the strength of PC system with age. It is considered that under normal conditions the strength of PC system slowly increases in the course of several months. The strength of the sample hardened with warming up practically does not change[23].

The PC system has found[21–24] to be impervious to water even at 14-16 atm. pressure. They are also impervious to petroleum products. PC systems are sufficiently resistant to water and frost with no decrease in their strength when subjected to these environments[2,23]. PC systems made with quartz sands have been shown[23] to degrade with weather with cosiderable strength losses, but with andesite and graphite aggregates when stored outdoors a continuous growth of strength is observed in the course of six months. PC systems are capable of working when heated up to 180-200°C. They possess good resistance to many acids, alkalies, solvents and petroleum products. The resistance to wear[21–23,25] of PC systems exceeds that of cement concrete by factor of ten.

In some PC systems[2,4,6] creep develops intensively already when the loads are 20% of breaking loads. Increased creep of PC systems may prevent these materials from being used in bending structures. The coefficient of thermal expansion[21,22] of PC system is the same as for steel and cement concrete, which makes it possible to reinforce PC and also to use it as an insulation coating for steel and concrete structures.

Premixed PC overlays incorporating vinyl ester or polyester and epoxy resins have been placed using concrete paving machines[27]. PC composites combine the premix characteristics of portland cement concrete with a unique set of properties[27–29].

These include; (a) rapid curing at ambient temperatures, (b) high strength, (c) good adhesion to concrete surfaces, (d) long term durability to freeze-thaw cycling, and (e) negligible permeability to water and de-icing salts. PC appears suitable for use in repair of concrete structures where traffic (bridges and runways) conditions restrict closing of the repair site to only a short periods.

In 1974, US and USSR established[25] a joint US/USSR polymer concrete team to address the "utilization of polymer concrete" in wear and cavitation resistant linings of hydrotechnical structures and for the repair of concrete structures.

In Soviet Union not only have they used polymer concrete materials to repair older structures[21,23], they have incorporated PC and PIC slabs in new hydrotechnical projects[25]. By late 1970s, a few stilling dam basins in USA[25] which were cavitated or eroded were repaired using PIC system containing epoxy resin. Also two concrete drop structures of Water and Power Resource services in USA were repaired using PC systems containing vinyl ester. In these the erosion damages were resulted from abrasive sediments carried by flowing water. A series of abrasion test results indicated that, the abrasion erosion loss of the PC systems was less than PIC and PPCC with conventional concrete having the greatest loss relatively to the polymeric systems.

The indoor and outdoor electrical insulators, and other electric utilities may provide a very large market for the polymer concretes in a wide variety of applications. In USA and Mexico, this has already been put to practice[30,31]. An example of these is the electric power transmission poles, transformer concrete foundation and substation structure that normally would use concrete, metal and wood for mechanical support requirements and insulator for electrical protection. In Mexico[32], PC formulations using native materials and techniques have resulted in PC devel-

opments to replace electrical porcelain for high voltage outdoor insulators. Two systems have been developed, one with MMA polymer and the other with polyester polymer as a binder (15%) with 85% silica sands and fines. The aggregate materials for such usage ought to be better than 97% silica which is not contaminated with any materials which might reduce the dielectric strength of the finished product. The overall test results of these type systems were comparable to those of porcelain and epoxy insulator. In these, the polymer concrete systems may be used with its combined mechanical and insulator properties, thus serving most effectively the industry in an economical manner.

Laboratory studies have shown[33] that PC systems consisting of a mixture of high molecular weight Siloxane copolymer (semi inorganic polymer) as a binder and silica-cement mixture as a filler, meet the requirements for geothermal well cementing materials in temperatures as high as $300°C$. With organic polymers this cannot be achieved since the PC systems made from them at temperatures above $250°C$ may become soft and crack or swell because of the evolution of gas. In addition the molecular chains of Siloxanes (Si-O-Si bonds) are more rigid[34] than those of organic polymers (C-C bonds). Other PC systems have also been developed[35] for use in high-temperature geothermal environments. These are formed from composition of one monomer system containing styrene, acrylonitrile, acrylamide, and divinyl benzene as binder with fillers consisting of silica sand and portland cement. The system has produced a compressive strength of 159 to 207 MPa at $20°C$ and is thermally stable to about $240°C$.

An extensive work in USA has been carried out[28] on development of PC systems which would be utilized in rapid all-weather pavement repairs. A technique has been devised with commercially available German product Sililal R7/BW for rapid

spall repair. The methyl-methacrylate (MMA) polymer concrete systems have also been devised for rapid repairs of cracks and spalls in pavements and airport runways. In these, aggregates coated with "silane" coupling has considerably influenced an increase in strength and with steel fibres improved strength of MMA system made with wet aggregates have been reported. Since the condensation polymers are compatible with completely saturated aggregates, use of "furfuryl alcohol" has shown excellent results regarding the compressive strength of PC system made with saturated aggregates. The short, medium, and long term applications, ambient temperature, weather and moisture tolerances have been considered in the developments of such PC systems.

In other work in the USA, several techniques, including chemical additives, aggregate treatment, and addition of fibres, have been investigated[29] for improving the strength of PC systems. The systems were formulated from MMA polymer as binder with wet aggregate as the filler. The important findings were; (a) PC systems made with cement possessed better flexural strength with compressive and tensile strength being approximately twice as large when compared to the system without cement. It is thought that hydration played a major role in the strength increase. (b) Silane coupling agent used for aggregate coating produced PC systems with excellent strength compared to those systems with uncoated aggregates. (c) The increased level of promoters and initiators was found to yield significant increases in strength. (d) Steel fibres proved to be effective in reducing the strength loss of PC systems made with wet aggregates.

Over 40000 large manholes made of polyester resin concrete have been mass produced in Japan[36]. A plant in West Germany[37] has been manufacturing wall panels, cable channels, facades, drains and curb stones. The PC system is made

with MMA monomer. Another manufacturer[38] has utilized continuous casting machines which were capable of producing a wide range of products including sewer channels, sanitary ware, facing panels, floor tiles, and window sills. These products made of PC systems with various monomer compositions.

Since 1958, precast polymer concrete building panels made with polyester have been in production[20]. These have been incorporated with exposed aggregate facings, fibre glass cloth reinforcing and insulation. More recently at Durham University[40], research work has been undertaken on the development of PC system using polyester resin with silica sands and other fine fillers. This work was in corelation to the polyester resin concrete (Fypol) developed by Kubase Construction Ltd.[39] in conjunction with BP Chemicals Ltd.. In its initial state the "Fypol" is capable of being poured, thus a vast variety of mould shapes and sizes are within its scope. Once set "Fypol" possesses great inherent strength, it is virtually distortion free, is non absorbent, easy to clean and simple to repair. For the building and construction industry, it provides a superior and economic alternative to brick, precast concrete, GRP, tiling and many other traditional materials. "Fypol" is currently available as various sized, double skined and insulated building system panels, in sheet form for cladding purposes and in reinforced section for use as permanent shattering.

During 1980-1985, various dwellings (domestic, school and shopping arcades) were built in Nigeria and Trinidad using pre-engineered "Fypol" building system panels. The most favoured advantages of the use of "Fypol" panels are their continuous precast production and their ease of handlling and speedy construction of the building assembled from them. The surfaces of the panels may be textured and coloured during manufacturing to simulate brick, stone or rough-cast walling. The

panels comprise of a lamination of Fypol resin concrete, reinforced with glass fibre and encapsulating a fire resistant, lightweight foam insulating core.

The Fypol bridge-panel is immensely strong and has been used as permanent shuttering in the construction of bridges over the M62 and A19 in the North of England. An other application of "Fypol" cladding has been the facial claddings to various office buildings for aesthetic purposes. The most craftsman application, of which the author has seen in production, is the "Fypol" resin concrete used in costructing a whole pool table. Using various gel coatings available the entire facial area is made from "Fypol" concrete to desired colouring. Fypol concrete is also used to construct the body of the pool table and the flat slabs replacing the conventional wooden frame and slate slabs for their accurate flatness requirements. Most of the "Fypol" developments are based on patents[41,42].

Thus the polymer concrete systems appear to becoming of use with their applications in many specific areas irrespective of their cost-effectivness. This is justified by their unique properties. Most of the developed PC systems are taylor made and based on patents. However, much more research and development work is still needed before such materials and systems can be generally accepted in wider range of engineering applications.

As in any other engineering materials and their applications, the PC systems have also their disadvantages. The major disadvantages are;

1. PC system is limited to special applications where its higher cost can be justified.
2. The troublesome procedure and the special equipments required for its application.
3. In manufacturing, the workers have to be protected from the dangers of coming into contact with the chemical or inhaling fumes during casting operation.

4. The creep can be high in PC systems, although this may be controlled to some degree by selection of the type of polymer and incorporation of fibrous and/or steel reinforcements.
5. The fire hazards of some PC systems, restricts their use to other than domestic or indoor (closed) applications.

1.4. Purpose and Scope of present work

The development of polymer-aggregate concrete is relatively recent but is continuously increasing in scope and intensity. In spite of abundant use of concrete as a construction material, it is only very recently that, impelled by competitive considerations and continued research efforts, a group of new materials in concrete construction have been developed. Polymer concretes form one of this group of materials. Several investigations of the recent past have concentrated on the techniques of development of this new material, property characterization and potential product application in the technological industry.

The reason for the ever increasing application of these materials does not rest only in the increasing knowledge, also with regard to the mechanics of materials, and in the decreasing price of resins due to their increasing production, but also in the increase of the assortment of resins enabling the satisfaction of the most varied users requirements. Prudent management of energy and natural resources demands ever higher levels of performance especially of lightweight systems. Although portland cement concrete is one of the most remarkable and versatile construction materials, a clear need is perceived for a material to produce lightweight structures with improved strength, toughness, ductility and durability. In general if polymer resin is used instead of cement to make a precast structural element, then that element could be

lighter in weight, easier to handle and install, and give other desirable characteristics not found in normal cementitious materials.

So far a vast range of work has been reported in the investigations of the properties of the various types of resin concrete. It is still a relatively new product and requires further research work before it can become generally accepted and understood with respect to design and material selection. Particular attention should be given to the Phenolic resin concrete, based on continuously available raw materials, of equivalent mechanical properties, superior fire resistance and superior chemical resistance to all other types of resin concrete used to date.

The objective of this work was to develop a Phenolic Concrete cold-set system from which structurally viable elements could be produced. The research work conducted here on the Phenolic Concrete is for a closer examination of the techniques of development of Phenolic Concrete and its mechanical properties and durability aspects. In the course of research work the methods of construction were developed and improved in order to produce distortion-free elements. This work investigates the formulation of various mix compositions, consisting of a phenolic matrix with sand and micro-fillers. It also investigates the effects of individual constituents of the whole system with respect to the physical and material properties of the developed system. Specifically, the project sought to optimize the formulation of a resin-aggregate system, with optimization in curing rate and manufacturing process to produce materials with high strength in flexure and which would be economically viable. In addition to confirming the behaviour of material as generalized by earlier investigations it was realized that it would be necessary to study the mechanism of strength mobilization and failure of Phenolic Concrete as well as improvement of the highly brittle nature of this material. Specimens from the most promising

formulations were tested and compared with respect to physical and mechanical properties.

Initially several phenol-formaldehyde resol cold-set system resins were used in the formulations which were commercially available and recommended by their suppliers to take on non-fibrous fillers. These claims proved not to be valid and this resulted in the development of a modified resin system suitable for this work. The work also entailed an investigation into the use and the effect of various fillers and their mix gradation on the flexural and other properties of the developed systems. A computer programme was developd for the purpose of filler mix design which enabled up to 14 granular materials of known grading to be combined into the closest possible approximation to a defined target grading.

The material properties of the developed phenolic concrete systems were also obtained using linear elastic fracture mechanics (LEFM) applied to the specimens tested in double torsion. The use of both fibrous (fibre glass mats) and steel (bars) materials as reinforcements to Phenolic Concrete, was studied with respect to increase in ductility and improved carrying capacities. Finally, structural elements such as box beams, bridge deck panels, etc., were produced using the developed Phenolic Concrete mixes and construction techniques. These were tested and their behaviour under flexural loadings up to failure were studied.

Chapter Two

2. Phenolic Resin Concrete

2.1. Introduction

Phenolics today are irreplaceable materials for selective high technology applications offering high reliability under severe circumstances. New products and applications continue to demonstrate the versatility and uniqueness of phenolics and their potential to cope and adjust to the ever changing requirements of present industrial society. As a result of increasing interest and growing successes in polymer concrete products, and their applications much attention is given to polymers such as polyester and epoxy resins. A wide range of application have been, or are being, commercialized generally through out the world[2,11-13]. The resulting products are tough and durable. A major drawback with these polymer concretes, and one which has restricted their growth in many areas, is their behaviour in fire. Although so called fire retarded resins can be used in special classes of applications, polymer concrete must generally be considered combustible, emitting considerable quantities of dense and toxic fumes whilst burning. For this reason, their uses must be restricted to situations where this disadvantage is not critical.

Many newly developed acid cured phenolics, on the other hand, if used in polymer concrete, would offer the same virtues of high strength, versatility of manufacture and application, whilst suffering none of the fire related disadvantages of other resin systems. In general phenolic resin products are very difficult to ignite and do not readily support combustion; when burning, there is very low smoke evolution combined with minimal emision of toxic fumes. Other advantages include the ma-

terial's high temperature performance, good resistance to corrosion, and resistance to microbiological attack. They are not water-absorbent and have high resistance to a range of common chemicals.

2.2. Materials

2.2.1. Phenolic Resin

Phenolic resins are probably the oldest commercial man made polymeric materials, discovered in 1872. They were first developed by Leo Baekeland in 1907 and immediately used as "composites" in the form of phenolic moulding materials (Bakelite) and similar materials continue to be manufactured today. These resins had found numerous applications in the electrical industry and also in laminated products where wood, fabric or paper are used as a fibrous reinforcement. Besides the insulating properties common to plastics, the main benefit from using phenolic resins is their superior fire resistance and low smoke emission.

The basic chemistry of phenolic resins, recent developments and their applications are well documented[43,44]. Today, phenolic resins find applications in foundry casting sands, brake friction linings, grinding wheels, heat shields, furnace taphole clays, fire resistant insulation and many other places where high temperature is a problem.

Early efforts in 1960s and 1970s to produce phenolic resins suitable for hand lay lamination "GRP" work were generally unsuccessful[45]. As a consequence the material did not make a serious market impact despite its obvious advantages over its competitors in fire and smoke emission properties[45]. In the late 1970s and early 1980s, a second generation of liquid phenolic resols[46–51] for "GRP" began to be

offered to the market which had several advantages over their predecessors. These advantages were; (a) lower viscosity, (b) low free monomer, particularly formaldehyde, and (c) high reactivity.

In phenolic resins two principle classes are recognised, novolacks, with a phenol to formaldehyde molar ratio of greater than unity, and resoles, with a ratio less than unity. It is this second group, the resoles, which is of concern in present work. Resoles are available as aqueous, alcoholic or alkaline solutions. In general, the cross linking may be determined by two methods; (a) thermal cross linking which is carried out normally at 120-180°C and involves the evolution of water of condensation, and (b) acid catalyst low temperature cross linking. The reaction occurs when a high methylol phenol content phenolic resol is treated with strong acid which is discussed in references [52,53].

The recent developments in liquid resol phenolic resins and the modern catalysts have made it possible for many manufactures to formulate systems for "cold set" uses of the phenolics. In spite of the apparent variety, the developed resins are basically similar but some may be more suited to one process than another, owing to their various specific properties. The lower viscosity enables better and quicker wetting out of the fibrous or non-fibrous components and also opens up mechanical production methods if needed. The low free formaldehyde makes the material more pleasant to work with and easier for the user to obtain atmospheric concentrations of formaldehyde possibly below the current working regulations. The high reactivity offers a truly "cold set" system if required when previous materials had required some external energy input.

With this new generation of phenolic resins, so far, considerable successes have been achieved[46–51] with regard to reinforced fibre glass/phenolic resin products.

The present work is aimed at devising a system which would allow the incorporation of these types of resins in phenolic concrete compositions. The ability to take fillers is a matter of chemical surface interaction of phenolic resins and fillers, and inter particle forces in the dispersed filler. Some fillers agglomerate and precipitate, some stay finely dispersed. Only experimentation will prove the suitability or otherwise of any given filler.

There exists a number of phenolic resol resins formulated by various manufactureres. It is therefore recommended that any resin selection to serve specific requirements should refer to the relevant manufacturer's property and technical specification.

For the purpose of the present work, initially, the two "cold set", J2018L and J2027L resol resins were used which were manufactured[45–47,51,54] and recommended by BP Chemicals claiming their ability to take non-fibrous fillers. Their relevant catalysts were Phencat 10, a weak acid and Phencat 15, a stronger acid. In addition, few similar phenolic resol resins were also used which were produced by other manufactureres, such as; XDF-4252 and XDF-4151 resol resin by Ciba Geigy, and PA104 resol resin with PX13 catalyst by Borden Chemicals, etc.

For a period of almost one year, various filler formulations, compositions, construction and curing procedures were used in developing phenolic concrete systems using the above resins. Unfortunately, the specimens produced from these phenolic concrete systems proved to have developed no bond between the binder (resol resins) and the aggregates (silica sands and fine filler composition). The flexural test results, showed very little or no enhanced flexural properties of the filled systems when compared to those results from non-filled systems (i.e. cast catalysed resin). It took over a year of experimental and development work to convince BP

Chemicals that their resin would not bond to the fillers. Therefore, alternatives were sought and resin modifications were proposed which would satisfy bondability requirements. Resin modification or filler treatment became eminent. In the latter, pre-coated filler, epoxy and polyurethane primers were used in order to achieve the bond requirements. Micro-filler coated with silane coupling (i.e. Spheriglass 5000 CP03) offered an expensive solution and yet did not afford the system sufficiently significant strength and possibly bond enhancement. Even the use of silane coupling substance in the resin matrix as an integral part of the resin would be uneconomical in production of the phenolic concrete composite system. The use of primer and adhesive, such as polyurethane and epoxy proved a tedious and uneconomical process and diverged from the original goal of producing solely a phenolic resin based concrete system. The only simple and economical solution was the use of "Furfuryl Alcohol" in the resin in order to modify the phenolic resin. The furfuryl alcohol was directly mixed with the resol resins J2018L and J2027L at various ratios forming modified resins of lower viscosity than the original resol resins. Furfuryl alcohol which itself is an aldehyde becomes an integral part of the resol resin, and with a co-reaction in the presence of strong acid catalyst as a result of polymerization larger and stronger cross linking chains will develope in the filled resin system. The specimens made from resol/furfuryl resin and filler compositions possessed considerable flexural strength and stiffness under flexural loading. This proved that the furfuryl alcohol had enhanced the bond and possibly provided good wetability to the filler composition in the mixed matrix.

In Section 2.3., some important points are explained which were derived from the investigations conducted in the preliminary part of this work on phenolic concrete composition and resulting specimens.

In the course of this work, two "cold setting" phenolic resins were introduced to the author which were produced by Fordath Chemicals Ltd. of B.I.S[55]. These were derivatives of phenolic resins with acquired physical/chemical properties; (a) Urea Formaldehyde Phenolic Furane Resin with the brand name "IR1271", and (b) Phenolic Furane Resin with a brand name of IR1270. The relevant catalyst was an aqueous solution of para toluene sulphonic acid with a brand name of CS30. Later four more resins by Fordath, known as IR1272, IR1273, IR1274, and IR1275 were also offered as improved versions of the IR1271 resin. However, that was not the case and the original IR1271 resin performed in superior manner to them all. For further increases in fillable media, furfuryl alcohol was added to both IR1271 and IR1270 resins which not only helped to reduce their viscosity, thus allowing more filler loadings, but also improved the flexural properties of the end products (see Chapter 3).

BP Chemicals, also succeeded in developing the phenolic resin named J50/010L to suit the acquired physical/chemical properties. The acid catalysts compatible with this resin were Phencat 10 and Phencat 15. The phenolic concrete mixes made using this new BP resin, also provided specimens with high flexural strength and stiffness. A chemical analysis of the IR1271 and J50/010L resins conducted by BP Chemicals (Applied Phenolic Resin Division) is provided in Table 2.4, which shows their chemical composition comparativeness. For physical and chemical properties of the above resins, references should be made to the manufacturers' specifications.

2.2.2. Furfuryl Alcohol

Furfural, sometimes called furfurol, is a colourless liquid with chemical properties similar to benzaldehyde. Commercial production starts with residues of annual plants like maize cobs, bagasse or rice hulls. These naturally occurring pentosans are hydrolyzed by dilute sulfuric acid to furfural which is then isolated by steam distillation. With alkaline catalysts the first step in the reaction with phenol is similar to that of formaldehyde, yielding α-(o-or ρ-hydroxyphenyl) - furfuryl alcohol[44,45,54]. Furfuryl alcohol/PF resin blends and acidic catalysts are used[44] in the foundry industry for the no-bake and hot-box core making process and for the preparation of acid resistant cements. Furfuryl alcohol is also used for the production of furane resins. For chemical/physical properties, reference should be made to the manufacturers "QO Chemical Inc.", for technical data[56].

2.2.3. Fillers (Sands and Micro-Fillers)

In a PC system the strength and other properties, as well as its durability are essentially affected by the mineral-petrographic and chemical characteristics of the aggregates. These aggregate properties however, do not usually influence the properties of cement concrete to such a great extent. Aggregates (fillers) should be tough, clean, free of dirt, and other organic materials. They should be dry (oven dry), with a moisture content as near as possible to zero, in order to ensure adequate bond to the polymer. Chemically, the fillers to be used, should be compatible with the resin polymer, otherwise, setting and curing may be retarded or inhibited. They should also be resistant to acid attack since the preferred method of mixing in phenolic resin systems requires prior mixing of the fillers with the prescribed amount of catalyst.

The aggregate gradation varies according to the application, but generally the gradation should provide a relatively low-void volume and have sufficient fines to provide workability. In polymer concrete, generally, aggregates in use are sand fillers. In selecting the sand fillers care should be given to their characteristics which determine their suitability for engineering purposes. The most important of these are:

(a) Chemical composition, which determines their compatibility with resin polymer.

(b) Solubility, the aggregate must not be soluble either in the cementation which is to be used with them or in any of other substances with which they may come into frequent contact.

(c) Hardness, this is a desirable quality and it may override other even more desirable qualities such as low weight.

(d) Obduracy, which is the geological term for the durability of the aggregate as well as the product. Obdurate aggregates are generally composed of a very few natural minerals in crystaline form.

(e) Grain shape, which is important in determining good workability and hence resin loading requirements. The grain shape defines the "sharpness" of the grains, and the degree of elongation of the grains.

(f) Particle size distribution, which is often refered to as grading, is by far the most important characteristic of an aggregate from the user's point of view. It can be easily modified to suit specific combined grading requirements.

At present, there are commercial suppliers available who offer a varied range of sand gradings. It is not possible for them to supply sands which can contain almost all particle sizes required to represent a desired grading. It is, therefore, common practice to obtain single size sands of various particle sizes in order to design the

desired grading. Aggregate gradation is of importance, since it has a great effect on all engineering properties of the finished product such as density, water absorption, heat transmission and, above all, strength. To design the aggregate gradation of a desired grading, it is essential to determine the particle size distribution of any defined component aggregate grading. A proper selection of particle sizes is also of importance; otherwise a poor selection will have a deleterious effect on the mechanical properties of the end product.

The proper selection and gradation of the aggregate (fillers) can afford the PC system some enhanced properties. The presence of fillers can influence crazing, shrinkage, the coefficient of expansion, and porosity. In the finished product, surface appearance, dimensional stability, and resistance to abrasion, moisture and temperature change, fire retardancy and creep can be improved by correct selection of the appropriate filler materials. However, care must be taken in the selection of these filler materials. For instance non-acid resistant carbonates cannot be used where the best corrosion resistance is necessary. The choice of given fillers is dictated by the advantages and benefits which are desired in the application, of the finished products. Fillers can also be used for cost reduction

To produce a "Phenolic Concrete" system, good quality silica sands in the particle size range of 2400, 1200, 600, 300 microns were selected from various suppliers. A good quality of silica sand would permit easy mixing and handling. The selection of these sizes was based on two essential reasons. Firstly, the need for production of micro-products requires a micro-resin concrete, and secondly, silica sands in the range used contain least impurities. The silica content (S_iO_2) in these sands was over 97% and in some as high as 99%. In accordance to the suppliers technical data, these sands were all pre-washed to remove clay and other impurities with no chem-

ical treatment and then oven dried and screeded to produce the single size graded sands. The grade sizes and place of supply of these sands and their measured specific gravity (SG), density and PH values are given in Table 2.1. The grading of each individual component was obtained in accordance with B.S. sieve analysis[57], (see Table 2.2(a) for fraction sizes), and graphically presented as grading curves in Figures 2.1a and 2.1b.

As in any aggregate gradation design, smaller particles would be needed to fill the smaller voids between the neighbouring aggregate particles. This would provide the graded aggregate to produce a material which is more dense, less porous and absorptive. It will allow a much smaller amount of resin to be needed to fill the voids between the sand particles, thus forming stronger and impervious composite. For this reason various fine fillers of micro size, i.e micro-filler, with a maximum size of 150 microns were also used in determining the filler gradation matrix. These micro-fillers, their place of supply and physical properties are presented in Table 2.1. The particle gradings of these fine fillers were obtained in accordance with B.S. pipette analysis[58], (see Table 2.2(b) for particle sizes), and these are presented graphically in Figure 2.2. For their chemical and other properties references should be made to their suppliers' technical data. The silica content (S_iO_2) of silica flour fillers was as high as 99.2%, and 65% for Ballotini, Fillite and Spheriglass micro-fillers.

2.3. Preliminary Work, "Some experiences with filled Phenolic Resol Resins"

The production of high-strength phenolic resin concrete requires special attention to a number of factors. These include filler/resin ratio, catalyst type and dosage, gradation and minerology of the fillers, composition and fineness of the micro-filler. In addition, mixing, casting, setting, and curing processes also greatly influence the strength development in the finished product. The characteristics of the fillers regarding their bonding potential with phenolic resin and low water absorption capacity are also important in the production of high strength phenolic resin concrete.

In the early part of the research work, as explained before, a number of different phenol-formaldehyde resol resins produced by various resin manufacturers were used in formulating the phenolic concrete mixes. The filler compositions of these were designed in the manner given in Chapter 3.

In general, the flexural test results revealed the fact that the specimens made from the devised mixes, possessed insufficient stiffness and flexural strength. Therefore, the phenolic resol resins (i.e. J2018L, J2027L, XDF 4252, XDF 4151, PA104, etc.) were not suitable for developing any high strength phenolic concrete system. It was also found that the flexural strength of the finished specimens decreased with their stiffness deteriorating with time. From visual examination of the fractured surfaces of the specimens, it was seen that there was no bond developed between the resin matrix and the silica sand grains. This also became clearer using a Scanning Electron Microscope (SEM) technique.

Attempts were made to understand the causes of such weak bond developments and also how to improve the strength, and how to control strength losses. For this purpose, three categories of thin rectangular specimens were made using the

above mentioned resins. In category one specimens, the resins were filled with only micro-fillers, and in category two, the resins were filled with designed mixed graded aggregate (i.e. silica sands and micro-filler mix grading). In category three, the specimens were cast from only pure resins mixed with their relevant acid catalyst. These specimens were tested in flexure and their flexural strength and modulus values were deduced from their corresponding recorded load-deflection graphs (see Chapter 3 for test details). The specimen categories, their variables and brief remarks based upon their composition, construction, test results, and visual observation are provided in the following sections.

2.3.1. Specimens made using resol resin mixes filled with micro-fillers

A series of specimens in the form of coupons (5-7mm thickness) were made using phenolic resol resin and various available micro-fillers; such as different brand Silica-Flours, Ballotini, China Clay, Fillite, and Spheriglass 5000 and 3000). Mixes with one part resin to one part micro-fillers were prepared and cast subject to vibration. The variables were the catalyst type (weak and strong) and its content, postcuring temperature (i.e. $40\pm5°C$ and $70\pm5°C$), and age of specimens after postcuring. The manufacturing procedure was kept constant throughout. The specimens were tested in flexure and hence their flexural strength and modulus values were obtained. The percentage weight losses and percentage shrinkage of the specimens were determined due to postcuring at elevated temperature. The following statements were drawn from the mix composition, test results, and visual observations.

1- Using acid catalyst at lower levels, required a longer period of time for samples to set. The period of time was considerably increased with the use of the weaker acid catalyst.

2- The mixes made using the stronger acid catalysts, produced specimens with highest flexural strength and modulus values. The flexural strength values varied between 5.2 to 6.8 N/mm^2 with modulus values between 3.9×10^3 to 6.3×10^3 N/mm^2.

3- The specimens made using mixes produced from Silica Flour and China Clay exhibited greater stiffness with higher flexural strength and modulus values.

4- From the flexural testing of similar specimens immediately after, and 7 days after curing, it was found, that there were considerable losses in both flexural strength and modulus values. This was clearly noticed from the specimens with high acid catalyst dosage. The surfaces of these specimens had become multi-crazed after being kept at room temperature over the period of 7 days after curing.

5- All the specimens after being cured, exhibited some weight and shrinkage losses. These losses were more in the specimens made using weaker acid catalysts. The weight losses were between 3.8% to 4.5% with shrinkages in the order of 0.4% to 1.1%.

6- With $70 \pm 5°C$ curing temperature, higher flexural strength but lower flexural modulus values were obtained when compared with the results obtained from similar specimens cured at $40 \pm 5°C$. In this part similar specimens were subjected to two cycle curing. This did not improve or control the flexural properties. However, the losses seemed to be less or possibly at a lower rate at the age of 7 days after final curing cycle. Insignificant weight losses and shrinkages were noticed after the final curing cycle.

7- Some specimens were cured at $100 \pm 5°C$. They developed excessive crazing on their surfaces 7 days after curing. These specimens, in general, possessed lower

strength and modulus values.

8- Voids in the form of air pockets could be seen at fractured surfaces of these tested specimens, which were greater in number in specimens made with higher catalyst dosages.

9- The optimum strength and modulus values were found with specimens made using 6% or 8% acid catalyst by weight of resin content. With increase in catalyst, a small reduction in the values was noticed, but mix working time (gel time) had decreased considerably.

10- For samples made with 3% and 4% catalyst, setting was subjected to both pressure (i.e. weights were applied using a lid to the moulds), and heat (i.e. by placing the closed top moulds in the oven at $40 \pm 5°C$ for 5 hours). The flexural test results obtained from these specimens were lower than those obtained from specimens with 6% and 8% catalyst content for which setting was conducted at room temperature in an open top mould. Overall the specimens subject to heat and pressure at the time of setting, were distortion free and exhibited better flatness.

2.3.2. Specimens made using resol resin mixes filled with silica sands and micro-filler composition

The main concern at this stage was not to devise or justify the designed mix composition which would have the best workability and produce high strength specimens. The main objective was to assess and understand the reasons behind the low flexural strength and modulus values developing in the mature specimens, and also to develop methods of construction, i.e. mixing, casting, compacting, setting, and curing.

A large number of mix compositions were formulated from which phenolic resin concrete coupon specimens (6-8mm thickness) were made with variables similar to the previous specimen category. The following statements are based upon the mix composition, flexural test results and visual observations.

1- The flexural strength values of the specimens varied between 4.6 to 6.8 N/mm^2, with flexural modulus values ranging between 2.8×10^3 to 7.5×10^3 N/mm^2.

2- Specimens tested 4 to 7 days after oven curing exhibited lower flexural strength and modulus values than the specimens of similar composition tested immediately after oven curing. The strength losses in some were as high as 45%.

3- Cycle curing showed some improvement and perhaps some control in the rate at which their flexural properties deteriorated.

4- Curing in oven at lower temperature ($40 \pm 5°C$) over a longer period, provided higher strength values than for those cured at higher temperature ($70 \pm 5°C$ and $100 \pm 5°C$) but of shorter duration.

5- At fractured sections, a considerable number of voids (air pockets) were visible. These voids seemed to be less in the specimens made using mixes with less catalyst content and also in those cured at lower temperature irrespective of catalyst content.

6- Using agents Byke W980 and A525 (void release agents) showed no effect on void development, and no effect on flexural properties. In some mixes a low percentage of these agents were used to adjust the mix consistency. Addition of these agents had no delay action either on working time nor on setting time.

7- At a fractured section of all the samples, it was clearly noted that the sand grains flaked off easily by applying a small pressure. At the points where sand grains had flaked off a smooth pocket could be seen representing the sand grain

nesting. This suggested that no bonding had been developed between the sand particles and the enveloping resin matrix.

8- The ambient temperature greatly influenced the period of gel time (working time). At higher ambient temperature, the working time was shortened. This was more noticeable with the mixes having catalyst content higher than 8%. In the mixes with higher filler loadings, the working time seemed to have increased. The optimum flexural properties were obtained from the specimens made using highly filled mix systems with 8% to 10% of catalyst.

9- In all the test specimens, failure was of a brittle type. No surface crazing of the specimens was noticed even after 8 weeks irrespective of catalyst dosage. Instead, these samples possessed even lower flexural strength and modulus values than the specimens tested 7 days after cycle curing.

2.3.3. Specimens made from casting pure catalysed resins

A series of coupon specimens were cast using resin/catalyst mixtures, with catalyst at 1%, 2% and 3% by weight of resin. Higher catalyst content mixtures were also prepared and their polymerization was observed with regard to volume, surface/volume ratio and ambient temperature in a given volume of mixture. The following observations are based on visual observations and coupon flexural test results.

1- The resin/catalyst mixtures with different catalyst contents were placed in various size containers. The mixtures (except with 1% catalyst) were all hardened into a low density expanded aerated foam. These aerated foams were strong and tough containing a great number of small and large air pockets with many pin-holes. The mixture with 1% catalyst content turned into paste form over a

period of approximately 4 hours and then slightly expanded in volume forming into a semi solid mass which hardened to a solid mass with heat. The rate and extent of volume expansion of these aerated foams, reduced as the mixture surface area increased with its volume decreasing (i.e. increasing container size). This became more apparent when coupon specimens of 6mm thickness were cast. Coupon specimens cast using mixtures with 1% and 2% catalyst had all set into paste form after 24 hours. The cast coupons with 3% catalyst had set with some volume expansion into a semi solid.

2- The polymerization of these mixtures was initiated with condensation process as a result of high exothermic temperature, thus causing foamation. The polymerization of these mixtures was initiated at a free surface due to ambient temperature. This was clearly seen as the foamation started from the top surface progressing downwards and hence entrapping the gases released and therefore causing an expansion in volume.

3- Mixtures with 3% catalyst, were cast in closed top moulds. The mould lid allowed the cast mixtures to set evenly into solid masses with no foamation or volume expansion. This showed how effective is the direct ambient temperature in initiating the polymerization and increasing the rate of exotherm.

4- The volume expansion increased as percentage catalyst increased (i.e. more and larger gas pockets developed).

5- Time taken for polymerization to proceed decreased with increase in ambient temperature and/or percentage catalyst.

6- No delay in polymerization, or significant decrease in volume expansion and air pockets were observed with addition of W980 and A525 agents.

7- The coupon specimens made using mixtures with 1% to 3% catalysts were placed

in the oven after they had formed into paste form and cured at $70 \pm 5°C$. It took approximately 3 hours for these to be cured with no volume expansion. Similar coupons were also cured at $35 \pm 5°C$ which took almost 5 hours. The curing was accomplished with the specimens becoming tough with reddish pink colour. These coupons were tested in flexure with flexural strength values ranging between 5.8 to 6.1 N/mm^2 and modulus values between 2.9×10^3 to 3.4×10^3 N/mm^2.

The surface topography of the fractured sections of the specimens from all three mix categories was studied using the SEM technique. The elemental composition of the specimens made using resin/catalyst mixtures was also determined using Energy Dispersion Analysis by X-ray (E.D.A.X.). A brief review of the conclusive findings are described in the following;

1- Plates 1 to 3, represent the SEM images of the fractured surfaces of the specimens made using resin/catalyst mixtures with 1%, 2% and 3% catalysts respectively. From these images, it may be seen that there are two major phenomena. These are, firstly, the presence of a great many micro-voids (pin-holes), secondly, the presence of lines in the form of striations which are joining the neighbouring micro-voids. These may, in fact, not allow enough strength and stiffness of the specimens to be developed. These images also show loosely dispersed particles of crystal shape which are housed in the voids or present on the fractured surface. It may also be seen with increase in catalyst, the voids have increased considerably (see Plates 1 to 3).

2- Plates 4 and 5, represent the images of the fractured surfaces of the filled resin systems with fibrous filler (sawdust), and non-fibrous filler (sands and ballotini composition) respectively. From Plate 4, it may be seen that the fibrous filler

is well bonded to the resin. In this image, an aerated-foamed patch can also be seen which is thought to have formed because of local catalyst concentration due to poor mixing or excessive catalyst dosage. It is, therefore, of importance not to over-dose and to adopt a mixing technique which would uniformly disperse the catalyst in the matrix. Plate 5, shows that silica sand particles and ballotini smooth sphere particles, are loosely dispersed with no apparent bonding to the resin matrix. The large apparent void in this image, indicates that a sand grain has fallen out without tearing or peeling off any of the surrounding resin matrix. The E.D.A.X. study, in general, indicated unaccounted impurities present in the catalysed resins.

Later in the course of research Furfuryl Alcohol, as part of the resin, was used in the devised mixes which when cast provided high strength phenolic concrete systems. Sample flexural test results are presented in Figure 2.3. showing the increase in flexural strength and modulus values of the cast coupons with increase in Furfuryl Alcohol content in the mix. To achieve the modified mixes, the mix resin was composed partly of phenolic resol resin (J2027L) and partly Furfuryl Alcohol. The results clearly indicated that the polymer/filler bond increases with the addition of Furfuryl Alcohol. However, too high a level of furfuryl alcohol in the mix matrix provides a brittle system, decreasing the flexural strength capacity. The flexural strength and modulus values obtained from testing the coupon specimens and their relevant modified phenolic resin concrete mixes are presented in Table 2.3..

From the preliminary work, the methods of construction (i.e. mixing, casting, setting, and curing) and other useful techniques were developed which helped in producing the phenolic concrete systems given in Chapter 3. These developed techniques are recommended in the following sections of this Chapter.

2.4. Construction techniques

2.4.1. Mixing

The phenolic concrete product is a composite material. It is of importance to achive a uniform homogeneous material. This may be achieved if a proper mixing procedure is adopted, otherwise it will directly influence the strength and behaviour of the end product. Since the phenolic resins used are "cold set" systems which need a strong acid based catalyst to polymerize, care should be given to the order in which the concrete constituent materials are to be mixed. The polymerization is exothermic and the degree and rate of polymerization for a given resin concrete mix is greatly influenced by; resin loading, catalyst type and its dosage, temperature, time, and volume of the mix.

The weighed filler constituents should be mixed thorougly to achieve uniformly graded filler. The prescribed catalyst amount should then be added and the catalysed filler, mixed further for not less than approximately 3 minutes, depending on the mix volume, until uniform dispersion of catalyst. The resin and mixed catalysed filler temperatures should be kept equally constant, and reduced if necessary, before the two are brought together. This will ensure a constant mixing period of similar batches, and constant working time (gel time).

The material temperature should be kept at as low as possible to avoid shortening of the working time span, especially in larger mixing volumes. With reference to the type of end product and mould shape, in larger mixing volumes, it is recommended to conduct the final mixing in batches to avoid any difficulties.

The time allowed for catalysed filler/resin mixing is determined from the working time of a given situation. For instance, with highly filled systems, the presence

of filler tends to retard the polymerization and decrease its rate by reducing the exothermic temperature while contributing to working time. However, a period of 1 to $1\frac{1}{2}$ minutes is sufficent and practical in any mixing, (with reasonable mix volume and catalyst dosage), to achieve a uniform matrix. The mixing can be conducted in any clean, dry and grease free conventional pan type mixer.

2.4.2. Casting

Casting the phenolic concrete mix matrix is crucal, since a short period of working time is left for it to be compacted, screeded and levelled off before setting. Thick section or mass volume casting should be avoided, otherwise due to high exothermic temperature development, it may become impossible or form into an aerated product containing large voids with considerable volume expansion. Instead, if necessary, it can be cast in thin layers (using several mixing batches) to form the desired thickness or volume. If cast in layers, time should be allowed for the previous layer to have cooled before the next layer is prepared and laid.

The compaction is vital for both releasing the entrapped air bubbles and easing the casting process. It is also of prime importance to achieve a uniform thin section micro-product. The compaction may be in the form of vibration which should be of low amplitude and high frequency (i.e. 1200 r.p.m.) to avoid any possibility of segregation, creating unnecessary voids (air bubbles) and surface resinous products. Screeding and levelling can be conducted while vibrating or performed on their own depending on the cast mix consistency.

Casting can be either hot or cold depending on the required product physical property and feature, availability of equipment and production technique. The cold casting is done as explained above with any catalyst level in the mix matrix. The

hot casting is only suitable for the mix matrix having low catalyst level which is followed by a hot setting process subject to pressure (see section 2.4.3.).

2.4.3. Setting

The cast mix matrix should be allowed to set into a hardened solid before it can be demoulded without being damaged. The time taken for the matrix to solidify is the setting period. The method of casting (i.e. cold or hot) determines the required method and period of setting. If it is cold casting and therefore cold setting, a period of over night or 24 hours (as customary) should be allowed before demoulding. If it is subjected to hot casting (i.e. cast in a preheated mould), normally, hot setting procedures should be adopted which would require a short period of time i.e. minutes. Using either method, the casting and setting should be conducted in a closed top mould with pressure applied to the cast matrix. In cold setting, the pressure may be applied using weights and with hot setting, a hot press platen may be used. This will produce a dense product with smooth surfaces while squeezing out the excess resin and minimizing the void content. It will also control the exothermic heat dissipation and produce a product with minimum distortion.

In hot casting and setting, the temperature of the press platen should be kept below the water boiling temperature in order to avoid occurence of any flow to the system. This method of setting will reduce the setting period required to as little as 15 minutes and produce the best result regarding the physical and mechanical properties of a given system.

2.4.4. Postcuring

Generally, in any polymer concrete system, the hardened product should be

postcured at an elevated temperature. In a phenolic concrete system the postcuring temperature and period controls the strength development. Postcuring, at elevated temperature, releases the volatiles in the matrix, thus enhancing the properties of the end product. These volatiles may be aldehydes, water, etc.

The rate of curing determines the period needed for the product to achieve its highest strength and stiffness properties. For the phenolic concrete specimens produced in this work an optimum level was found to be an oven temperture at $120°C$ for a period of 2 hours (see Chapter 3). Higher curing temperatures may be detrimental or produce brittle end products, and lower temperature will require a much more uneconomical curing period. For an end product which is to be free from distortion curing should be carried out free standing in a fan-blow oven.

2.5. Reinforcement

2.5.1. Fibre reinforcement

There has been an ever increasing interest in using fibre-glass in concrete technology in improving certain properties. It has been suggested that fibre-reinforced concrete is superior in wear resistance to conventional concrete, but, although superior performance in pavements has been demonstrated, this improved performance is largely the result of superior crack resistance rather than resistance to abrasion[59]. In the case of phenolic resin concrete, which is a brittle composite, the fibre reinforcement may be used for enhanced mechanical and physical properties. For its increased carrying capacity, enhanced ductility, early cracking and impact resistance, fibre glass in the form of laminated chopped-strand mat (CSM) or other types may be used as reinforcement. Since the resin used in developing the phenolic concrete

systems (see Chapter 3) had properties different from those for use with the fibre glass mats available, a method of pre-lamination using the resin suitable for fibre glass wet out was used to incorporate the pre-laminates with the phenolic concrete systems.

The recent developments on fibre glass/phenolic resin composites have made it possible to adopt lamination techniques for various applications[46,51]. The methods suitable[47] for the purpose of the present work are "hand lay up" and "spray up". The latter may be regarded as automation of the former technique.

The selection of suitable glass for fibre glass/phenolic composite requires their compatibility. Most glasses available in the market have been developed for polyester and epoxy resins. The sizes and binders used on these glasses do not effect polyester or epoxy chemistry but some have adverse effects on that of phenolics. In general powder bound chopped strand mats are compatible whilst emulsion bound materials are less satisfactory[47,60]. Most woven roving glasses appear acceptable but a somewhat higher degree of rolling is required to achieve good wetting of the bundles than with polyester.

The fibre glass/phenolic resin composite in the form of laminates acting as reinforcement to the phenolic concrete system should be employed on both faces for symetrical responses to the system. This would in fact avoid any differential shrinkages of the extreme faces which otherwise would produce distorted laminated fibre glass reinforced phenolic concrete products. This was clearly seen from the specimens made having fibre glass/resin laminates laid only on their tension faces. These became distorted (concaved) at the end of the system's curing period. The prelaminates can be laid on the faces of the phenolic concrete matrix in either wet or semi dry form. The construction technique and physical shape and dimensions of

the product may determine the wet or semi dry form of use.

In using the fibre glass mat laminates for reinforcing the elements produced in this research work, a single cold-cure phenolic resole resin system, BP Cellobond J2018L was used with its recomended catalyst Phencat 10. It is worth noting that where there is lamination, there is possibility of delamination. However, the testing of the fibre glass reinforced phenolic concrete product clearly showed that full composite action was achieved and that the specimens which failed in flexure did not delaminate, and also similar samples tested after a two year period responded similarly.

A comprehensive study of phenolic resin fibre glass reinforced laminates using J2018L resin and various glass types is reported by BP Chemicals[47,51]. Table 2.5. shows thermal and typical physical properties obtained on a three-ply hand laid laminate using $450g.m^{-2}$ chopped strand mats at 2:1 resin to glass ratio. The water absorption of a phenolic fibre glass laminate system is higher than that of similar materials based on polyester or epoxy resin. However, with a phenolic system the loss in mechanical properties due to water absorption is not as high as in a polyester system. It has been shown[47,48,51] that a typical loss of flexural strength after one year immersion is 25%. The mechanical properties of a phenolic fibre glass reinforced laminate system are influenced considerably by glass:resin ratio and type of reinforcement. It has also been shown[47] that whilst the flexural strength of a polyester fibre glass laminate is reduced by 50% at $140°C$, a phenolic system retains 50% strength to $225°C$.

More recently, there has been research work conducted on the assessment of chopped-strand fibre glass mat reinforcements for hand lay up with J2018L resin and their compatibility at the University of Bath[60]. The systems were assessed by the

mechanical properties of laminates determined using tensile and short-beam shear tests. The latter test has provided evaluation between competing reinforcements, both in the quality of the fibre-resin bond, and in its retention after a 16 hour exposure of the laminates to boiling water. The reduction in interlaminar shear strength has been found to be 25% with small variation from one system to another.

2.5.2. Steel reinforcement

Steel bars may also be used as reinforcements in the phenolic concrete systems. The bond may only be achieved by mechanical means since there is no chemical bond capability between the steel and the phenolic system. Therefore deformed steel bars, having for instance ribs, can benefit the system by mechanical bonding. However, care should be given to the dosage of strong acid catalyst in the cold set phenolic concrete system. The high catalyst dosage may cause long term problems i.e. excessive creep due to corrosion in the embedded steel reinforcement. It is also suspected that the degree of condensation as a result of polymerization of phenolic system may influence the bond properties. This area is one which would need some long term research work before it can be otherwise justified.

The bond properties of the phenolic concrete and the steel bars were studied using a series of pull-out type tests. The pull-out tests, were intended to determine the adhesion of round and deformed steel bar reinforcements to the phenolic concrete. In these tests, a bar incorporated in a phenolic concrete cube along a defined length was strained at one end by a tensile force. The relation between the tensile force and the relative displacement was determined between the steel bar and the phenolic concrete. The load was increased up to failure of the adhesion. The test specimens were cubes of phenolic concrete cast in cubic polypropylene moulds with

the steel bars incorporated on their central axis (see Figure 2.4(b)). The bars to be tested were extended beyond the two sides of the cubes, with the longer end subject to tension and the shorter end remaining without stress. The displacement between the steel bar and the phenolic concrete was measured using three dial-gauges. One was set on the steel bar shorter end with the other two set against the corresponding cube face (see Figure 2.4(c)). The bars used in these tests were: 12, 10, 8, and 6 mm diameter ribbed high yield steel bars and also a 10mm diameter plain-surface round mild steel bar.

The size of the phenolic concrete specimens were 10D with D being the relevant steel bar diameter. The effective adhesion lengths were: (10D), 3/4(10D), 1/2(10D) and 1/4(10D) for each bar size. The longer bar end was 450mm long and the shorter end was 50mm (see Figure 2.4(a) for specimen description). The bars were degreased using an acetone solution. The non-adhering part situated in the phenolic concrete was wrapped with a mastic tape to which was applied a thin layer of industrial wax. To cast the phenolic concrete cubes, the mix formulation E1 (see Chapter 3) was used with a filler:resin ratio of 6:1. The resin IR1271 was used in the mixes with acid catalyst CS30 at 4% by weight of resin. This catalyst level served two purposes. Firstly, to be able to cast a bulky volume of phenolic concrete cubes and also to ensure minimum acid attack to the embedded steel bar. The cubes with steel bars aligned in their axis (see Figures 2.4(a) and 2.4(b)) were cast in 20mm thick layers, i.e. for instance with 12mm dia. steel bars phenolic concrete cubes of $120 \times 120mm^2$ were cast in six layers. The mix matrix to form the specimen was placed in layers which were horizontal with the bar in the vertical axis of the mould, with each layer subjected to a very short period of low amplitude vibration. The cast specimens were kept at room temperature overnight subject to pressure by applying weights via mould top lids. The following day, these were placed in the

oven at $70 \pm 5°C$ for a period of six hours for setting to complete. Once set, the specimens were demoulded and placed in the oven $70 \pm 5°C$ for a further period of 24 hours which helped the phenolic concrete to cure. The specimens were tested in a Denison Testing machine in the manner shown in Figure 2.4(c). The tension force (P) was applied to the upper face of the cube while the longer end of steel bar tightened in the jaws of the Denison. The displacement between the steel and the phenolic concrete was recorded at three points at 0.25 (kN) intervals.

The adhesion stresses B_p (tensile force exerted on the encased bar surface) was determined using the following equation;

$$B_p = \frac{P}{\pi.D.L}$$

where,

P is the applied force (kN)

D is the bar diameter (mm)

L is the adhesion length (mm)

The test results indicated clearly that greater bond strengths were developed with ribbed bars in comparison to plain surface round bars (see Table 2.6). The pull-through slip in round bars was sudden with no prior warning. The form of slip curves presented in Figures 2.5 and 2.6 are similar for all the ribbed bars. In Table 2.6, the slip stresses developed at 0.1mm, 0.25mm, 0.50mm, and pull-through are given for each bar and its relevant adhesion lengths. Figure 2.7, presents the effect of bond (embedment) length on the maximum bond stress development for various sizes of h.y.s. ribbed bars at failure (pull-through). Table 2.6, indicates that greater slip bond stresses are developed with shorter adhesion lengths. This suggests that the bond stresses are not uniformly distributed along the bond length, but are concentrated near to the end at which tension is applied. The stress distribution is

thought to be an exponential zone over the embedded length as illustrated in Figure 2.8.

2.6. Moulds and mould releasing agents

Steel, polypropylene, and wooden moulds can all be used for casting phenolic concrete mixes. Polypropylene moulds are most favoured due to their non-chemical reactions with cast phenolic systems. However, under continuous use, this type of mould exhibits some distortion particularly if used in hot casting and setting processes. They may be used when cold casting is required with a smooth surface finish. With this material, an industrial wax or any mould releasing agent (i.e. Freecoat) may be used for ease of demoulding.

Wooden moulds of any size or shape can be used providing a good deal of care is given to protect it against direct contact with the phenolic system. Phenolic systems adhere to wood. They may be used in casting product where surface finish is not of importance. Industrial wax, grease or moulding oil in conjunction with a Melinex film lining should be used with a thin layer of mould releasing agent (i.e. Freecoat) applied to the lining. A wax, grease or oil type of material placed on the wooden mould would protect it against phenolic concrete and at the same time will provide means of holding the Melinex film in place while casting on to it.

Steel moulds may be used, where a good surface finish and greater dimensional accuracies of the end products are required. It should be noticed that care should be given to avoid acid attack in repetitive use of steel moulds with catalysed phenolic systems. For this reason a mould releasing agent should be used which would also provide protection for the steel surface in continuous usage. Steel moulds can be used with both cold and hot casting and setting processes.

A study of mould releasing agents has been conducted[61] for polyester (or polymer) concrete. Mould-releasability of silicon and fluorine containing agents are recommended. No matter how excellent, any mould-releasing agent may be considerably affected by vibrating compaction. This may generally arise as a result of the scraping action of aggregates on the mould surfaces.

In the present research work, the best solution which provided good mould-releasability, easy application, protection to the mould material, and also enhanced surface finish was the use of Teflon Coated Glass Cloth with silicone adhesive coating on one face (TCGC). This mould releasing lining can be adhered to the mould surfaces. For extra precaution a spray of, let's say Freecoat, should be applied to the TCGC surface. TCGC as lining on any mould made of any material, results in a very satisfactory surface of the end product.

Table 2.1.

(Fillers and their Physical Properties)

Sands					
Sample	Grade	Designation (Place of Supply)	Measured		
			Specific Gravity	Uncompacted Dry Dencity ($g.cm^{-3}$)	PH Value
A	8/16	J.A.	2.59	1.56	7.30
B	16/30	J.A.	2.62	1.55	7.15
C	No.14	J.A.	2.60	1.57	7.15
D	No.80	Ch.	2.61	1.56	8.15
E	.....	T.	2.62	1.57	7.20
A1	8/16	J.A.	2.59	1.55	7.15
B1	16/32	T.	2.65	1.55	7.15
C1	No.14	J.A.	2.60	1.58	7.15
D1	No.81	J.A.	2.60	1.56	8.10
E1	.....	T.	2.63	1.57	7.30
F	6/14	L.B.	2.60	1.57	7.10
G	14/25	L.B.	2.59	1.58	7.15
H	16/30	T.	2.54	1.50	7.15
I	No.21	L.B.	2.60	1.53	7.30
J	.....	N.S.	2.58	1.55	7.20
K	.....	N.S.	2.60	1.57	7.15

Micro Fillers						
Trade Name	Designation (Place of Supply)	Measured			Specified	
		Specific Gravity	Density in Toluene (g/ml)	PH Value	Specific Gravity	Bulk Density ($kg.m^{-3}$)
E. CHINA CLAY (D)	D.U.	2.62	0.293	7.40	.....	.....
BALLOTINI	F.	2.43	0.685	9.80	2.55	1080
a)SILICA FLOUR L.G.3/300	T.	2.60	0.656	4.75	2.52	930-1010
b)SILICA FLOUR L.G.3/300	T.	2.59	0.678	4.80	2.52	1089-1169
c)SILICA FLOUR C.W.5/300	B.I.S.	2.51	0.695	4.80	2.55	1050
d)SILICA FLOUR C.W.5/300	B.I.S.	2.55	0.680	4.70	2.55	1150
e)SILICA FLOUR H.P.F.5	B.I.S.	2.56	0.910	4.90	2.65	1442
FILLITE	F.R.Ltd.	.....	.....	7.50	.....	180-450
SPHERIGLASS 3000	C.G.	2.50	0.712	7.15	2.45	1150
SPHERIGLASS 5000	C.G.	2.56	0.718	7.20	2.50	1180

Key : J.A.= Joseph Arnolds D.U.=Durham University T.=Tilcon
L.B.= Leighton Buzzard N.S.=Natural Sand F.=Fypol
B.I.S.= British Industrial Sands C.G.= Craxton & Garry Ch.= Chelford
F.R.Ltd.= Fillite (Runcorn) Ltd.

Table 2.2 Filler Components (measured gradings)

Sieve Sizes (micron)	Percentage Passing (%)																
	SANDS																FILLITE
	A	B	C	D	E	A1	B1	C1	D1	E1	F	G	H	I	J	K	
2400	99.20	100.00	100.00	100.00	93.14	99.34	100.00	100.00	100.00	98.71	71.10	100.00	100.00	100.00	100.00	100.00	100.00
1200	19.70	99.77	100.00	100.00	29.64	24.08	99.87	100.00	100.00	15.81	0.45	99.00	85.00	100.00	100.00	100.00	100.00
850	4.50	56.77	100.00	100.00	21.68	1.65	76.49	100.00	100.00	0.67	0.20	45.10	53.60	100.00	100.00	100.00	100.00
600	2.50	13.27	99.25	100.00	20.96	0.34	11.92	99.50	100.00	0.37	0.10	0.60	20.00	91.90	100.00	100.00	100.00
300	0.40	0.40	26.50	98.00	18.80	0.00	0.00	31.16	96.68	0.00	0.06	0.10	0.22	11.30	79.00	95.25	100.00
150	0.10	0.28	0.50	23.20	8.91	0.00	0.00	0.50	25.59	0.00	0.00	0.00	0.11	1.20	4.40	21.75	52.17
90	0.03	0.18	0.40	2.10	3.71	0.00	0.00	0.00	2.37	0.00	0.00	0.00	0.06	0.10	0.20	7.88	22.81
75	0.00	0.03	0.25	1.00	3.19	0.00	0.00	0.00	1.42	0.00	0.00	0.00	0.00	0.00	0.20	6.50	15.50
63	0.00	0.00	0.13	0.30	0.36	0.00	0.00	0.00	0.50	0.00	0.00	0.00	0.00	0.00	0.05	1.00	5.47

(a) Sieve Analysis of the "Sands" in accordance to B.S. 1377 Test 7(b)

Micro Fillers (Particle Sizes in micron)																
E.CH.C.(D)		BALLOTINI		SPHERIGLASS 5000		SILICA FLOUR										
						(a) L.G.3/300		(b) L.G.3/300		(c) C.W.5/300		(d) C.W.5/300		(e) H.P.F.5		
Particle Size	(%) Passing	Particle Size	(%) Passing	Particle Size	(%) Passing	Particle Size	(%) Passing	Particle Size	(%) Passing	Particle Size	(%) Passing	Particle Size	(%) Passing	Particle Size	(%) Passing	
63.00	100.00	63.00	92.00	63.00	99.60	150.00	100.00	63.00	100.00	63.00	98.00	63.00	100.00	300.00	100.00	
60.00	100.00	60.00	86.50	60.00	98.00	90.00	99.70	60.00	100.00	60.00	97.00	60.00	100.00	150.00	89.00	
30.00	99.41	35.00	60.00	30.00	95.81	75.00	96.00	35.00	90.02	30.00	80.00	30.00	80.00	63.00	61.00	
24.00	99.41	24.00	41.50	24.00	94.00	63.00	93.00	24.00	77.28	20.00	61.00	20.00	67.50	40.00	45.00	
19.00	98.25	19.00	32.50	19.00	88.25	60.00	92.80	19.00	64.44	15.00	47.00	15.00	49.50	30.00	36.00	
13.00	95.03	15.00	22.50	13.00	60.00	28.00	74.00	13.00	50.19	13.00	39.50	13.00	40.50	20.00	28.00	
11.00	90.33	11.00	11.50	11.00	48.00	22.00	62.00	11.00	43.33	11.00	35.50	11.00	38.00	15.00	23.00	
8.00	78.72	8.00	9.00	8.00	28.12	15.00	50.00	8.00	32.25	8.00	27.00	8.00	30.00	10.00	18.00	
5.00	64.54	5.00	7.00	5.00	11.50	11.00	40.00	5.00	21.58	5.00	20.00	5.00	20.50	6.00	10.50	
3.00	49.76	3.00	2.50	3.00	4.00	6.00	25.00	3.00	16.92	3.00	10.00	3.00	14.00	4.00	7.00	
2.60	46.00	2.60	1.50	2.60	3.50	5.00	23.00	2.60	16.03	2.60	7.50	2.60	13.00	3.00	4.50	
2.00	43.16	2.00	0.50	2.00	0.56	4.00	18.00	2.00	12.72	2.00	6.00	2.00	11.50	2.00	3.50	
1.00	33.49	1.00	0.00	1.00	0.00	2.00	13.50	1.00	6.86	1.00	3.50	1.00	7.50	1.00	2.00	

(b) Pipette Analysis of the "Micro Fillers" in accordance to B.S. 1377 Test 7(c)

Table 2.3 Flexural strength and modulus of Furfuryl Alcohol modified Phenolic Concrete mixes (using J2027L resin + Furfuryl Alcohol)

Mix		J2027L : Furfuryl ratio	Filler : Resin ratio	Catalyst Content (%)	Flexural	
No.	Formulation				Strength σ_{fu} $\times 10^6$ $(N.m^{-2})$	Modulus E_f $\times 10^9$ $(N.m^{-2})$
1	34.8% Sand A	100:0	5:1	6	6.52	5.22
	17.5% Sand B	90:10			9.73	7.55
	15.7% Sand C	80:20			13.67	8.05
	14.0% Sand D	70:30			14.02	8.27
	18.0% Ballotini	60:40			14.35	8.49
		50:50			17.22	8.72
		40:60			16.48	8.82
		30:70			14.06	9.25
		20:80			13.12	9.85
2	34.8% Sand A	100:0	5:1	8	5.88	6.23
	17.5% Sand B	90:10			8.96	8.10
	15.7% Sand C	80:20			13.82	8.65
	14.0% Sand D	70:30			13.79	8.85
	18.0% Ballotini	60:40			16.86	9.35
		50:50			17.67	9.95
		40:60			16.82	9.72
		30:70			16.89	10.6
		20:80			12.35	11.1
3	34.8% Sand A	100:0	5:1	8	5.85	4.66
	17.5% Sand B	80:20			14.23	8.85
	15.7% Sand C	60:40			16.35	9.33
	14.0% Sand D	50:50			18.26	9.86
	18.0% S.F. L.G.3/300	40:60			17.92	10.1
		20:80			15.45	11.9
4	34.8% Sand A	100:0	5:1	8	5.28	4.10
	17.5% Sand B	80:20			10.12	7.26
	15.7% Sand C	60:40			12.24	7.85
	14.0% Sand D	50:50			15.66	8.68
	18.0% ECC (D)	40:60			15.10	8.72
		20:80			11.80	8.06

Resin Type : BP's Resin J2027L
Catalyst : Phencat 15
ECC (D) : English China Clay
S.F. LG.3/300 : Silica Flour LG.3/300

Casting: Cold Mould
Setting : 24Hrs. @ Room Temp. subject to pressure
Curing : 24 hrs. in oven @ $70 \pm 5°C$

Table 2.4 Comparative measured Physical/Chemical properties of BP-J50/010L and Fordath-IR1271 resins (by BP Chemicals, Applied Phenolic Resin Division-Sully)

Properties		BP-J50/010L		FDTH-IR1271	
		Specification	Measured	Specification	Measured
Viscosity @ 25°C	(cP)	50.0 - 80.0	57.50	70.0	22.0
Specific Gravity @ 25°C	(gml^{-1})	1.18 - 1.20	1.19	1.2	1.17
pH value		5.0 - 6.5	6.20	5 - 8	6.5
Pot life	(minutes)	1.5 - 3.0	1.90	....	2.5
Solids	(%)	28.0 - 36.0	33.95	....	28.0
Water Content	(%)	6.0 - 9.0	7.80	8.0	8.5
Free Phenol	(%)	3.0 - 5.0	3.27	....	3.35
Free Furfuryl Alcohol	(%)	47.0 - 53.0	48.10	....	55.0
Free Formaldehyde	(%)	4.0 - 4.5	4.00	0.8	1.0
Nitrogen	(%)	2.80	2.80	2.8	2.8

Table 2.5 Typical physical and thermal properties of fibre glass reinforced laminate (by BP Chemicals, Applied Phenolic Resin Division-Sully)

Physical and Thermal Properties		
Flexural strength	150 - 200	$MN.m^{-2}$
Flexural modulus	4500 - 6000	$MN.m^{-2}$
Tensile strength	90 - 120	$MN.m^{-2}$
Tensile modulus	5000 - 5500	$MN.m^{-2}$
Elongation at break	2.0 - 2.5	%
Izod impact	550 - 700	$J.m^{-1}$
Coefficient of linear thermal expansion	10 - 25	$\times 10^{-6} °C^{-1}$
Thermal conductivity	0.12 - 0.17	$W.m^{-1} °C$
Heat distortion temp. (BS 2782 Pt.121A):		
Cast resin	90 - 150	$°C$
Laminate	up to 250	$°C$

The specimens used in the tests were made from 3 ply hand lay laminate using $450g/m^2$ CSM at 2:1 resin:glass ratio. BP-J2018L resin was used with different content levels of Phencat 10 catalyst.

Table 2.6. Results of developed bond stress at various slip levels with different bond-lengths (using pull-out test)

Steel bar			Embeded Length (mm)	Developed bond stress MN/m^2			
Type	Diameter (mm)			Slip (mm)			
	Spec.	Measured		0.10	0.25	0.50	Pull-through
A	12.0	12.22	120	1.0	1.2	1.6	10.20
A	12.0	12.22	90	1.7	2.3	3.1	14.80
A	12.0	12.22	60	0.7	1.1	1.9	17.20
A	12.0	12.22	30	2.6	3.4	4.7	30.40
B	12.0	12.08	120	0.3	....	....	1.40
A	10.0	10.24	100	0.1	0.2	0.3	10.60
A	10.0	10.24	75	2.6	4.0	....	17.90
A	10.0	10.24	50	0.9	1.6	3.5	19.80
A	10.0	10.24	25	3.2	4.7	8.1	37.40
B	10.0	9.98	100	0.1	0.6	....	2.40
A	8.0	8.26	80	1.0	1.4	1.8	10.80
A	8.0	8.26	60	3.1	4.7	....	15.50
A	8.0	8.26	40	2.7	4.4	....	18.80
A	8.0	8.26	20	4.8	9.3	14.7	35.20
B	8.0	8.12	80	0.2	0.3	1.1	4.70
A	6.0	6.24	60	2.8	3.8	5.2	11.20
A	6.0	6.24	45	3.0	4.9	....	14.40
A	6.0	6.24	30	3.6	4.6	6.1	15.90
A	6.0	6.24	15	8.5	10.2	11.9	25.70
B	6.0	6.06	60	2.2	2.6	3.1	4.40

Bar type A - Ribbed high yield steel bar

Bar type B - Plain-round mild steel bar

Failure - All failed in pull-through manner, with type "B", the failure occured suddenly at low stress.

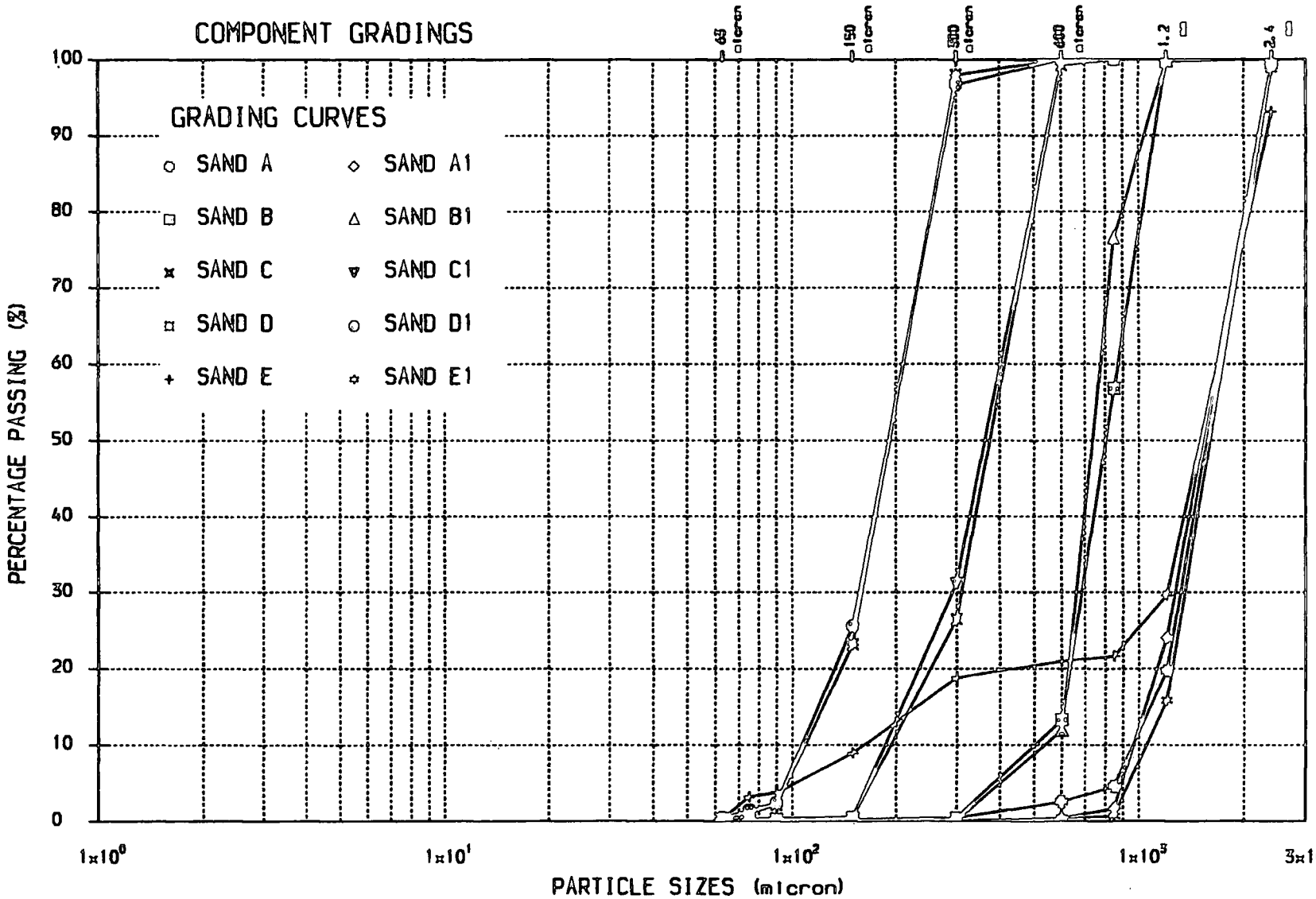

Figure 2.1a Grading curves of the sand filler components (from sieve analysis)

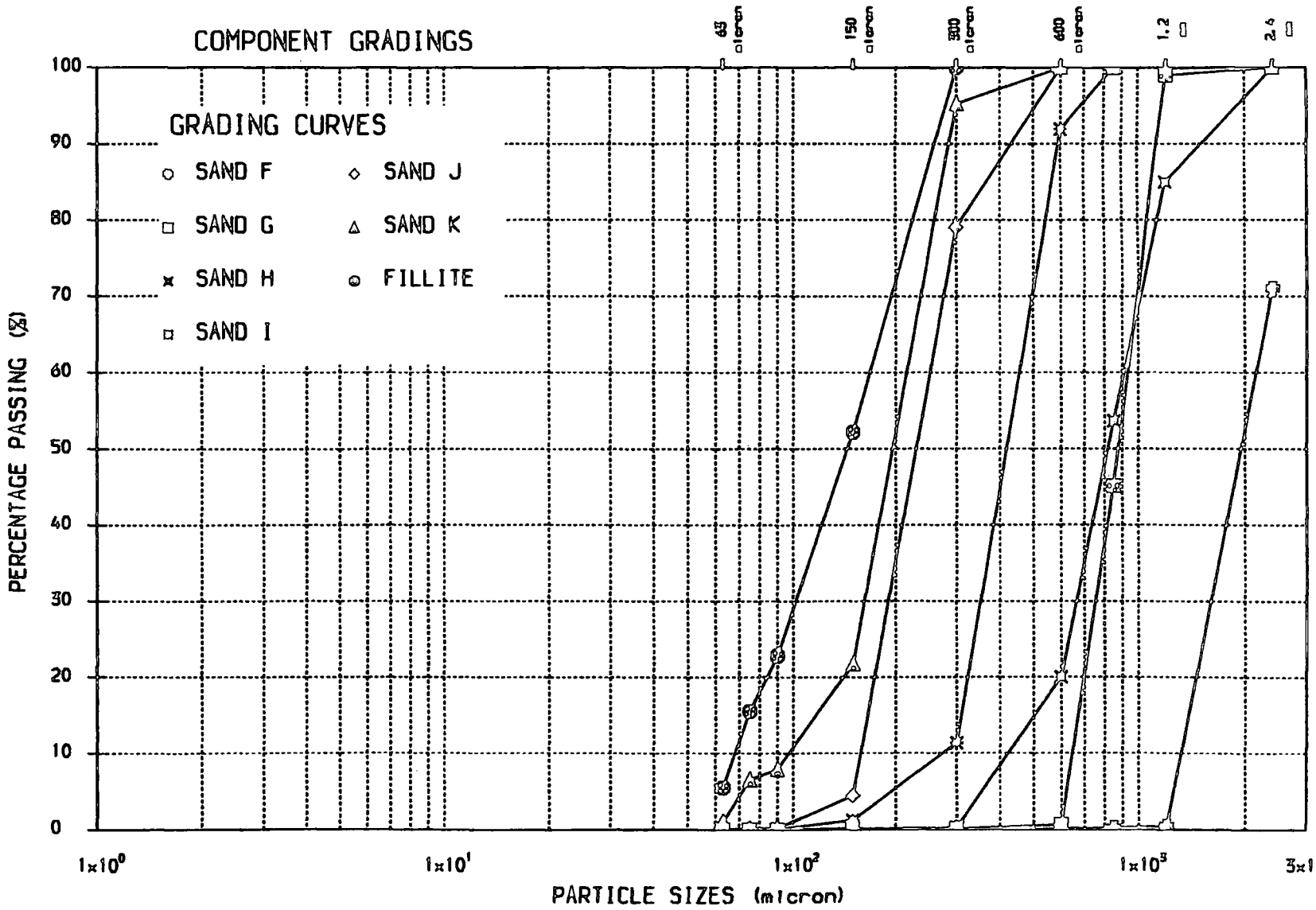

Figure 2.1b Grading curves of the sand filler components (from sieve analysis)

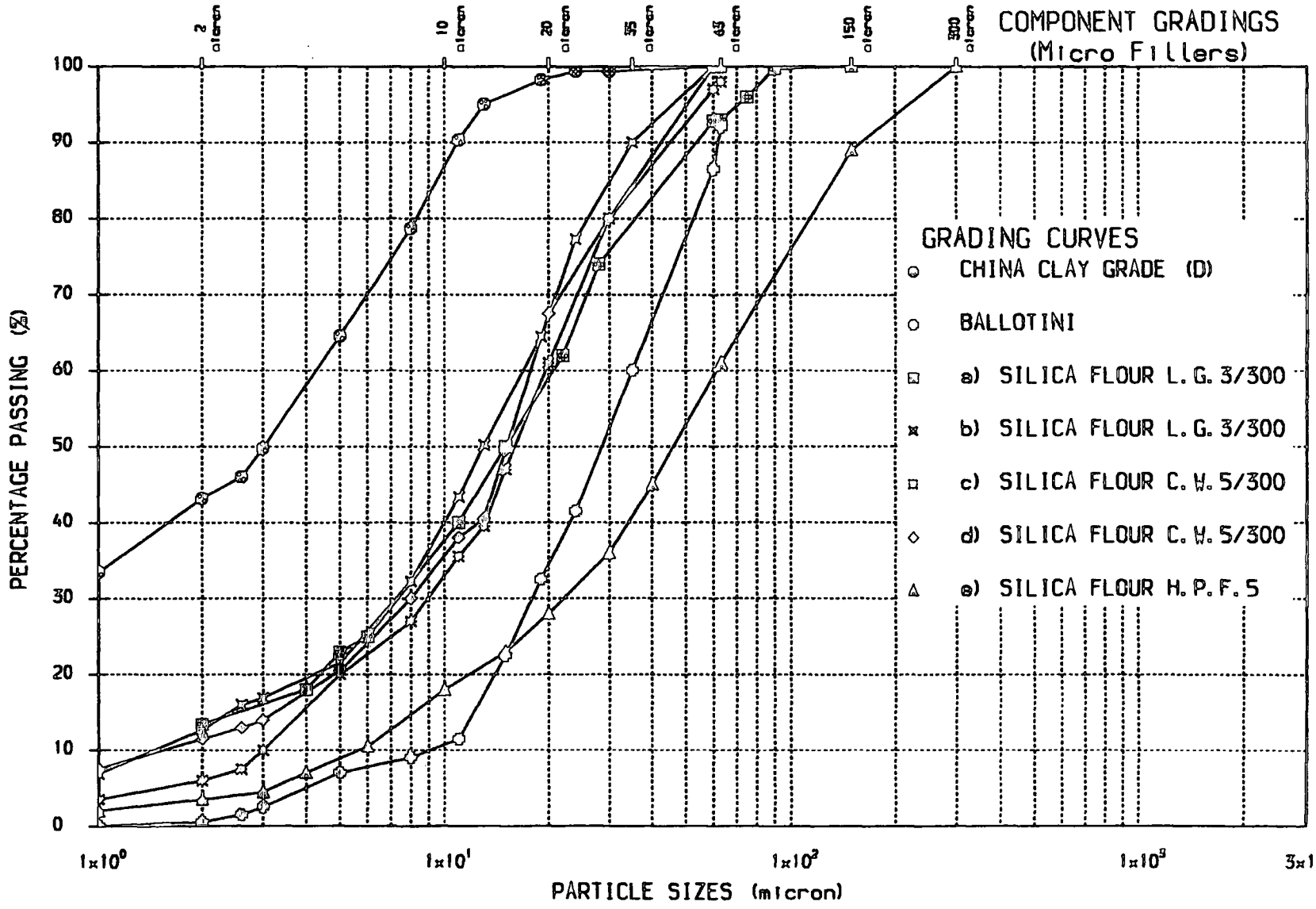

Figure 2.2 Grading curves of the micro filler components (from pipette analysis)

Figure 2.3 Performance of J2027L/Furfuryl Alcohol modified resin concrete

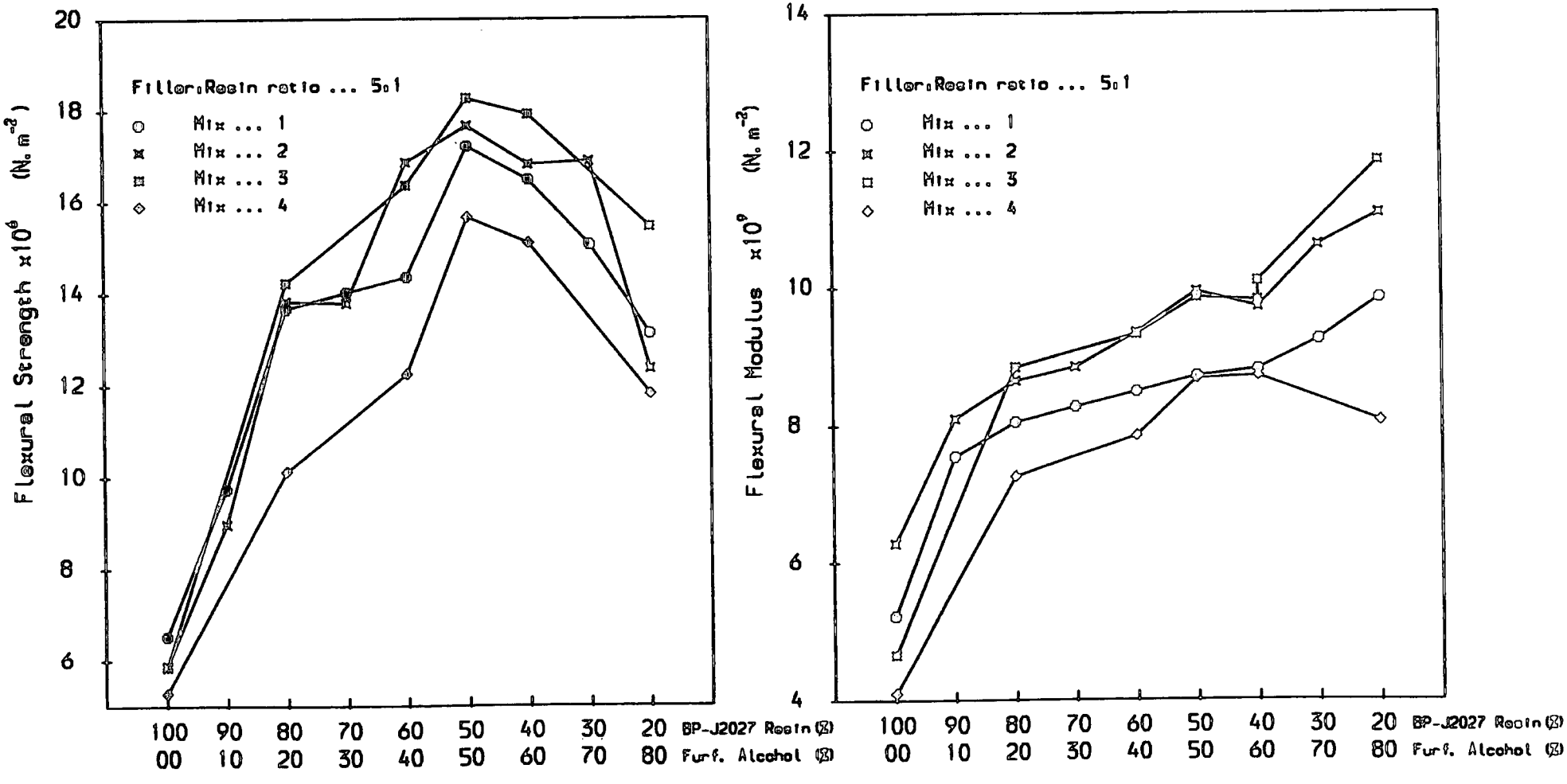

Effect of Furfuryl Alcohol on flexural properties of the Phenolic Concrete coupon specimens

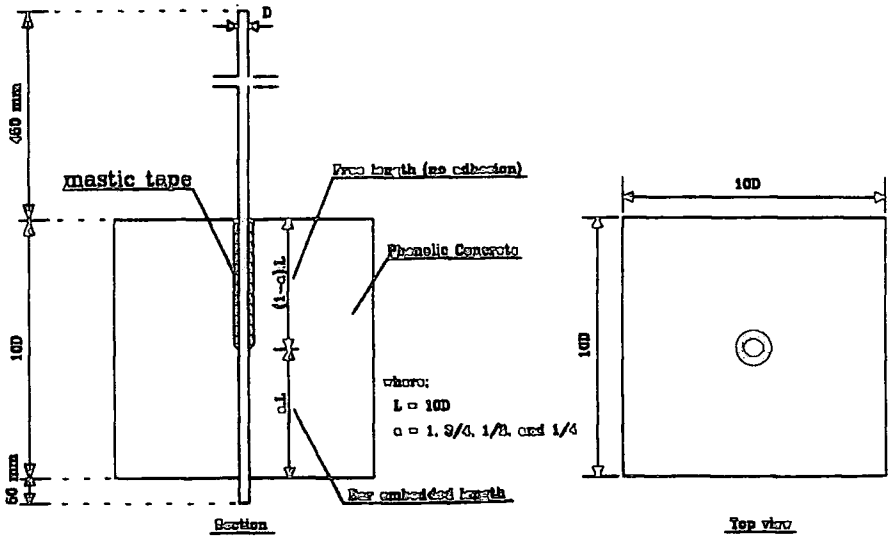

(a) Details of test specimens for pull-out test

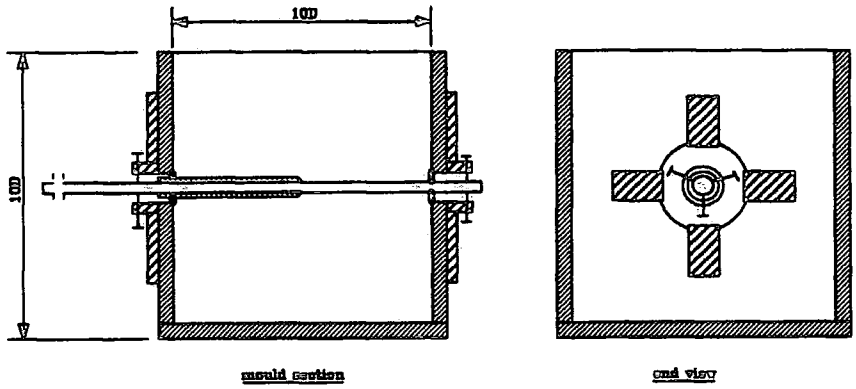

(b) Details of the mould and positioning of the steel bar

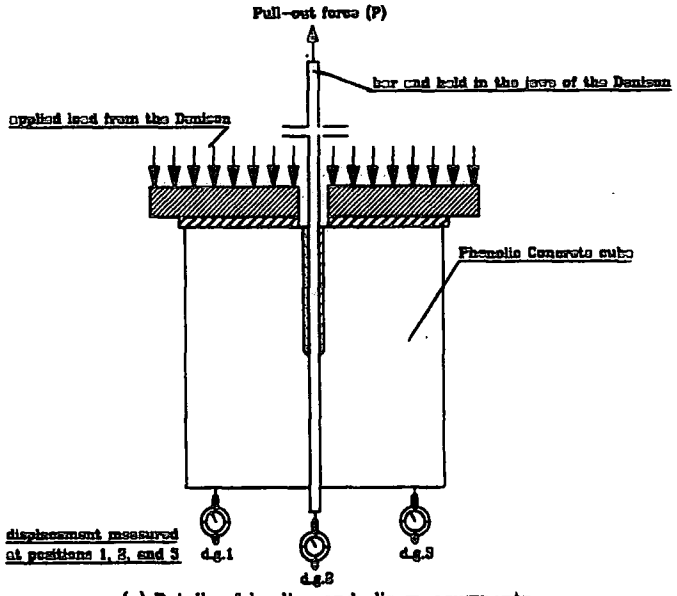

(c) Details of loading and slip measurements

Figure 2.4 Pull-out test specimen and testing arrangement

Figure 2.5 Results of pull-out tests on ribbed steel bars with various embedment lengths

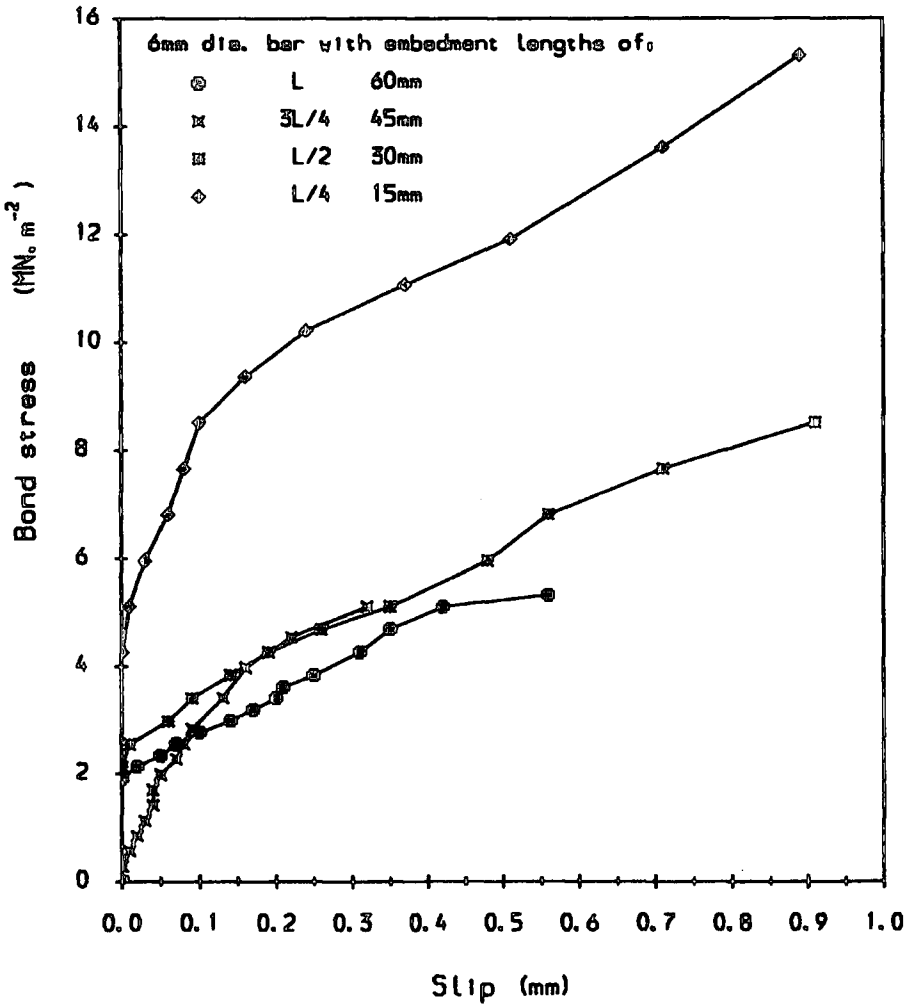

(a) Results of pull-out tests on 6mm diameter bars

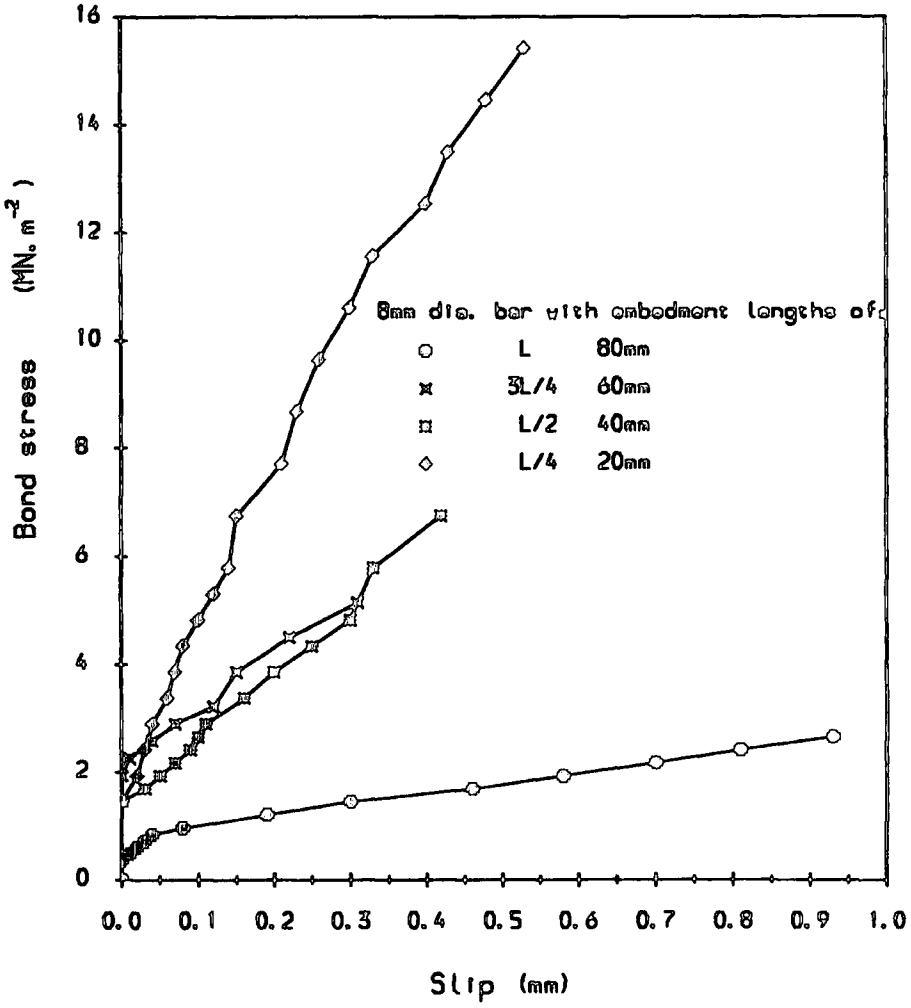

(b) Results of pull-out tests on 8mm diameter bars

Figure 2.6 Results of pull-out tests on ribbed steel bars with various embedment lengths

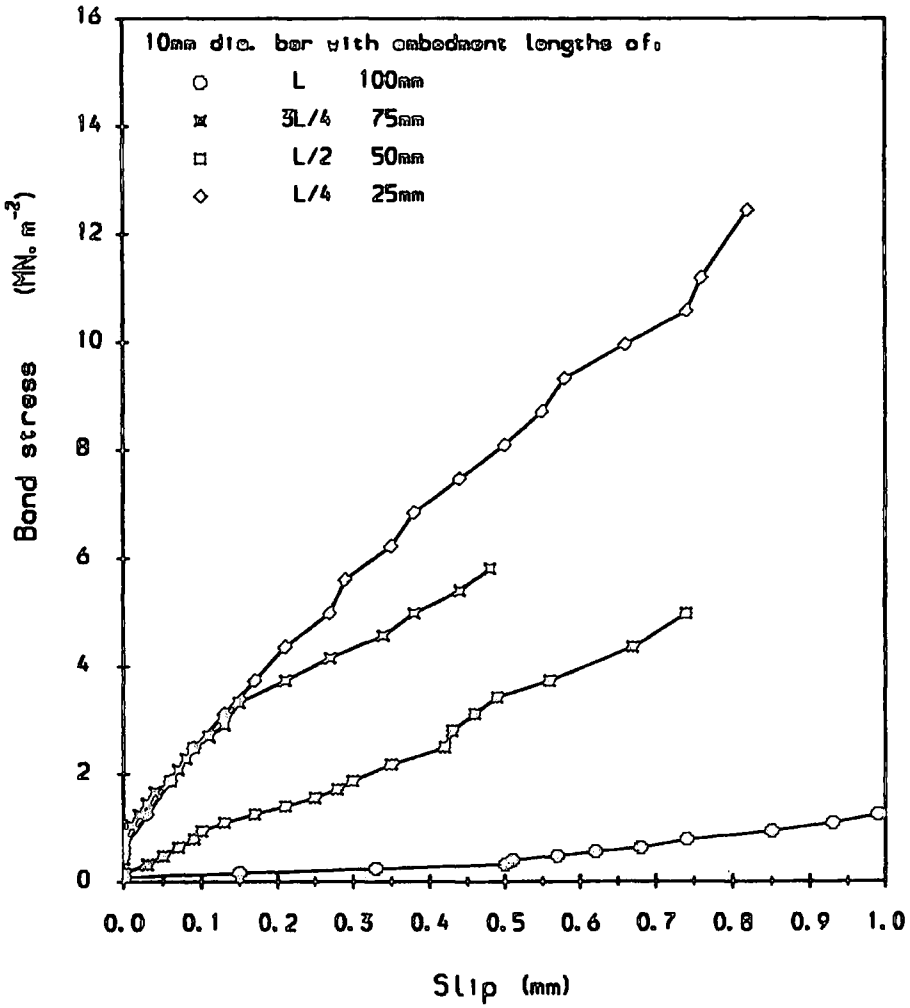

(a) Results of pull-out tests on 10mm diameter bars

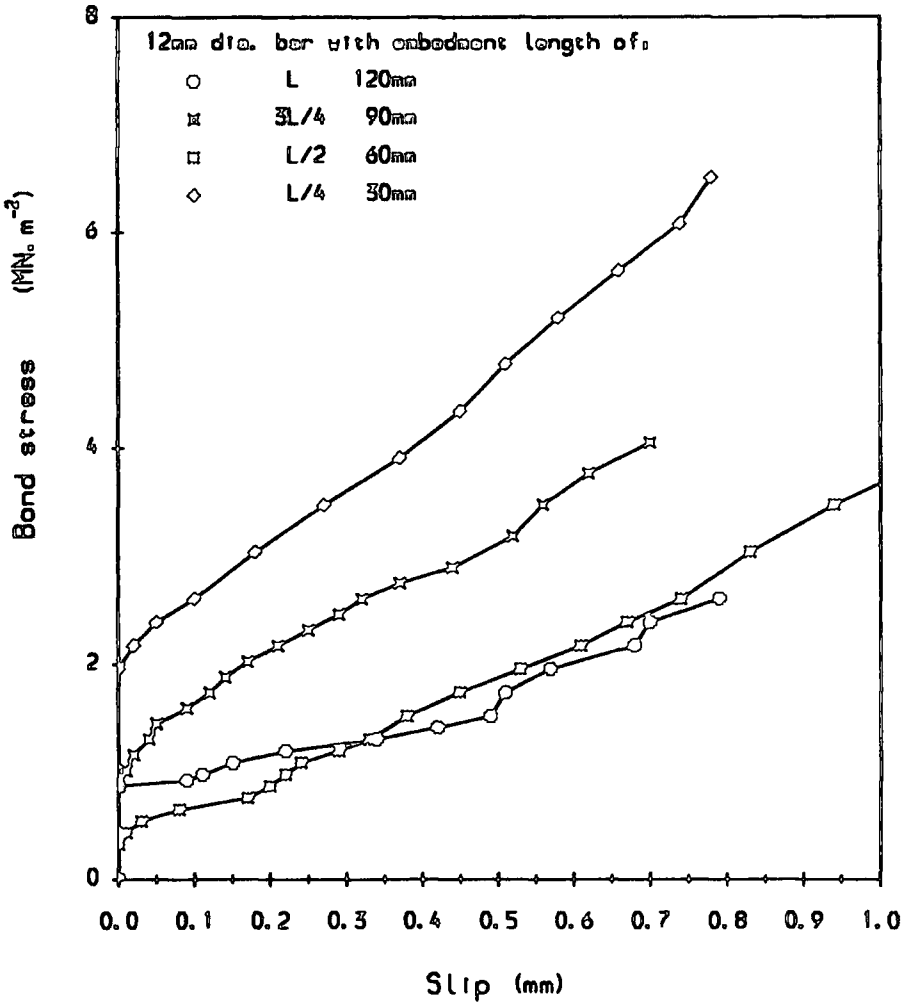

(b) Results of pull-out tests on 12mm diameter bars

Figure 2.7 Effect of bond (embedment) length

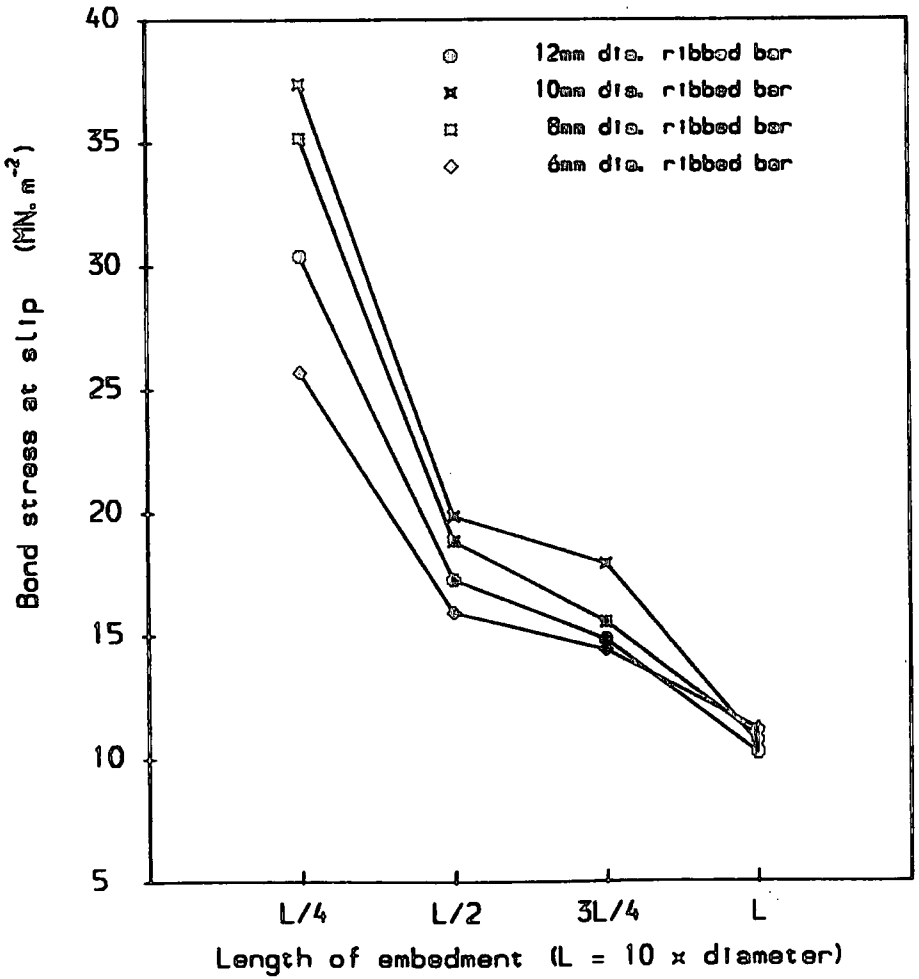

Variation of bond stress development with embedment length of ribbed steel bars

Figure 2.8 Intensity of bond stress developed along the embedded length

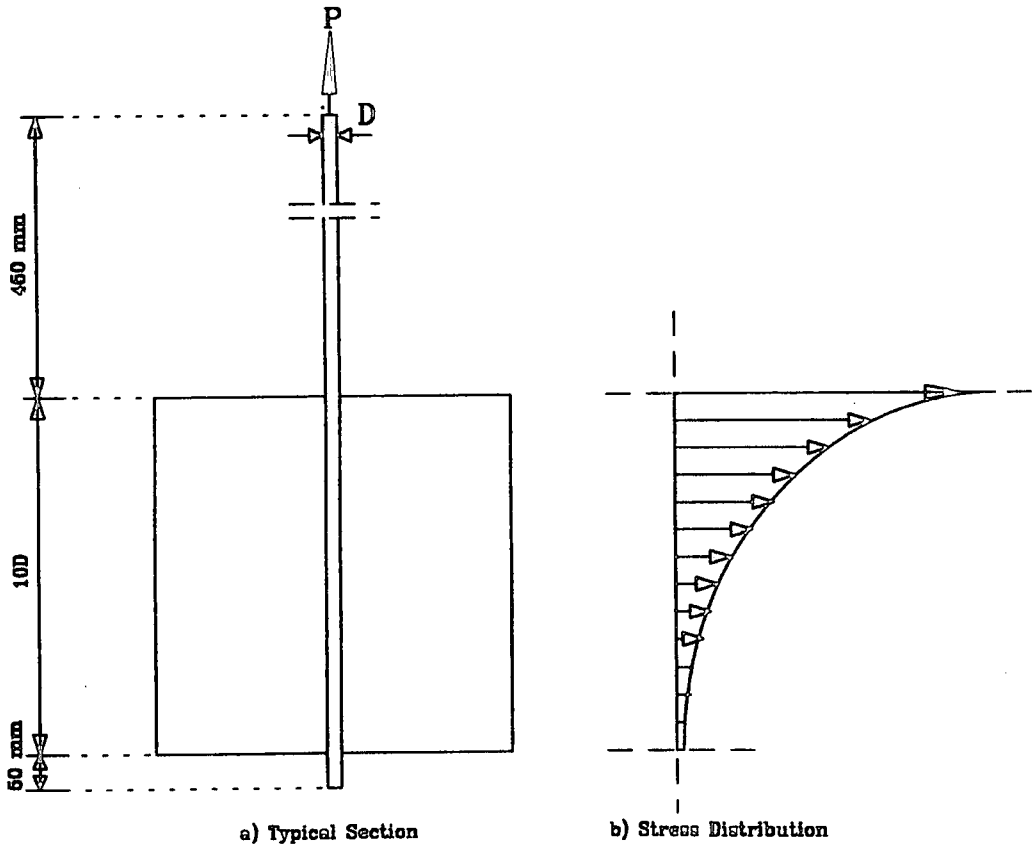

a) Typical Section

b) Stress Distribution

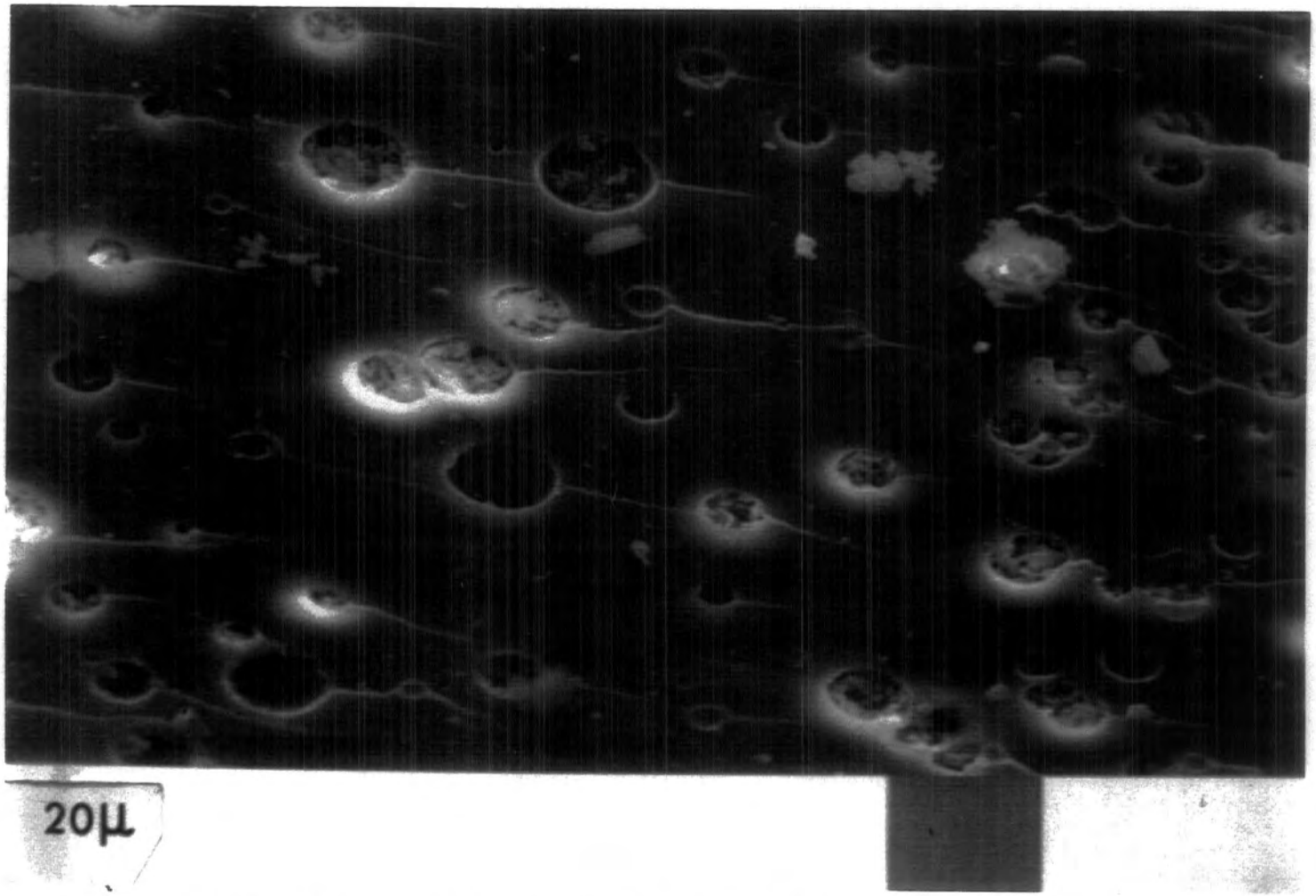

Plate 2.1 SEM image of fractured surface of specimens made from catalysed phenolic resol resin J2027L with 1% acid catalyst Phencat 15.

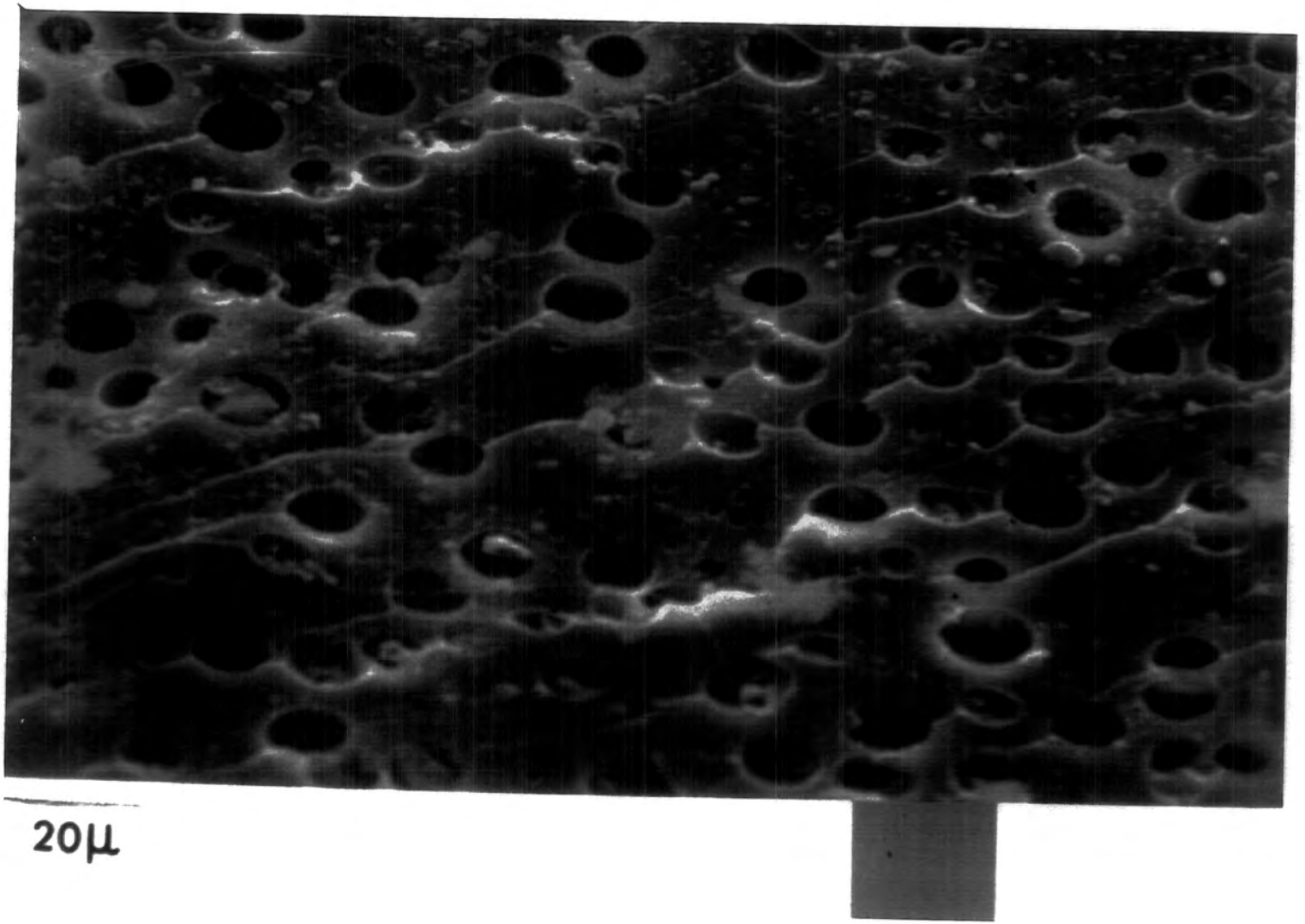

Plate 2.2 SEM image of fractured surface of specimens made from catalysed phenolic resol resin J2027L with 2% acid catalyst Phencat 15.

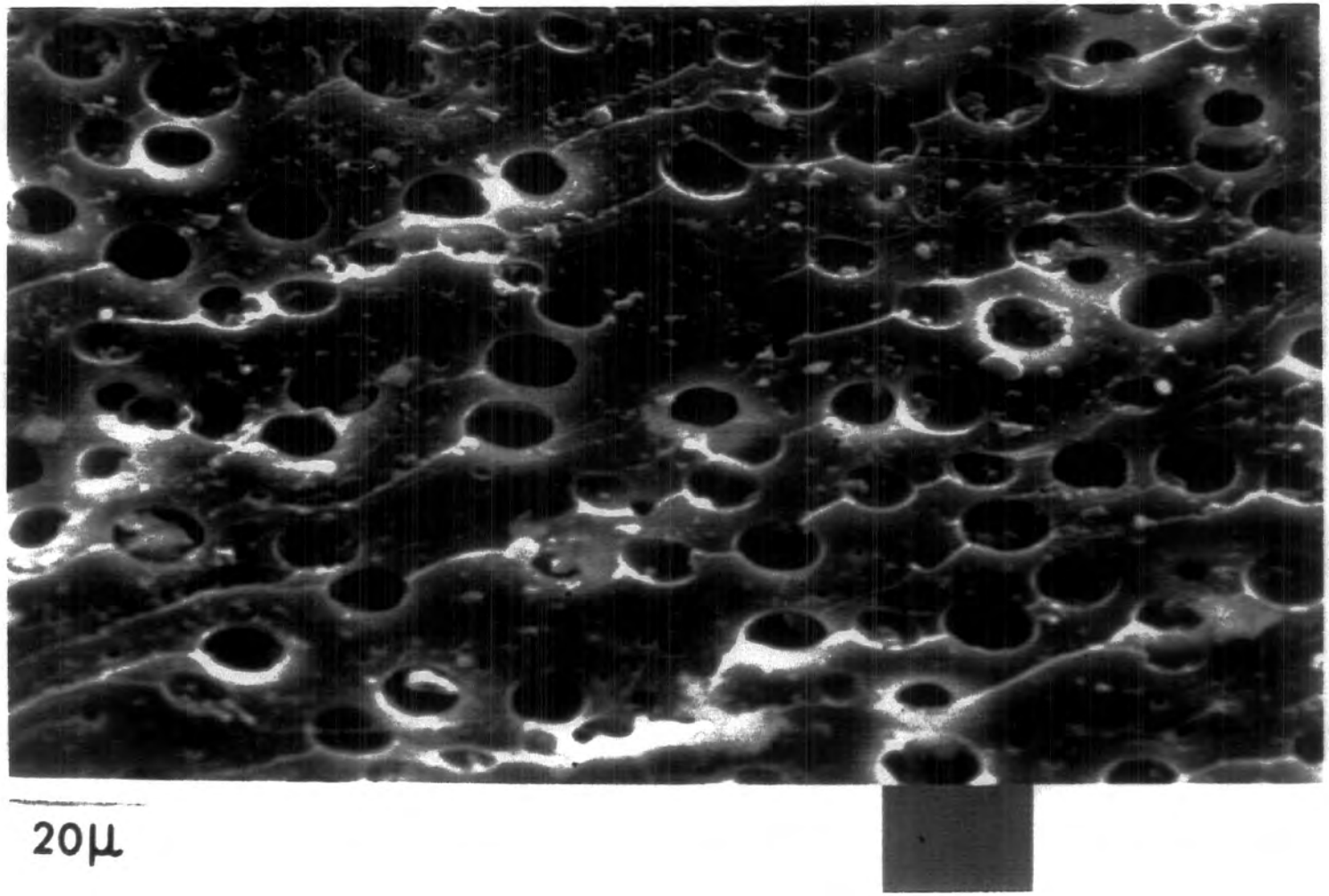

Plate 2.3 SEM image of fractured surface of specimens made from catalysed phenolic resol resin J2027L with 3% acid catalyst Phencat 15.

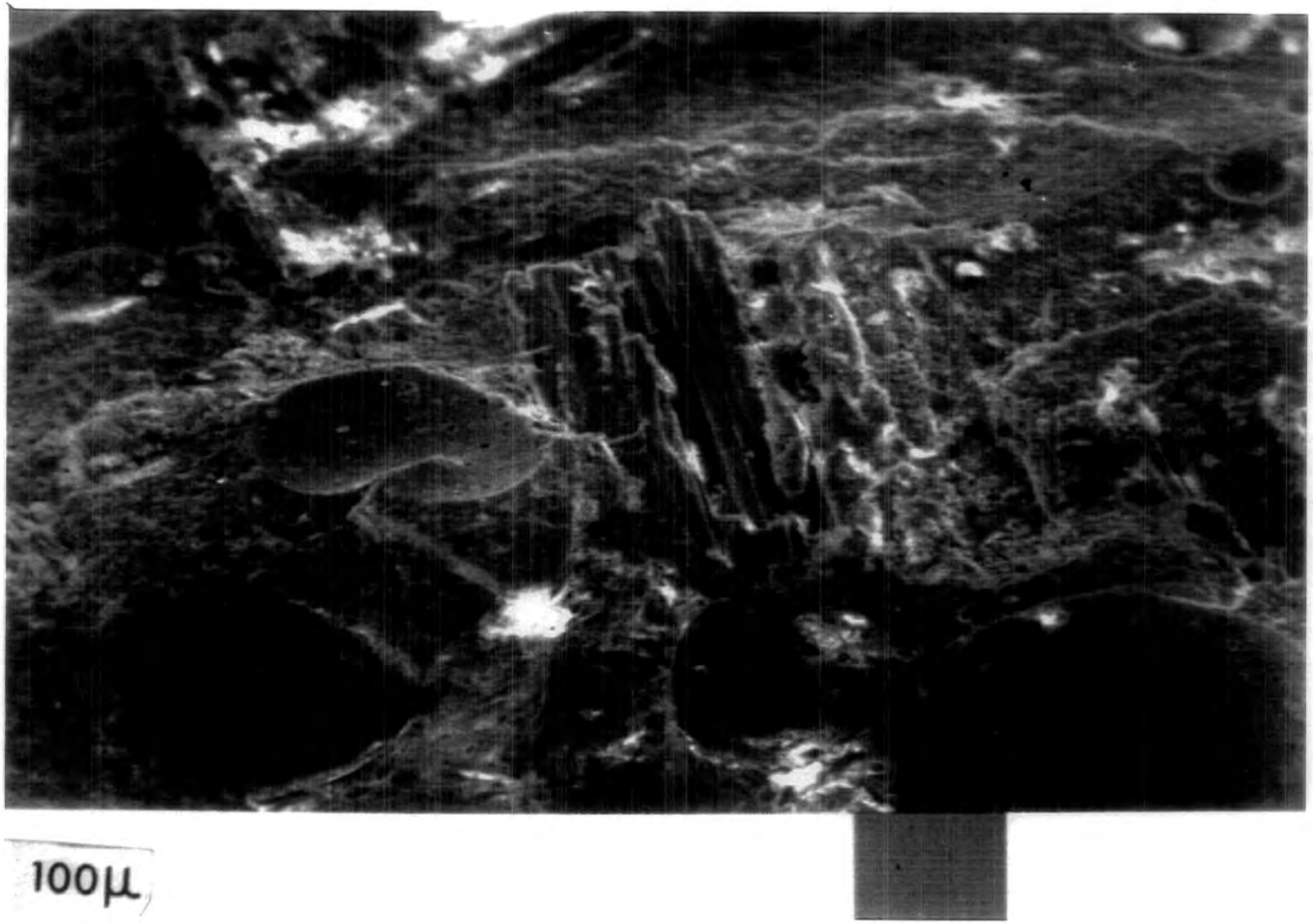

Plate 2.4 SEM image of fractured surface of specimens made from fibrous filler sawdust + resin composition (exhibiting the perfect bond development).

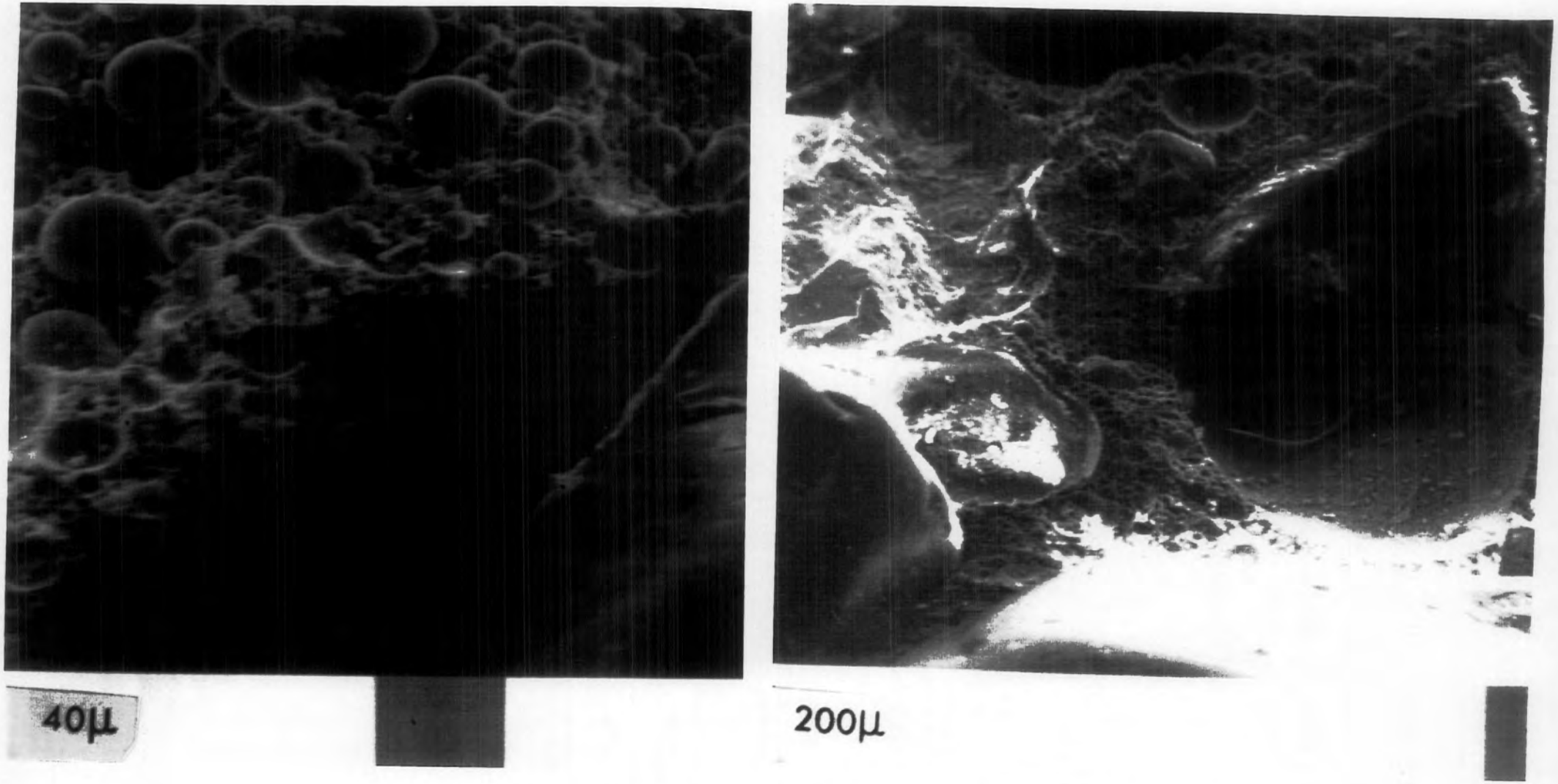

Plate 2.5 SEM image of fractured surface of specimens made from granular sand and ballotini + resin composition (exhibiting no bond to have developed between the granulars and the resin matrix with ballotini particles loosely dispersed on the surface).

Chapter Three

3. Phenolic Concrete Mixes and Properties

3.1. Mix Design

3.1.1. Introduction

Resin concrete, often refered to as polymer concrete, is produced using polymer as a binder for the aggregate. A wide range of aggregates and monomers may be used, although the cost and properties of the polymer concrete may be strongly influenced by the gradation of the aggregate and monomer.

For a given polymer (resin), and the aggregate components available, it is necessary to design a mix grading which would give the best workability with maximum aggregate/resin ratio. Because of the large range of aggregate particle sizes available to the commercial suppliers, it is not possible to obtain any reliable graded aggregate which would satisfy a desired mix grading. It is therefore common practice, to combine a series of aggregate fractions in order to achieve the desired mix grading. This would be achieved more easily and consistently, by using "single-sized" aggregate than the graded ones.

In Phenolic Concrete mix design the objectives should be to satisfy the following three main requirements;

1. To determine the most appropriate proportions in which to use the constituent materials to meet the needs of producing thin faced elements and their construction process. That is, to use a micro-concrete mix which in its slurry state, is

capable of being easily mixed, handled, placed and compacted efficiently within its working time. This, therefore, requires that the Phenolic Concrete mix should be sufficiently workable and to have reasonable work time (i.e. gel time), before the wet mix becomes semi soft, soft and then solid.

2. To make a Phenolic Concrete which, in its hardened state, will possess the required physical and mechanical properties. This means, that the product must have the desired structural strength, satisfactory durability in the environment in which it is to be used, and to have satisfactory surface finishes where it will be exposed to view.
3. Not the least important, the Phenolic Concrete mix must be designed for minimum cost to achieve the above characteristics.

3.1.2. Determination of the aggregate (filler) mix grading

Polymers, in general, are not economically viable for large scale structures. In designing polymer concrete mix, its constituent materials should be selected and fabricated in a manner which would result in an economically viable product. Therefore, in such mixes, the aggregate (filler), which is considerably less costly than the resin, should occupy the largest possible volume.

The aggregate gradation which refers to the distribution of the particle sizes in the mix grading, should also provide a relatively low void volume. At the same time the distribution of the particle sizes in the mix matrix should be designed to provide a material which is more dense, less porous and absorptive. This may be achieved by designing the mix grading to contain sufficient smaller particles to fit into the interstices between their larger particles present, without preventing the latter from being compacted as closely as possible. A proper mix gradation would

ensure a good workability, providing that the proportioning of the aggregate (filler) constituents are based on a particle size distribution with sufficient fines present in the mix matrix. The preceding combinations would provide closely packed particles in the mix grading which may also satisfy the strength criterion. As the greater the amount of solid particles that can be packed into a given volume of a polymer concrete the higher will be its strength.

A poorly graded mix may result in undue waste of the resin and/or result in a poor workability which may indeed require greater work in the moulding and compacting process. Therefore, determination of the grading of the filler mix in polymer concrete is of importance and is both economically and practically the major factor in improving the workability, compaction and the constituent material content of the mix matrix. It is important to produce a mix that can be compacted to a maximum density with a reasonable amount of work.

Based on the packing style of the particle fractions present in a mix grading (i.e. the inter-particle voids of the larger sizes to be filled with the next smaller sizes present), two approaches have been devised to solve the problem of how to achieve the best grading in satisfying the preceding requirements. One is the "through" grading and the other is "gap" grading, and both are concerned to produce mix grading which will give the greatest density with the least effort and the least resin. The former is designed with a suitable proportion of all sizes present in the mix matrix, and is best achieved by using the Fuller grading rules. Fuller has defined the "through" grading by an empirical formulation, which allocates proportionate volumes of all aggregate fractions as a simple function of particle size. He suggested that the best grading containing all sizes would be achieved if the proportion by weight of the material passing any particular mesh (sieve) size were in inverse pro-

portion to the square root of its particle size. This theory has been widely accepted as a basis for mix design. The grading of filler matrix based on this principle will be represented as a parabolic curve on the grading chart, which can be expressed as;

$$P_n = 100 \times \left(\frac{D_n}{D_{max}}\right)^{-1/2}$$

where;

P_n is the percentage passing size D_n

D_n is the seive size

D_{max} is the maximum particle size

"Through" grading is probably the most appropriate in the case of Phenolic Concrete mix grading from which micro elements may be produced and thus fine aggregates (sands) will be the largest particles used in the matrix.

The "gap" graded mix is designed on the principle that the largest aggregate size present must be allowed to pack closely, so that one or more "interference size" is totaly omitted, and the small size is choosen to fit the interstitial voids of the close packed matrix of the larger particles. On a grading chart, the grading of a filler matrix based on the "gap" grading principle will be of a stepped curve form, with the range of sizes omitted represented by a straight line. The geometrical analysis of close-nested spherical particles suggests that the diameter of the small filler particle must be equal or less than one sixth of the diameter of the larger filler particles. This suggests that the volume ratio of the larger particles to the smaller ones in the mix matrix will be about 70% to 30%. Although, the grading of the aggregate mix may be determined on the basis of the preceding principles, experimental adjustment based on much trial mix experimentation would be required to achieve the best results with the aggregates available in any successful mix design.

In determining a mix grading, it is of some importance to assess and compare

the aggregate specific surface of the gradings. This is a function which estimates the total aggregate surface area of the mix. The total surface area of the aggregate particles will directly affect the amount of resin needed in the polymer concrete to produce a certain workability, since the resin must coat all the particles and act as lubricant between them to ease the moulding and compacting processes. The specific surface area is primarily a function of the particle size. For a given weight of aggregate in a polymer mix matrix as the size of particles decreases the total surface area increases and thus more resin is required for ease of moulding and compaction processes. This therefore can be used as a means of comparing workability and/or resin requirements. For a given workability a lower specific surface value requires less resin and for a given amount of resin as specific surface increases workability decreases.

In this work, to determine a Phenolic Concrete mix grading, the selection of the mix proportions is based upon the achievement of highest filler/resin ratios from the type and the sizes of the available sands and micro fillers to be used. The silica sands were provided from various commercial suppliers. Although, the specification in some claimed to be of single-size, the seive analysis[57] showed some variation in the particle sizes with some fines present in their gradings. The definition of the term "single-size", in particle analysis is that the grains will all pass one sieve size and all be retained on the next size down. The corresponding grading curves obtained from sieve analysis on sands and pipette analysis[58] on micro-fillers are presented in Figures 2.1a to 2.2. The source of supply of the fillers and their physical properties are given in Table 2.1.

3.1.3. Proportioning of Fillers (mix proportions)

The scope of this work was concerned in producing a Phenolic-bound micro-concrete from a mix constituent which was designed to give low voids with high workability at maximum filler/resin ratio. Therefore, the aggregate mix grading was designed by combining at least four "single-size" sand components (with nominal particle sizes of 2.4mm, 1.2mm, 600μm and 300μm) and a fine filler referred to as micro-filler with maximum particle size of 150μm. The main factor concerned in choosing the type of the fillers was their chemical compatibility with the phenolic resin. Their gradings determined their likely mix proportions.

There are several numerical and graphical techniques available for determining the proportion of aggregate constituents required to produce a desired aggregate mix grading. These techniques will provide a reasonable approximation depending upon the number of aggregates being combined and the gradings of each. With some of these techniques[62,63] initially two components may be proportionally combined followed by repeating the procedure several times to determine the mix grading of more component combinations. However, there is a more direct method which will produce, with reasonable approximation, a solution to the proportioning of the aggregate components to achieve the desired grading. This method, which is by a graphical procedure[64] is appropriate to as many sizes of aggregate as required.

In this work, the graphical method was used in conjunction with trial and error procedures which resulted in producing the desired grading to a close approximation. Initially in determining the required mix grading of the Phenolic micro-concrete mix, the above combined method gave quite a precise solution but proved to be a lengthy procedure. This is the disadvantage of the method. It also becomes particularly tedious when graded aggregate components are to be used in obtaining the

desired grading. In this method, using the graphical procedure (see Appendix A1) the required proportions of each size of filler components (i.e. four sand and one micro filler components) were obtained which approximated the deduced combined grading as nearly as possible to the Fuller grading (in this case being the target grading). The results were checked both on a grading chart and also arithmatically, by comparing the deduced combined grading (%age passing) with the target grading (%age passing). The differences were obtained between the two gradings with correspondence to the fraction sizes of the individual filler components present in the combined grading. The differences outlined the presence of the relevant fraction sizes of which more and/or less are present in the combined grading. The proportion of each filler component was then adjusted accordingly with respect to the ratios of their preceding deduced %age proportions. New proportionate values were calculated and the procedure was repeated until the combined grading curve almost coincided with the target grading. At the same time, using experimental judgement, the best of the combined mix gradings, which closely approximated to the target grading, were used in casting Phenolic micro-concrete specimens for flexural strength tests. At filler/resin ratio of 6:1, the deduced filler proportions were selected to give the desired mix grading, on the basis of having the best workability with the least effort in moulding and compacting, and which also resulted on the highest flexural strength values obtained from testing the made samples.

In the light of such lengthy and complicated procedures, there was a need to devise a method with least work but best results in designing such mix gradings (see Appendix A1). Nevertheless, a computer based solution had been reported[65] for mix proportioning of various aggregate components. In this, however, the results had not been optimized to a unique solution. Therefore, a computer programme based on a "least square" method, was written to give the best possible combination

of up to 14 different sizes of aggregate components in order to simplify and reduce the work involved in designing mix gradings. The programme produces the best possible approximation to a prescribed grading by quantifying and minimising the variation of the designed grading from the target grading with a comparison between their surface area indices. The procedure is reported in the published paper[66] elsewhere. The mix grading results obtained using the graphical method in conjunction with trial and error procedures were in most cases in close agreement with the results obtained using the computer based solution. Using both methods, several mix gradings were designed from four sand filler and one micro filler components provided from several different commercial suppliers. The grading curves of these filler mix gradings are presented in Figures A1.2 to A1.13 of Appendix A1.

3.1.4. Grading Curves

From a vast number of gradings formulated in this work, only those are reported here which resulted in casting the Phenolic Concrete specimens with highest flexural strength capacities. The determined proportionate weights of the selected designed gradings are given in Table 3.1.

The resultant gradings A to K series plotted in Figures A1.2 to A1.13 of Appendix A1, were determined using various single size sand gradings and micro fillers listed in Table 2.1. Several mix combinations were devised using up to five filler components, the component gradings of which are given in Table 2.2. and shown in Figures 2.1a, 2.1b and 2.2.

The designed gradings based on through grading using the two methods are comparatively plotted in Figures A1.2 to A1.7 from which their variations from their corresponding target Fuller grading can be seen. The surface indices of the

gradings obtained for any particular mix grading using both methods are comparatively included in Table 3.1, from which it may be possible to compare the particle specific surface area resulted from the two approaches.

The component materials (sand and micro fillers) were selected on the basis that their combined grading produce a curve closely coinciding with the target Fuller curve. With the "graphical" method, using the "Fuller" grading option, the relative proportions of the component materials were determined so that the coincidence is best for the part of the curve representing the sand particle sizes. This procedure becomes neccessary for combined gradings having micro filler with relatively low density, since in the "Fuller" expression, all the component fillers are considered to be of same density. This will provide a grading with lower surface area which would in turn need less resin in the mix matrix. This may be seen from the grading curves C1, C2, C3 and C4, (shown in Figure A1.4 with their mix proportions and surface indices given in Table 3.1), in which China Clay is the micro filler with low density as compared to the silica sand fillers. From the resultant grading C series, it was found that not necessarily those gradings which required least resin produced elements with highest flexural strength capacities. This was the case with grading C1 which possessed high surface area in comparison to grading C2, C3 and C4, and consequently resulted in a resin rich mix matrix, from which specimens were produced with higher flexural properties (see Tables 3.2 and 3.3).

Using the "graphical" method, the obtained resultant grading curve at each stage was compared to the target grading curve on the grading chart. If the resultant curve fell above the target curve, the mix grading was more finely graded and therefore contained a higher proportion of micro filler. If it fell below the target curve, the mix grading was coarsely graded and contained a higher proportion of

larger sand sizes. To adjust the mix grading, the algebric differences between the two curves were deduced. The differences were then adjusted using a trial and error procedure by distributing the algebric differences over the component fraction sizes in the ratios of the preceding proportions of each component filler. As a result the preceding proportionate values were adjusted algebrically in accordance with the increase or decrease requirements of any particular component filler size. This procedure was repeated with the new resultant grading curve being compared to the target grading curve until the best coincidence of the two was achieved.

Figures A1.8 to A1.10, show the grading curves achieved for "gap" grading formulation. The gap grading formulation was based on determining a mix matrix with best workability which would produce elements with highest flexural properties.

In studying the effect of the micro-filler content, grading curves were plotted from the designed gradings which fell below or above the target Fuller grading curve representing lower or higher micro filler content respectively. The variation of these grading curves from the target Fuller grading curve can comparatively be seen from Figure A1.3. For mixes I, J, and K (see Table 3.1), the filler mix propotions were determined using the sand component proportions of mix E1, with their micro-filler proportions deduced using equivalent volume of 19.5% Silica Flour present in the mix grading E1. This was done in order to assess the effect of micro-filler type. The grading curves representing these filler gradations are shown in Figures A1.11 to A1.13.

3.2. Workability and its dependence on mix parameters

The important factor of concern, in producing any Phenolic Concrete product, is the amount of resin to be used in the mixes. From the economy point of view, the required mix should be designed for maximum possible filler/resin ratio with ease of moulding and compaction. From many trial mixes, it was found that filler/resin ratio and the combination of filler constituents directly affected the strength of the product. For a given resin and fillers, specimens produced from "through" grading mixes which closely approximated the Fuller grading, distinctly exhibited higher flexural strength values when compared to the specimens made of other grading mixes. At the same time flexural strength values increased with increase in filler/resin ratios. This, therefore, initiated the search for an optimum mix ratio produced from "through" grading filler combinations, which would have fair workability. From many trial mixes the optimum ratio was found to be 6:1 weight by weight of filler to resin. At this ratio the mixes, produced from the various fillers obtained from several commercial suppliers, gave reasonable workability and were easily cast and compacted using vibration technique. Therefore, using this mix ratio as a base, the filler constituents could be adjusted and trial mixes made in order to assess comparatively the workabilities. Trial mixes were also produced from the mixes fractionaly less than the optimum 6:1 ratio using similar mix constituents. The results cleary indicated a fair increase in the workability with negligible effect on the flexural properties of the made specimens. However, it should be noted that in real terms when the mix matrix is catalysed, the workability becomes time and temperature dependent, besides other factors. This, therefore, suggests that for a given condition from prescribed filler constituents the Phenolic Concrete mixes should be designed for an optimum mix ratio and then adjusted accordingly for the required workability which would serve particular casting requirements. This set

aside the need to conduct any workability tests. Nevertheless, the author is aware of the technique available which was devised and used in "polyester concrete" research work. But as the research work is not available to the author therefore due reference cannot be made to it. It should be noted that the method of measuring workability for fresh concrete cannot be suitable for the Phenolic Concrete, as the mixes are designed in the form of micro-concrete to construct thin face elements. It is also obvious that workability may vary from one batch of Phenolic Concrete mix to the next, depending on the methods and care with which batching and mixing are undertaken. Therefore the workability measurements should not be ruled out for polymer concrete in general, but for each particular polymer used the factors affecting the workability should be observed and weighed in such assessments. As the phenolic resin is a thermosetting polymer and the filled mixes made from this resin may only be suitable to construct uniform thin elements it is important to outline the factors influencing the workability of such mixes:

1. Size, Grading, Shape and Texture of the sands and micro fillers.

In a given mix matrix, the workability of the Phenolic Concrete mix is directly influenced by the total surface area of the fillers. The surface area is a function of particle size. For a given weight of fillers as the size of particles decreases the surface area increases. This means that workability would decrease with increase in the specific surface. As a result of increase in surface area more resin would be required for wetting the particles present and, thus for a given amount of resin, this will reduce the resin lubricative effect for particles to flow easily in the mix which will inversly affect the workability.

The gradation of the fillers in which the particles would nest allowing the particles to be compacted well into a maximum density and less voids is a major factor

in improving the workability.

Fillers having round shape and smooth texture will result in a higher workability. Angular, elongated or flaky particles with poor surface quality would result in a greater void ratio and therefore require considerably greater proportion of resin for a given mix composition. Consequently mixes having a high proportion of such particles would result in greater difficulties when handling.

2. Type of Resin

The viscosity of the resin is the factor of prime importance in achieving high workability. It is a function of both time (i.e. pot life of resin) and also solvent and water contents in the phenolic resin.

3. Temperature

The Phenolic Concrete mix matrix is quite sensitive to temperature. Temperature increase will have two completely different effects on any given mix matrix. Initially it may decrease viscosity of the resin, and at the same time reduce the time required for catalyzation of the mix matrix to initiate. The former may increase the workability while the latter decreases it. It is therefore important for a consistant mix, to maintain a constant working time (i.e. gel time, which is time taken for the mix to gel). This is achieved by the constituent materials of the mix matrix being maintained at a constant temperature at all time during the period of preparation for the mixing process.

4. Filler/Resin Ratio

As described earlier, the Phenolic Concrete mix may be designed for the highest possible mix filler/resin ratio. An increase in such ratio beyond the optimum ratio will decrease the workability. For a given mix matrix there is a limit where beyond this optimum ratio the uniform mixing becomes difficult and handling, moulding

and compacting becomes impossible even with the aid of vibration. At ratios lower than the optimum ratio the workability will increase. Care must be given to the process of casting and compacting in order to avoid possibility of segregation and disorder of the particles nesting.

5. Catalyst Content and Time

For a given mix matrix which is catalysed, there is a time limit during which the matrix can be mixed, poured and compacted. The time limit depends on the catalyst type and content. With time, as a result of chemical interaction, the workability of the mix will decrease with the mix forming into a semi-soft matrix. The time taken is called working time (gel time) which may be increased if desired by using a weaker catalyst or lower catalyst content.

6. Additives and Solvent

There was only one type of pigment (T_iO_2) which helped to increase the workability of the mix matrix. This was achieved by reduction in the viscosity of the resin and increase in gel time due to the retarding effect of Titanium Dioxide on the polymerisation reaction of the resin matrix. Using the correct amount of this pigment, it was found that T_iO_2 had an insignificant effect on the flexural strength of the made specimens although it had changed the colour of the produced specimens. This colour change could only be reproduced if the correct proportion of T_iO_2 is used in the Phenolic Concrete mixes with special procedure followed in the setting and postcuring processes. There was also only one solvent, "Furfuryl Alcohol", which helped to increase mix workability and at the same time increased the flexural properties of the specimens made from the phenolic concrete mixes. This is simply achieved by replacing a proportion of the resin content by Furfuryl Alcohol which has lower vicosity than the resin and therefore increases the matrix workability.

7. Type of Moulds

The Phenolic micro-concrete product may only be of thin sections and/or faces. Therefore their mixes should be cast in a manner to achieve as uniformly homogeneous section as possible. In this case the physical configuration may require complicated moulding. It is therefore of great importance for the Phenolic Concrete mixes to be designed for high workabilities in order to achieve full compaction with a reasonable amount of effort.

8. Compaction

The process of compaction, by means of vibration, serves two purposes in casting the Phenolic Concrete mixes. First is the elimination of the entrapped air, and second is to assist the moulding process. Compaction in the form of vibration is especially useful in easing the placement of the mixes with higher filler/resin ratios. The vibration should be of high speed but relatively of low amplitude and be sustained for a short period of application well within the gel time. It may be detrimental if applied at high amplitudes to any state of mix be it dry or wet since it can easily produce a porous and resinous surface.

All of the above factors must be considered and invariably a compromise must be made during a particular mix grading design and mix proportioning for a desired production process to achieve a successful result.

3.3. Determination of the Phenolic Concrete Characteristics

3.3.1. Introduction

The mechanical properties of the Phenolic Concrete may vary in its hardened state. This variation may be assessed relatively easily, using the criterion of strength and the factors affecting it. In this work the factors affecting the variability of strength of the hardened Phenolic Concrete has been investigated in relation to the mix constituent materials and their proportions. This assessment has also helped to adjust the mix proportioning to some degree in order to achieve an optimum level of resin requirement in a mix which would result in a product with high flexural strengths. The determination of the Phenolic Concrete properties has been used, to some extent, in describing the indicative inter-relation between the mix constituents, mix proportionings, and criteria of both strength and economy.

The properties of the Phenolic Concrete have been determined in terms of the following;

1. Flexural strength and modulus by testing thin rectangular specimens subject to four point bending.
2. Tensile strength and modulus of elasticity by testing specimens subject to direct tensile loading.
3. Tensile strength by testing disc form specimens using the brazillian disc test method.
4. Compressive strength using cored cylinder tests.
5. Density measurments and water absorption tests.

3.3.2. Flexural Tests

3.3.2.1. Specimen Preparation and Testing

To investigate the flexural properties of the Phenolic Concrete, specimens in the form of rectangular coupons were constructed and tested under four point loading. Steel and polypropylene moulds having internal dimensions of 600×100 mm with 4 to 10 mm adjustable depths were constructed for casting the flexural specimens. A total of 3 to 6 specimens were cast for each particular mix composition. The mixing, casting, vibrating, setting and curing procedures, and the period of time allocated for each process, were all kept constant and were conducted in the manner as explained in Chapter 2. The temperature of the mix constituents at the time of mixing was monitored for all the mixes and kept constant to $\pm 3°C$.

Once the specimens were ready, their geometrical dimensions were measured and then they were placed in a test rig mounted in the Instron testing machine type 1195. The test rig was attached to a load cell (100 kN capacity) which was resting on top of the Instron spreader beam and the base of the rig was connected to the Instron cross-head through universal hinge joints. The specimens were tested subject to four point loading with their span and loading point positions kept constant for all the test specimens. This therefore ensured that the test specimens were tested under constant spans between the loading positions. The test was conducted at a constant rate of Instron cross-head displacement of 20mm/minute. The load-deflection response of each specimen was plotted directly on an X-Y recorder with a deflection scale of 1:1. From the load-deflection plots, the slope of the graphs and the ultimate sustained load at failure of the test specimens were deduced. Using the deflection equations obtained from the bending theory (see Appendix A1) the

flexural modulus value of each specimen was calculated using its deduced load-deflection slope value and calculated I value. The ultimate flexural strength of each specimen in terms of its extreme fibre tension stress was also calculated from its measured ultimate failure moment and calculated I value.

Various Phenolic Concrete mix compositions were used in casting many coupon specimens. The effect of these variables on strength development of the Phenolic Concrete samples was investigated in terms of their flexural properties using this equipment and analysis.

3.3.2.2. Effect of Filler/Resin Ratio on Flexural Properties

Coupon specimens were cast using mix formulations A, B, C, D, E, and F series with filler mix gradings as presented in Appendix A1. In these specimens the only variable was the filler/resin ratio of the mixes. These ratios were 4:1, 5:1, 6:1 and 7:1 weight by weight of the total filler to resin content. The mixes up to 6:1 ratios were satisfactorily workable and could be easily moulded using a small pressure from a premade screed to level them off. The 7:1 ratio mix was not so workable. However, all the mixes were cast subject to vibration and then levelled off by screeding. Once the cast specimens were postcured they were tested accordingly. The average calculated results which are given in Table 3.2 and shown graphically in Figures 3.1a and 3.1b. From these results it may be seen that as the filler content increases with resin content decreasing, both flexural strength and modulus values increase accordingly. The rate of increase at lower ratios seems to be greater and between 6:1 to 7:1 ratios the increase in flexural properties is not significant. This suggests that having excessive resin in a mix (i.e. in this case 4:1 and 5:1 ratios) not only is economically not viable but also results in products with lower flexural properties.

As a result of excessive resin, the system may become surface resin rich. This may therefore account for lower values in flexural properties of the samples made from lower filler loading systems. The resin on its own would have lower flexural properties than the filled composite. Therefore, the surface resin layer would contribute to the specimen thickness which would adversely affect the computed flexural properties. Higher modulus and strength values may be obtained with just enough resin in the composite matrix to act as cementation for the fillers. It is suspected that as the resin content increases the filler particles become less well nested irrespective of their mix grading and this produces a porous product with more voids and possibly other defaults which may be present in the resin matrix. It produces a material with physical properties which are more like the lower modulus and strength of the unfilled resin matrix. It is worth noting that thorough optical observation of the surfaces at fracture sections of these tested specimens showed no segregation in resin rich specimens. The important point to notice was that in specimens of lower filler/resin ratio no fractured sand particle could be observed whereas in specimens of higher ratios a greater number of fractured sand particles were apparent. It seems that in the specimens of lower mix ratios the fracture at failure due to bending was mostly through the resin matrix rather than the composite matrix, whereas, in systems with higher filler loadings, a greater number of fractured sand grains were noticed at fractured surfaces.

3.3.2.3. Effect of Catalyst Content on Flexural Properties

For this section of tests coupon specimens were cast using a mix with various catalyst content levels. The mix formulations C1, C2 and C3 were used in this excercise, the mix filler grading of which are shown in Figures A1.4.

The catalyst level varied between 4% to 14% by weight of the resin content. The initial tests revealed that the samples cast from the mix with 4% catalyst content would not set at room temperature. For this reason the effect of the catalyst level was investigated between 6% to 14% content at two postcuring temperatures. The first group of specimens were postcured in the oven at $120°C$ for a period of 2 hours with second group being cured at room temperature for a period of 45 days prior to testing. During the catalyst content investigation it was found that specimens made from the mixes with low resin content showed ambiguous results with respect to strength and modulus values when tested under flexure. Therefore, for this reason and also from the trial experiments, mix formulations C1 and C2 at 4.5:1 filler to resin ratio was used with good workability and with its matrix containing more resin than mixes used in other sections. The average calculated test results are given in Table 3.3 and graphically presented in Figure 3.2. It can be noted that the modulus and strength values increase as the acid catalyst level increases from 6% to 8%. For specimens (postcured in an oven) with 8% to 12% catalyst contents there is insignificant variation between their flexural properties. The specimens which were cured at room temperature show steady increase in their flexural properties with increase in catalyst up to 12% content level and above this level there seems to be little difference. Those specimens with 14% catalyst content postcured in an oven showed considerable decrease in their strength and modulus values. This may be due to the development of unaccountable high stresses in the matrices during postcuring in the oven due to high acid content. It is also noticable that specimens develop better and higher flexural properties if postcured in the oven for the shorter period than at room temperature over a longer period.

It is obvious that the polymerisation of a phenolic matrix is exothermic and by a condensation reaction leads to a polymer crosslinking reaction. Concurrently

the crosslinking reaction causes an increase in viscosity which yields the gelation of the matrix. It is suspected that when sufficient catalyst is introduced in the resin matrix, it will initiate the exothermic effect fully, which would then accelerate the condensation reaction and produce stronger crosslinks by initiating stronger H bonds in the resin matrix before gelation.

The postcuring treatment in an oven is neccessary to obtain a Phenolic Concrete element with higher strength values and also to remove the entrapped volatiles. This may be the reason for samples cured at oven temperature to posses higher flexural properties when compared to those cured at ambient temperature. If high acid concentration is introduced to a phenolic matrix it will only be used partially and the remaining acid may be extruded, during the high temperature curing, as additional volatiles causing dangerous stress development and hence inversly affecting flexural properties. This may, therefore, account for the reduced flexural strength and modulus values of the specimens made from mixes containing 14% catalyst. Also, with increase in catalyst the work time (i.e. gel time) decreases considerably.

3.3.2.4. Effect of Micro Filler Content on Flexural Properties

In designing the mix grading, the aim was to obtain a grading with least void which would approximate as closely as possible to a Fuller grading. In doing so the micro filler which represented the lower part of the grading curve had a great effect on the proportioning of the fillers combined to produce the resultant filler mix grading. Also it was of importance to obtain a product with highest strength as a result of low void content. It was expected that the presence of the correct amount of the fine filler (micro-filler) particles would fill the interstical voids between the larger sand particles. To investigate such effect the amount of micro-filler present

was proportionally decreased or increased, below or above its designed level present in the most desirable grading (i.e. to more or less than would approximate to the Fuller grading curve). The grading curves obtained for these combinations of various micro-filler contents are presented in Figure A1.3. Two groups of specimens were cast from two mixes having filler/resin ratios of 7:1 and 8:1 for each combination of mix grading formulations. In the mixes the micro-filler content varied from 8% to 30% by weight of the total filler. The reason why the high mix ratios (i.e. 7:1 and 8:1) was used, was to optimise the resin content since with mixes having low micro filler content, at optimum filler/resin ratio 6:1, the mixes were resin rich and with higher micro filler content the mixes were stiff. Therefore higher filler/resin ratios were used in conjunction with furfuryl alcohol which reduced the resin viscosity resulting in more workable mixes. This combination optimised both extremes of the mixes being resin rich or stiff by bringing the two extremes closer by being able to cast mixes with higher filler/resin ratios.

The flexural tests, of the specimens made from the above formulations in both filler/resin ratio groups, clearly indicated that there was an optimum level of micro filler content which would result possibly in fewer voids and consequently in higher strength and modulus values. Concurrently, the results favoured the desired grading deduced which contained 18% Silica Flour L.G.3/300 by weight of total mix filler content. The grading of the relevant mix closely approximated the Fuller grading. The flexural test results are tabulated in Table 3.4 and graphically presented in Figure 3.3.

In this part of the work, several coupon specimens were also made from various mixes with mix ratios of 6:1 (filler/resin). The mixes were formulated using four different micro-fillers (Silica Flour, Ballotini, Chaina Clay and Spheriglass 5000).

The mix proportioning for all the mixes was based on mix E1 which was designed using Fuller grading with its micro filler being Silica Flour. Therefore, the required amounts of the other micro fillers were obtained so as to fill the equivalent volume of 19.5% Silica Flour content of the desired mix grading. The flexural test results of these specimens (see Table 3.5) showed that the mixes with Silica Flour and Spheriglass 5000 as their micro-filler produced specimens with highest flexural properties. This suggests that the type of micro filler has an effect on the flexural properties of the Phenolic Concrete specimens.

3.3.2.5. Effect of Postcuring Time and Temperature on Strength Development

A serious of coupon specimens were cast using mix E1, which were postcured at five different temperature levels over different periods of time. The flexural strength and modulus values obtained from testing these specimens are given in Table 3.6 and shown in Figure 3.4. It is evident that with increase in curing temperature the time taken for strength development decreases. Figure 3.4 suggests that it would be economical if the Phenolic Concrete specimens were cured at high temperature but of short duration. It also shows that at high temperature prolonged curing is detrimental to strength development. This may be due to the fact which the samples cured at $120°C$ above 6 hours started spalling on their surfaces and as a result sustained lesser bending moments. Between the 2 to 6 hours periods of curing at this high temperature level insignificant variation in strengths were developed. Similarly using a higher curing temperature ($140°C$) resulted in surface spalling of the samples. This was also experienced with Phenolic Concrete samples having large surface area cured at high temperatures in tests which were conducted concerning other work at B.P. Chemicals laboratories.

The optimum curing temperature and the optimum curing time needed for any Phenolic Concrete product may therefore be $120°C$ over a 2 hours period.

3.3.2.6. Effect of Additives and Solvent on Flexural Properties

The effect of Titanium Dioxide R-CR2 on the flexural properties of the Phenolic Concrete specimens was investigated by testing several coupon specimens made from mixes containing various T_iO_2 content levels. Mix E1 was used with 1% to 5% R-CR2 in increments of 1% weight by weight of the total filler content. The presence of T_iO_2 at higher percentages, i.e. 3%, 4% and 5%, showed a distinguishable effect in the mixes by increasing their workabilities. It is suspected that the increase in the workability of the mixes was due to possible reduction in the viscosity of the resin matrix. It is fair to note that Tioxide R-CR2 has been recommended as a pigment for use in resin bonded concrete by the Tioxide Group Plc[67] because of its rheological characteristics in the Polyester and Phenolic resin, as reported elsewhere[68].

The R-CR2 at 1% and 2% showed insignificant effects on the mix preparation, casting, setting and curing procedures of the coupon specimens. At these levels, also, insignificant effects were noticed on the flexural properties as can be seen from Table 3.2. However, at 3% T_iO_2 content the polymerisation and hence setting of the cast mix was considerably retarded. With 4% and 5% T_iO_2 content, the samples failed to set and even in the oven at high temperature curing was inhibited. After the mix with 3% T_iO_2 was cast, as soon as the cast coupon specimens formed into gel, they were placed in the oven at $70°C$ subject to pressure until they set after a period of 6 hours. The specimens were then demoulded and placed in the oven at $120°C$ for a period of 2 hours for postcuring. These cured specimens had become beige in colour as in comparison to the normal dark colour of cured Phenolic Concrete

specimens. These specimens were tested in flexure and showed little differences in their flexural properties when compared to other specimes made of similar mix formulation but without Tioxide R-CR2 (see Table 3.2). For the purpose of their colour and strength stability a set of specimens of similar composition were made and after being postcured they were kept at room temperature for a period of 30 months. At the end of this period the specimens were inspected and found to have kept their colour and when tested under flexure they showed approximately 4.5% decrease in their flexural strength values. Their flexural modulus values, however, showed insignificant variations (see Table 3.2). Further investigation concerning the effect of Tioxide R-CR2 on the Phenolic Concrete was not carried out since it was beyond the scope of the present work.

From the experimental trials of the early work (see Chapter 2) and also the preferential needs to produce higher filler/resin ratio mixes with good workabilities, "furfuryl alcohol" was found to enhance both the mix workability and also the Phenolic Concrete flexural strength. In this section of the work, several coupon specimens were made from the mixes whose resin content was comprised of partly phenolic resin and partly furfuryl alcohol. Various mixes were devised by replacing 20% to 55% of the phenolic resin with weight by equivalent weight of the furfuryl alcohol. For a given mix the workability increased with increase in furfuryl alcohol. Economically the cost per tonne of both resin and furfuryl alcohol was similar and therefore the equivalenet weights were used rather than volumes. When the specimens were tested under flexure, it was found that mixes with up to 55:45 IR1271 resin:furfuryl alcohol ratio had the effect of increasing the flexural properties of the Phenolic Concrete specimens. In the case of J50/010l resin the optimum ratio was found to be 60:40 resin:alcohol. Above these ratios the flexural properties seem to decrease. The test results are given in Table 3.7 and presented graphicaly in Figure

3.5.

Formaldehyde is virtually the only carbonyl component in the synthesis of technically relevant phenolic resin. Furfuryl alcohol itself, which is also an aldehyde, can be used to produce special phenolic resin[44]. It has a similar reaction to formaldehyde in the presence of alkaline catalysts. It has been shown[44] that phenol-furfural resins show enhanced flexibility, low melt viscosity and a low viscosity index. The high formaldehyde evolution of phenolic resin during polymerisation proccessing is a disadvantage. The high nitrogen content and low temperature resistance of formaldehyde lead to the formation of pinholes. With foundry resins containing furfuryl alcohol the bond strength developed between the resin and sand has been shown[44] to be high. In the test samples, therefore, replacing the phenolic resin content by furfuryl alcohol would in fact increase the flexural capacity. The reason for the drop in flexural capacities at above 55% and 40% alcohol with IR1271 and J50/010L resin respectively, could be due to over-riding the enhanced flexibility property of the higher furfuryl alcohol content. Additionaly, the volatile components in the phenolic matrix consist mainly of water, formaldehyde and phenol. The content of these will therefore be reduced by replacing the resin by furfuryl alcohol in a Phenolic Concrete mix matrix. This reduction in volatile component is thought to enhance the system strength. The results from these tests, made it possible to devise mixes with higher filler/resin ratios with improved workabilities. Therefore, further specimens were constructed using mix ratios of 7:1, 8:1 and 9:1 with 35% and 45% furfuryl alcohol to 65% and 55% IR1271 phenolic resin respectively. The flexural test results showed even more enhanced strength and modulus values (see Table 3.8 and Figure 3.6). The improved properties may be accounted for allowing more filler particles to be packed in to the mix matrix volume by introducing furfuryl alcohol. The high bond strength property of the furfuryl alcohol to the sand

and further reduction in volatile exclusion during postcuring process due to lesser resin content may also account for such increases in flexural properties.

3.3.2.7. Comparison of IR1270, IR1271 and J50/010L Phenolic Resins

During the course of this work B.P. Chemicals had succeeded in developing a phenolic resin which was intended to be competetive with the existing IR1271 resin produced by Fordath Chemicals. The latter was used in most of the preceding experimental work.

Preliminary mix designs and flexural tests on coupon specimens made of J50/010L resin showed that B.P.'s resin behaved almost as well as Fordath's IR1270 resin. Many coupon specimens were made from mix E1 using all three resins at filler/resin ratio of 6.5:1. In this experimental trial also three available catalysts, Phencat 15 and Phencat 10, B.P.'s product, and CS30 which is Fordath's product, were used which were compatible with both resins. Phencat 15 and CS30 were strong, highly concentrated acids, with Phencat 10 a weaker and less concentrated acid having higher water content. The results from the flexural tests on coupon specimens are tabulated in Table 3.9 and presented graphically in Figure 3.7. Overall, using the stronger catalysts in the mixes with all three resins lead to producing specimens with higher flexural properties. The specimens made from the mixes with IR1271 were shown to possess higher flexural strength and modulus values. With stronger acids the flexural properties of the made specimens improved with catalyst increase from 6% to 10% and with insignificant variations between 10% to 12% catalyst content. However, using Phencat 10 showed an increase in flexural properties with increase in catalyst level. With 12% Phencat 10 in the mixes made from the three resins, a sharp increase in flexural strengths of the specimens became evident. Using Phencat

10 at similar content level to either of stronger catalysts provided increased working time. The weaker the catalyst the longer it takes to promote and initiate the polymerisation and also the presence of more water retards the process of polymerisation thus giving greater work time.

Considering Figure 3.7 it is therefore recomended that IR1271 and IR1270 should be used with CS30 and J50/010L with Phencat 15 at not greater than 10% and not less than 8% by weight of Phenolic Concrete resin content. These catalyst levels may be used if cold casting (i.e. cold moulding and cold setting) is used; otherwise lower catalyst levels may be used (see 3.3.2.8). However, where in cold casting method more attention may be required for the casting process in complicated moulds, Phencat 10 at not less than 10% by weight of resin can be used, which would provide ample work time while at the same time ensuring the required strength development. A property analysis of the two resins, which was conducted by B.P. Chemicals[54], indicated that IR1271 resin is less viscous than J50/010L (see Table 2.4 of Chapter 2). In the latter the amount of free formaldehyde and free phenol is greater than in the former resin. This suggests that more volatiles would be removed in postcuring of the specimens made from the mixes using J50/010L resin. This therefore may account for better performance of the samples made with Fordath's IR1271 resin which contains less volatiles to be removed during the postcuring process. Fordath Chemicals later introduced four other resins (IR1272, IR1273, IR1274, and IR1275 resins) with lower viscosities and better mechanical properties which were the derivatives of their original IR1270 resin.

3.3.2.8. Effect of Hot-Casting and Laminated Fibre Glass mats

In the early experimental trials, the Phenolic Concrete specimens were produced

using an open cast method i.e. with their top surfaces exposed during casting and setting processes. Consequently the specimens suffered from two distinct faults. Firstly, at the end of their setting period they tended to curl up slightly and this became even more obvious when specimens were postcured in the oven. This suggested that the specimens extreme faces were subject to different temperatures while setting. It is thought that the top surfaces of the cast specimens, which were exposed, lost the exothermic heat at a greater rate than their bottom faces. Therefore, during the condensation reaction the top face becomes more porous (i.e. more pineholes) which may assist further volatiles (i.e. water) to be removed at top surface easily and rapidly while being postcured in an oven. This action may have caused differential shrinkages between the extreme faces resulting in a concave product. Secondly, the flexural test results showed a large variation from one batch of specimens to another. These faults were later controlled to considerable extent by casting the samples in closed moulds (i.e. mould with lids on) while allowing the samples to set under pressure by means of placing weights on top of the mould lids. This procedure overcame the stresses developed as a result of possible differential shrinkage, but still some variation in the test results remained. It was therefore decided to cast specimens in hot moulds and allow them to set under hot press pressure. This procedure gave the system further advantages, the most important of which was the use of lower catalyst levels, which provides a more controllable mixing process. It also speeded up the process of setting to a maximum time of approximately 15 minutes, before demoulding.

The work on the hot casting method was carried out at B.P. Chemical laboratories. Several coupon specimens were made, using both "through" and "gap" graded mixes E1, B and G2, G3 respectively. The mixes were formulated at 6:1, 7:1 and 8:1 filler/resin ratios using J50/010L resin plus Furfuryl alcohol with Phen-

cat 15 catalyst at 4% by weight of the total resin content. The temperature of the mix constituents was kept constant at all times during mixing processes. The steel mould coated with TCGC lining was pre-heated between the hot platens of a press to temperatures of $85 - 90°C$. This was controlled by frequent temperature measurments and adjusted as necessary. Once the mix was ready the pre-heated mould was placed on a vibrating table of low frequency and casting was performed subject to vibration. The cast mix was screeded and levelled. The mould lid was placed on top and the closed mould was placed in between the hot press platens at the controlled temperature. A constant pressure (150 psi) was applied for a period of 15 minutes while the press temperature was maintained constant. At the end of this period the specimens were demoulded and immediately placed in an oven for a period of 2 hours at $120°C$ for postcuring. The specimens constructed in this manner were quite flat with good smooth surface finishes. The specimens from different batches when tested under flexure showed very little variation in their flexural properties. The flexural test results of the hot-pressed specimens are given in Table 3.10 and shown graphically in Figure 3.8. From these results, it can be seen that for specimens made using the "through" grading mix formulation both flexural strength and modulus values increase with increase in filler/resin ratio. For those made from the "gap" grading mix formulation these values increase with increase in filler/resin ratio from 6:1 to 7:1 and flexural strength value decreases with the ratio increasing to 8:1 while its flexural modulus value having insignificant variation. The results also indicate that the specimens made from the former mix grading formulation have better flexural properties than the specimens made from the latter mix grading formulation.

Using the hot-casting technique the effect of fibre glass lay-up as a means of primary reinforcement was also investigated on Phenolic Concrete specimens made

of both mix grading formulations. The construction procedures for reinforced specimens were similar to those of plain specimens as explained above.

Three types of fibre glass mats (see Table 3.11) were used in the form of hand lay-up laminates. For each coupon specimen two layers of fibre glass mat were cut around a 600×100 mm rectangular templet, and weighed. The resin J2018L (B.P.'s product for lamination) was prepoured in two batches using 1.5:1 resin to glass ratio. They were mixed with catalyst, (Phencat 10 at 6% by weight of resin), individually as required. The first glass layer to go at the bottom face was wetted out on a glass plate covered with Melinex release film, with hand rolling to remove entrapped air. The second fibre glass layer to go on the top face was wetted out in a similar manner but on another glass plate covered with Melinex release film. The lay ups were left to become stiff so that when they were placed in the preheated mould there should be no movement or entrapment of air during vibration. When the mix was ready the bottom lay up layer was placed in the mould and the mix was immediately poured on top and vibrated. When the cast mix was levelled off, the top lay up layer was placed on top and the mould lid was gently placed above it. The construction, setting and curing procedures of the Phenolic Concrete composite reinforced with fibre glass laminates were similar to those of the plain specimens. These coupon specimens with laminated glass mat reinforcements on both faces were tested under flexure similarly to previous test specimens. The results showed that woven roving fibre glass mat (800 g/m^2) enhances the flexural strength of the Phenolic Concrete specimens considerably. And of the two chopped strand mats (SCM) of 450 g/m^2 the Powder Bounded mat had the effect of increasing the flexural strength capacity of the coupon specimens. All three types of fibre glass mat laminates in the form of reinforcement had increased the flexibility of the Phenolic Concrete. This is noticed when the flexural modulus values of the plain specimens are compared to those of

the mat reinforced ones. However, this is expected as in the theoretical calculation the shift in the neutral axis of the mat reinforced specimens is not considered and also laminated lay ups as reinforcment should increase the flexibilty thus resulting in lower modulus values.

Failure of the coupon specimens reinforced with the laminated glass mats was of composite failure. Full composite action existed throughout the test with the specimens failing in rupture undergoing large deflections at failure. With fibre glass reinforced specimens, at failure, deflection values as high as 45 to 50 mm were recorded whereas with plain specimens the ultimate deflection values were of order of 4 to 6 mm.

3.3.3. Tensile Test

3.3.3.1. Direct Tensile Test

Specimens in the form of "T-bones" were constructed using various Phenolic Concrete mixes. The specimens were cast in a series of steel moulds having three studs which provided the cast samples with three cast-in holes near each end. These were symmetrically positioned about the centre line of each mould. Each mould had a lid which enabled the operater to apply pressure by means of weights to the cast samples throughout their setting period. The inner faces of the moulds were all lined with sheets of TCGC. The samples were cast with their end widths greater than their gauge length width, to provide greater cross-sectional area at each end in order to prevent premature failure of the samples in these end areas when subjected to applied stresses.

From each mix composition, several samples were cast with cross-sectional di-

mensions of 58 × 8 mm^2 along the gauge length (centre section) and 100 × 8 mm^2 at each end. Once the samples were cured, the faces were fixed with a pair of demec studs of 200 mm gauge. Additionally four e.r.s. gauges of size 10 mm were also fixed to either faces. Two of these were in the longitudinal direction along the centre axis and the other two transversly. The demec studs and the e.r.s. gauges were glued to the faces using araldite adhesive. Because of the possibility of load eccentricity the strain gauges were used on both sides of the tensile specimens. The ends of the samples were clamped using two steel plates. These were tightened against the sample ends using three bolts passing through the precast holes.

The samples were loaded in tension using the Denison testing machine (model T4284). The tensile load was transfered to the specimens through the steel clamps which were connected to the jaws of the Denison machine by hinge joints. With the test specimens kept in their vertical position, the initial grip loads were applied prior to recording any strain readings. The load was applied in equal increments until failure. At each load interval strain readings were recorded from two pairs of demec studs and four e.r.s. gauges. Two of the e.r.s. gauges were used in measuring the lateral strains, the results of which were used in determining the Poisson's ratio. To ensure axiality of the specimens the strain readings were rejected if their opposite face readings differed by more than 10%. In some cases the samples had to be rejected totaly since the recorded strains revealed eccentric loading. The deduced longitudinal strains over the elastic range were plotted against the applied tensile stresses for each sample. From these plots the tensile modulus values were determined for each sample. The average tensile modulus and the ultimate tensile strength values are tabulated in Table 3.12.

The deduced lateral strains were plotted against the corresponding longitudinal

strains. These values were obtained from early loading stages. Although the values presented scattered points on the graph a best fit line method was used which enabled the author to represent these strain results linearly, the slopes of which determined the Poisson's ratio. Sample plots are shown in Figure 3.9. From these plots an average Poisson's ratio of 0.27 was found for the Phenolic Concrete composite systems.

The tensile test results indicated that the tensile modulus of the Phenolic Concrete composite increases as the filler loading increases in the system up to 6:1 ratio. Above this level of filler loading, the system required addition of Furfuryl alcohol for higher filler loadings. This inversely affected the tensile modulus values. The enhanced flexibility effect of the Furfuryl alcohol to the system may account for this phenomenon. However, the tensile strength seems to have only increased as filler/resin ratio increased from 4:1 to 5:1 ratio. Above this level the test results showed insignificant variation of the tensile strength values with respect to filler loading. The test results also clearly showed that the Phenolic Concrete has the lowest tensile properties when the mixes are cast using 6% catalyst. With 8%, 10% and 12% catalyst levels there was little variation in tensile properties of the specimens.

3.3.3.2. Brazilian Disc Test

Discs of 50 mm diameter × 25 mm thickness were prepared using various Phenolic Concrete mix compositions. They were made in two forms of cast-in discs and cored discs from larger specimens. These were tested subject to diametral compression using the Brazilian disc test method in order to obtain the appropriate tensile strength of the Phenolic Concrete.

To construct the cast-in discs, prescribed Phenolic Concrete mixes were cast in a row of six drilled shallow cylinderical holes in a 600 × 75 × 25 mm^3 thickness polypropylene rectangular block. A flat sheet of similar material was fastened to the bottom face of the block acting as a base to these cylinderical holes.

The Phenolic Concrete mixes were cast in these cylinderical holes subject to vibration. A flat polypropylene strip was placed on top acting as a lid which made it possible to apply pressure by means of weight to these cast cylinders while setting. The cast specimens were stripped after 24 hours and then postcured in the oven at 120° C over a period of 2 hours.

Additionally a series of discs were cut from cored cylinders. Several cylinders of 50 mm dia. × 75 mm height were cored from precast Phenolic Concrete mix composition (see section 3.3.4.). Two 50 mm dia. × 25 mm thickness discs were cut from each cored cylinder using a diamond tipped rock cutter saw.

The geometrical dimensions of all cast-in and cored discs were carefully measured using a micrometer. These specimens were tested in accordance with the Brazilian test[69] for rock specimens. The disc specimens were progressively compressed under the increased loading at a constant rate of strain until failure occurred with the specimens splitting vertically through the centre as it can be seen from Plate 3.1. The diametral compression induces a uniform tensile stress across most of the ver-

tical diameter of the disc specimen. This therefore causes the disc specimen to fail in tension rather than in compression.

The tensile strength is given by;

$$\sigma_t = 0.636 \times \frac{P}{dt}$$

where

σ_t is the tensile strength.

P is the load to cause failure.

d is the disc diameter.

t is the disc thickness.

The tensile strength of the Phenolic Concrete made using various mix formulation was determined using the above procedure. The average results obtained from testing both types of prepared disc specimens are given in Table 3.13. These tensile test results indicated that the tensile strength values obtained from the disc tests were higher than the values obtained from the direct test. This may be due to the fact that in the direct tensile test it was not possible to apply the loading free of eccentricity and this as a result may yield lower values. Also in the direct tensile test the larger volume of the specimen is subject to tensile stresses which may entail a greater number of defects.

3.3.4. Compressive Test

Phenolic Concrete specimens of right circular cylinders were tested in compression. These cylinders were of sizes 20 mm diameter × 60 mm length. The compressive strength of the Phenolic Concrete was obtained from the maximum compressive load carrying capacity of these cylinder specimens.

The cylinders were cored from a number of Phenolic Concrete prism blocks of $75 \times 75 \times 150\ mm^3$ which were cast using various mix compositions. The type of resin, type of catalyst and procedures of mixing, casting, setting and postcuring were all kept constant and similar to the construction of coupon specimens. The prism blocks were cast in box type moulds made from polypropylene with a lid of similar material. Since the Phenolic Concrete due to its exothermic reaction could not be cast in a bulk, therefore, the prism blocks were cast in layers of approximately 15 mm thickness. Several of these right circular cylinders were cored from these prism blocks using rock coring techniques. The ends of the cored cylinders were trimmed using a diamond tipped rock cutter saw. These ends were then gradually lapped on a "Lapping" machine untill flatness and parallelism of these ends were achieved. The prepared specimens were tested in a standard concrete compression testing machine "ELE" in accordance with the ISRM[70] testing method at a constant rate of loading 200 N/s. The compressive strength values obtained from these tests are tabulated in Table 3.13. The prepared cylinder core specimens are shown in Plate 3.1 with thier failure mode after compression testing.

3.3.5. Density Measurements and Water Absorption Test

The Phenolic Concrete is almost impermeable and water absorption due to surface porosity would have very little effect on density measurements. Therefore, the method of immersion in water was used in accordance with B.S. 1881[71] to determine the Phenolic Concrete density. A cylinderical watertight container filled with water was placed and weighed on a scale. Dry samples were weighed to the nearest 1g from cored cylinders and discs, prism blocks and coupon specimens which were cast from various Phenolic Concrete mix compositions. These samples were individually suspended in the water free from contact with the container. The

increase in weight of water was noted as the weight of the immersed solid occupying the equivalent volume of water. The density of the specimens was then calculated from the equation:

$$\rho_b = \frac{m_s}{V_s} \times 10^3$$

in which

$$V_s = m_{ws}$$

where;

ρ_b is the bulk density of the specimen (kg/m^3).

m_s is the dry mass of the specimen (g).

V_s is the water volume occupied by the specimen (cm^3).

m_{ws} is the apparent mass of the specimen when immersed in water (g).

The cored cylinder and disc specimens representing the body mass of the Phenolic Concrete casting were used to determine water absorption. The direct cast specimens could not have been used since the surfaces of the cast specimens were in contact with mould releasing agents and somtimes with industrial wax or grease, which might have influenced the possible absorptivity. The water absorption tests were conducted in accordance with B.S. 1881[72] for testing concrete specimens and also B.S. 6431[73] for testing ceramic tile specimens. The selected samples were weighed to the nearest $0.01g$ at their dry state prior to their placement in water. The specimens representing Phenolic Concrete cast from various mix compositions were placed in water tanks over a period of 48 hours. At the end of this period the samples were removed and using a cloth they were dried of any surface water. These were then weighed to the nearest $0.01g$. The results clearly showed that the Phenolic Concrete is impermeable, having zero water absorption. In systems with higher filler loadings some water absorptivity was detected which was thought to be

due to their fine surface pitting, which were apparent on inspection.

The properties of the Phenolic Concrete in terms of density, water absorption, cylinder compressive strength, and disc tensile strength are given in Table 3.13, in correspondance to its mix formulation, mix composition, and mix workability at time of casting.

3.4. Conclusion

In formulating a Phenolic Concrete mix, one of the prime factors influencing the quantity of the resin required and consequently all resulting properties is the correct selection of the fillers. To produce a Phenolic Concrete it is of prime requirement to use silica sands as the granular filler components which contain the least impurities and are graded between $300\mu m$ to 2.4mm. In order to fill the inter-particle voids of the granular components (i.e. sands) it becomes necessary to use a fine filler component in the form of micro filler. The system upon mixing, yields a matrix which most resembles fine concrete in its uncured and later cured solid state.

The filler components will, in practice, consist of at least three gradings and preferably of five gradings, includuing the micro filler. This is obviously in accordance with the requirements of the discrete granulogmetric curves of "gap" grading and also "through" grading respectively. To achieve a desired mix grading, be it gap or through grading, the use of single size filler components will result in an efficient design and ensure a very close approximation to the target grading and minimise porosity.

The mix grading design on the basis of correctly proportioning of the combined filler components ensures the most effective compaction of the system, the maximum reduction of the necessary amount of resin required and the best workability of the

mix. The selection of micro filler type and particle size, other than reducing porosity, will enhance the workability, contribute to maximum reduction in resin content and also provide the system with further enhanced strength and stiffness properties.

For a given mix volume and mix filler/resin ratio, gap graded filler mix design may result in a more workable system when compared with through graded design. However, the latter grading tends to provide a system with enhanced flexural properties at its hardend state.

The Phenolic Concrete in its solid state, proved to be a non-absorptive composite irrespective of its level of porosity. Theoretically with increase in filler/resin ratio porosity may increase. Water absorptivity was only detected at a negligible level with samples made from high filler/resin ratio mixes. This was due to the rough surface texture and the apparent surface voids in high filler loaded systems. The increase in filler/resin ratio resulted in change of practically all investigated properties, density, strength and modulus values. These properties were found to be affected by mix composition variations. The optimum flexural property results lie between filler/resin ratios of 6:1 to 9:1. These ratios would favour the use of such filled Phenolic composites for bulding purposes due to the lower requirements of the more expensive component i.e. the Phenolic resin content in the composite matrix. With increase in filler/resin ratio, the tested samples showed an increase in both flexural strength and also in flexural modulus. It is demonstrated that a Phenolic Concrete with high resin loading will be less stiff and therefore may undergo larger deflections when compared to composites from lesser resin loading. It was clearly seen from inspection of the fractured sections, strong bond had been developed between the fillers (sand grains) and the resin matrix. At the fracture surface, sand grains had also fractured with no apparent debonding. This may be the reason for

increase in the flexural strength of the highly filled systems as in such systems more of tougher grains have to fail in fracture. However, the optimum filler/resin ratio was found to be at 6:1 filler to resin ratio and above this level, at 7:1 ratio, the increase in flexural properties was insignificant. Using furfuryl alcohol as a solvent in the mix formulation produced a further optimization. It became possible to produce and cast workable mixes up to and including 9:1 filler to resin ratio. The furfuryl alcohol due to its lower viscosity than resin increased the workability of a given mix matrix system by proportionally replacing the resin content thus allowing further increases in filler loading for a given mix system. Replacing considerable quantities of resin content of a system by stronger crosslinking furfuryl alcohol agent improved the physical properties of the Phenolic Concrete matrix, resulting in stronger and stiffer composites. The mix compositions containing furfuryl alcohol showed an increasing effect on the flexural properties of the made specimens. Furfuryl alcohol is a crosslinking agent and developes larger chains in the habitat matrix and it may be used as an integral part of the resulting Phenolic Concrete matrix.

In selecting a Phenolic resin for the production of filled composites, the factors of importance are both its chemical composition and its physical characteristics. These factors affect its bonding properties to fibrous and non-fibrous fillers and its viscosity, which influences the workability of the composite mix system. All of the resins investigated in this part of the work showed suitability for producing Phenolic Concrete composites. However, the mixes composed of IR1271 resin resulted in more workable mixes and at the same time produced elements with higher strength values in flexure.

The catalyst content was important in determining both the rate and the extent of the polymerization. Either too much or too little catalyst resulted in material with

lesser flexural strength capacities. Generally the specimens' shape, size, the resin loading in the mix system and resin type, the temperature, as well as the catalyst type, controls the catalyst requirements. Less catalyst is required with high resin loading due to increased polymerisation exothermics per unit volume. Less catalyst is required with larger or compact sections because of lower heat dissipation rates, due to the lower surface to volume ratios of the specimens. However, from the made test specimens it was noticed that excess catalyst in the mix system introduces internal defects due to early local polymerisation as a result of local high catalyst concentration. This may be easily detected from the surface finishes, as in the cases experienced in this work.

In producing a Phenolic Concrete composite, postcuring is neccessary to achieve full curing in order to produce an element with enhanced physical properties. From the economy point of view an optimum level of curing temperature and time was found to be $120°C$ over a period of 2 hours. It should be noted that a higher curing temperature and prolonged curing at high temperatures may result in a damaged or a more brittle composite, resulting in a less stronger and less stiffer system.

Both cold and hot casting methods may be used in conjunction with pressure. The latter affords the system further specific properties. It will result in a more stable composite system with reasonable flatness and with much improved smoothness of surface even with higher filler loadings. It will also optimise the period needed for the composite to set prior to demoulding by reducing the setting process time to as low as 15 minutes. In cold setting, the process may need a period of 12 to 24 hours depending on the storage condition and catalyst level used in mixing process. It is of importance in hot casting, to keep the casting temperature below water boiling temperature in order to avoid any flaw occurring in the system during the

setting process. It is recommended in either casting methods to apply a constant pressure to the cast matrix while setting. This may help to densify the system and improve physical shape and surface texture. As a result the system has to be cast in a closed top mould which would provide the system with steady and equal rate of exothermic temperature dissipation and also a steady and stable rate of setting This will prevent the faces of the system from possible differential shrinkages.

To provide reinforcement to the Phenolic Concrete composite, fibre glass lay-up laminates may be used. The lay-up laminates should be provided on either faces of a particular element for two reasons. Firstly, to keep the composite material symmetry, and secondly, to prevent any problem arising from the differential rate of setting and curing. The reinforcement by means of fibre glass mat lay-up laminates would considerably increase the flexural strength capacity of the system depending on the type and density of the fibre glass mat. However, the test results clearly showed that it may decrease the stiffness of the system (i.e. lower flexural modulus values). The fibre glass lay-up laminates provide a great deal of flexibility to the system and increase the ductility of the brittle Phenolic Concrete. This may be as a result of larger void ratio in the laminate matrix since it requires a hand lay-up procedure. Furthermore, because the composite modulus is much greater than the resin modulus, therefore the direct contribution of the resin to the ability of a fibre glass reinforced resin to assist flexural deformation would be small, and can be neglected. Therefore, layers of resin on the outer surfaces of the composite reinforced with fibre laminates would have little effect on the deflection of a latterally loaded element. However, surface resin layers do contribute to the composite thickness used in computing flexural modulus and can have a significant effect on the computed flexural modulus.

It was seen from the test results that the flexural tests produced higher strength and modulus values when compared to the values obtained from direct tensile tests. It is fair to say that flexural tests measure the flexural properties of the composite rather than the material property. A good test for material mechanical property should have a single uniform stress component in the gauge section, particularly when the principal objective of the test is to determine strength values. Flexure tests satisfies neither criteria. Generally, the flexural stress at failure appears to be greater than the ultimate tensile strength of the material from which it is composed. This may be explained by the non-uniformity of stress in the flexure test. The maximum tensile and compressive stresses exist only in the outer fibres of the element under flexure. Therefore for a given stress level, it is more likely for failure to occur in a larger volume of a material than in a smaller volume.

In an element subject to direct tension, a greater volume of such an element would be subjected to the maximum stress when compared to the element under flexure. In the former, therefore, the probability of a weak element occurring is higher.

Table 3.1 Mix proportions

Mix Formulation	Filler Grading	Design Method	Percentage by weight of fillers						Surface Index
			Silica Sands				Micro Filler		
			No.1	No.2	No.3	No.4	Content	Type	
A1	*Through*	G.T.E.	35.6%A	17.0%B	15.0%C	9.0%D	23.4%	S.F.(b)	1.970
A2		A.M.P.	36.6%A	16.4%B	15.7%D	8.5%D	22.8%		1.920
A3		A.M.P.	35.3%A	15.9%B	14.9%C	9.1%D	24.8%		2.090
B	*Through*	G.T.E.	34.8%A	17.5%B	15.7%C	14.0%D	18.0%	S.F.(b)	1.510
B2		A.M.P.	36.8%A	16.7%B	14.7%C	11.7%D	20.2%		1.702
B8		P.	39.0%A	19.7%B	17.6%C	15.7%D	8.0%		0.673
B13		P.	36.9%A	18.6%B	16.7%C	14.8%D	13.0%		1.090
B15		P.	36.1%A	18.1%B	16.3%C	14.5%D	15.0%		1.260
B20		P.	33.9%A	17.1%B	15.3%C	13.7%D	20.0%		1.680
B25		P.	31.8%A	16.0%B	14.4%C	12.8%D	25.0%		2.100
B30		P.	29.7%A	15.0%B	13.4%C	11.9%D	30.0%		2.520
C1	*Through*	G.T.E.	34.0%A	16.4%B	16.0%C	9.6%D1	24.0%	E.Ch.C.	8.690
C2		A.M.P.	35.9%A	16.2%B	14.6%C	10.6%D1	22.7%		8.220
C3		G.T.E.	36.8%A	16.5%B	15.0%C	24.7%D1	7.0%		2.540
C4		A.M.P.	36.7%A	16.8%B	13.4%C	15.3%D1	17.8%		6.450
D	*Through*	G.T.E.	39.5%E	21.0%B1	13.5%C1	8.0%D1	18.0%	S.F.(a)	0.753
D1		G.T.E.	41.8%E	21.4%B1	14.2%C1	9.6%D1	13.0%		0.546
D2		A.M.P.	45.1%E	18.9%B1	16.7%C1	6.2%D1	13.1%		0.552
E1	*Through*	G.T.E.	36.8%A1	16.0%B1	15.7%C1	12.0%D1	19.5%	S.F.(a)	0.792
E2		A.M.P.	37.2%A1	14.8%B1	16.3%C1	11.4%D1	20.3%		0.823
F1	*Through*	G.T.E.	35.0%E1	17.5%B1	15.5%C1	14.0%D1	18.0%	S.F.(c)	0.831
F2		A.M.P.	35.7%E1	17.8%B1	16.3%C1	11.2%D1	19.0%		0.877
G1	*Gap*	G.T.E.	65.0%E	.....	20.0%C1	5.0%D1	10.0%	Ballot.	0.059
G2		G.T.E.	.....	64.0%B1	.....	11.0%D1	25.0%	S.F.(a)	0.101
G3		G.T.E.	60.0%E	.....	17.0%C1	7.0%D1	16.0%	S.F.(a)	0.675
I	*Through*	P.	36.8%A1	16.0%B1	15.7%C1	12.0%D1	21.3%	Sph.G.	1.160
J		P.	36.8%A1	16.0%B1	15.7%C1	12.0%D1	8.8%	E.Ch.C.	1.200
K		P.	36.8%A1	16.0%B1	15.7%C1	12.0%D1	20.3%	Ballot.	0.545

A.M.P. : Aggregate Mix Programme
G.T.E. : Graphical plus Trial and Error procedure
P. : Proportioning
S.F.(a) : (a) Silica Flour L.G.3/300
S.F.(b) : (b) Silica Flour L.G.3/300
S.F.(c) : (c) Silica Flour C.W.5/300
E.Ch.C : English China Clay (D)
Ballot. : Ballotini
Sph.G. : Spheriglass 5000

Gradings I, J & K are derived from grading E1 with their micro filler %age determined using the equivalent volume of 19.5% Silica Flour present in the E1 grading.

Table 3.2 Filler/resin ratio effect

Coupon Set	Mix Formulation	Filler: Resin ratio	Specimen thickness variation (mm)	Flexural	
				Strength σ_{fu} $\times 10^6$ $(N.m^{-2})$	Modulus E_f $\times 10^9$ $(N.m^{-2})$
a_{1-4}	A1	4:1	6.16±0.11	16.17	22.06
b_{1-4}		5:1	6.33±0.30	17.85	24.22
c_{1-6}		6:1	6.34±0.21	21.20	26.34
d_{1-4}		7:1	6.54±0.06	22.85	28.10
a_{1-6}	A2	4:1	6.21±0.06	17.01	21.88
b_{1-6}		5:1	6.32±0.15	16.88	24.05
c_{1-6}		6:1	6.18±0.11	20.79	25.90
d_{1-6}		7:1	6.43±0.13	22.63	27.88
a_{1-5}	A3	4:1	6.51±0.10	17.15	21.92
b_{1-5}		5:1	6.47±0.09	18.01	24.50
c_{1-4}		6:1	6.47±0.15	21.41	26.42
d_{1-6}		7:1	6.33±0.20	23.10	27.33
a_{1-5}	B	4:1	6.22±0.08	18.01	22.10
b_{1-6}		5:1	6.37±0.06	18.66	23.96
c_{1-6}		6:1	6.19±0.16	22.12	25.88
d_{1-5}		7:1	6.42±0.23	24.62	27.92
a_{1-6}	B2	4:1	6.18±0.32	17.88	22.82
b_{1-6}		5:1	6.27±0.21	19.02	24.76
c_{1-6}		6:1	6.72±0.05	21.75	26.12
d_{1-6}		7:1	6.05±0.18	24.82	28.30
a_{1-4}	C3	4:1	6.55±0.16	15.61	18.34
b_{1-6}		5:1	6.13±0.21	17.10	19.02
c_{1-6}		6:1	6.63±0.11	20.71	22.44
a_{1-5}	C4	4:1	6.31±0.10	17.25	19.48
b_{1-5}		5:1	6.09±0.19	17.88	20.16
a_{1-5}	D	4:1	6.27±0.20	19.11	20.89
b_{1-4}		5:1	6.48±0.04	19.68	22.46
c_{1-6}		6:1	6.37±0.11	22.39	25.83
d_{1-5}		7:1	6.52±0.08	24.95	27.12

Resin Type : Fordath's Resin IR1271
Catalyst : CS30 @ 10% by weight of resin

Casting: Cold Mould
Setting : 24Hrs. @ Room Temperature subject to pressure
Curing : 2Hrs. in oven @ 120°C

Table 3.2 Filler/resin ratio effect (Contd....)

Coupon Set	Mix Formulation	Filler: Resin ratio	Specimen thickness variation (mm)	Flexural	
				Strength σ_{fu} $\times 10^6$ $(N.m^{-2})$	Modulus E_f $\times 10^9$ $(N.m^{-2})$
a_{1-4}	D1	4:1	6.41±0.05	18.10	20.44
b_{1-6}		5:1	6.59±0.12	18.92	21.93
c_{1-6}		6:1	6.38±0.17	21.95	23.14
d_{1-5}		7:1	6.19±0.14	24.50	24.88
a_{1-6}	D2	4:1	6.70±0.06	18.38	20.14
b_{1-6}		5:1	6.61±0.08	19.03	22.16
c_{1-6}		6:1	6.75±0.13	22.18	22.80
d_{1-5}		7:1	6.44±0.21	24.39	24.36
a_{1-6}	E1	4:1	6.38±0.12	18.92	22.28
b_{1-6}		5:1	6.41±0.25	19.85	24.27
c_{1-5}		6:1	6.33±0.08	23.44	26.17
d_{1-6}		7:1	6.61±0.15	25.05	28.55
a_{1-6}	E2	4:1	6.15±0.13	18.63	22.66
b_{1-5}		5:1	6.09±0.12	18.95	25.05
c_{1-5}		6:1	6.23±0.21	22.35	26.42
d_{1-5}		7:1	6.29±0.05	24.67	28.12
a_{1-5}	F1	4:1	6.35±0.10	17.95	22.01
b_{1-5}		5:1	6.53±0.16	18.88	23.96
c_{1-6}		6:1	6.40±0.22	22.81	25.10
d_{1-5}		7:1	6.48±0.28	24.51	27.80
a_{1-6}	F2	4:1	6.40±0.11	18.02	21.86
b_{1-6}		5:1	6.16±0.18	19.36	24.02
c_{1-6}		6:1	6.32±0.07	23.12	26.27
d_{1-5}		7:1	6.09±0.30	24.81	27.92
a_{1-6}	E1 +1%T_iO_2	6:1	6.44±0.17	23.85	26.72
b_{1-6}	E1 +2%T_iO_2	6:1	6.50±0.08	23.27	27.02
c_{1-5} ⊙	E1 +3%T_iO_2	6:1	6.17±0.22	23.33	26.26
d_{1-3} ⊙⊙	E1 +3%T_iO_2	6:1	6.48±0.14	22.28	26.44

Resin Type : Fordath's Resin IR1271
Catalyst : CS30 @ 10% by weight of resin
Casting: Cold Mould
Setting : 24Hrs. @ Room Temperature subject to pressure
Curing : 2Hrs. in oven @ 120°C

The specimens, ⊙ & ⊙⊙, were placed in the oven for a period of 6hrs. at 70°C for setting to complete.

The specimens, ⊙⊙, were tested 30 months after the postcuring.

Table 3.3 Catalyst content effect

Coupon Set	Mix Formulation	Filler: Resin ratio	Catalyst content %	Specimen thickness variation (mm)	Flexural Strength σ_{fu} $\times 10^6$ $(N.m^{-2})$	Flexural Modulus E_f $\times 10^9$ $(N.m^{-2})$
Postcuring 2 hours in oven at 120°C						
a_{1-4}	C1	4.5:1	6	6.71±0.19	22.19	20.36
b_{1-6}			8	6.55±0.38	25.72	24.65
c_{1-5}			10	6.47±0.10	26.97	25.62
d_{1-6}			12	6.64±0.61	26.88	25.58
e_{1-6}			14	7.28±0.33	24.38	22.16
a_{1-6}	C2	4.5:1	6	6.39±0.06	21.36	20.00
b_{1-6}			8	6.72±0.18	24.67	23.42
c_{1-6}			10	6.28±0.28	24.79	24.68
d_{1-5}			12	6.39±0.17	24.52	24.14
e_{1-6}			14	6.50±0.31	22.16	22.83
a_{1-6}	C3	6:1	6	6.47±0.10	17.34	18.19
b_{1-6}			8	6.62±0.09	21.06	22.23
c_{1-5}			10	6.58±0.42	21.23	22.98
d_{1-4}			12	6.71±0.31	21.19	22.36
e_{1-4}			14	6.42±0.27	20.07	21.05
Postcuring 45 days at room temperature						
a_{1-6}	C1	4.5:1	6	6.33±0.28	12.04	14.07
b_{1-6}			8	6.48±0.15	16.13	16.25
c_{1-6}			10	6.27±0.16	16.47	17.64
d_{1-5}			12	6.81±0.16	17.65	18.04
e_{1-6}			14	6.69±0.41	18.12	19.26
a_{1-6}	C2	4.5:1	6	6.18±0.19	11.64	14.25
b_{1-6}			8	6.32±0.31	14.72	16.06
c_{1-4}			10	6.55±0.08	15.97	17.88
d_{1-4}			12	6.10±0.23	18.46	18.67
e_{1-6}			14	6.63±0.15	18.91	19.50
a_{1-5}	C3	6:1	6	6.52±0.31	12.87	14.28
b_{1-4}			8	6.45±0.22	15.33	16.09
c_{1-6}			10	6.60±0.29	16.13	17.81
d_{1-6}			12	6.35±0.17	17.87	19.12
e_{1-6}			14	6.39±0.32	18.49	19.50

Resin Type : Fordath's Resin IR1271
Catalyst : CS30 (as in table)
Casting : Cold Mould
Setting : 24Hrs. @ Room Temperature subject to pressure
Curing : (as in table)

Table 3.4 Micro filler content effect

Coupon Set	Mix Formulation	Filler: Resin ratio	Micro Filler content %	Specimen thickness variation (mm)	Flexural	
					Strength σ_{fu} $\times 10^6$ $(N.m^{-2})$	Modulus E_f $\times 10^9$ $(N.m^{-2})$
Resin : Furfuryl Alcohol @ 65 : 35				*Micro filler : Silica Flour L.G.* 3/300		
a_{1-6}	B8	7:1	8	6.42±0.36	22.08	22.45
b_{1-6}	B13		13	6.53±0.35	22.62	22.82
c_{1-6}	B15		15	6.73±0.44	24.65	26.16
d_{1-6}	B18		18	6.67±0.06	26.97	28.44
e_{1-6}	B20		20	6.44±0.49	26.85	27.98
f_{1-6}	B25		25	6.73±0.18	26.27	27.45
g_{1-6}	B30		30	6.12±0.11	25.80	27.01
a_{1-6}	B8	8:1	8	6.87±0.16	25.23	23.85
b_{1-6}	B13		13	6.10±0.04	25.78	24.04
c_{1-6}	B15		15	6.36±0.52	28.50	25.10
d_{1-6}	B18		18	6.96±0.21	29.69	30.42
e_{1-6}	B20		20	6.83±0.07	29.55	30.13
f_{1-6}	B25		25	6.42±0.48	28.65	29.44
g_{1-6}	B30		30	6.28±0.31	27.80	27.56

Table 3.5 Micro filler type effect

Coupon Set	Mix Formulation	Filler: Resin ratio	Micro Filler Filler	Specimen thickness variation (mm)	Flexural	
					Strength σ_{fu} $\times 10^6$ $(N.m^{-2})$	Modulus E_f $\times 10^9$ $(N.m^{-2})$
a_{1-6}	E1	5:1	Silica Flour	7.02±0.27	20.06	25.15
b_{1-6}	$(E_{s.f.})$	6:1	a-L.G.3/300	7.23±0.19	23.77	26.44
c_{1-4}		7:1		6.98±0.36	25.42	29.06
a_{1-5}	I	5:1	Sphereglass	7.16±0.17	19.87	24.82
b_{1-5}	$(E_{sph.g.})$	6:1	5000	6.97±0.25	24.06	25.44
c_{1-5}		7:1		7.02±0.07	25.38	28.50
a_{1-6}	J	5:1	China Clay	7.25±0.29	19.22	22.20
b_{1-6}	$(E_{ch.c.})$	6:1	(D)	6.89±0.38	22.63	23.78
c_{1-3}		7:1		6.78±0.43	24.18	25.12
a_{1-6}	K	5:1	Ballotini	7.14±0.24	19.97	23.00
b_{1-5}	$(E_{ballo.})$	6:1		7.28±0.10	23.92	23.96
c_{1-6}		7:1		6.77±0.31	25.40	26.70

Resin Type : Fordath's Resin IR1271
Catalyst : CS30 @ 10% by weight of resin
Casting : Cold Mould
Setting : 24Hrs. @ Room Temperature subject to pressure
Curing : 2Hrs. in oven @ 120°C

Table 3.6 Effect of postcuring period and temperature

Coupon Set	Mix Formulation	Filler: Resin ratio	Postcuring		Specimen thickness variation	Flexural	
			Period (*hours*)	Oven Temperature	(*mm*)	Strength σ_{fu} $\times 10^6$ $(N.m^{-2})$	Modulus E_f $\times 10^9$ $(N.m^{-2})$
a_{1-3}	E1	6:1	4	$70°C$	7.21±0.12	.....	.....
b_{1-3}			8		7.06±0.07	19.22	20.28
c_{1-3}			12		7.35±0.23	23.01	24.16
d_{1-3}			24		7.16±0.41	23.79	27.02
a_{1-5}	E1	6:1	4	$80°C$	7.28±0.18	15.67	14.87
b_{1-6}			8		7.53±0.26	19.06	21.08
c_{1-6}			12		7.19±0.22	23.42	25.72
d_{1-5}			24		7.48±0.37	23.52	26.94
a_{1-6}	E1	6:1	2	$100°C$	7.13±0.21	17.20	17.06
b_{1-6}			4		7.45±0.08	20.73	22.84
c_{1-6}			6		7.42±0.11	23.63	26.95
d_{1-6}			8		7.09±0.20	23.59	27.20
a_{1-4}	E1	6:1	1	$120°C$	7.41±0.40	20.43	21.42
b_{1-4}			2		7.38±0.21	23.82	27.56
c_{1-4}			3		7.52±0.17	23.61	27.70
d_{1-4}			4		7.21±0.38	23.52	26.99
e_{1-4}			6		7.10±0.09	23.65	27.40
a_{1-6}	E1	6:1	1	$140°C$	7.47±0.32	20.60	23.42
b_{1-6}			2		7.06±0.19	23.06	27.08
c_{1-4}			3		7.60±0.28	22.92	27.68
d_{1-5}			4		7.32±0.18	23.10	27.02
e_{1-6}			6		7.50±0.09	19.04	25.10

Resin Type : Fordath's Resin IR1271
Catalyst : CS30 @ 10% by weight of resin

Casting: Cold Mould
Setting : 24Hrs. @ Room Temperature subject to pressure
Curing : in oven (as in table)

Table 3.7 Phenolic Resin : Furfuryl Alcohol ratio effect

Coupon Set	Mix Formulation	Resin: Furfuryl ratio	Specimen thickness variation (mm)	Flexural	
				Strength σ_{fu} $\times 10^6$ $(N.m^{-2})$	Modulus E_f $\times 10^9$ $(N.m^{-2})$
a_{1-4}	A3	100:0	6.33±0.20	23.10	27.33
b_{1-4}		80:20	7.51±0.37	24.54	28.20
c_{1-5}		65:35	6.38±0.14	25.16	28.95
d_{1-6}		55:45	7.20±0.41	25.10	27.67
e_{1-6}		45:55	6.88±0.14	24.97	26.31
a_{1-5}	B	100:0	6.42±0.23	24.62	27.92
b_{1-5}		80:20	6.51±0.07	25.20	28.20
c_{1-6}		65:35	6.60±0.20	26.10	28.55
d_{1-5}		55:45	6.32±0.15	26.38	28.60
e_{1-6}		45:55	6.44±0.25	25.45	26.87
a_{1-5}	D	100:0	6.52±0.08	24.95	27.12
b_{1-5}		80:20	6.81±0.17	25.70	27.90
c_{1-6}		65:35	7.01±0.12	26.62	29.20
d_{1-5}		55:45	7.06±0.14	27.15	29.72
e_{1-5}		45:55	6.97±0.11	25.30	27.01
a_{1-6}	E1	100:0	6.61±0.15	25.05	28.55
b_{1-6}		80:20	6.51±0.39	25.31	29.00
c_{1-4}		65:35	6.62±0.29	27.16	29.66
d_{1-6}		55:45	6.23±0.08	28.45	28.10
e_{1-5}		45:55	6.77±0.34	27.30	26.92

Resin Type : Fordath's Resin IR1271
Catalyst : CS30 @ 10% by weight of resin
Filler/Resin ratio : 7:1

Casting : Cold Mould
Setting : 24Hrs. @ Room Temperature subject to pressure
Curing : 2Hrs. in oven @ 120°C

Table 3.8 Filler/(resin + alcohol) ratio effect

Coupon Set	Mix Formulation	Filler: Resin ratio	Specimen thickness variation (mm)	Flexural	
				Strength σ_{fu} $\times 10^6$ $(N.m^{-2})$	Modulus E_f $\times 10^9$ $(N.m^{-2})$
Resin : Furfuryl Alcohol @ 65 : 35					
a_{1-5}	A3	7:1	6.38±0.14	25.16	28.95
b_{1-6}		8:1	6.47±0.10	26.09	28.80
c_{1-6}		9:1	6.53±0.47	29.10	30.65
a_{1-6}	B	7:1	6.60±0.20	26.10	28.45
b_{1-4}		8:1	6.81±0.41	28.95	29.81
c_{1-6}		9:1	6.45±0.23	28.63	29.70
a_{1-6}	D	7:1	7.01±0.12	26.62	29.20
b_{1-6}		8:1	7.11±0.06	27.86	31.30
c_{1-5}		9:1	6.85±0.32	28.90	31.32
a_{1-4}	E1	7:1	6.62±0.29	27.16	29.66
b_{1-4}		8:1	6.38±0.11	28.28	30.22
c_{1-4}		9:1	6.45±0.25	29.75	31.75
Resin : Furfuryl Alcohol @ 55 : 45					
a_{1-6}	A3	7:1	7.20±0.41	25.10	27.67
b_{1-6}		8:1	7.31±0.19	27.55	29.72
c_{1-6}		9:1	7.06±0.28	28.86	29.66
a_{1-5}	B	7:1	6.32±0.15	26.38	28.60
b_{1-5}		8:1	6.85±0.22	27.75	29.88
c_{1-4}		9:1	6.59±0.24	28.08	31.48
a_{1-5}	D	7:1	7.06±0.14	27.15	29.72
b_{1-5}		8:1	6.82±0.07	27.67	30.62
c_{1-6}		9:1	6.45±0.16	28.56	30.44
a_{1-6}	E1	7:1	6.23±0.08	28.45	28.10
b_{1-5}		8:1	6.52±0.21	29.96	31.82
c_{1-6}		9:1	6.64±0.17	31.77	31.64

Resin Type : Fordath's Resin IR1271
Catalyst : CS30 @ 10% by weight of resin

Casting: Cold Mould
Setting : 24Hrs. @ Room Temperature subject to pressure
Curing : 2Hrs. in oven @ 120°C

Table 3.9 Flexural test results of coupon specimens made using Phenolic Resins IR1270, IR1271 and J50/010L

Coupon Set	Mix Formulation	Phenolic Resin type	Catalyst type & content	Coupon thickness variation (mm)	Flexural	
					Strength σ_{fu} $\times 10^6$ $(N.m^{-2})$	Modulus E_f $\times 10^9$ $(N.m^{-2})$
a_{1-3}	E1	IR1271	CS30 6%	7.42±0.30	23.13	23.46
b_{1-3}			8%	7.51±0.37	25.04	26.20
c_{1-3}			10%	7.06±0.14	25.85	27.43
d_{1-3}			12%	6.97±0.43	25.13	27.11
a_{1-3}	E1	IR1271	Ph.15 6%	7.19±0.28	23.08	23.77
b_{1-3}			8%	7.94±0.07	24.84	25.78
c_{1-3}			10%	6.32±0.12	25.44	26.88
d_{1-3}			12%	6.79±0.33	25.20	26.34
a_{1-3}	E1	IR1271	Ph.10 8%	6.55±0.10	17.72	18.52
b_{1-3}			10%	6.42±0.03	22.16	22.50
c_{1-3}			12%	6.85±0.21	24.85	21.87
a_{1-3}	E1	IR1270	CS30 6%	6.18±0.18	22.45	23.08
b_{1-3}			8%	6.77±0.12	24.18	24.32
c_{1-3}			10%	7.03±0.10	25.24	25.90
d_{1-3}			12%	6.70±0.11	24.49	25.31
a_{1-3}	E1	IR1270	Ph.15 6%	6.54±0.25	22.42	23.12
b_{1-3}			8%	6.49±0.31	24.27	25.90
c_{1-3}			10%	6.85±0.11	25.17	25.62
d_{1-3}			12%	6.50±0.28	24.66	24.88
a_{1-3}	E1	IR1270	Ph.10 8%	6.74±0.22	18.23	17.96
b_{1-3}			10%	6.23±0.16	21.70	22.60
c_{1-3}			12%	6.72±0.14	24.11	22.46
a_{1-3}	E1	J50/010L	CS30 6%	6.25±0.07	21.76	23.92
b_{1-3}			8%	7.09±0.23	24.06	24.44
c_{1-3}			10%	6.56±0.18	24.89	25.78
d_{1-3}			12%	6.68±0.21	24.12	25.60
a_{1-3}	E1	J50/010L	Ph.15 6%	6.60±0.42	21.77	22.56
b_{1-3}			8%	6.77±0.11	23.31	26.08
c_{1-3}			10%	7.11±0.19	24.62	26.74
d_{1-3}			12%	6.46±0.31	23.87	26.22
a_{1-3}	E1	J50/010L	Ph.10 8%	7.10±0.22	18.81	17.40
b_{1-3}			10%	6.34±0.06	21.13	21.68
c_{1-3}			12%	7.23±0.33	23.37	22.07

Filler/Resin Ratio : 6.5:1
Catalyst : (as in table)

Casting: Cold Mould
Setting : 24Hrs. @ Room Temperature subject to pressure
Curing : 2Hrs. in oven at $120°C$

-5mm

Table 3.10 Setting subject to heat and pressure using a hot press (plain specimens)

Coupon Set	Mix Formulation	Filler: Resin ratio	Resin: Furfuryl ratio	Specimen thickness variation (mm)	Flexural	
					Strength σ_{fu} $\times 10^6$ $(N.m^{-2})$	Modulus E_f $\times 10^9$ $(N.m^{-2})$
a_{1-6}	E1	6:1	.....	8.66±0.12	24.79	27.88
b_{1-6}		7:1	80:20	8.33±0.03	28.38	29.36
c_{1-6}		8:1	60:40	8.15±0.06	30.18	30.80
a_{1-6}	B	6:1	.....	8.42±0.09	23.44	26.98
b_{1-6}		7:1	80:20	8.51±0.08	26.88	27.72
c_{1-6}		8:1	60:40	8.32±0.12	28.60	29.04
a_{1-6}	G2	6:1	.....	8.39±0.06	24.07	26.80
b_{1-6}		7:1	80:20	7.78±0.17	26.82	27.86
c_{1-6}		8:1	60:40	8.52±0.08	25.05	27.14
a_{1-6}	G3	6:1	.....	8.17±0.07	24.65	27.02
b_{1-6}		7:1	80:20	8.44±0.11	27.12	28.60
c_{1-6}		8:1	60:40	8.38±0.10	26.11	28.56

-5mm

Table 3.11 Setting subject to heat and pressure using a hot press (reinforced specimens with laminated fibre glass)

Coupon Set	Mix Formulation	Filler: Resin ratio	Resin: Furfuryl ratio	Fibre Glass type	Specimen thickness variation (mm)	Flexural	
						Strength σ_{fu} $\times 10^6$ $(N.m^{-2})$	Modulus E_f $\times 10^9$ $(N.m^{-2})$
a_{1-6}	E1	6:1	.....	P.B.(csm)	9.31±0.15	45.30	18.03
b_{1-6}			80:20	E.B.(csm)	8.93±0.23	40.46	17.96
c_{1-6}			60:40	W.R.	9.34±0.07	59.17	18.35
a_{1-6}	B	6:1	.....	P.B.(csm)	9.22±0.18	43.07	18.10
b_{1-6}			80:20	E.B.(csm)	9.35±0.09	40.12	17.38
c_{1-6}			60:40	W.R.	9.11±0.20	57.82	17.87
a_{1-6}	G2	6:1	.....	P.B.(csm)	9.08±0.26	38.54	17.78
b_{1-6}			80:20	E.B.(csm)	9.87±0.22	35.90	17.62
c_{1-6}			60:40	W.R.	9.03±0.06	56.61	17.04
a_{1-6}	H	6:1	.....	P.B.(csm)	8.95±0.11	39.05	18.01
b_{1-6}			80:20	E.B.(csm)	8.96±0.18	35.67	17.88
c_{1-6}			60:40	W.R.	9.01±0.09	55.98	17.55

Fibre glass lay-up laminate:

P.B. (csm) : $450g/m^2$ Powder Bounded mat
E.B. (csm) : $450g/m^2$ Emulsion Bounded mat
W. R. : $800g/m^2$ Woven Roving mat
Fibre Glass Type : as in table
Fibre Glass : 1 Layer Top & Bottom
Prewetting : J2018 Resin + 6% Phecat10
Resin/Glass Ratio : 1.5:1

Mix matrix & construction procedure:

Resin type : J50/010L B.P.'s resin
Catalyst : Phencat 15 @ 4%
Casting : Preheated Mould
Setting : Subject to heat & pressure
Time : 15 minutes under press
Temperature : $87 - 90°C$ press platens
Curing : 2Hrs. in Oven @ $120°C$

Table 3.12 Tensile test results from T-Bone specimens

Specimen Set	Mix Formulation	Resin type	Catalyst type & content	Filler: Resin ratio	Resin: Furfuryl ratio (mm)	Tensile	
						Strength σ_{tu} $\times 10^6$ $(N.m^{-2})$	Modulus E_t $\times 10^9$ $(N.m^{-2})$
a_{1-5}	E1	J50/010L	Ph.15 @ 10%	4:1	.....	5.40	15.77
b_{1-4}		(B.P.)		5:1	.....	6.54	17.26
c_{1-6}				6:1	.....	6.98	17.72
d_{1-5}				7:1	80:20	6.72	17.41
e_{1-5}				8:1	60:40	7.08	16.33
a_{1-5}	E1	IR1271	CS30 @ 10%	4:1	.....	6.22	16.46
b_{1-3}		(Fordath)		5:1	.....	7.09	17.45
c_{1-5}				6:1	.....	7.05	17.86
d_{1-5}				7:1	65:35	7.15	17.21
e_{1-6}				8:1	65:35	7.32	17.06
f_{1-5}				9:1	55:45	6.95	16.75
a_{1-6}	E1	J50/010L	Ph.15 @ 6%	6:1	.....	5.66	14.64
b_{1-3}		(B.P.)	8%		.....	6.07	16.44
c_{1-6}			10%		.....	6.98	17.72
d_{1-6}			12%		.....	6.37	17.65
a_{1-5}	E1	IR1271	CS30 @ 6%	6:1	.....	6.63	15.73
b_{1-5}		(Fordath)	8%		.....	6.97	16.92
c_{1-5}			10%		.....	7.05	17.86
d_{1-4}			12%		.....	7.02	17.65
a_{1-5}	G2	IR1271	CS30 @ 10%	5:1	.....	5.65	16.02
b_{1-5}		(Fordath)		6:1	.....	6.10	15.84
c_{1-5}				7:1	.....	6.02	16.16
a_{1-5}	G3	IR1271	CS30 @ 10%	5:1	.....	5.70	15.65
b_{1-5}		(Fordath)		6:1	.....	5.95	16.38
c_{1-5}				7:1	.....	6.18	16.12

Resin Type : (as given in table)
Catalyst : (as given in table)

Casting: Cold Mould
Setting : 24Hrs. @ Room Temperature subject to pressure
Curing : 2Hrs. in oven @ $120°C$

Table 3.13 (Physical properties of the Phenolic Concrete mixes)

Mix Formulation	Mix Composition					Workability	Density ρ (g/cm^3)	Water Absorption (%)	Cylinder Compressive Strength (N/mm^2)	Disc Tensile Strength (N/mm^2)
	Resin Type	Filler: Resin ratio	Resin: Furfuryl ratio	Catalyst type & content	Micro Filler Type					
E1	J50/010L (B.P.)	4:1	.....	Ph.15 8%	S.F. (a)	V.W.	2.09	0.00	79.6	8.3
		5:1	.....			V.W.	2.12	0.00	80.8	8.1
		6:1	.....			W.	2.14	0.00	84.3	8.4
		7:1	80:20			W.	2.19	0.01	84.5	7.9
		8:1	60:40			W.	2.22	0.03	82.4	8.8
E1	IR1271 (Fordath)	4:1	.....	CS30 8%	S.F. (a)	V.W.	2.11	0.00	81.3	8.3
		5:1	.....			V.W.	2.13	0.00	83.1	8.6
		6:1	.....			W.	2.16	0.00	86.5	8.4
		7:1	65:35			W.	2.19	0.00	88.3	8.7
		8:1	65:35			W.	2.24	0.02	87.4	7.6
		9:1	55:45			W.	2.28	0.03	84.6	7.8
G1	J50/010L (B.P.)	5:1	.....	Ph.15 8%	Balloti.	V.W.	2.08	0.00	77.9	7.8
		6:1	.....			V.W.	2.16	0.00	80.4	7.4
		7:1	.....			W.	2.21	0.02	81.1	7.9
G2	J50/010L (B.P.)	5:1	.....	Ph.15 8%	S.F. (a)	V.W.	2.10	0.00	78.2	7.6
		6:1	.....			V.W.	2.14	0.00	81.6	7.8
		7:1	.....			W.	2.20	0.01	83.6	8.1
G3	J50/010L (B.P.)	5:1	.....	Ph.15 8%	S.F. (a)	V.W.	2.10	0.00	75.5	7.6
		6:1	.....			V.W.	2.15	0.00	75.8	7.4
		7:1	.....			W.	2.19	0.00	79.3	7.8
E1	J50/010l (B.P.)	6:1	.....	Ph.15 4%	S.F. (a)	V.W.	2.15	0.00	77.7	7.1
			.....	6%		V.W.	2.13	0.00	78.1	7.3
			.....	8%		W.	2.14	0.00	77.9	7.9
			.....	10%		W.	2.14	0.02	79.2	7.8
$E_{Ch.C.}$	J50/010L (B.P.)	6:1	.....	Ph.15 8%	China Clay	W.	2.12	0.08	74.6	7.8
$E_{Sph.G.}$	J50/010L (B.P.)	6:1	.....	Ph.15 8%	Sph.glass 5000	W.	2.12	0.08	74.6	7.8

V.W.= very workable, self-levelling with the aid of tapping on the mould and use of screed.

W.= workable, levels with the aid of small vibration and use of screed.

Casting : Cold mould

Setting : 24hrs. at R.T. subject to pressure

Curing : 2Hrs. in oven at $120°C$

Figure 3.1a Effect of Filler/Resin ratio

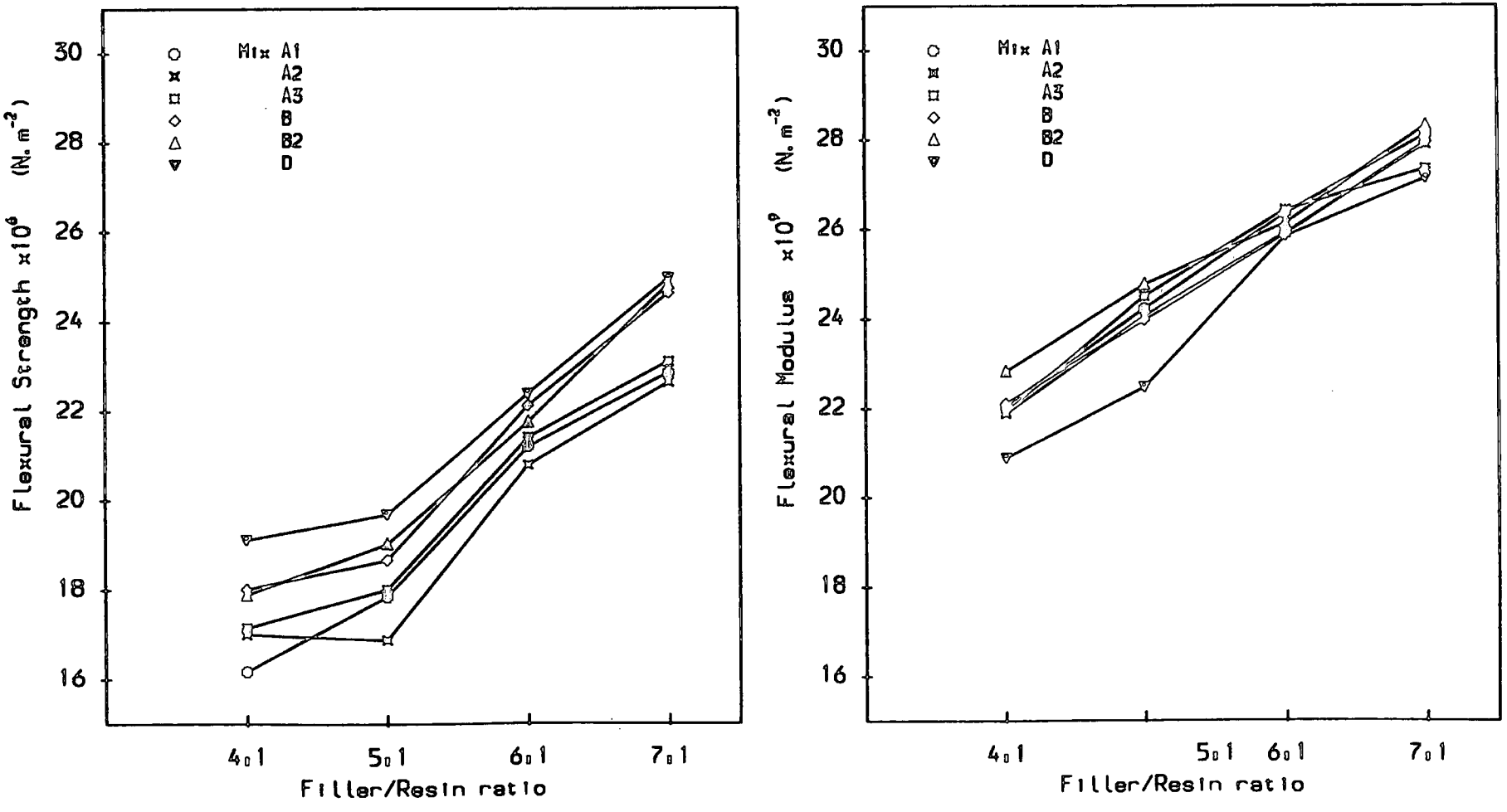

Effect of filler/resin ratio on flexural strength and modulus values of the Phenolic Concrete coupon specimens

Figure 3.1b Effect of Filler/Resin ratio

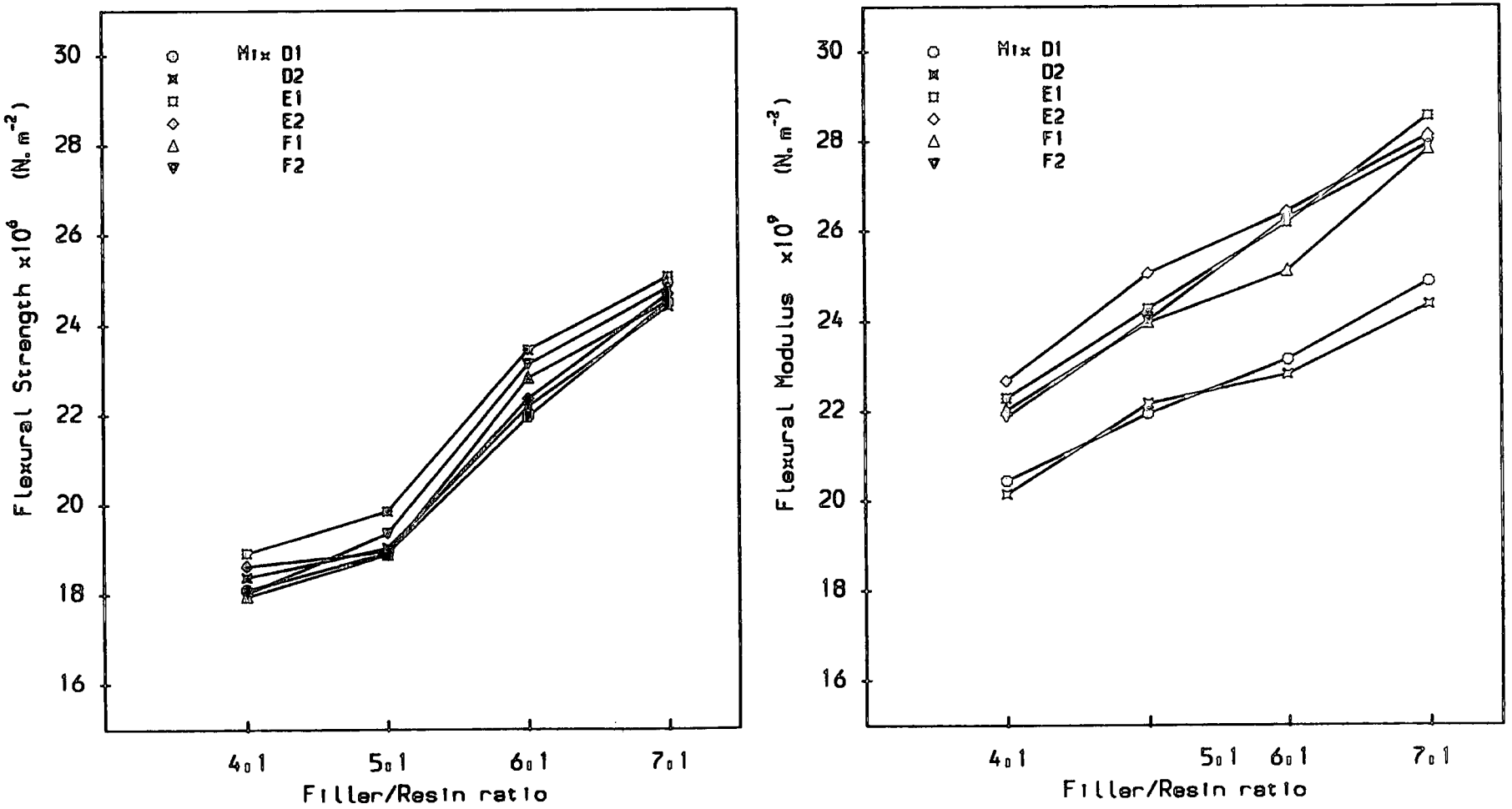

Effect of filler/resin ratio on flexural strength and modulus values of the Phenolic Concrete coupon specimens

Figure 3.2 Effect of Catalyst Content with different Curing methods

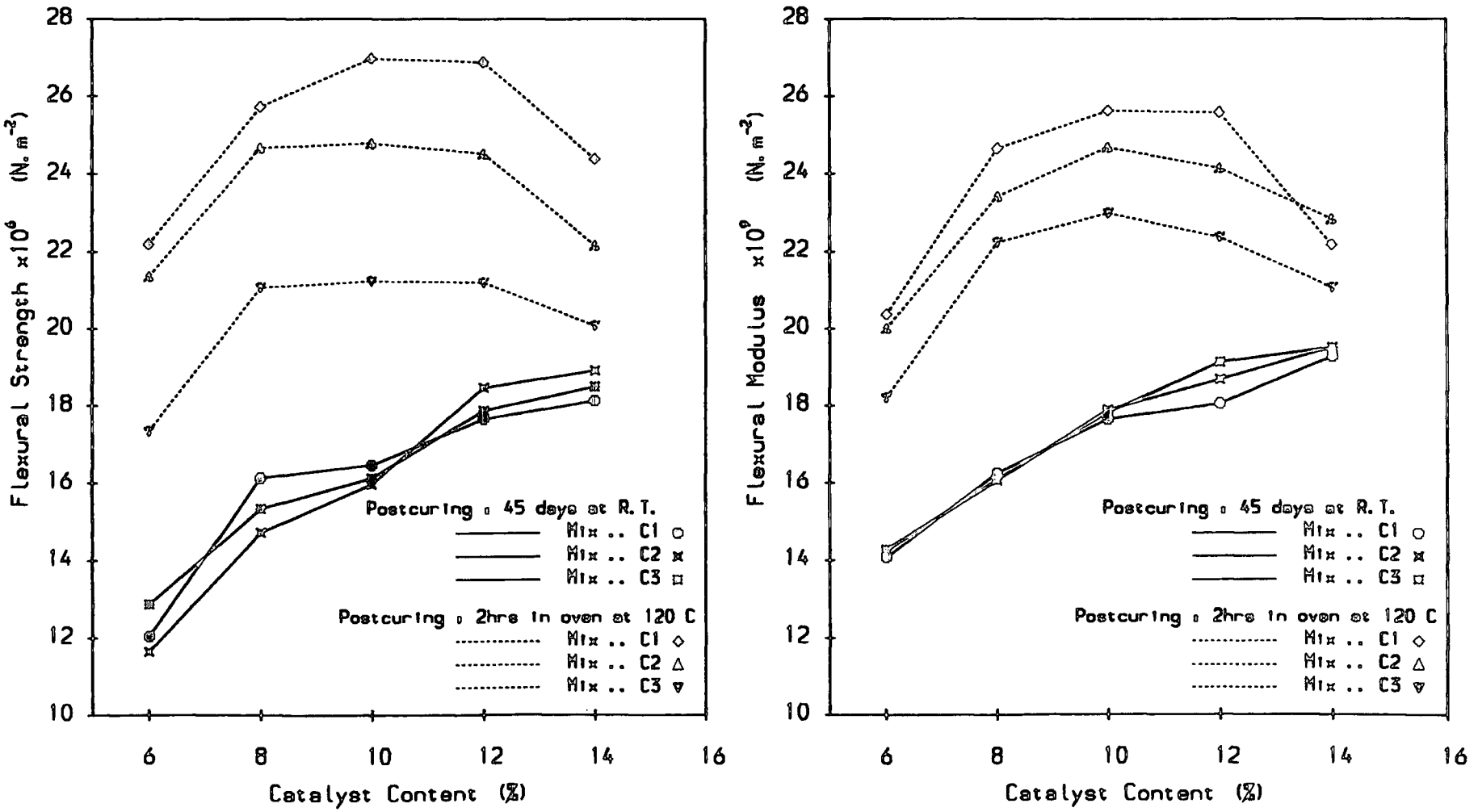

(a) Flexural Strength v Catalyst Level

(b) Flexural Modulus v Catalyst Level

Effect of Catalyst level on flexural properties of Phenolic Concrete coupon specimens

Figure 3.3 Effect of Micro Filler content

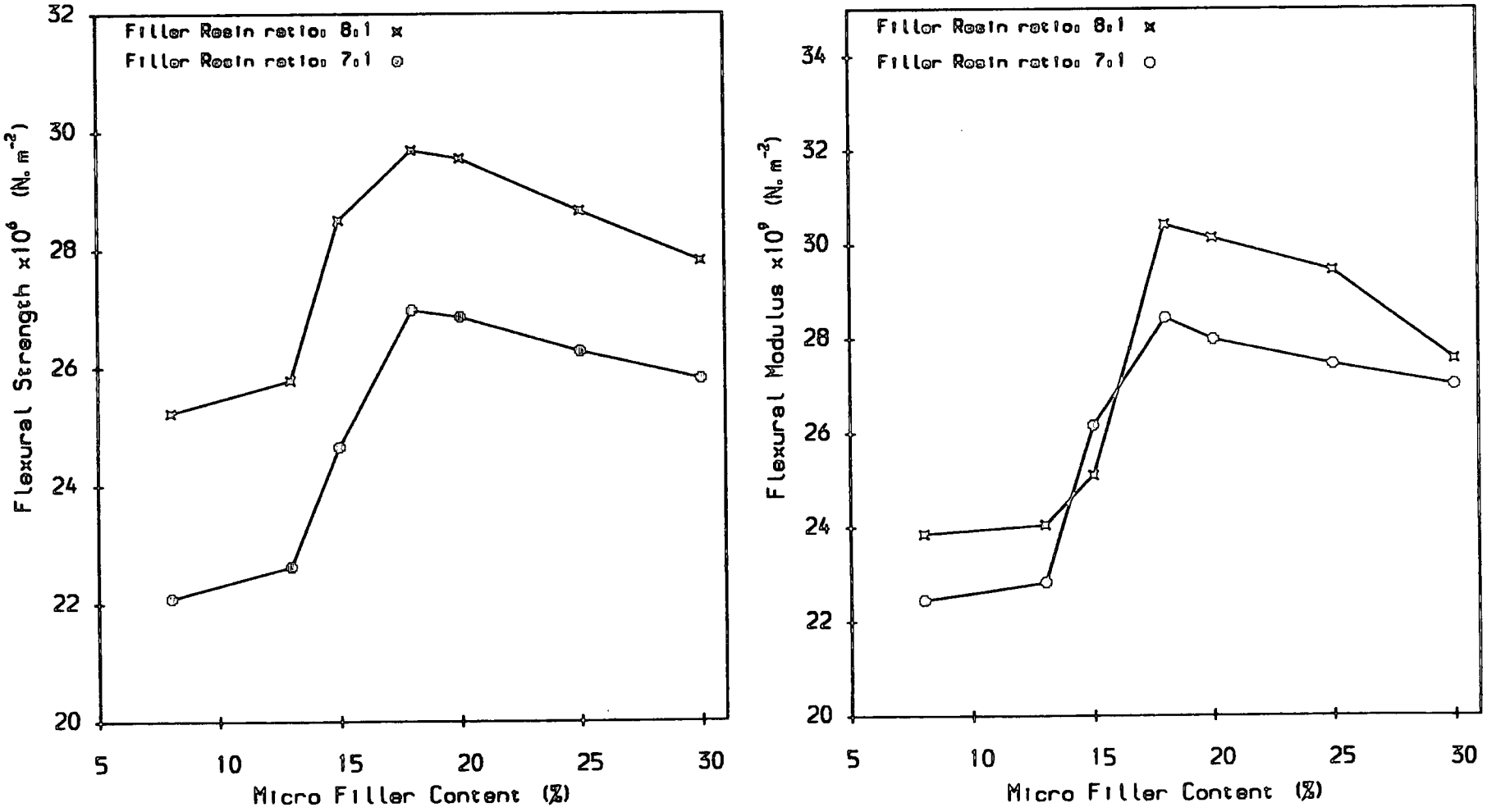

Effect of Micro Filler content on flexural strength and modulus values of Phenolic Concrete coupon specimens

Figure 3.4 Effect of Postcuring rate

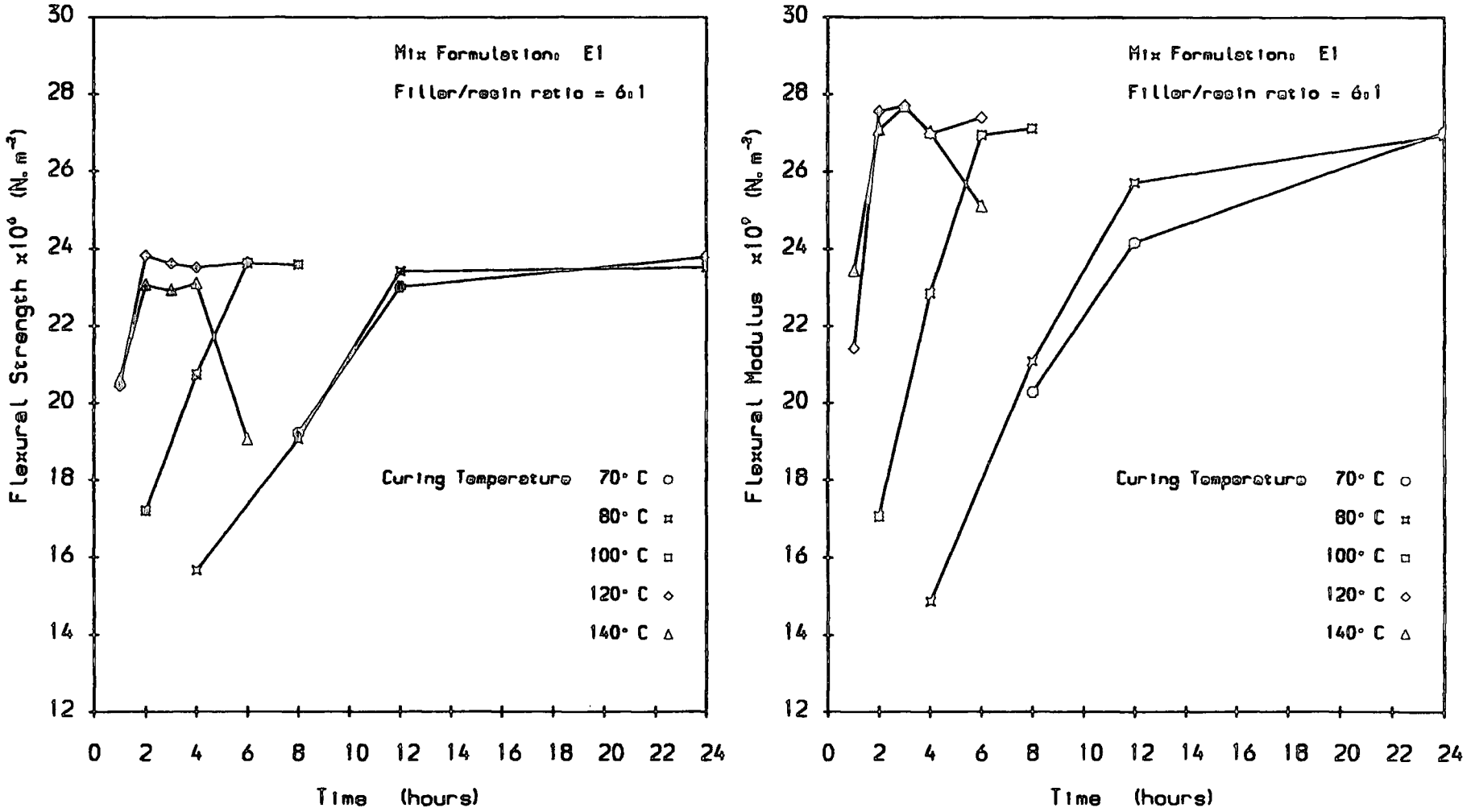

Effect of postcuring period and temperature on flexural properties of Phenolic Concrete coupon specimens

Figure 3.5 Effect of Resin/Furfuryl Alcohol ratio

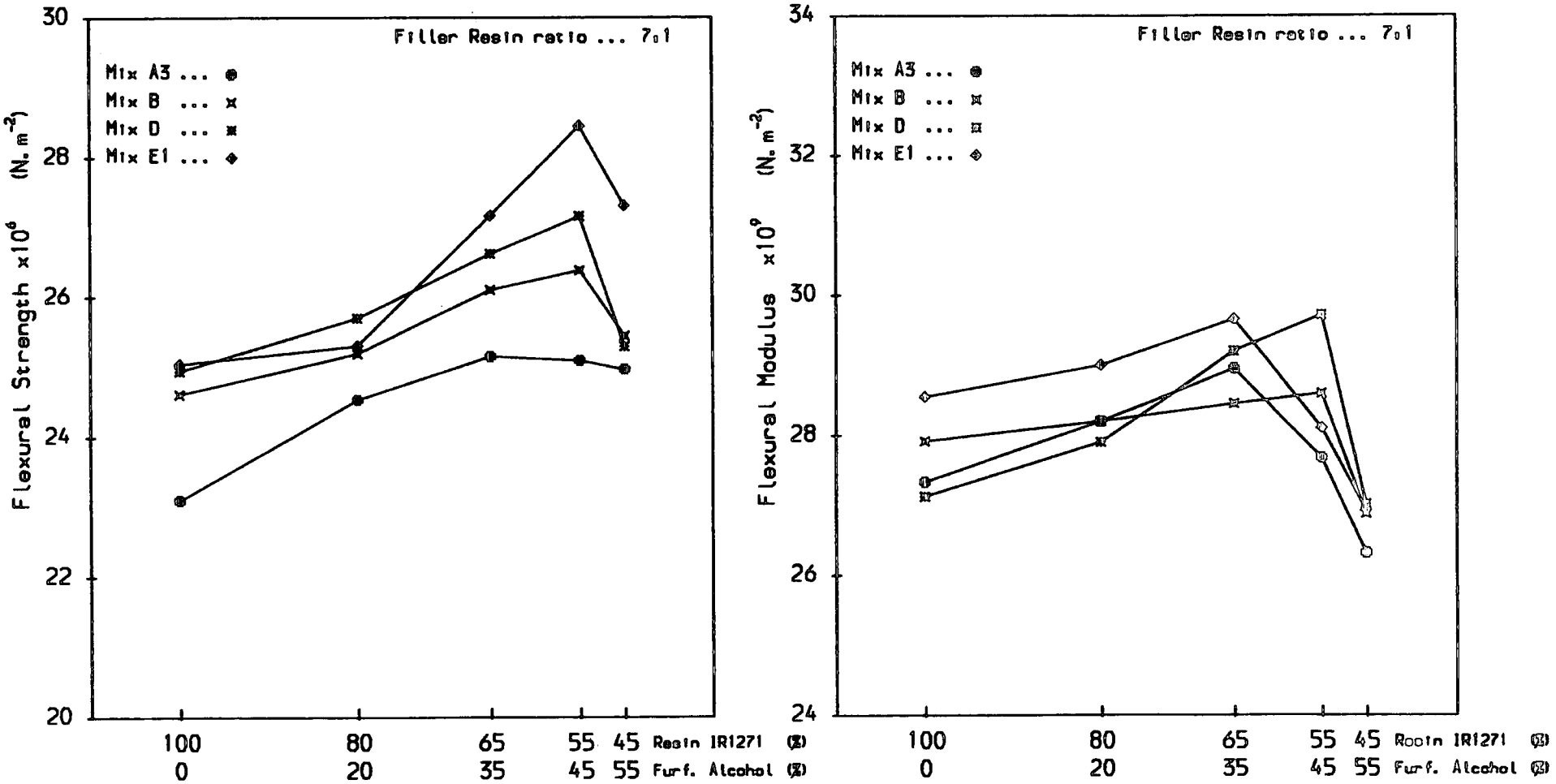

Effect of Furfuryl Alcohol on flexural properties of Phenolic Concrete coupon specimens

Figure 3.6 Effect of Filler/(Resin + Furfuryl) ratio

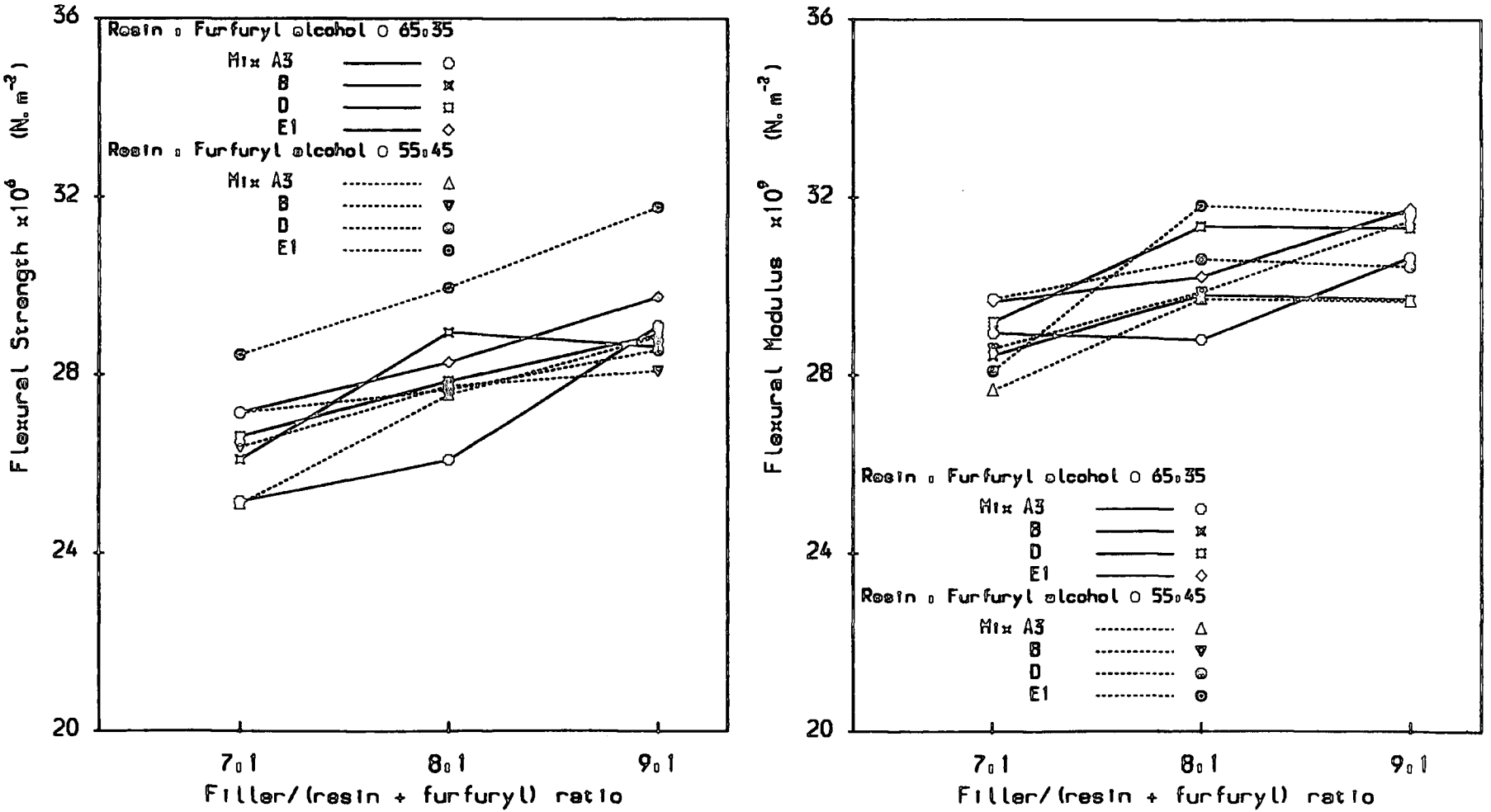

Effect of furfuryl alcohol on flexural strength and modulus values of the Phenolic Concrete coupon specimens

Figure 3.7 Resin Performance

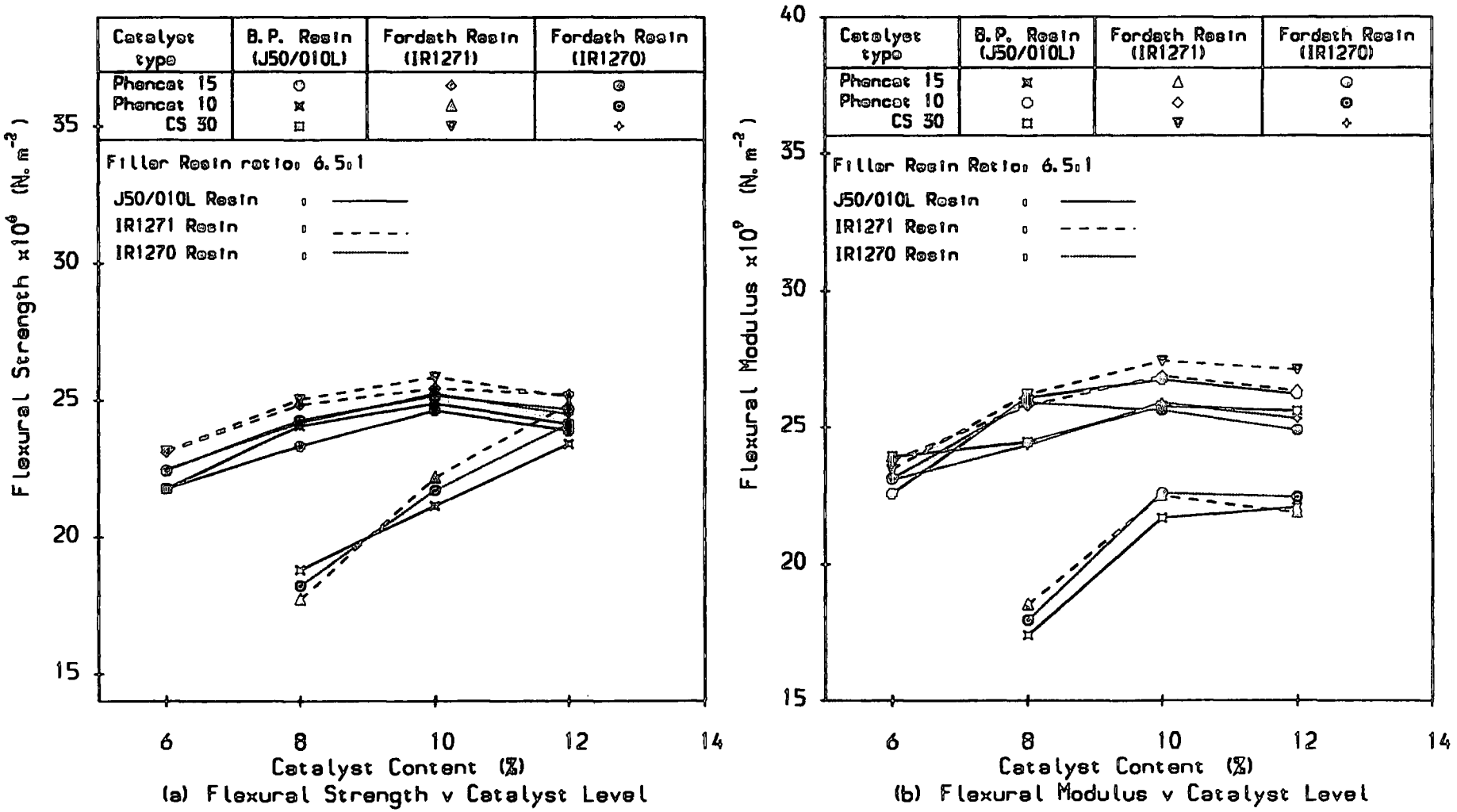

Comparison between J50/010L, IR1271 and IR1270 resins used with different catalysts at various content levels

Figure 3.8 Effect of Filler/Resin ratio (hot casting)

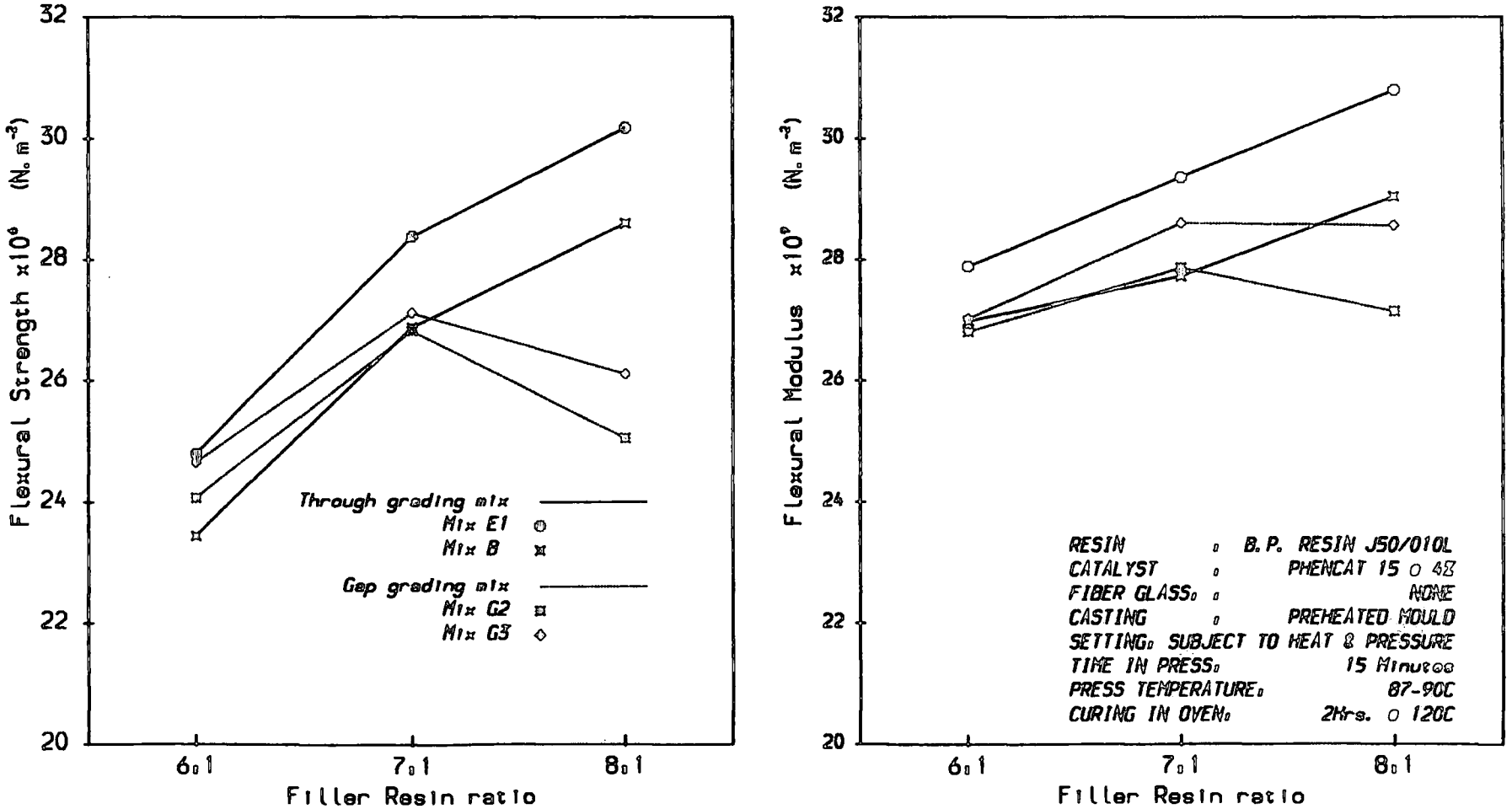

Flexural Strength and Modulus values of Phenolic Concrete coupon specimens cast in preheated moulds. "Setting subject to heat and pressure using a hot press"

Figure 3.9 Determination of Poissons Ratio

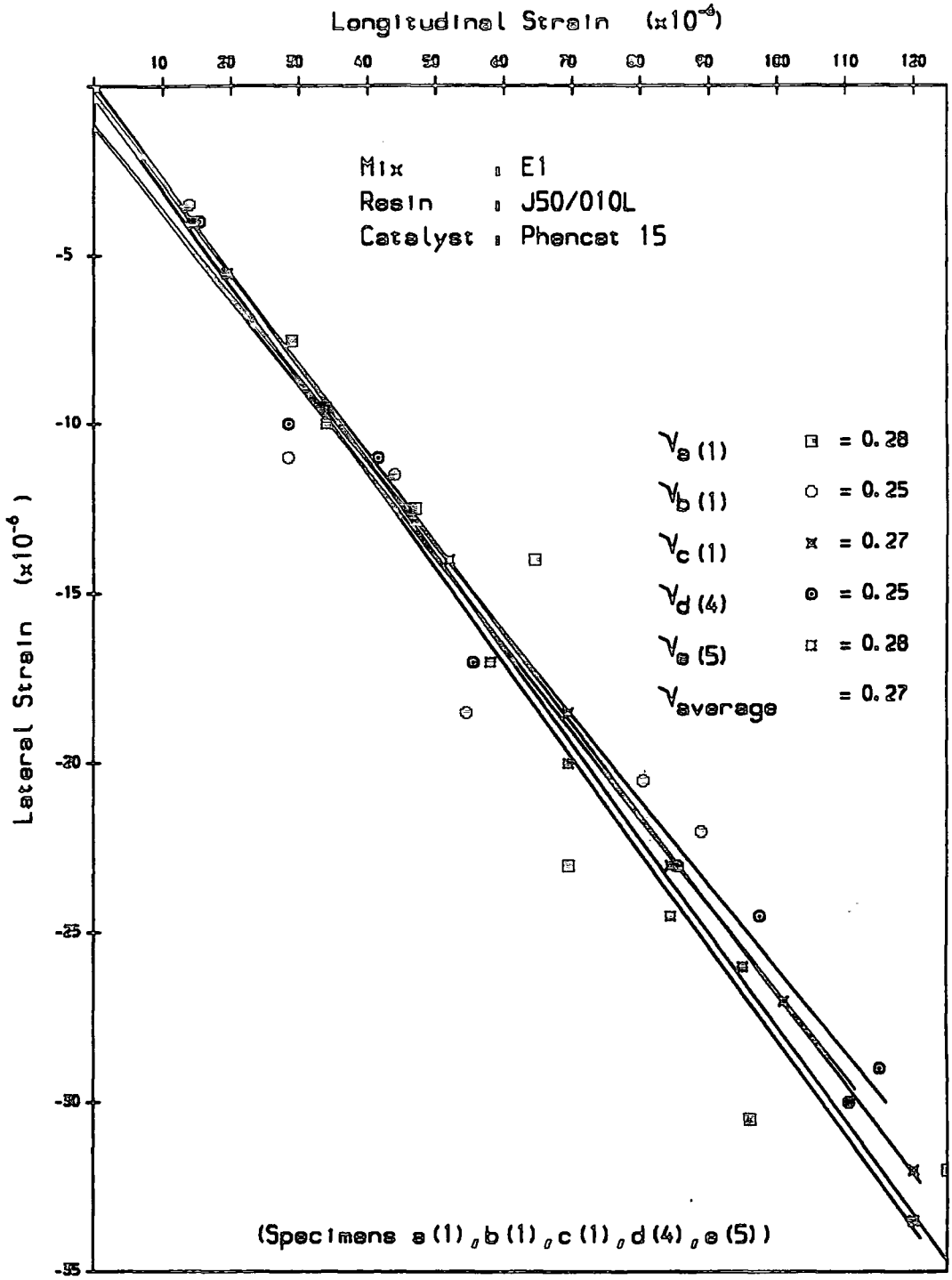

Longitudinal strains versus Lateral strains
(Measured strains from T-Bone specimens)

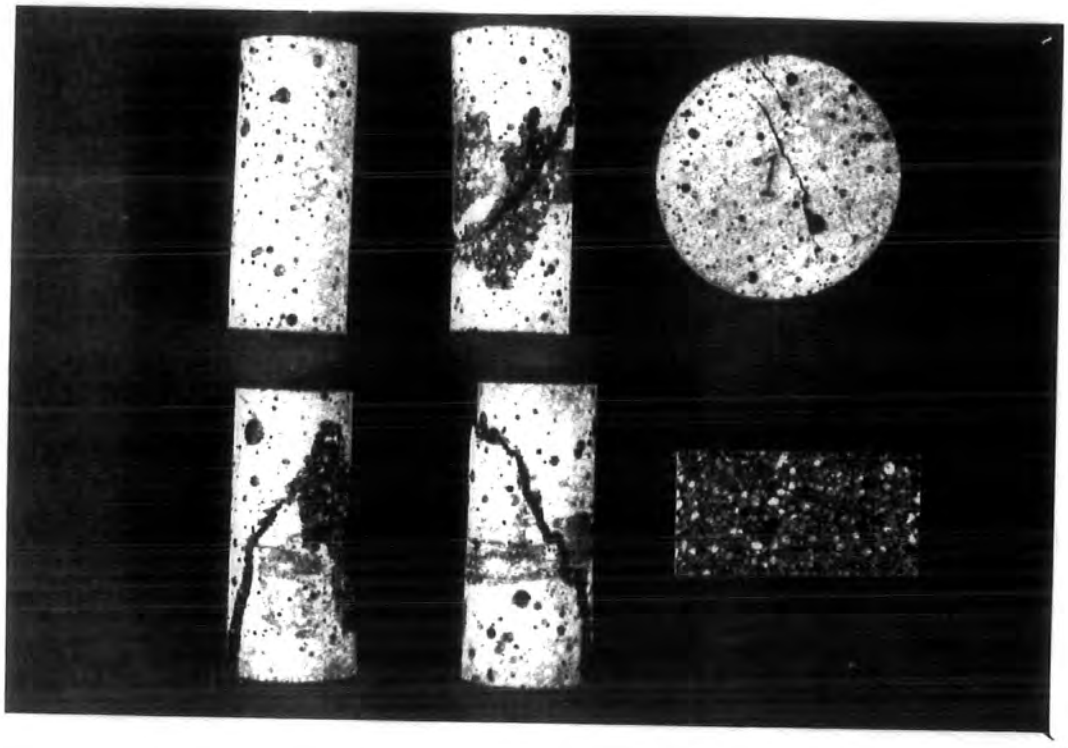

Plate 3.1 Typical phenolic resin concrete compressive cylinder and tensile disc test specimens and their plane of failure.

Chapter Four

4. Fracture Toughness of Phenolic Concrete

4.1. Introduction

In the preceding chapters, investigation of the Phenolic Concrete has concentrated on mix design with optimization of the mix matrix resin content and also on defining its macro-properties such parameters as, the type and content of fillers, the type and content of resin and its catalyst, filler/resin ratios and other parameters effecting the flexural strength and stiffness of the manufactured product.

The load versus deflection curves of the coupon specimens subject to flexural loading and also stress versus strain curves of the specimens subject to direct tensile tests, revealed the fact that the Phenolic Concrete is a brittle material and failure of components made of such material is of brittle type. In the study of the flexural strength and modulus of the Phenolic Concrete matrix, made up of the mix compositions as defined in previous chapters, large variations were originally noticed from one specimen to another. These variations, however, were to some considerable extent restrained by practising more controllable mixing, casting, setting and curing procedures.

In the mixes, the effect of polymerization at the time of mixing and casting may introduce many internal defects in the form of voids to the end product. These defects would be due to the condensation produced as a result of resin and catalyst exothermic reaction. This will, later in the process of setting and curing, form microstructure pores and void clusters which may coincide with filler grain boundaries, and thus may well be the source of brittle fracture failure of the Phenolic Concrete

products.

It was also found that the flexural strength and modulus of the Phenolic Concrete specimens were in excess of the tensile strength and modulus of the same size specimens subject to direct tensile tests. The reason is that the effective size is smaller when failure is by bending than by direct tension because only part of the specimen is subjected to tension in bending. This simply implies that more defects may be present among the greater number of defects in the full section when subjected to direct tension. Information is therefore needed about the matrix in order to relate the short term strengths of the optimum Phenolic Concrete strength (as measured from flexural or even tensile tests) to the material properties and microstructure of the operational component made from the same material.

The fracture mechanics approach provides a knowledge of the properties of the engineering material and the pertinent failure criterion for the load-bearing member made of such material. The important circumstance which justifies the application of fracture mechanics theory to engineering structures, is probably that all engineering materials contain cracks or crack-like defects and other inhomogeneities; thus the failure occurs because of crack propagation and resultant preferential bond breakage. The fracture theory developed has concentrated on these defects and in the forces which act upon them, and is applied to linear elastic brittle materials or even to common engineering materials in which plastic deformation may occur and is known as linear elastic fracture mechanics (LEFM). Since the basic tenant of fracture mechanics theory is that the strength of most real solids is governed by the presence of crack like defects, and since the theory enables the manner in which they propagate under stress to be analysed mathematically, the application of the theory to brittle material has received considerable attention. Fracture mechanics

seeks to quantify the critical combination of stress and crack size for crack extension. This governs the condition for fracture. Fracture occurs when sufficient energy is released (from the stress field) by the growth of the crack to supply the requirements of the fracture surface. The energy released comes from stored elastic or potential energy of the loading system and can, in principle, be calculated for any type of test piece. This, therefore, provides a measure of the energy required to extend a crack over unit area, and it is termed the fracture energy or strain energy release rate and is denoted by G_I. Fracture cannot take place until G_I reaches a critical value G_{IC} which equals the required energy (per unit area of crack advance), that is needed to derive the microstructural fracture processes near the crack tip. The applied load to do the work of causing the crack to travel across the specimen or structure and attain the separation, is partly measured by G_{IC}. Therefore G_I is a variable parameter derived from solid mechanics, but G_{IC} is an important property of the material and depends on the microstructure. The stress field around a crack is defined by a parameter named the stress-intensity factor, K_I, and fracture occurs when the value of K_I exceeds some critical value K_{IC}. The value of K_I is therefore a stress field parameter independent of the material whereas K_{IC}, often referred to as the fracture toughness, is a material property. It should be noted also that the plain-strain values of fracture energy or stress-intensity factor for a given mode of loading is independent of the geometry of the brittle elastic specimens employed for their evaluation. It is for this reason that these parameters become material properties.

Fracture of a component containing a defect or crack occurs in several stages. After severe local deformation at the crack tip, the first separation or initiation of fracture is followed by a period of slow stable growth and then by complete rapid separation. The period of stable growth is controlled both by the toughness of

the material and the nature of the loading system, so that in brittle material with load increase the final rapid propagation may be nearly inseparable from the first initiation.

Fracture mechanics applied to brittle materials, such as bulk ceramics, rocks and concrete, in order to characterise and understand the important parameters relating to the current fracture mechanics models, is finding an important place in predicting the failure of such important engineering materials[74–76]. The strength of most real solids is governed by the presence of flaws inherent in them. The application of fracture mechanics to structural adhesive joints (polymeric adhesive) whose failure criterion is based upon the initiation and propagation of such flaws inherent in the joint, has recently received considerable attention[77]. The theory has also been used in hostile enviroments such as high temperature which would affect the long term performance of products such as ceramics and polymers and, recently, the theory has been adopted to determine fracture toughness of some adhesive cements in high temperature ranges[78,79].

Various types of laboratory tests and experimental specimen models and procedures have been devised with regard to the materials (brittle, semi-brittle and even moderately tough) in using the theory to understand the complex problem of brittle fracture[74,80–84] and its characteristics in evaluating the relevant properties. Amongst all the available experimental techniques and test specimen models, the double-torsion specimen, with its longitudinal, crack directing centre groove, has become the most successful specimen in crack propagation in testing the brittle materials. This preference is because of its relative simplicity of fabrication and testing and also suitability for testing in high temperatures where materials such as ceramic frequently find application[78–79,84–88]. For such a geometry, the frac-

ture toughness K_{IC} and the critical strain energy release rate G_{IC} can be evaluated with no requirements for crack length measurements. In double-torsion method the strain energy release rate, G_I, does not change with crack length. The strain energy can be evaluated experimentally or mathematically[77,89]. The former can be quite a tedious method, and in the latter numerical methods in conjunction with various techniques of the elastic theory with the aid of computer can be used to calculate compliance and hence the strain energy. However, well established expressions of the strain energy release rate are now known for a large number of specimen geometries. For these reasons, therefore, the double-torsion method in applying LEFM theory has been adopted in this work to evaluate the material properties of the Phenolic Concrete as a function of its microstructure and of the microscopic processes that take place at the crack tip as the fracture begins.

4.2. Test specimens and Test Variables

Assuming a linear-elastic body, the knowledge of the rate of change of the specimen's compliance (reciprical of load/displacement) at any crack length allows the determination of the strain energy release rate and the stress intensity factor of the material. A double-torsion specimen possesses a constant rate of change of compliance with crack length. In this work, therefore, a double-torsion specimen was used which consisted of a rectangular plates with a shallow centre groove cast-in along both faces of the specimen, and containing a centre edge-notch in the form of a saw slot.

For each mix composition (see Table 4.1), three sets of specimens were made in the form of coupon geometry ($600 \times 100 \times 8\ mm^3$ thick). Each set, after being cured accordingly, was cut (using a diamond tipped rock cutter saw) into three

rectangular plates of approximately 200 × 100 × 8 mm^3 thick, bringing the total of test pieces for each test variable to nine specimens. Each specimen set was cast using Phenolic Concrete mix, as defined in Table 4.1, in a rectangular steel mould lined with mould releasing cloth (TCGC). Longitudinal thin PVC strips serving as prefabricating groove formers to the centre faces of the specimens were positioned longitudinally at the centre of the top and bottom faces of the steel mould prior to casting. The full specimen thickness was controlled to ± 1 mm by introducing spacers between the two faces of the moulds at extreme ends.

The groove formers were $1mm$ deep and $2mm$ wide positioned longitudinally at the centre faces of the moulds beneath the mould releasing lining. This made it possible to keep the geometry and position of the central face grooves constant throughout. Prefabrication of the cast-in shallow grooves served the purpose of ensuring that the crack would propagate along the specimens' axis.

The objective of this work was twofold, firstly, to furnish unambigious experimental information that compares the various strength values for the different mix formulations and mix constituents and, secondly, to obtain the material properties using the fracture mechanics theory by which one can correlate the brittle failure of the Phenolic Concrete with its microstructure.

The objectives were accomplished by designing the mix filler grading to follow the fuller grading curve for mix series E (see Table 4.1), except for mix G2 which was a gap-grading mix. The Phenolic Concrete mixes in all the test specimens were made to achive the same final 2.15 g/cm^3 bulk density. Thus by controlling the grading curve of the mix constituents (filler grading curve) for mix series E and the final density of the samples, the variables were; the resin type and its relevant catalyst, resin/filler ratio, catalyst content, resin/furfuryl alcohol ratio, micro-filler

type and its content. In mix formulation G2, a gap graded mix design was used with only resin/filler ratio and resin/furfuryl alcohol ratio as variables. The two mix formulations of series E1 (fuller grading) and G2 (gap grading) were themselves equivalently considered also as test variables. In these specimens, the resin, catalyst and furfuryl alcohol contents were maintained to correspond with the filler/resin ratios.

In mixes $E_{Ch.C.}$ and $E_{Sph.G.}$, the equivalent volumes of China Clay and Spheriglass 5000 to volume of 19.5% Silica Flour of mix E1 were used respectively.

The twenty one different combinations of the Phenolic Concrete mix compositions used in casting of the test specimens are presented in the self-explanatory Table 4.1.

4.3. Specimen Construction and Material

The matrix composition of the Phenolic Concrete double-torsion specimens used in the tests are referred to in Table 4.1, with their individual technological properties defined in Chapter 2.

The required weights of the silica sand fillers, micro fillers, phenolic resin, the relevant catalyst and furfuryl alcohol (as neccessary) for the given mix formulation were carefully weighed. The mix composition weights were based upon the requirement that all the material should achieve the same final 2.15 g/cm^3 bulk density; thus the mixes were designed for the volume necessary to achieve the desired full specimen thickness. For each test variable, the constituents were weighed to produce three specimens of $600 \times 100 \times 8$ mm^3 thickness. The measured fillers (dry weights) were mixed in a Hobart mixer for a period of five minutes to achieve approximate homogeneity. The required weight of the catalyst was then added to the mixed fillers

and mixed for a further three minutes. The catalysed filler mix temperature was constantly observed by a temperature probe in order to keep a constant temperature (for all the twenty one mixes) at the time of introducing the required resin for final mixing, and hence to avoid introducing any primary heat which may accelerate the resin/catalyst reaction of the mix matrix. This was done in order to have constant mix reaction time with respect to the corresponding catalyst levels through-out the mixes.

For casting the Phenolic Concrete mixes, three rectangular steel moulds were constructed having internal dimensions of $600 \times 100 \times 20\ mm^3$ from 10 mm thick steel plate. The four side walls and the bottom face were fixed using c/s studs and therefore could be easily dismantled at the time of demoulding the set specimens. The bottom and the top face (or lid) of the moulds were degreased and thin PVC strips ($600 \times 2 \times 1\ mm^3$ thick) positioned longitudinally at the centre of these two faces. A teflon coated glass cloth (TCGC) with silicon adhesive on one side was then glued to these faces while keeping the groove formers (PVC strips) in position. Using mould releasing (freecoat) sprays, the side walls and the coated surfaces were sprayed prior to casting.

The required weights of the Phenolic resin (either J50/010L B.P.'s resin or IR1271 Fordath's resin) with required weights of furfuryl alcohol, if necessary, were carefully weighed and mixed in a container using a glass stirrer prior to final mixing. The temperature of the resin to be used in the mixes was also monitored and kept constant at the time of mixing. The prepared resin was added to the catalysed filler mix and mixed at room temperature in the Hobart mixer for a period of two minutes until a homogeneous mix matrix was observed. Instantaneously the mix was poured into the prepared moulds and compacted with the aid of a vibrating table; and using

a premade screed the cast mix was levelled off to the required pre-marked depths. With the spacers at either ends of the moulds in position, the top face (lid) of the mould was gently placed on top of the cast matrix. By applying weights to the top of the lid, pressure was applied to the cast mix in order to assist the setting, which also helped the excess mix to be squeezed out through the side gaps while helping the densification of the Phenolic Concrete.

A period of 24 hours was allowed for setting of the specimens subject to pressure at room temperature, except for mixes with 4% catalyst content. Setting of the latter mixes were subject to both heat and pressure by placing the moulds in the oven at $80 \pm 5°C$ for a period of two hours. This was done in order to assist the condensation reaction and also to ensure crosslinking of the matrix.

The moulds were stripped off at the end of the 24 hour period and the set specimens were placed in the oven at $120 \pm 5°C$ for a period of two hours for final curing to complete. After the cured samples had been removed from the oven and reached room temperature, each was correctly marked and cut into three almost equal rectangular plates of approximately $198 \times 100 \times 8\ mm^3$ thickness, using a diamond tipped rock saw cutter.

The specimens were constructed in the manner explained with the constant pressure (weights) applied to the cast mixes during their setting. This assisted the densification of the mixes to some extent in ensuring that the final Phenolic Concrete densities would be over a common range. However, samples were taken from the tested double torsion specimens to obtain their actual densities using a submerged weight in water method. The average results of densities for corresponding Phenolic Concrete specimens are tabulated in Table 4.2. In this table, are also given the relevant observed mix workabilities at the time of casting. As seen from Table 4.2, a

common density range was achieved, except for lower filler/resin ratio (4:1 and 5:1) mixes, as would have been expected.

Phenolic Concrete specimens of similar mix formulation and similar construction procedures to double torsion specimens were prepared for both flexural and direct tensile testing, details of which are referred to in previous chapter. The summary of the results obtained from these tests with regard to strength and modulus values of the specimens constructed from the relevant mix formulation are also presented in Table 4.2.

Surface topography of samples taken from fractured sections of the flexural specimens was studied using the Scanning Electron Microscop (ESM) technique. Sample SEM images are provided in Plates 4.1, 4.2 and 4.3. As a result of the construction process the Phenolic Concrete fracture surface exhibits a 'contiguous' structure with no apparant particle boundaries (see Plate 4.3). The voids in the matrix are well rounded having sizes approximately equal the size of the micro filler particles as can be seen from these images. Also from Plate 4.2 it can be seen that resin/filler interface seems to have developed perfect bond. At the fractured surface, sand particles have fractured with no bond breakage, thus suggesting the sand grains cracked right through, with crack propagation through the composite matrix.

4.4. Specimen preparation

To determine the strength of a brittle material, if a small strip is used it would show a larger strength than if a larger sample was tested. This is due to the fact that the strength in brittle materials is controlled by crack development and crack propagation. It is therefore possible to measure the strength and crack development for a given loading in order to relate these two properties to define the real strength

of the material of the element. It therefore becomes neccessary to prepare a specimen which would simulate the above state of material.

Rectangular plates of approximately $200 \times 100 \times 8\ mm^3$ thickness, as explained in the previous section, were prepared for use in double-torsion tests. The plates contained shallow cast in grooves on either face in order to ensure that the crack propagates centrally along the plate axis. The provision of a centre slot has been in some cases argued as not quite well understood as to what other effects it may entail. Therefore, a modified double torsion method, totally avoiding the centre edge slot and centre groove and instead providing only an edge notch has been devised[84] and successfully used in determining the characteristic properties of the monolithic ceramics at elevated temperatures. In this work, however, as a result of unsatisfactory precracking of the double-torsion specimens initially having only one cast-in groove on the lower centre face, grooves were introduced on both faces with a centre edge slot. This resulted in satisfactory and more stable precracking using an indentation technique along the specimen centre axis.

At one end of the double-torsion specimens, at centre edge, a crack starter notch ($15\ mm$) in the form of a slot, was introduced using a diamond tipped circular saw (cutting wheel). The details of this are shown schematically in Figure 4.1. As this does not in effect represent a real natural crack in the specimen, therefore, precracking was required. It has been shown[78,79] that precracking prior to testing is neccessary in order to obtain valid G_{IC} values, otherwise the deduced values could be overestimated. Also in double torsion specimens, it has been shown that the stress intensity factor, K_I, at the crack tip is independent of crack length[77–79,85,86] and thus the specimen possesses linear compliance (reciprocal of load/displacement).

Precracking was achieved by using a wedge-indentation technique[78,79,90]. The

major advantage of this technique is that it produces stable precracks with crack tips that are sharp and stress-free. It has been shown[90] that the factors governing the stability of cracks formed by this technique appear to be:, the fracture toughness of the indented material, the apex angle of the indenter, the applied load, and possibly the elastic properties and coefficient of friction of the indenter material.

A steel wedge of 30° angle was slowly penetrated into the saw cut notch at the end of the double torsion samples in a vertical direction, as shown in Figure 4.2 and Plate 4.4. This was performed under constant crosshead displacement speed of the Instron 1195 testing machine, with rate of loading being monitered on an X-Y plotter which recorded the values of load as a function of penetration displacement in response to the wedge-indenter. The load applied to the wedge was stopped as soon as a load drop was detected. This indicated the initiation of a precrack. At the same time, the precracking was optically monitered using a magnifying glass. For this purpose, the centre grooves were painted white prior to precracking.

4.5. Double-Torsion Apparatus and Test Procedure

The double-torsion Phenolic Concrete test specimen and its loading geometry are illustrated in Figure 4.3 and shown in Plate 4.5. The rectangular pre-cracked specimen was supported on two parallel steel rollers. The steel rollers were 90 *mm* center to center, 200 *mm* long sitting on two longitudinal grooves of a 20 *mm* thick bottom supporting steel plate. The steel plate was resting immediately above the compression load cell of the Instron 1195 testing machine. The loading was transmitted via two parallel 35 *mm* wide by 50 *mm* high vertical steel plates of 10 *mm* thickness, positioned at 19 *mm* centre to centre. These were semi-circular at their lower ends at the point of contact with the specimen, having a radius of

5 mm, with their top ends being attached to the upper plate, at the centre top face of which a steel sphere was positioned in a semi-spherical nest. Immediately above the steel sphere bearing was the secondary top steel plate which was connected to the bottom face of the Instron crosshead. The schematic arrangement of the double-torsion apparatus is illustrated in Figure 4.4.

The double-torsion apparatus was loaded in the Instron 1195 testing machine at a crosshead speed of $2mm/min$. The vertically applied load was transmited to the double-torsion apparatus through the nested frictionless steel sphere bearing. The load versus displacement of the crosshead was recorded directly on the X-Y plotter (as shown in Plate 4.6). The load and the displacement could be read to the nearest $2.5N$ and 0.005 mm respectively.

4.6. Results and Discussion

A total of 189 precracked specimens were tested in double-torsion, with nine specimens representing each composite Phenolic Concrete matrix. From these, some were rejected, either due to the specimen containing apparent surface defects as a result of casting, and/or their calculated fracture energy G_{IC} values, which are partly a measure of the load to cause crack propagation, differed by more than $\pm 10\%$ in the relevant group results. The geometrical dimensions of the double-torsion specimens were measured using a vernier and a micrometer. The test results, geometrical dimensions and the calculated fracture energy "G_{IC}", fracture toughness "K_{IC}" and the defect size "a" of the Phenolic Concrete specimens are presented in Tables 4.3 to 4.8.

The load-displacement curves of the precracked double-torsion specimens, which were recorded instantaneously during the tests on the X-Y plotter of the Instron

1195, exhibited a brittle crack propagation. At maximum loads the curves became almost flat, for specimens made of low filler/resin ratio, with increasing displacement at a constant load. As the filler/resin ratios in the specimens increased the corresponging curves at maximum loads gradually changed from flat to stick-slip type. This behaviour is typical of a brittle crack propagation which occurs at a constant load with rate of crack propagation being dependent upon the rate of crosshead displacement.

The failure of the specimens occurred with a sudden drop in load followed by complete separation i.e. the specimen splitting in two through its centre axis (see Plate 4.7). The precrack in low filler/resin ratio Phenolic Concrete had propagated centrally along the specimen axis with no apparent crack arresting. This type of crack propagation is known as 'stable' crack growth. With high filler/resin ratios the crack propagation changed from 'stable' to 'unstable' crack growth exhibiting crack initiation and arrest. In the specimens with low filler/resin ratios the higher resin content possibly allows the crack to propagate and pass around the grains through the resin matrix continuously at constant maximum load. However, in specimens with higher filler contents with increase in strain energy crack propagation may well pass through the larger filler grains. Sample load-displacement traces representing the typical recorded curves for specimens with various filler/resin ratios and also with various micro-fillers are presented in Figures 4.6 to 4.12. From these figures it can be seen that at maximum loads, the curves oscillate. The average of the load values at maximum and minimum oscillations is considered as the maximum load P_{max} to have caused failure of the specimens.

In measuring the fracture toughness of a material several successful techniques have been devised in introducing naturally sharp precracks into the specimen. The

importance of crack tip sharpness with regard to the developed component stresses ahead of the crack tip has been established in brittle materials.

Fracture toughness measurement in brittle materials relies mostly on linear compliance design. The geometry of the double-torsion specimens which are used in this work possesses linear compliance. It has been shown[78,79] that with precracking introduced to double-torsion specimens a valid G_{IC} value can be expected providing that the crack tip is in the region where the rate of change of compliance with crack length is linear. Therefore, to ensure the crack tip to be in the critical region, and at the same time to achieve crack tip sharpness, a starter crack of $15mm$ in the specimens was employed which assisted precracking using a wedge-indentation technique.

Phenolic Concrete fracture toughness K_{IC} for plain-strain value was calculated using the following expression[77,89]:

$$K_{IC}{}^2 = \frac{E.G_{IC}}{(1-\nu^2)}$$

In which G_{IC} is the fracture energy, and was calculated using the following expression[77,89]:

$$G_{IC} = \frac{P_{max}^2}{2D}.\frac{(1+\nu)}{E}.\frac{S^2}{ZWD^3}$$

where,

P_{max} is the maximum load to cause propagated crack to break the DT specimen in two.

D is the full specimen thickness.

$2W$ is the specimen total width.

S is the distance between the loading point and the support roller.

Z is a function of W/D ratio[89,91].

E is the Young's mdulus.

ν is the Poisson's ratio.

In the specimens of Table 4.3, in which the samples were cast using $J50/010L$, B.P.'s resin, the value of fracture energy increases with the filler/resin ratio. These values are in good correlation with those of the specimens cast using $IR1271$ Fordath's resin (see Table 4.7). It is thought that the reason for the increase in the G_{IC} values of the specimens is that as the crack propagates forward from the crack tip there are more filler grains as the filler content increases. Thus, more work is needed to propagate the crack through the stiffer filler grains. The examination of the SEM images of the fractured surface showed that at the apparent fracture the crack propagates right through the sand grains (see Plate 4.1). This therefore causes higher stress concentration at crack tip with larger strain energy stored in the filler grains as filler content increases. At the same time with increase in filler/resin ratios (see Table 4.3 and 4.7) the fracture toughness values of these specimens increases. The increases in G_{IC} and K_{IC} values of the specimens with increase in filler/resin ratios are presented graphically in Figure 4.5. From this figure it may be seen that the pattern of increase in G_{IC} values with increase in filler content of both resin composites is similar whereas this is not so for their K_{IC} values. This may be as a result of using one value of Young's modulus in the $IR1271$ resin composite. It is evident from Table 4.2 that the modulus values of the $J50/010L$ resin composites increase with increase in filler content.

Considering the acid catalyst content (Table 4.4), there is an increase in both G_{IC} and K_{IC} values of the specimens as the catalyst content of the composition increases. This may be due to the fact that the resin matrix in the process of polymerization which is exothermic produces a greater rate and quantity of con-

densation with increase in catalyst level, thus producing (as seen from earlier work) more spherical voids, and at the same time the matrix inhibits stronger and larger crosslinks. From early work on Phenolic resins using the SEM technique it was found that specimens made from the resin matrix with low catalyst content have defects in the form of striation and with increase in catalyst content these striations disappear, but the number of spherical micro voids increases. The increase in acid level will in effect increase the fracture toughnes of the filled resin matrix. These spherical micro voids (see Plate 4.2 and 4.3) may arrest the crack tip and therefore the crack may indeed require higher stresses for it to propagate.

Table 4.5, shows the G_{IC} and K_{IC} values determined for the specimens with different micro filler content, but of similar mix formulation. There is a little evidence to show that Silica Flour has a superior effect on the fracture toughness of the Phenolic Concrete as opposed to the other micro fillers of different chemistry but compatiblity. However, the K_{IC} value of the material depends on the microstructural feature and is generaly insensitive to the chemical properties of the surrounding environment.

In Table 4.6, the micro filler content (Silica Flour) in the mix composition seems to have a significant effect on the fracture toughness of the Phenolic Concrete. This was also found from the flexural tests (see Chapter 3) with regard to the strength and the stiffness values. At 19.5% S.F. content, the filler mix grading curve follows the Fuller grading curve and hence provides a more uniformly packed (i.e. more homogeneous) filler in the matrix. Above or below this level (see Table 4.6) the composite fracture toughness value decreases. Therefore, the mix/filler grading to satisfy the Fuller grading specification seems to be the optimum design in attaining optimum fracture toughness of the composite.

The fracture toughness of the gap-graded specimens (see Table 4.8), is lower than the values for similar specimens constructed using the Fuller grading mix design (Tables 4.3 and 4.7). This may in effect be as a result of less homogeneous filler packing than in the latter mix. It has been shown[82] that in concrete, the larger the grain sizes the higher is the value of fracture energy, and the fracture toughness increases with increase in the lower range of grain sizes, with no significant increase with increase in the larger grain sizes. However, with graphite, it has been shown[83] that as its mode of failure excludes its implicit description as a linear brittle material, its crack growth is independent of particle size, while its total fracture strain increases with reduced particle size. In the gap-grading mixes reported in this work the larger sand grains (i.e. passing 2.4 mm B.S. sieve) are not present, as they are in Fuller grading mixes. It may therefore be valid to assume that the lower toughness values in the specimens made of this composite are due to larger grain size exclusion. At a mix ratio of 7:1 of the gap-grading mix (see Table 4.8) the fracture toughness value has decreased. It is reasonable to suppose that this is due to insufficency of resin to fill the intersticial voids between the larger particles, resulting in the development of 'star-voids', with resulting stress enhancement.

For all the double-torsion specimens from their average fracture toughness values, the sizes of the possible defects in the matrix of the Phenolic Concrete were calculated using the following expression[77,89]:

$$K_{IC} = \psi\sigma\sqrt{\pi.a}$$

where,

σ is the nominal stress (here it is considered as the flexural strength obtained from coupon specimens).

a is the defect size.

ψ is the dimensionless factor that depends on the shape of the specimen[89].

The calculated defect size in all the specimens made from Fuller grading mixes (see Tables 4.3 to 4.8), falls below the maximum grain size (i.e. maximum size passing B.S. seive 2.4 mm) available in the composite matrix of the Phenolic Concrete. This suggests that the mix and casting processes have been successfully controlled and no defects other than those associated with the filler grains (sands) themselves are present in the composite. However, the calculated defect sizes in the specimens constructed from the gap-grading mixes seems to be some-what larger than the maximum sand grains present in the matrix (i.e. maximum size passing B.S. seive 1.2 mm). Therefore, using a gap-grading mix may prevent the production of a homogeneous Phenolic Concrete which may cause a reduction in fracture toughness of the matrix.

4.7. Conclusion

The use of double-torsion specimens having centre face shallow grooves has been successfully used in determining the fracture energy G_{IC} and the fracture toughness K_{IC} values of the Phenolic Concrete. It was found that the fracture toughness of Phenolic Concrete will be in the range of $1.8 - 2.2\ MNm^{-3/2}$ with the fracture energy as high as $220\ J.m^{-2}$. The fracture toughness and fracture energy of the Phenolic Concrete obtained from the preceding tests were compared with the values of some engineering materials given in reference [80]. It was found that the Phenolic Concrete is tougher and stiffer than ordinary portland cement concrete and is equally as tough as polyester concrete.

The fracture energy G_{IC} appears to be affected by filler/resin ratio. The higher the ratio, the higher the values of the fracture energy. This shows that the increase

of work was used to propagate the crack right through the filler grains.

Precracking using the wedge-indentation technique can be successfully introduced to the Phenolic Concrete double-torsion specimen with a crack starter as a centre edge saw cut slot. This technique provided a sharp precrack tip which, under double-torsion loading, propagated along the specimen axis with 'brittle' crack propagation.

In designing a Phenolic Concrete mix references can be made to the microstructures of the Phenolic Concrete with the microscopic changes that can occur at the crack tip. It was shown that the Fuller grading mix design, provides an optimum mix which would result in higher fracture toughness values of the Phenolic Concrete. A comparison of this type of mix to a gap-grading mix suggested that in the latter defects are evident and that they would result in a less tough Phenolic Concrete. The type of resin would have no significant effect on the fracture toughness as would be the case with any compatible micro filler. The level at which the acid catalyst can be used in Phenolic Concrete is dictated by the mix and casting process, the type of catalyst and the temperature. From the double-torsion tests it became clear that increase in catalyst level would have, to some degree, the effect of improving the material properties of the composite Phenolic Concrete matrix.

Table 4.1 (Mix-Composition of the speciemens used in Double-Torsion Tests.)

Mix	Filler Formulation					Resin Type	Catalyst	Resin: Filler Ratio	Resin: Furfuryl Ratio
	Sand(A1)	Sand(B1)	Sand(C1)	Sand(D1)	Micro Filler				
E1	36.80%	16.00%	15.70%	12.00%	S.F. @ 19.5%	J50/010L (B.P.)	Phencat 15 @ 8%	4:1 5:1 6:1 7:1 8:1	.... 80:20 60:40
E1	36.80%	16.00%	15.70%	12.00%	S.F. @ 19.5%	J50/010L (B.P.)	Phencat 15 @ 4% @ 6% @ 10%	6:1	....
E3	38.86%	16.89%	16.58%	12.67%	S.F. @ 15%	J50/010L (B.P.)	Phencat 15 @ 8%	6:1	....
E4	34.29%	14.90%	14.63%	11.18%	S.F. @ 25%	J50/010L (B.P.)	Phencat 15 @ 8%	6:1	....
$E_{Ch.C.}$	36.80%	16.00%	15.70%	12.00%	** Ch.C. @ 19.5%S.F.	J50/010L (B.P.)	Phencat 15 @ 8%	6:1	....
$E_{Sph.G.}$	36.80%	16.00%	15.70%	12.00%	** Sph.G. @ 19.5%S.F.	J50/010L (B.P.)	Phencat 15 @ 8%	6:1	....
E1	36.80%	16.00%	15.70%	12.00%	S.F. @ 19.5%	IR1271 (Fordath)	CS-30 @ 8%	4:1 5:1 6:1 7:1 8:1	.... 80:20 60:40
G2	.....	64.00%	.....	11.00%	S.F. @ 25.0%	J50/010L B.P.	Phencat 15 @ 8%	4:1 5:1 6:1 7:1	.... 80:20

Note:

S.F.= Silica Flour L.G.3/300 Ch.C.= English China Clay (D) Sph.G.= Spheriglass 5000

** equivalent volumes of Ch.C. and Sph.G. 5000 to volume of 19.5% S.F. are used in the Mix

Casting: Cold Mould subject to vibration .

Setting: 24 Hrs. @ R.T.(15 – 20°C), subject to "Pressure" and for those with 4% Catalyst setting was acomplished subject to both "Heat and Pressure".

Curing : 2 Hrs. in oven @ 120°C.

Table 4.2 (Properties of the speciemens used in Double-Torsion Tests.)

Mix	Mix Composition				Workability	Density	Flexural Test		Tensile Test	
	Resin Type	Catalyst	Resin: Filler ratio	Resin: Furfuryl ratio		(g/cm^3)	Strength $\sigma_{UF} \times 10^6$ (N/m^2)	Modulus $E_F \times 10^9$ (N/m^2)	Strength $\sigma_{UT} \times 10^6$ (N/m^2)	Modulus $E_T \times 10^9$ (N/m^2)
E1	J50/010L (B.P.)	Phencat 15 @ 8%	4:1	.....	V.W.	2.09	22.10	23.89	5.90	14.775
			5:1	.....	V.W.	2.12	24.89	25.12	6.14	16.258
			6:1	.....	W.	2.14	25.10	25.87	6.98	17.115
			7:1	80:20	W.	2.19	29.25	27.46	7.67	18.717
			8:1	60:40	W.	2.22	30.51	28.92	7.85	19.642
E1	J50/010L (B.P.)	Phencat 15	6:1	.....						
		@ 4%		.....	W.	2.15	23.85	24.45	5.59	15.636
		@ 6%		.....	W.	2.13	21.25	23.52	6.14	16.436
		@ 10%		.....	W.	2.14	27.68	28.77	7.67	18.696
E3	J50/010L (B.P.)	Phencat 15 @ 8%	6:1	....	V.W.	2.10	21.70	22.15	4.70	14.540
E4	J50/010L (B.P.)	Phencat 15 @ 8%	6:1	....	W.	2.17	22.68	23.98	5.41	15.259
$E_{Ch.C.}$	J50/010L (B.P.)	Phencat 15 @ 8%	6:1	....	W.	2.12	24.29	23.99	7.02	17.113
$E_{Sph.G.}$	J50/010L (B.P.)	Phencat 15 @ 8%	6:1	....	W.	2.15	25.72	26.02	7.19	17.116
E1	IR1271 (Fordath)	CS-30 @ 8%	4:1	.....	V.W.	2.05	22.18	23.39	....	.....
			5:1	.....	V.W.	2.11	23.40	24.57	6.65	16.670
			6:1	.....	V.W.	2.14	25.57	27.89	7.10	16.880
			7:1	80:20	W.	2.16	28.62	29.40	....	.....
			8:1	60:40	W.	2.20	31.40	32.40	....	.....
G2	J50/010L B.P.	Phencat 15 @ 8%	4:1	.....	V.W.	2.08	21.32	24.55	....	.....
			5:1	.....	V.W.	2.10	22.61	24.62	....	.....
			6:1	.....	V.W.	2.13	24.74	25.68	5.85	14.940
			7:1	.....	V.W.	2.15	26.48	27.85	5.88	15.560

Note:

V.W.= very workable, self-leveling with the aid of tapping on the mould and use of screed.

W.= workable, levels with the aid of small vibration and use of screed.

Table 4.3 (Filler/Resin Ratio Effect)

Mix Ratio	Sample	(Dimensions) L (mm)	D (mm)	Z=f(W/D) W/D	Z	Failure Load P_{max} (N)	Fracture Energy G_{IC} ($J.m^{-2}$)		Stress-Intensity Factor K_{IC} ($MN.m^{-3/2}$)		Defect Size a (mm)
4:1	a	200.75	8.11	6.17	0.296	470.0	186.9	Av.	1.7		
	b	197.00	8.02	6.23	0.296	442.5	173.2	180.7	1.7	Av.	
	c	204.50	7.63	6.55	0.298	400.0	171.6		1.7	1.70	1.88
	d	194.75	7.80	6.41	0.297	427.5	180.1	s.d.	1.7		
	e	200.25	7.90	6.33	0.297	447.5	187.5	±7.0	1.7		
	f	195.00	8.13	6.15	0.296	470.0	185.0		1.7		
5:1	a	202.00	8.03	6.23	0.296	490.0	192.1	Av.	1.8		
	b	197.00	8.49	5.89	0.295	520.0	173.7	187.2	1.7	Av.	
	c	196.00	8.01	6.24	0.296	470.0	196.4		1.9	1.82	1.70
	d	198.00	8.18	6.11	0.296	500.0	184.7	s.d.	1.8		
	e	198.00	8.44	5.92	0.295	520.0	177.8	±10.2	1.8		
	f	201.00	8.08	6.19	0.296	505.0	198.6		1.9		
6:1	a	194.00	7.99	6.26	0.296	508.0	199.9	Av.	1.9		
	b	200.50	7.92	6.31	0.297	495.0	196.1	197.0	1.9	Av.	
	c	201.50	7.63	6.55	0.298	460.0	195.9		1.9	1.90	1.82
	d	199.75	8.03	6.23	0.296	510.0	197.6	s.d.	1.9		
	e	199.50	8.00	6.25	0.296	500.0	192.8	±2.6	1.9		
	f	200.75	8.05	6.21	0.296	515.0	199.5		1.9		
7:1	a	198.50	8.63	5.79	0.294	625.0	204.8	Av.	2.0		
	b	201.50	8.51	5.88	0.295	630.0	219.4	211.9	2.1	Av.	
	c	196.75	8.13	6.15	0.296	563.5	210.0		2.1	2.08	1.61
	d	200.75	8.42	5.94	0.295	610.0	214.6	s.d.	2.1		
	e	200.50	8.59	5.82	0.294	630.0	212.0	±4.9	2.1		
	f	195.00	8.57	5.83	0.294	625.0	210.6		2.1		
8:1	a	202.00	8.51	5.88	0.295	620.0	202.5	Av.	2.1		
	b	198.00	8.60	5.81	0.294	677.0	232.2	213.6	2.2	Av.	
	c	195.5	8.50	5.88	0.295	632.0	211.4		2.1	2.12	1.54
	d	198.00	8.40	5.95	0.295	620.0	213.3	s.d.	2.1		
	e	198.00	8.55	5.85	0.295	640.0	211.7	±9.9	2.1		
	f	197.50	8.57	5.83	0.294	640.0	210.5		2.1		

Note:

2W = 100.0 (mm)

S = 35.5 (mm)

E = refer to Table 4.2.

Poisson's Ratio =0.27

Resin : J50/010L (B.P.)

Catalyst: Phencat 15

Mix Formulation: E1

Maximum load P_{max} is deduced from the average loads recorded at failure (i.e. average of the maximum and minimum oscillation points on x-y plotter at failure).

Table 4.4 (Catalyst Content Effect)

Catalyst Content (%)	Sample	(Dimensions) L (mm)	D (mm)	Z=f(W/D) W/D	Z	Failure Load P_{max} (N)	Fracture Energy G_{IC} (J.m^{-2})		Stress-Intensity Factor K_{IC} (MN.m$^{-3/2}$)		Defect Size a (mm)
4	a	198.00	8.47	5.90	0.295	500.0	168.6	Av.	1.7		
	b	192.00	8.19	6.11	0.296	452.0	157.0	156.6	1.6	Av.	
	c	199.00	8.47	5.90	0.295	465.0	145.8	s.d.	1.5	1.60	1.43
	d	198.00	8.20	6.10	0.296	450.0	154.9	±9.4	1.6		
6	a	195.75	8.70	5.75	0.294	540.0	168.6	Av.	1.7		
	b	196.75	8.75	5.71	0.294	530.0	158.8	162.8	1.7	Av.	
	c	195.00	8.69	5.75	0.294	522.0	158.3	s.d.	1.7	1.68	2.00
	d	195.00	9.09	5.50	0.293	560.0	152.7	±8.1	1.6		
	e	196.25	8.85	5.65	0.294	550.0	163.3		1.7		
	f	198.75	8.49	5.89	0.295	525.0	175.2		1.7		
8	a	194.00	7.99	6.26	0.296	508.0	199.9	Av.	1.9		
	b	200.50	7.92	6.31	0.297	495.0	196.1	197.0	1.9	Av.	
	c	201.50	7.63	6.55	0.298	460.0	195.9	s.d.	1.9	1.90	1.82
	d	199.75	8.03	6.23	0.296	510.0	197.6	±2.6	1.9		
	e	199.50	8.00	6.25	0.296	500.0	192.8		1.9		
	f	200.75	8.05	6.21	0.296	515.0	199.5		1.9		
10	a	200.25	8.57	5.83	0.294	620.0	207.5	Av.	2.0		
	b	198.75	8.89	5.62	0.294	665.0	206.2	203.2	2.0	Av.	
	c	201.75	8.45	5.92	0.295	600.0	204.9	s.d.	2.0	2.0	1.66
	d	195.75	8.87	5.64	0.294	650.0	198.8	±7.8	2.0		
	e	199.50	9.06	5.52	0.293	690.0	206.5		2.0		
	f	198.75	9.02	5.54	0.293	665.0	195.2		2.0		

Note:

2W = 100.0 (mm)

S = 35.5 (mm)

E = refer to Table 4.2.

Poisson's Ratio =0.27

Mix Ratio: 6:1

Resin : J50/010L (B.P.)

Catalyst : Phencat 15

Mix Formulation: E1

Maximum load P_{max} is deduced from the average loads recorded at failure (i.e. average of the maximum and minimum oscillation points on x-y plotter at failure).

Table 4.5 (Micro-Filler Type)

Micro Filler Type	Sample	(Dimensions) L (mm)	D (mm)	Z=f(W/D) W/D	Z	Failure Load P_{max} (N)	Fracture Energy G_{IC} ($J.m^{-2}$)		Stress-Intensity Factor K_{IC} ($MN.m^{-3/2}$)		Defect Size a (mm)
China Clay (D)	a	193.50	8.06	6.20	0.296	520.0	202.4	Av.	1.9		
	b	205.50	7.94	6.30	0.296	500.0	198.7	200.8	1.9	Av.	
	c	191.00	8.38	5.97	0.295	540.0	187.4		1.9	1.92	2.05
	d	194.75	8.42	5.94	0.295	565.0	201.3	s.d.	1.9		
	e	200.25	8.22	6.08	0.296	540.0	201.8	±8.3	1.9		
	f	195.00	8.07	6.20	0.296	535.0	213.2		2.0		
Spheri Glass 5000	a	200.00	7.65	6.54	0.293	470.0	205.9	Av.	1.9		
	b	198.75	7.69	6.50	0.297	485.0	211.8	210.3	2.0	Av.	
	c	192.25	7.33	6.82	0.299	450.0	219.4		2.0	1.97	1.98
	d	198.00	7.56	6.61	0.298	455.0	198.9	s.d.	1.9		
	e	198.00	7.64	6.54	0.297	485.0	217.4	±7.6	2.0		
	f	201.00	7.68	6.51	0.297	480.0	208.5		2.0		
Silica Flour L.G.3 /300	a	194.00	7.99	6.26	0.296	508.0	199.9	Av.	1.9		
	b	200.50	7.92	6.31	0.297	495.0	196.1	197.0	1.9	Av.	
	c	201.50	7.63	6.55	0.298	460.0	195.9		1.9	1.90	1.82
	d	199.75	8.03	6.23	0.296	510.0	197.6	s.d.	1.9		
	e	199.50	8.00	6.25	0.296	500.0	192.8	±2.6	1.9		
	f	200.75	8.05	6.21	0.296	515.0	199.5		1.9		

Table 4.6 (Micro-Filler Content Effect)

Micro Filler Content	Sample	(Dimensions) L (mm)	D (mm)	Z=f(W/D) W/D	Z	Failure Load P_{max} (N)	Fracture Energy G_{IC} ($J.m^{-2}$)		Stress-Intensity Factor K_{IC} ($MN.m^{-3/2}$)		Defect Size a (mm)
Silica Flour @ 15%	a	197.00	9.18	5.45	0.293	530.0	126.2	Av.	1.4		
	b	196.00	8.71	5.74	0.294	495.0	135.4	137.7	1.5	Av.	
	c	198.00	8.79	5.69	0.294	525.0	146.9		1.5	1.48	1.48
	d	196.00	8.53	5.86	0.295	480.0	138.0	s.d.	1.5		
	e	194.50	8.95	5.59	0.293	530.0	139.7	±6.8	1.5		
	f	196.00	8.85	5.65	0.294	520.0	140.2		1.5		
Silica Flour @ 19.5%	a	194.00	7.99	6.26	0.296	508.0	199.9	Av.	1.9		
	b	200.50	7.92	6.31	0.297	495.0	196.1	197.0	1.9	Av.	
	c	201.50	7.63	6.55	0.298	460.0	195.9		1.9	1.90	1.82
	d	199.75	8.03	6.23	0.296	510.0	197.6	s.d.	1.9		
	e	199.50	8.00	6.25	0.296	500.0	192.8	±2.6	1.9		
	f	200.75	8.05	6.21	0.296	515.0	199.5		1.9		
Silica Flour @ 25%	a	202.50	9.20	5.43	0.293	540.0	129.9	Av.	1.5		
	b	192.00	9.55	5.24	0.292	555.0	118.6	128.8	1.4	Av.	
	c	191.00	9.08	5.51	0.293	530.0	131.9		1.5	1.47	1.34
	d	200.00	8.76	5.71	0.294	505.0	137.8	s.d.	1.5		
	e	200.75	9.30	5.38	0.293	550.0	129.1	±6.5	1.5		
	f	199.55	9.24	5.41	0.293	535.0	125.3		1.4		

Note:

2W = 100.0 (mm)

S = 35.5 (mm)

E = refer to Table 4.2.

Poisson's Ratio =0.27

Mix Ratio: 6:1

Resin : J50/010L (B.P.)

Catalyst : Phencat 15

Mix Formulation: refer to Table 3.7.1

Maximum load P_{max} is deduced from the average loads recorded at failure (i.e. average of the maximum and minimum oscillation points on x-y plotter at failure).

Table 4.7 (Filler/Resin Ratio Effect)

Mix Ratio	Sample	(Dimensions) L (mm)	D (mm)	Z=f(W/D) W/D	Z	Failure Load P_{max} (N)	Fracture Energy G_{IC} (J.m^{-2})		Stress-Intensity Factor K_{IC} (MN.m$^{-3/2}$)		Defect Size a (mm)
4:1	a	198.75	7.96	6.28	0.296	495.0	196.7	Av.	1.9		
	b	199.00	8.12	6.16	0.296	505.0	189.1	187.8	1.8	Av.	
	c	199.50	8.04	6.22	0.296	495.0	189.0		1.8	1.82	2.14
	d	198.75	8.10	6.17	0.296	497.5	185.3	s.d.	1.8		
	e	199.25	8.02	6.23	0.296	490.0	187.1	±5.6	1.8		
	f	198.00	7.98	6.27	0.296	480.0	179.5		1.8		
5:1	a	199.75	8.24	6.07	0.295	520.0	189.7	Av.	1.9		
	b	198.00	8.15	6.13	0.296	510.0	190.0	191.7	1.9	Av.	
	c	200.25	8.16	6.13	0.296	500.0	181.7		1.8	1.87	2.03
	d	199.50	7.96	6.28	0.296	485.0	188.9	s.d.	1.8		
	e	200.00	7.88	6.35	0.297	500.0	208.3	±8.8	1.9		
	f	199.00	7.97	6.27	0.296	490.0	191.8		1.9		
6:1	a	198.75	8.03	6.23	0.296	505.0	197.7	Av.	1.9		
	b	199.50	8.11	6.17	0.296	505.0	190.0	201.7	1.9	Av.	
	c	198.50	8.21	6.09	0.296	550.0	214.6		2.0	1.92	1.80
	d	198.75	8.25	6.06	0.295	540.0	203.6	s.d.	1.9		
	e	198.50	8.09	6.18	0.296	520.0	203.5	±8.1	1.9		
	f	197.75	8.12	6.16	0.296	520.0	200.5		1.9		
7:1	a	197.50	8.41	5.95	0.295	565.0	206.4	Av.	1.9		
	b	199.50	8.78	5.69	0.294	615.0	206.6	208.8	1.9	Av.	
	c	198.75	8.22	6.08	0.296	540.0	205.9		1.9	1.93	1.45
	d	197.75	8.14	6.14	0.296	535.0	210.1	s.d.	1.9		
	e	198.50	8.36	5.98	0.295	565.0	211.4	±2.8	2.0		
	f	199.00	8.46	5.91	0.295	580.0	212.4		2.0	Av.	
8:1	a	200.75	8.12	6.16	0.296	540.0	216.2	Av	2.0	1.98	1.27
	b	196.75	8.63	5.79	0.294	595.0	207.1	220.7	1.9		
	c	199.50	8.42	5.94	0.295	590.0	224.0		2.0		
	d	201.00	8.38	5.97	0.295	585.0	224.4	s.d.	2.0		
	e	200.50	8.49	5.89	0.295	600.0	224.1	±7.8	2.0		
	f	201.50	8.21	6.09	0.296	567.0	228.4		2.0		

Note:

2W = 100.0 (mm)

S = 35.5 (mm)

E = 16.7755 $\times 10^9$ (N.m^{-2})

Poisson's Ratio =0.27

Resin : IR1271 (Fordath)

Catalyst: CS-30

Mix Formulation: E1

Maximum load P_{max} is deduced from the average loads recorded at failure (i.e. average of the maximum and minimum oscillation points on x-y plotter at failure).

Table 4.8 (Filler/Resin Ratio Effect)

(Gap-Grading Mix)

Mix Ratio	Sample	(Dimensions) L (mm)	D (mm)	Z=f(W/D) W/D	Z	Failure Load P_{max} (N)	Fracture Energy G_{IC} ($J.m^{-2}$)		Stress-Intensity Factor K_{IC} ($MN.m^{-3/2}$)		Defect Size a (mm)
4:1	a	196.25	8.50	5.88	0.295	480.0	157.0	Av.	1.6		
	b	195.75	8.52	5.87	0.295	485.0	158.8	153.6	1.6	Av.	
	c	196.00	9.14	5.47	0.293	540.0	149.7	s.d.	1.6	1.60	1.79
	d	195.75	9.13	5.48	0.293	537.5	148.9	±4.4	1.6		
	e	195.25	9.00	5.56	0.293	530.5	153.6		1.6		
5:1	a	195.00	8.55	5.85	0.295	502.5	168.1	Av.	1.7		
	b	195.50	8.91	5.61	0.294	525.0	156.1	160.2	1.6	Av.	
	c	196.75	8.54	5.85	0.295	495.0	163.9	s.d.	1.6	1.62	1.63
	d	196.25	9.05	5.52	0.293	540.0	155.7	±5.5	1.6		
	e	195.25	9.01	5.55	0.293	538.0	157.3		1.6		
6:1	a	195.75	8.71	5.74	0.294	510.5	161.6	Av.	1.6		
	b	195.25	8.86	5.64	0.294	520.0	156.6	163.2	1.6	Av.	
	c	195.25	8.46	5.91	0.295	510.0	179.3	s.d.	1.7	1.62	1.37
	d	198.00	9.02	5.54	0.293	540.0	157.8	±9.2	1.6		
	e	195.50	8.85	5.65	0.294	525.0	160.7		1.6		
7:1	a	196.50	8.40	5.95	0.295	465.0	154.5	Av.	1.6		
	b	195.00	8.92	5.61	0.294	515.0	149.6	152.4	1.6	Av.	
	c	195.75	8.73	5.73	0.294	505.0	147.7	s.d.	1.6	1.60	1.16
	d	195.75	8.86	5.64	0.294	515.0	153.6	±3.7	1.6		
	e	196.50	8.95	5.59	0.293	530.0	156.8		1.6		

Note:

2W = 100.0 (mm)

S = 35.5 (mm)

E = 15.2504×10^9 ($N.m^{-2}$)

Poisson's Ratio =0.27

Resin : J50/010L (B.P.)

Catalyst: Phencat 15

Mix Formulation: G2

Maximum load P_{max} is deduced from the average loads recorded at failure (i.e. average of the maximum and minimum oscillation points on x-y plotter at failure).

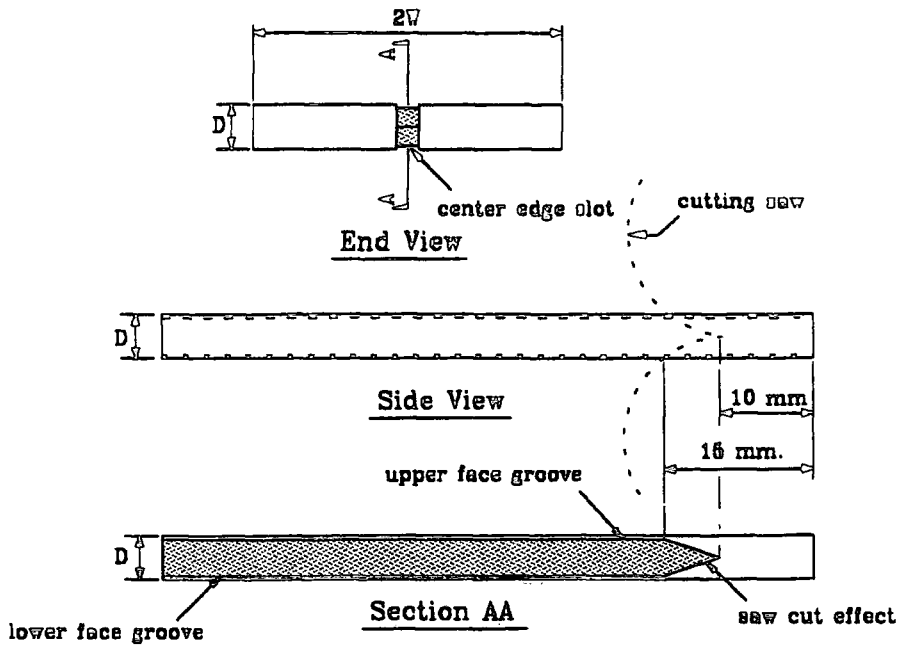

Figure 4.1 Details of center grooves and center edge slot.

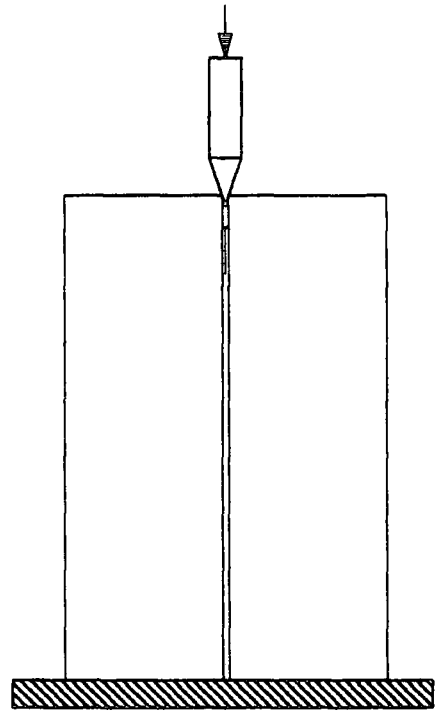

Figure 4.2 Details of wedge indentation technique used in initiating the starter crack.

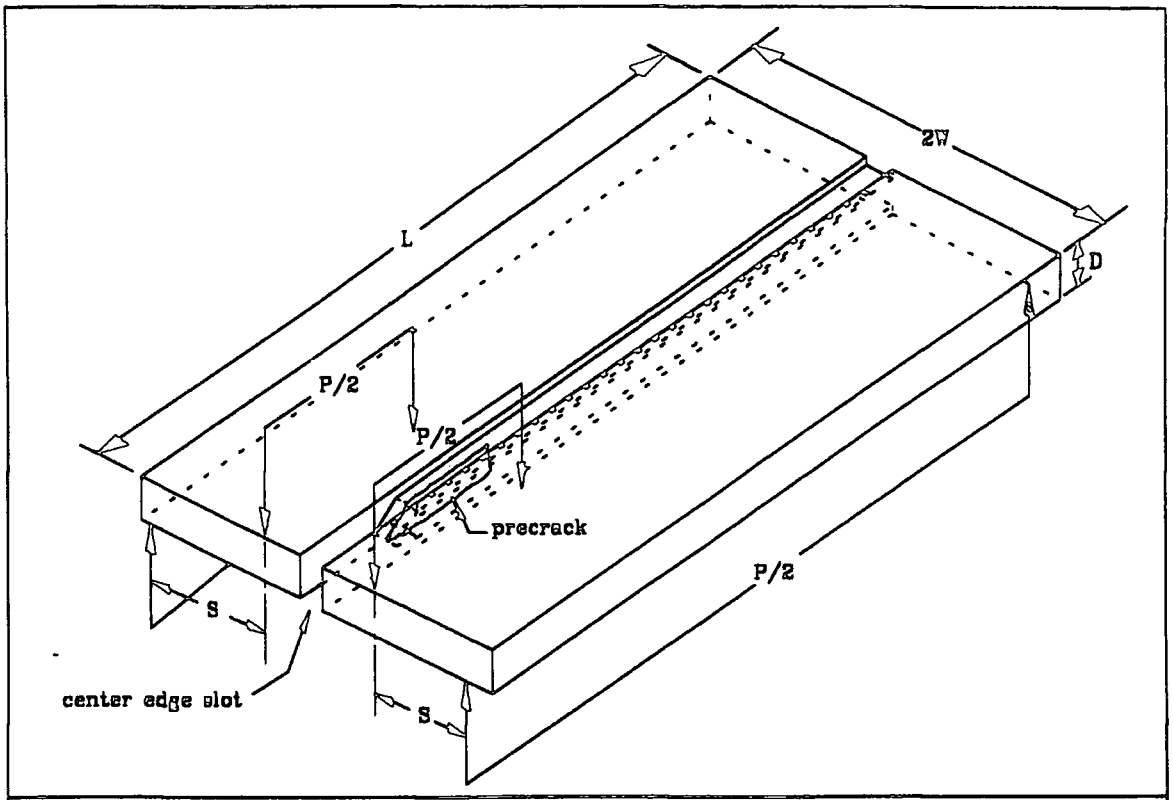

Figure 4.3 The double-torsion test specimen and the loading geometry.

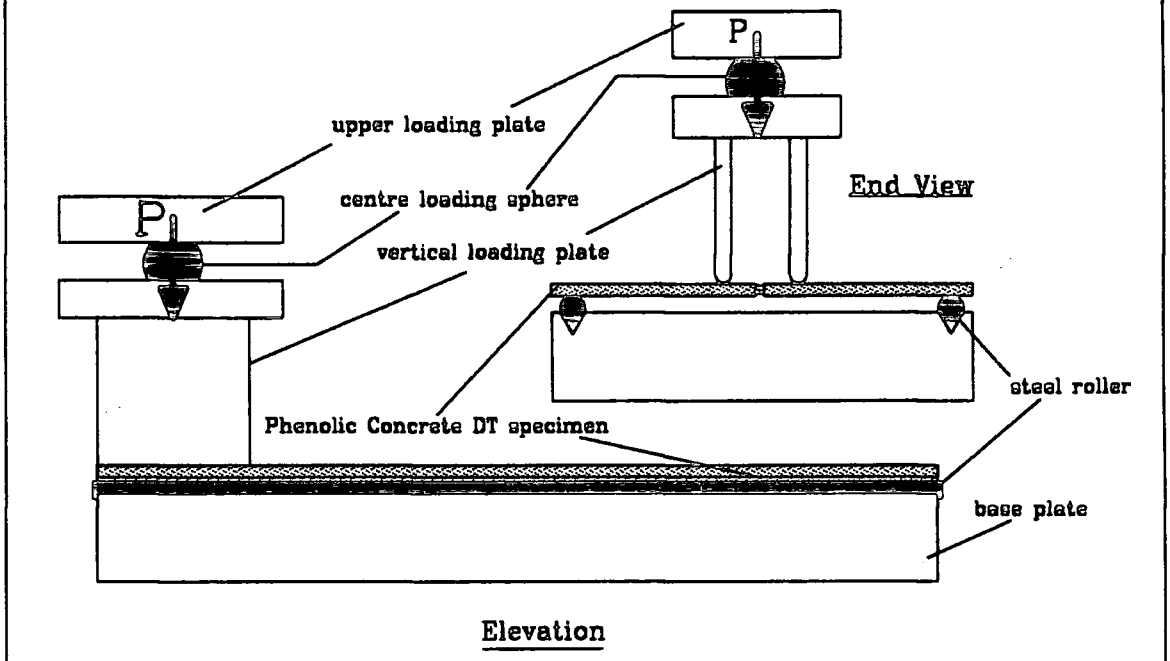

Figure 4.4 Schematic arrangement of the double-torsion apparatus.

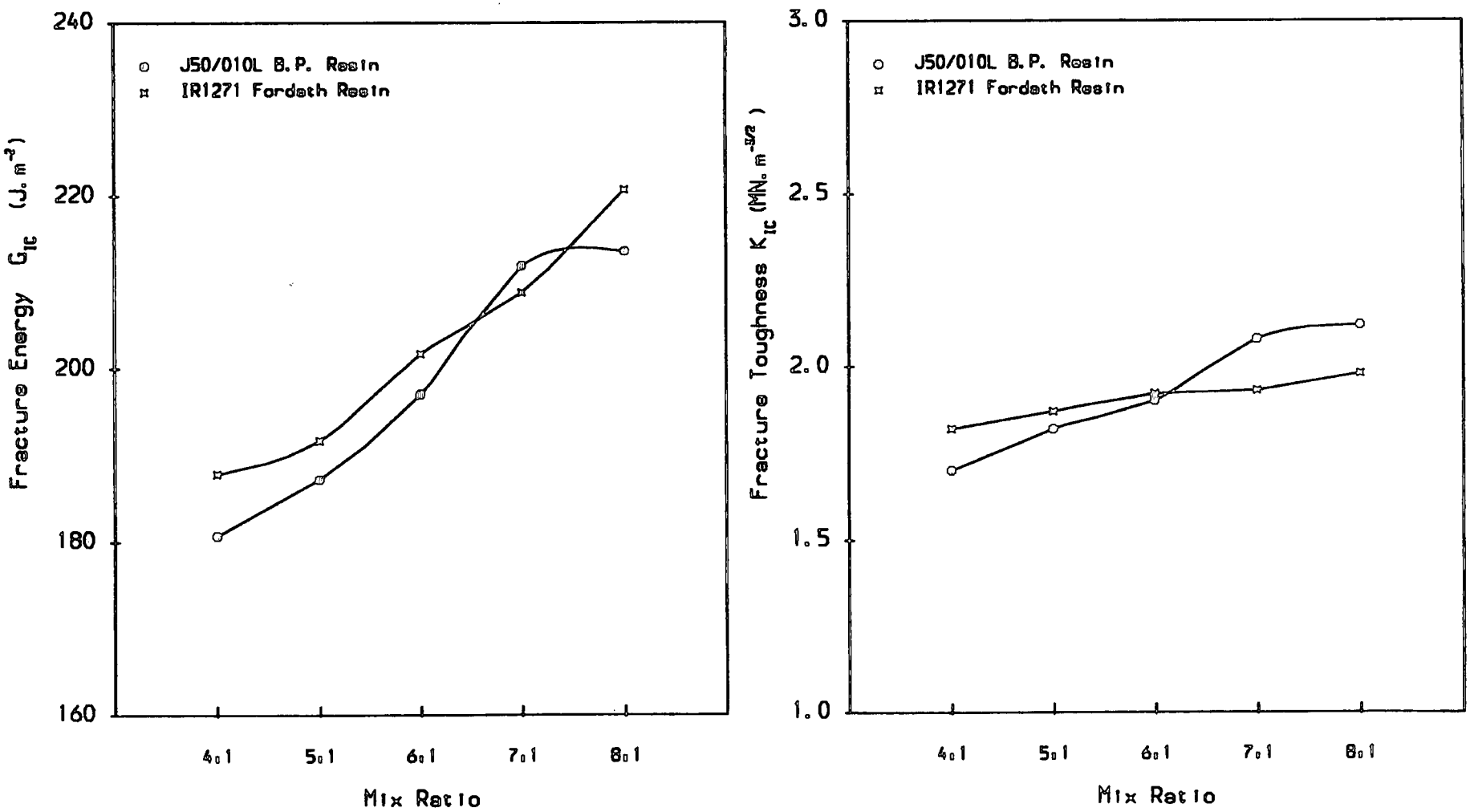

Figure 4.5 Effect of filler/resin ratios on Fracture Energy and Fracture Toughness of the Phenolic Concrete.

Figure 4.6

Recorded plot of load v displacement from double-torsion test

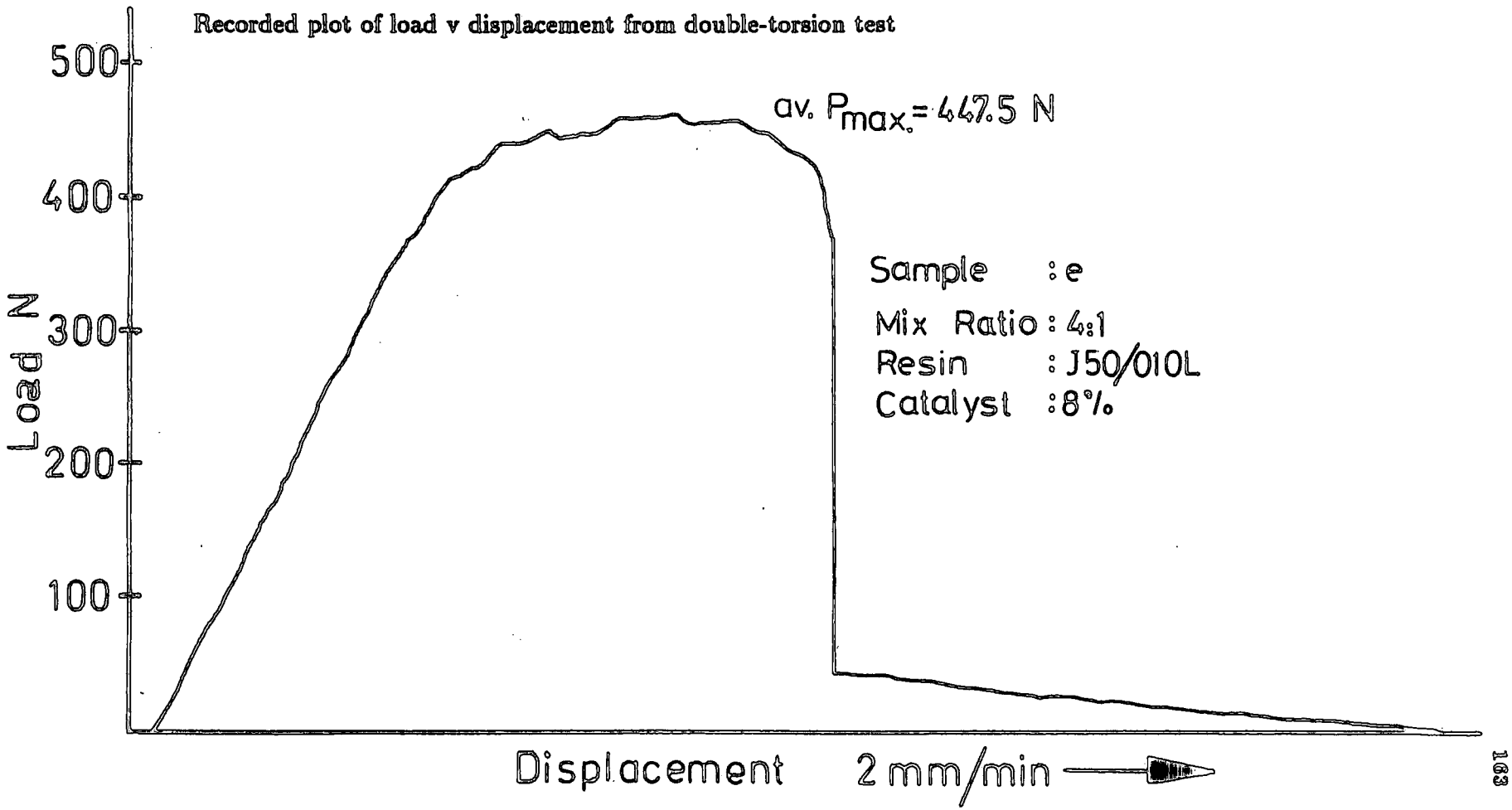

Figure 4.7

Recorded plot of load v displacement from double-torsion test

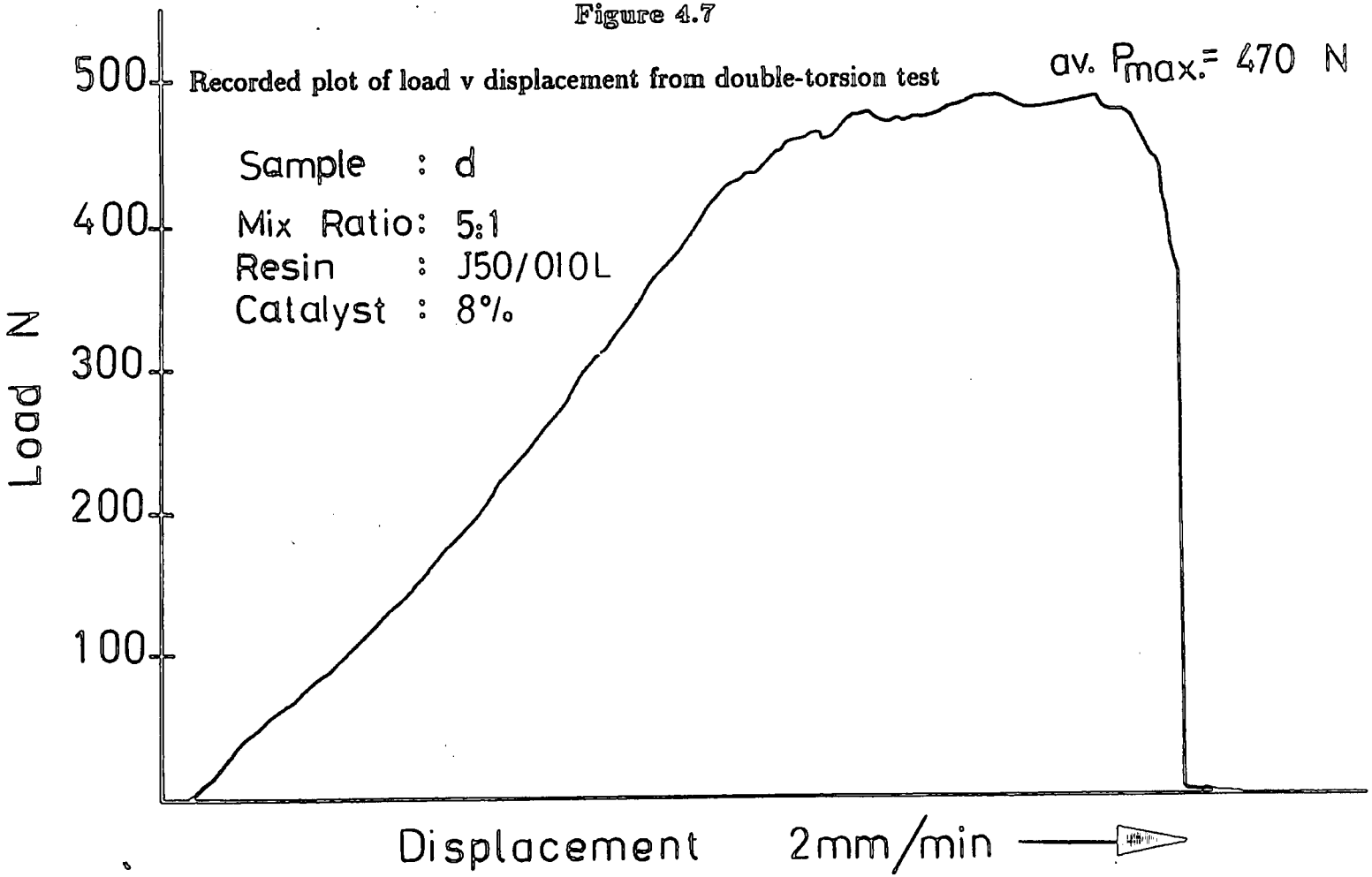

Figure 4.8

Recorded plot of load v displacement from double-torsion test

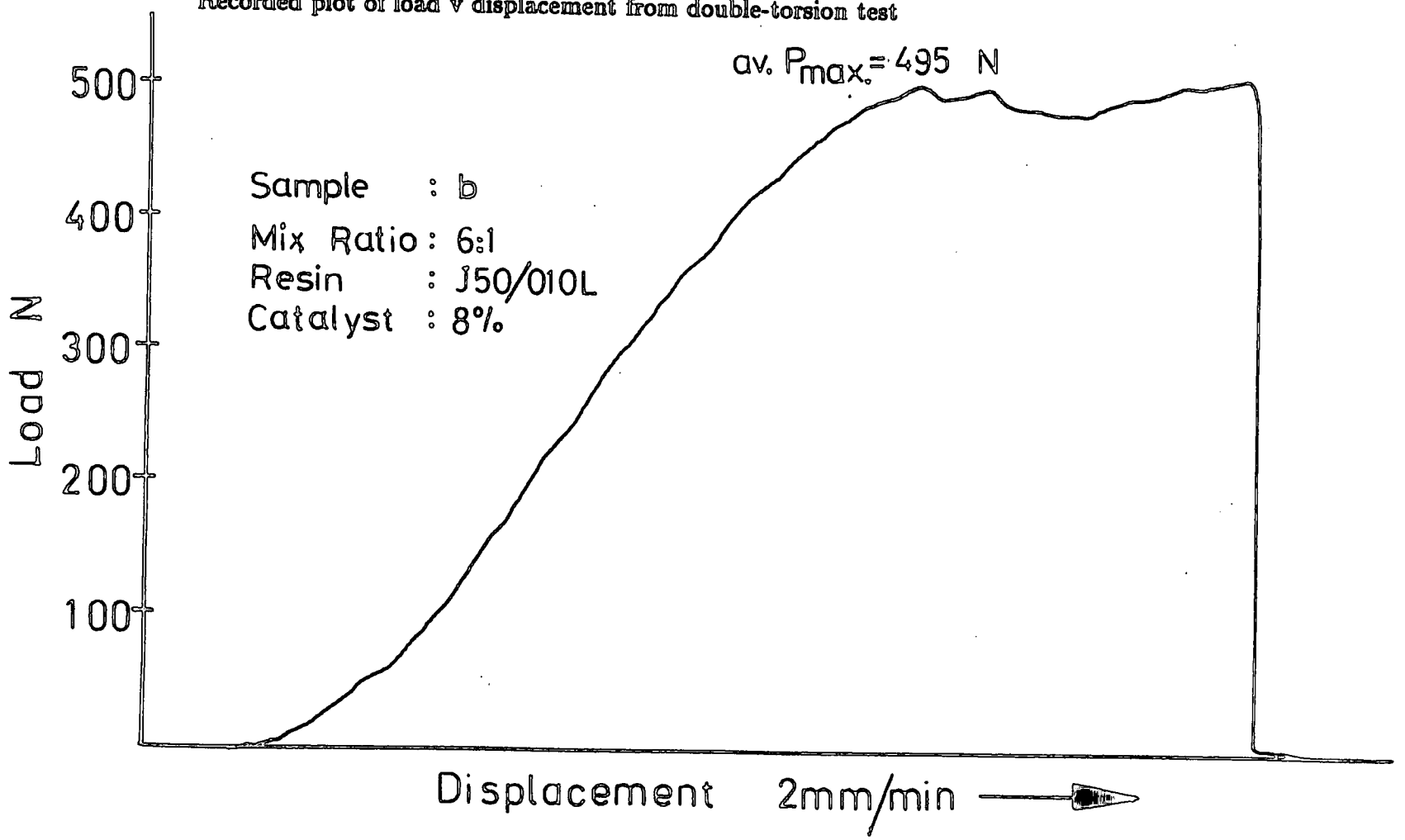

Figure 4.9

Recorded plot of load v displacement from double-torsion test

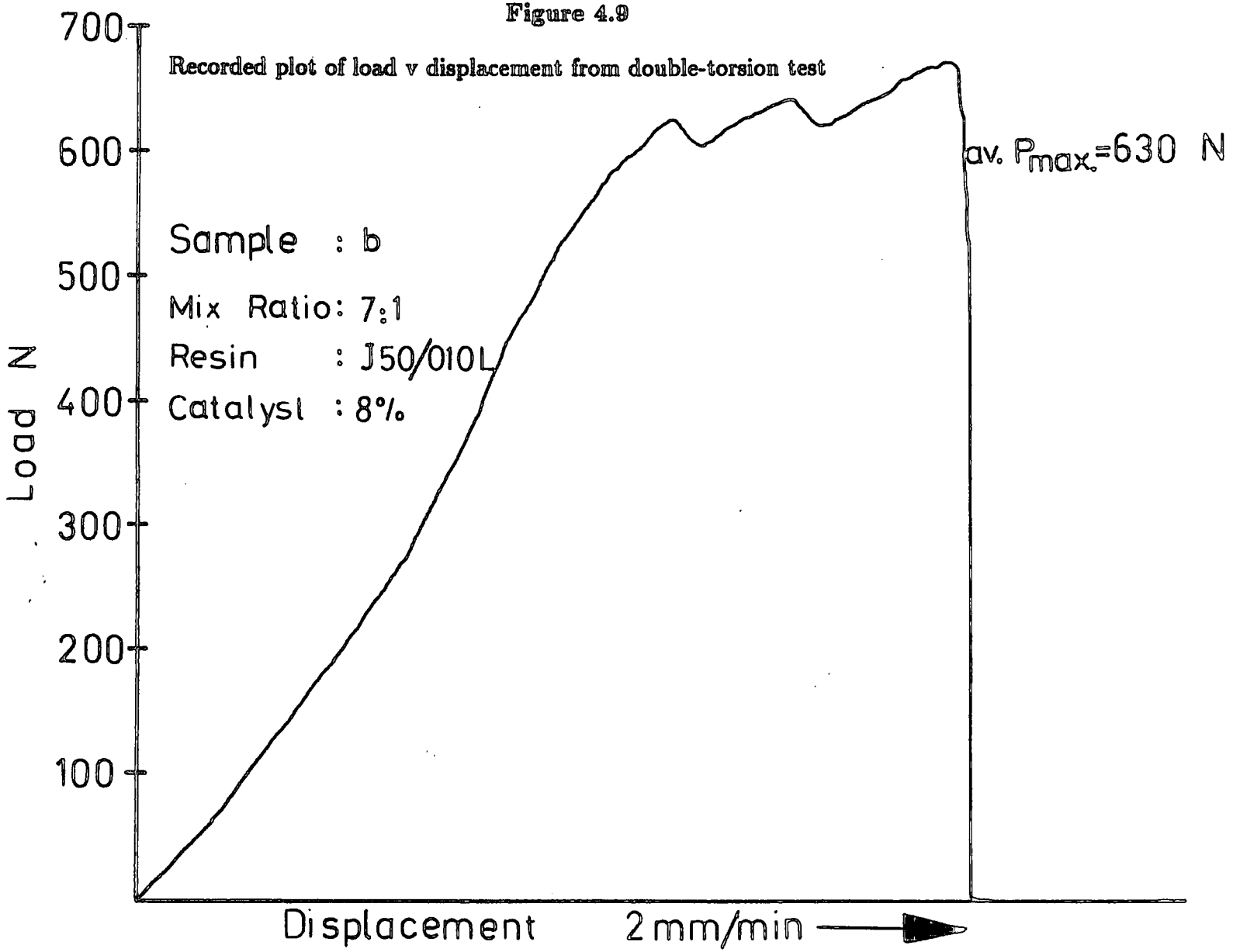

Figure 4.10

Recorded plot of load v displacement from double-torsion test

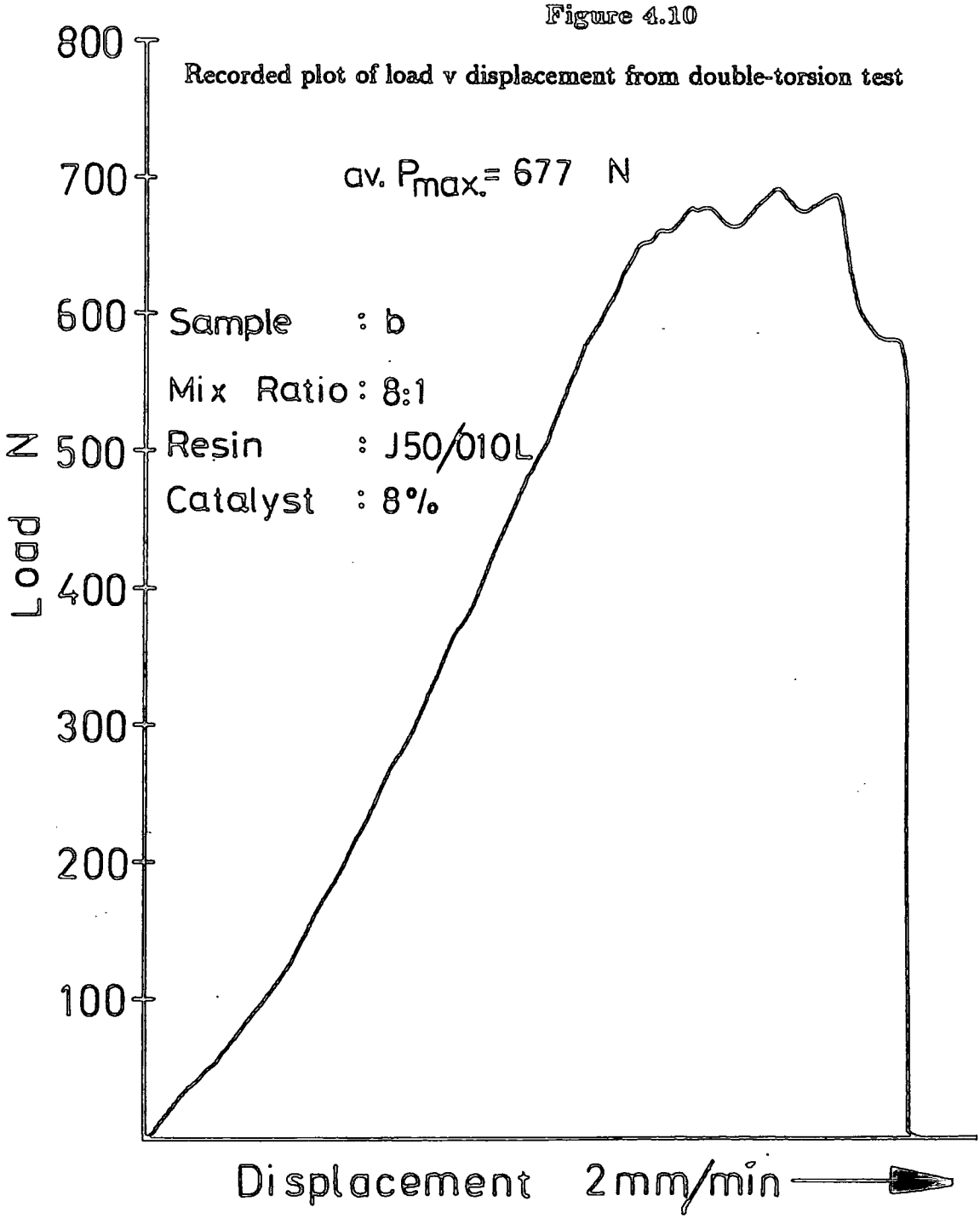

Figure 4.11

Recorded plot of load v displacement from double-torsion test

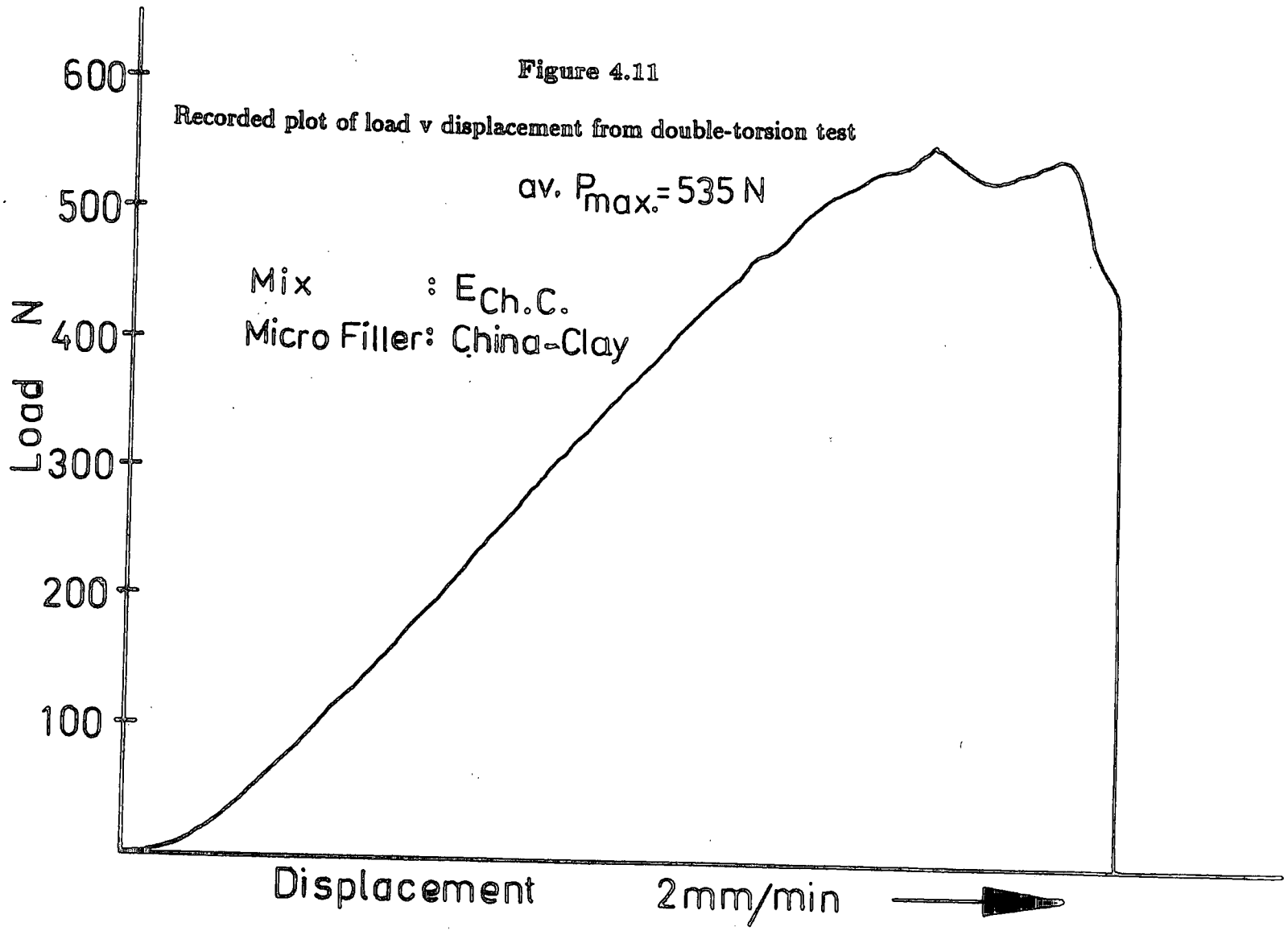

Figure 4.12

Recorded plot of load v displacement from double-torsion test

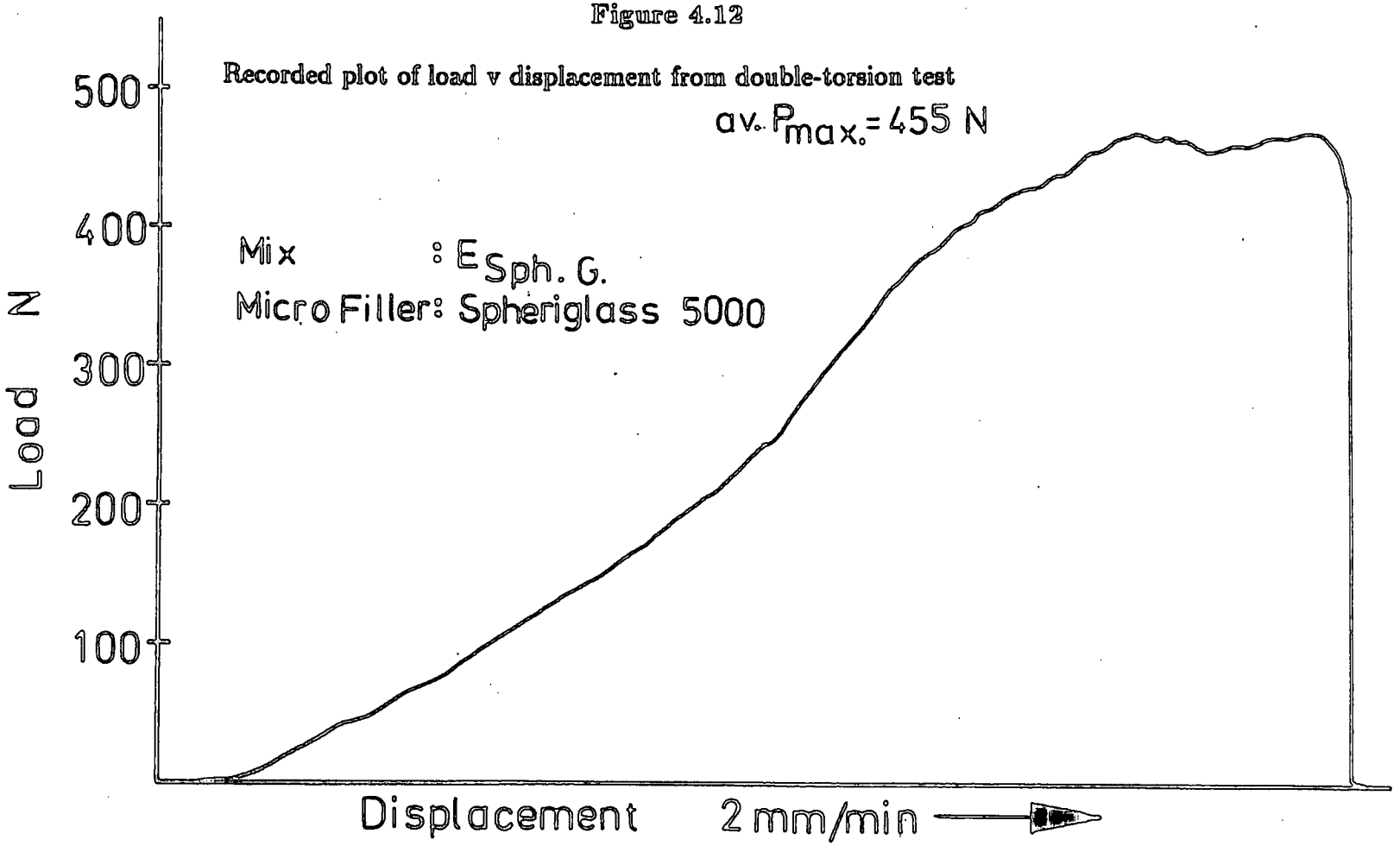

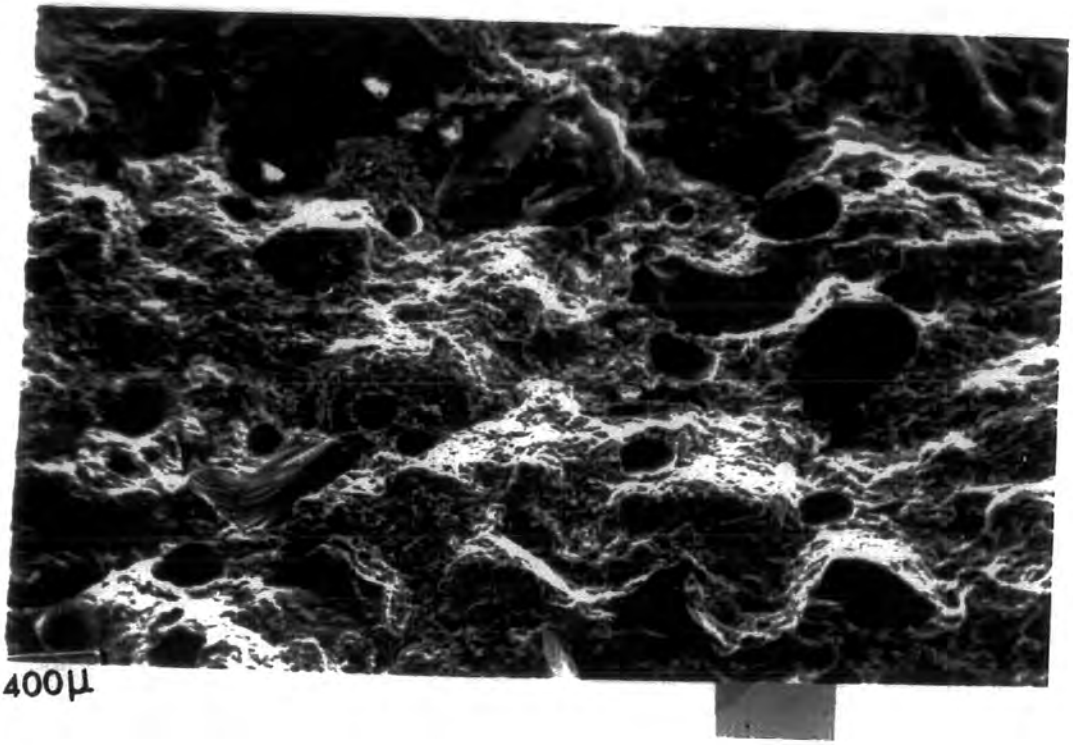

Plate 4.1 SEM image of fractured phenolic concrete specimen showing the plane of fracture through the sand grains with no bond breakage between the grains and resin matrix.

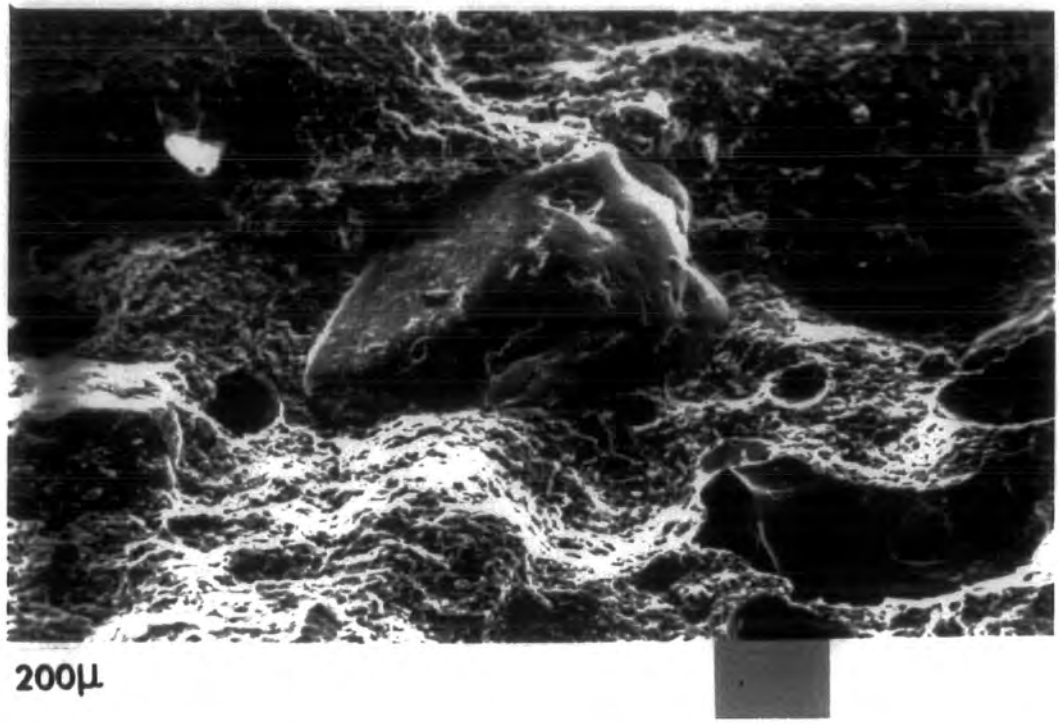

Plate 4.2 SEM image of fractured surface of phenolic concrete specimen showing the resin/filler interface to have developed perfect bond.

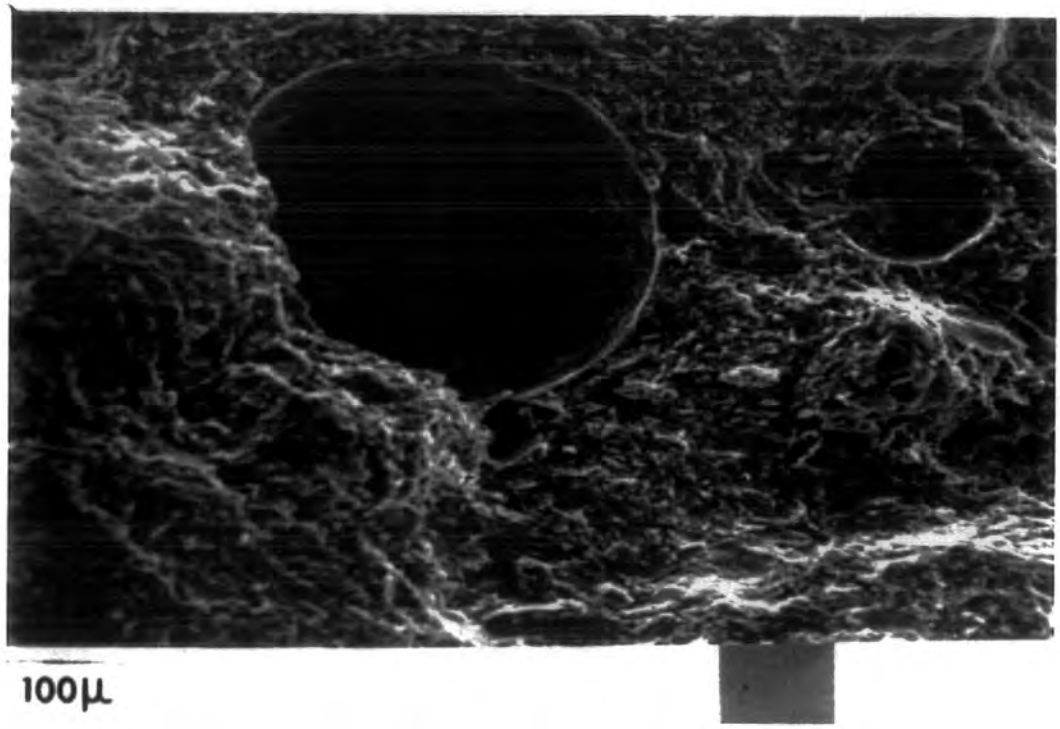

Plate 4.3 SEM image of fractured surface of phenolic concrete specimen exhibiting no apparent particle boundaries.

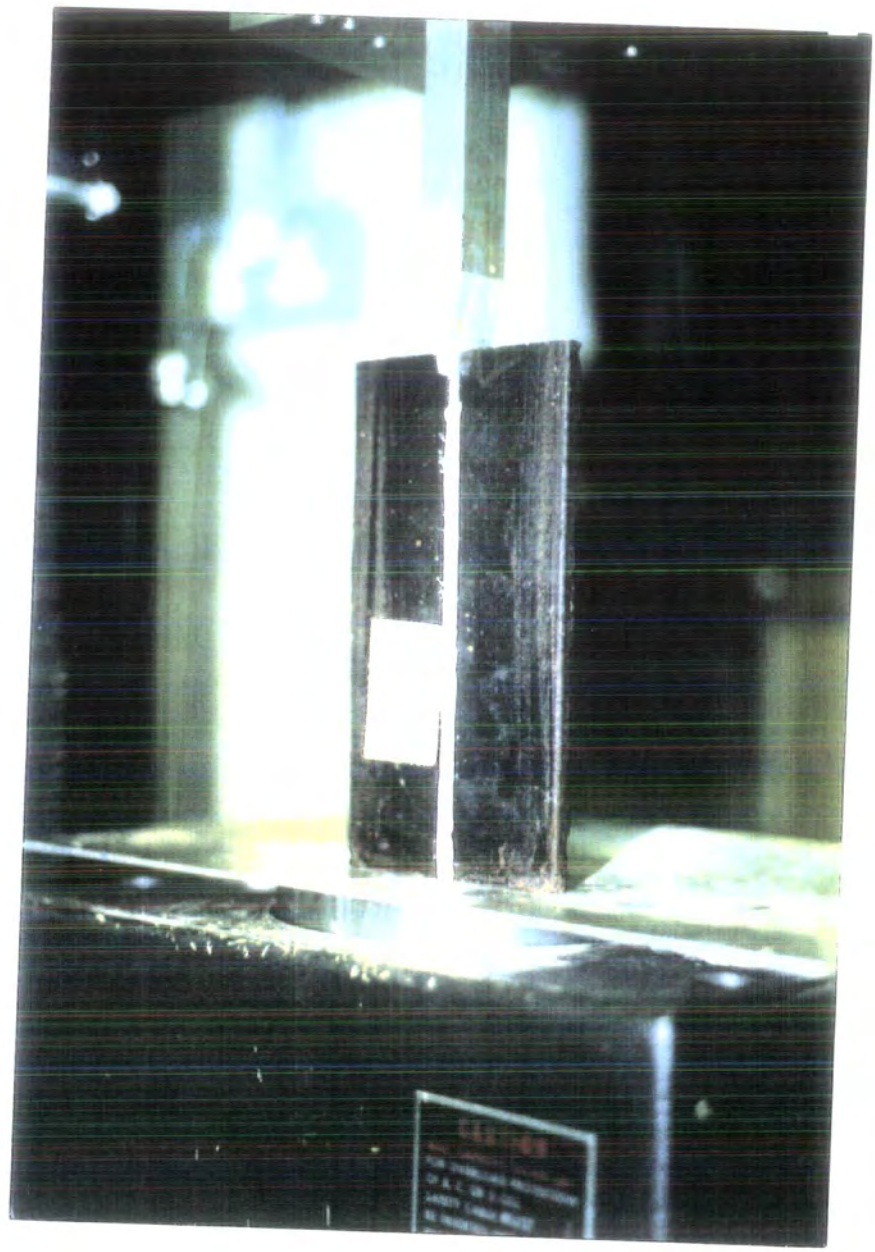

Plate 4.4 The use of steel wedge in indentation technique in precracking the double-torsion phenolic concrete specime in Instron 1195.

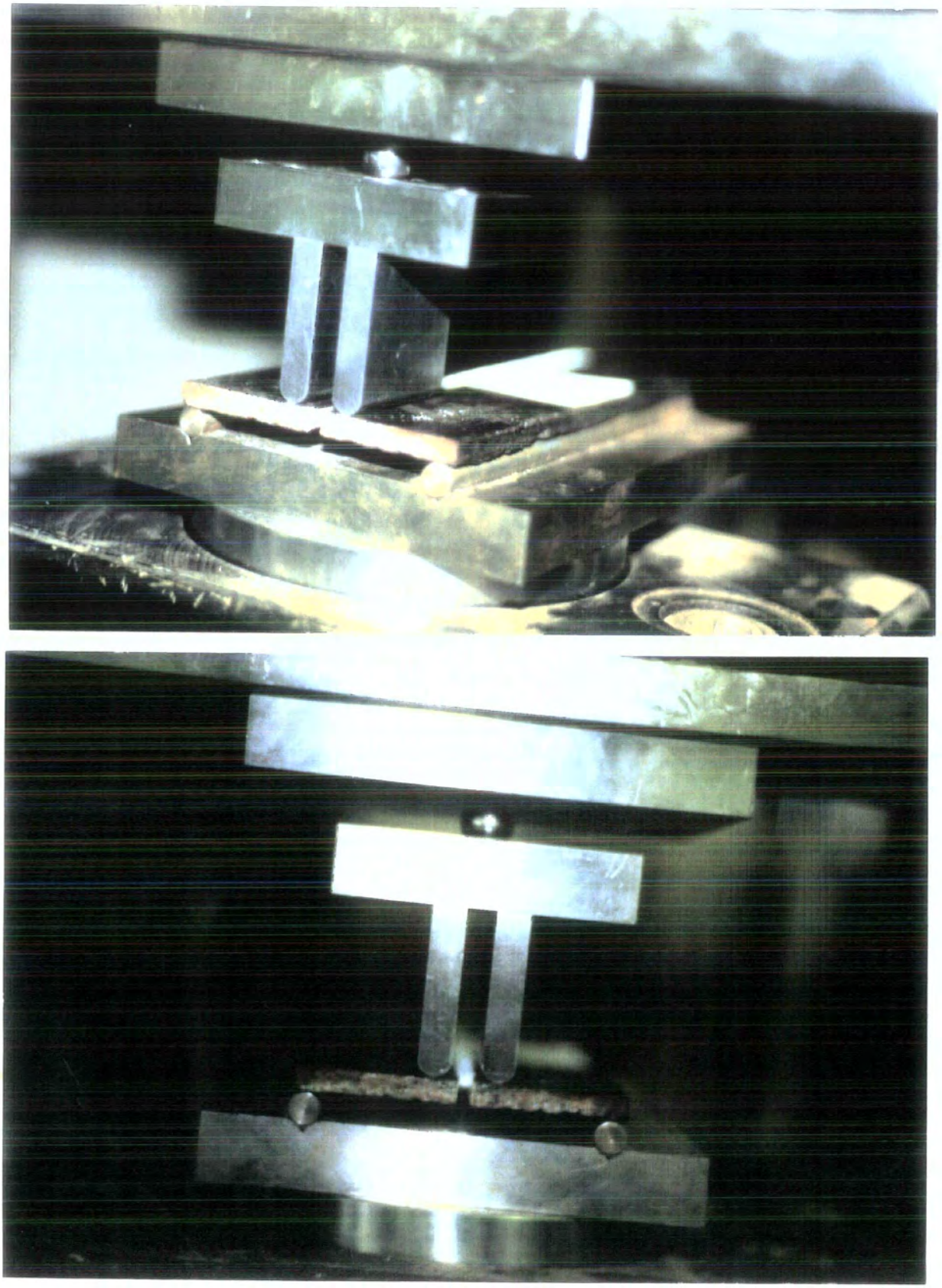

Plate 4.5 The double torsion phenolic concrete test specimen and its loading geometry.

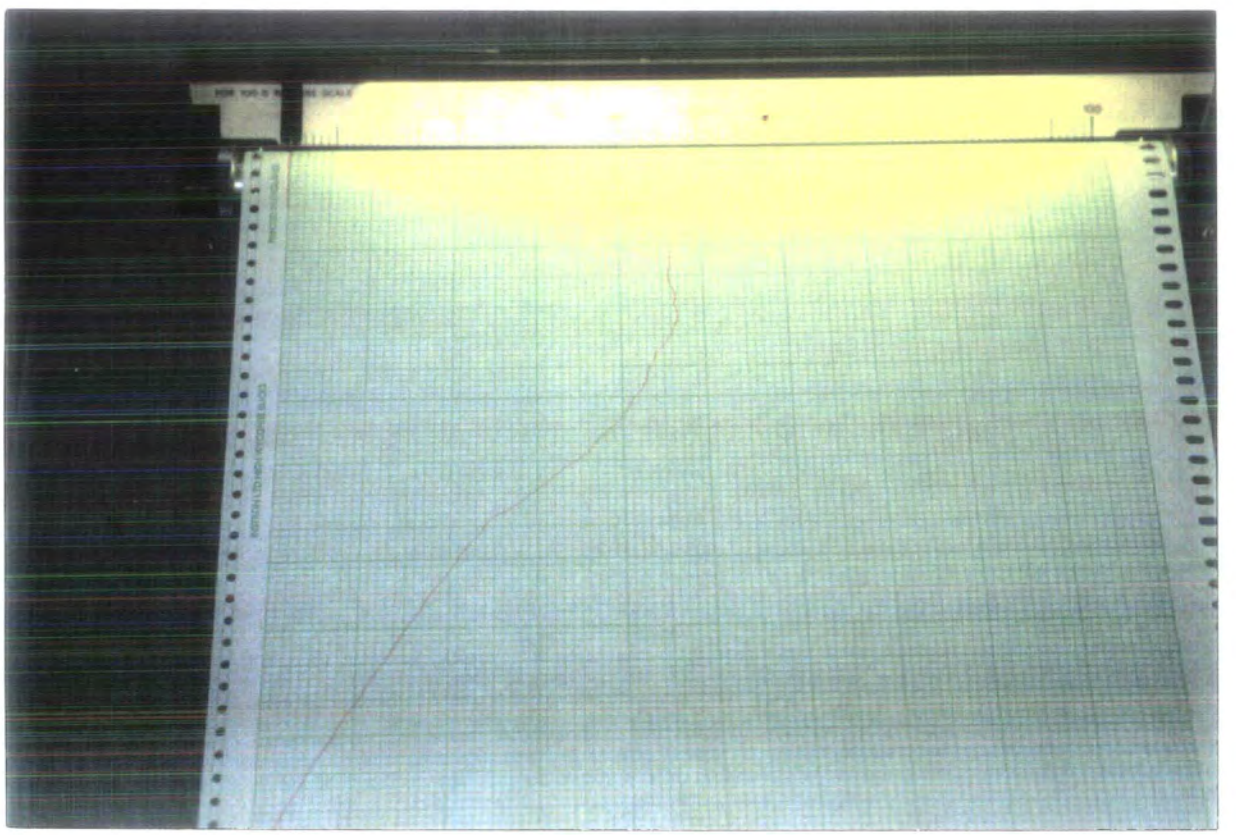

Plate 4.6 Typical load-displacement response from double torsion testing as recorded directly on X-Y plotter of the Instron 1195.

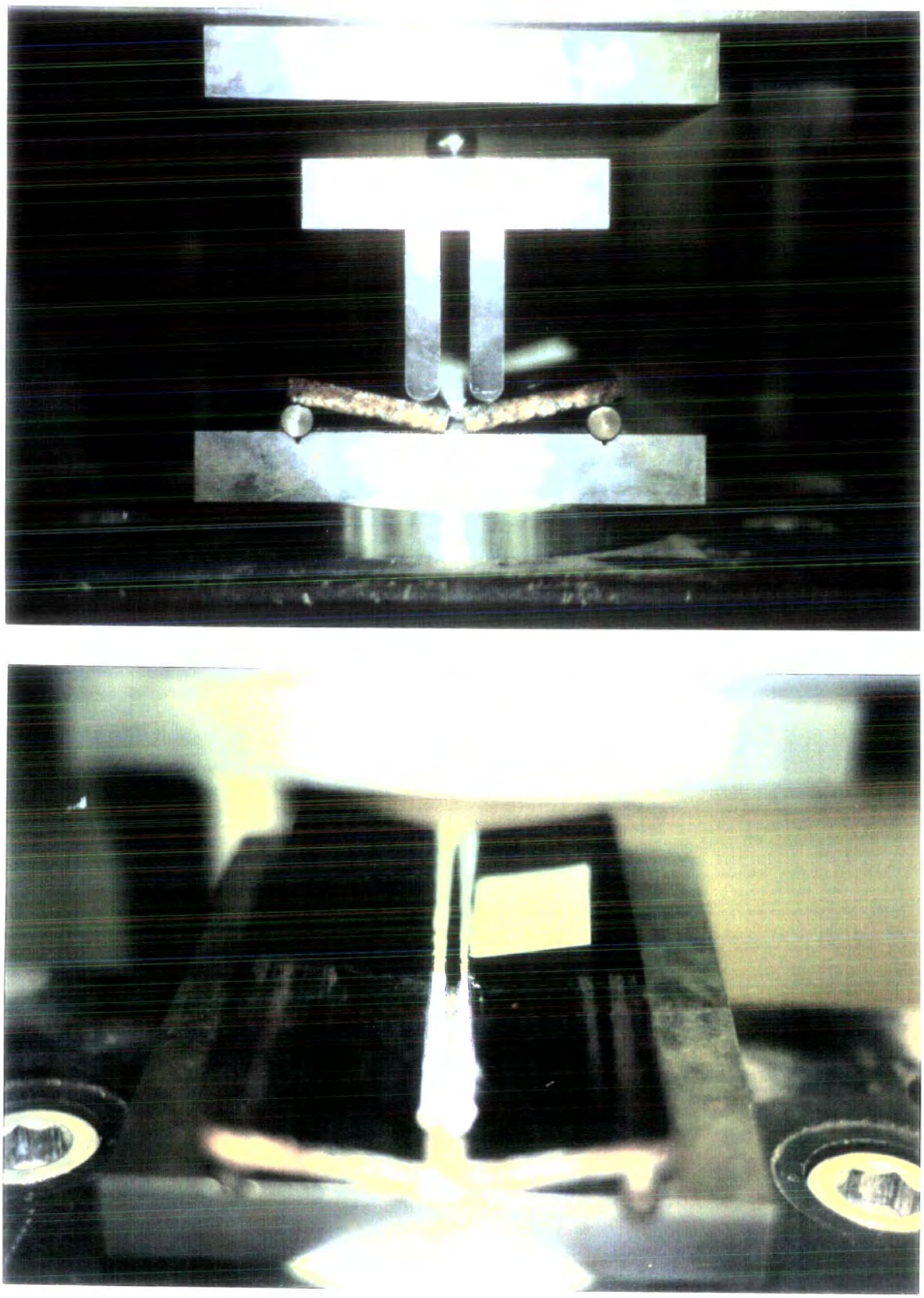

Plate 4.7 The failure of phenolic concrete double torsion specimen through its centre axis by complete seperation.

Chapter Five

5. Phenolic Concrete Beam

5.1. Introduction

In building structures there is often the need to increase the effective tensile or compressive strength of some materials used in the construction of a particular element. This leads to the utilization of secondary materials of higher strength, in order to enhance the strength capacity of the element concerned, providing certain vital conditions are met. The element therefore needs to be composed of two or more materials, constructed in a particular geometry before it can fulfil its required functions efficiently. Also, special configurations of structural elements have been devised to increase efficiency. Some of the most effective in practice are sandwich beams, slabs and panels; all of which have been used for many years. Examples of early construction are wood box beams, glulam beams and also welded and rolled steel box girders. In earlier sandwich construction the materials have been conventional ones such as timber joists sandwiched between two metal sheets.

Glass-fibre reinforced polymer composites have been known and used for some time and extensive work has been carried out on them. Thin layers of GRP composites have been used in forming the faces of sandwich slabs with polymer foam as their cores. Extensive work has also been carried out on fibre-glass reinforced concrete in producing thin panels[92–96] and other applications. This has lead to recent work which has been carried out in the construction of sandwich beam and slab faces using cement-based materials reinforced with fibre glass[97,98], with unsatisfactory results due to insufficient bond being achieved between the core and the faces. The

recent work in which cement- based material was used, adopted mesh reinforcement in the faces with a polystyrene concrete core. This has been successful in producing sandwich beams[99].

The theory behind the sandwich element is to have thin stiff faces of high density and stiffness separated by a less stiff, thick layer of low density material with the assumption that the assemblage will behave as a single member, thus producing an element with greater bending stiffness, but low weight.

The work reported here outlines the use of a newly developed polymer composite matrix in the construction of sandwich beams in the form of closed box beams. The successful development of the Phenolic Concrete matrix in this research, enabled the author to use this polymer matrix in a composite structural element with phenolic laminated fibre glass mat (in the form of phenolic GRP) as reinforcement, to form thin faces. Assemblage of these faces with polymer foam (i.e. Polyurethane or Phenolic) as the core, proved to be an effective method of construction of sandwich box beams. The Phenolic Concrete matrix utilizes the high tensile strength of the phenolic laminated fibre glass mat to increase both the stiffness and the strength of the composite thin faces of the beam. The laminated glass fibre mat provides a well distributed and well bonded means of reinforcement to the thin faces.

The technique of construction together with the geometrical arrangement of the sandwich box beams, makes it possible for any type of low density polymer foam to be used as the core.

Beams of similar geometry to those constructed for this work were also made of Polyester Concrete composites at Durham University[40]. Some Polyester Concrete sandwich beams had already been constructed and utilized in the construction of houses assembled of Polyester Concrete sandwich panels in South-Africa, prior to the

work carried out at Durham University. However, since the results of the research work were not made available to the author a comparison is not possible.

Phenolic Concrete composite sandwich box beams made for this research work, have several advantages. They are light in weight with inherently good sound, heat loss and weather insulation. A characteristic which gives an important advantage is, the superior fire resistant and smoke emission properties of the Phenolic Concrete matrix, providing safeguards to building regulations concerning fire resistance requirements. These box beams can be used, with wall panels of similar materials, as lintel beams spanning across door, window or corridor openings to form a stiff structure.

5.2. Test Specimens

A total of twelve Phenolic Concrete box beams were constructed and studied in this research. These beams consisted of six shallow beams, series A, and six deep beams, series B (Figure 5.1 and 5.2 respectively).

All the beams had the four longitudinal sides of glass reinforced polymer concrete cored by low density foam. In shallow beams the core was of Polyurethane foam and in deep beams it was of Phenolic foam. The upper and the lower sides of the beam in each series were joined by the two longitudinal vertical sides, acting as 'ribs'. The ends of the beams were also ribbed similarly to the sides.

The beams had a cross-section of approximately $205 \times 97mm^2$ and a total length of 1.5m with an effective span of 1.35m (Figure 5.3). The sides of the box beams were of approximately 10-20mm thickness, dependent upon casting and core formation. The sides were made up of Phenolic Concrete Mix (see 5.4.1.).

All the beams were reinforced with laminated fibre glass mat at the inner faces of

their tops, bottoms and sides, and in some there was additional internal tensile steel bar reinforcement. The internal longitudinal tensile steel bars were of the 'ribbed' type, consisting of two 6mm or two 10mm diameter, in both beam series.

Cross-sectional schematics of the test beams are shown in Figures 5.1 and 5.2, with their cross-sectional dimensions in Table 5.1 .

5.3. Specimen and Test Variables

The purpose of this work was to demonstrate possible techniques and methods of construction of Phenolic Concrete beams and also to investigate their behaviour under flexural loading as structural elements. For this purpose, these beams were designed in box form, internally cored by foam to give light weight and at the same time to overcome the high cost of the materials. Also, it had become evident that Phenolic Concrete can only be cast as a thin face in order to develop sufficient strength.

In the experiments, it was also demonstrated that pre-laminated fibre glass mat, in the form of GRP, can be used to reinforce the Phenolic Concrete matrix. In these beams the inner fibre glass mat was wrapped around the foam (core) and acted as inner face reinforcement for all the beams (see 5.5.).

After failure of the test beams, cross sectional examination clearly showed no debonding of these pre-laminated fibre glass mats from the Phenolic Concrete matrix. The bond was similarly unaffected in the case of the outer laminated fibre glass mats which were laid wet at the time of the Phenolic Concrete mix being poured.

The main variables in the tests were the type of the test beam (Shallow and Deep beams) and the internal longitudinal tensile reinforcement.

In both series, two groups A-1 and B-1 were constructed without internal steel

reinforcement and tested as reference beams. Beams group A-2 and B-2 were each reinforced internally by $2 \times 6mm$ diameter high yield steel bars and beams group A-3 and B-3 with $2 \times 10mm$ diameter high yield steel bars.

5.4. Properties of the Materials

5.4.1. Phenolic Concrete Matrix

The twelve Phenolic Concrete Beams, were cast using the mix E1 (see Appendix A1). The mix constituents and the mix ratio were kept constant for all the beams and their control specimens. The mix ratio (Filler:Resin ratio) was 5.5:1 by weight. This ratio was adopted to have easy flow (good workability) and hence control of mixing and casting. The resin used was J50/010L Phenolic Resin produced by BP Chemicals. The acid catalyst Phencat 15 was used at 8% by weight of the resin. This level of catalyst provided sufficient time to proceed with mixing and casting in the construction of each beam.

Two types of mixers were used in mixing the Phenolic Concrete mix. A 'Hobart' mixer with a capacity of 20kg and a non-tilting pan type of mixer with a maximum capacity of 170kg, the latter is normally used for mixing conventional concrete.

Control specimens were also cast along with the beams. Due to the time limit in the construction of each beam before the Phenolic Concrete mix could gel, it was decided that these control specimens would be cast separately but from random sampling of mix constituents taken from the actual beam mixes prior to their being mixed with resin. All the control specimens were mixed, cast, set and cured in the same manner and for the same period of time as of the actual beams.

A total of twelve coupon specimens ($100 \times 600 \times 7 - 10mm^3$), were made for each mix, six of which had and the remaining six had not laminated fibre glass mat on their inner and outer faces when cast. These coupon specimens were tested in flexure in the Instron 1195 Testing Machine, as explained in Chapter 3.

The compressive, tensile and flexural moduli of the first six coupons with fibre glass mat were calculated from the test results. Compressive and tensile moduli were determined using the strain measurements. The strains at the centre of span of the upper and lower faces of these coupons were measured at each loading interval using 10mm e.r.s. gauges which were bonded to these faces with 'Araldite' prior to testing. The loading interval was controlled by stopping the movement of the cross-head on the Instron 1195 with the load magnitude being measured from the paper-chart. At the same time a digital read out of the deflection (cross-head travel) was also recorded and compared with those ploted on the paper-chart at corresponding load stages. The result of load against deflection and bending stress against bending strain are presented in Figure 5.4, and Figures 5.5a to 5.5f, respectively. For the remaining six coupons without fibre glass mat only load-deflection readings were recorded.

The computed results from these flexural tests are produced in Table 5.3 . The mean flexural modulus for coupons with fibre glass mat was $12.43 \times 10^9 N/m^2$ and that of coupons without was $22.40 \times 10^9 N/m^2$, with mean ultimate flexural strength of $45.94 \times 10^6 N/m^2$ and $24.82 \times 10^6 N/m^2$, respectively.

The compressive and tensile moduli of the coupons with fibre glass mat are also shown in Table 5.3 . The ratio of the flexural modulus obtained from the load-deflection graphs to the tensile modulus of each coupon obtained from the bending stress-strain relations, clearly indicates that the laminated fibre glass mats were in

good bonding order with the Phenolic Concrete matrix in the elastic region. This was also the case through the remaining part of the test as visual inspection of the failed sections made it evident that the section had undergone flexural failure as a composite section and not because of the failure of the interface between the laminated fibre glass mat and the matrix.

Similarly twelve T-bone specimens were cast, six with and the remaining six without laminated fibre glass mat. These were constructed and prepared for testing at the same time as the coupon specimens. The T-Bone specimens were tested in direct tensile stress in the Denison T42B4 Testing Machine. To ensure axiality of the specimens, both e.r.s. gauges and demec studs were bonded to both their faces prior to testing. The strains on both faces of these specimens at corresponding applied stresses were measured using 10mm e.r.s. gauges and also demec gauges with a nominal gauge length of 200mm. The sets of readings which differed by more than 15% on opposite faces were rejected. The stress-strain relationship from these strain results (e.r.s. gauges) together with their deduced properties are shown in Figures 5.6 and 5.7, and the calculated tensile moduli and corresponding ultimate tensile strengths of these specimens are presented in Table 5.4 .

To obtain the values of the compressive and tensile strength of the Phenolic Concrete mix used in construction of the beams, a number of blocks in the shape of prisms ($75 \times 75 \times 150mm^3$) were cast. These were cast in layers of approximately 25mm thickness, as it is not possible to cast the Phenolic Concrete in a bulk, due to volume expansion which would be caused by the polymerization process, and also premature setting due to the exotherm effect. If cast in bulk, the above effects would produce an expanded aerated solid block with the presence of large voids (see Chapter 2). These prism blocks were cast in moulds constructed as polypropylene

boxes with a lid of the same material. All the processes of mixing, casting, setting and curing were similar to those of other control specimens and also the actual beams. However, the physical dimensions of these blocks required larger pressure to accompany their setting in the mould as opposed to the other thinner samples. After these prism blocks were cured, a total of nine right circular cylinders of approximately 60mm length × 20mm diameter and nine discs of approximately 25mm thick × 50mm diameter were cored from them. The cored Phenolic Concrete cylinders were trimed at their ends using a diamond saw and then placed on a 'Lapping Machine' until the required flatness of ends were obtained. These right circular cylinders were prepared and tested in accordance with the ISRM[70] method and their average unconfined compressive strength was found to be $85.5 N/mm^2$.

The cored Phenolic Concrete discs were tested in accordance to the Brazilian Test[69] for rock specimens, and hence the average tensile strength of these specimens was found to be $8.15 N/mm^2$.

5.4.2. Reinforcement

From early results it became evident that the Phenolic Concrete on its own behaves in a brittle manner and failure under flexure is sudden since cracking occurs in the extreme tension fibres of the element. To overcome this weakness the best possible means of reinforcement which would comply with both chemical and mechanical bonding criteria would be the employment of suitable fibre materials as means of reinforcement. This, therefore, led to the incorporation of fibre glass mat in the tension side of a Phenolic Concrete element in the form of Phenolic GRP[47]. However from early trial procedures adopted in construction of Phenolic Concrete samples with fibre glass mats only on their tension faces, it was found that once the

curing of the sample is completed the element tendes to curl, possibly due to the differential rate of curing of the Phenolic GRP and that of the Phenolic Concrete matrix. This phenomenon was overcome by symmetrical application of the Phenolic GRP laminated mat on either face of a Phenolic Concrete element.

It is of importance to select an appropriate type of glass for lamination in Phenolic GRP. It has been found[51] that certain binders and/or 'size' on glasses interfere with the curing chemistry, either retarding or effectively stopping the curing process. In the case of chopped strand mats, powder bound (P.B.) varieties are generally acceptable. Overall, however, it is not difficult to find glasses of all types which are compatible with phenolic resin and some manufacturers have recently developed mats specifically for cold set Phenolic GRP Lamination.

In the construction of the test beams the fibre glass mat with a brand name of Supermat P.B. $450g/m^2$ of chopped strand type was used. The resin used in hand-lay lamination was J2018L, produced by BP Chemicals, in conjunction with acid catalyst Phencat 10. This resin and its acid catalyst is recommended by BP Chemicals for cold set hand-lay lamination Phenolic GRP[51,54]. A ratio of 1.5:1 by weight of resin to glass mat with 6% Phencat 10 by weight of resin was used. This level of catalyst gives ample time to hand-lay lamination.

The technique of use of fibre glass mat in the form of laminated Phenolic GRP mat as reinforcement can be adopted in two forms. It can either be pre-laminated and pre-set or it can be applied in the form of wet lamination at the time of its application to the Phenolic Concrete matrix (see 5.5.).

In order to obtain the physical properties of the laminated fibre glass mats used in the test beams, samples of 4-ply hand layed laminated Supermat P.B. $450g/m^2$ at 1.5:1 ratio of resin to glass mat were made in the form of coupon specimens(100 $\times$

$600 \times 6mm^3$). A number of these coupon specimens were tested in flexure (see Chapter 3) and from remaining coupon specimens, samples in the form of T-Bone specimens were cut and tested in direct tension in Hounsfield Tensometer Testing Machine.

The Physical properties as given below were deduced from the corresponding tests.

Flexural Modulus	$5800 - 6300$	MN/m^2
Flexural Strength	$160 - 185$	MN/m^2
Tensile Modulus	$5500 - 6000$	MN/m^2
Tensile Strength	$110 - 130$	MN/m^2
Elongation at break	2.5%	

The above means of reinforcement enhances the ductility of the Phenolic Concrete element, and at the same time increases its load carrying capacity to some extent. Furthermore the fibre glass mat provides an effective means of crack entrapment thus increasing the loads to cause early cracking of the Phenolic Concrete.

To increase further the load carrying capacity of such elements, it was decided to use steel rods which were to be embedded longitudinally on the tension side of the Phenolic Concrete test beams. From early work it was found that the plain steel rods have little effect, as no bond (grip) is developed between Phenolic Concrete and round steel rods and they have a tendency to slip under flexure. It was therefore decided to use high yield steel bars of 'ribbed' type. The curing shrinkage of the Phenolic Concrete Matrix causes the matrix to grip the steel by its ribs in order to bring about a mechanical means of bonding.

In the test beams, two sizes of h.y.s. bars were used. Samples from these steel bars were prepared and used in tensile tests in accordance with the recommendation of BS 18: Part $2^{(100)}$, in order to determine their stress-strain characteristics, modulus of elasticity and ultimate strength. The steel specimens tested were of $6.39mm$

and $10.43mm$ diameter with their corresponding properties of:

		$6mm\ \phi$	$10mm\ \phi$
Elastic Modulus	(E)	200.0 kN/mm^2	207.0 kN/mm^2
Ultimate Tensile Strength	(σ_{Tu})	712.3 N/mm^2	629.0 N/mm^2
Proof Stress	(σ_{ps})	610.0 N/mm^2	557.0 N/mm^2
Strain at Proof Stress	$(\epsilon_{p.s.})$	4250×10^{-6}	4250×10^{-6}

A detailed cross-sectional layout of the reinforcement (laminated fibre glass mat and steel bars) of the Phenolic Concrete beams is shown in Figures 5.1 and 5.2 .

5.4.3. Foam (Core of the Test Beams)

The beams which were constructed for this part of the research, were of composite type in the form of box beams with four longitudinal sides and two ends. The prime requirement of a sandwich beam is to have as its core a thick layer of low density material separating the thinner stronger faces of stiff and dense materials. This, therefore, dictates the vital properties which the core has to possess. The core has to ensure that the faces remain the correct distance apart. It needs to be of low density but must be stiff enough to keep the faces as flat as possible in order to avoid any premature local buckling of the faces due to their local slenderness. In true sandwich beams the core must also be able to transmit the bending shear between the two extreme faces. However, in the case of the box beam only the slenderness control of the faces is really significant, since the rigid sides of the beam take over the other functions.

Two types of foam were adopted in the construction of the test beams, which complied with these requirments. Polyurethane foam in shallow beams and Phenolic foam in deep beams.

The polyurethane foam was used, irrespective of its poor coherence to the phenolic concrete. The method of construction enabled any type of foam to be used in

so far as it complies with the properties outlined above. The polyurethane foam was available in block or slab shapes, easily cut to the required shapes and dimensions. It was of closed cell structure, with low density $(25 - 30kg/m^3)$.

The phenolic foam[101] was also of closed cell micro-structure with low density $(35kg/m^3)$. It was available in block or slab shapes. It also complied with the requirments and had advantages over the polyurethane foam, as the slab blocks could be bonded together by use of a little catalysed phenolic resin J2018L to obtain any thickness required. This had to be done, since the thicknesses required the use of two slabs of foam to be bonded together before cutting to the required shapes and dimensions.

The important properties[101] of the phenolic foam used are outlined below:

Density	35	kg/m^3
Compressive Strength	$140 - 110$	kPa
Cross break Strength	$160 - 210$	kPa
Thermal conductivity	0.033	$W/m°C$
Corrosivity to metal	*Negligible*	
Closed cell content	*Greater than*	75%

5.5. Method of Construction, Casting, Setting and Curing

A mould was constructed using wood lined internally with $20mm$ polypropylene sheets. The mould was designed so that eight clips fastened the side and end walls to the base, thus enabling the mould to come apart very easily. The mould was thoroughly waxed and the polypropylene sheets were sprayed with mould releasing agents prior to casting. G-Clamps were used to keep the side walls of the mould the correct distance apart once the beams were cast and left to set under applied pressure.

The mix constituents (i.e. Fillers) were carefully weighed, taking into account

the required extra mix to be used in casting the control specimens. The fillers were mixed dry in a non-tilting pan type mixer until a uniform mix was achieved. The required amount of catalyst Phencat 15 (at 8% by weight of the total resin required in the mix), was added to the mixed fillers, and mixed for further five minutes.

The required weight of catalysed filler to form the first (i.e. bottom face) skin of the beam was weighed and transfered to a small mixer (i.e. Hobart Mixer). also, the required weight of catalysed filler to cast the control specimens was weighed and kept in a closed bucket, leaving the remaining material in the pan mixer for the final mix for the beam.

Before any casting operation, the foam and the fibre glass mat were cut to the required shape and dimensions. The fibre glass mat consisted of three sections, one to be used on extreme inner faces of the beam sides to be wraped around the foam, other to be used on the extreme outer faces of the bottom and two side skins with the last section to be used on the outer face of the top skin. The amount of resin (J2018L) and its corresponding acid catalyst (Phencat 10) for hand lay up lamination (wetting) of these fibre glass mats were all carefully measured and kept in individual containers. The resin and catalyst for hand lay up were brought together and mixed as required by means of a stirrer. The wetting out of the fibre glass mat was achieved using a brush and a roller which enabled catalysed resin to soak into the chopped strand mat uniformly.

After the first section of glass mat was wetted, it was wrapped around the cut foam and gently rolled on with a little hand pressure using the roller to release any trapped air bubbles. This was then left over an hour to set. The second section of glass mat was placed in the mould, covering the bottom and two side faces of the mould. The required catalysed resin was then applied, in the same manner as

explained above. At this stage the pre-weighed phenolic resin J50/010L was added to the catalysed filler in the 'Hobart' mixer and mixed for a period of two minutes. This Phenolic Concrete mix was then poured into the mould over the laminated fibre glass mat and vibrated to remove any trapped air. With the aid of a pre-made wooden screed the poured mix was levelled and formed the required thickness of the first skin of the beam. The cut foam wrapped in pre-laminated fibre glass mat was then placed over the first skin, maintaining equal clearances in all directions from the mould. For this purpose spacers made up of pre-cured laminated fibre glass mats were placed at either ends of the mould. These spacers were also used as guides in positioning the longitudinal steel bars in the internally reinforced Phenolic Concrete beams. This process was followed by mixing the remaining catalysed filler in the pan mixer with the required amount of phenolic resin (J50/010L) for two minutes. The remaining and final mix was poured carefully into the mould and vibrated in stages until all the spaces were filled and air bubbles removed. The top skin was screeded and levelled, and final laminated glass mat section was laid on the top face. A flat sheet of plywood ($25mm$ thick), lined with Melinex release sheet with mould releasing agent (Freecoat) sprayed over it, was placed on top surface. Pressure by means of weights was applied to this flat wooden sheet to assist setting of the Phenolic Concrete beam subject to pressure. This pressure insured proper bonding of the Phenolic Concrete matrix with the laminated glass mat.

In internally reinforced beams, the steel bars were carefully cleaned with grease free steel brushes and grease removing agent prior to casting. For ease of casting, in shallow beams the tension face with steel bars was cast upper-most in the mould, and in deep beams it was cast to the side.

At all stages, prior to the mixing of the catalysed filler with phenolic resin, the

temperature of the catalysed filler was noted and decreased or increased in order to have a constant temperature of $15 - 17°C$, and thus to have constant activating time in casting the beams. Photographic evidence of beam construction is given in Plates 5.1, 5.2, 5.3, and 5.4.

The control specimens were all constructed accordingly from random catalysed constituents kept from beam mixes.

Each beam and also the control specimens were kept in the mould for a period of 24 hours subject to pressure while setting before being stripped. All the test specimens were transferred to an industrial site where a large oven was available. They were placed and cured in the oven for a period of three hours at $120 \pm 5°C$.

5.6. Test Rig, Instrumentation and Test Procedure

The general loading arrangement of the test beams is illustrated in Figure 5.3 . The experimental Phenolic Concrete beams were tested in a loading frame with a capacity of 200tons. The loading was applied by a hydraulic ram, driven by a Denison Testing Machine (Model TLB). An electro mechanical load cell was situated immediately below the hydraulic ram with the casing of the ram being mounted on a bearing suspended from the spreader beam of the loading frame. Mounted immediately below the load cell, was a universal bearing thus allowing unrestrained rotation and translation to take place at the loading position.

The beams were supported at their ends on two steel support rollers suspended from the loading frame, with an effective span of 1.35m. The beams were tested in four point loading. The load was transferred to the beams through a steel load spreader rested on two steel loading rollers, each 25mm in diameter and 210mm long, positioned across the beam width at 310mm centre to centre. Each loading

roller was positioned at 165mm away from beam centre.

The positions of the loading and the support points on each beam relative to its centre were marked carefully prior to preparation for testing.

The vertical deflections at mid-span and at the loading points were measured using three dial gauges. These gauges were located centrally at the bottom (Tension) face of the beam at pre-marked positions. Strains in Phenolic Concrete over the depth of the beams, at mid-span were measured using a 150mm demec gauge. The position of the dial gauges and demec studs are illustrated in Figure 5.3 .

The beams were loaded by lowering the hydraulic ram onto the steel load spreader. With the load cell being connected to a Direct Reading Transducer Meter, the applied load was controlled and measured. Because of its original calibration the load was incremented in pounds at constant intervals. Two load cells of capacity 10000lb and 25000lb were used as required, with their calibration being confirmed regularly. Each load increment was maintained for a short period of time for dial gauges to become steady while recording the deflections and strain readings. As the pre calculated ultimate failure load was approached, the dial gauges were removed and loading was continued at a slow rate until failure occurred. Sustained load at failure and the type of failure were recorded. At cracked sections, the steel bar reinforcement of the beams was examined for any slip as well as the bond between laminated glass mat and that of Phenolic Concrete Matrix. Failed beams were then cut at three sections along the beam length and the appropriate cross-sectional dimensions measured using a micrometer (see Table 5.1). The photographic evidence of beam tests is given in Plate 5.5, with beam sections after failure in Plate 5.6 .

5.7. Discussion of Test Results

5.7.1. Introduction

In sections 5.4 and 5.6, the readings recorded during the tests are described. The test beam dimensions and schedules, theoretical and experimental properties of the test beams (uncracked sections) together with their failure criterion are presented in Table 5.1 and Table 5.2 respectively. The theoretical calculations are based on the derived equations in Appendix A2, in conjunction with material properties obtained from testing the control specimens.

The experimental deflection, and the theoretical deflections computed for each beam at corresponding applied loads, are shown in Tables A2.2a to A2.2l. In these tables, the deduced neutral axis positions at all loads from measured strain results, with computed values for the moment-curvature relationship and their derived deflection values for the test beams, are also shown.

Theoretical and experimental load-deflection curves, with their computed values of slopes (W/y) over the elastic regions, are presented in Figures 5.8a to 5.8l.

The neutral axis variation of the test beams shown by strain distribution profiles of the Phenolic Concrete composite matrix over the depth of the beam sections at mid-span are illustrated in Figures 5.9a to 5.9f .

The moment-curvature curves for all the test beams are presented in Figures 5.10a to 5.10f .

5.7.2. Control Specimens

The stress-strain curves defining the control T-bone specimens in tension, (Figure 5.6), show brittle behaviour of the Phenolic Concrete matrix. This was also evi-

dent from the load-deflection curves, obtained from flexural testing of non-laminated coupon specimens, recorded on the paper-chart of the Instron 1195. The strain at fracture or deflection at rupture for the brittle Phenolic Concrete matrix is considerably smaller than that of the reinforced matrix with laminated fibre glass mat (e.g. refer to Figure 5.7, and Figure 5.6 respectively). When the brittle Phenolic Concrete matrix reinforced with laminated fibre glass mat is loaded, the matrix will crack long before the laminated fibre mat can be fractured. Even after cracking of the matrix, the composite continues to carry increasing tensile stresses. The peak stresses and the peak strains or deflections of the composite are far greater than those of the matrix alone, and during the inelastic range (between the first cracking and the ultimate peak) multiple cracking or possibly a restraining action of the widening of the developed cracks in the matrix, occurs before failure takes place. The stress- strain curves in tension and the load-deflection curves in flexure of the control specimens show that considerable increase in the toughness of the composite matrix (area under the curve) is obtained, compared with that of the brittle Phenolic Concrete matrix. It is clear that failure in this mode, results in the optimum performance of both the Phenolic Concrete matrix and the laminated fibre glass mat.

The observed failure modes of the flexural specimens (laminated coupon composites) which represented the faces of the actual test beams, suggested that failure is a tension failure. This criterion was later revealed from examination of the bending stress-strain curves for these coupons (Figures 5.5*a* to 5.5*f*). They show larger tensile strains develop in comparison to compressive strains, as failure approaches.

5.7.3. Failure of the Test Beams

All the test beams failed in sudden tension failure mode. The geometry in which the beams were designed clearly overruled possibility of compression failure. The ultimate tension face strains were well in excess of the compression face strains, thus allowing the tension failure to occur. From mid-span strain distribution over the beam section (Figures 5.9*a* to 5.9*f*) and corresponding load-deflection curves (Figure 5.8*a* to 5.8*l*), it became evident that the tension faces of the beams had undergone larger strains at the highest loads. This criterion and also the lower tensile strength possessed by the tension face, supports the likelyhood of a tension mode of failure.

The crack initiation was not visible due to the laminated fibre glass mat. The tension crack became apparent at very high load near failure. This is explained by the restraining action which the fibre glass mat provided on the partially cracked Phenolic Concrete matrix (i.e. the laminated fibre mat carried larger tensile strains before fracture). In all the internally reinforced beams, at failure the progressive deflection with no increase in sustained load indicated yielding of the internal tension steel bars. The failure of these beams was typical of an under reinforced section loaded in flexure. The main crack always developed across the width of the tension face almost at mid-span, widened with increasing applied load. At failure it extended vertically through the depth of the side ribs towards the compression zone.

The tension faces in reference beams series A-1 and B-1 underwent quite large strains with beams deflecting excessively at ultimate failure loads. The failure occurred with the sudden development of a tension crack accompanied by a loud fracture noise of the tension face, with a single crack propogating upwards over the side ribs towards the compression zone.

In beams series A-2 and B-2, both reinforced internally with $6mm\phi$ h.y.s. bars,

failure also occurred in the tension face in a similar pattern to the reference beams with the exception of the noise. The sudden tensile fracture of the tension face was followed by snapping of the longitudinal tensile steel reinforcement bars.

With beam series A-3 and B-3, both internally reinforced with $10mm\phi$ h.y.s. bars, failure again occured as sudden tensile fracture of the tension face. Only in beam series B-3 (deep beam) the sudden tensile failure was followed by snapping of the steel bar reinforcement, whereas in beam series A-3 (shallow beam) at failure the steel bars did not snap although large deformations were observed. Extensive shattering of the Phenolic Concrete matrix was observed in the vicinity of the tension crack at the fractured tension face of the beams. The cracked sections, in these beams (series A-3), were carefully examined for possible slip of the steel bars; but none was observed.

After failure, all the cracked beam sections were examined carefully and no debonding of the phenolic laminated fibre glass mat from the Phenolic Concrete matrix was observed. The tension crack on tension faces of all the beams had occurred in the maximum moment area of the beam, near to the mid-span (see Table 5.2). Predictably, the failure in the deep beam series occurred at higher failure loads than for the shallow beam series. They exhibited greater bending stiffness than the shallow beams.

5.7.4. First Crack Load

The loads (W_C) at which the first crack in the Phenolic Concrete of the composite beams occurred, were deduced from the experimental load-deflection curves and the neutral axis variation (strain profiles). These first crack loads for all the beams are given in Table 5.2 . In both series of the test beams, from deduced first

crack loads, it is evident that the delay in first crack is relatively increased due to the presence of the internal reinforcement when compared with that of the relevant reference beam. The delay of the first crack increases with increase in steel area. It is also evident that in the deep beam series the first crack is initiated at higher loads than those in relevant shallow beams. This is explained by the deep beams exhibiting greater bending stiffnesses than the shallow beams.

The theoretical first crack load in the Phenolic Concrete matrix based on uncracked transformed sections was calculated assuming that a uniform tensile stress distribution exists across the tension face of the beams. From comparison between the theoretical and the experimental values (see Table 5.2), it was revealed that, with the exception of beam A-1b, the theoretical first crack load (W_C) values are in close agreement with the experimental values. In the case of beam A-1b, the presence of a defect or fault in the Phenolic Concrete matrix is anticipated to have caused the first crack to appear at a fairly early stage of loading.

5.7.5. Ultimate Moment of Resistance

The ultimate failure of the test beams was due to tensile failure. The crack restraining capability of the laminated fibre glass mat incorprated in the test beams enabled the Phenolic Concrete matrix of the internally reinforced sections to remain intact until after the steel bars had yielded considerably and then snapped in most of the beams at failure. In the case of unreinforced sections (the reference beams), the Phenolic Concrete composite remained viable until the laminated fibre glass mat on the tension face fractured causing the ultimate failure of the section.

Therefore, the cracked transformed section method normally adopted in the analysis of a concrete section can not be used with these sections. As the earlier

failure of the Phenolic Concrete in tension does not occur in these composite sections, (as would be the case with a concrete section), the sections were considered partially cracked with maximum utilization of the tensile strength of the laminated fibre glass mat at failure.

In calculating the theoretical ultimate moment of resistance, for all the beams, the effect of the Phenolic Concrete composite in tension was considered (see Appendix A2). An empirical method based on the geometrical properties of the test beams made it possible to establish a relationship (see Figure A2.6) between the degree of the effect of the Phenolic Concrete composite in tension (i.e. the tension zone), with the relevant neutral axis position for all the beams. Using these relationships and a triangular stress distribution, the value of the tension zone coefficient (α) and hence the corresponding depth of the neutral axis at failure for each beam were obtained. In this way it was possible to calculate the moment of resistance of the relevant beam sections.

In the reference beams it was assumed that for the failure to occur, the stresses on the the tension face of the beams would reach the ultimate tensile strength of the laminated fibre glass mat. In the case of the internally reinforced sections, the theoretical analysis was based on the internal steel bars to have reached both their yield stresses and also their ultimate tensile strengths.

The theoretical ultimate moment of resistance of the test beams based on the above assumptions was in close agreement with the corresponding experimental values of the sustained ultimate moment at failure. The theoretical and experimental values of the moments at failure of the reference and internally reinforced test beams are presented in Table A2.1 .

5.7.6. Strain Distribution

The strains in the composite matrix, over the depth of the test beams were measured at mid-span as described in section 5.6 . Mid-span strain profiles of the test beams are presented in Figures 5.9a to 5.9f. From these diagrams it can be seen that all the beams, with the exception of deep beam series B-3, behaved as under reinforced sections with neutral axes position moving upwards into the compression zone as failure was approached. Strain profiles for deep beam series B-3 represent a balanced section.

From strain distribution profiles it is noted that, at a given loading level, the tensile strains are considerably reduced with increase in internal steel reinforcement in both series of the test beams.

In all the beams, the strain distribution profiles over the beam section at mid-span, showed a linear strain-distribution, becoming slightly non-linear only at higher loads when failure approached. This suggests that plane sections remained plane during the test. From these profiles, positions of the neutral axis depth over the beam sections at all loads, were deduced and tabulated in Tables A2.2*a* to A2.2*l*. The theoretical neutral axes depth of the uncracked transformed section for all the beams were found to be in a very close agreement with the relevant deduced neutral axis depth.

5.7.7. Deflection

The experimental and theoretical load-deflection curves for all the beams are presented in Figures 5.8*a* to 5.8*l*. From experimental curves it became evident that the test beams behaved in two stages. The first stage represented an elastic behaviour, with the second stage representing an inelastic behaviour (non-linear).

Theoretical deflection values were calculated using the well known bending theory. A relation was derived between the bending stiffness (EI) and the slope (W/y) of the linear part of the load-deflection curves, from which the flexural modulus values for each test beam was calculated (see Appendix A2.4.).

The observed neutral axis depth at all loads of the test beams was used in extrapolating the tension zone coefficient (α) from the Figure A2.6 and hence, the effective second moments of area of the relevant sections were calculated at all loads. The deflection values at mid-span and load points of the test beams were then calculated using the effective transformed sections, considering the effect of the tension zone contribution to the stiffness of the sections (see Appendix A2). The average values for flexural modulus obtained from testing control laminated coupon specimens were used in the calculations.

The linear sections of the load-deflection data were plotted using the best fit line method and then their slopes were computed; as shown in Figures 5.8a to 5.8*l*. A comparison between these slope values, shows the variation of the theoretical values in general, for shallow beams to be between 6% to 31% and for deep beams to be between 10% to 50% in excess of the experimental values. This consequently suggests an under estimation of the theoretical flexural stiffness of the beams. This variation is thought to be due to two reasons. Firstly, in the theoretical computation of the effective transformed sections, the effect of the laminated fibre glass mat was

not considered. Secondly, only one value of flexural modulus was used for all the beams. This value may well not represent the actual value for each individual beam. This is supported by the fact that the flexural moduli obtained by elastic analysis from the load-deflection results were found to be on average 9% in shallow beams and almost 23% in deep beams less than the value used in theoretical calculations. Three flexural moduli values for each beam based on elastic analyses using load-deflection curves were computed. These were from deflection results obtained at mid-span and two loading point positions on the beams. The average value from the three flexural moduli values and their relavant load-deflection slope values are given in Table 5.2.

However, the theoretical and experimental load-deflection curves show a very close trend over the elastic regions. In non-linear parts of these curves, the theoretical and experimental deflection values, specially those of deep beams, differ by larger amounts. This could well be due to the possible local buckling of the side walls in the deep sections.

The presence of the laminated fibre glass mat prevented the visual inspection and determination of the degree of the developed cracks in the Phenolic Concrete matrix while contributing its tensile strength to the stiffness of the composite section. The crack restraining capability of the fibre glass mat may have caused the Phenolic Concret matrix to have developed excessive scattered tension cracks, as it can be seen from the fluctuation of the experimental load-deflection graphs, thus resulting in a reduction in the stiffness and an increase in the deformation of the composite beam subject to bending. This may also be the possible reason to some extent for the inconsistencies between the theoretical and the experimental deflection values over the non-linear sections observed in the load-deflection graphs.

Provision of the internal tension reinforcement increased the flexural stiffness of the beams at all loads, and consequently reduced deflections at corresponding loads. In shallow beams the increase in flexural stiffness was 6% and 68% for beams with $6mm\phi$ and $10mm\phi$ h.y.s. bars respectively. The increases in deep beams were 44% and 55%. Change of geometry from shallow to deep beam had also considerable effect on increase in flexural stiffness. On average, the increase in flexural stiffness, for the reference beams from shallow to deep section, was 214%.

5.7.8. Moment-Curvature Relationship

The position of the neutral axis (zero strain surface) is usually determined from strains measured on the surface of the beam compression and tension zones. Assuming that the initially plane sections remain plane during the bending process, then the curvature can be geometrically calculated.

The relation between applied moment and curvature is derived in Appendix A2.5 . The moment-curvature relationship is adopted in computing the bending stiffness of the test beams at all applied moments. The relevant beam deflections are then computed from bending theory using these stiffness values for corresponding beams (see Tables A2.2*a* to A2.2*l*).

In most of the approximate procedures available to compute deflections for uncracked sections under service loads, linearly elastic stress-strain curves are assumed for the brittle material in tension and in compression. For cracked sections, the tensile strength of the brittle material is neglected, while the material in compression is considered linearly elastic. Since most of the brittle material sections in a beam are partially cracked, transition values are required between these two extreme limits for deflection calculation. The moment-curvature relationship can be used for a more

accurate calculation of member deflections with material nonlinearities in tension and compression.

Extensive work has been carried out on moment-curvature theory in determining concrete member stiffness and hence deflections at all loading stages. Mathematical approaches have been made[104] in computation of moment- curvature relations adopting concrete nonlinearities in tension and compression. Stiffness equations for flexural members have been presented for computation of member deflections using a moment-curvature relationship[103]. Moment- curvature relationships have been developed in accurate assessment of r.c.beam sections ductility[104] by accounting for a curvature ductility factor method, which could be used in sesmic design.

In this work a simple moment-curvature relationship has been adopted in computation of Phenolic Concrete beam deflections. Limited available data did not permit the developement of model curves. However, from the measured strains of the Phenolic Concrete beams in their compression zones, and deduced positions of zero strain surfaces, the average curvature at all applied moments for all the beams were computed. A third degree polynomial was used in curve fitting of the data to present the moment-curvature relationship for the internally reinforced test beams (see Figures 5.10b,c,e,f). The flexural rigidity (stiffness) of the beams at all applied moments were determined from the linear elastic theory, using the slopes of the secants computed from the corresponding moment-curvature curves. For the reference beams the slopes of the moment-curvature graphs representing straight lines (see Figures 5.10a,d) over various stages of applied moments were used in determining their relevant flexural rigidity.

The flexural rigidity obtained for each beam (at all applied moments), was used in the deflection equations, (derived from bending theory Appendix A2.4.),

to compute the relevant deflections. These values are tabulated under moment-curvature relationship headings in Tables A2.2*a* to A2.2*l*. It is evident that the beam deflections computed from this method, even at higher applied moments, are in close agreement with the experimental mid-span deflection values, for all the beams.

It should be born in mind that curvature computation is very much dependent on strain measurements. The strains are affected by the position at which they are measured, the gauge length in which they are measured and also the elapsed time between loading and the strain measurements. It is therefore obvious that the strains measured in this work may be affected by inherent lack of precision and repeatability. For these reasons the simple method of analysis is adopted in computation of the flexural rigidity and hence deflection values are more of a qualitative representation than a strictly quantitative one.

5.8. Conclusions

In simple terms the work carried out justifies the use of a Composite Phenolic Concrete matrix reinforced with laminated fibre glass mat in the construction of cored box beams with thin faces. The technique by which the test beams were constructed proved to be reliable and repeatable.

The limited number of tests, described in this work, have been concerned with the behaviour of internally reinforced and unreinforced Composite Phenolic Concrete box beams. From the behaviour of the box beams tested and the results obtained the following general conclusions can be drawn. It is emphasised that the following statements are based on elastic calculation and test observation.

1. At lower loads the beams behaved as box beams exhibiting elastic behaviour.

Their behaviour can be predicted from simple elastic theory.

2. The beam experiments demostrate that, due to the technique of construction and also the geometry of the beams, the comparative properties of the foam to the phenolic matrix are not of importance in formation of the beam core. The core can be made of any foam type in so far as it remains stiff enough to prevent local buckling of the thin faces.

3. It was seen that full composite action was achieved between the phenolic laminated fibre glass mat and the Phenolic Concrete matrix up to failure. The fibre glass mat used as reinforcement on the beam faces provided an adequate dispersion of reinforcement with an excellent bond and ease of application. It also introduced a good degree of ductile behaviour to the brittle Phenolic Concrete matrix.

4. Internal steel reinforcement bars made a significant contribution to the ultimate strength of the beams, in both series. They increased the stiffness of the beams in all cases. The strength enhancement was increased relatively with the percentage of internal reinforcement. This increase in strength was relatively higher with deep beams. At failure it was revealed that good mechanical bond had been achieved between Phenolic Concrete and the steel bars.

5. Bending theory can be applied to predict the first crack load in the Phenolic Concrete matrix. The first cracks in the test beams were not apparent due to the restraining action of the laminated fibre glass mat on the beam faces. The cracks became obvious due to the fracture of the glass mat at higher loads as failure was approached. This delay in visual crack appearance of the beam has the disadvantage that it masks any visual display of the crack until the beam is near to fracture. However, it demonstrates optimum performance of the Phenolic Concrete and laminated fibre glass mat.

The crack initiation, in the Phenolic Concrete matrix of the internally reinforced beams, was delayed due to presence of internal bars. This was relatively increased in deep beams.

6. From the strain distribution in the Phenolic Concrete composite over the beam depths, it was seen that internal reinforcement reduced the tensile strains in the composite. The reductions in tensile strains were relatively increased with increase in internal steel bar areas. The strain distribution profiles showed that plane sections remained plane through the testing process.

In general the failure mechanism of both shallow and deep beams was similar. The deep beams, however, exhibited stiffer behaviour than shallow beams. The moment-curvature relationship obtained from strain analysis of the test beams, indicated that the stiffness of these box beams can be predicted even in the case of the cracked sections.

7. This work justifies the use of beams of this type in situations where similar sizes and strengths are appropriate such as the lintels and joists required in domestic construction.

Also, the success obtained with the beams, in construction, practical behaviour and analysis, justifies the expansion of the work to cover larger sections required in structural members such as longer span beams, columns and portal frames.

Table 5.1 (Dimensions and Schedules of the Test Beams.)

Test Beams	Beam Dimensions (mm)																Type of Foam	Internal Reinforcement
	B	D	B_f	D_f	T_t	T_b	T_{ls}	T_{rs}	W_{fl}	W_{fr}	H_{fl}	H_{fr}	W_{sl}	W_{sr}	H_{sl}	H_{sr}		
A-1a	204.0	97.0	167.7	68.6	12.2	16.2	19.3	17.0	....	....	....	....	....	....	....	....	Polyester	None
A-1b	204.0	97.0	169.3	68.1	14.9	14.0	18.4	16.3	....	....	....	....	....	....	....	....	Polyester	None
A-2a	202.0	97.0	179.8	72.2	8.3	16.6	10.3	11.9	17.7	27.1	32.5	25.2	15.0	18.0	12.0	11.0	Polyester	$2 \times 6mm\phi$ H.Y. Steel Bar
A-2b	202.0	97.0	167.8	68.9	15.4	12.7	14.8	19.4	21.2	17.7	27.9	30.2	17.0	20.0	25.0	21.0	Polyester	$2 \times 6mm\phi$ H.Y. Steel Bar
A-3a	203.0	97.0	173.0	69.1	15.8	12.1	15.5	14.5	23.5	28.5	28.6	23.6	17.0	17.0	24.0	20.0	Polyester	$2 \times 10mm\phi$ H.Y. Steel Bar
A-3b	203.0	97.0	170.0	68.6	16.1	12.3	15.8	17.2	21.2	18.8	27.8	29.5	25.0	25.0	18.0	16.0	Polyester	$2 \times 10mm\phi$ H.Y. Steel Bar
B-1a	97.0	204.0	70.2	172.9	13.8	17.3	10.3	16.5	....	....	....	....	....	....	....	....	Phenolic	None
B-1b	97.0	204.0	69.7	169.5	18.6	15.9	12.1	15.2	....	....	....	....	....	....	....	....	Phenolic	None
B-2a	97.0	205.0	67.1	171.9	14.1	17.0	8.0	21.9	15.1	22.1	26.4	27.1	20.0	18.0	16.0	24.0	Phenolic	$2 \times 6mm\phi$ H.Y. Steel Bar
B-2b	97.0	205.0	68.4	172.9	18.0	14.1	12.6	16.0	19.4	16.0	29.2	31.1	22.0	16.0	16.0	28.0	Phenolic	$2 \times 6mm\phi$ H.Y. Steel Bar
B-3a	98.0	206.0	69.0	169.3	20.1	16.6	14.9	14.1	17.1	15.9	30.6	31.2	24.0	19.0	20.0	23.0	Phenolic	$2 \times 10mm\phi$ H.Y. Steel Bar
B-3b	98.0	206.0	66.8	168.0	14.9	23.1	15.2	16.0	14.8	17.0	31.7	30.6	18.0	18.0	21.0	15.0	Phenolic	$2 \times 10mm\phi$ H.Y. Steel Bar

Note: See Figures 5.1 , 5.2 and 5.3 for beam dimensions.

All the dimensions are the average measurments taken from 3 cross-sections for each beam.

Table 5.2 (Test Beams)

Test Beam	Uncracked Section									Sustained Load at Failure (W_F) (lb)	Mode of Failure
	N.A.Depth (Y)		2nd Momt. of Area Uncracked Section $I_{uc} \times 10^{-4}$ (m^4)	Load at first Crack (W_C)		Experimental Load - Deflection					
	Theoretical (mm)	Observed (mm)		Theoretical (lb)	Observed (lb)	($W/\ y_c$) ($N.mm^{-1}$)	($W/\ y_{l1}$) ($N.mm^{-1}$)	($W/\ y_{l2}$) ($N.mm^{-1}$)	Flexural Modulus $E_{fg} \times 10^9$ ($N.m^{-2}$)		
A-1a	51.28	51.00	0.1089399	1711	1500-1700	2503	2592	2527	10.43	3500	Tension Failure T.C. @ 90mm from ctr.
A-1b	47.87	47.00	0.1105414	1616	800-1000	2178	2322	2273	9.14	3450	Tension Failure T.C. @ 100mm from ctr.
A-2a	60.36	61.50	0.0997412	1955	2000-2200	2115	2239	2233	9.71	5900	Tension Failure T.C. @ 110mm from ctr.
A-2b	50.40	49.00	0.1189193	1833	1700-1800	2741	2946	2956	10.81	5050	Tension Failure T.C. @ 150mm from ctr.
A-3a	53.29	52.50	0.1265452	2079	1500-2000	3836	4227	4208	14.45	7550	Tension Failure T.C. @ 140mm from ctr.
A-3b	53.83	54.94	0.1319631	2195	1500-2000	3832	4063	4015	13.40	7500	Tension Failure T.C. @ 80mm from ctr.
B-1a	104.78	105.50	0.3829149	2772	2000-2500	7202	7558	7447	8.64	6200	Tension Failure T.C. @ 35mm from ctr.
B-1b	100.00	103.00	0.4028606	2865	2000-2500	7458	7863	7641	8.49	7500	Tension Failure T.C. @ 120mm from ctr.
B-2a	114.30	110.00	0.4750926	3856	3000-3500	11852	12280	12218	11.40	10000	Tension Failure T.C. @ 35mm from ctr.
B-2b	110.20	110.65	0.4827139	3657	3500-4000	11479	11935	11780	10.86	12000	Tension Failure T.C. @ 85mm from ctr.
B-3a	119.56	123.70	0.5754929	4782	4000-5000	11808	12262	12066	9.36	18000	Tension Failure T.C. @ 50mm from ctr.
B-3b	124.94	123.35	0.5712551	5062	4000-5000	11159	11717	10742	8.77	17500	Tension Failure T.C. @ 10mm from ctr.

Note: T.C.= propagated tension crack at failure.

Experimental W_C are deduced from N.A. variation(i.e. Strain Diagrams) and also Load-Deflection graphs.

Flexural Modulus for each beam is averaged from three calculated values obtained from the slopes of the Load-Deflction graphs at ctr. point and Ldg. points.

Table 5.3 (Results from Flexural Testing of the Coupon Specimens)

Coupon Specimen	Fibre Glass Type	Av. Thickness d (mm)	I_{xx} $\times 10^{-12}$ (m^4)	Sustained Loads at: Onset of Crack W_C (N)	Sustained Loads at: Failure W_F (N)	Ult. Flexural Strength $\sigma_{Fu} \times 10^6$ ($N.m^{-2}$)	Deflection Measurments: Slope W/y ($N.mm^{-1}$)	Deflection Measurments: Flexural Modulus $E_{Fg} \times 10^9$ ($N.m^{-2}$)	Strain Measurments: Compressive Modulus $E_{Cg} \times 10^9$ ($N.m^{-2}$)	Strain Measurments: Tensile Modulus $E_{Tg} \times 10^9$ ($N.m^{-2}$)	Ratio $(E_{Fg})/(E_{Tg})$
1A	$450g.m^{-2}$ P.B. Supermat	10.61	9962.63	500.0	1400.0	41.93	120.9	11.52	10.65	12.09	0.95
1B		10.98	11031.28	500.0	1435.0	40.17	134.3	11.56	11.14	13.13	0.88
1C		10.54	9757.53	500.0	1400.0	42.53	130.1	12.66	9.51	13.63	0.93
1D		9.45	7032.52	500.0	1550.0	58.58	105.1	14.18	12.34	15.90	0.89
1E		10.76	10381.39	500.0	1480.0	43.09	138.1	12.63	10.00	13.63	0.93
1F		10.80	10497.60	500.0	1580.0	45.72	132.9	12.02	10.81	13.20	0.91
2A	none	7.80	3954.60	455.0	455.0	25.24	90.0	21.60	$E_{Fg} = C \times (W/y) \times (1/I_{xx}) \times 10^3$		
2B		7.76	3894.07	440.0	440.0	24.66	88.0	21.45	$C = 949218.75 \times 10^{-9}$ (m^3)		
2C		7.55	3586.41	430.0	430.0	25.46	86.0	22.76	$\sigma_{Fu} = \bar{y} \times (M_F/I_{xx}) \times 10^{-3}$		
2D		7.90	4108.66	440.0	440.0	23.79	88.0	20.33	$M_F = 0.5 \times (W_F) \times 0.1125$		
2E		7.72	3834.16	445.0	445.0	25.20	98.0	24.26	$\bar{y} = d/2$, $Z = (I_{xx})/\bar{y}$		
2F		7.64	3716.20	425.0	425.0	24.57	94.0	24.01	E_{Cg} or $E_{Tg} = (M/Z)/\epsilon$		

Table 5.4 (Results from Tensile Testing of the T-Bone Specimens)

T-Bone Specimen	Fibre Glass Type	Av. Thickness d (mm)	Av. Breadth b (mm)	c.s.a. $(b \times d)$ $\times 10^{-6}$ (m^2)	Ult. Failure Load W_F (N)	Ult. Tensile Strength $\sigma_{Tu} \times 10^6$ ($N.m^{-2}$)	Tensile Modulus $E_{Tg} \times 10^9$ ($N.m^{-2}$)
1A	$450g.m^{-2}$ P.B. Supermat	9.43	48.67	458.96	5600.0	12.20	13.62
1B		9.97	48.12	479.76	5180.0	10.80	12.31
1C		8.56	48.29	413.36	5300.0	12.82	13.13
1D		9.68	48.45	468.99	4970.0	10.60	13.16
1E		9.60	48.41	464.74	5200.0	11.19	14.74
1F		9.51	48.50	461.24	5800.0	12.58	13.97
2A	none	8.56	48.32	413.62	2700.0	6.53	15.54
2B		8.55	48.35	413.39	2800.0	6.77	14.24
2C		8.09	49.26	398.51	2800.0	7.03	18.30
2D		7.38	48.49	357.86	2500.0	6.99	16.41
2E		7.74	48.88	378.33	2600.0	6.87	16.26

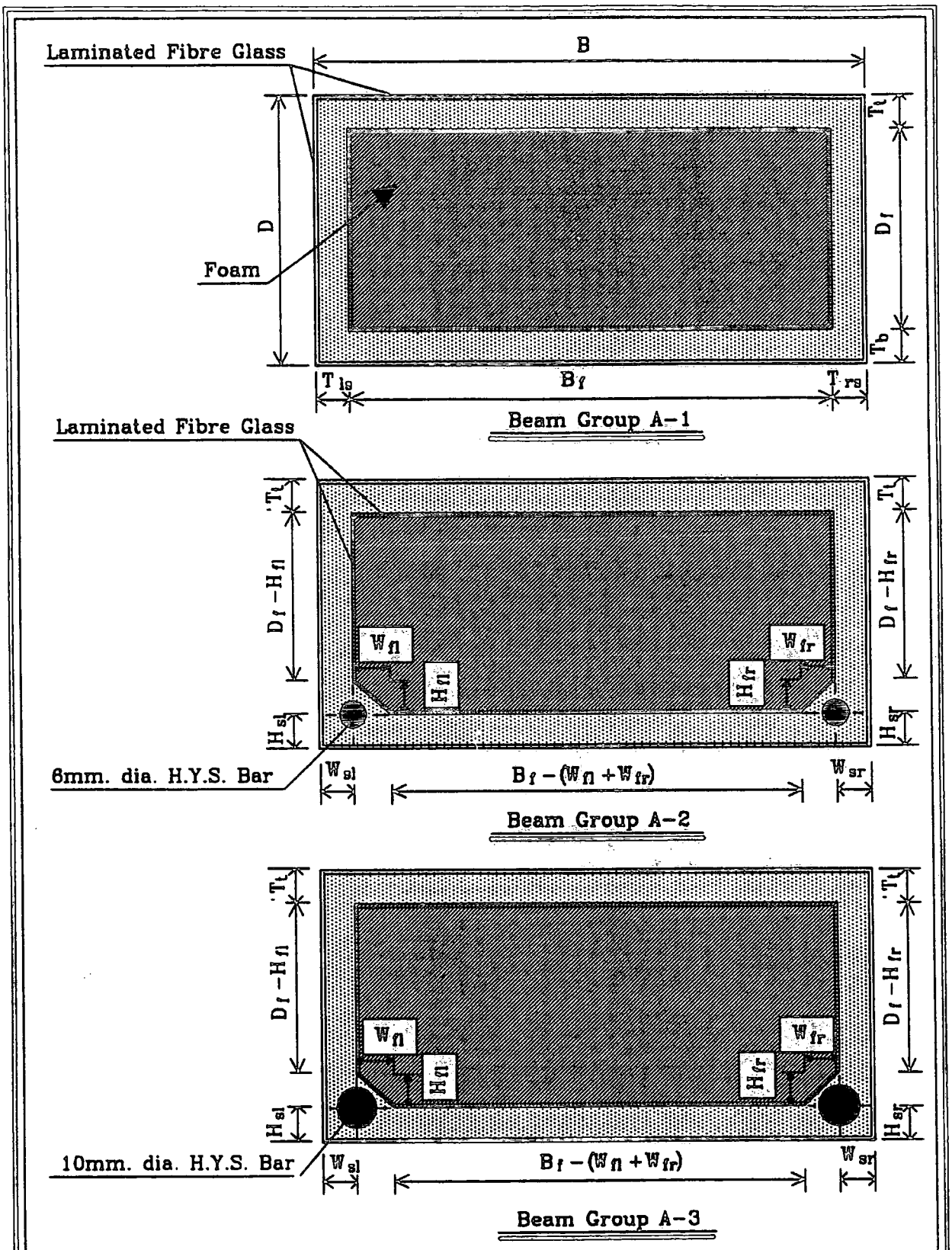

Figure 5.1 Cross-Sectional Schematic of Shallow Beam Series (A)

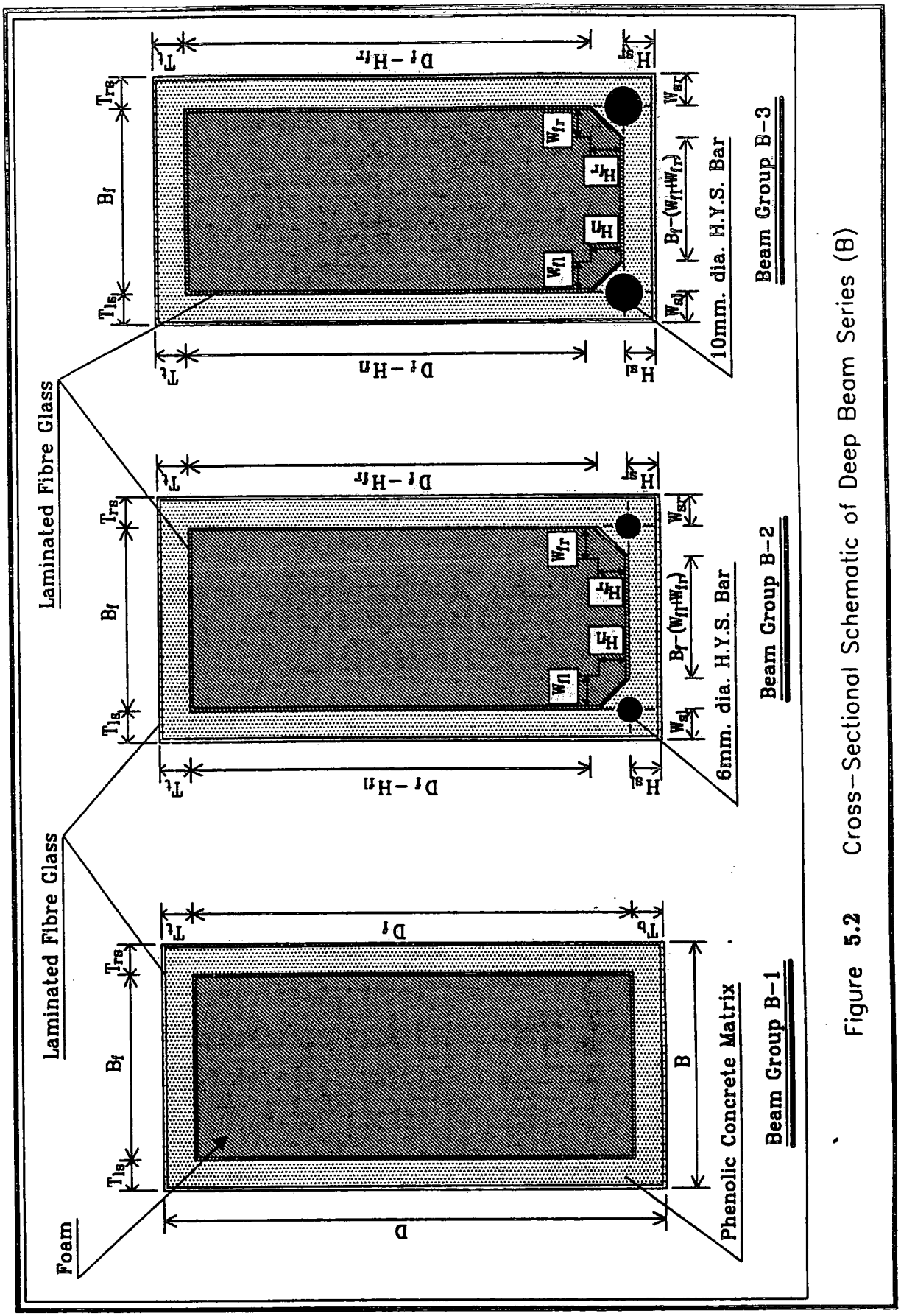

Figure 5.2 Cross-Sectional Schematic of Deep Beam Series (B)

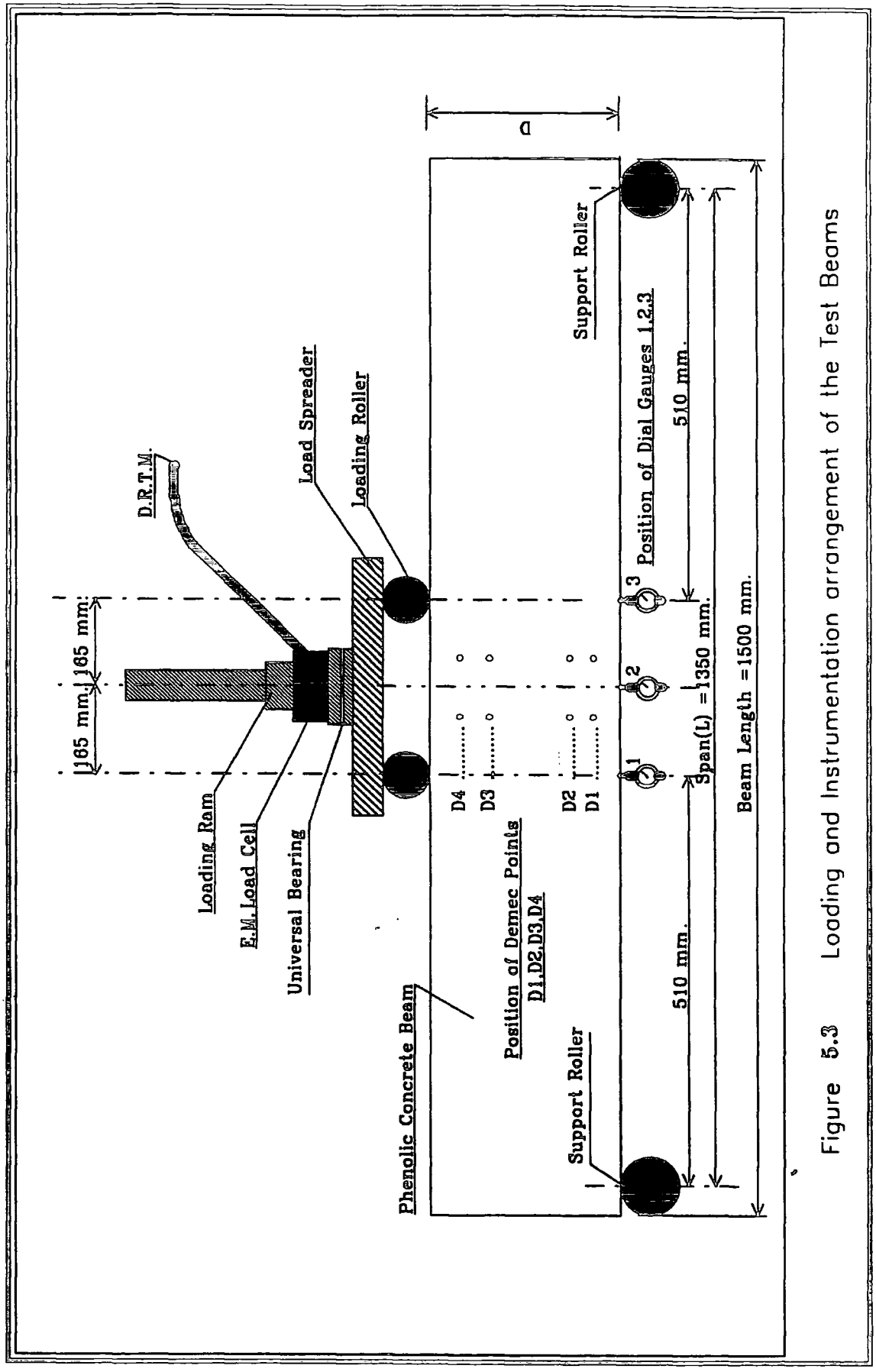

Figure 5.3 Loading and Instrumentation arrangement of the Test Beams

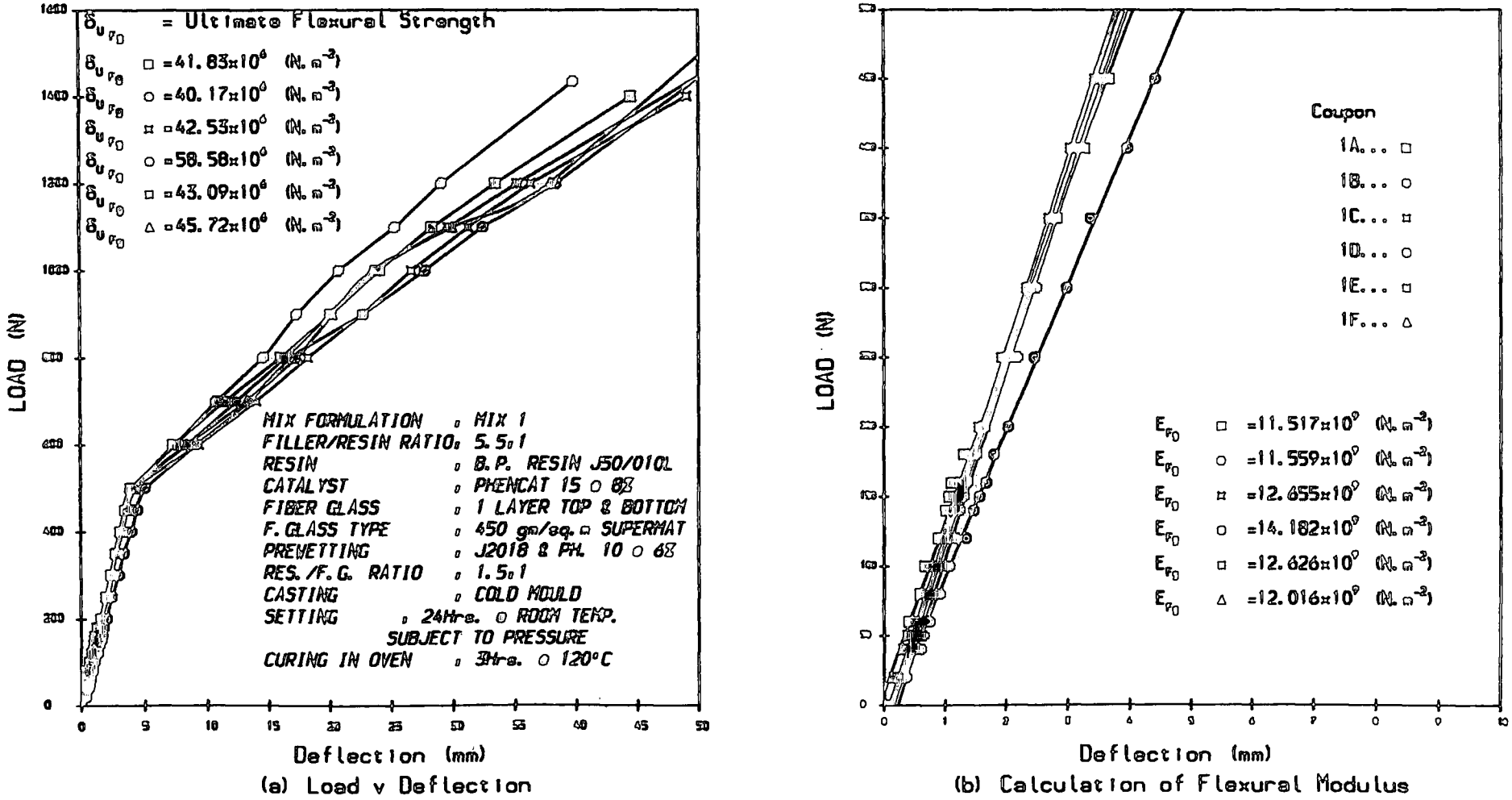

(a) Load v Deflection

(b) Calculation of Flexural Modulus

Fig 5.4 Flexural Testing of Coupon Specimens, with Laminated Fibre Glass on both faces, Subject to 4 point Flexural Loading. (Tested on Instron °1195°)

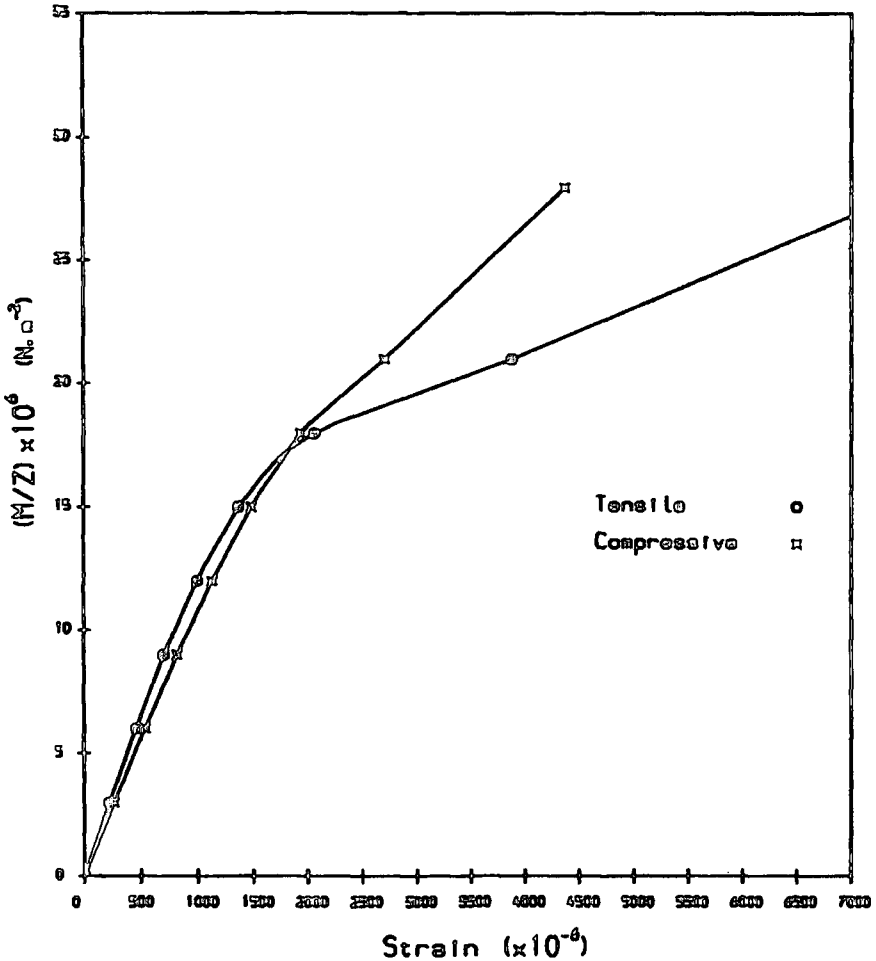

(a) Stress v Strain

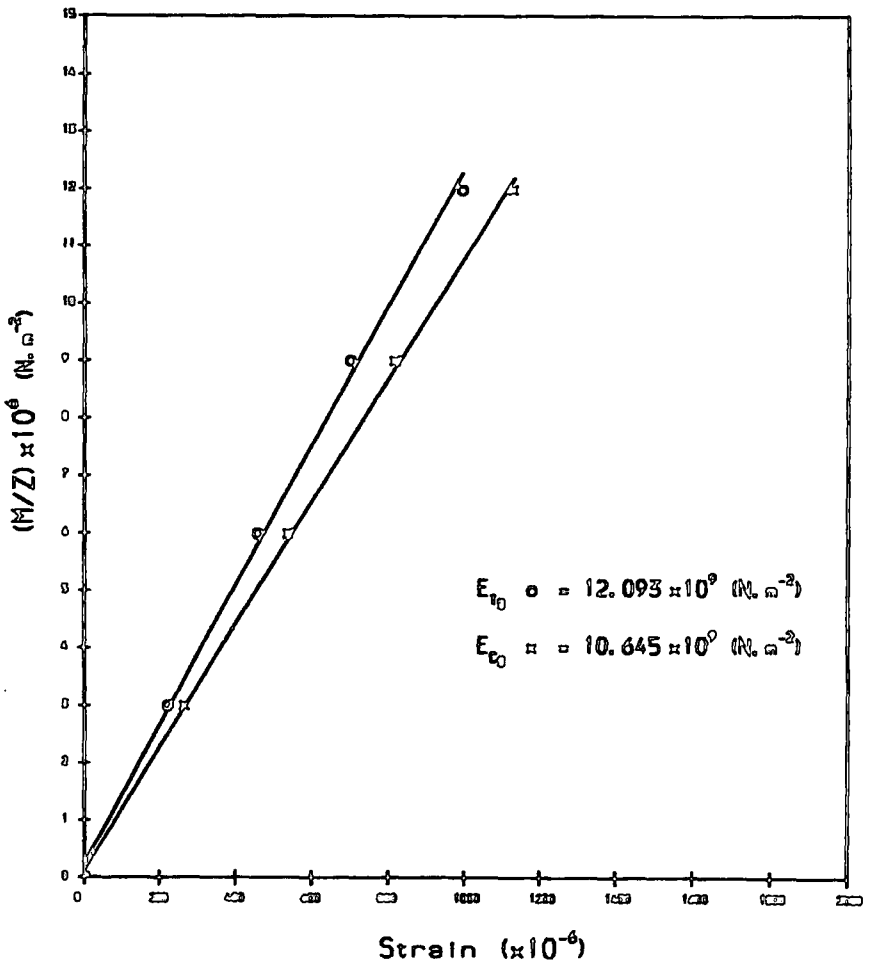

(b) Calculation of Tensile & Compressive Moduli

Fig. 5.5a Measured Strains on both faces of Laminated Coupon Specimen (1A) Subject to 4-Point Flexural Loading. (Tested on Instron "1195")

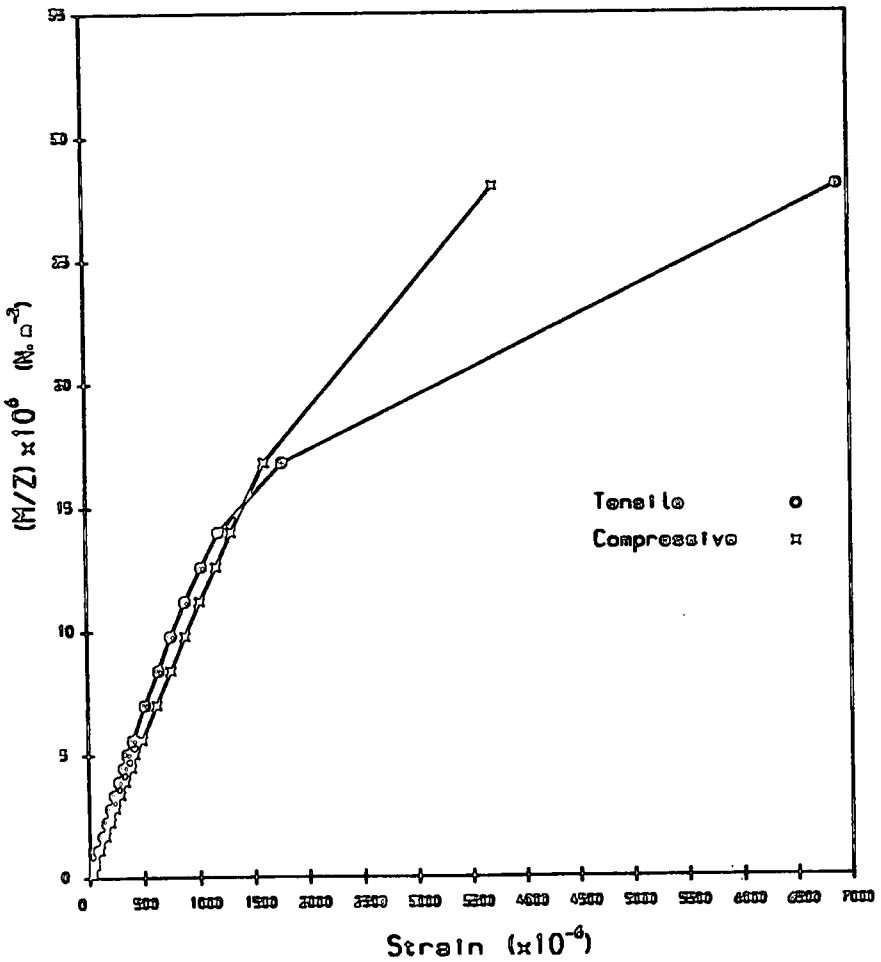

(a) Stress v Strain

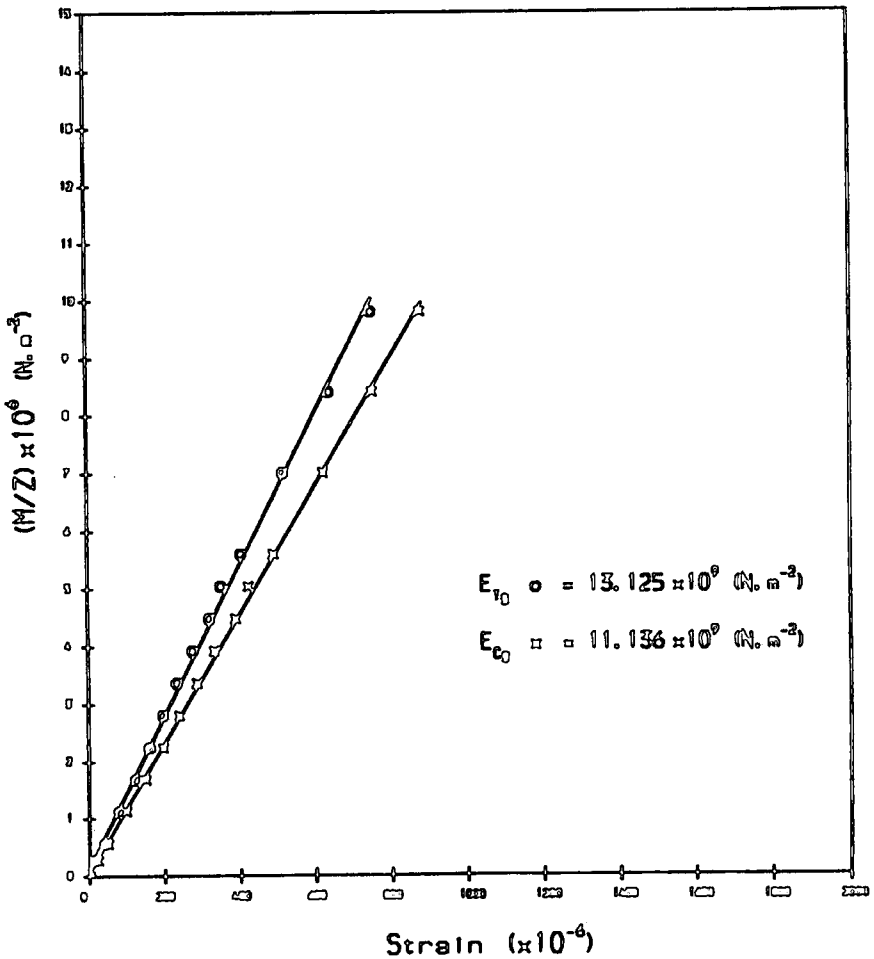

(b) Calculation of Tensile & Compressive Moduli

Fig. 5.5b Measured Strains on both faces of Laminated Coupon Specimen (1B) Subject to 4-Point Flexural Loading. (Tested on Instron °1195°)

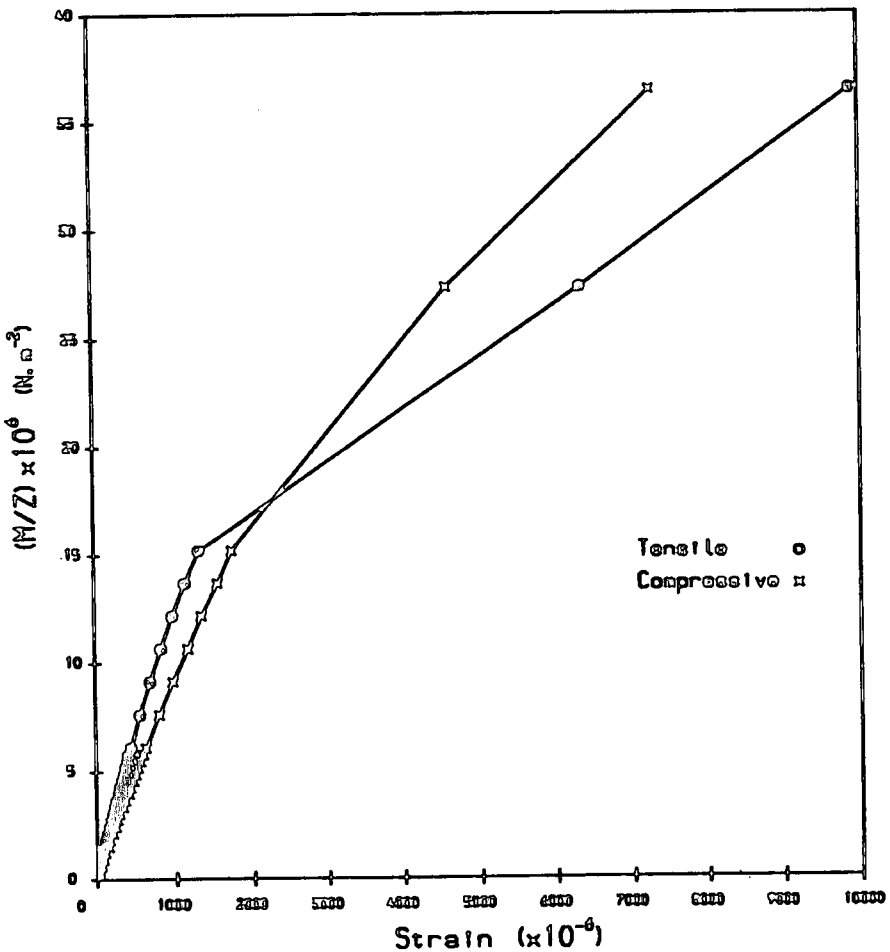

(a) Stress v Strain

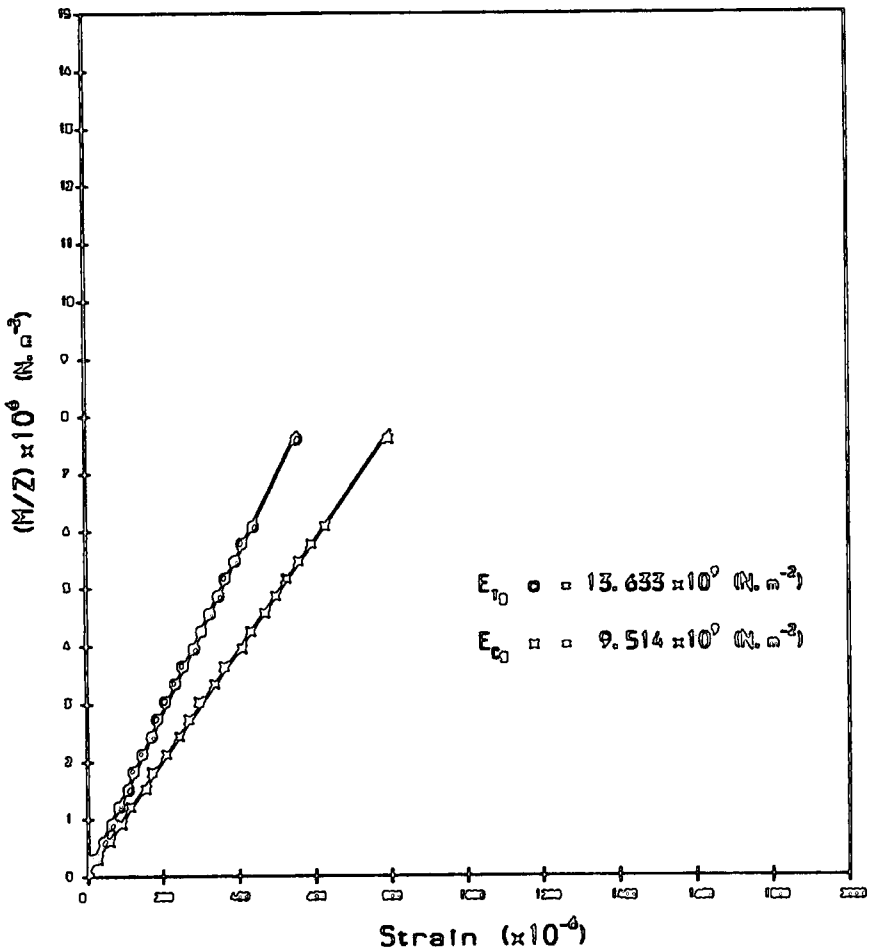

(b) Calculation of Tensile & Compressive Moduli

Fig. 5.5c Measured Strains on both faces of Laminated Coupon Specimen (1C) Subject to 4-Point Flexural Loading. (Tested on Instron °1195°)

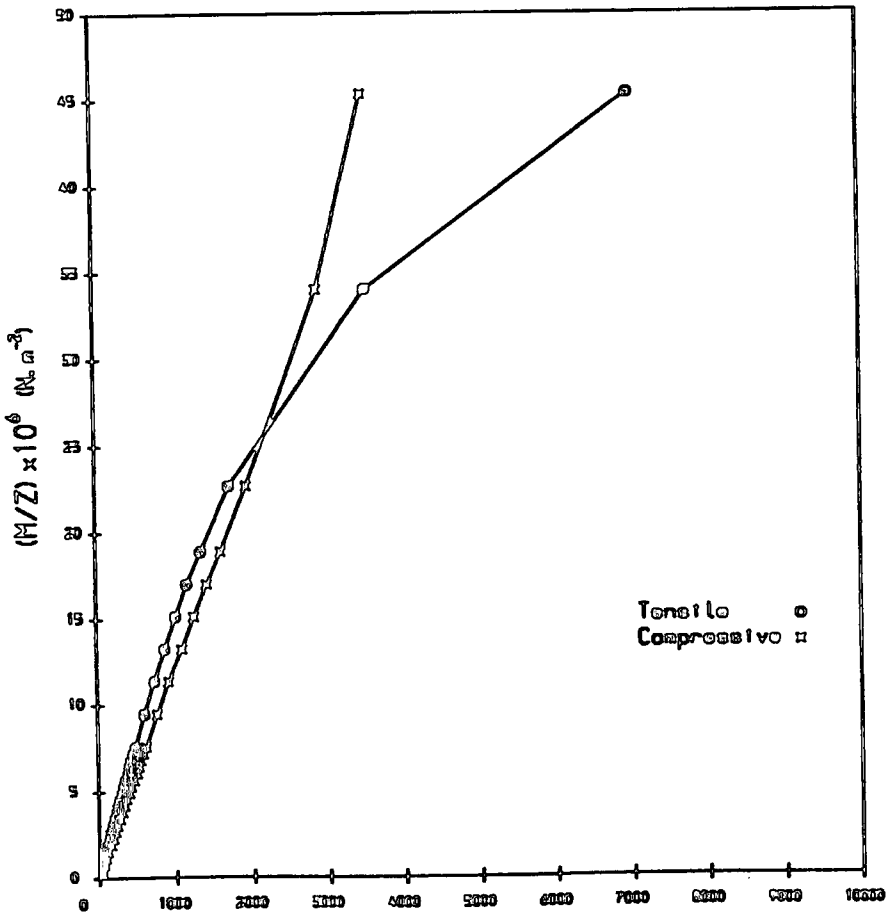

(a) Stress v Strain

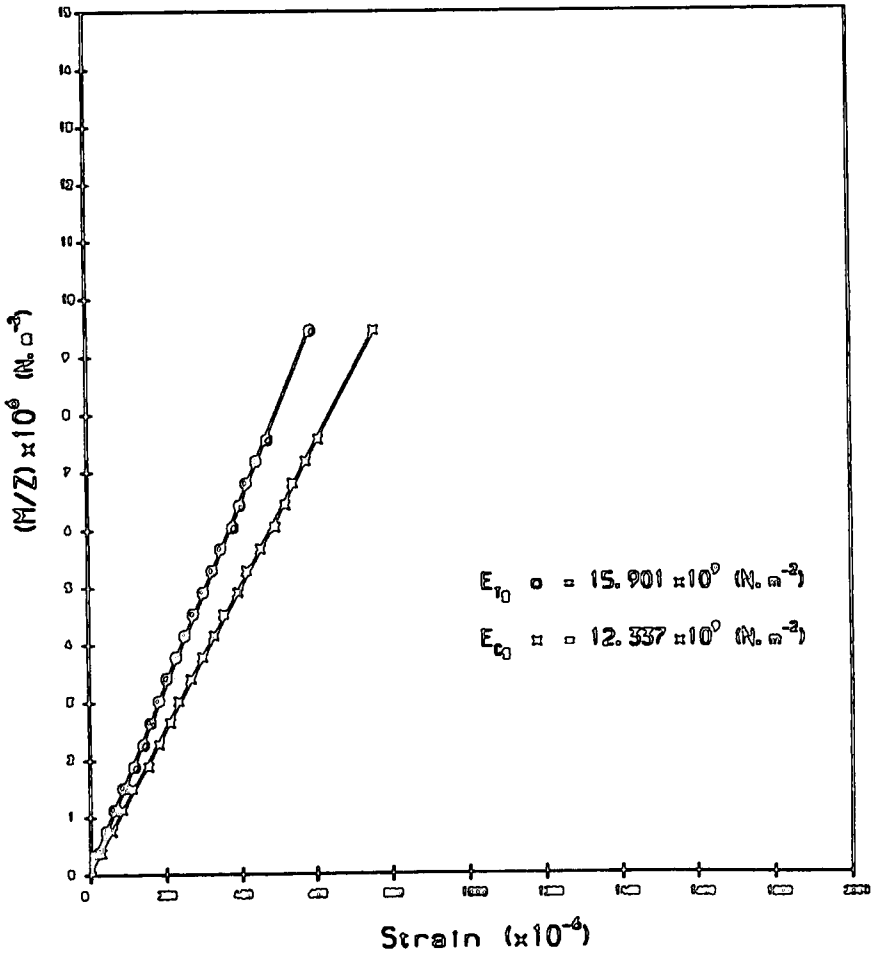

(b) Calculation of Tensile & Compressive Moduli

Fig. 5.5d Measured Strains on both faces of Laminated Coupon Specimen (1D) Subject to 4-Point Flexural Loading. (Tested on Instron '1195')

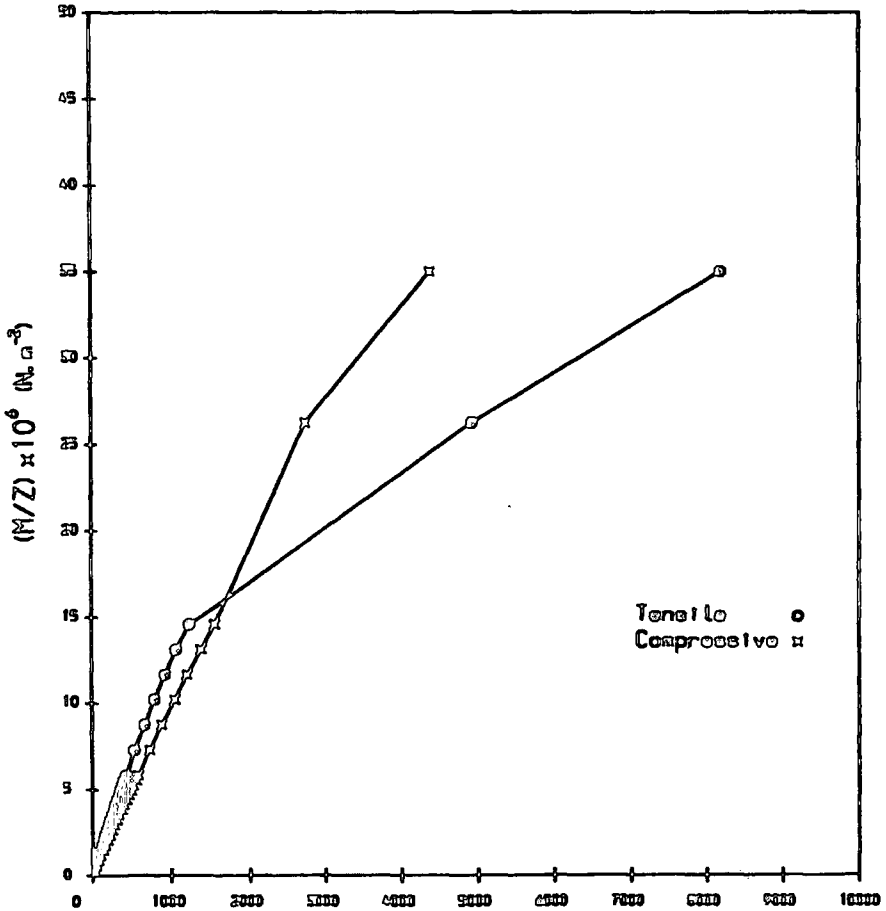

(a) Stress v Strain

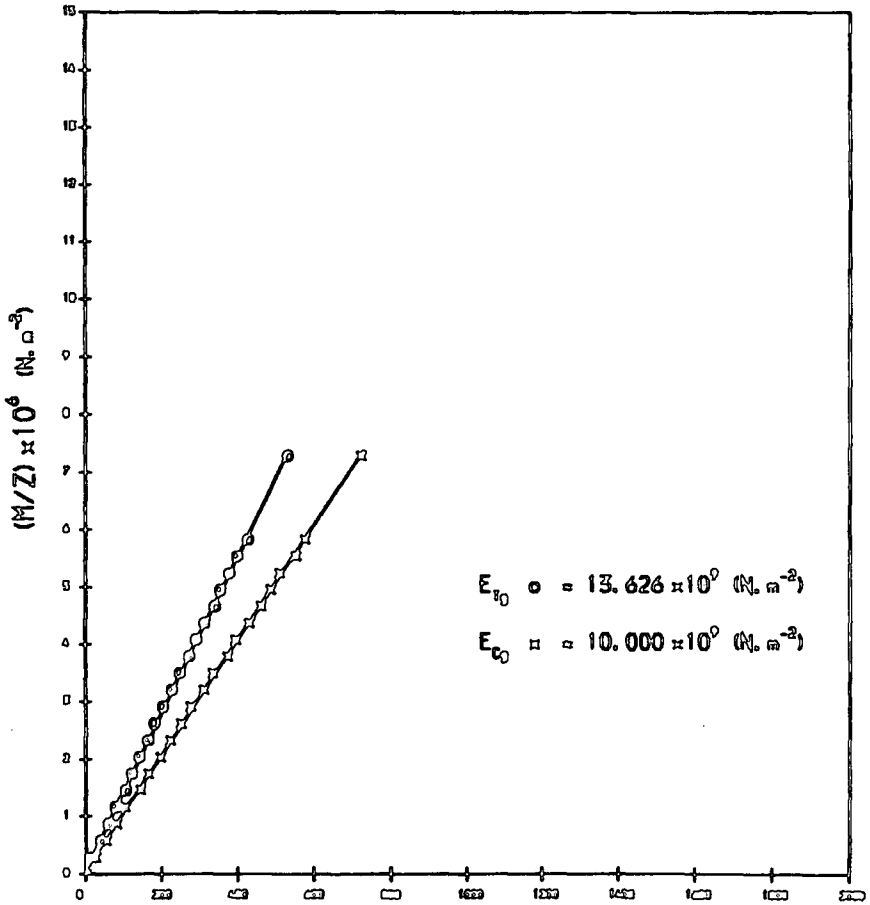

(b) Calculation of Tensile & Compressive Moduli

Fig. 5.5e Measured Strains on both faces of Laminated Coupon Specimen (1E) Subject to 4-Point Flexural Loading. (Tested on Instron '1195')

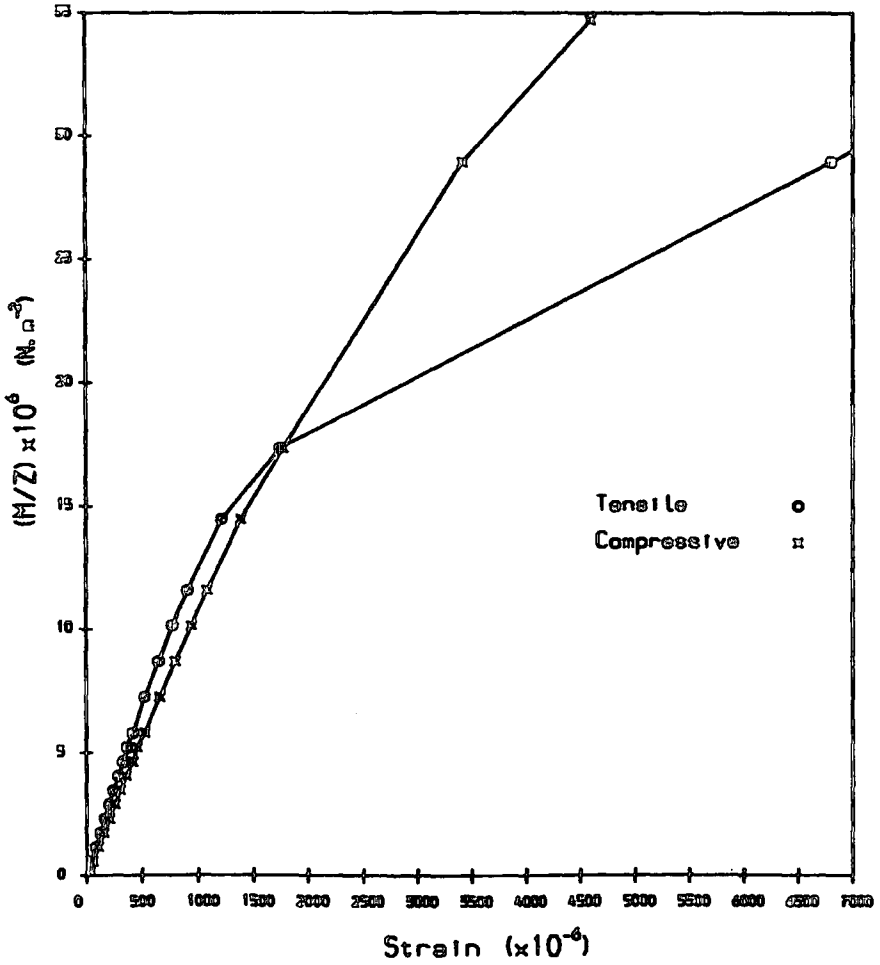

(a) Stress v Strain

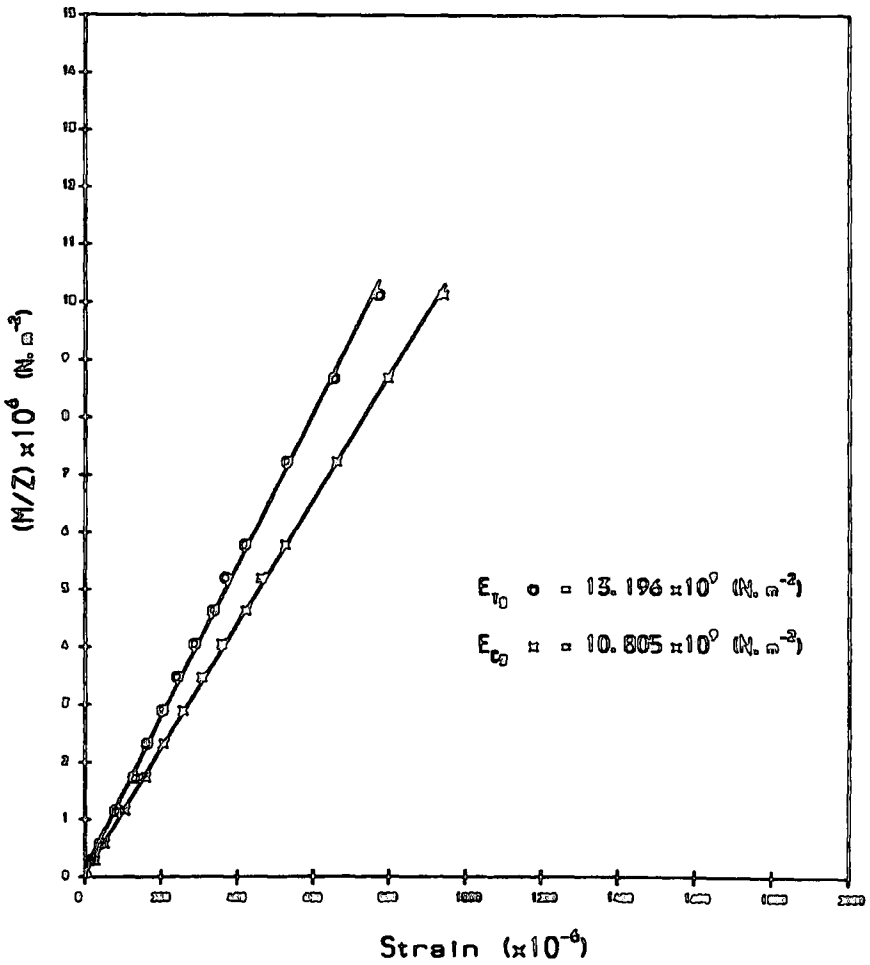

(b) Calculation of Tensile & Compressive Moduli

Fig. 5.5f Measured Strains on both faces of Laminated Coupon Specimen (1F) Subject to 4-Point Flexural Loading. (Tested on Instron °1195°)

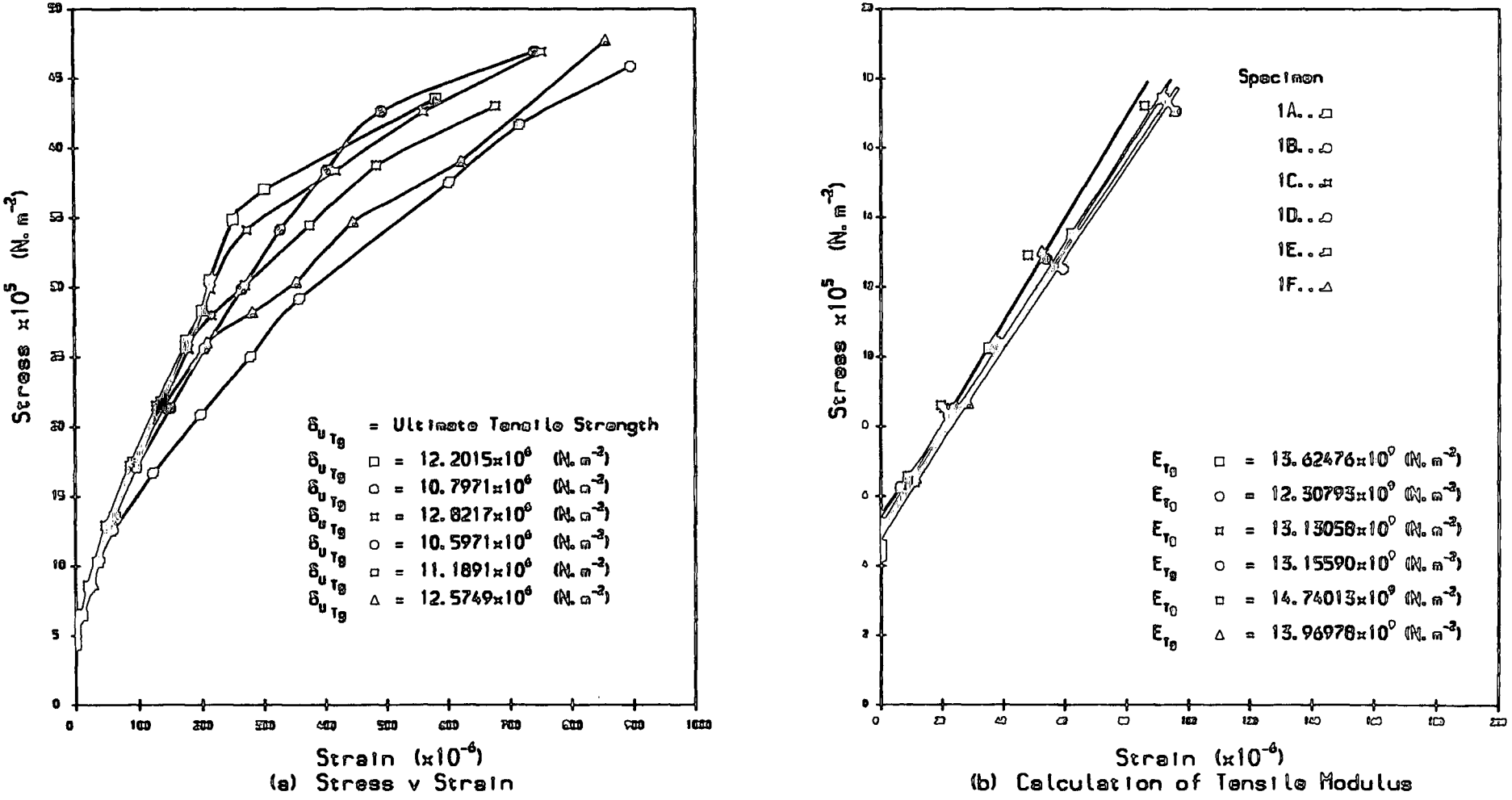

(a) Stress v Strain

(b) Calculation of Tensile Modulus

Fig. 5.6 Tensile Testing of T-Bone Specimens, with Laminated Fibre Glass on both faces, Subject to Direct Tensile Test. (Tested on Denison Model "T42B4")

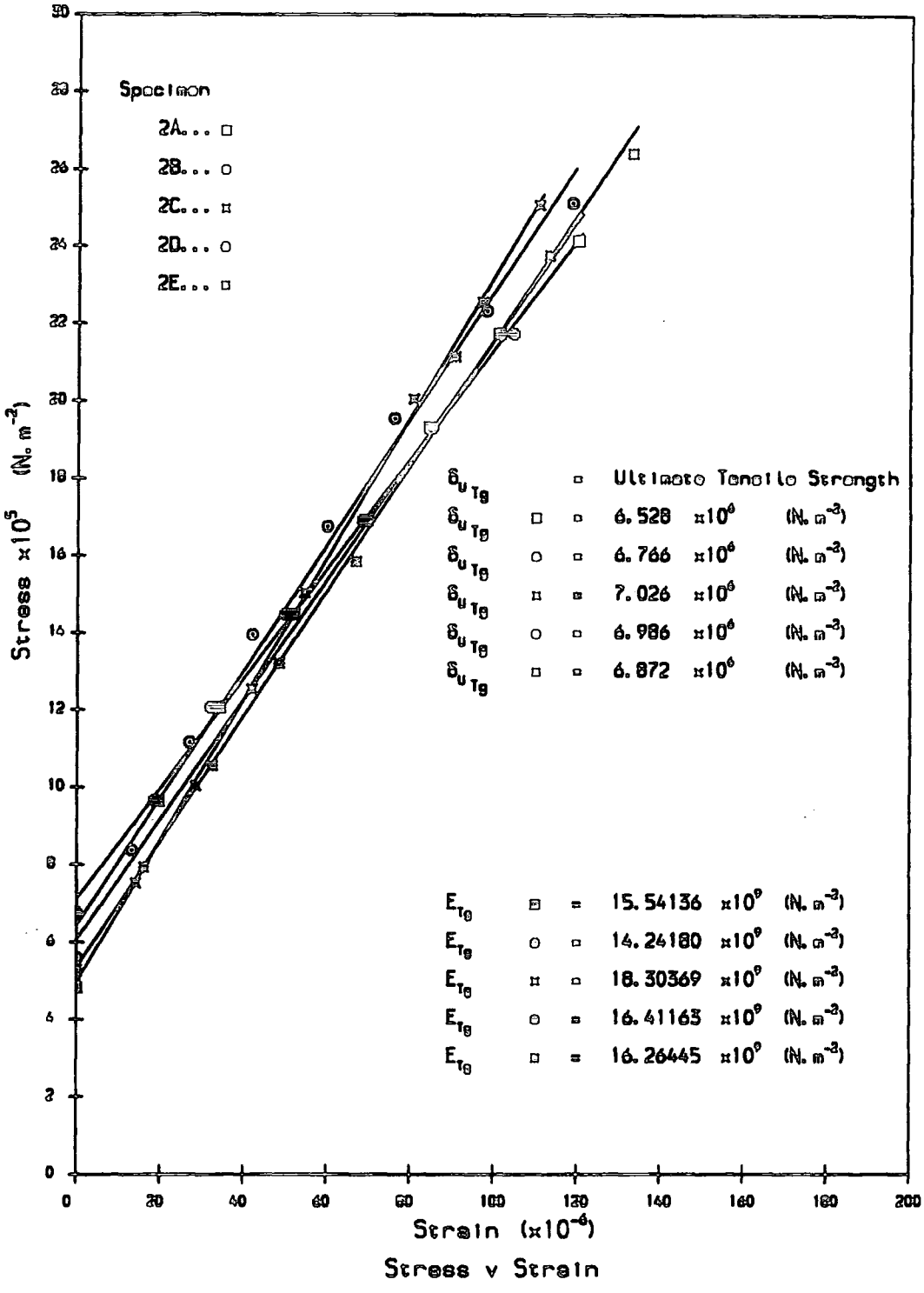

Stress v Strain

Fig. 5.7 Tensile Testing of T-Bone Specimens, with no Fibre Glass, Subject to Direct Tensile Test. (Tested on Denison Model "T42B4")

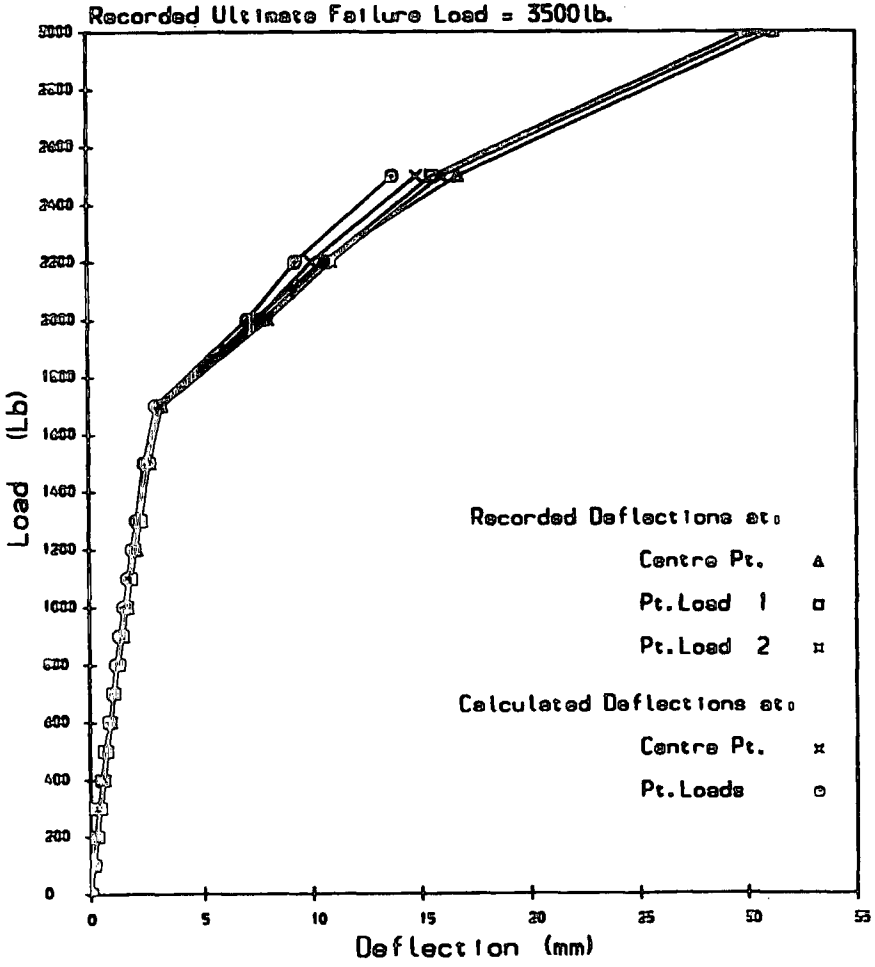

(a) Load v Deflection

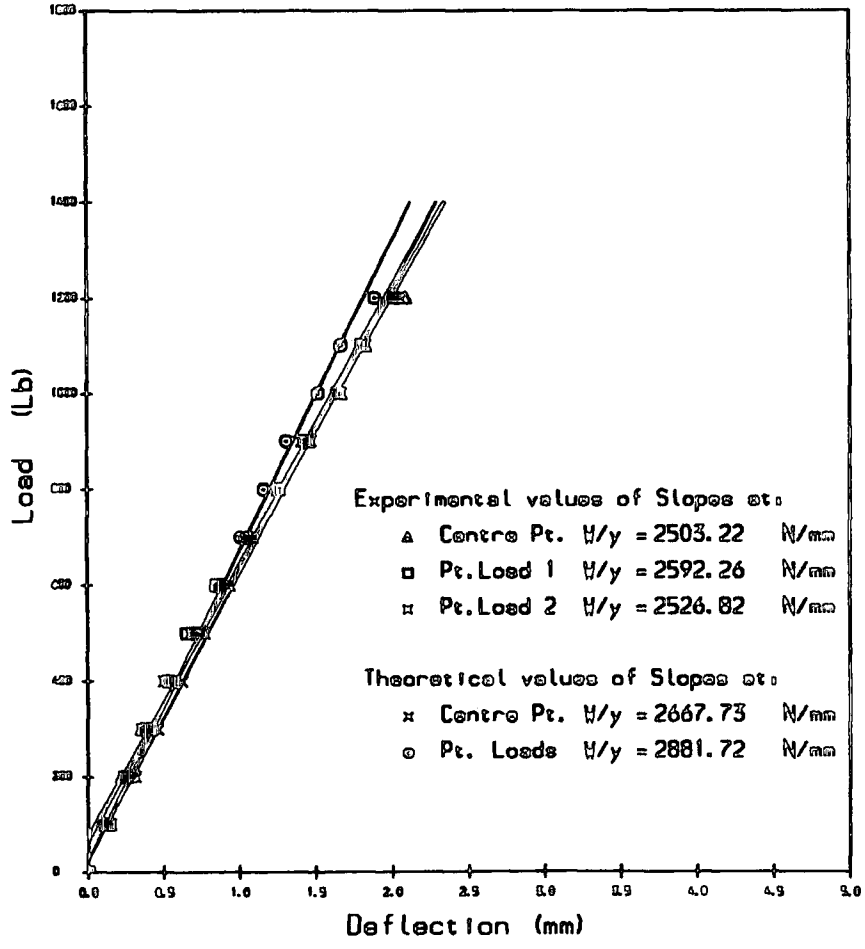

(b) Evaluation of Slopes

Figure 5.8a Recorded and Theoretical Load v Deflection for Beam A-1a

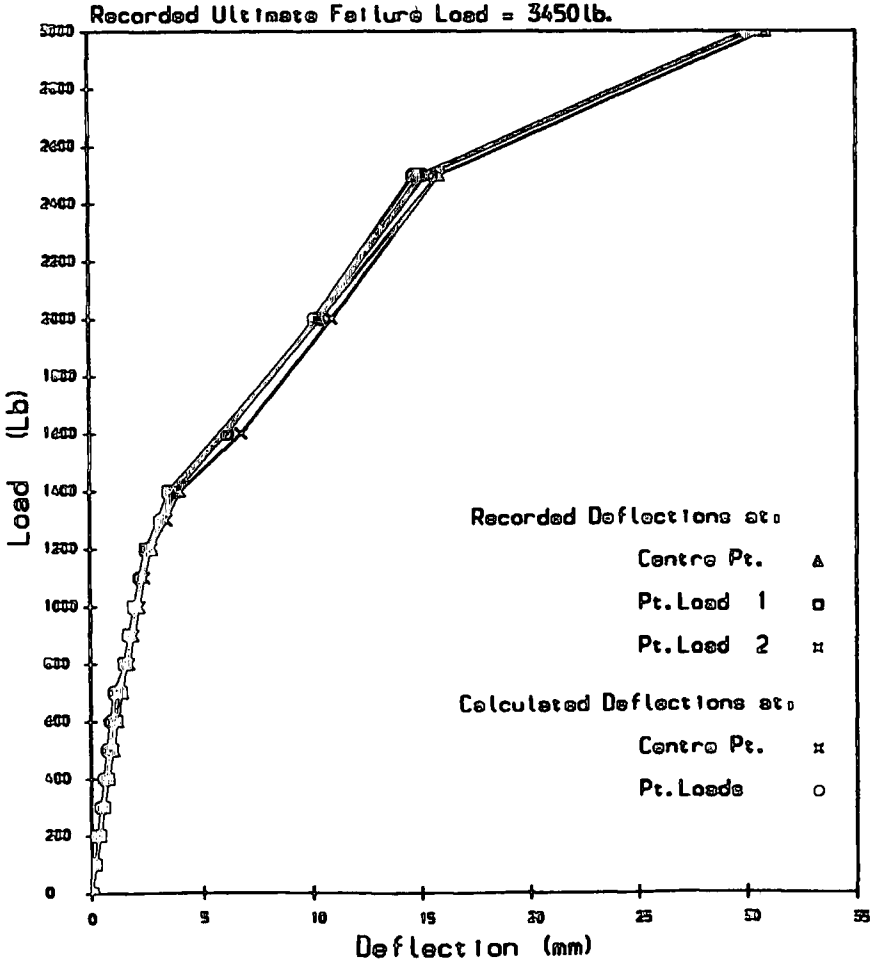

(a) Load v Deflection

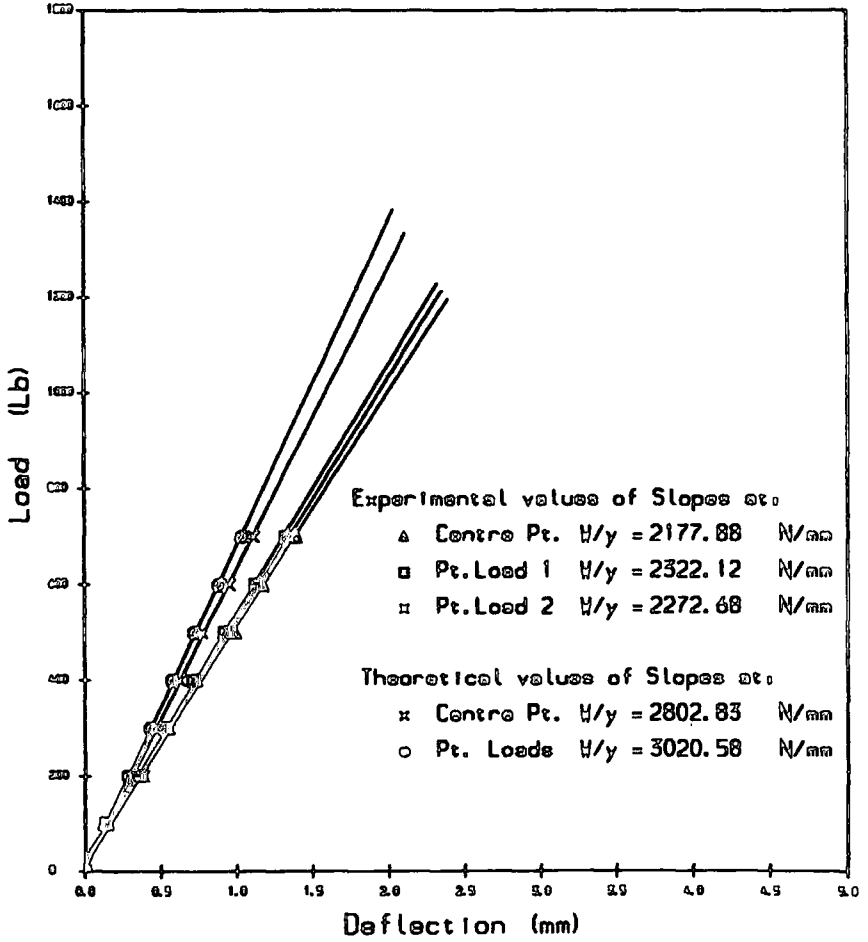

(b) Evaluation of Slopes

Figure 5.8b Recorded and Theoretical Load v Deflection for Beam A-1b

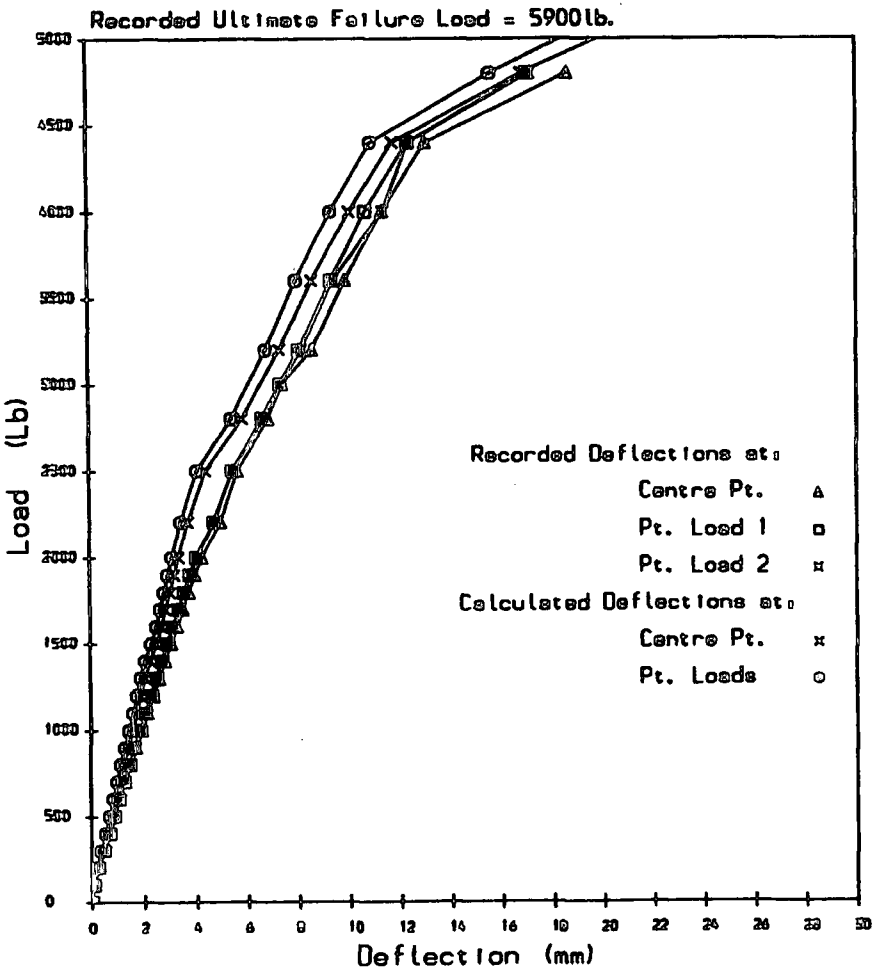

(a) Load v Deflection

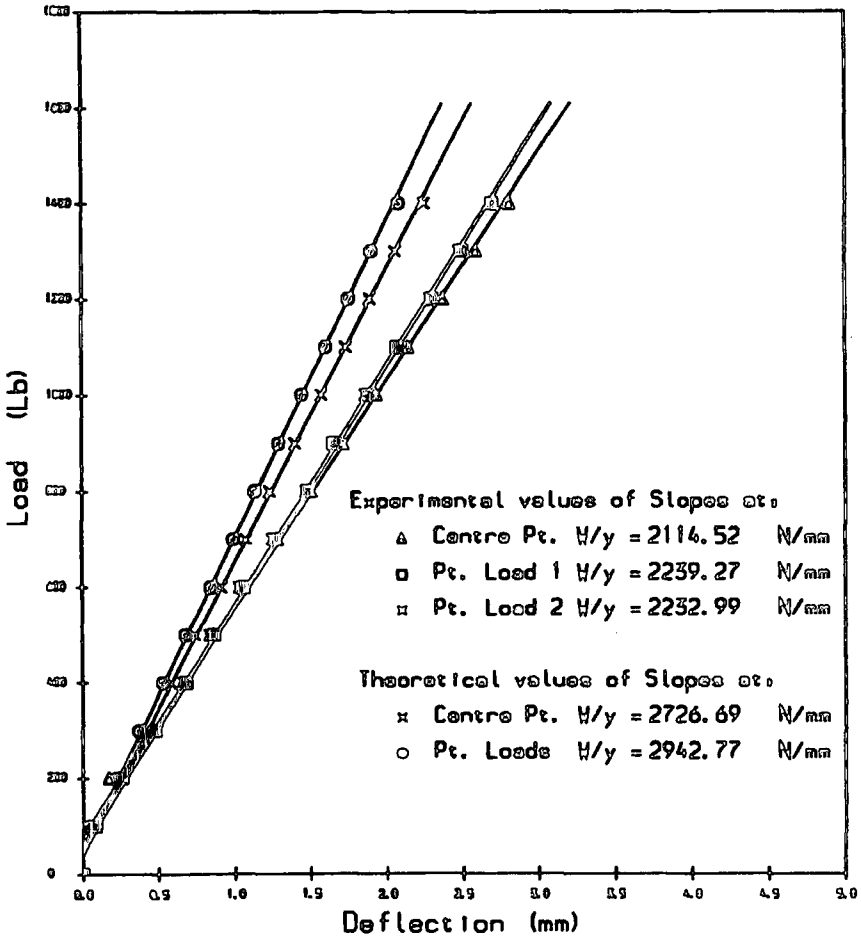

(b) Evaluation of Slopes

Figure 5.8c Recorded and Theoretical Load v Deflection for Beam A-2a

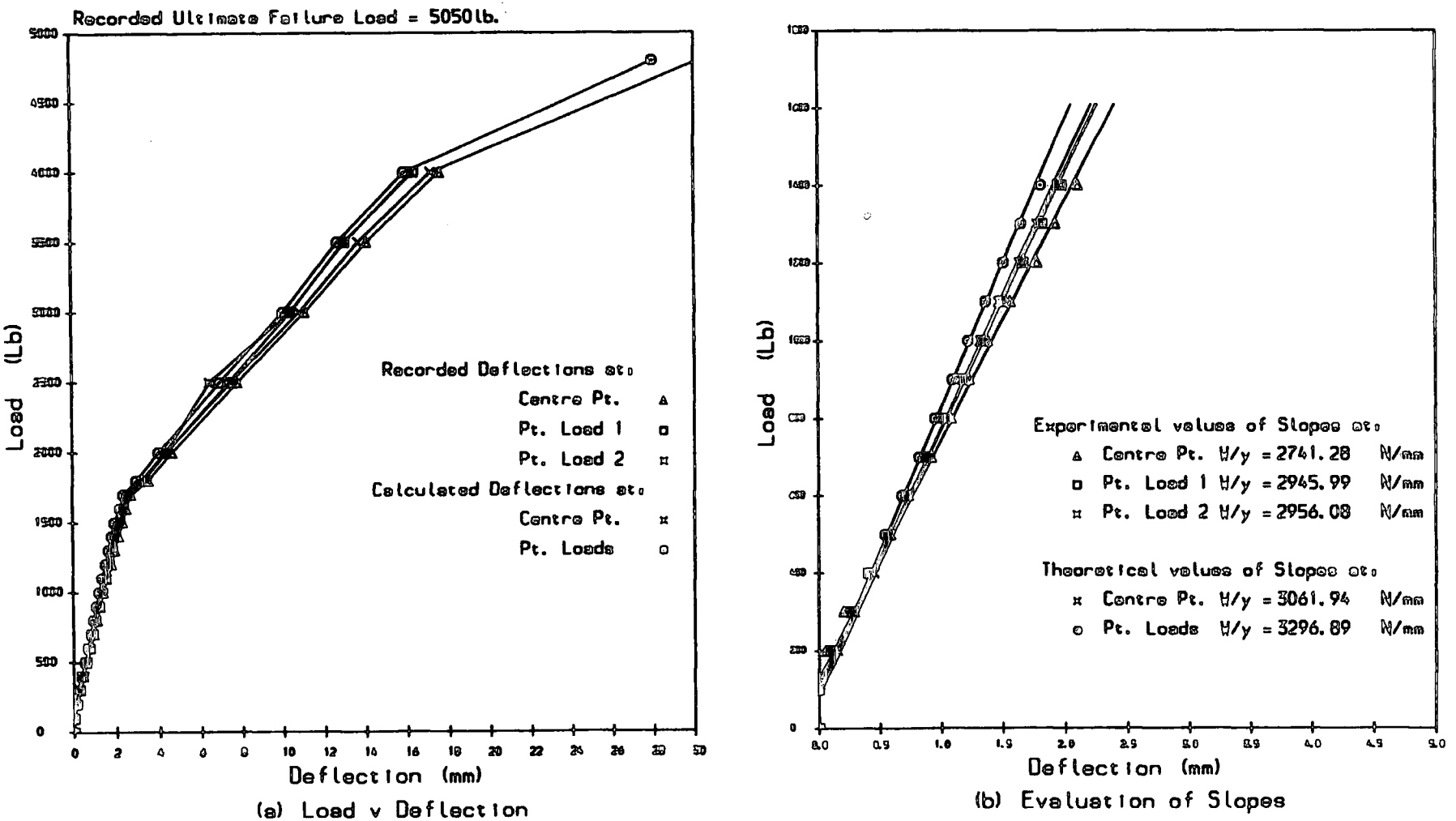

(a) Load v Deflection

(b) Evaluation of Slopes

Figure 5.8d Recorded and Theoretical Load v Deflection for Beam A-2b

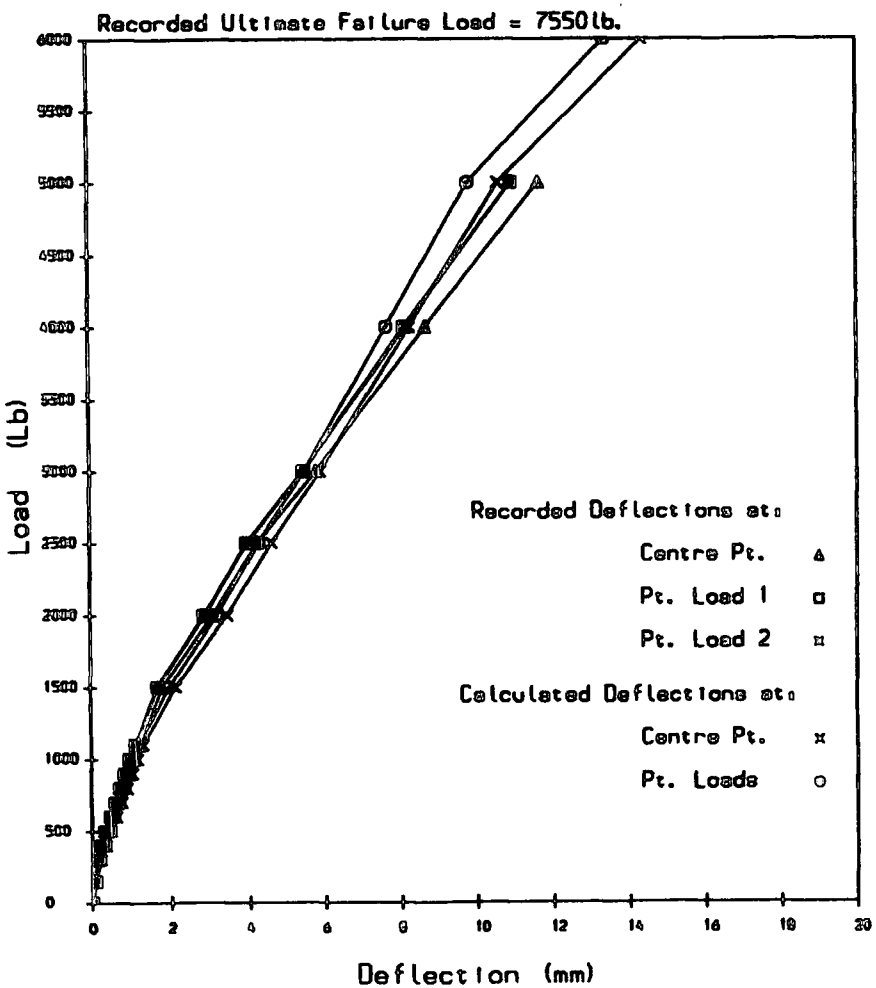

(a) Load v Deflection

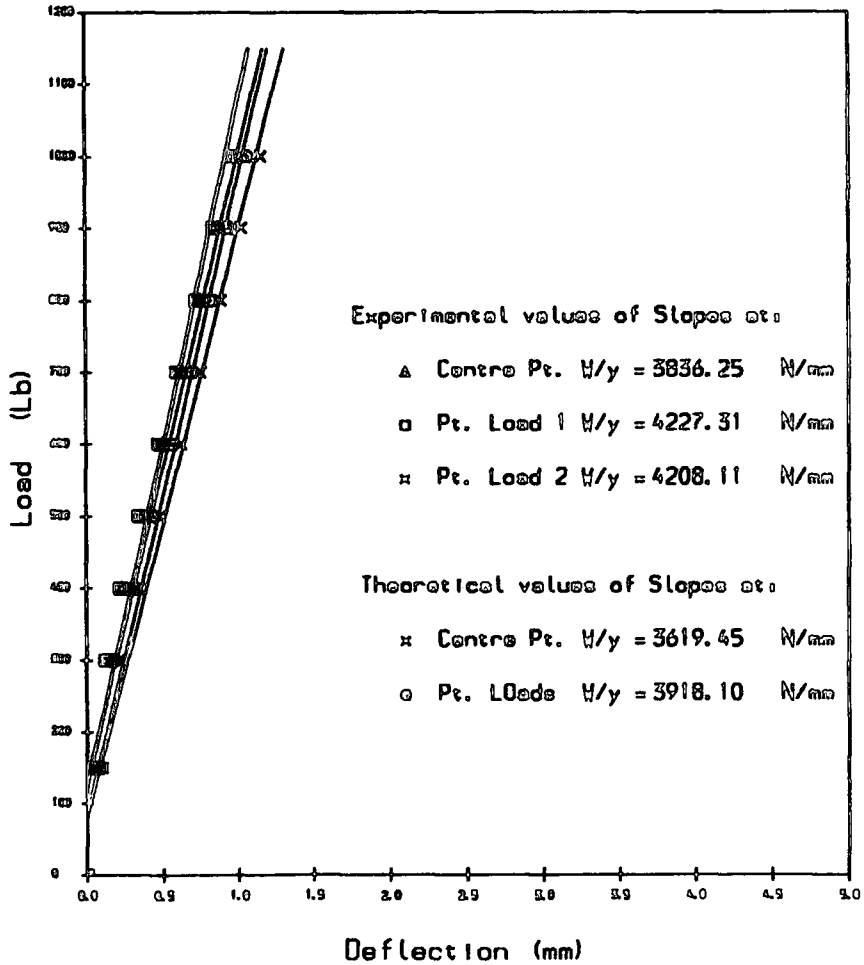

(b) Evaluation of Slopes

Figure 5.8e Recorded and Theoretical Load v Deflection for Beam A-3a

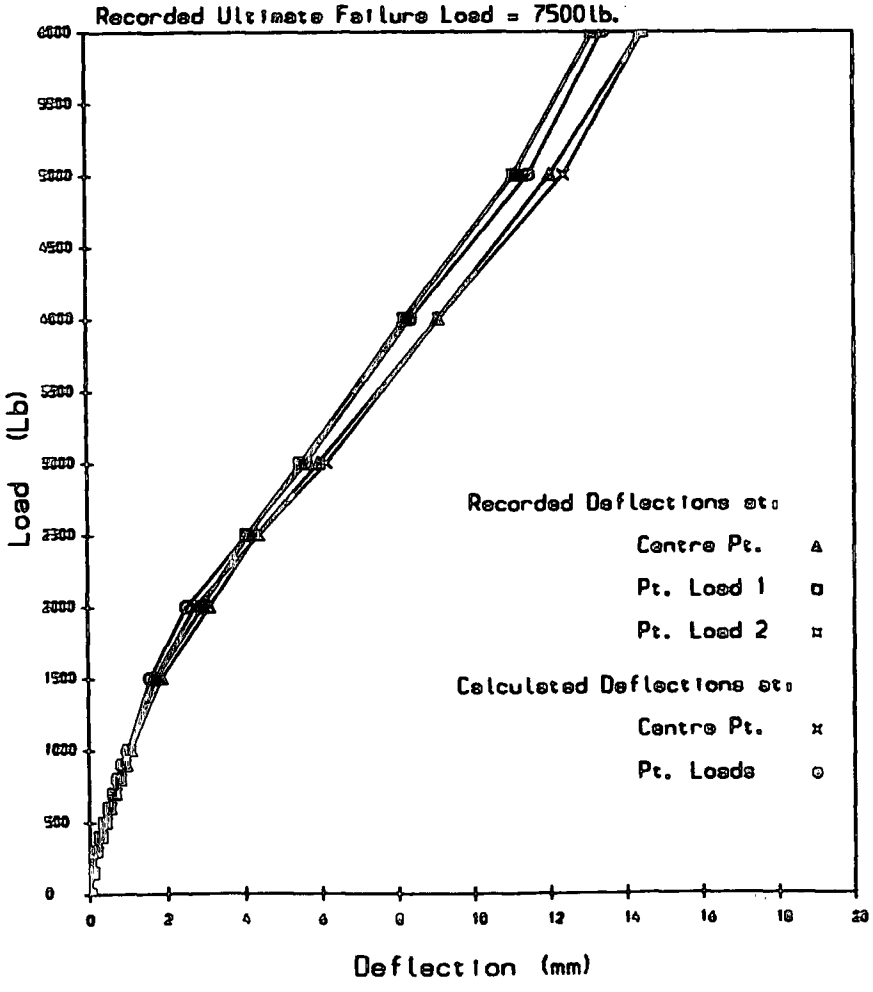

(a) Load v Deflection

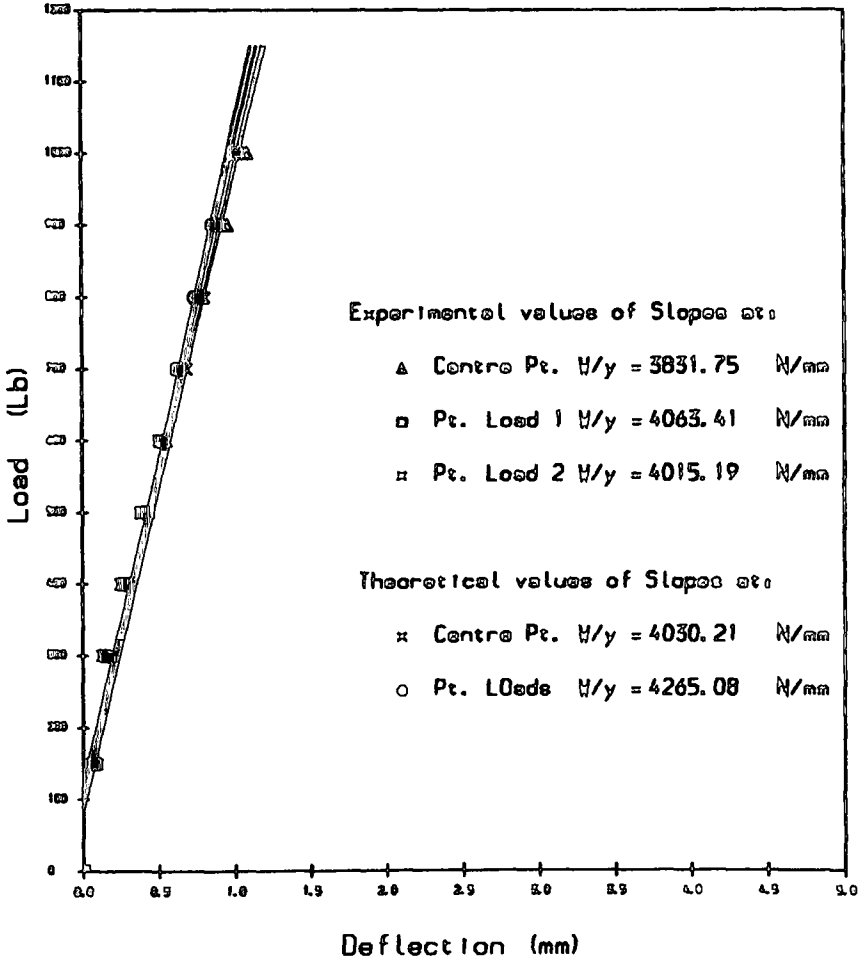

(b) Evaluation of Slopes

Figure 5.8f Recorded and Theoretical Load v Deflection for Beam A-3b

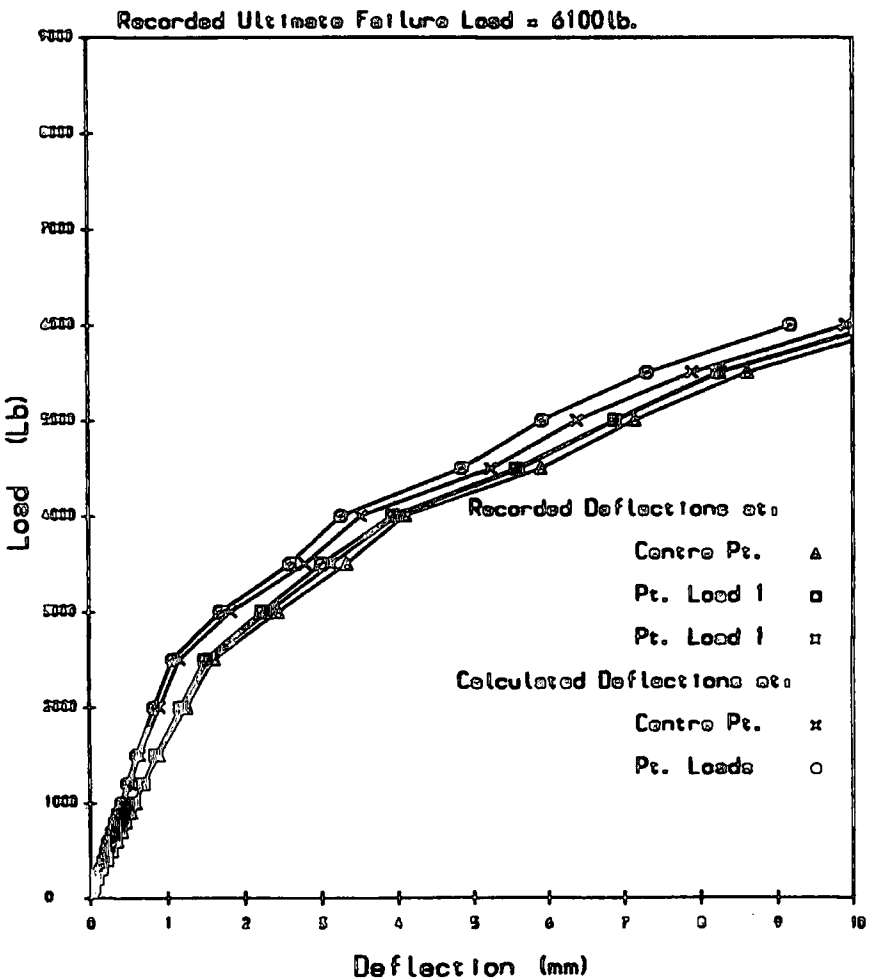

(a) Load v Deflection

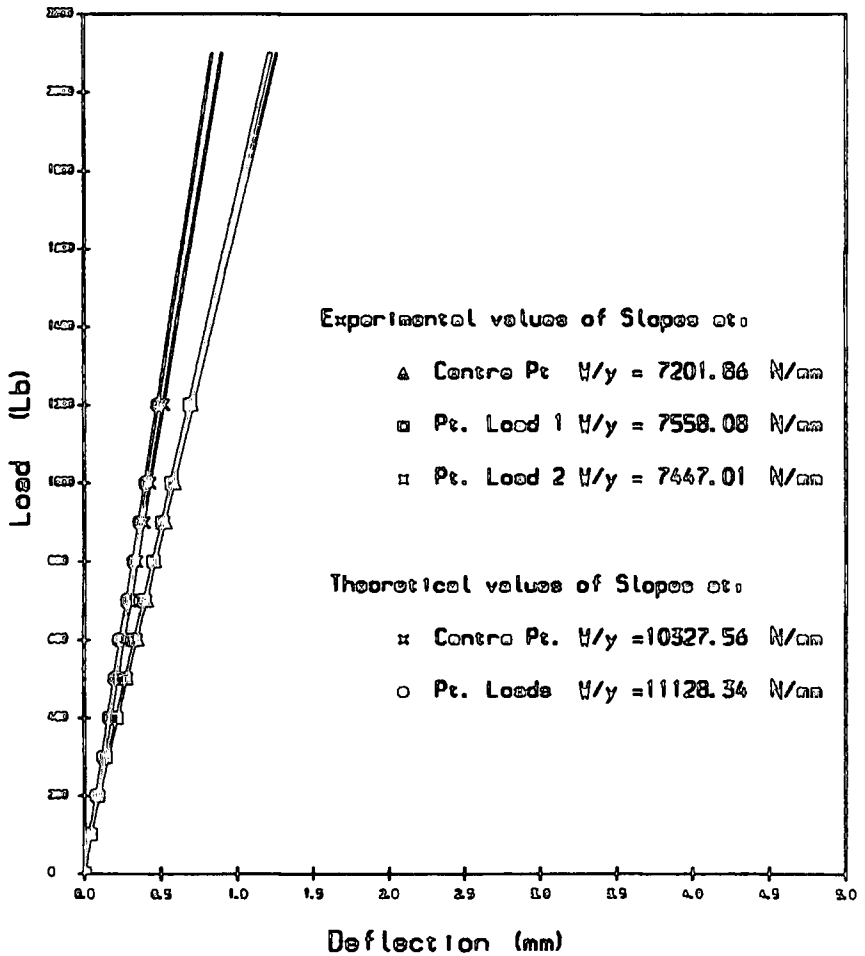

(b) Evaluation of Slopes

Figure 5.8g Recorded and Theoretical Load v Deflection for Beam B-1a

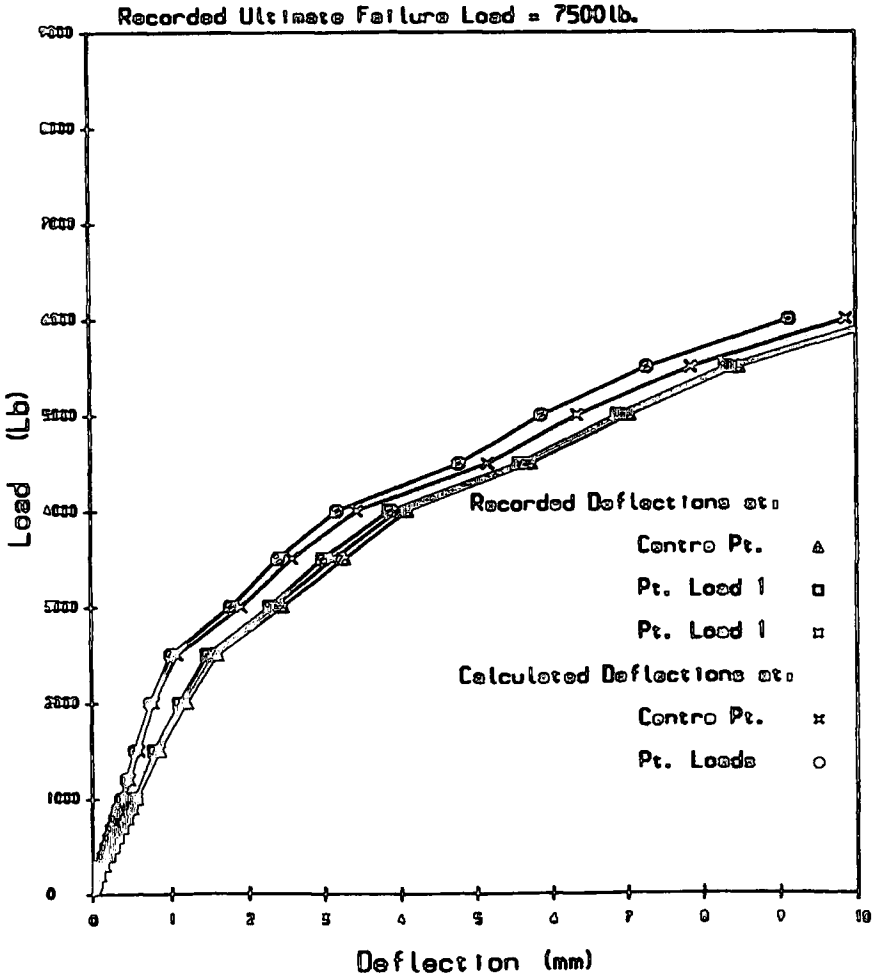

(a) Load v Deflection

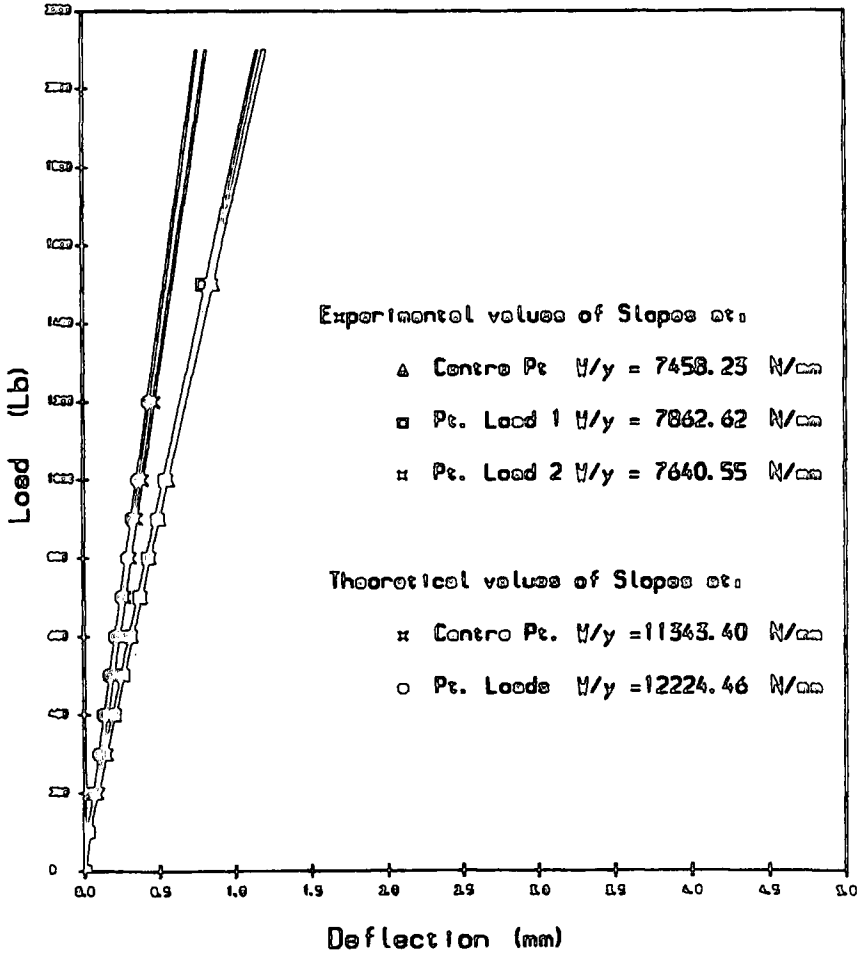

(b) Evaluation of Slopes

Figure 5.8h Recorded and Theoretical Load v Deflection for Beam B-1b

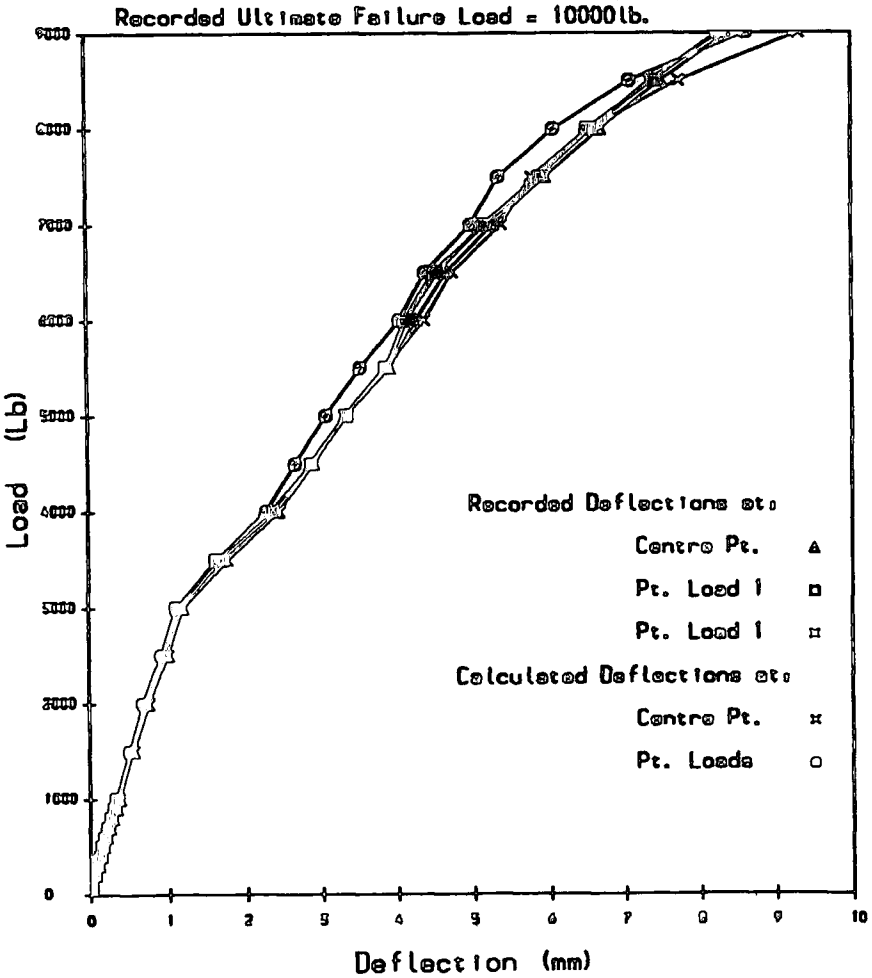

(a) Load v Deflection

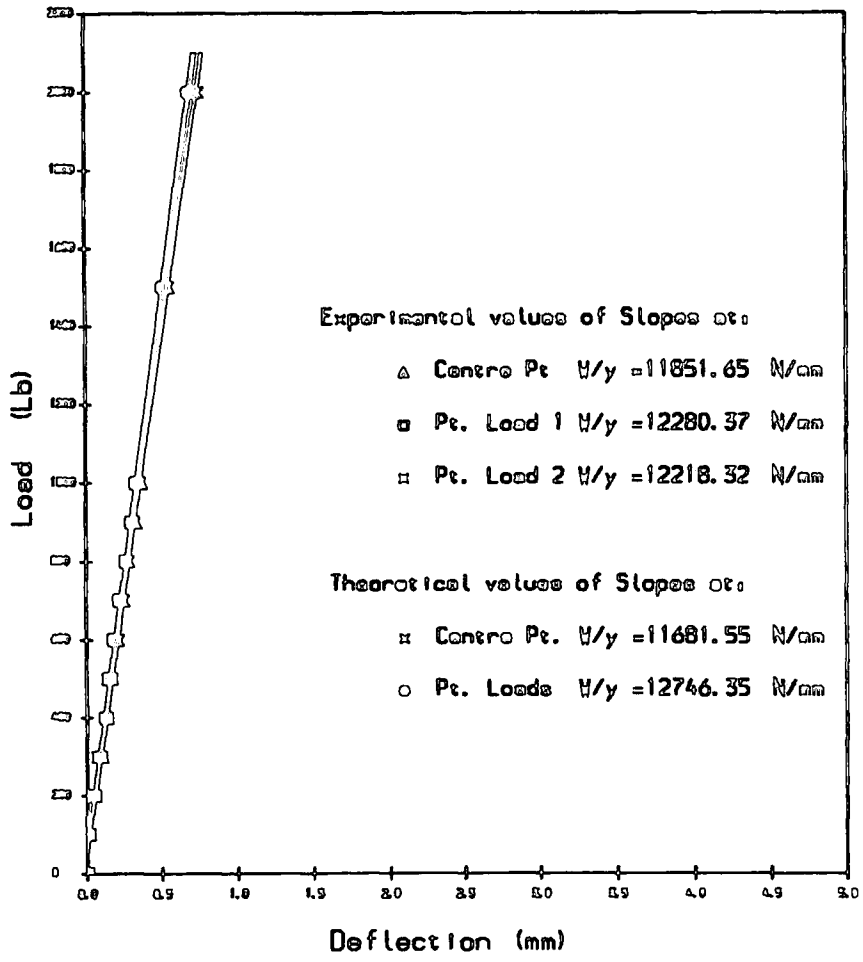

(b) Evaluation of Slopes

Figure 5.81 Recorded and Theoretical Load v Deflection for Beam B-2a

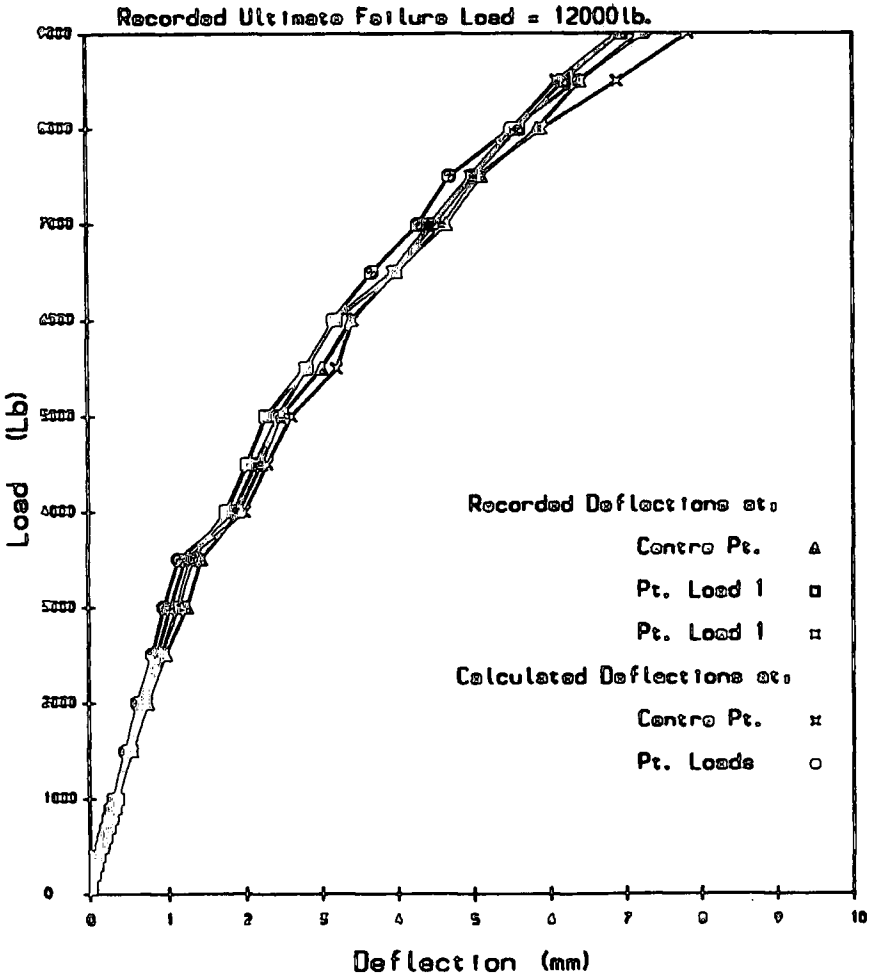

(a) Load v Deflection

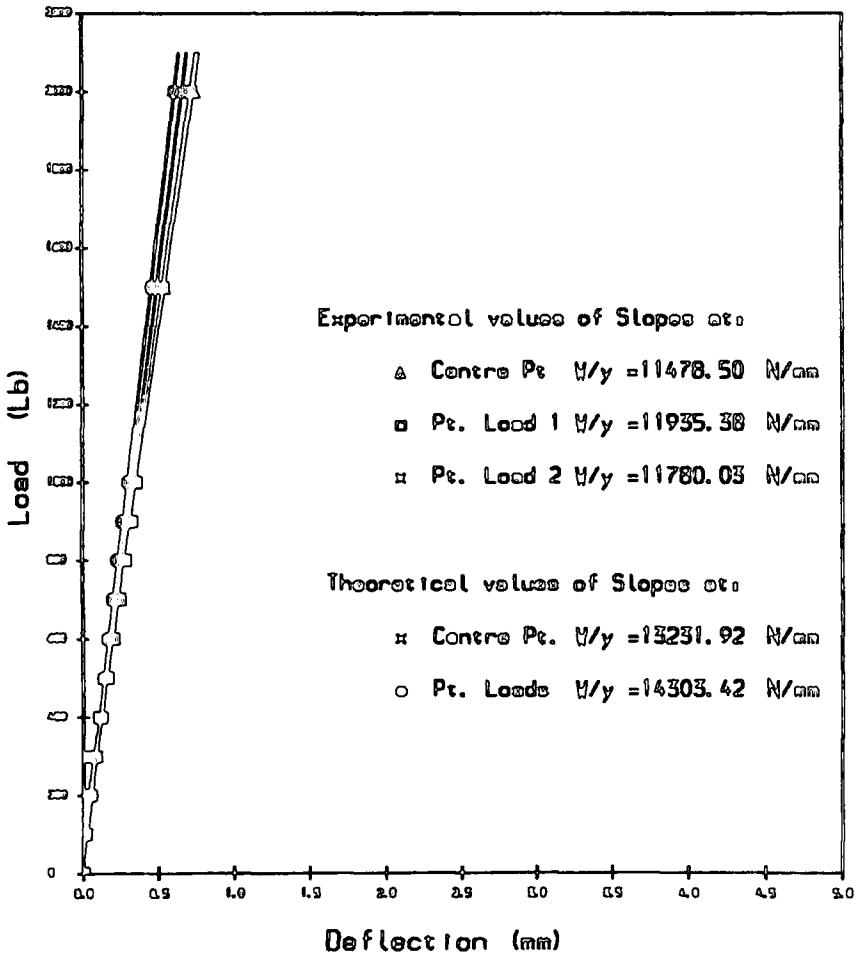

(b) Evaluation of Slopes

Figure 5.8j Recorded and Theoretical Load v Deflection for Beam B-2b

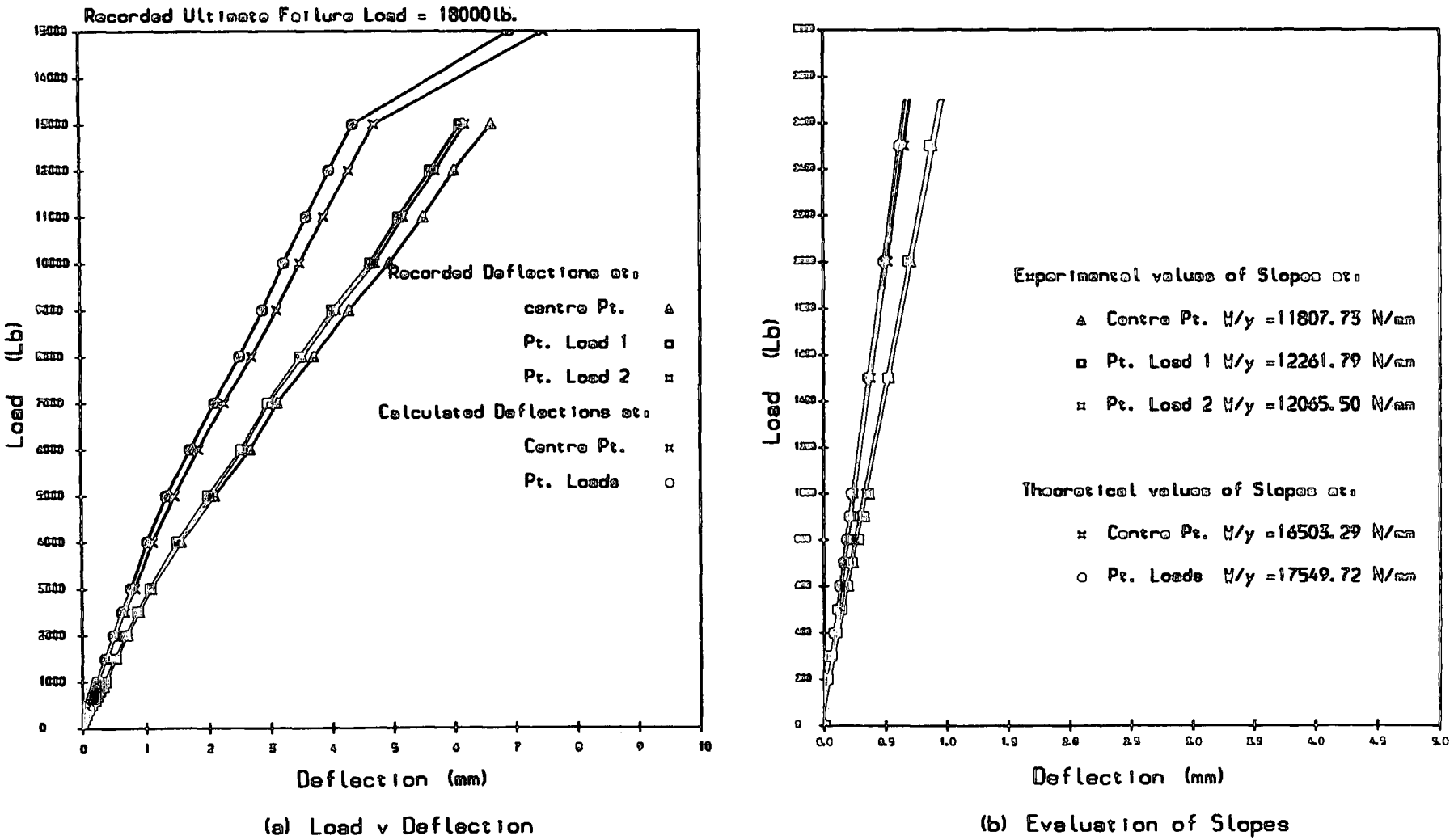

(a) Load v Deflection

(b) Evaluation of Slopes

Figure 5.8k Recorded and Theoretical Load v Deflection for Beam B-3a

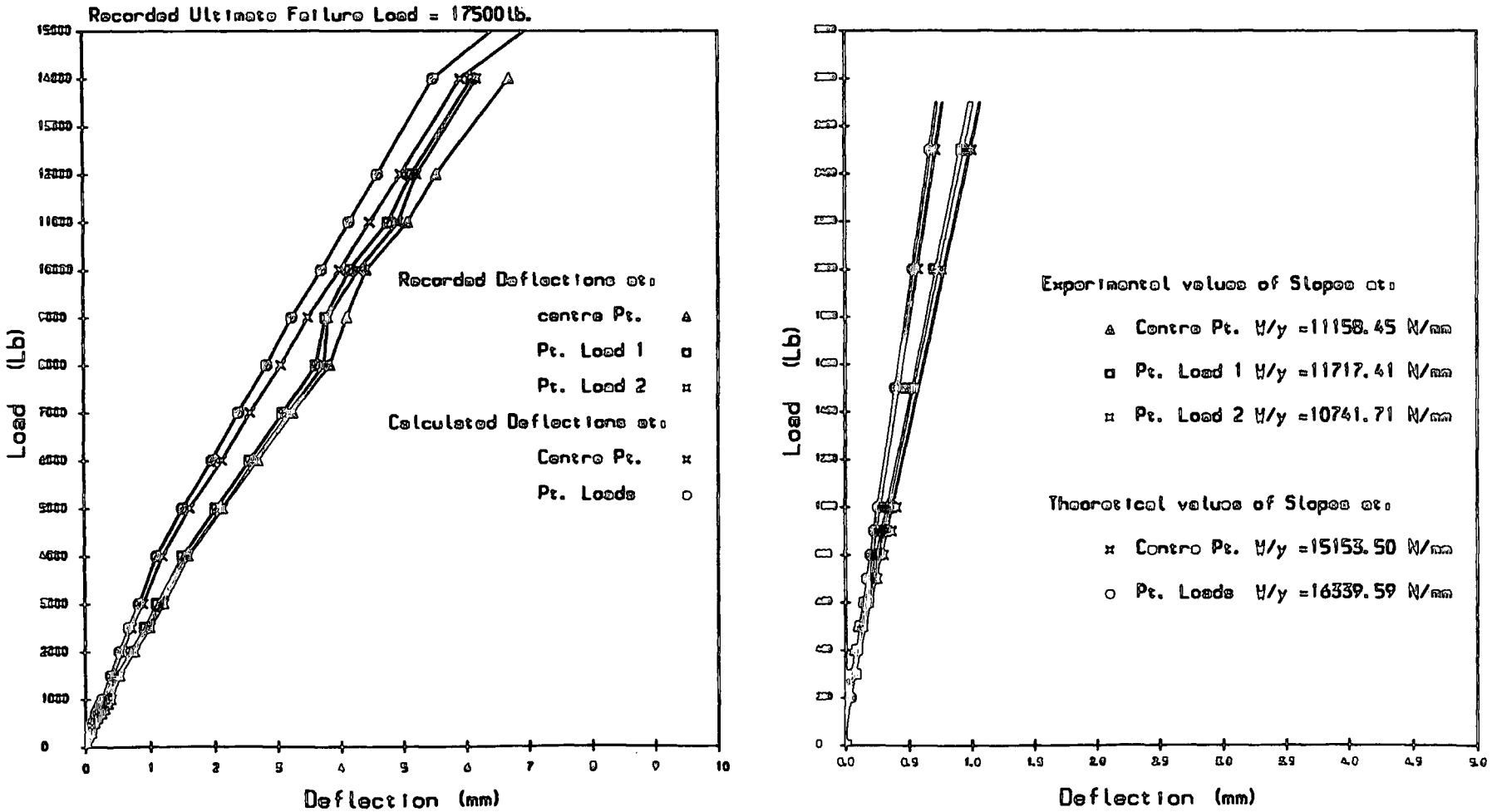

(a) Load v Deflection

(b) Evaluation of Slopes

Figure 5.81 Recorded and Theoretical Load v Deflection for Beam B-3b

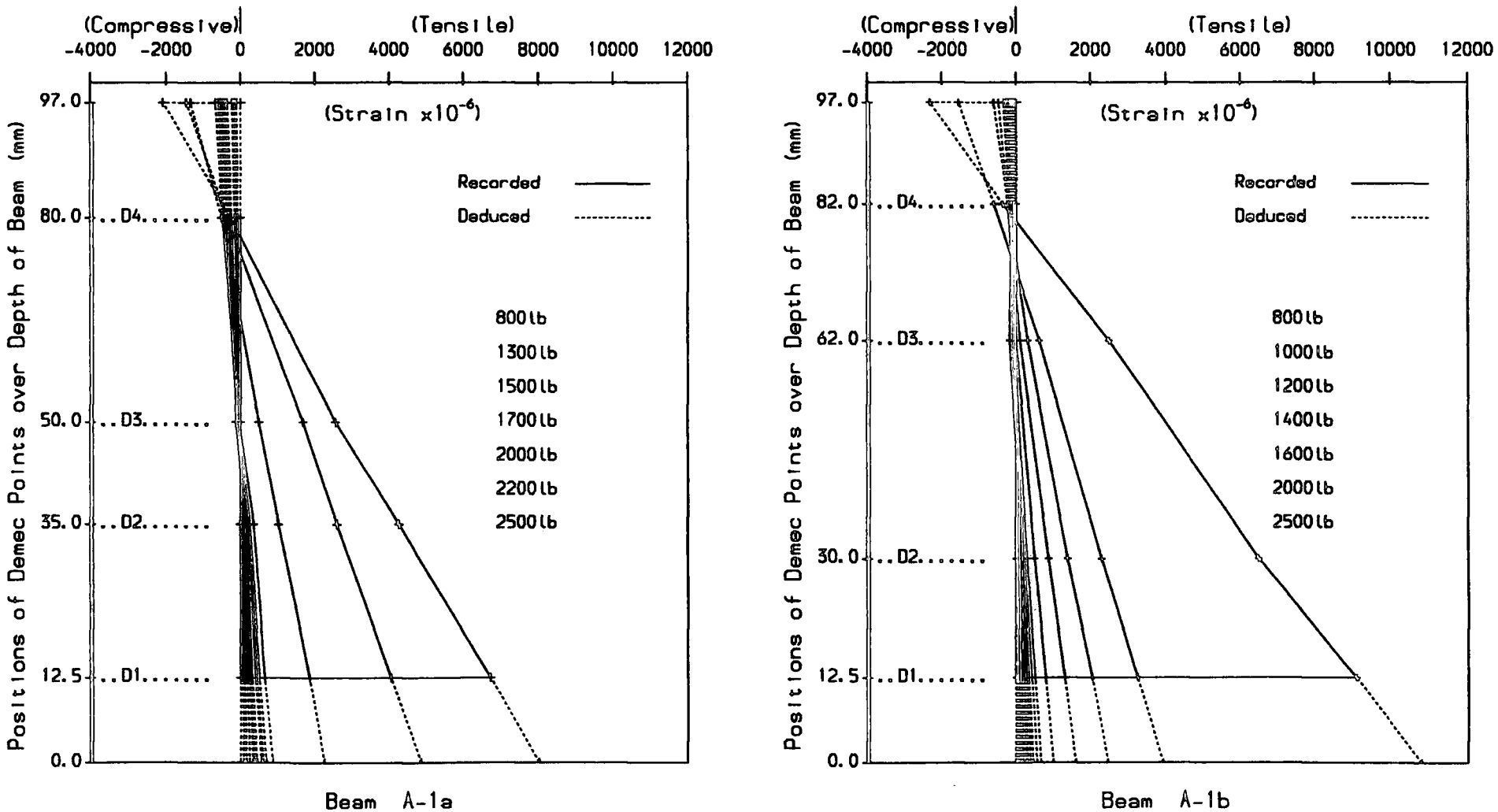

Fig. 5.9a Variation of Neutral Axis position with load.

Shallow Beam A-1 (no internal steel reinforcement).

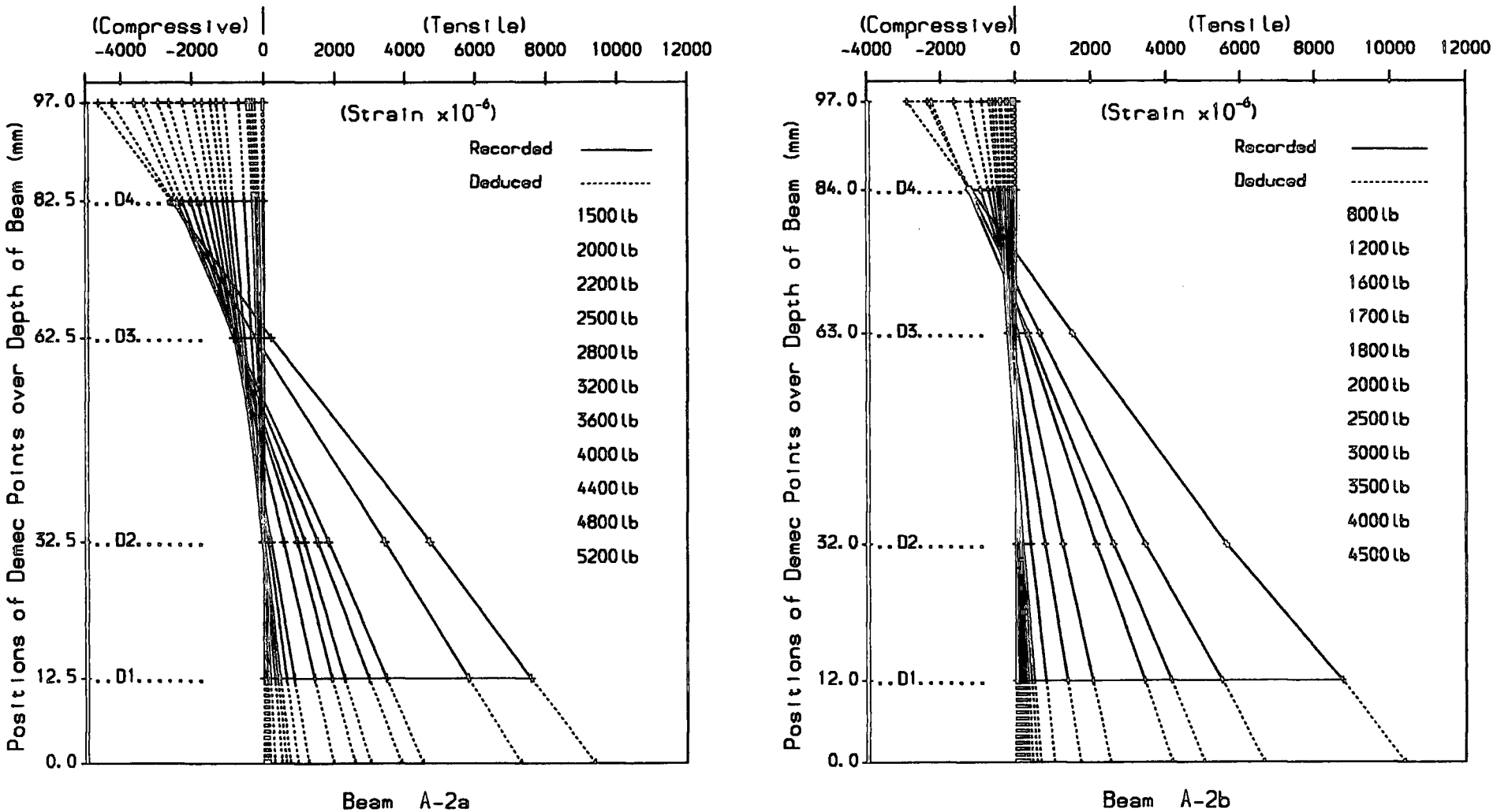

Fig. 5.9b Variation of Neutral Axis position with load.

Shallow Beam A-2 (Internal reinforcement: two 6mm dia. High Yield Bars).

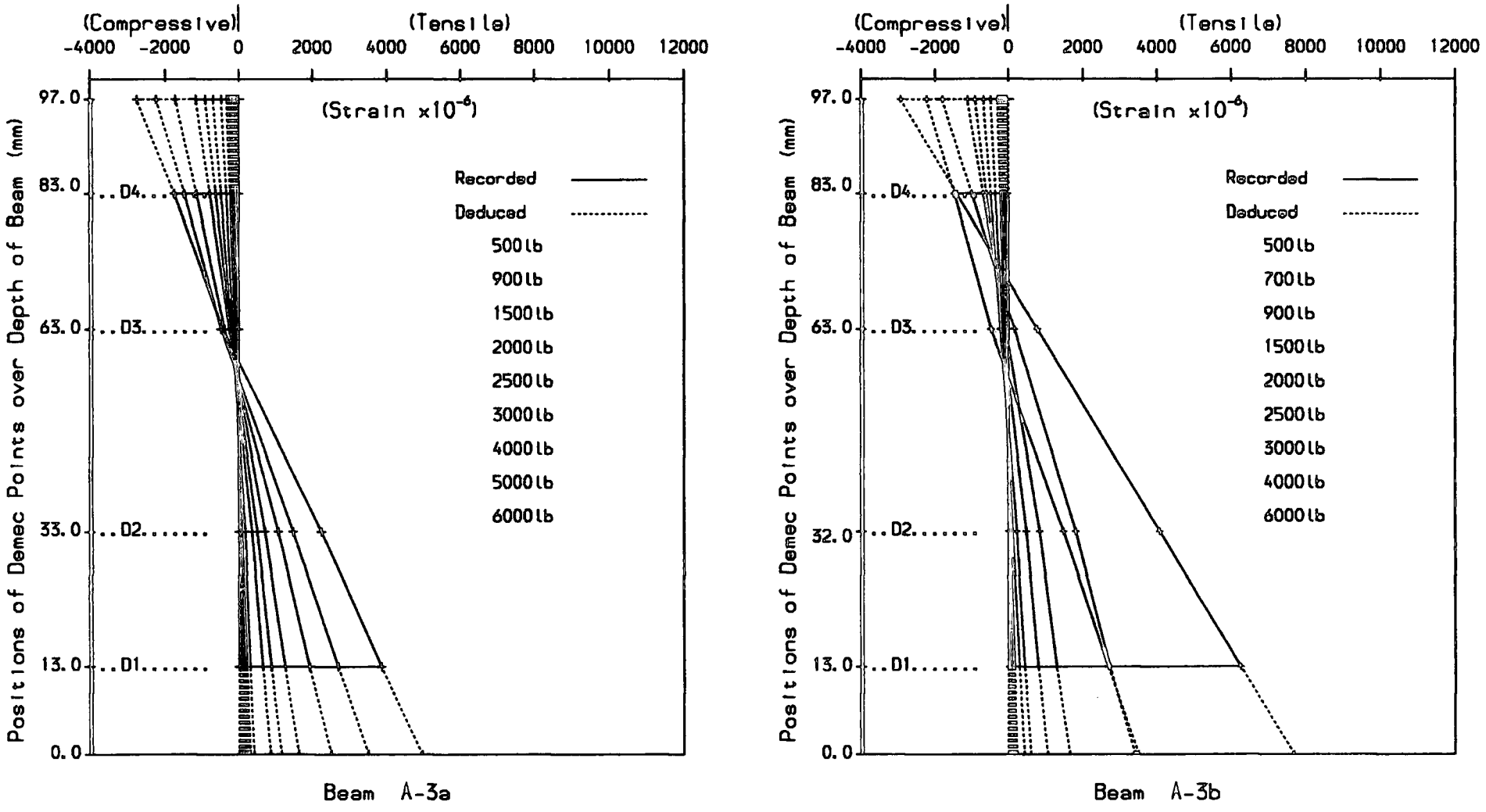

Fig. 5.9c Variation of Neutral Axis position with load.

Shallow Beam A-3 (internal reinforcement: two 10mm dia. High Yield Bars).

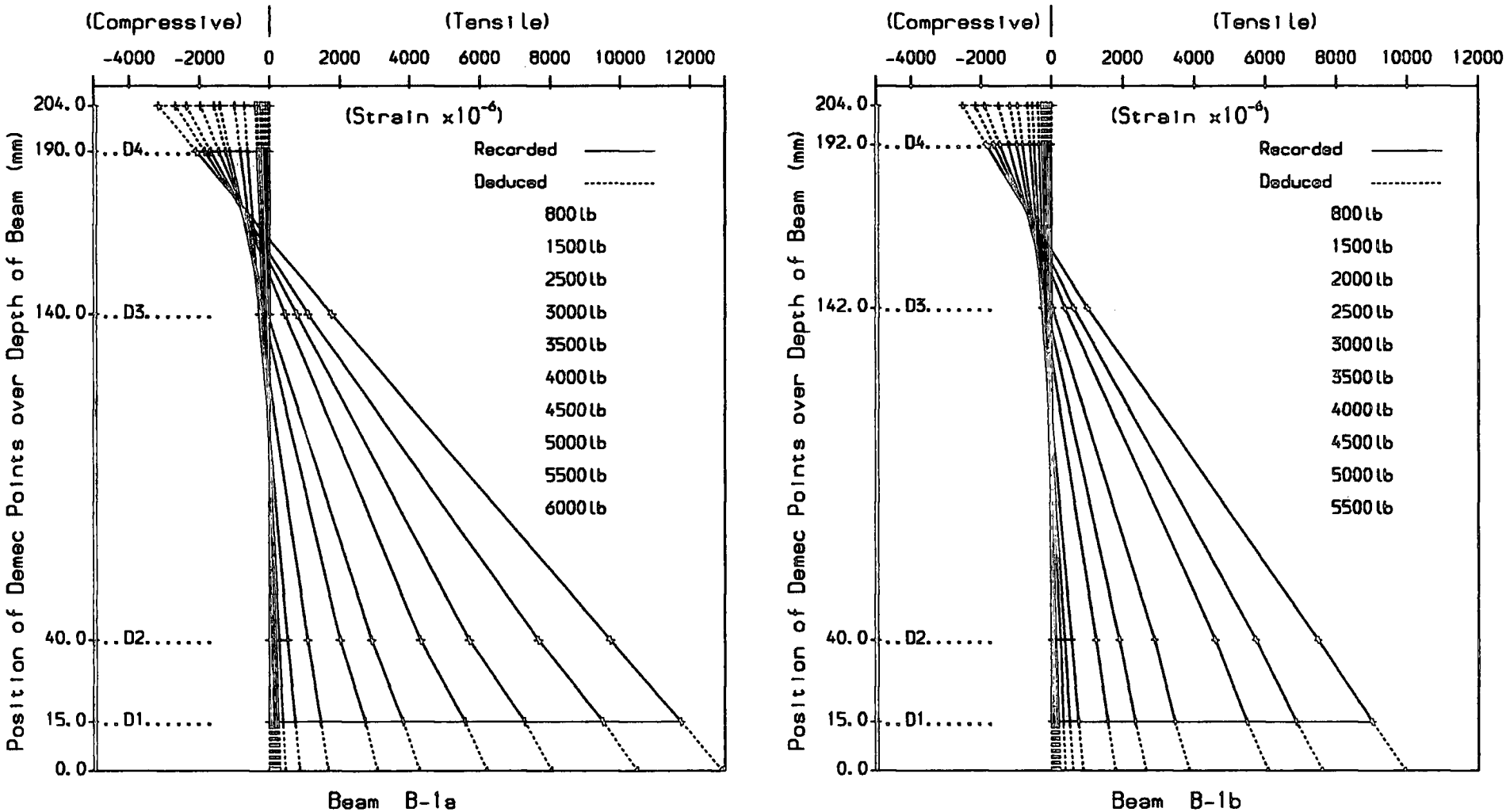

Fig. 5.9d Variation of Neutral Axis position with load.
Deep Beam B-1 (no internal steel reinforcement).

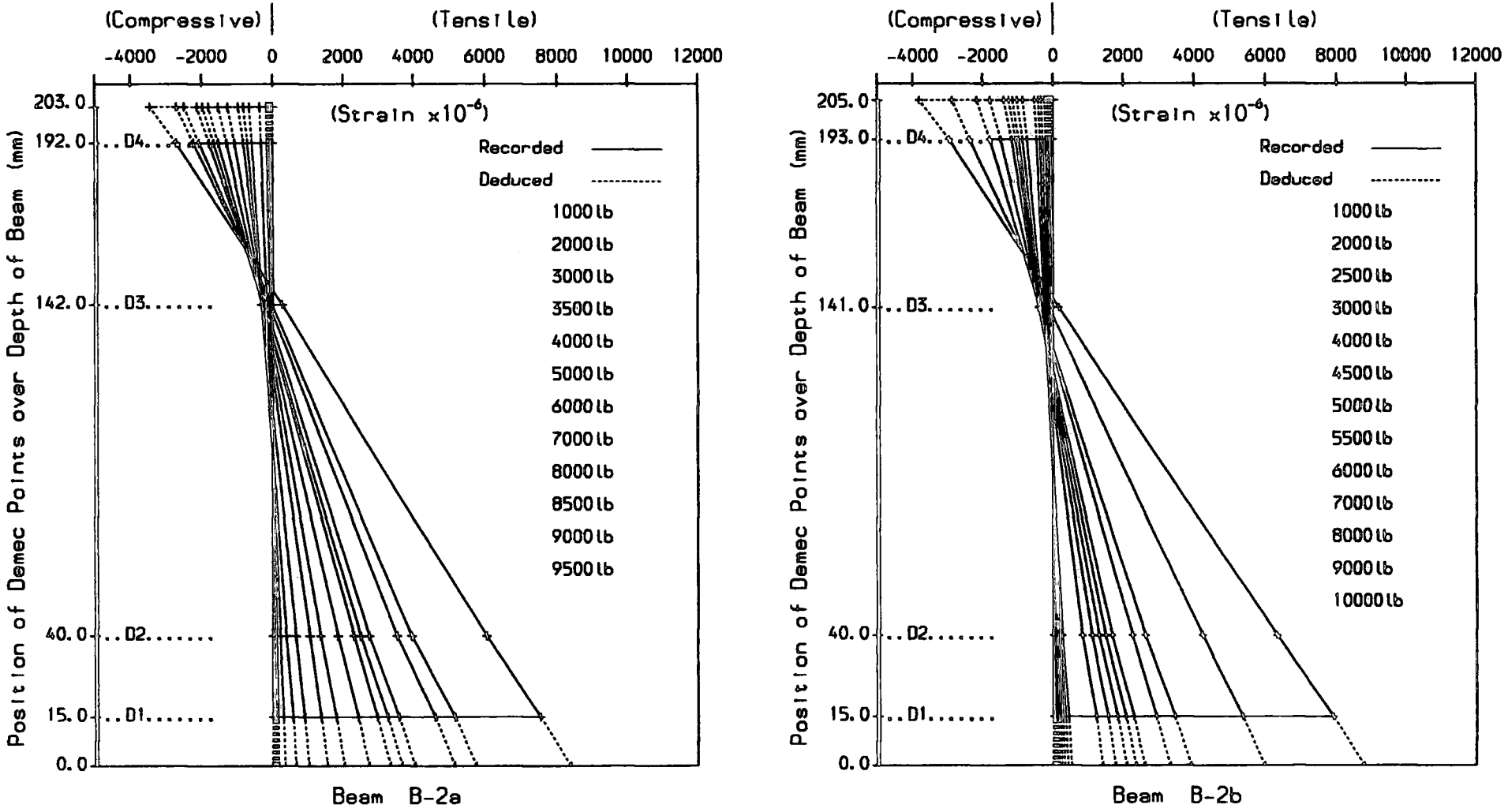

Fig. 5.9e Variation of Neutral Axis position with load.
Deep Beam B-2 (internal reinforcement -two 6mm dia. High Yield Bars).

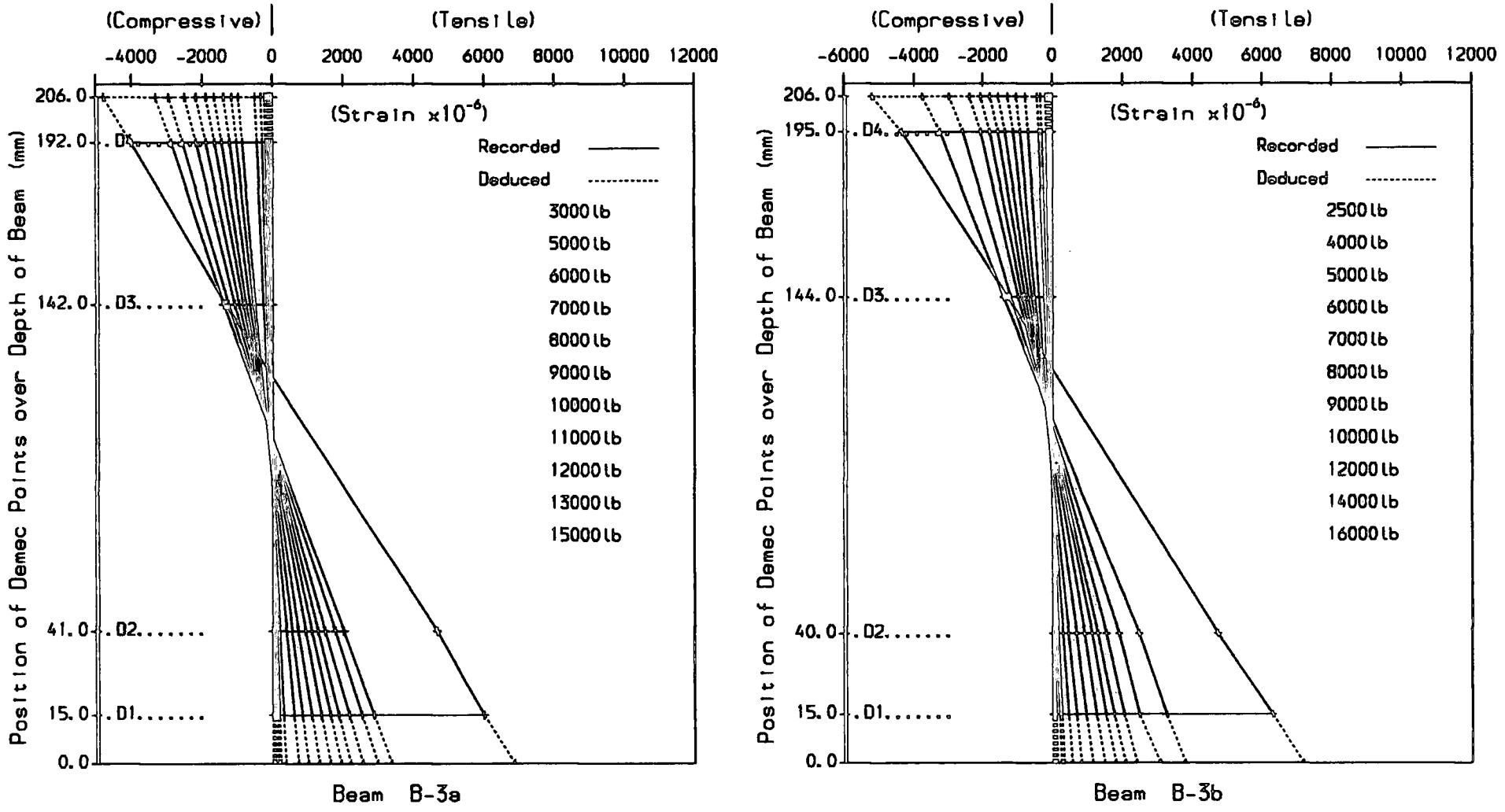

Fig. 5.9f Variation of Neutral Axis position with load.
Deep Beam B-3 (internal reinforcement -two 10mm dia. High Yield Bars).

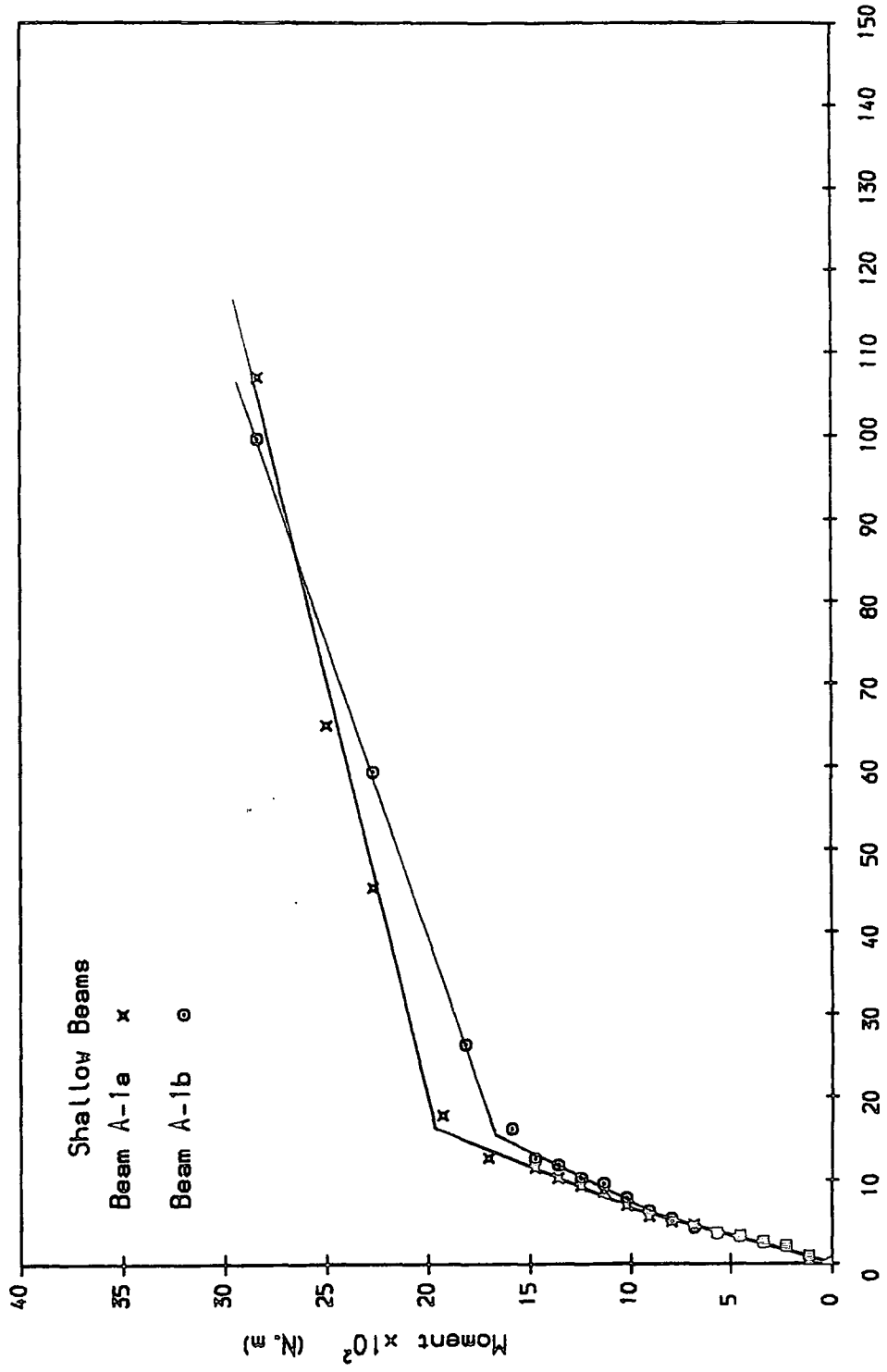

Fig 5.10a Moment - Curvature Relationship for Phenolic Beams.
(Internally Unreinforced)

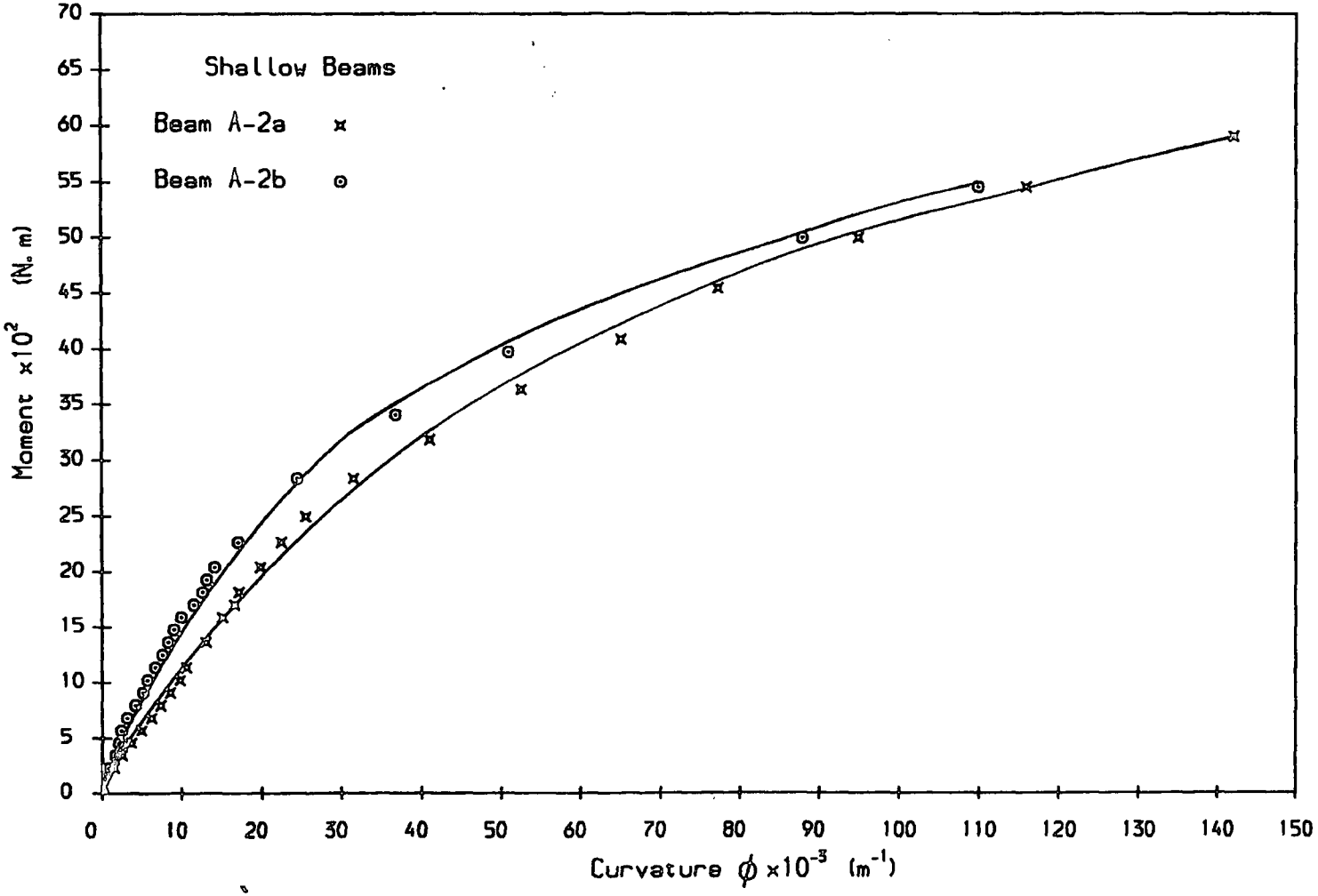

Fig 5.10b Moment - Curvature Relationship for Phenolic Beams.

(Internal Reinforcement 2x6 mm dia. h.y.s. bars)

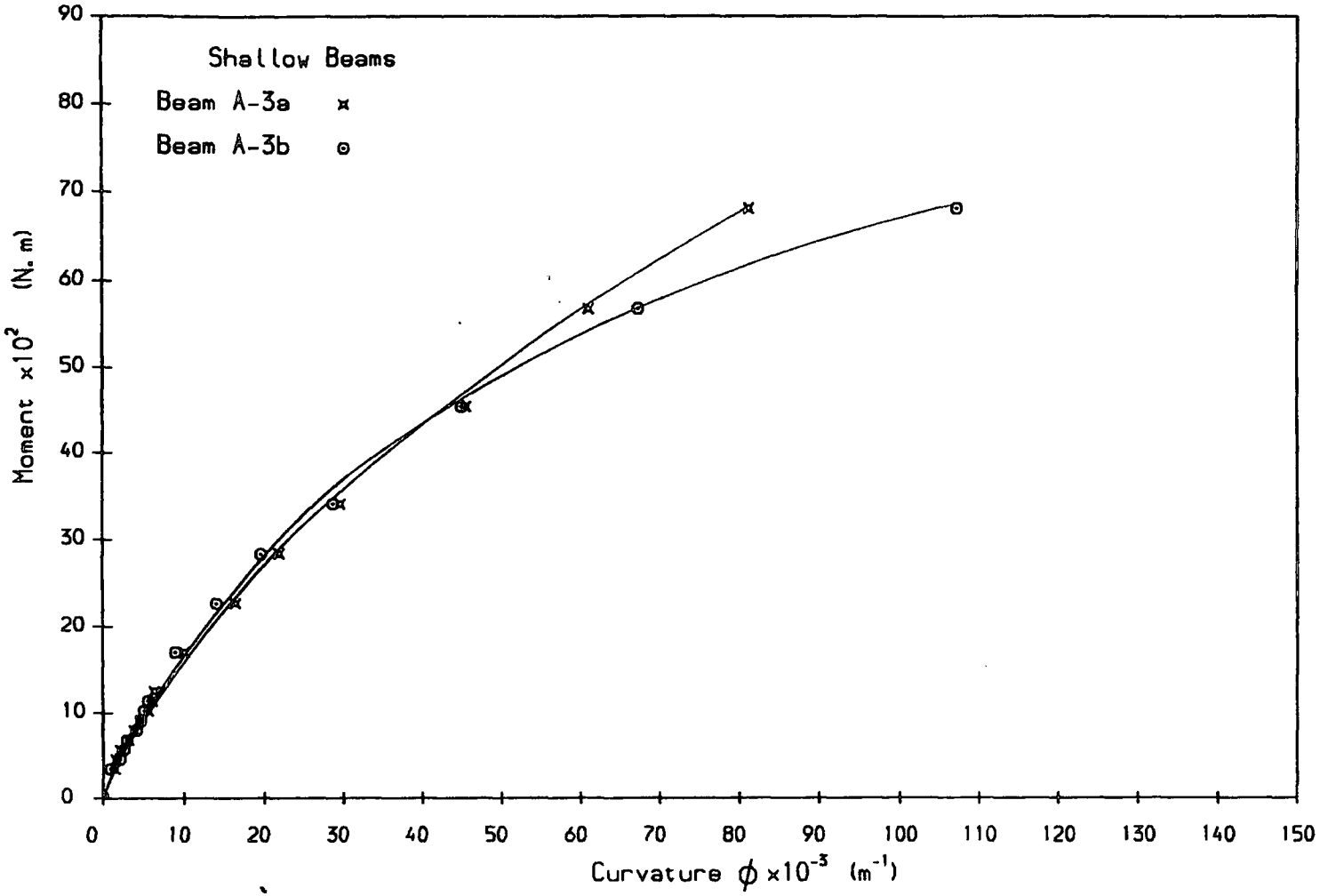

Fig 5.10c Moment - Curvature Relationship for Phenolic Beams.

(Internal Reinforcement 2x10 mm dia. h.y.s. bars)

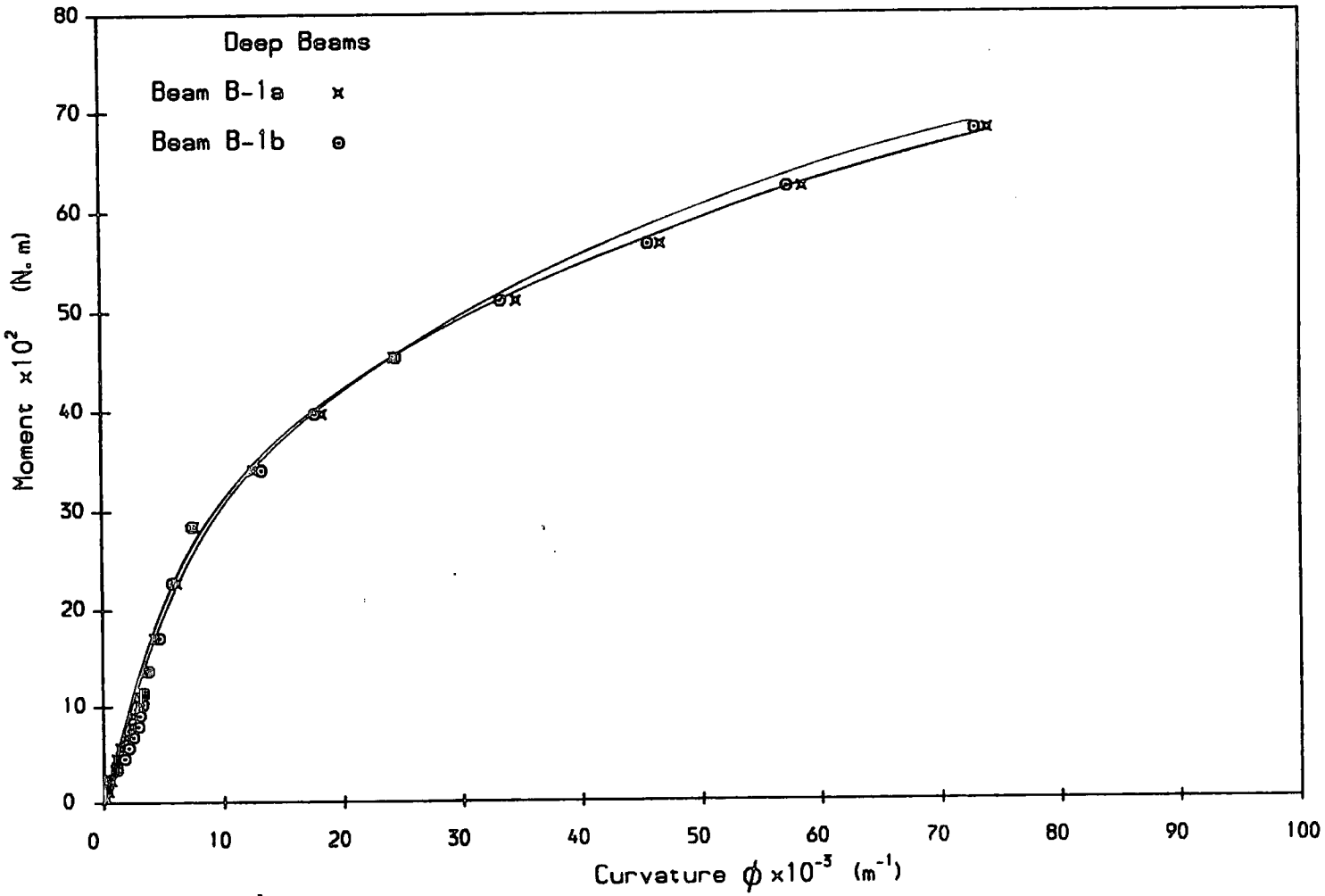

Fig 5.10d Moment - Curvature Relationship for Phenolic Beams.

(Internally Unreinforced)

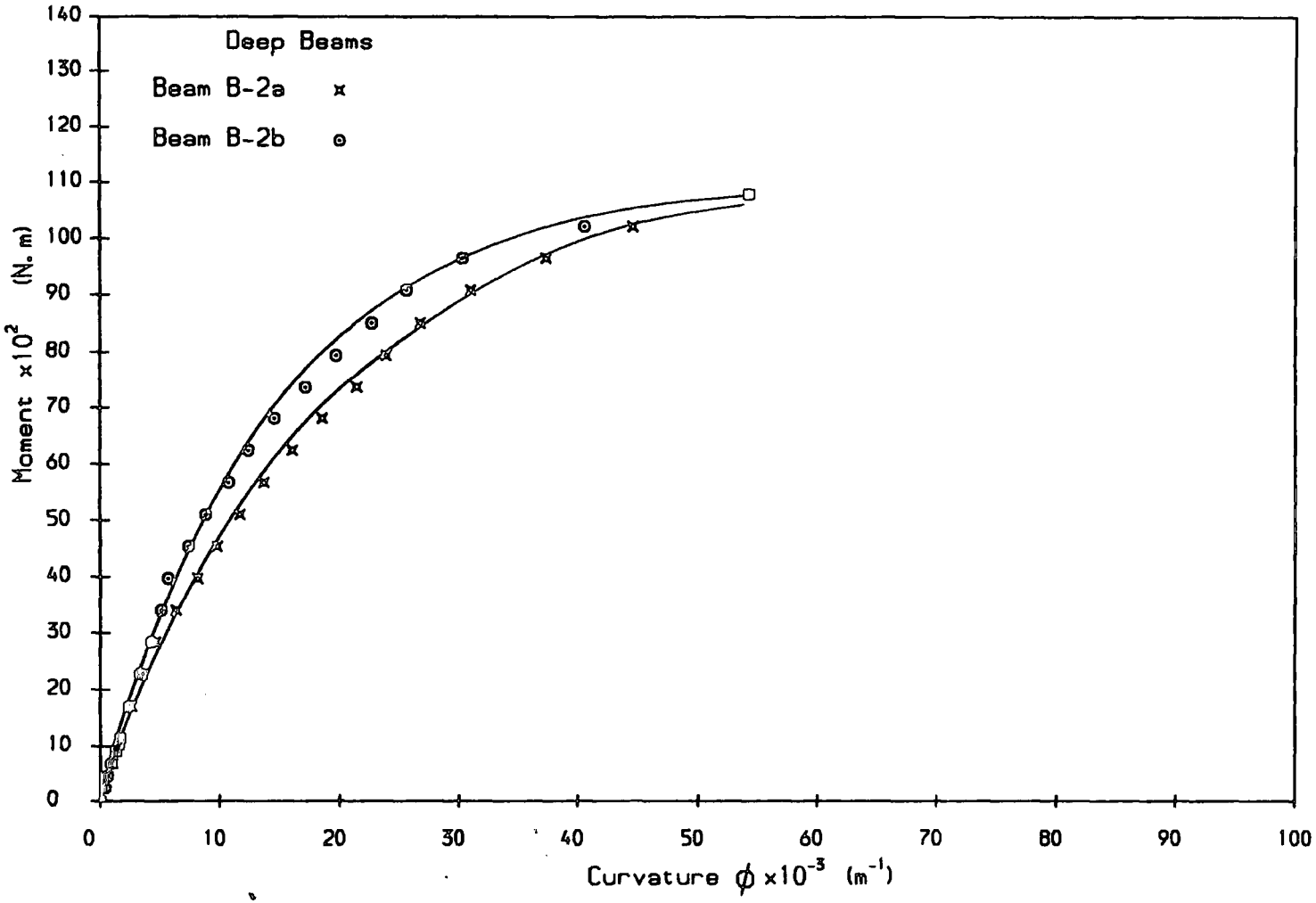

Fig 5.10e Moment - Curvature Relationship for Phenolic Beams.
(Internal Reinforcement 2x6 mm dia. h.y.s. bars)

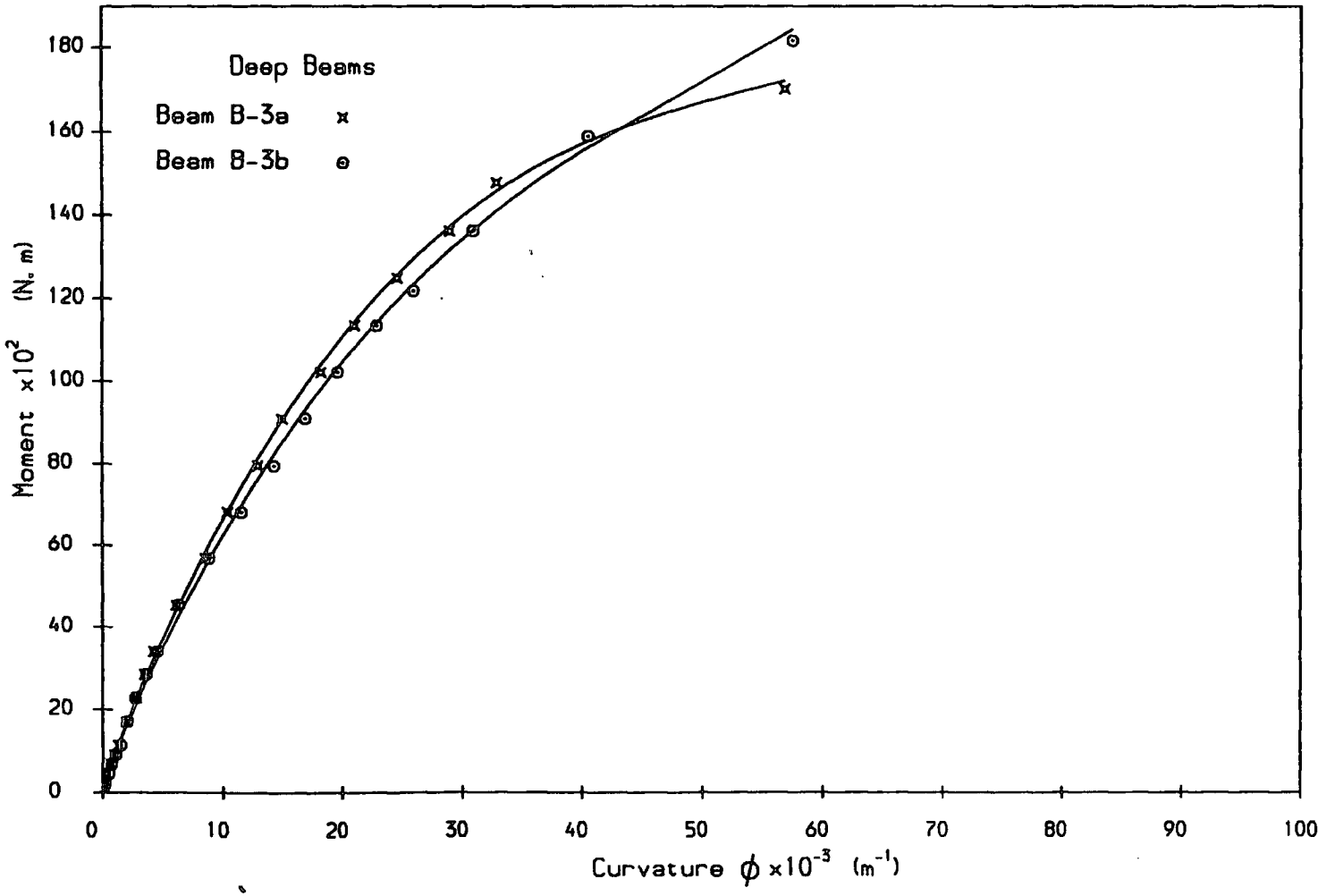

Fig 5.10f Moment - Curvature Relationship for Phenolic Beams.

(Internal Reinforcement 2x10 mm dia. h.y.s. bars)

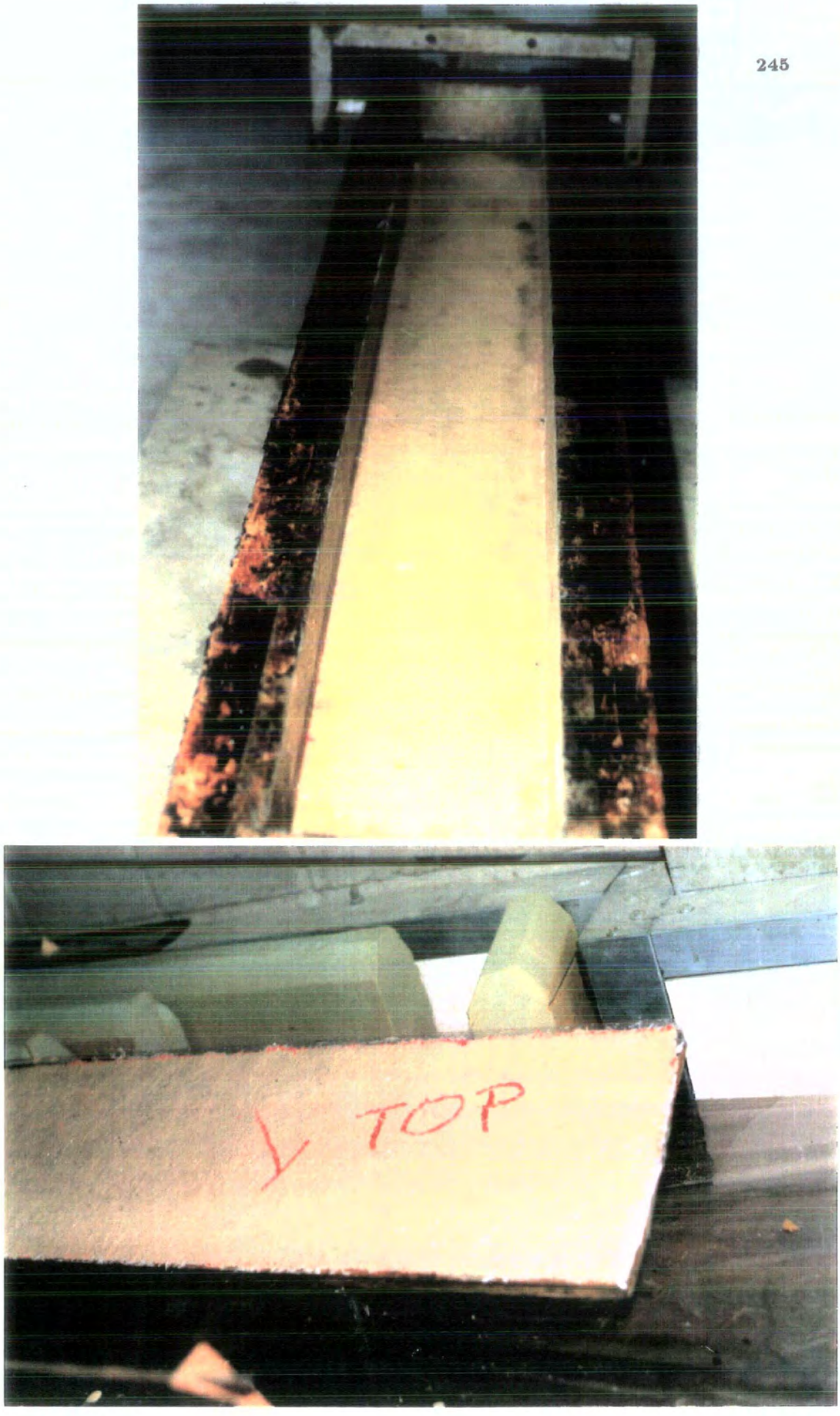

Plate 5.1 Formation of the outer lay-up laminates and the pre-cut foam to form the inner core of the test box beams.

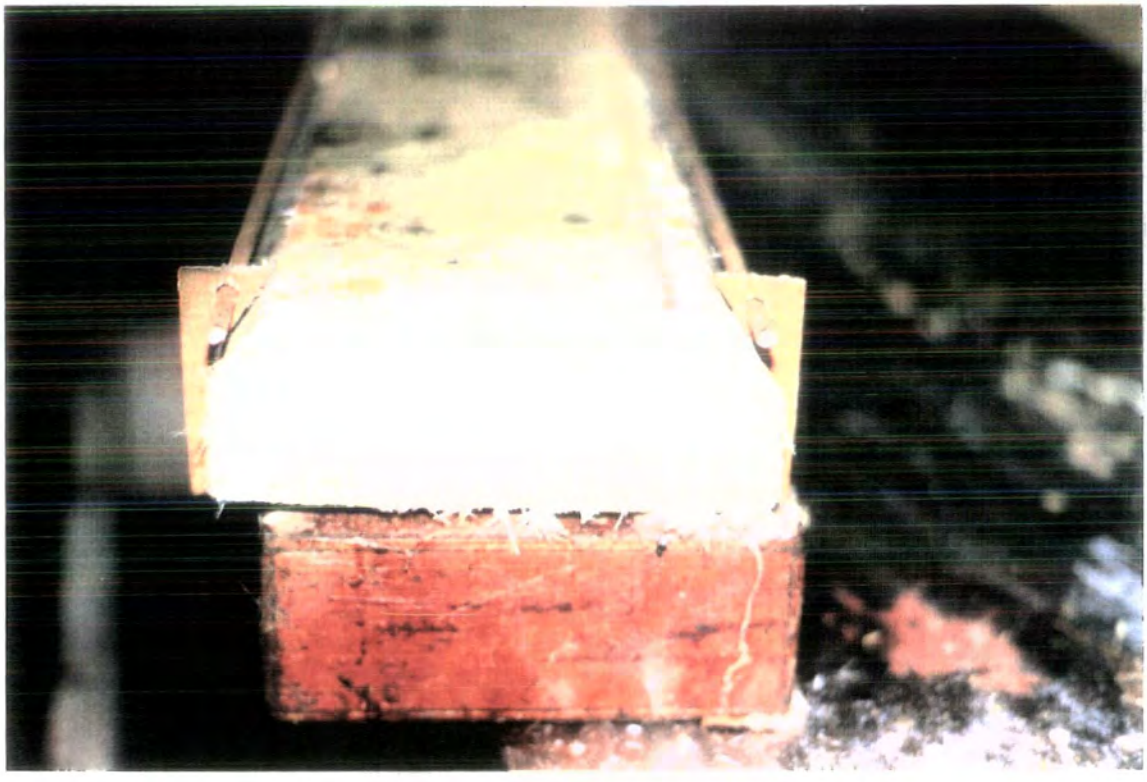

Plate 5.2 Formation of the inner lay-up laminates enveloping the pre-cut foam (inner core). Showing the prepared core and the longitudinal steel bars in pre-cured laminated fibre glass formers cut to the required geometry to act as spacers and steel bar guides.

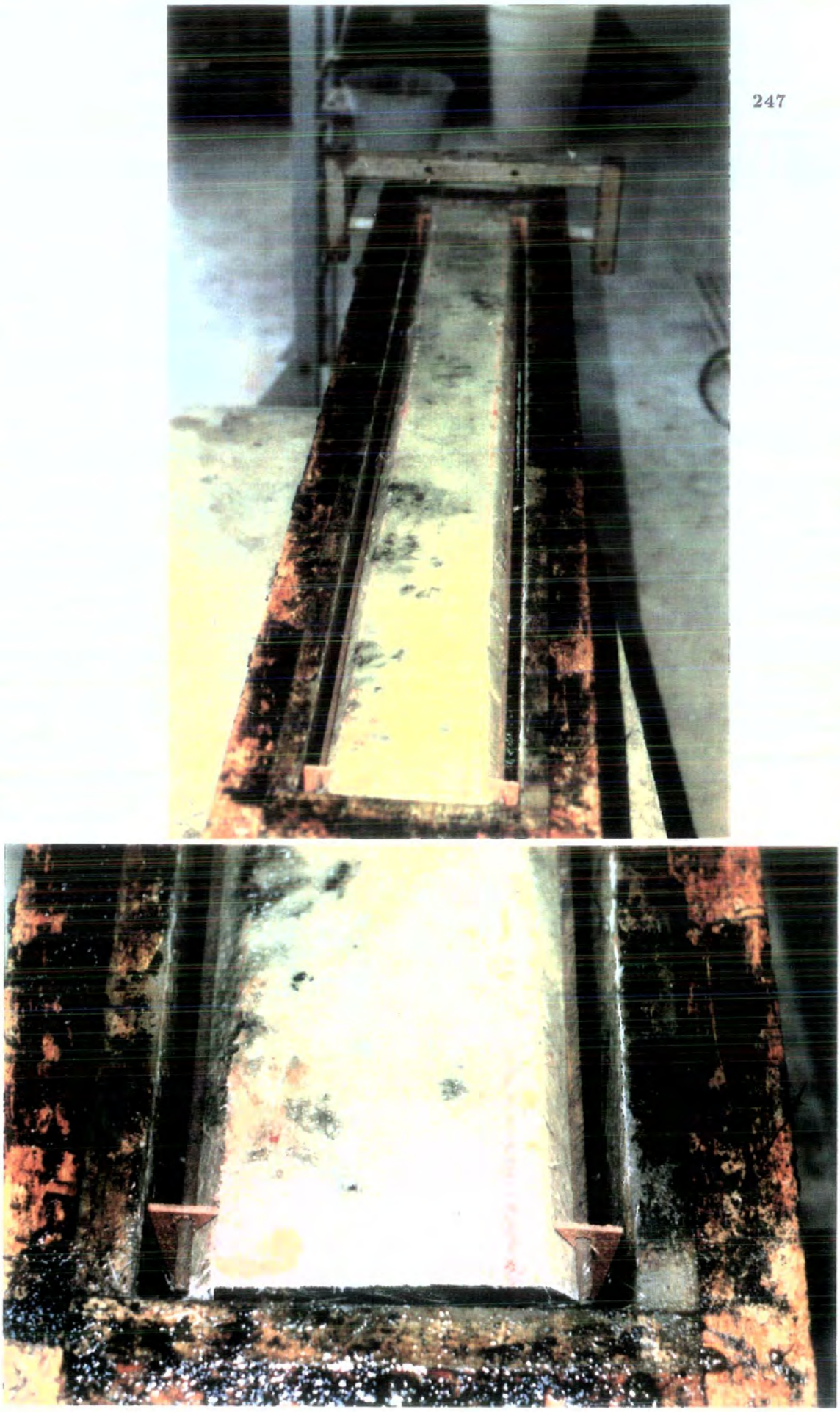

Plate 5.3 Positioning the core and the steel bars in the mould over the first cast phenolic concrete skin.

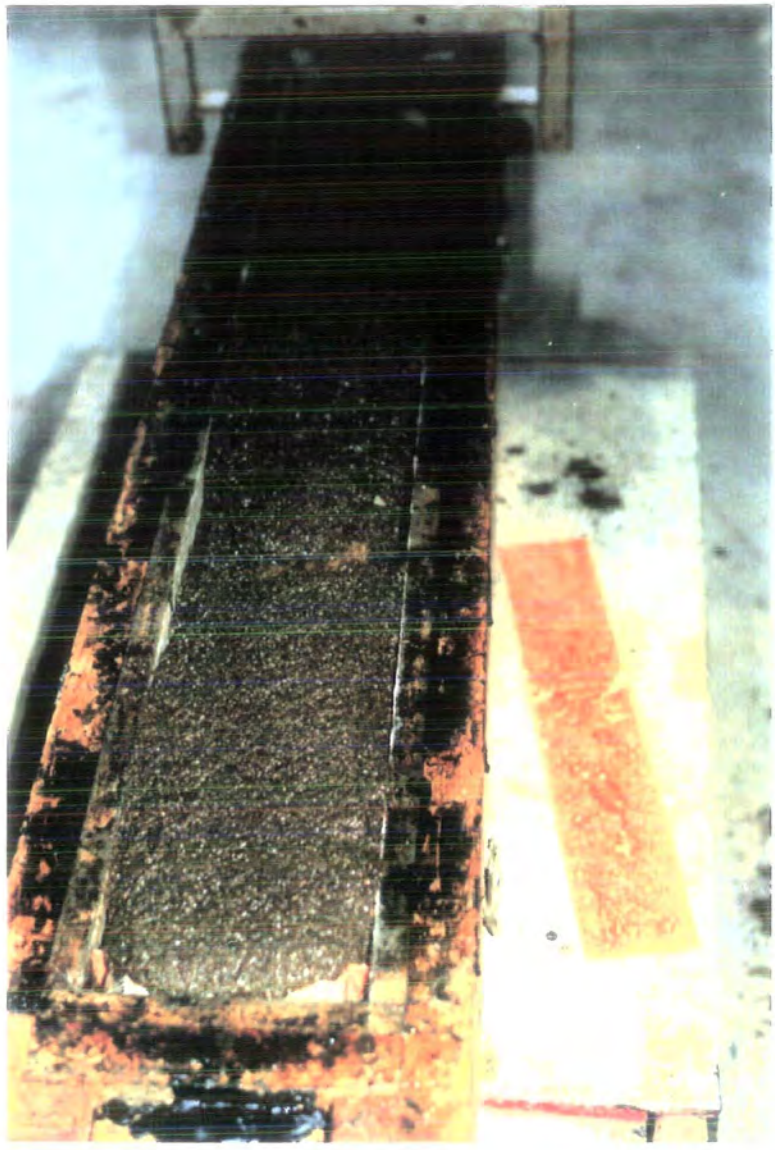

Plate 5.4 Casting the final batch of the Phenolic Concrete mix over the positioned core and the longitudinal steel bars.

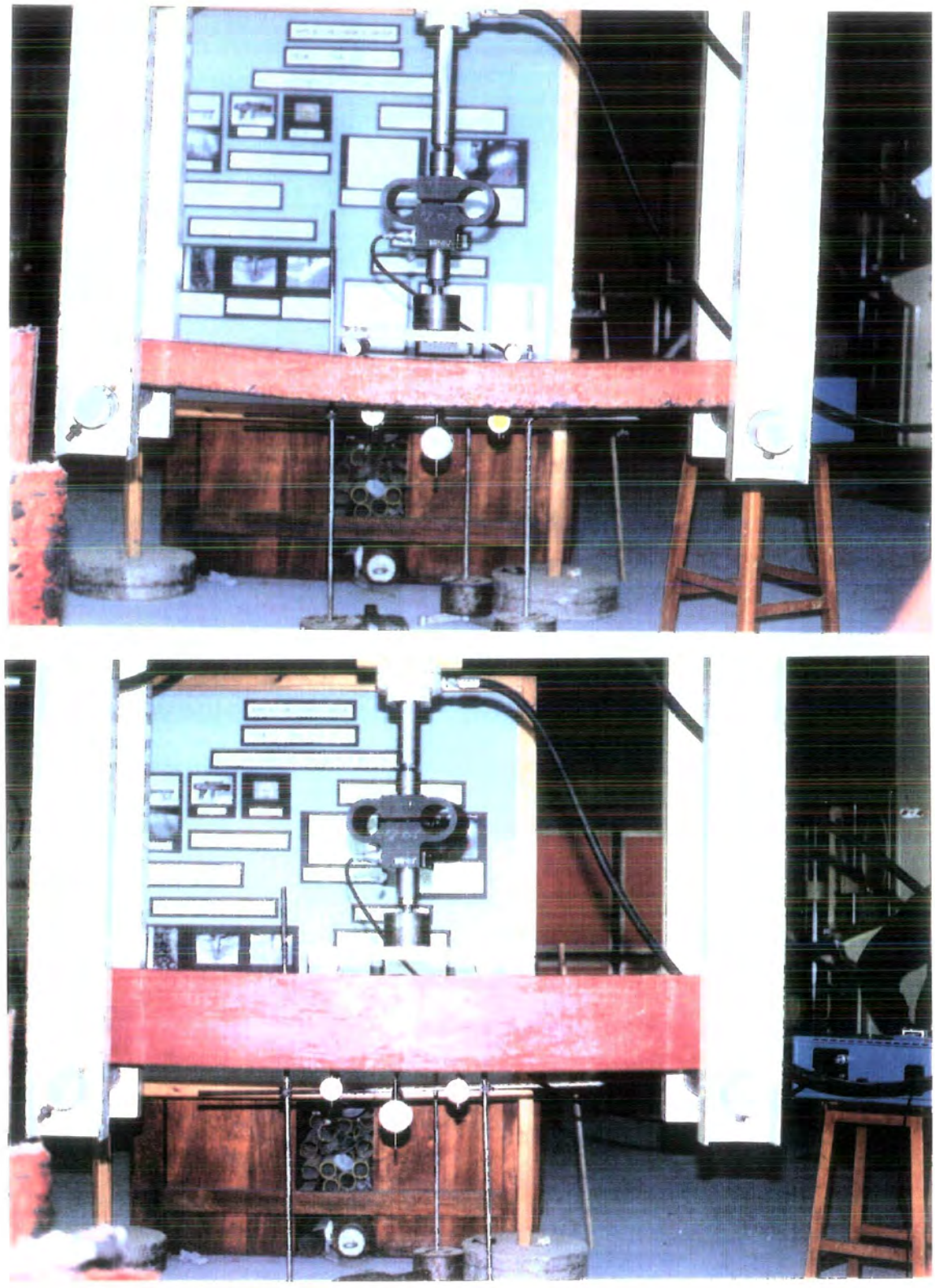

Plate 5.5 General loading, support and instrumentation arrangement of the test beams.

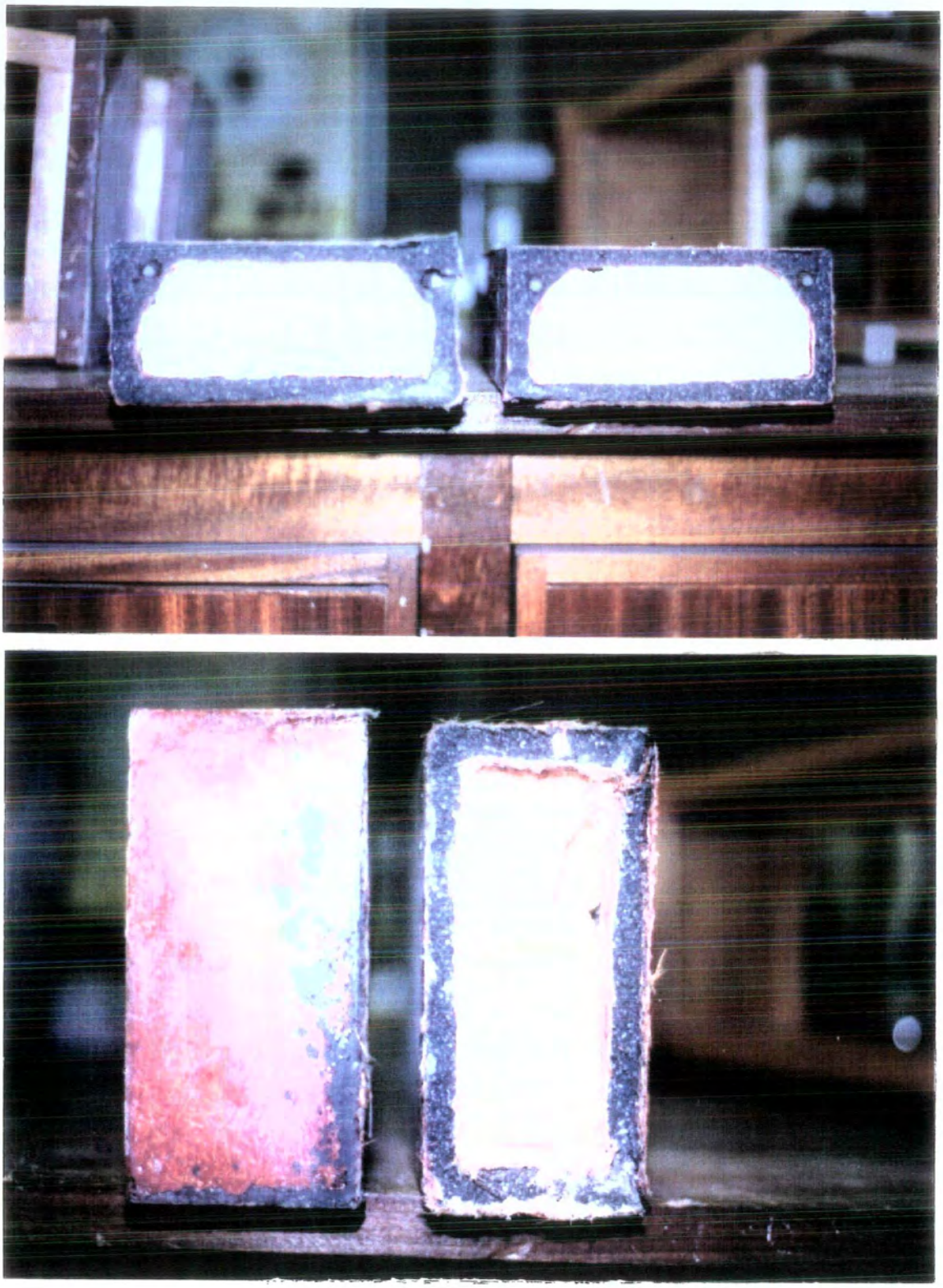

Plate 5.6 Cross section of the box beams after failure at the plane of failure.

Chapter Six

6. Phenolic Concrete Bridge-Deck Panel

6.1. Introduction

Polymer concrete panels have been in use for sometime. An important development was a resin concrete product which was developed using filled polyester resin by Kubase Construction Ltd. in conjunction with B.P. Chemicals Ltd.. The panels could be constructed in a variety of shapes and sizes. The form of use determines their physical arrangements. They could be used in the construction and civil engineering industry, providing a superior and economic alternative to the traditional materials.

Panel assemblies can be in the form of double skined sandwich panels encapsulating a rigid foam core for housing costruction, in sheet form for cladding purposes and in reinforced sections for use as permanent shuttering or as self-supporting floor structures.

The panel constructed for this work can be for use as permanent shuttering, retaining walls, security fencing and cladding to factories and warehouses and possibly for roofing sheets. This type is known as bridge-deck panel, which has already been used in the form of internally reinforced filled polyester resin concrete in the construction of the bridges over the M62 and A19 in N.E. of England. However, the filled polyester concrete used in the construction of these panels falls short of fire regulation requirements for use in domestic buildings. It is primarily for this reason that the filled Phenolic Concrete developed in this research has been used in the

construction of such panels for this work.

The polymer concrete bridge-deck panel consists of a thin flat sheet stiffened on one face by a number of equi-distant longitudinal ribs.

The panel comprises a lamination of resin concrete, reinforced with fibre glass mat on extreme faces. Additionally the ribs can be internally reinforced using steel bars longitudinally cast into the top and bottom of each rib.

The Phenolic Concrete bridge-deck panels constructed for this work, were long thin slabs stiffened on one face by two ribs. In these the Phenolic Concrete matrix was reinforced using laminated fibre glass mat/Phenolic resin lay-ups (in the form of Phenolic GRP) on its extreme faces, with the ribs internally reinforced with high yield deformed steel bars.

6.2. Test Specimens and Test Variables

Four groups (A,B,C and D) of the Phenolic Concrete Composite bridge-deck panels were constructed and tested in this work. Groups A, B, and C, each consisted of three sets (1,2, and 3), with group D consisting of only one set (i.e. ten sets in total). Each group is identified by its section rib depth. The depths were 65, 58, 46 and 35 mm. respectively. All the panels were composed of Phenolic Concrete matrix. In all the panels the primary reinforcement was by means of fibre glass mat/Phenolic resin lay-ups to top and bottom faces. The secondary reinforcement in Sets 2 and 3 of the panel groups A, B and C was by pairs of deformed high yield steel bars of 'ribbed' type cast in each of the ribs.

Each set consisted of two identical samples thus bringing the total of the number of the test samples to twenty specimens. The panels were of $3m$ length with $300mm.$ width, with two symmetrically disposed longitudinal ribs stiffening a thin flat slab

(flange) of 7 to 9 mm. thickness.

Once all the panel sets ($3m$ length) were constructed and cured, they were cut into two equal lengths approximately $1.5m$ long using a diamond tipped rock cutter saw, and then tested in pairs as two individual panel specimens. Set 1, in each group was constructed as internally unreinforced section and tested as reference panels, with Sets 2 and 3 being internally reinforced with a pair of steel bars in each rib. The reinforcement in each rib consisted of a pair of $6mm\ \phi$ in Set 2 and a pair of $10mm\ \phi$ in Set 3, with one of the bars at the top of the ribs and the other approximately at the centre of thickness of the thin slab (flange) of the panel section.

Cross-sectional schematics and schedules of the test panels are illustrated in Figures 6.1 and 6.2, with bridge-deck panel schedules and their cross-sectional dimensions as measured from the tested panels in Tables 6.1 and 6.2 respectively.

6.3. Properties of the Materials

The panels were cast using the mix E1 (see Chapter 3 and Appendix A1). The Phenolic Concrete matrix contained the fillers and the phenolic resin in the ratio of 5.5:1 by weight. The mix constituents and the mix ratio were kept constant for all the panels and their control specimens.

The resin used in the mix was J50/010l Phenolic Resin produced by B.P. Chemicals, with its relevant acid catalyst, a derivation of paratoluene sulphonic acid commercially known as Phencat 15 at 8% by weight of the resin.

A non-tilting pan type of mixer, normally used in concrete mixes, was used in mixing the Phenolic Concrete mixes. Each mixing capacity was designed to provide for one bridge deck panel of $3m$ long and four control coupon specimens ($100 \times 600 \times 8mm^3$.). The mixing, casting, setting and curing procedures and their

time span for all the panels and the control specimens were kept constant.

The coupon specimens were cast with and/or without fibre glass mat /Phenolic resin lay-ups at their extreme faces. These were tested along with the panel specimens in the manner explained in Chapter 3 and 5, under flexure. The results of these control specimens are outlined in Table 6.3.

The primary reinforcement in all the panels and their relevant control specimens was of laminated fibre glass mat of chopped strand type known as Supermat P.B., of weight $450g/m^2$. The resin used in hand-lay lamination of the glass mat was $J2018L$ with its relevant acid catalyst Phencat 10 produced by B.P. Chemicals. The formation and material properties of the laminated fibre glass mat used in these panels were similar to those used in beam construction. These are explained in Chapter 5. The properties of the secondary reinforcement which was of steel deformed bars of 'ribbed' type cast in the ribs of Set 2 and Set 3 of group panels A, B and C, are referred to in Chapter 5.

6.4. Method of Construction, Casting, Setting and Curing

Four wooden moulds having inverted ribs, each with different rib sizes (depths) were constructed and used in casting the panels. They were designed so that the thin slabs of the panels could be cast uppermost and the ribs to the bottom face of the moulds. The moulds were designed to cast panels of $3m$ length, $300mm.$ wide with two symmetrical ribs. For ease of stripping the set panels and also to avoid any possibility of the Phenolic Concrete matrix or any excess resin being bonded to the mould, special care and preparation was needed prior to any casting. The moulds were thoroughly waxed using an industrial wax, then a thin layer of gel type grease was applied to all surfaces followed by placing thin Melinex release sheets, which

had been previousely cut to the required sizes, over the greased surfaces and pushed down into place inside the inverted ribs. The grease layer acted as an adherent between the mould surface and the Melinex release sheets. A brush pressure was applied to the Melinex lining to remove any trapped air. Over the Melinex lining a mould releasing agent was sprayed which enabled the Melinex release sheets to be pilled off easily once the set specimens were stripped.

The fibre glass mat which had been prepared to the required size was then placed in the prepared mould and pushed down into the ribs. Once the glass mat had taken the shape of the ribbed face, using a brush and steel roller, the relevant catalysed resin was uniformly applied soaking the chopped strand mat to form the laminated lay-up. This was left to set before any casting was poured. Otherwise the glass mat in a wet state would allow air to be trapped during casting while the mould is subjected to vibration.

The required lengths of the steel bars prepared previously were positioned inside the ribs using formers acting as spacers in the form of templets made up of pre-cured laminated fibre glass mat.

The mix constituents were mixed in the pan mixer in a similar procedure to that explained in Chapter 5. The Phenolic Concrete mix was then poured into the mould over the laminated fibre glass mat and the positioned steel bars. During casting the panel was subjected to vibration, and the cast mix was levelled off with a flat screed. The bottom fibre glass mat which had been already hand-layed on a flat wooden panel with a Melinex release lining, was placed over the levelled mix and the trapped air was removed with the aid of a steel roller. The flat wooden panel (acting as the lid to the mould) was positioned on top and pressure by means of weights was applied to it in order to assist the setting of the composite bridge deck

panel. The corresponding control coupon specimens were constructed accordingly along side each panel.

The panels and the coupon specimens remained in the mould subject to pressure for a period of 24 hours while setting before being stripped off. All the test specimens after being stripped off were transferred to N.E.I. Parsons of Durham City where they were placed and cured in a large walk in oven for a period of three hours at $120 \pm 5°C$.

6.5. Test Rig, Instrumentation and Test Procedure

The general loading and support arrangement of the test panels is illustrated in Figure 6.3, with its photographic evidence in Plates 6.1*a* and 6.1*b*. Each $3m$ panel was cut into two $1.5m$ long panels and tested over an effective span of $1.3m$.

For the cut panels the internal steel bars cast in their ribs were exposed at both ends (see Plate 6.2), thus showing their position and enabling any possible slipage to be noticed after completion of the test.

The panels were tested in a loading frame with their ribs upper most (i.e. the ribbed face in compression and the thin slab face in tension). The loading was applied by a hydraulic ram, driven by a Dartec Testing Machine (model M1000 K1). An electro-mechanical load cell with a capacity of $35kN$ was situated immediately below the hydraulic ram. The ram casing was suspended from the spreader beam of the loading frame with the hydraulic pressure to drive the ram downwards onto the test panel. The panels were supported at their ends on the wooden rails positioned centrally on two runners $1.3m$ apart across the main beams of the loading frame.

The panels were tested under two point loading. The load was transfered to the panels through a load spreader rested on two identically symmetrical wooden saddles

made to encase the ribs of the panel. The wooden saddles were positioned on the ribs across the panel width $300mm$ apart (see Figure 6.3).

The vertical deflection, at mid-span of the panels at the centre of the tension face (centre of the bottom thin slab face) and at the loading points over four points on the ribs (two per rib) of the compression face, were measured at all loading stages using five transducers with $75mm.$ and $100mm.$ travel lengths (see Figure 6.3 and Plates 6.1*a* and 6.1*b*). The calibration of the load cell and those of the transducers was confirmed regularly during the testing of the panels.

The panels were loaded by applying a constant rate of loading. The load intensity and rate were controlled by the Dartec. The load cell and the five transducers were connected to a data logger in which over a time span of 2 second intervals the applied load and the corresponding deflection readings were recorded until failure occurred. From the recorded values on the data logger, the loading and the corresponding deflection values and the maximum sustained load at failure were determined.

At cracked sections and at the exposed panel ends, the steel bars were examined for any slippage. The bond between the Phenolic Concrete matrix and the laminated glass mats on the top and bottom faces of the panels at cracked sections were also examined. Tested panels after failure were cut into sections and the appropriate cross-sectional dimensions were measured using a micrometer and a vernier. The averaged measured cross-sectional dimensions of the panels are tabulated in Table 6.2.

6.6. Results and Discussion

The measured deflection values at the corresponding loading levels for all the panel specimens are presented graphically in Figures A3.3 to A3.22 of Appendix A3. The deflection values for each panel were recorded up to where the relevant transducers travel length permitted.

In general the load-deflection curves of the internally reinforced panels initially exhibit a two stage linear section comprising of two straight lines with different slopes. It is suspected that the early cracking of the Phenolic Concrete matrix of the composite section restrained by the crack resistance effect of the laminated fibre glass mat introduces a change in the slope of the primary straight line of the load-deflection curves while maintaining the linearity up to next stage of the curve. The initial straight line of these curves represents linear elastic behaviour of the panel composite sections. The two stage linear section of the preceeding curves is followed by a curved section which indicates the onset of the yield in the reinforcement of the lightly reinforced sections and slipping of the reinforcement in heavily reinforced sections.

Examining the ends of the tested panels reinforced with 10 mm ϕ steel bars (panel sets A3, B3 and C3) exhibited that some movement of tension steel bars had occurred, thus suggesting the bars had slipped under flexure. This was later supported by studying the relevant load-deflection curves. The fluctuation of load with increasing deflection for these panels at higher loading levels clearly suggests the Phenolic Concrete/steel bars bond had not remained intact. The tension steel bars in these sections were slipping before the compression steel bars reached their yield strengths. The bond failure is thought to have caused the tensile force component to be provided by the effective partially cracked Phenolic Concrete composite

thus introducing extensive cracking or possibly crazing of the matrix. This would therefore cause premature failure of the panels at low Phenolic Concrete strains. These sections are thought to be over reinforced, with the failure being a bond failure between the Phenolic Concrete matrix and the steel bars followed by bending failure of the Phenolic Concrete/laminated fibre glass mat in tension (see Plate 6.3).

The second stage of the load-deflection graphs of the lightly reinforced panels (panel sets A2, B2 and C2) is terminated by a short curved section indicating the onset of yield in the steel bars. This is followed by a long horizontal section representing larger increases in deflection, (also observed from test), with no increase or even some decrease in loading thus suggesting the steel reinforcement is yielding.

From observation it was also revealed that the internally reinforced panels continued deflecting with a sudden drop in load. This was supported from the recorded loading values although deflection measurements were ceased. This could well have been due to the widening of the tension crack or possibly development of multiple cracking i.e. crazing in the Phenolic Concrete matrix across the bottom face of the flat slab (flange) within the maximum bending moment area. Although the cracking was invisible due to the crack resistance effect of the laminated fibre glass mat due to its larger strain capabilities, the continued deflection of the specimens with drop in load suggested that the tensile force components were provided by the tension steel and also effective partially cracked Phenolic Concrete composite of the tension zone while the compressive force components were still being provided by the uncracked Phenolic Concrete composite of the compression zone coupled with the compression steel at the top of the panel section possibly yielding. The failure of these panels occurred by a sudden crack becoming visible (i.e. fibre glass mat fracturing) across the bottom face of the thin flat slab (flange) of the section. This was followed by

rapid widening of the visible crack and snapping of the tensile steel bars in lightly reinforced panels.

The load-deflection graphs of the reference panels (unreinforced sections), exhibited a two or three stage linear section leading to a shallower sloped straight line section with larger increases in deflections at higher loads. The first part of these graphs also represented linear elastic behaviour.

From the test observations it was noted that the reference panels underwent considerable deflections (as can be seen from Plate 6.4) representing plastic behaviour as the failure approached. The failure of these panels occurred by a sudden tensile fracture of the sample through a section across the panel width near to the mid-span at ultimate sustained load with total collapse of the panel specimen.

For all the panel specimens, using their relevant load-deflection graphs and the recorded values, the load at first cracking of the Phenolic Concrete matrix (W_{C1}), the load at start of the curved section of the load-deflection graph (W_{C2}) and the ultimate sustained load at failure (W_U) are tabulated in Table 6.4.

The slopes of the initial linear elastic section of the load-deflection graphs of the relevant panels were obtained using a computer '@ogramme based on a best fit line method (see Figures A3.3 to A3.22). Using the slope values (W/y_l) the experimental bending stiffness values (EI) for all the panels were calculated from the expression,

$$EI = C \times \frac{W}{y}$$

where;

C is the constant.

$\frac{W}{y}$ is the slope of load-deflection graph.

EI is the bending stiffness.

The slopes of the load-deflection graphs and the corresponding bending stiffness of the panels are given in Table 6.6.

For the internally reinforced sections, using the equivalent transformed section method, and reducing the Phenolic Concrete composite to the equivalent steel area, the experimental second moment of area I_e of the sections with respect to the steel modulus from the bending stiffness relationship was calculated and tabulated in Table 6.5.

A computer program B/DECK based on the geometrical properties of the bridge deck panel using the equivalent transformed section method was written (by G.M. PARTON) to provide a numerical model for various bridge deck panel configurations. This program made it possible to calculate the theoretical second moment of area I_t of all the panel specimens.

A comparison was made between the theoretical and experimental bending stiffness (calculated with respect to steel modulus) of the internally reinforced panel specimens. It can be seen from the results obtained during testing of the coupon specimens that the application of laminated fibre glass mat as primary reinforcement has two opposing effects on their behaviour. The coupons with the primary reinforcement exhibited lower bending modulus (stiffness) and higher ultimate strength than the coupons without mat reinforcement. Therefore, it was difficult to decide on the modulus which should be used for the Phenolic Concrete in the bridge-deck panels, and a similar procedure was adopted to that which was used in the investigation of the Polyester Concrete panels in a previous study. The theoretical I_t values were plotted (see Figure 6.2), for a range of modular ratios from 10 to 40, so that the effective modular ratio or in effect the effective modulus values of the Phenolic Concrete composite of the test panel could be determined. From the graphs in

Figure 6.3 and the experimental I_e values (calculated with respect to steel modulus) it became clear that a modular ratio of 30 is a reasonable general approximation to make for all the internally reinforced panel sections. The theoretical I_t values of reinforced panels based on modular ratio 30 and those of reference panels are given in Table 6.6. The modulus value E based on the theoretical I_t values, using the bending stiffness relationship derived from the relevant experimental load-deflection graphs for all the panels, were obtained (see Table 6.5). The validity of the modular ratio 30 used in computation of I_t values for internally reinforced sections is confirmed when the deduced E values for both internally reinforced and unreinforced panels are compared.

For all the panels, using the tensile strength of the Phenolic Concrete matrix (8.15 $N.mm^{-2}$) obtained from Brazilian Disc Tests in Chapter 5, the theoretical load to cause first cracking (W_{C1}) in the matrix was computed from bending theory based on the equivalent transformed section method. It was assumed that a uniform tensile stresses existed across the bottom face of the thin flat slab of the panels. The theoretical values were found to be in close agreement with the experimental values (see Tables 6.4 and 6.5).

With the assumption that $E_s = 30 \times E_f$, the loads to cause the development of the yield stress in the compression steel bars of the lightly reinforced sections, were calculated and tabulated in Table 6.5. It can be seen that for lightly reinforced sections where Phenolic Concrete/steel bar bond has remained viable up to steel yielding, the failure load can be predicted by calculating the moment to cause the development of the yield stress in the steel bars (see Tables 6.4 and 6.5 for comparison).

The load at failure of the unreinforced sections (reference panel sets A1, B1, C1

and D1) was calculated considering the corresponding Phenolic Concrete strength at tensile fracture obtained from flexural testing of the coupon specimens. The calculated failure loads of the relevant panels were in close agreement with the corresponding experimental ultimate sustained load at failure (see Tables 6.4 and 6.5).

The ultimate failure moments of the panels were calculated using the section modulus determined from the equivalent section method. The use of the equivalent section method in the design of the bridge deck panel section together with the output of the computer program B/DECK are given in Appendix A3.

As the failure of the heavily reinforced panels occurred due to Phenolic Concrete/steel bond failure, it is therefore suggested that limiting steel strain values and hence Phenolic Concrete strain values should be obtained in order to predict the premature failure of these panels. Therefore, from the recorded loads at the onset of the steel bars slipping and also at the ultimate sustained loads, the developed strains in the compression steel and in the corresponding Phenolic Concrete of extreme panel tension faces were calculated.

These strain values are tabulated in Table A3.2 and they may be used as failure strain limits. These strain values suggested that the failure of the heavily reinforced panels occurred at uneconomically low Phenolic Concrete/fibre glass mat strains. It is also evident that the compression steel strains developed at failure were too low in comparison to its yield strain and hence the steel strength capacity was not completely utilized. Similarly the relevant strain values of the lightly reinforced panels are also calculated and tabulated in Table A3.2, in order to study the Phenolic Concrete strains at failure. When the developed compression steel strain values are compared with the steel yield strains it is evident that the steel had well reached the

steel yield strain with the Phenolic Concrete strain at steel yield strain not being high enough to have caused complete tensile failure. It is therefore suspected that the Phenolic Concrete had not failed until the steel had reached its hardening stage (see Table A3.2).

From the calculated strains of the lightly reinforced panels (see Table A3.2), there is a clear correlation between "the yield strain ϵ_{ys} (i.e proof stress/modulus)" and the strain ϵ_{2ts} in the steel at the end of the elastic range of the bridge-deck panels and at the onset of the plastic hinge. The strain ϵ_{Uts} in the steel at panel fracture is approaching the fracture strain in the tensile specimen but infact never reaches it. It may not be possible to correlate these as clearly, however, under these circumstances it is fair to say that fracture strains of the tensile specimens and the steel in the panels are similar. The calculated Phenolic Concrete strains (ϵ_{2bp}) at the end of the elastic range of the lightly reinforced panels are low as one would expect, but in general the strains at fracture (ϵ_{Ubp}) are inconsistent with the strains at fracture (ϵ_{Fp}) of the coupon specimens. These inconsistencies are clear in deeper sections, but only in the shallow sections of the panels set C2 there is a clear correlation between ϵ_{2bp} and ϵ_{Ubp} strain values of the panels and strain (ϵ_{Fp}) at fracture of the relevent coupon specimen. It is, however, obvious that the coupon specimens represent a different structural element as opposed to the panels, and therefore their test results cannot justify the true behaviour of the panels but can only represent a guide as test control specimens.

6.7. Conclusion

It was demonstrated that the effective failure of the heavily reinforced (over reinforced) panel section was caused by the bond failure between the Phenolic Concrete and the steel bars leading to a tensile failure of the Phenolic Concrete/laminated fibre glass mat in bending at uneconomically low strains. However, with the lightly reinforced sections, from the elastic-plastic behaviour of the bridge deck panel (as seen from load-deflection curves), the effective failure was caused by the development of yield in the steel reinforcement, causing the formation of a plastic hinge in the vicinity of the maximum bending moment. The ultimate failure of the lightly reinforced sections was then reached, when the hinge effect had suffered considerable deformation. This was when the Phenolic Concrete/laminated fibre glass mat failed in tension along a section across the bottom face of the thin slab within the maximum bending moment area. Therefore, in designing Phenolic Concrete bridge deck panel, if a suitable weight of reinforcement is used, the failure can be predictable. The crack resistance capability of the laminated fibre glass mat and the high modular ratio allows the composite section to remain intact until after the steel has yielded with the Phenolic Concrete/steel bar bond remaining viable until the steel yield.

The effect of the laminated fibre glass mat as primary reinforcement on the Phenolic Concrete matrix of the panels impedes the early cracking of the composite section as a whole. This in effect simplifies the use of the equivalent section method in the design of the panel section. It also provides sufficient flexibility (ductility) to the Phenolic Concrete of the bridge-deck panels making them viable structures. Even in the internally unreinforced panels some plastic behaviour was observed prior to failure, which in effect gives sufficient warning before ultimate failure occures.

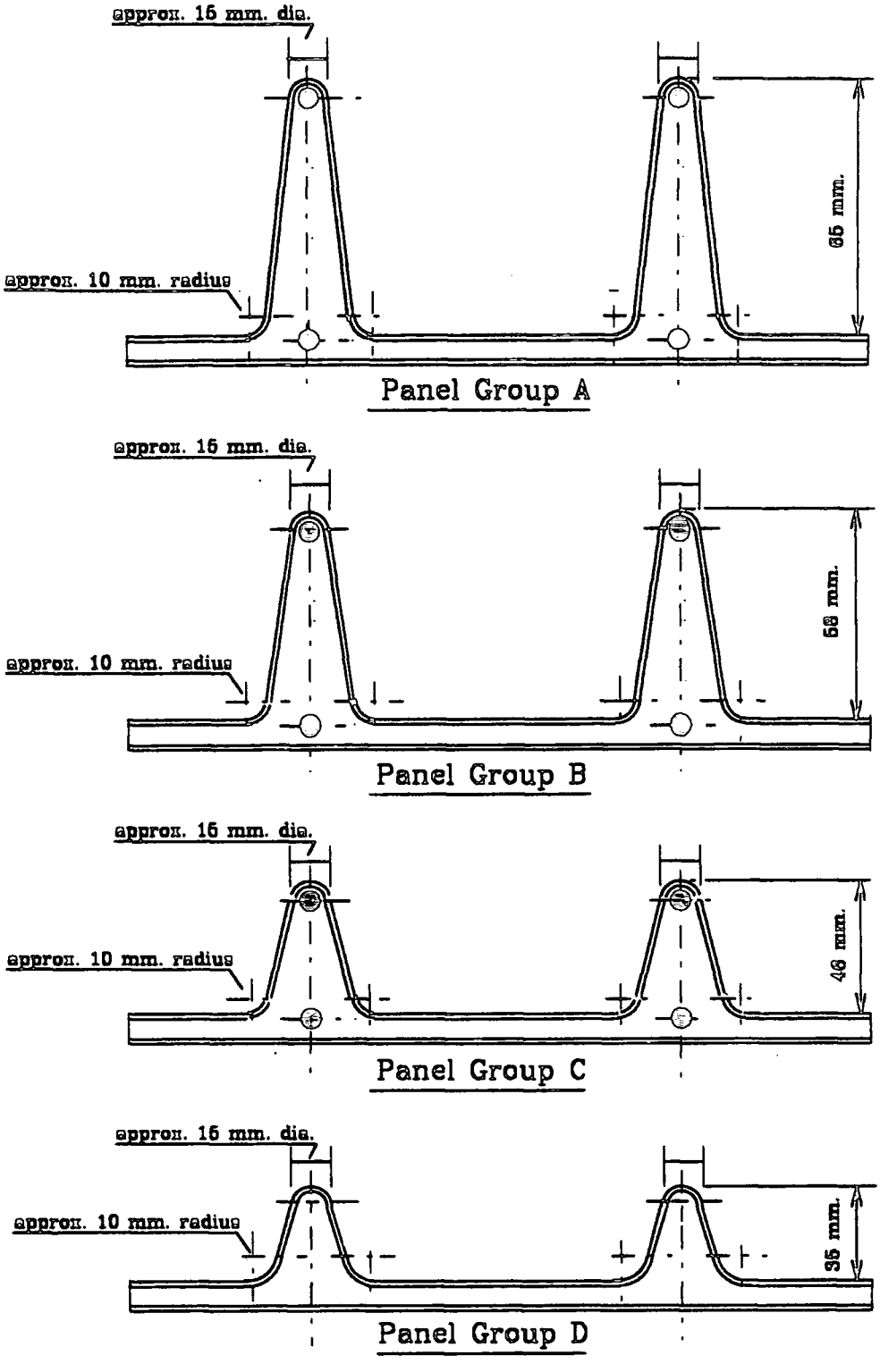

Figure 6.1 Schematic layout of the Phenolic Concrete bridge deck panels.

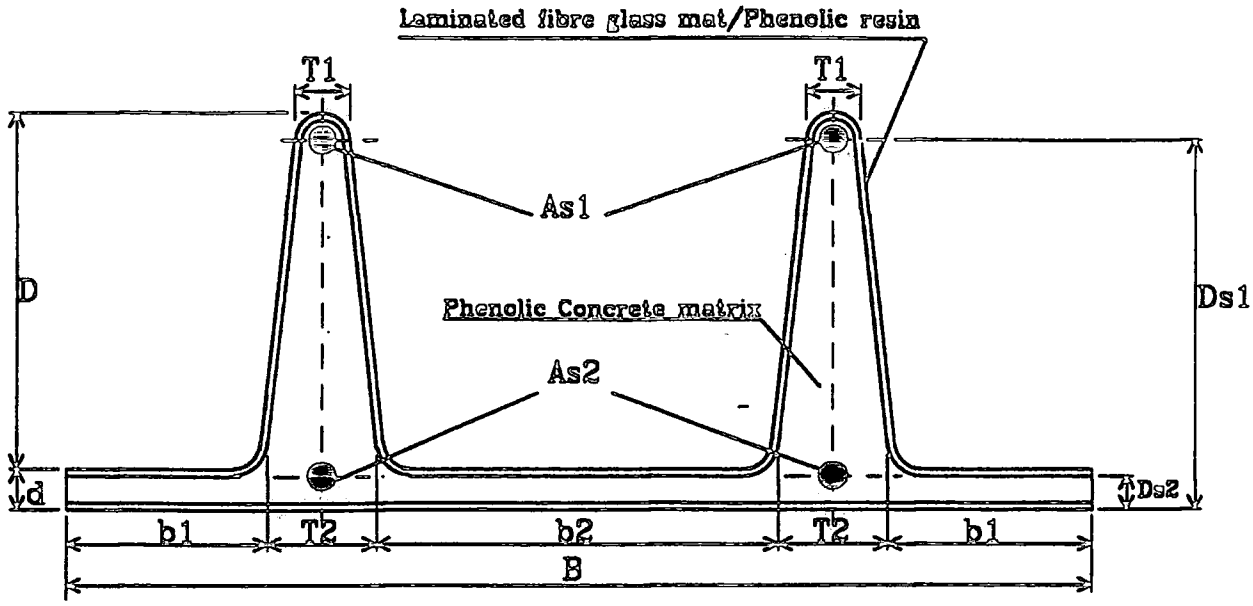

Figure 6.2 Cross-sectional schedule of a typical Phenolic Concrete bridge deck panel.

Panel Group	Rib Depth (mm.)	Internal Reinforcements (two bars per rib)		
		Set 1 (a & b)	Set 2 (a & b)	Set 3 (a & b)
A	65	no reinforcement	8 mm. dia. h.y. steel bars	10 mm. dia. h.y. steel bars
B	58	no reinforcement	8 mm. dia. h.y. steel bars	10 mm. dia. h.y. steel bars
C	46	no reinforcement	8 mm. dia. h.y. steel bars	10 mm. dia. h.y. steel bars
D	35	no reinforcement	———	———

Table 6.1 Phenolic Concrete Bridge Deck Panel Schedule.

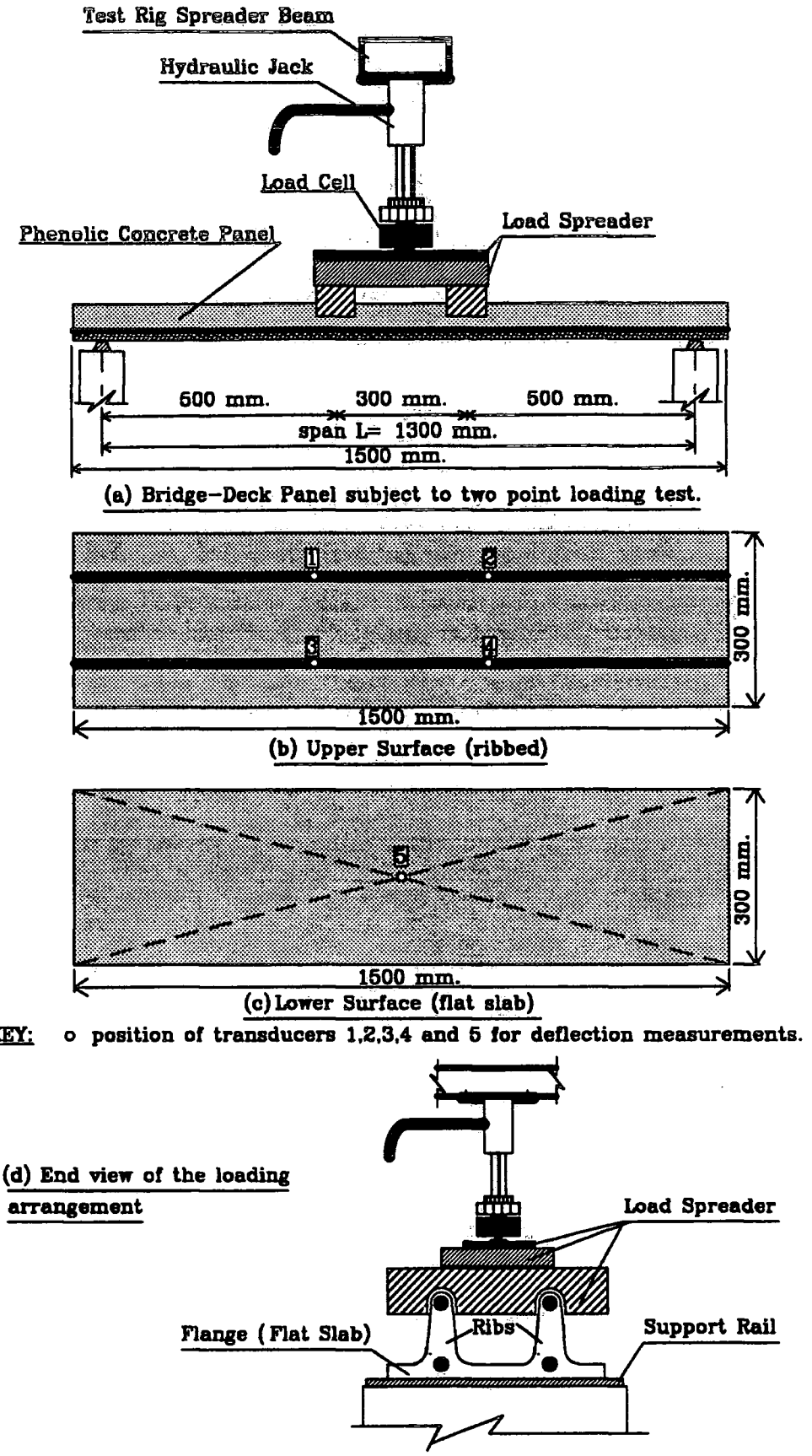

Figure 6.3 Loading and Instrumentation arrangement of the Phenolic Concrete Test Panels.

Table 6.2 (Cross-Sectional Dimensions and Schedules of the Test Panel.)

Test Panels	Panel Dimensions (mm)									Internal Steel Bar Reinforcement
	B	b1	b2	T1	T2	D	d	Ds1	Ds2	
A-1a	300	60	124.30	16.24	27.85	65.50	7.87	.....	.....	*none*
A-1b	300	60	124.44	16.27	27.78	65.92	7.74	.....	.....	
A-2a	300	60	124.46	16.17	27.77	65.95	8.95	58.36	19.99	2 × 6 *mm* ϕ *h.y.s. per rib*
A-2b	300	60	124.08	16.09	27.96	65.92	8.82	57.94	17.70	
A-3a	300	60	124.22	16.05	27.89	65.63	8.98	51.96	17.89	2 × 10 *mm* ϕ *h.y.s. per rib*
A-3b	300	60	124.52	16.07	27.74	65.94	8.91	53.46	15.88	
B-1a	300	60	123.86	16.10	28.07	58.40	8.22	.....	.....	*none*
B-1b	300	60	123.22	16.09	28.39	58.62	8.55	.....	.....	
B-2a	300	60	123.10	16.08	28.45	58.88	9.10	56.72	20.85	2 × 6 *mm* ϕ *h.y.s. per rib*
B-2b	300	60	123.98	16.01	28.01	58.82	8.48	55.10	20.93	
B-3a	300	60	122.18	16.14	28.91	58.85	9.73	45.04	17.71	2 × 10 *mm* ϕ *h.y.s. per rib*
B-3b	300	60	122.20	16.06	28.90	58.82	9.31	46.72	20.39	
C-1a	300	60	123.60	16.01	28.20	46.35	7.35	.....	.....	*none*
C-1b	300	60	122.60	16.03	28.70	46.84	7.66	.....	.....	
C-2a	300	60	122.42	16.01	28.79	46.83	8.52	38.20	19.83	2 × 6 *mm* ϕ *h.y.s. per rib*
C-2b	300	60	123.44	16.10	28.28	46.88	8.64	38.45	20.76	
C-3a	300	60	122.22	16.17	28.89	46.78	8.79	30.30	18.10	2 × 10 *mm* ϕ *h.y.s. per rib*
C-3b	300	60	122.32	16.16	28.84	48.80	8.76	30.80	18.22	
D-1a	300	60	123.90	16.01	28.05	34.79	7.36	.....	.....	*none*
D-1b	300	60	123.14	16.09	28.43	34.90	7.73	.....	.....	

Note: See Figures 6.1 and 6.2 for panel dimensions.
All the dimensions are the average measurments taken from 3 cross-sections for each panel.

Table 6.3 (Results from Flexural Testing of Control Coupon Specimens)

Coupon Test		Laminated Fibre Glass $450g/m^2$ Supermat P.B.	Av. Thickness d (mm)	Sustained Loads at:		Ult. Flexural Strength $\sigma_{Fu} \times 10^6$ ($N.m^{-2}$)	Load-Deflection Graphs	
Group	Specimen			Onset of Crack W_C (N)	Failure W_F (N)		Slope W/y ($N.mm^{-1}$)	Flexural Modulus $E_{Fg} \times 10^9$ ($N.m^{-2}$)
A-1	a	top & bottom	9.55	550	1550	57.36	110	14.59
	b	top & bottom	9.40	540	1510	57.68	118	16.18
	c	none	7.80	460	460	25.52	96	23.04
	d	none	7.64	440	440	25.45	96	24.52
A-2	a	top & bottom	9.42	570	1485	56.48	120	16.35
	b	top & bottom	9.65	550	1485	53.82	125	15.84
	c	none	7.75	460	460	25.85	92	22.51
	d	none	7.63	450	450	26.09	92	23.59
A-3	a	top & bottom	10.02	580	1540	51.77	120	13.59
	b	top & bottom	10.10	530	1520	50.29	115	12.71
	c	none	7.83	455	455	25.05	88	20.88
	d	none	7.62	420	420	24.41	86	22.14
B-1	a	top & bottom	10.14	510	1530	50.22	115	12.56
	b	top & bottom	10.21	590	1560	50.51	110	11.77
	c	none	7.79	460	460	25.58	88	21.20
	d	none	7.82	465	465	25.66	88	20.96
B-2	a	top & bottom	10.01	520	1520	51.20	120	13.63
	b	top & bottom	9.92	530	1550	53.16	110	12.84
	c	none	7.21	410	410	26.62	86	26.14
	d	none	7.44	415	415	25.30	86	23.79
B-3	a	top & bottom	9.88	560	1510	52.21	110	12.99
	b	top & bottom	9.75	560	1480	52.54	130	15.98
	c	none	7.80	440	440	24.40	86	20.64
	d	none	7.49	410	410	25.57	88	24.74
C-1	a	top & bottom	9.66	510	1500	54.25	115	14.53
	b	top & bottom	9.72	530	1510	53.94	115	14.26
	c	none	7.10	405	405	27.11	82	26.10
	d	none	7.25	410	410	26.33	88	26.30
C-2	a	top & bottom	9.89	500	1480	51.07	130	15.31
	b	top & bottom	9.91	540	1470	50.52	130	15.21
	c	none	7.29	440	440	26.67	88	25.87
	d	none	7.12	420	420	26.63	86	27.14
C-3	a	top & bottom	10.22	520	1460	47.18	125	13.34
	b	top & bottom	10.15	540	1450	47.50	125	13.62
	c	none	7.65	450	450	25.95	90	22.90
	d	none	7.41	430	430	26.43	90	25.20
D-1	a	top & bottom	9.72	540	1490	53.23	120	14.88
	b	top & bottom	9.94	550	1485	50.73	120	13.92
	c	none	7.34	420	420	26.31	88	25.35
	d	none	7.50	445	445	26.70	88	23.76

Note: The results are extrapolated from the load-deflection graphs obtained from flexural testing of the coupon specimens subject to 4 point flexural loading on Instron "1195".

Table 6.4 (Experimental results from flexural testing of the Bridge-Deck Panels.)

Panel		Experimental			
Group	Specimen	W_{C1} (kN)	W_{C2} (kN)	W_U (kN)	Observed Failure Mode
A	1a	4.264	.....	10.310	Bending Failure
	1b	4.470	.....	11.257	(Tension Cracking)
A	2a	6.521	13.000	14.985	Steel Yielding followed
	2b	5.651	14.459	15.953	by Tension Failure
A	3a	7.746	19.402	21.497	Steel Slipping followed
	3b	7.731	18.310	21.261	by Tension Failure
B	1a	3.748	.....	8.710	Bending Failure
	1b	3.216	.....	7.445	(Tension Cracking)
B	2a	5.356	12.570	14.290	Steel Yielding followed
	2b	5.282	12.526	14.857	by Tension Failure
B	3a	6.344	15.225	17.538	Steel Slipping followed
	3b	6.197	15.521	17.749	by Tension Failure
C	1a	1.638	.....	6.875	Bending Failure
	1b	1.623	.....	6.733	(Tension Cracking)
C	2a	3.128	10.097	10.549	Steel Yielding followed
	2b	3.157	10.136	10.947	by Tension Failure
C	3a	3.570	10.475	11.523	Steel Slipping followed
	3b	3.570	10.549	11.705	by Tension Failure
D	1a	1.534	.....	4.180	Bending Failure
	1b	1.415	.....	4.470	(Tension Cracking)

Notes:

W_{C1} - Load at first cracking of the Phenolic Concrete matrix of the composite section.

W_{C2} - Load at the onset of yield or slip of the steel bar reinforcements of the relevant section.

W_U - Ultimate sustained load at failure.

Table 6.5 (Predicted first crack and ultimate failure loads of the Panels.)

Panel		Section Modulus					
Group	Specimen	Z_{ts} (mm^3)	Z_{bs} (mm^3)	Z_{tp} (mm^3)	Z_{bp} (mm^3)	W_{C1} (kN)	W_U (kN)
A	1a	.....	.....	49294	-111183	3.625	11.350
	1b	.....	.....	49629	-111132	3.623	11.313
A	2a	5963	-18755	114063	-178022	5.804	14.550
	2b	5981	-15860	113912	-182506	5.950	14.594
A	3a	12743	-21801	186197	-269830	8.796	.....
	3b	12991	-20762	202380	-296813	9.676	.....
B	1a	.....	.....	40897	-96769	3.155	9.901
	1b	.....	.....	41763	-99606	3.247	10.224
B	2a	5173	-21237	112443	-160524	5.233	12.622
	2b	5129	-20994	106513	-152815	4.982	12.515
B	3a	11702	-21575	150715	-227588	7.419	.....
	3b	11471	-24411	156713	-213893	6.973	.....
C	1a	.....	.....	26668	-65236	2.127	7.074
	1b	.....	.....	27658	-67917	2.214	7.153
C	2a	4236	-60522	61763	-93837	3.059	10.336
	2b	4239	-56740	62408	-95129	3.101	10.343
C	3a	10351	-26489	79956	-126415	4.121	.....
	3b	10239	-26312	82202	-127818	4.167	.....
D	1a	.....	.....	16547	-43237	1.410	4.550
	1b	.....	.....	17057	-44724	1.458	4.777

Notes:

W_{C1} -Load at first cracking of the Phenolic Concrete matrix of the composite section is based on the tensile strength of the Phenolic Concrete obtained from Brizilian Disc tests.

W_U -The ultimate failure load for panel sets A2, B2 and C2 is based on the steel yield stress and for the reference panels it is based on the strength of the Phenolic Concrete at tensile fracture.

Table 6.6 (Theoretical and Experimental second moment of area of the Panels)

Panel		Experimental				Theoretical		
		Slope of Load-deflection curves		Bending Stiffness	Second Moment of Area	Modular Ratio	Second Moment of Area	Modulus value
Group	Specimen	W/y_l $(N.mm^{-1})$	W/y_c $(N.mm^{-1})$	$EI \times 10^3$ $(N.m^2)$	I_e (mm^4)	E_s/E_f	I_t (mm^4)	$E \times 10^9$ $(N.m^{-2})$
A	1a	630.63	370.91	24.9624	3744360.0	.....	2505742.0	9.962
	1b	632.45	480.50	25.0345	3755175.0	.....	2527131.0	9.906
	2a	947.27	602.04	37.4961	187480.5	30	173568.0	7.201
	2b	929.47	603.82	36.7915	183957.6	30	174733.0	7.019
	3a	1354.63	882.10	53.6208	268103.9	30	273998.0	6.523
	3b	1315.56	877.11	52.0743	260371.3	30	300229.0	5.782
B	1a	398.96	260.61	15.7922	2368830.0	.....	1915165.0	8.246
	1b	403.43	313.67	15.9691	2395365.0	.....	1976498.0	8.080
	2a	738.49	619.60	29.2319	146159.5	30	149177.0	6.532
	2b	713.37	602.88	28.2376	141187.8	30	140803.0	6.685
	3a	1043.71	800.31	41.3135	206567.6	30	207273.0	6.644
	3b	1127.98	743.25	44.6492	223246.0	30	205403.0	7.246
C	1a	184.01	119.26	7.2837	1092555.0	.....	1016509.0	7.165
	1b	166.69	161.21	6.5982	989730.0	.....	1071141.0	7.160
	2a	343.79	327.61	13.6083	68041.8	30	68721.0	6.601
	2b	367.97	349.59	14.5655	72827.4	30	69743.0	6.962
	3a	448.46	446.90	17.7515	88757.7	30	90724.0	6.522
	3b	460.98	372.93	18.2471	91235.6	30	92652.0	6.565
D	1a	84.17	77.81	3.3317	499755.0	.....	504420.0	6.605
	1b	85.47	78.14	3.3832	507480.0	.....	526388.0	6.427

Notes:

W/y_l -slope value determined from the load-deflection curves relating to the loading points on the panels.

W/y_c -slope value determined from the load-deflection curves relating to the mid-span on the panels.

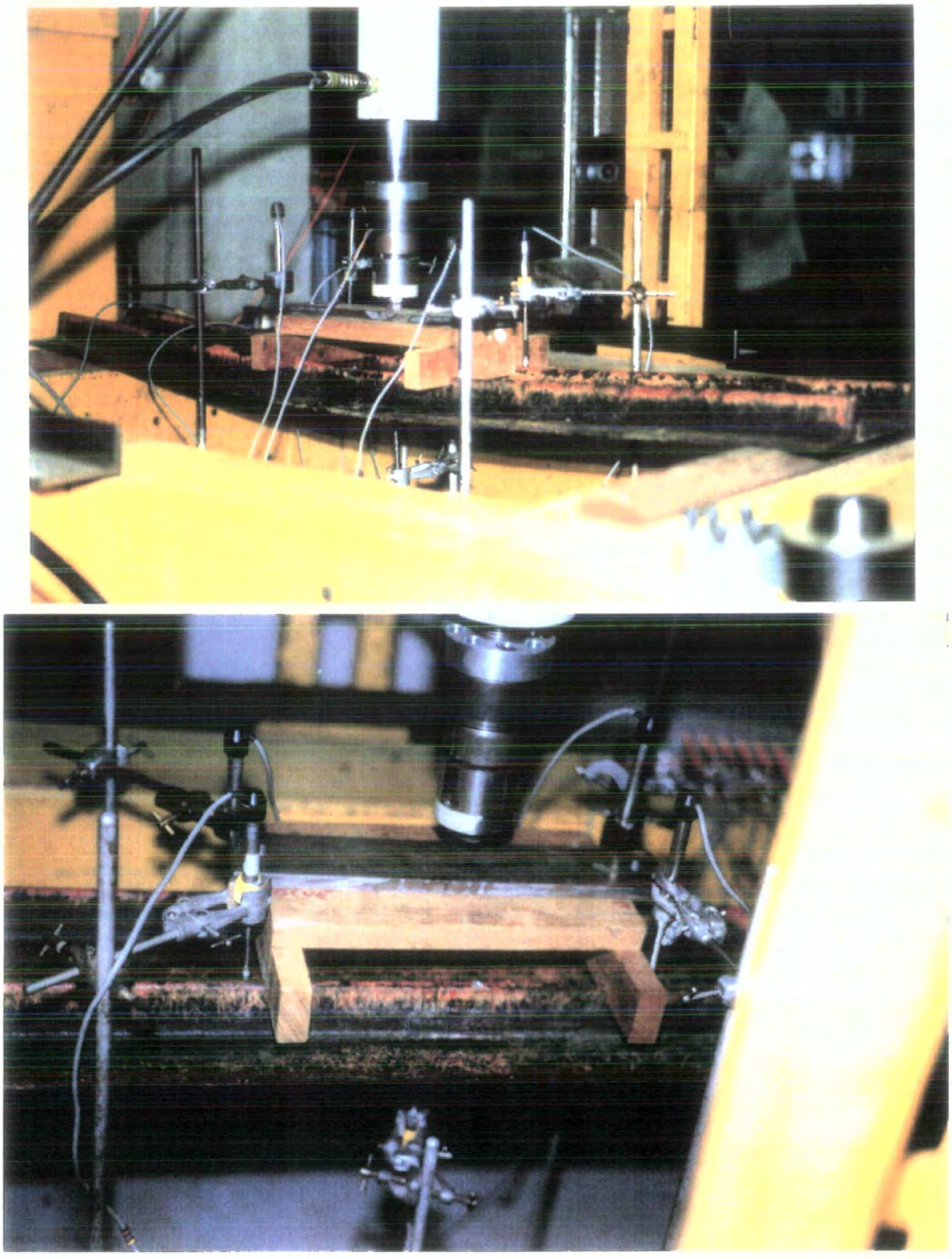

Plate 6.1 General loading, support and instrumentation (i.e. position of the transducers for vertical deflection measurements) arrangements of the test bridge deck panels.

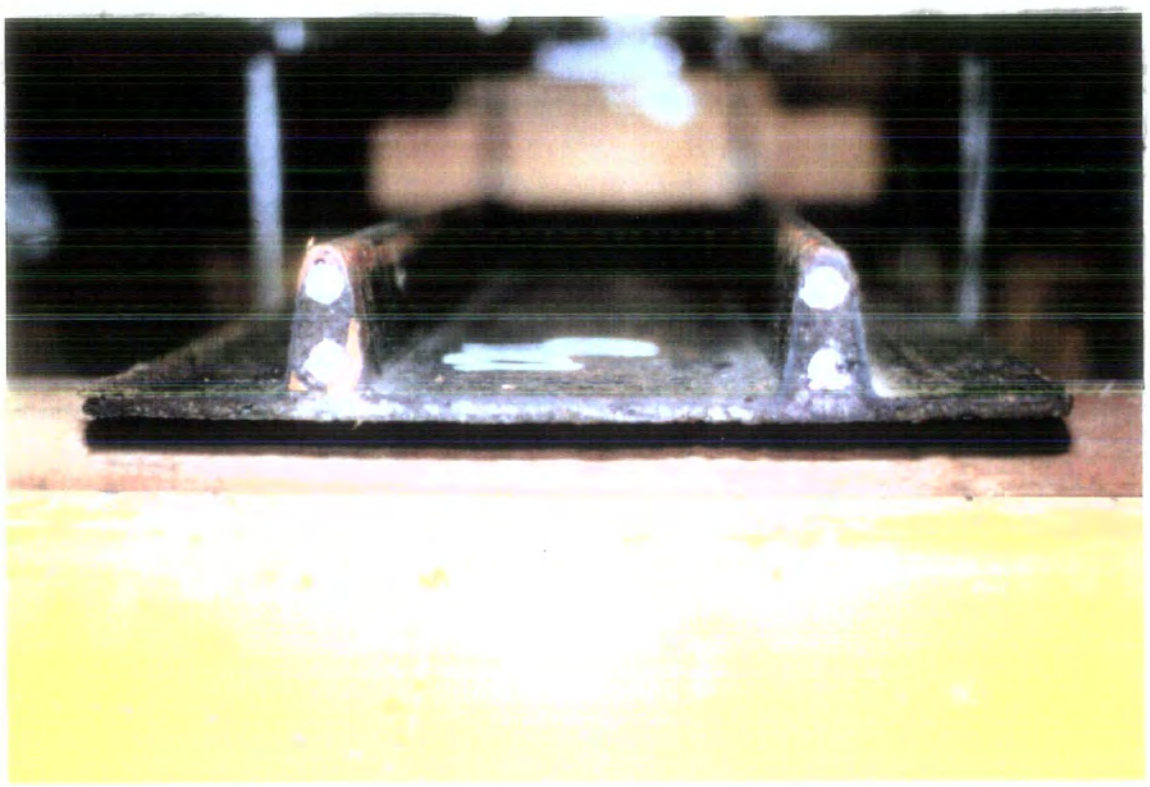

Plate 6.2 Exposed end of b/deck panel, showing the position of the embeded internal steel bars.

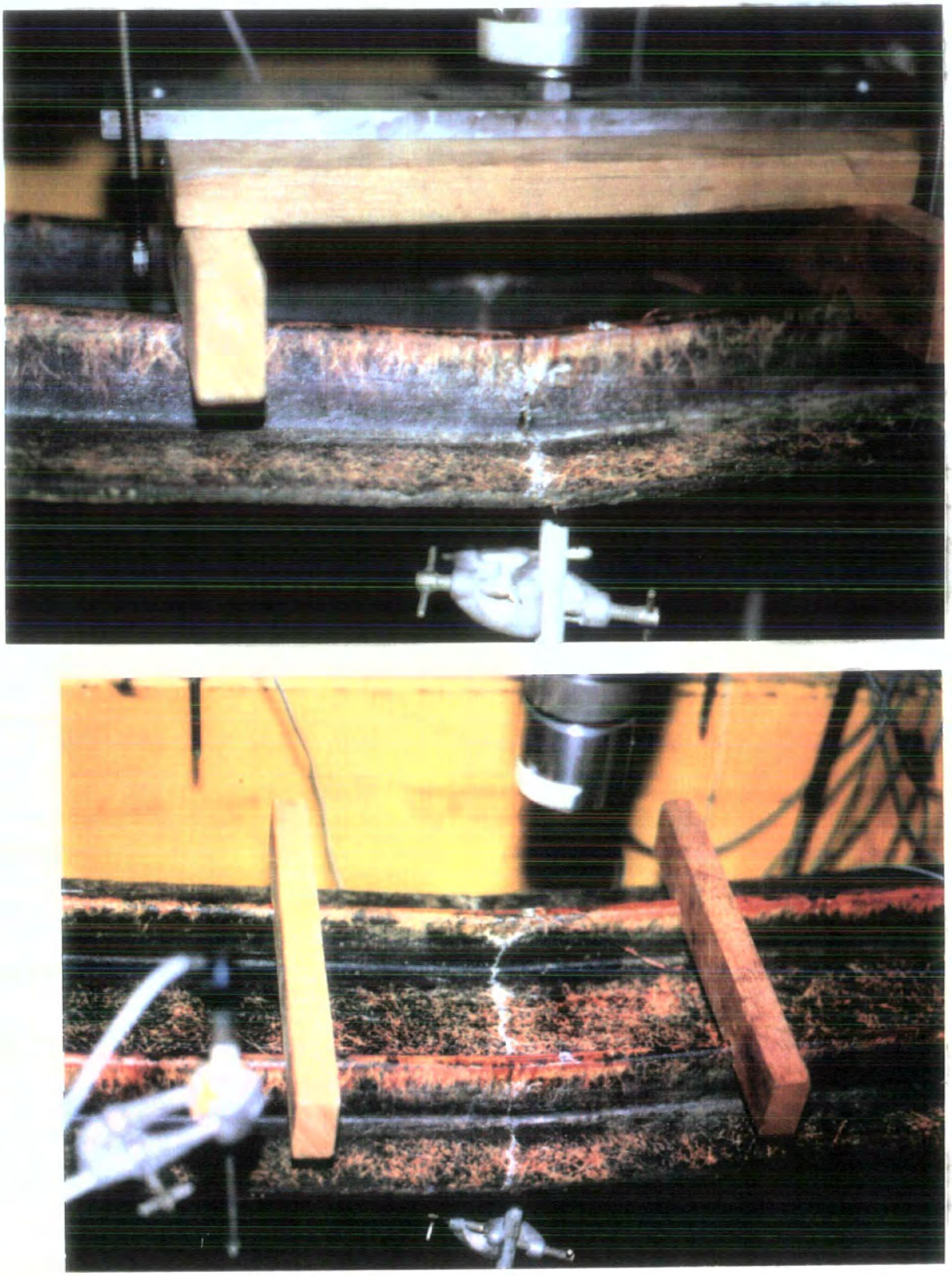

Plate 6.3 Failure mode of the internally reinforced b/deck panels (failure of phenolic concrete/laminated fibre glass mat in bending).

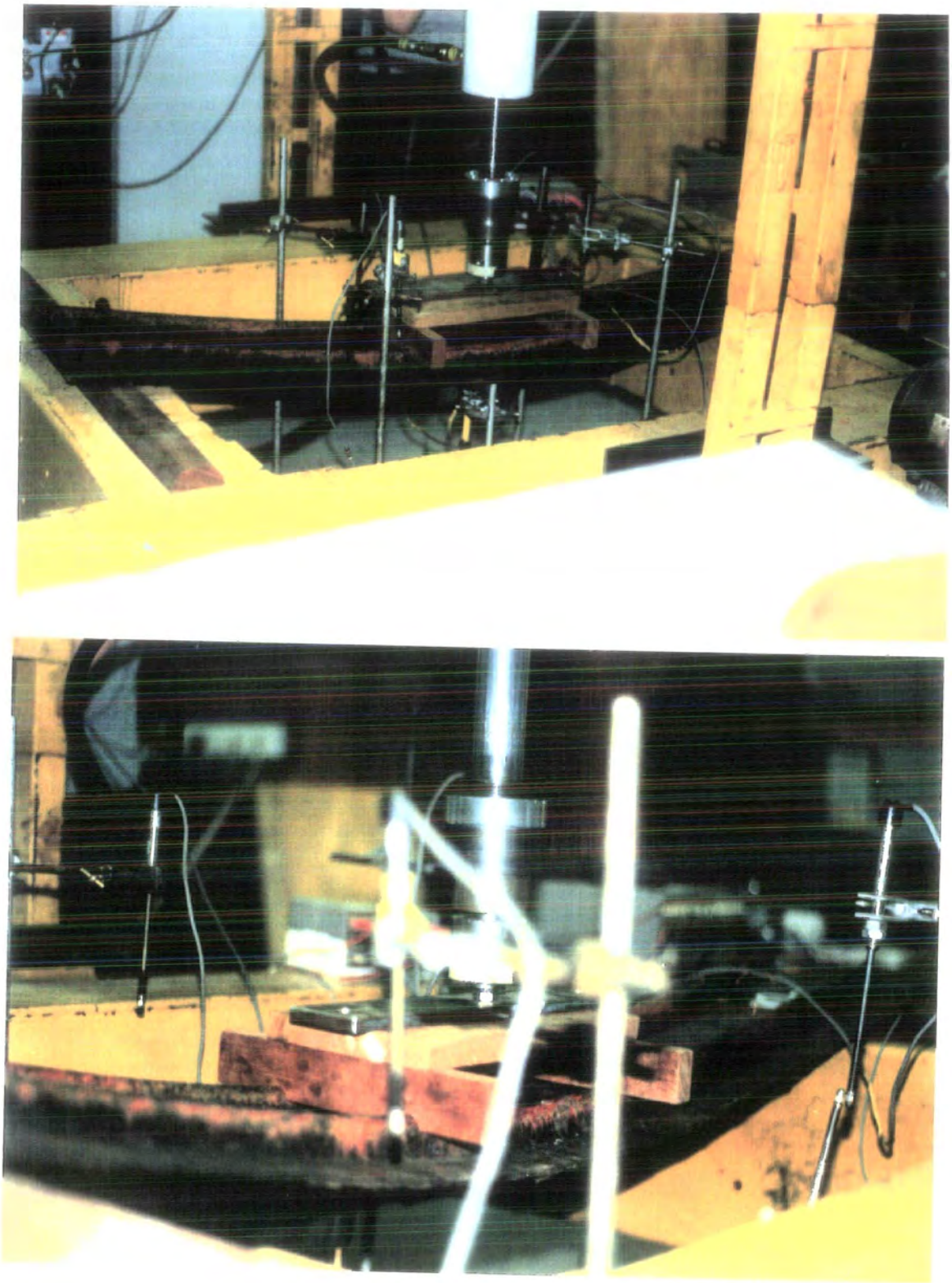

Plate 6.4 Excessive deflection of the reference b/deck panels (internally unreinforced sections) under 4 point flexural loading.

Chapter Seven

7. Conclusions

7.1. General

In spite of the persistent claims of the phenolic resin manufacturers such as BP Chemicals, the phenol-formaldehyde resol resins J2018L and J2027L did not provide a strong binder for the compatible non-fibrous fillers. With these types of phenolics no bond was developed between the granular fillers and the resin irrespective of the type and gradation of the fillers, mix formulation and the developed techniques of construction with regard to mixing, casting and curing procedures. With fibrous fillers such as sawdust, inevitably, some bond was established. A microscopic study of the fractured sections using the SEM technique, clearly revealed the bondability of these resol resins to fibrous fillers but not to the non-fibrous granular fillers. However, the experimental work with phenol-formaldehyde resol resins provided this research work with basic knowledge and some useful information. The influence of particle size and filler gradation on resin loading was clearly demonstrated in these experiments. The mixes with only fine fillers (i.e. max. size less than $150\mu m$) required much more resin to achieve a workable mix than a similar mix with larger size silica sands and micro-filler combinations.

It is clearly important, for any worker in this field to aquire fundamental knowledge of the chemistry of the binder, aggregate and the surface chemistry involved in binder-aggregate interaction. However, the research work intended here was limited in scope and the work was concerned with developing a phenolic concrete system from commercially available phenolic resins. With the resol resins, normally used in GRP systems, the lower flexural strength values developed when the resins were

filled with granular fillers were realized to be due to both lower strength of resin matrix and poor or no bonding strength. The cross-linking agent such as furfuryl alcohol used with these resol resins acted as an integral part of the resin and provided the modified resin with enhanced bondability to the filler composition. The increase in flexural strength values of the specimens made using the modified resol/furfuryl alcohol resins were due to enhanced resin matrix and bond strength.

In principle, development of high strength concrete depends upon the type of aggregates, water cement ratio and other admixtures which either strengthen the matrix and bonding or fill up the void spaces. In phenolic concrete both the matrix strength and the bonding are greatly improved by the selection of suitable resin formulation, proper filler sizes and careful aggregate gradation. These aspects would contribute to the overal strength of the phenolic concrete provided that the strength of aggregate (filler) matches with matrix strength and bonding is such that the material exhibits better synergistic effects. With increase in the furfuryl alcohol of the modified resin in the phenolic concrete mix matrix, the filler wettability increases as well as the resin matrix strength, thus developing higher bonding between the filler and resin matrix.

The phenolic resins which were later developed by Fordath (IR1270 and IR1271), and BP Chemicals (J50/010L) met the needs of this research work. It was found that in the phenolic concrete materials developed in this work, the failure in bending has been invariably through fracture of the filler grains (i.e. sand grains). Thus, the better bonding in the material was reflected in higher tensile and flexural strength mobilized by the highly filled resin systems. With increase in filler loading an increase in flexural properties was noticed which was accompanied by improvement in the compressive and tensile strengths. For the same system, with increase in resin loading lower strength values were obtained. This is attributed to the low strength of the resin matrix as a result of possible flaw occurance in the higher resin loaded

system. With higher filler loading, it is suspected that there is full mobilization of strength of the filler while the occurance of flaws in the matrix reduces with lesser resin loading. With higher resin loadings the failure tends to occur through the resin matrix only. The increase in filler loading, increased the strength and fracture energy in bending with little sacrifice of workability. This was achieved by proper filler gradation, use of further furfuryl alcohol in the system and mix design formulation as given in the text.

Plain phenolic concrete specimens exhibited brittle behaviour. The specimens reinforced with laminated fibre glass mats sustained loads even under larger deformation and remained as integral units (composites) without marked disintegration up to failure in flexure. Addition of laminated fibre glass mat to the phenolic concrete system, in the form explained in the text, provided high strength but reduced moduli, and conferred a high degree of ductility.

The working-time (gel time) of fresh phenolic resin concrete is a variable of time, ambient temperature, mix volume, surface to volume ratio of cast mix, resin loading and catalyst type and content. The usual penetration or pull-out resistance methods are not applicable as they are with polyester resin concrete. Instead, a finger-touching method may be applicable to a representative sample, especially in the mixes devised with higher filler loadings (i.e. greater than 85% by weight of total mix).

In a preferred application of the produced phenolic concrete material, the order of combining the constituents is, filler, e.g. silica sand, and micro-filler, e.g. silica flour, a catalyst which is conventional and commercially available, a phenolic resin, compacting by vibration and allowing the mixture to set and then be cured. The curing temperature may be in the range of $70°C$ to $120°C$ and determines the curing time. The ratios of total filler (i.e. filler plus micro-filler) to resin, may be less than

or equal to 6:1 without furfuryl alcohol, but less than or equal to 9:1 with furfuryl alcohol, a preferred ratio being 7:1. The percentage of filler used is dependent upon the particle size distribution of the particular filler. These percentages differ from the values used in normal practice with other resins. To achieve a uniformly homogeneous phenolic concrete matrix, the fillers should be mixed thoroughly and then the required acid catalyst should be added and mixed with the pre-mixed filler for even and uniform dispersion of the catalyst before the resin is added.

The advantages of a phenolic resin concrete prepared using the materials and the developed methods explained in the text include:

1. Filled phenolic resins are much stronger weight for weight than cement based concretes.
2. Phenolic resins exhibit great resistance to fire, and when they do degrade, under extreme conditions of fire, they degrade to water and carbon dioxide only, without forming a noxious smoke and, thus, can be used for building materials. The combination of silica sands and micro-fillers such as silica flour used in the formulation permits the composite's serviceability at even higher temperature.
3. The additional strength introduced with the method developed, makes filled phenolic resins suitable for use as structural, as opposed to purely decorative, building components.
4. Phenolic resins without a high proportion of inert filler are expensive and not viable for use as building materials but, when combined with fillers according to the method developed here, in proportions which would otherwise compromise the product's strength, their economic viability as building materials significantly improves.
5. The increased filler ratios achieved using the developed method occurs such that the bonding of the fillers to the resin matrix is improved, resulting in the

improvement of the important mechanical properties of strength and stiffness of the filled phenolic resin with increasingly high filler loadings.

6. The developed method allows phenolic products to be made in a permanent colour other than the natural dark burgundy, making them more aesthetically acceptable and resulting in an increase in their market range. The Titanium Dioxide powder used in some formulations, was very effective in imparting a stable beige-yellow colour to the normally dark burgundy. Adding 3% T_iO_2 by weight of total filler during the mixing increased workability and, by special casting, setting and curing procedures, produced material with the alternative colour appearance.

7. The choice of suitable materials allows the developed methods to be used commercially in a simple but controlled way at, or near to ambient temperatures, which allows the use of conventional casting techniques.

8. By appropriate choice of conditions in order to obtain an increase in physical strength with increased filler loading, a significantly high proportion of filler can be introduced which makes the resulting mixes compatible with those achieved by the use of other polymers.

9. With the developed method, one can achieve the faster curing time (2 to 24 hours depending on curing temperature) for faster production and recycling of moulds.

10. The light-weight phenolic concrete component provides an economical alternative technique in the production of precast members. Consequently, in design the cost of the phenolic resin concrete structure, could be reduced even further to reflect reduction in the structure's dead load with a corresponding reduction of frame and foundation requirements.

The physical and mechanical properties of the phenolic resin concrete specimens

were used in determining the characteristics of the material. The material properties were determined using the fracture toughness and fracture energy measurements of the double-torsion test specimens. From these material properties, it is evident that the developed Phenolic Concrete is both tougher and stiffer than ordinary concrete. The results of these investigations are briefly tabulated below;

Table 7.1 Physio-Mechanical Properties of the Phenolic Concrete

Filler : Resin Ratio (weight by weight)	4:1 - 9:1	
Compressive Strength (cylinder)	74.6 - 88.3	N/mm^2
Flexural Modulus	17.4×10^9 - 32.4×10^9	N/m^2
Flexural Strength	15.6×10^6 - 30.5×10^6	N/m^2
Elastic Modulus	14.6×10^9 - 19.6×10^9	N/m^2
Tensile Strength (direct test)	5.4×10^6 - 7.7×10^6	N/m^2
Tensile Strength (disc test)	7.1×10^6 - 8.9×10^6	N/m^2
Fracture Toughness (K_{IC})	1.48 - 2.12	$MN/m^{3/2}$
Fracture Energy (G_{IC})	152.4 - 220.7	J/m^2
Density	2.08 - 2.28	g/cm^3
Water Absorption	0.01 - 0.08	%
Poisson's Ratio	0.27	

These investigated material properties and the developed construction techniques were used in the construction of structural elements such as box beams and bridge deck panels which were tested under flexure. The results clearly showed that their behaviour can be predicted by simple elastic analysis. In producing such elements, the repeatability of the construction technique was proved, as was the potential versatility in formulation and in processing the phenolic concrete to offer a wide range of applications.

Electrical properties, such as permittivity, loss factor and electrical conductivity of the Phenolic Concrete samples were measured at radio frequecy of 500Hz to 15KHz. This was conducted in other work the details of which are not included in the text. The results obtained clearly support the application of the developed

Phenolic Concrete for specific areas of use such as computer rooms, comunication rooms and electrical shieldings.

The properties investigated and the construction techniques developed resulted in production of viable and valuable structural units such as access floor tiles. Details of this development are not included in the text because they did not fall within the scope of this project. However, in general two types of medium grade access floor tiles of 600x600 mm were constructed comprising of solid panels and ribbed panels primarily reinforced with laminated fibre-glass lay-ups. The latter was with or without internal steel reinforcement. The developed access floor tiles weighed between 16.5 - 20kg having 24 - 28.5mm thickness with reasonable material cost thus offering a competitive alternative to the existing processed timber and steel systems. The developed tiles were tested by an independent testing body and proved to perform well to the requirements of DOE Performance Specification set by MOB 08/801 dated August 1985, regarding physical dimensions, weight, static and dynamic loading, factor of safety and deflection criteria. In some the test results well exceeded the required Performance Specification concerning the deflection, factor of safety and the ultimate sustained load. From these tiles the solid panel offers the most versatility for use on site where cutting and fitting at margins is required. In the course of developing the Phenolic Concrete access floor tiles, the object was proved unattainable without some form of reinforcement. This required the use of fibre glass lay-ups which employ a large number of manufacturing operations and could well be costly. The work in hand is the development of a technique to meet the needs of mass production. It is also intended to further reduce the cost of material, without sacrifising the strength, by alternative design or use of materials, so that the end product should be within reasonable economy in order to be able to compete in the market. Other projects include the development of other components such as roof tiles in the form of imitation slate and others are also in progress.

The one weak link in the chain is acceptable construction technique. It is hoped

that this development will achieve the technological break-through needed to meet the future needs. Once this material is developed it is hoped that a ready market will exist in producing precast Phenolic Concrete members. Obviously those who pioneer in this field will be the ones who reap the potentially large rewards as more uses are found for Phenolic Concrete in the technological industry.

7.2. Suggestions for Future Work

In addition to the work reported in this research it would be of value to investigate the use of Phenolic Concrete in load-bearing applications subject to a combination of static, cyclic, or impact (high stress) and agressive environment (water, high temperature, and chemicals).These applications would need a sound base of research.

In spite of the knowledge that creep can be high in polymer concretes, there have been few studies in this field. The effect of higher loads should be studied. As in cement based concrete, it should be assessed whether the creep in phenolic concrete reduces as the specimen's size increases. This has been shown to be otherwise with other polymer concrete systems. This reflects the difference in creep mechanism, that of the polymer involving molecular (segmental) motions.

As with ordinary concrete the use of steel reinforcement may become neccessary in Phenolic Concrete members. The effect of acid catalyst attack and possible corrosivity due to condensation as a result of polymerization should be carefully investigated and long term performance of the reinforced members studied. The long term performance of the members reinforced with laminated fibre glass lay-up should be observed and possible rate of delamination or degradation of the composite should be assessed with time lapse. Furthermore, the development of a controllable technique by which the large number of manufacturing proccess could be reduced in the use of fibre glass lay-up laminates as the primary reinforcement.

7.3. Conclusion points (Itemised summary of conclusions).

1. The work has established well defined knowledge of the bonding characteristics and limitations of the original phenol-formaldehyde resins to granular fillers.
2. It has shown the variation in resin requirements of mixes with a range of different aggegate particle sizes and gradings, from fine to coarse.
3. It has demonstrated the beneficial effects on both resin strength and aggregate bonding when the resol resins are mixed with furfuryl alcohol.
4. It has demonstrated how the introduction of high aggregate contents of suitable grading can improve the strength and stiffness properties of the composite .
5. It has shown how the brittle behaviour of the plain resin concrete was modified by the introduction of glass fibre reinforcement, producing the effect similar to yield or ductility, and higher fracture strengths.
6. Much useful experience was gained in the practical techniques of mixing, casting and curing the Phenolic Concrete in making a wide range of components.
7. Double torsion tests have demonstrated the fracture toughness and fracture energy of the heavily filled phenolic resin concrete.
8. Theoretical work has been done to successfully model the stiffness of Phenolic Concrete flexural components such as hollow beams and ribbed sheets, before and after cracking and with and without steel bar reinforcement.
9. The limits of elastic, elastic-plastic and fracture behaviour of flexural components have been related to the known compressive and tensile strengths of the material.
10. A programme of further work has been suggested, which is necessary to enhance present knowledge of the material characteristics, and to develop further structural components and applications.

Appendix (A1)

A1. Phenolic Concrete Mixes

A1.1. Mix Design

As in ordinary concrete, it is important that the Phenolic Concrete is designed for greater strength at its hardened state. The strength is affected by the gradation of the aggregates (fillers), resin type and their ratio in the mix. The more densely the Phenolic Concrete is compacted and the lesser is the resin loading the greater is the strength. To obtain a dense Phenolic Concrete the voids in the made product should be a minimum. This may be achieved by properly selecting the filler gradation and its particle packing, and also proportioning of the filler to resin so that the mix is sufficiently workable to be properly compacted into a dense mass.

Design of the Phenolic Concrete mixes is essential both to achieve the required mechanical properties of the finished product and the necessary economy. In designing such mixes, since no past experience exists, the laboratory scale trial mixes are essential. The data needed for mix design cannot be standardized because the Phenolic Resin and the corresponding filler materials may have widely differing properties. However, the mix design procedure may become standardized. A suitable mix design may be achieved with the aid of trial mixes, and the results from the flexural strength tests.

The Phenolic Concrete mixes, may be described in terms of the proportions by weight of the materials which they contain. The mix design procedure favoured in this work is that which enables an estimate to be made of the required mix proportions, in as simple manner as possible, generally using parameters such as: type

of resin, type and grading of fillers, workability, filler/resin ratios and strength requirements. In these mix designs the knowledge of filler specific surface and particle packing manner are essential since these parameters determine the need for the most expensive component material, resin, contained in the mix matrix.

The variation of the Phenolic Concrete may be assesed by determining its required resin in the prescribed mixes and also by measuring the strength of the finished product. However, the following techniques are all that is needed for the initial filler gradation mix design, which would then determine the proportioning of filler to resin for workability requirements.

A1.1.1. Graphical procedure

The "Fuller" grading and "Gap" grading options were used in filler mix grading design. A graphical method of determining the actual proportions of fillers to give a combined grading approximating to a type grading is given in reference [64].
This procedure was adopted initially in this work. The variation of the resultant grading from the specified grading was determined from the plotted gradings on the grading chart and also arithmatically using their %age weight-fractions. Using a trial and error procedure the filler proportionings were adjusted so that the resultant grading approximated as closely as possible to the specified grading with the variation of particle size fractions being minimum both graphically and arithmatically. At the same time trial mixes, with constant filler/resin ratios, were made from each deduced mix filler grading in order to asses both the workability and the flexural strength of the finished products. Filler proportions were selected which resulted in a mix grading to coincide with the target grading and to produce improved workability when mixed with a given weight of resin, which also resulted in

finished products with highest flexural properties. This procedure in obtaining the filler mix grading was lengthy and somtimes tedious because of the large number of fillers involved. Therefore, a computer program was written to determine the initial filler proportioning of up to 14 fillers which would produce the best mix grading to closely approximate to the target grading.

A1.1.2. Aggregate Mix Design theory used in developing the computer program

The aggregate mix design programme was written in order to determine the mix proportions of known components to give a resultant mix grading which would approximate as closely as possible to previousely defined target grading.

The defined grading may be the "Fuller" grading or may be some other option, such as a "Gap" grading option. The procedure of the programme is explained fully in reference [66]. Here the theory is explained only briefly.

The theory is based on solving for the mixing proportions of "n" component aggregates of known gradings in order to achieve a defined grading. Component aggregates are defined by %age weight passing a given range of B.S. seive sizes. From these, the %age fraction weights (f_i) of these components can be determined, say f_1, f_2, f_3, ... and f_m. For each aggregate component (x) the %age fraction weights can then be defined as;

$$f_1x,\ f_2x,\ f_3x,\ ....\ and\ f_mx$$

so

$$\sum_{i=m}^{i=1} f_ix = 100\%$$

If the component aggregates are mixed in proportions:

$$p_1,\ p_2,\ p_3,\ .....\ and\ p_n$$

Such that;

$$\sum_{j=n}^{j=1} p_j = 100\%$$

to give the required %age weight fractions F_1, F_2, F_3, ... Then for any fraction,

$$\sum f_{ij} x . p_j = F_i + v_i$$

where F_i is the vector of desired %age weight fractions and v_i is the variation between %age weight fractions of the resultant and the defined grading. Thus, arranging these weight fractions of the component aggregates into a data matrix $[f]$ in which the columns are the components and the rows are the weight fractions, we can write;

$$\begin{bmatrix} f_{11} & f_{12} & f_{13} & . & . & . & f_{1n} \\ f_{21} & f_{22} & f_{23} & . & . & . & f_{2n} \\ f_{31} & f_{32} & f_{33} & . & . & . & . \\ . & . & . & . & . & . & . \\ . & . & . & . & . & . & . \\ . & . & . & . & . & . & . \\ f_{m1} & f_{m2} & f_{m3} & . & . & . & f_{mn} \end{bmatrix} * \begin{Bmatrix} p_1 \\ p_2 \\ p_3 \\ . \\ . \\ . \\ p_n \end{Bmatrix} = \begin{Bmatrix} F_1 \\ F_2 \\ F_3 \\ . \\ . \\ . \\ F_m \end{Bmatrix} + \begin{Bmatrix} v_1 \\ v_2 \\ v_3 \\ . \\ . \\ . \\ v_m \end{Bmatrix} \qquad (1.1a)$$

or

$$[f] \times \{p\} = \{F\} + \{v\} \qquad (1.1b)$$

This will produce too many equations to be solved. However, the best fit grading will be achieved if the condition is met that $\sum v^2$ is minimum in equation 1.1b. This will be achieved by differentiating the equation 1.1b, such that;

$$[f^T] \times [f] \times \{p\} = [f^T] \times \{F\} \qquad (1.2)$$

where, $[f^T]$ is the transpose of matrix $[f]$.

The equation 1.2 can be rearranged so that,

$$[G] \times \{p\} = \{C\} \qquad (1.3)$$

where

$$[G] = [f^T] \times [f]$$

and

$$\{C\} = [f^T] \times \{F\}$$

In equation 1.3, the general matrix G will, of course, be symmetrical and positive, definite and it will therefore be always possible to achieve some resultant grading even if $\sum v^2$ is large, i.e. the resultant grading is long way from the defined one. However, solving equation 1.3 will give the best value of mix proportion "p".

The programme will then evaluate the usual grading curve values and compute its own %age fraction sizes both for the component and the resultant gradings. It also identifies the large values of v_i, so that the "gaps" in the resultant grading can be seen, and the short-comings may be rectified by supplying another suitable component. Finally, the programme produces graphical output of the component, target and resultant gradings.

The programme converts the percentage passing data of both the target and the component gradings into weight fraction data. All the calculations are therefore performed on the weight fractions. An additional routine calculates the surface area index of each fraction and hence a comparison of the target and the designed grading may be made using their surface area indicies. The surface area of particles is roughly in inverse proportion to the square of the particle size (i.e. to the equivalent particle diameter). If the %age weight of each single-size fraction of a component aggregate is multiplied by the inverse of the square of the particle size, and all the resulting values for the whole aggregate are added together the final value is called the specific surface of the aggregate.

A1.2. Flexural testing of the Coupon Specimens

A four-point flexure test was used to determine the flexural strength and modulus values of the Phenolic Concrete coupon specimens. The test was a simple procedure which defined the material properties of the Phenolic Concrete composite with respect to bending. The Figure A1.1 shows the schematic representation of the test.

For an element subject to flexure, the mode of failure is strongly dependent on span to depth ratio, L/d. Short span beams usually fail in shear and long ones in tension or compression[105]. Generally, the flexural stress at failure is greater than either the tensile or compressive strength of the material from which it is composed[106]. This is explained by the nonuniformity of stress in the flexure test. The maximum tensile and compressive stresses exist only in the outer fibres of the beam. Because of the scatter in strength, the probability of failure in a small volume of material at a given stress level is lower than that in a large volume. Therefore, for equal probability of failure, the outer fibre stress in a flexure test must be higher than in the same specimen loaded in pure tension or compression. It has been shown[107] that span-to-depth ratio greatly influences the measured flexural strength and modulus values. It is therefore fair to say that the flexural test provides the component properties rather than the material properties. In specimens with higher L/d values the effect of shear deformation becomes negligible. In this work, the L/d ratio for plain Phenolic Concrete coupon specimens was in the range of 55/1 to 85/1, and for coupon specimens reinforced with laminated fibre glass lay-ups the L/d ratio was approximately 50/1.

The coupon specimens were tested in a rig mounted on the Instron testing machine at a constant rate of displacement. The flexural strength was deduced

using the bending theory such that;

$$\frac{M}{I} = \frac{\sigma}{\bar{y}} \tag{1.4a}$$

rearranging this equation we have;

$$\sigma = \frac{M}{I} \times \bar{y} \tag{1.4b}$$

where,

$$\bar{y} = \frac{d}{2} \qquad and \qquad I = \frac{bd^3}{12}$$

substituting for $\bar{y}$ and I in equation 1.4b we get

$$\sigma = \frac{3Wa}{bd^2} \tag{1.5}$$

where

σ is the maximum flexural strength at failure.

W is the maximum recorded load at failure.

b is the coupon specimen width.

d is the coupon specimen thickness.

a is the maximum moment lever arm.

The flexural modulus values were determined using the deflection formulae derived for similar loading arrangements as for the beams in Appendix A2 (equation 3.4.9.). Using the deflection formulae the EI values of the coupon specimens were calculated with respect to their deduced slopes of the load-deflection graphs recorded on the X-Y plotter of the Instron machine. From careful geometrical measurements of the coupon specimens the corresponding I values were calculated and hence the flexural modulus value for each sample was determined. The following equations were used;

$$EI = C_l \times \frac{W}{y} \tag{1.6}$$

where;

E is the flexural modulus.

W/y is the slope of the recorded load-deflection graphs.

C_l is the deflection constant w.r. to loading point position.

From the geometrical properties of the coupon specimen loading arrangement as a means of boundary conditions in solving for deflection equation the value of C_l was found to be;

$$C_l = 949218.76 \quad mm^3$$

The equation 1.6 used in calculating the flexural modulus implicitly assumes that all deformation results from bending and ignores shear deflection.

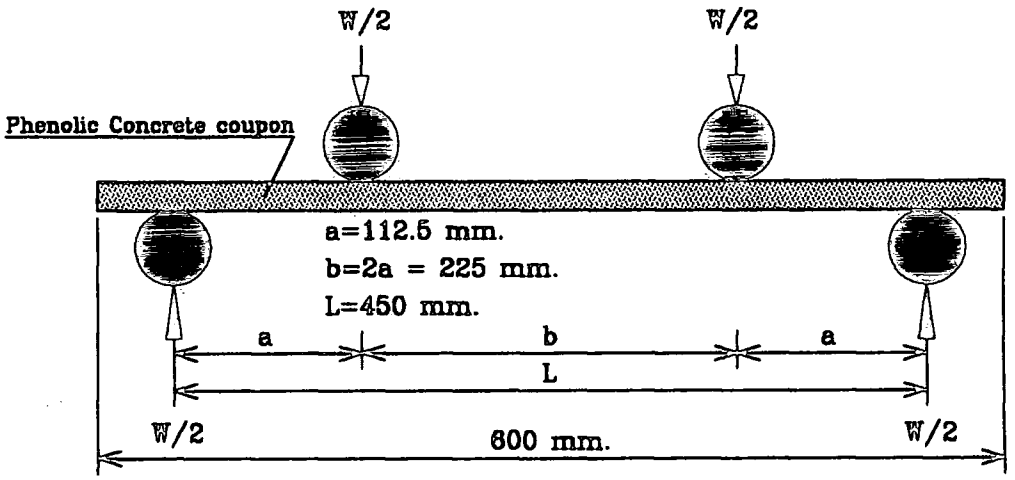

Figure A1.1 Phenolic Concrete coupon specimen and the loading geometry
(four point flexural loading on Instron 1195 testing machine)

Figure A1.2

Variation between Grading Curves obtained using 'Graphical Method' and Aggregate Mixing Programme 'Grade' from the target Fuller grading

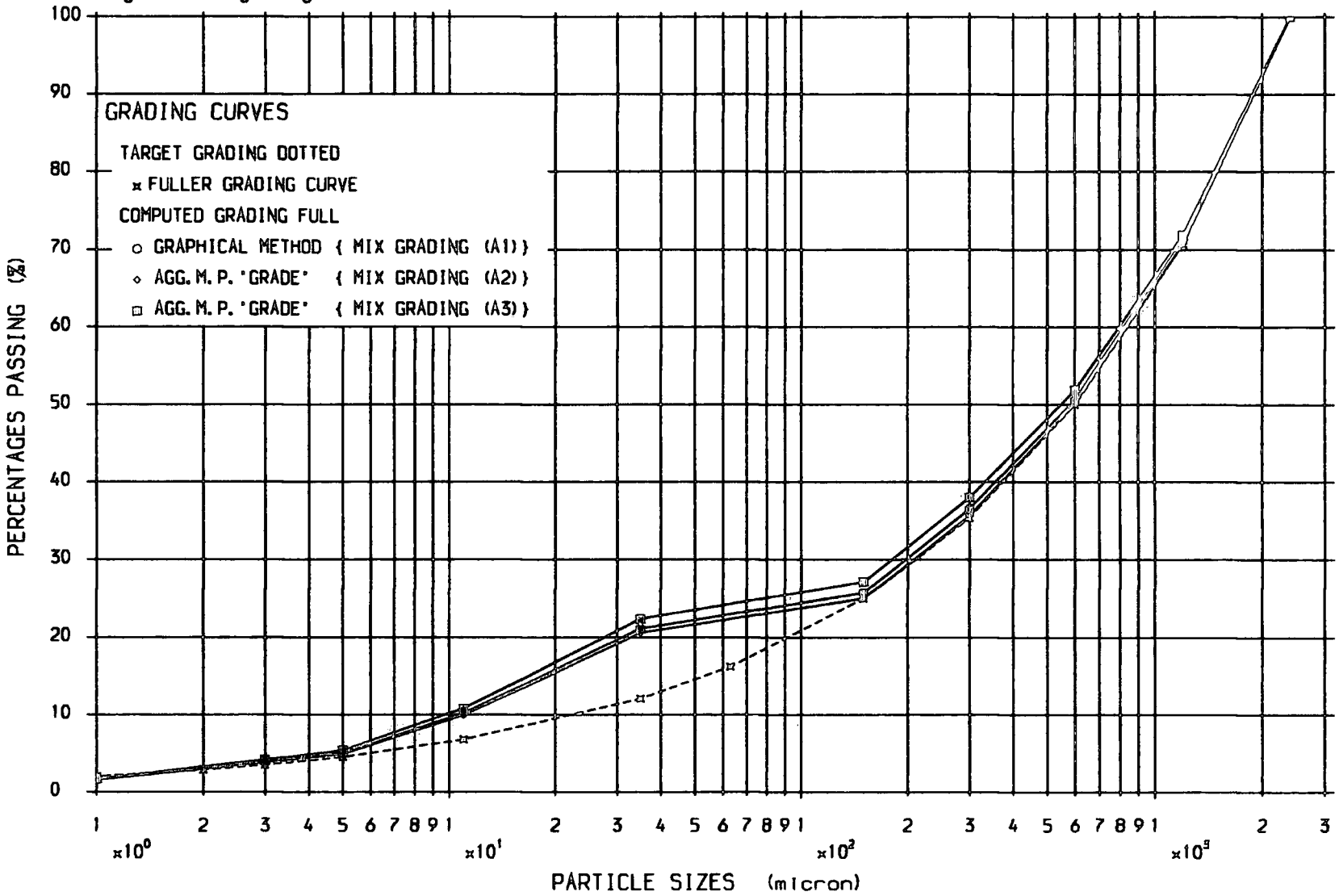

Figure A1.3

Variation of the designed grading 'B' with micro-filler content (%)$_0$ from the target Fuller grading
(Refer to Table 3.1 for Grading Constituents and their proportions)

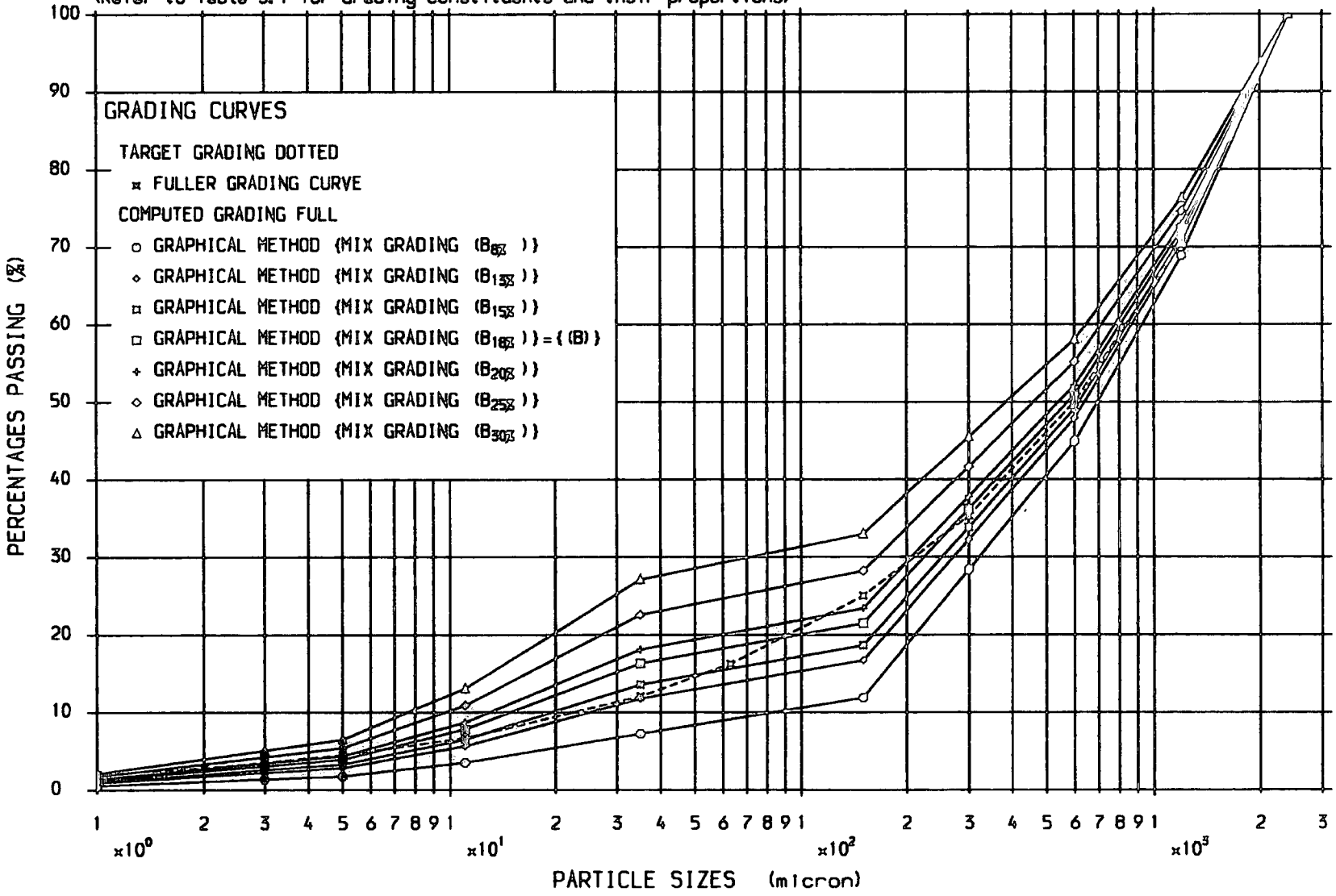

Figure A1.4

Variation between Grading Curves obtained using 'Graphical Method' and Aggregate Mixing Programme 'Grade' from the target Fuller grading

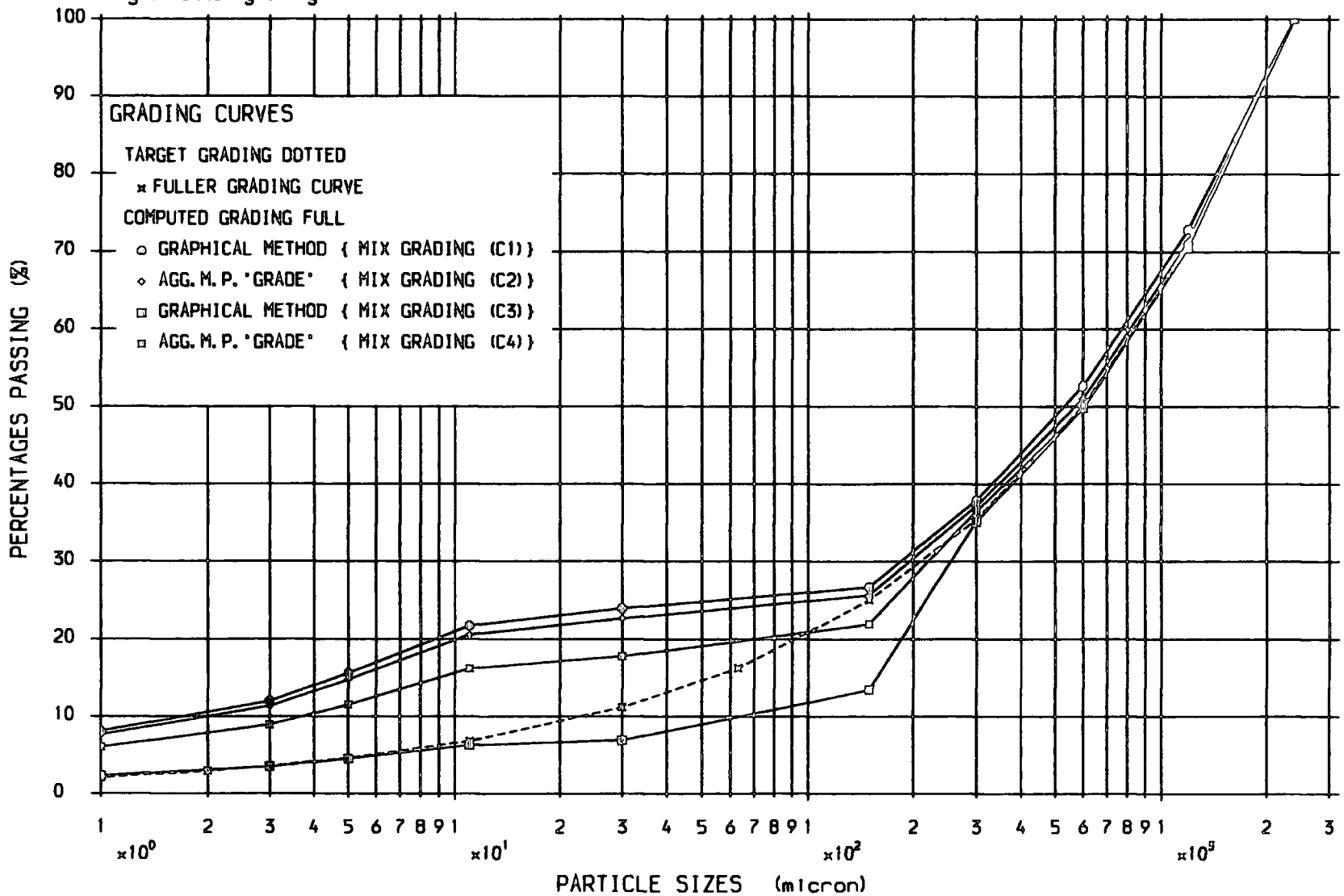

Figure A1.5

Variation between Grading Curves obtained using 'Graphical Method' and Aggregate Mixing Programme 'Grade' from the target Fuller grading

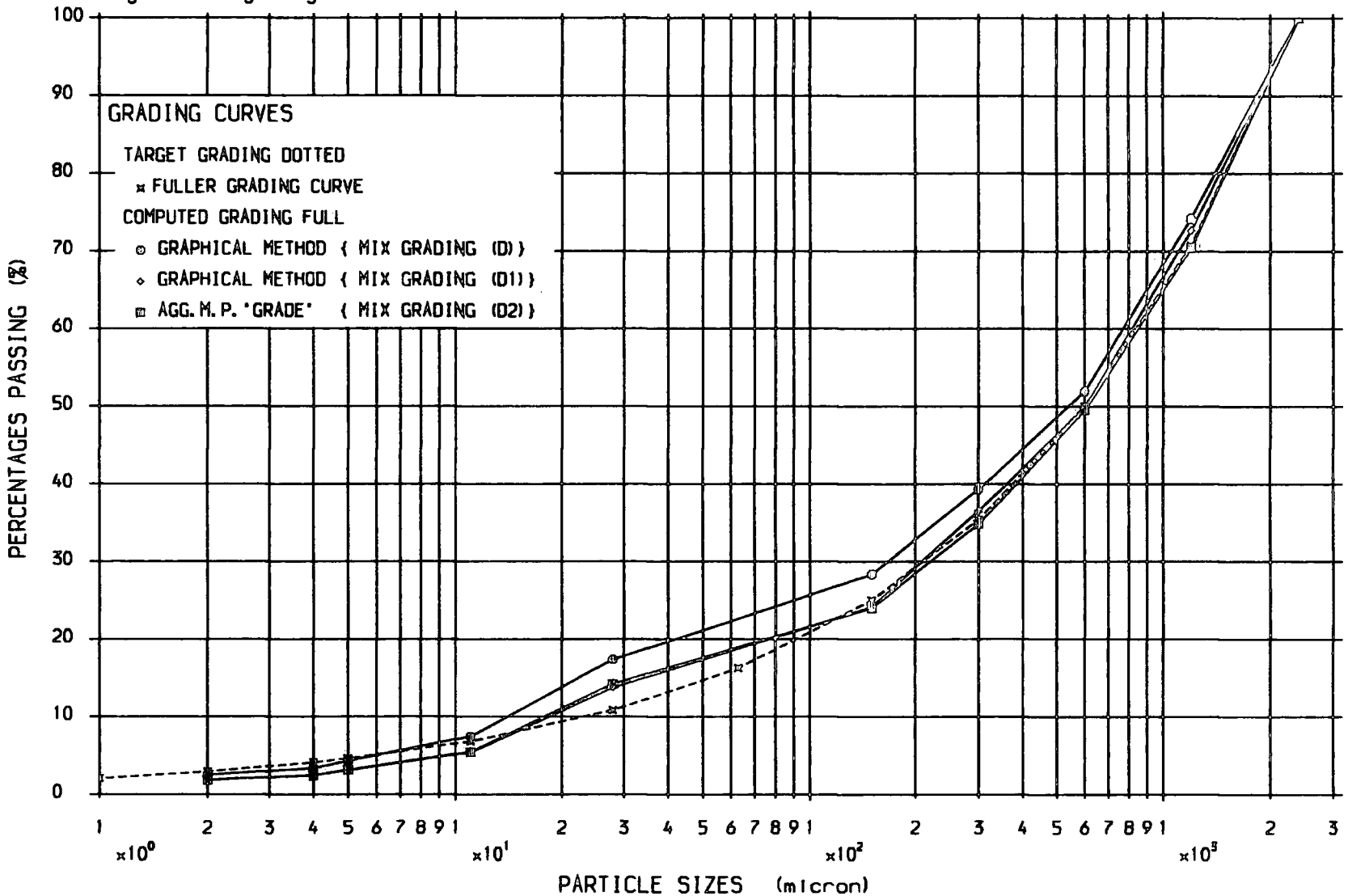

Figure A1.6

Variation between Grading Curves obtained using 'Graphical Method' and Aggregate Mixing Programme 'Grade' from the target Fuller grading

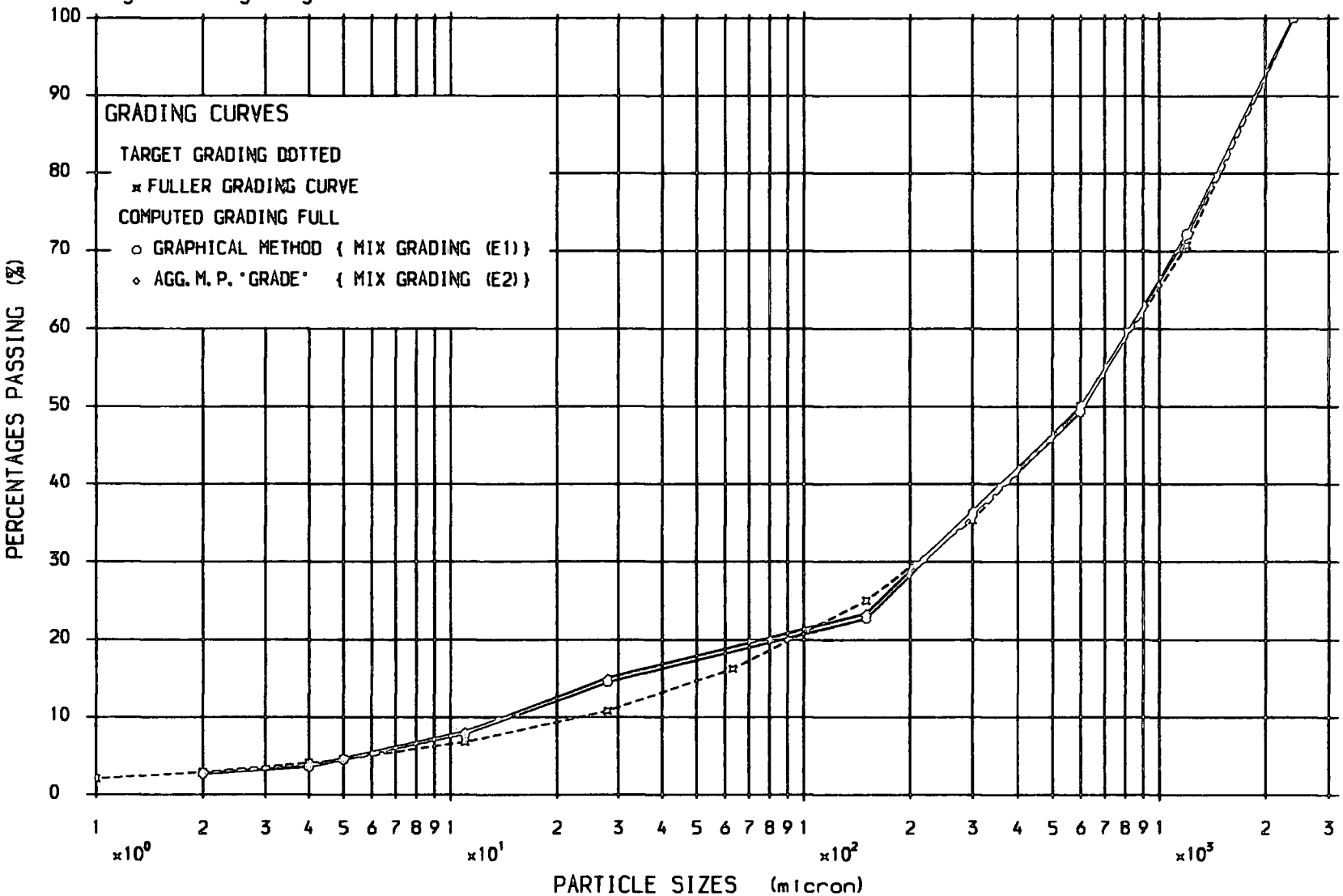

Figure A1.7

Variation between Grading Curves obtained using "Graphical Method" and Aggregate Mixing Programme "Grade" from the target Fuller grading

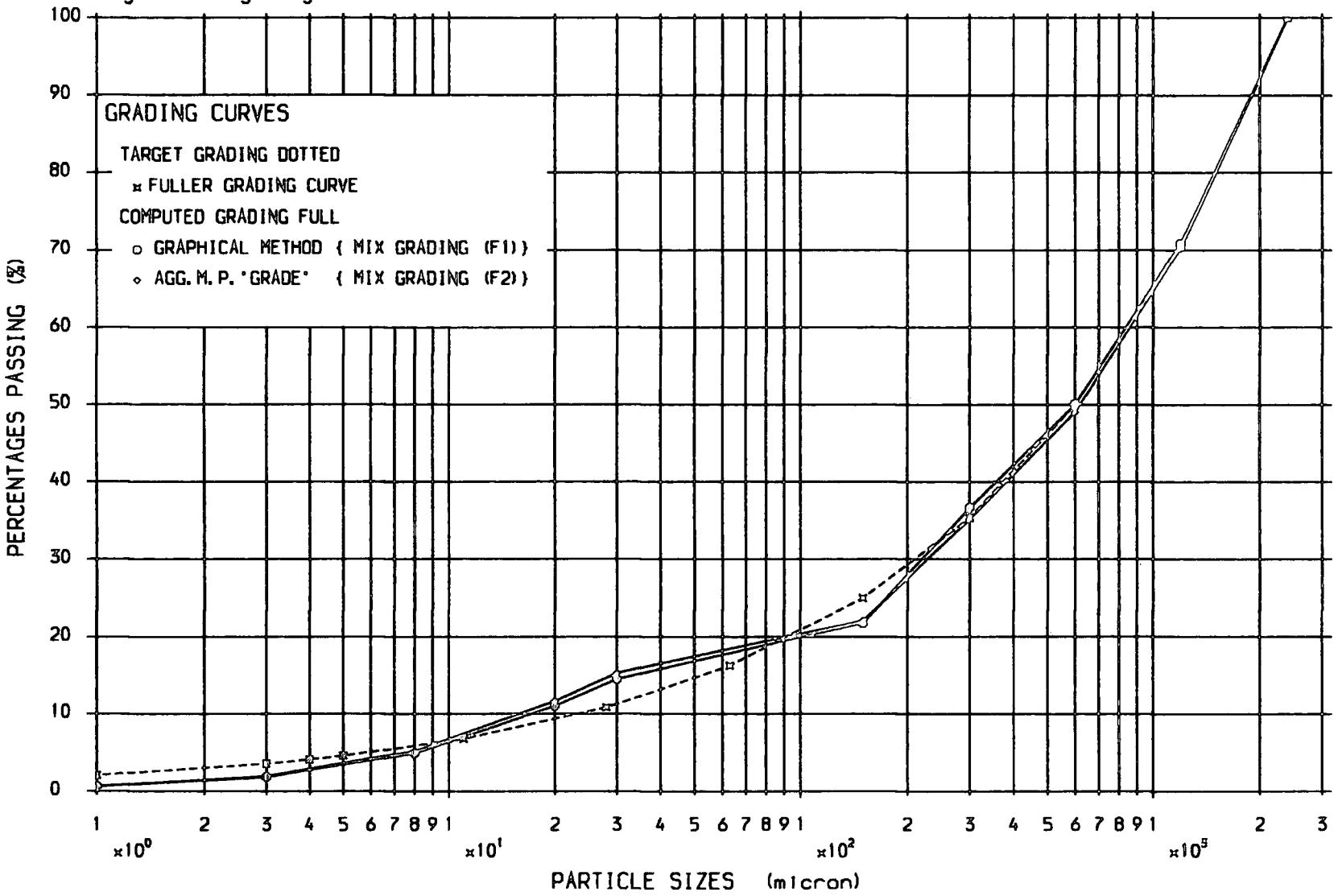

Figure A1.8

GRADING TASK NO. = 3

** The filler proportionates, to achive the mix grading, are based on laboratory trial and error procedure in order to obtain a mix with high workability which would result in specimens with highest 'Flexural Strength'

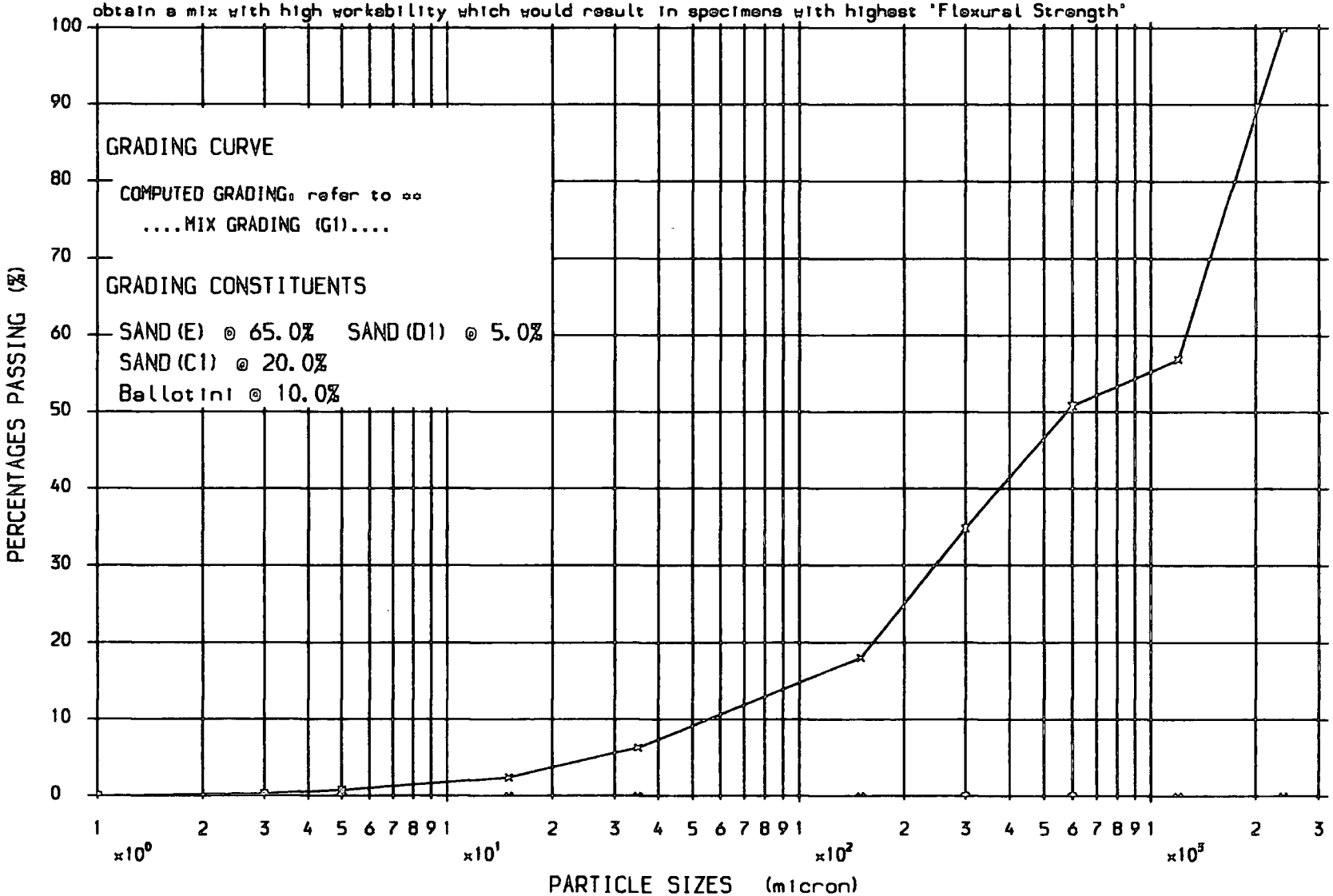

Figure A1.9

GRADING TASK NO. = 3

** The filler proportionates, to achive the mix grading, are based on laboratory trial and error procedure in order to obtain a mix with high workability which would result in specimens with highest "Flexural Strength"

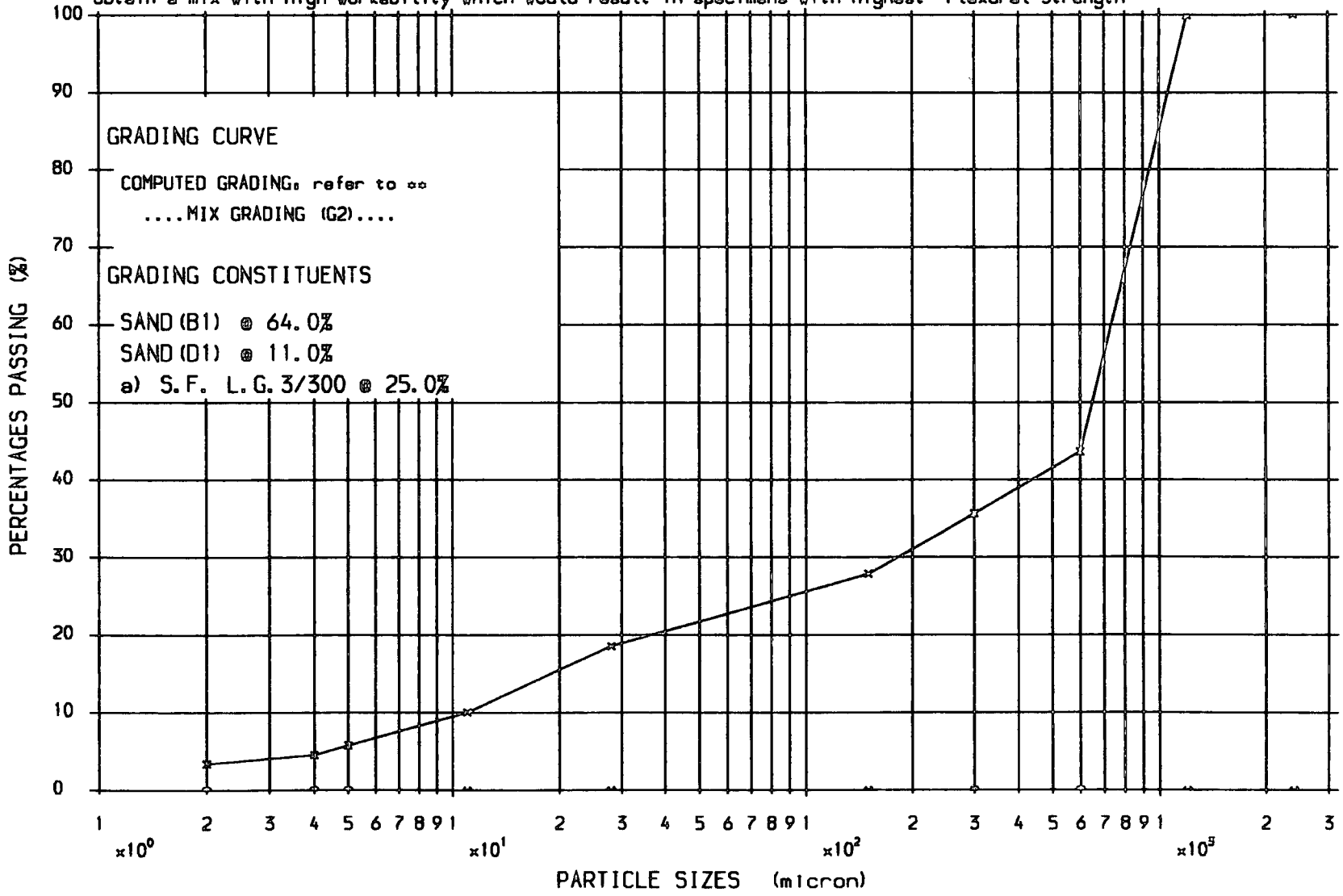

Figure A1.10

GRADING TASK NO. = 3

** The filler proportionates, to achive the mix grading, are based on laboratory trial and error procedure in order to obtain a mix with high workability which would result in specimens with highest 'Flexural Strength'

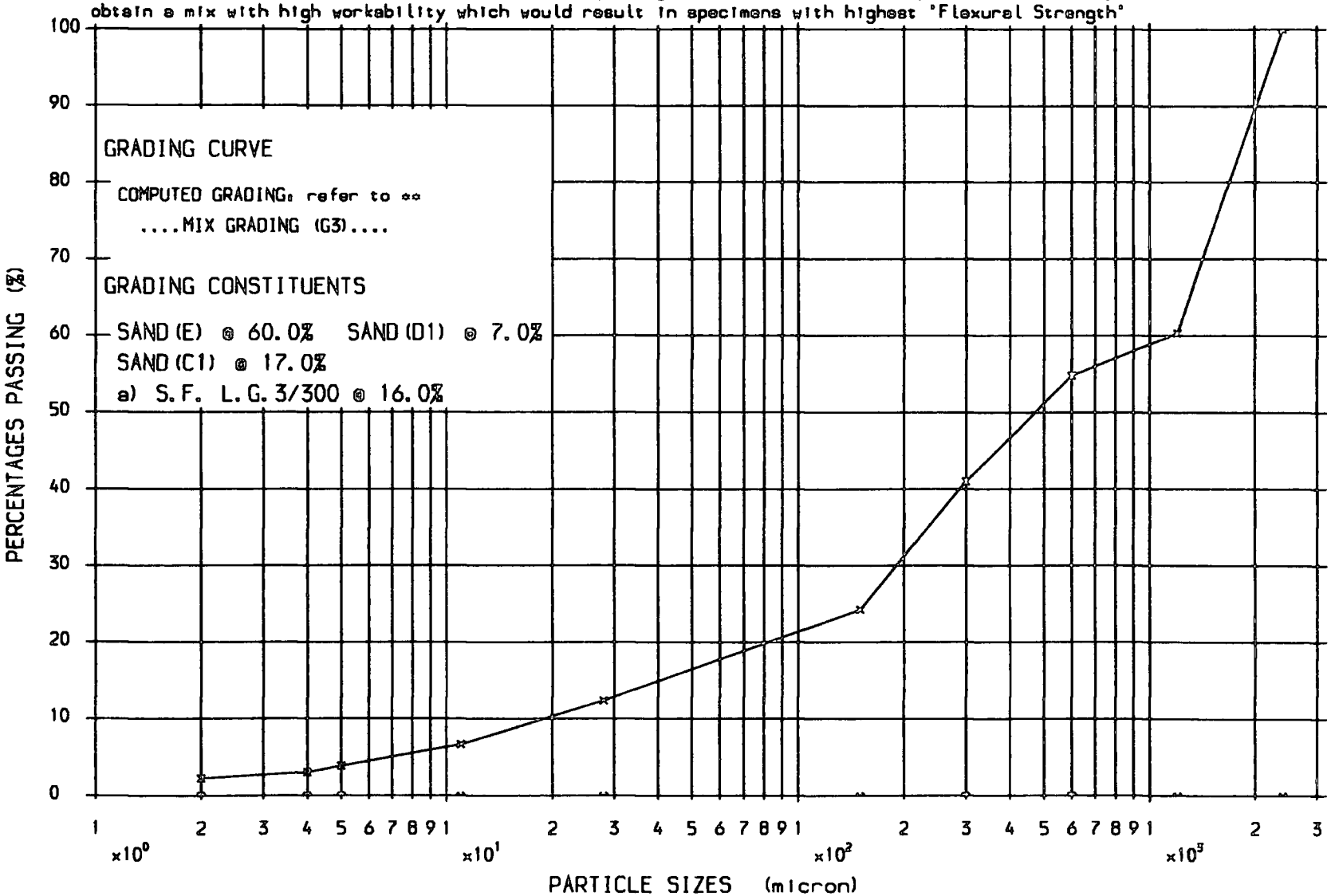

Figure A1.11

GRADING TASK NO. = 3

** The filler proportionates, to achive the mix grading, are based on 'E1' grading. The micro-filler content in the mix grading is based on equivalent volume of 19.5% Silica Flour present in the 'E1' grading

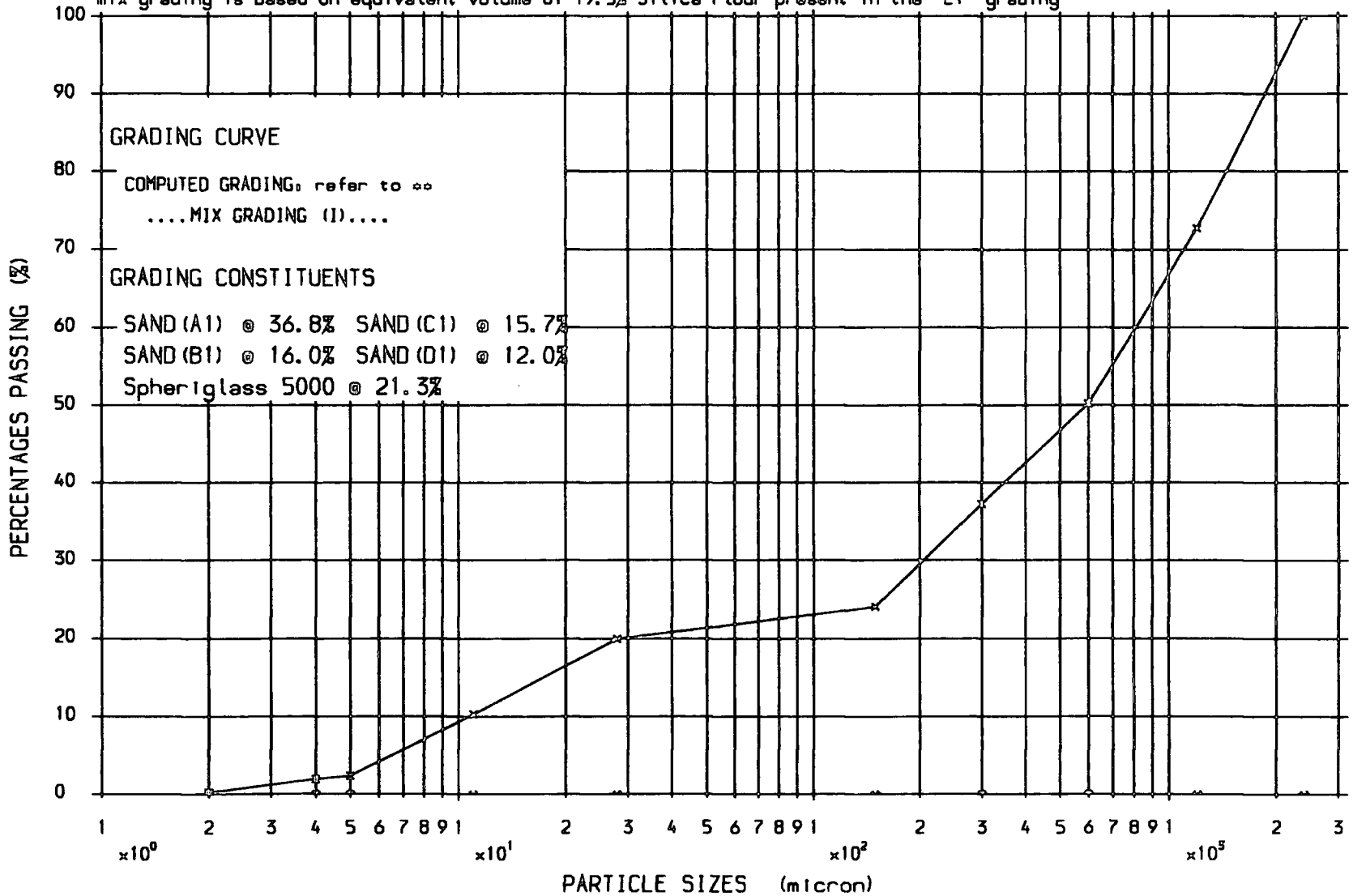

Figure A1.12

GRADING TASK NO. = 3

** The filler proportionates, to achive the mix grading, are based on 'E1' grading. The micro-filler content in the mix grading is based on equivalent volume of 19.5% Silica Flour present in the 'E1' grading

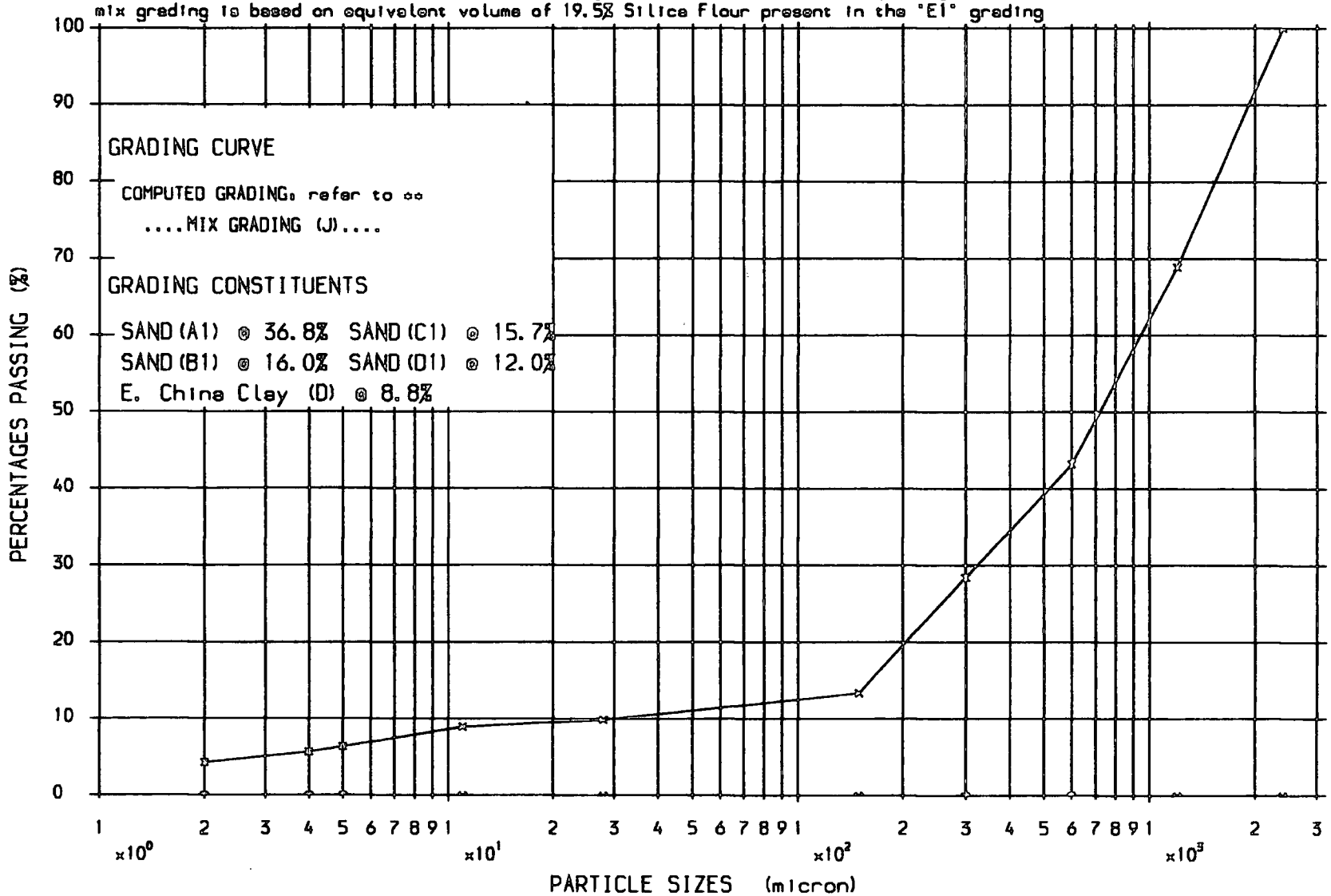

Figure A1.13

GRADING TASK NO. = 3

** The filler proportionates, to achive the mix grading, are based on "E1" grading. The micro-filler content in the mix grading is based on equivalent volume of 19.5% Silica Flour present in the "E1" grading

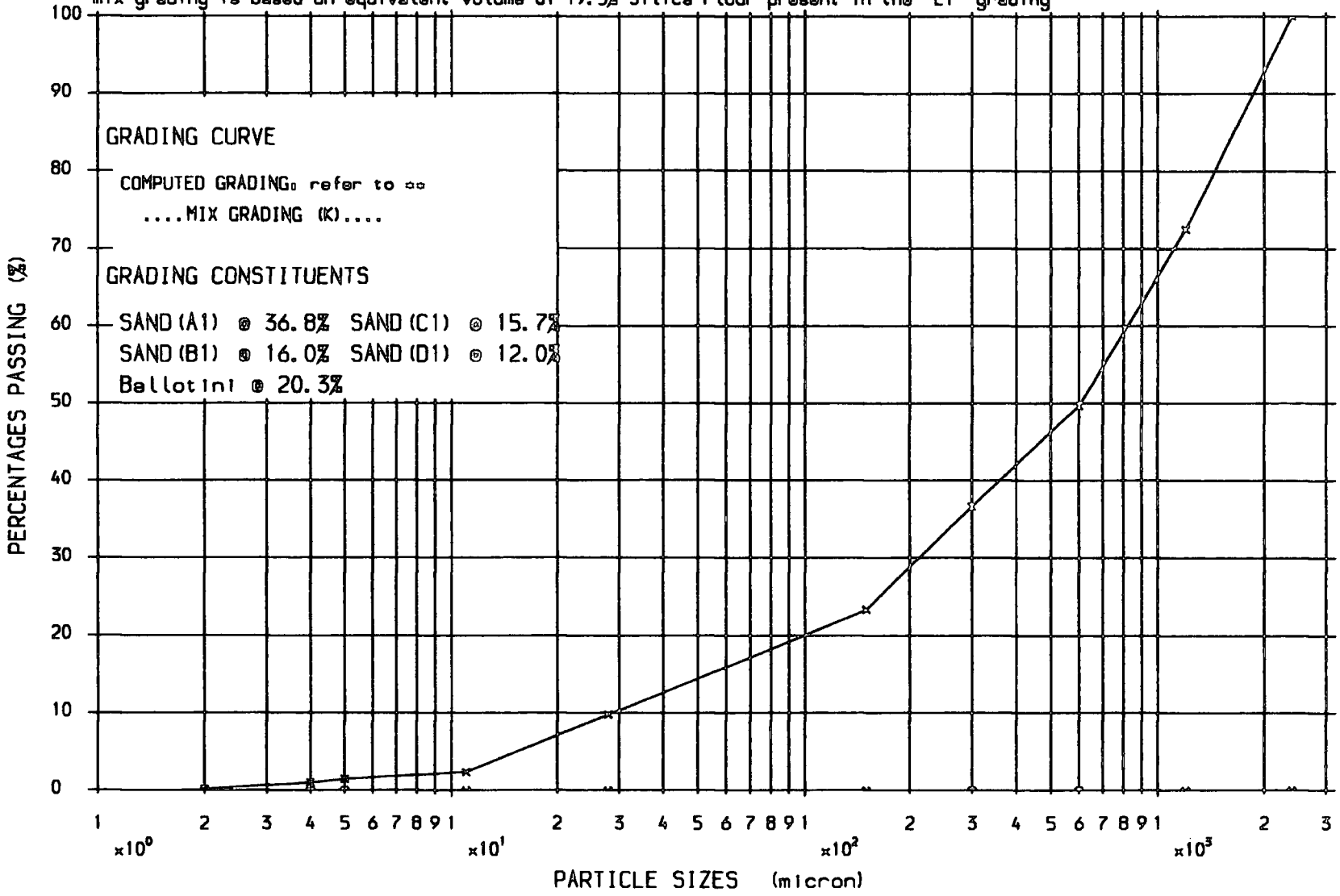

Appendix A2

A2. Theoretical Analysis of the Beams

A2.1. Introduction

Theoretical analysis of the test beams were based on elastic theory. In all the test beams, it was assumed that full composite action was achieved between the Phenolic Concrete matrix and that of the laminated fibre glass (Phenolic G.R.P.), and in internally reinforced beams the bond between the matrix and the steel bars remained viable up to failure. From the control specimen test results, it became clear that the materials of the test beams, behaved in linear elastic manner so that Hook's law is valid.

The test beams were all subjected to 'pure' bending over the central section of span. In the analysis the beam deformation was computed only due to bending and the effect of the shear deformation was not considered. However, shear stresses in beams whose effective cross-sectional dimensions are small in relation to their length are comparatively low so that for small displacements the bending theory can be used with reasonable accuracey. Theory of bending in analysing thin walled beams and sandwich panels is well known[108–112] . It was also assumed that the beams were of uniform homogeneous section and that plane sections of the beams remained plane under bending. This was the case from the strain distribution profiles measured over the heights of the beams. The strain distribution remained linear almost up to failure.

An empirical method based on the geometrical properties of the beams was adopted in the analysis, in which the neutral axis depth variation was related to the

degree of the effect of the composite section in tension.

A2.2. Tension Zone Coefficient (α)

From the test results and the behaviour of the test beams up to failure, it was noticed that the laminated fibre glass mat provided a restraining action on the cracked sections of the Phenolic Concrete matrix. The tension cracks were not visible until the fibre glass mat fractured at high loads near the failure. This consequently contributed to the strength and the stiffness of the composite sections. It is therefore, not valid to assume the sections fully cracked but to assume them to be partially cracked with a considerable contribution from the stresses developed in the tension zone, to the strength of the section. This phenomenon was also revealed, when from the elastic analysis, the condition of equilibrium was checked from the equations of static forces on the beam sections.

To establish the degree of the tension zone contribution to the strength and the stiffness of the composite sections, an empirical method was used. A simple computer programme made it possible to establish a relationship between the neutral axis depth variation and the degree of the tension zone contribution for each of the test beams. This was based on the geometrical properties of the transformed (equivalent) section, using the following expressions:

from the elastic theory

$$m = \frac{E_s}{E_f} \tag{2.2.1}$$

from condition of equilibrium

$$A1_C = \alpha A1_T + (m-1)A1_S \tag{2.2.2}$$

where,

$A1_C$ is the first moment of area of compression zone from N.A.

$A1_T$ is the first moment of area of tension zone from N.A.

$A1_S$ is the first moment of area of internal steel bars from N.A.

α is the tension zone coefficient

m is the modular ratio

E_s is the steel modulus

E_f is the Phenolic Concrete matrix modulus

from the geometry of the section (see Figure A2.1a);

$$A1_C = BT_t(Y_c - \frac{T_t}{2}) + \frac{T_l + T_r}{2}(Y_c - T_t)^2$$

$$A1_T = \alpha\{BT_b(Y_t - \frac{T_b}{2}) + \frac{T_l + T_r}{2}(Y_t - T_b)^2 + (\frac{H_r W_r}{2})(Y_t - (T_b + \frac{H_r}{3}) + (\frac{H_l W_l}{2})(Y_t - (T_b + \frac{H_l}{3})\}$$

$$A1_S = A_s(D_s - Y_c)$$

where,

D is the overall depth of the beam.

B is the breadth of the beam.

Y_c is the position of the neutral axis from compression face.

Y_t is the position of the neutral axis from tension face.

A_s is the total area of the internal steel bars.

D_s is the depth of the steel bars from the compression face.

T is the wall thicknesses.

H is the height of the left or right hand wedge.

W is the width of the left or right hand wedge.

For values of $0 \leq \alpha \leq 1$ in steps of 0.025, positions of the neutral axis depth from the equilibrium condition were computed for all the test beams. The relationship between these values is presented graphically in Figure A2.6. From the relevant graph for each of the test beams, the values of the tension zone coefficient (α) were extrapolated using the corresponding observed neutral axis depth values at all loads. The effective second moment of areas using these values were then computed from the following expressions:

$$I_E = I_C + \alpha I_T + (m-1)I_S \tag{2.2.3}$$

where,

I_E is the effective second moment of area of the section.

I_C is the second moment of area of the compression zone.

I_T is the second moment of area of the tension zone.

I_S is the second moment of area of the steel bars.

in which;

$$I_C = \frac{BT_t^3}{12} + BT_t(Y_c - \frac{T_t}{2})^2 + (Y_c - T_t)^3(\frac{T_l + T_r}{3})$$

$$I_T = \{\frac{BT_b^3}{12} + BT_b(Y_t - \frac{T_b}{2})^2 + (Y_t - T_b)^3(\frac{T_l + T_r}{3}) + \frac{W_l H_l^3}{36} + \frac{W_l H_l}{2}(Y_t - \frac{(H_l + T_b)}{3})^2 + \frac{W_r H_r^3}{36} + \frac{W_r H_r}{2}(Y_t - \frac{(H_r + T_b)}{3})^2\}$$

$$I_S = A_s(D_s - Y_c)^2$$

A2.3. First Crack Load and Ultimate Moment of Resistance

A2.3.1. Cracking of Phenolic Concrete Matrix

The theoretical load at first crack in the Phenolic Concrete matrix was calculated using the bending theory. It was assumed that uniform tensile stress distribution existed across the tension face of the beams.

Therefore, from the bending theory;

$$\frac{M}{I} = \frac{f}{Y} = \frac{E}{R} \tag{2.3.1}$$

hence;

$$M_{cracking} = \frac{f_{ct} I_{u.c.}}{D - Y_{u.c.}} \tag{2.3.2}$$

where,

$M_{cracking}$ is the moment to cause the first crack.

f_{ct} is the tensile strength of the Phenolic Concrete matrix obtained from Brazilian Disc Tests.

$I_{u.c.}$ is the second moment of area of the uncracked transformed section.

D is the overal depth of the beam.

$Y_{u.c.}$ is the position of the N.A. from the compression face of the uncracked section.

Using the expressions (2.2.2) and (2.2.3) in section A2.2., for the value of tension zone coefficient α equal to unity, the relevant neutral axis depth ($Y_{u.c.}$) and hence the second moments of area ($I_{u.c.}$) of the uncracked transformed (equivalent) sections were calculated.

The corresponding load at first crack was determined from the respective mo-

ment at first crack, such that;

$$W_C = \frac{2M_{cracking}}{a} \tag{2.3.3}$$

where,

W_C is the load at first crack

a is the maximum moment lever arm

The theoretical neutral axis depth and the second moment of area of the uncracked section with corresponding load at first crack of the test beams are given in Table 5.2 of Chapter 5.

A2.3.2. Ultimate Moment of Resistance

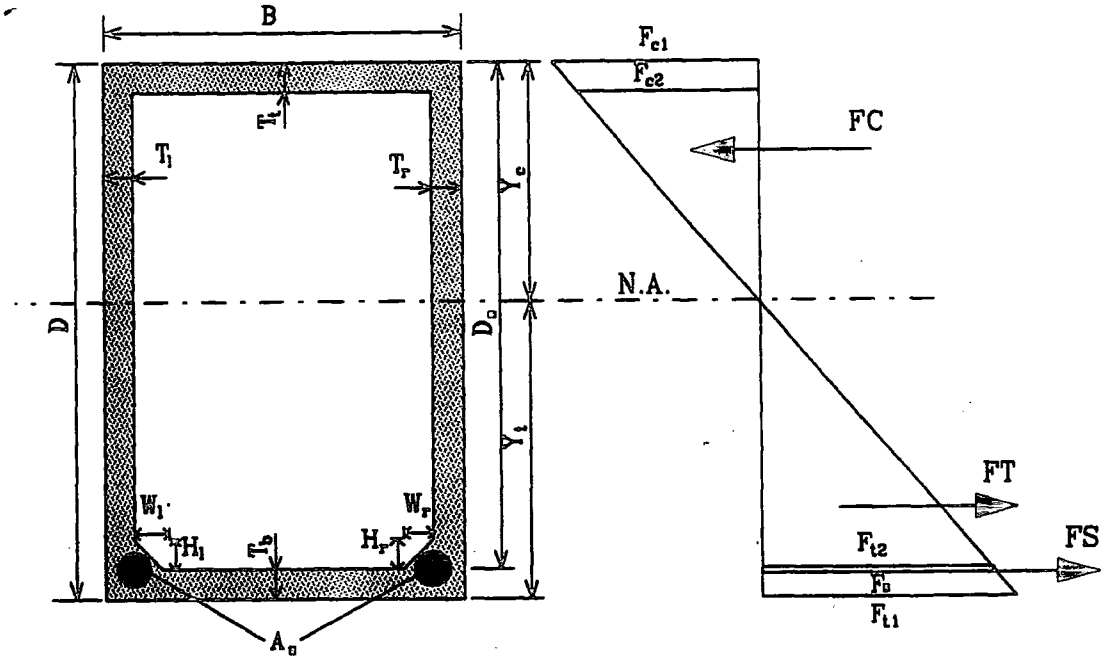

(a) Cross-Section (b) Stress Distribution and Forces Diagram

Figure A2.1

The ultimate moments of resistance of the beams were calculated using a triangular stress distribution. In all the beams, it was assumed that full composite action was

achieved between the laminated fibre glass mat and the Phenolic Concrete matrix up to failure, with the bond between the internal steel bars and the matrix remaining viable. It was also assumed that plane sections remained plane.

In the reference beams, the ultimate moment of resistance was computed on the basis that the stresses in the extreme tensile face of the beams had reached the ultimate tensile strength of the laminated fibre glass mat. In the internally reinforced beams the ultimate moment of resistance was computed for both steel stresses reaching their yield stress and also their ultimate tensile strength. The corresponding stress values of the laminated fibre glass and the steel bars are referred to in section 5.4.2. of Chapter 5.

Considering the stress distribution diagram (Figure A2.1b), from the condition of compatibility and the elastic theory, the stresses in the extreme faces of the beam section in Figure A2.1a, are given as;

$$F_{c1} = \frac{F_s}{m} \times \frac{Y_c}{D_s - Y_c} \tag{2.3.4}$$

$$F_{c2} = F_{c1} \times \frac{Y_c - T_t}{Y_c} \tag{2.3.5}$$

$$F_{t1} = F_{c1} \times \frac{Y_t}{Y_c} \tag{2.3.6}$$

$$F_{t2} = F_{t1} \times \frac{Y_t - T_b}{Y_t} \tag{2.3.7}$$

Considering the force diagram (Figure A2.1b), from the condition of equilibrium;

$$FC = \alpha FT + FS \tag{2.3.8}$$

where,

FC is the effective compressive force due to the compression zone.

FT is the effective tensile force due to the tension zone.

FS is the total steel tensile force due to the internal steel bars.

The effective compressive and tensile forces are obtained as:

$$FC = FC_{solid} - FC_{void} \tag{2.3.9}$$

$$FT = FT_{solid} - FT_{void} + FT_{\Delta L} + FT_{\Delta R} \tag{2.3.10}$$

where,

FC_{solid} is the total compressive force due to the whole section above the neutral axis position.

FC_{void} is the total compressive force due to the void section (core) above the neutral axis position.

FT_{solid} is the total tensile force due to the whole section below the neutral axis position.

FT_{void} is the total tensile force due to the void section (core) below the neutral axis position.

$FT_{\Delta L}$ is the tensile force due to the left hand wedge ($\frac{H_l W_l}{2}$).

$FT_{\Delta R}$ is the tensile force due to the right hand wedge ($\frac{H_r W_r}{2}$).

Taking moment of these forces about N.A. position ;

$$M_{1C} = FC_{solid}\frac{2Y_c}{3} - FC_{void}\frac{2(Y_c - T_t)}{3} \tag{2.3.11}$$

$$M_{1T} = \alpha\{FT_{solid}\frac{2Y_t}{3} - FT_{void}\frac{2(Y_t - T_b)}{3} + FT_{\Delta L}(Y_t - T_b - \frac{H_l}{3}) + FT_{\Delta R}(Y_t - T_b - \frac{H_r}{3})\} \tag{2.3.12}$$

$$M_{1S} = FS(D_s - Y_t) \tag{2.3.13}$$

The ultimate moment of resistance is therefore given as;

$$M_{UR} = M_{1C} + M_{1T} + M_{1S} \tag{2.3.14}$$

As explained before, the tension zone of the beam section subject to loading acts as though partially cracked as failure of the beam approaches. This therefore requires the evaluation of the degree of the tension zone contribution to the strength and the stiffness of the beam. For this reason a simple computer program based on an empirical method, which accounts for the tension zone contribution of the composite section, was used in computing the ultimate moment of resistace for each beam. The program and a trial execution for the test beam B-3a are presented in section A2.6 of this Appendix.

The theoretical ultimate moment of resistance and the experimental sustained ultimate moment at failure of the test beams are presented in Table A2.1. In this table the theoretical values of tension zone coefficient α, corresponding neutral axis position Y_c and the extreme face stresses at failure are also given for all the test beams.

The procedure used in computation of the ultimate moment of resistance of the beams is outlined as follows:

1. Consider the steel bars in the internally reinforced sections at failure to reach their yield or their ultimate tensile strength, and in the reference beams assume that the extreme tensile face reaches the ultimate tensile strength of the laminated fibre glass mat for failure to occur.

2. For internally reinforced beams, the stresses in the beam faces (top and bottom) when the steel yielded are evaluated using the stress distribution diagram and the condition of compatibility. In unreinforced beams and those where the tension steel was observed to fracture the force diagram has been used to satisfy the condition of equilibrim at beam failure, considering the ultimate tensile strengths of the laminated fibre glass and/or tension steel.

3. Using the geometrical properties of the sections in deriving the empirical method, for $0 \leq \alpha \leq 1$ in steps of 0.025 and the corresponding N.A. positions, the stresses are evaluated for each level of α value. Hence, from the force diagram and the condition of equilibrium the moment of resistance for each level of α is computed assuming failure occurs.

4. Check the ultimate moment of resistance values obtained in 3 against the actual (experimental) value, and find a range for α and hence neutral axis position.

5. Evaluate a new value of α by interpolation and hence, using Figure A2.6 (graph of α against neutral axis depth) the corresponding neutral axis position is found.

6. Using the new values obtained in 5 compute the ultimate moment of resistance (M_{UR}) of the section.

7. Repeat 4 to 7 until the ultimate moment of resistance approximately equals the actual ultimate moment sustained at failure. This will therefore determine the value of the α and the neutral axis position at which the failure would occur.

It is demonstrated (as can be seen from Table A2.1) that in general a value of α in the range of $0.0625 \leq \alpha \leq 0.2250$ may be used to calculate the effective ultimate moment of resistance of beams of this type.

A2.4. Deflection

Theoretical deflection values for all the beams at all loads, were calculated using the differential equation of the deflection curves derived from the theory of bending. The equations are based upon the geometric consideration; thus they apply to a beam of any material. The use of these equations provides no restriction on the magnitudes of the deflections and the slopes of the deflection curves. It is well known that a straight beam of uniform cross- section, when subjected to end couples M applied about a principal axis, bends into a circular arc of radius R.

The equation of the deflection curves in terms of angle of rotation can be written as;

$$K = \frac{1}{R} = \frac{\partial \theta}{\partial x} = \frac{\partial^2 y}{\partial x^2} \tag{2.4.1}$$

where,

K is the curvature.

R is the radius of curvature.

θ is the angle of rotation $(\frac{\partial y}{\partial x})$ of the axis of the beam at any point.

The equation (2.4.1) relates to the deflection y of the beam. It is valid for a beam of any material, provided the rotations are small.

If the material of the beam is linearly elastic and thus follows Hook's law, the curvature is:

$$K = \frac{1}{R} = -\frac{M}{EI} \tag{2.4.2}$$

where,

M is the bending moment.

EI is the flexural rigidity.

The Equation (2.4.2) is valid for large rotations as well as small rotations. In order

to evaluate deflection values of the test beams Equations (2.4.1) and (2.4.2) are combined;

$$\frac{\partial^2 y}{\partial x^2} = -\frac{M}{EI} \tag{2.4.3}$$

The eqution (2.4.3) can now be integrated in each particular case to find the deflection y, provided the bending moment M is known. In each order of integration, the constant of integration is being evaluated from the boundary condition of the beam. For this purpose the equations for the bending moment, using free-body diagram and static equilibrium are derived, in order to obtain the differential equation of the relevant deflection curve (considering Figure A2.2a,b,c).

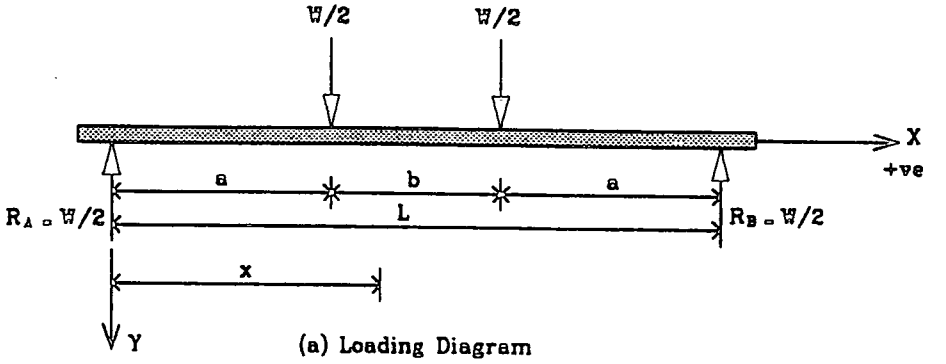

(a) Loading Diagram

(b) Bending Moment Diagram

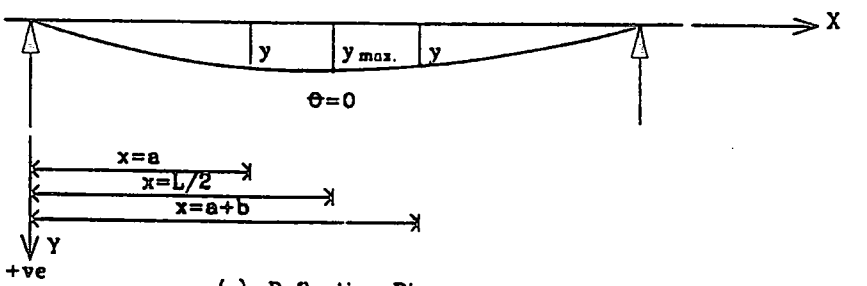

(c) Deflection Diagram

Figure A2.2

To obtain the deflections, we first must determine the expression for the bending moment in each part of the beam. From Figure A2.2a, due to symmetrical loading, the bending moment is only considered for $0 \leq x \leq a$ and $a \leq x \leq (a+b)$ parts of the beam. Therefore, sustituting the bending moments into Equation (2.4.3) will give;

for $0 \leq x \leq a$;

$$EI\frac{\partial^2 y}{\partial x^2} = -\frac{W}{2}x \tag{2.4.4}$$

and, for $a \leq x \leq (a+b)$;

$$EI\frac{\partial^2 y}{\partial x^2} = -\frac{W}{2}x + \frac{W}{2}(x-a) \tag{2.4.5}$$

First integration of these equations gives;

$$EI\frac{\partial y}{\partial x} = -\frac{W}{4}x^2 + C_1 \tag{2.4.6}$$

and,

$$EI\frac{\partial y}{\partial x} = -\frac{W}{4}x^2 + \frac{W}{4}(x-a)^2 + C_2 \tag{2.4.7}$$

Performing a second integration, we obtain;

$$EIy = -\frac{W}{12}x^3 + C_1 x + C_3 \tag{2.4.8}$$

and,

$$EIy = -\frac{W}{12}x^3 + \frac{W}{12}(x-a)^3 + C_2 x + C_4 \tag{2.4.9}$$

From the boundary conditions, the four constants of the integrations appearing in the preceding equations can be evaluated.

At at $x = a$, the slopes from both Equations (2.4.6) and (2.4.7) must be equal; thus,

$$-\frac{W}{4}a^2 + C_1 = -\frac{W}{4}a^2 + 0 + C_2$$

from which $C_1 = C_2$. At $x = a$, the deflections found from Equations (2.4.8) and (2.4.9) must be equal; thus,

$$-\frac{W}{12}a^3 + C_1 a + C_3 = -\frac{W}{12}a^3 + 0 + C_2 a + C_4$$

from which $C_3 = C_4$.

At $x = L/2$, the slope found from Equation (2.4.7) must equal to zero (i.e. $\frac{\partial y}{\partial x} = 0$);

$$0 = \frac{W}{4}\frac{L^2}{4} - \frac{W}{4}(\frac{L}{2} - a)^2 - C_2$$

which gives $C_2 = \frac{W}{4}(aL - a^2)$. Finally, when $x = 0$, the deflection obtained from Equation (2.4.8) becomes zero, and therefore $C_3 = 0$.

From the preceding results, we see that;

$$C_1 = C_2 = \frac{W}{4}(aL - a^2)$$

and,

$$C_3 = C_4 = 0$$

Substitution of these values into Equations (2.4.8) and (2.4.9) gives the equations for the deflection curve (Figure A2.2c), such that;

for $0 \leq x \leq a$

$$EIy = -\frac{W}{12}x^3 + \frac{W}{4}(aL - a^2)x \tag{2.4.10}$$

and, for $a \leq x \leq (a + b)$

$$EIy = -\frac{W}{12}x^3 + \frac{W}{12}(x - a)^3 + \frac{W}{4}(aL - a^2)x \tag{2.4.11}$$

The first part of these equations can be used to obtain the deflection at loading point $(W/2)$, and the second part can be used to obtain the maximum deflection which will be at mid-span $(L/2)$.

At $x = a$, the deflection (y_l) at loading point ($W/2$), from Equation (2.4.10) is;

$$y_l = \frac{WL^3}{12EI}[3(\frac{a}{L})^2 - 4(\frac{a}{L})^3] \tag{2.4.12}$$

At $x = L/2$, the maximum deflection at mid-span, from Equation (2.4.11) is;

$$y_{max.} = y_c = \frac{WL^3}{12EI}(\frac{a^3}{L^3} - \frac{3a}{4L}) \tag{2.4.13}$$

The Equations (2.4.12) and (2.4.13) can be written in terms of:

$$y_l = \frac{W}{EI}C_l \tag{2.4.14}$$

$$y_c = \frac{W}{EI}C_c \tag{2.4.15}$$

in which; from the loading geometry and the beam span, ($a = 510\ mm$, $b = 330\ mm$ and $L = 1350\ mm$), the deflection constants are;

$$C_l = 43.57 \times 10^6\ mm^3$$

$$C_c = 47.03 \times 10^6\ mm^3$$

The flexural moduli of the test beams were calculated from the Equations (2.4.14) and (2.4.15), using the slopes (W/y) of the corresponding load-deflection curves over the elastic region (see Table 5.2 of Chapter 5).

The tension zone coefficients (α) for all the beams at all loads using the observed N.A. depth were obtained. Then, from these values the effective second moments of area of the sections were calculated and hence the deflection at the corresponding loading stages for all the test beams using the Equations (2.4.14) and (2.4.15) were deduced (see Tables A2.2a to A2.2l).

A2.5. Moment-Curvature

It is usual that in a reinforced concrete member subject to bending, the section is considered to be uncracked up to and cracked beyond the service load. In calculating the deflection, for uncracked sections, linearly elastic stress-strain diagrams are assumed for the concrete in tension and compression. For cracked sections, the tensile strength of the concrete is neglected, while the concrete in compression is considered linearly elastic. These conditions are used to determine second moment of area I in terms of position of neutral axis depth Y_c from the compression face for both uncracked and cracked cases.

Uncracked and cracked values of I and Y_c are the only two conditions for which the linear stress-strain relationship is applicable. Since the Phenolic Concrete Composite beams tested in this work, can not be considered as cracked sections but can be considered partially cracked (if one can use the term), therefore transition values are required between these extreme limits for deflection calculations. This requires a method from which the $I_{effective}$ can be computed and then used in deflection calculations of the partially cracked sections.

The moment-curvature relationship is, therefore, adopted in computing the beam deflections. This enables us to establish a general method to determine the flexural rigidity of the beams at all applied moments, in terms of $I_{effective}$. From flexural theory, the assumptions are made that (a) plane sections remain plane and (b) there is no slippage between the Phenolic Concrete matrix and the internal reinforcements.

The section and the strain distribution for the composite member are defined in Figure A2.3.

From strain compatibility, the curvature ϕ and strain ϵ at any distance D from

extreme compression face are given in Equations (2.5.1 a,b,c).

$$\phi_1 = \frac{\epsilon_{c1}}{Y_c} \qquad (2.5.1\ a)$$

$$\phi_2 = \frac{\epsilon_{c2}}{(Y_c - D_{c2})} \qquad (2.5.1\ b)$$

$$\phi_3 = \frac{\epsilon_{c3}}{(Y_c - D_{c3})} \qquad (2.5.1\ c)$$

$$\phi = \frac{\phi_1 + \phi_2 + \phi_3}{3} \qquad (2.5.2)$$

where;

$\epsilon_{c1,c2,c3}$ is the measured strains over the height of the beam compression zone.

ϕ is the curvature.

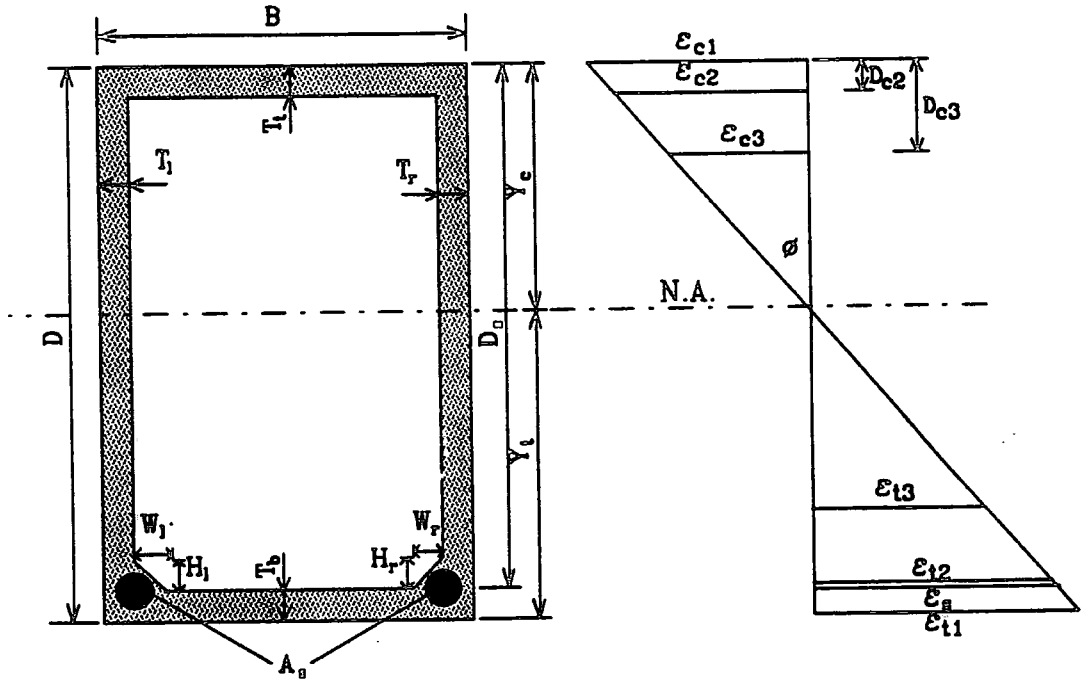

(a) Cross-Section (b) Strain Distribution Diagram

Figure A2.3

The experimentally measured strains over the height of the compression zone of the test beams were used in evaluating the curvature ϕ value. The corresponding

ϕ values were averaged accordingly for each level of applied moments and then tabulated in Tables A2.2*a* to A2.2*l* for all levels of applied moments.

The flexural rigidity of a reinforced member depends on the level of moments. At a higher level the development of cracks in the Phenolic Concrete matrix reduced the flexural rigidity of the composite section. This reduction in rigidity was greater for a lightly reinforced section, but smaller for a heavily reinforced section.

A typical moment-curvature relationship of the Phenolic Concrete composite section is given in Figure A2.4;

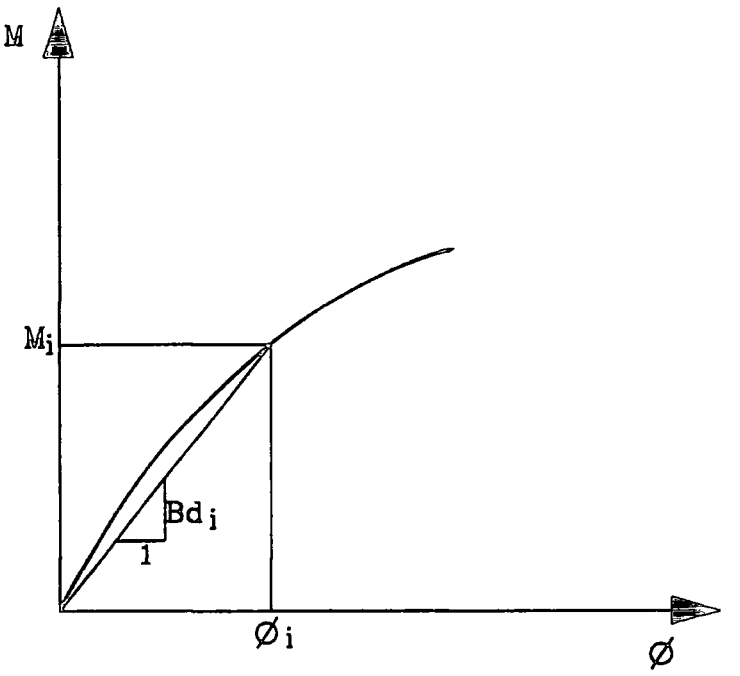

Moment–Curvature relationship for internally reinforced Phenolic Concrete beams.

Figure A2.4

At any level of applied moment the bending stiffness can be obtained from the slope

of the secant using the linear elastic relationship,

$$B_{di} = \frac{M_i}{\phi_i} \tag{2.5.3}$$

$$B_{di} = E_f I_e \tag{2.5.4}$$

where;

M_i is the applied moment (level i).

ϕ_i is the curvature at applied moment level M_i.

B_{di} is the bending stiffness at applied moment level M_i.

Using the effective bending stiffness values in deflection equations derived in Section A2.4, the corresponding deflection values at all levels of applied moment can be calculated.

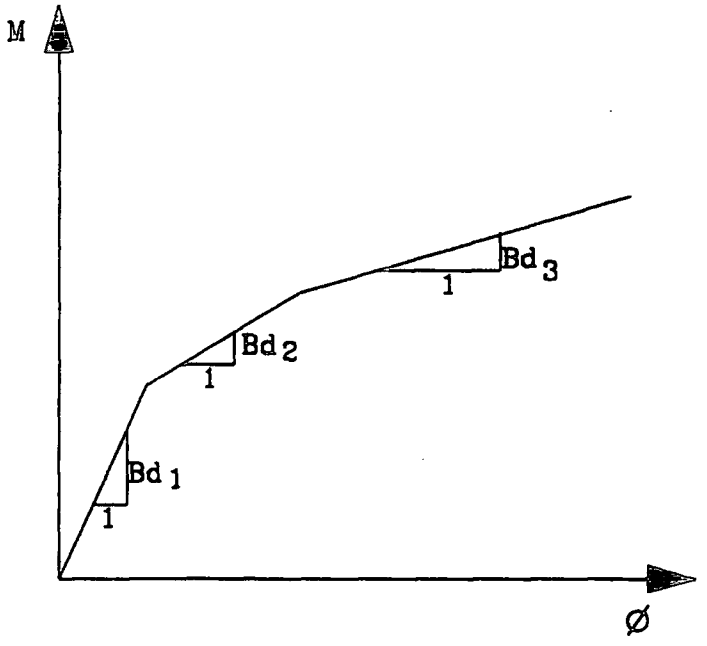

Moment–Curvature relationship for unreinforced Phenolic Concrete beams.

Figure A2.5

For the unreinforced section, the typical moment-curvature relationship was found to be of form as defined in Figure A2.5.

From the slopes B_{d1}, B_{d2} and B_{d3} the effective bending stiffness for each range of applied moments is determined and the corresponding deflection values from the deflection equations are then calculated for all levels of applied moments.

The applied moments M, the evaluated curvatures ϕ, the corresponding effective bending stiffnesses B_d and the deflection values at mid-span of the beams using the above procedure for all the beams are computed and presented in Tables A2.2a to A2.2l.

```
LIST
10 PRINT "SEEKING MOMENT OF RESISTANCE"
20 PRINT "READ IN BREADTH,DEPTH,WALL THICKNESSES"
30 INPUT B,D,TT,TB,TL,TR,WL,WR,HL,HR
40 PRINT "READ IN STEEL AREA,STEEL DEPTH,STEEL STRESS,MODULAR RATIO"
50 INPUT AS,DS,FS,H
60 YC1 = .1
80 FOR I = 1 TO 100
90 YC1 = YC1 + .025
100 YC = D*YC1
105 YT = D - YC
106 FC1 = (YC/(DS-YC))*(FS/H)
107 FT1 = (YT/YC)*FC1
108 FC2 = ((YC-TT)/YC)*FC1
109 FT2 = ((YT-TB)/YT)*FT1
111 A1C = (B*TT)*(YC-(TT/2)) + ((YC-TT)^2)*((TL+TR)/2)
112 M1C = (((FC1*B*YC^2)*1/3) - (FC2*(B-(TL+TR))*(YC-TT)^2)*1/3)
115 ALFA = -.025
120 FOR J = 1 TO 100
130 ALFA = ALFA + .025
135 A1T = ALFA*((B*TB)*(YT-(TB/2))+((YT-TB)^2)*((TL+TR)/2))
140 A1T = A1T +ALFA*(((HR*WR)/2)*(YT-(TB+(HR/3)))+((HL*WL)/2)*(YT-(TB+(HL/3))))
141 M1T = ALFA*(((FT1*B*YT^2)*1/3) -(FT2*(B-(TL+TR))*(YT-TB)^2)*1/3)
142 M1T = M1T +ALFA*FT2*(((WL*HL+WR*WR)*(YT-TB)*1/2)-((WL*HL^2)+(WR*HR^2))*1/6)
143 A1S = (AS*(DS-YC))*(H-1)
144 M1S = (AS*(DS-YC)*FS)
145 A1Z = A1T + A1S
150 IF A1Z>A1C GOTO 170
160 NEXT J
170 PRINT "YC =",YC ,"ALFA =",ALFA
172 DS1 =DS*3/4
175 IF YC>DS1 GOTO 190
176 IF ALFA>1 GOTO 190
177 MUR = M1C + M1T + M1S
178 PRINT "MOMENT OF RESISTANCE IF FAILING =",MUR
179 PRINT "EXTREME COMPRESSIVE STRESS(TOP) =",FC1
180 PRINT "EXTREME TENSILE STRESS (BOTTOM) =",FT1
185 NEXT I
190 STOP
Ok
```

```
RUN
SEEKING MOMENT OF RESISTANCE
READ IN BREADTH, DEPTH, WALL THICKNESS
? 98,206,20.1,16.6,14.9,14.1,17.1,15.9,30.6,31.2
READ IN STEEL AREA,STEEL DEPTH, YIELD STRESS,MODULAR RATIO
? 170.88,184.5,557,12.82
YC =          25.75        ALFA =        0
MOMENT OF RESISTANCE IF FAILING =        1.526136E+07
EXTREME COMPRESSIVE STRESS(TOP) =        7.047429
EXTREME TENSILE STRESS (BOTTOM) =        49.332
YC =          30.9         ALFA =        0
MOMENT OF RESISTANCE IF FAILING =        1.493341E+07
EXTREME COMPRESSIVE STRESS(TOP) =        8.749463
EXTREME TENSILE STRESS (BOTTOM) =        49.52929
YC =          36.05        ALFA =        0
MOMENT OF RESISTANCE IF FAILING =        1.455011E+07
EXTREME COMPRESSIVE STRESS(TOP) =        10.55097
EXTREME TENSILE STRESS (BOTTOM) =        49.74027
YC =          41.20001     ALFA =        0
MOMENT OF RESISTANCE IF FAILING =        1.426646E+07
EXTREME COMPRESSIVE STRESS(TOP) =        12.49161
EXTREME TENSILE STRESS (BOTTOM) =        49.96642
YC =          46.35001     ALFA =        0
MOMENT OF RESISTANCE IF FAILING =        1.404129E+07
EXTREME COMPRESSIVE STRESS(TOP) =        14.57693
EXTREME TENSILE STRESS (BOTTOM) =        50.20543
YC =          51.50001     ALFA =        0
MOMENT OF RESISTANCE IF FAILING =        1.388396E+07
EXTREME COMPRESSIVE STRESS(TOP) =        16.82375
EXTREME TENSILE STRESS (BOTTOM) =        50.47124
YC =          56.65001     ALFA =        0
MOMENT OF RESISTANCE IF FAILING =        1.380537E+07
EXTREME COMPRESSIVE STRESS(TOP) =        19.25158
EXTREME TENSILE STRESS (BOTTOM) =        50.75415
YC =          61.80001     ALFA =        0
MOMENT OF RESISTANCE IF FAILING =        1.381824E+07
EXTREME COMPRESSIVE STRESS(TOP) =        21.88322
EXTREME TENSILE STRESS (BOTTOM) =        51.06083
YC =          66.95001     ALFA =        0
MOMENT OF RESISTANCE IF FAILING =        1.393752E+07
EXTREME COMPRESSIVE STRESS(TOP) =        24.74544
EXTREME TENSILE STRESS (BOTTOM) =        51.39437
YC =          72.10001     ALFA =        0
MOMENT OF RESISTANCE IF FAILING =        1.41809E+07
EXTREME COMPRESSIVE STRESS(TOP) =        27.86996
EXTREME TENSILE STRESS (BOTTOM) =        51.75808
YC =          77.25001     ALFA =        0
MOMENT OF RESISTANCE IF FAILING =        1.456945E+07
EXTREME COMPRESSIVE STRESS(TOP) =        31.29454
EXTREME TENSILE STRESS (BOTTOM) =        52.15755
YC =          82.40001     ALFA =        0
MOMENT OF RESISTANCE IF FAILING =        1.512853E+07
EXTREME COMPRESSIVE STRESS(TOP) =        35.06459
EXTREME TENSILE STRESS (BOTTOM) =        52.59697
YC =          87.55002     ALFA =        0
MOMENT OF RESISTANCE IF FAILING =        1.588886E+07
EXTREME COMPRESSIVE STRESS(TOP) =        39.23518
EXTREME TENSILE STRESS (BOTTOM) =        53.08288
```

CONTINUED...

```
YC =          92.70001     ALFA =        .1
MOMENT OF RESISTANCE IF FAILING =        1.685392E+07
EXTREME COMPRESSIVE STRESS(TOP) =        43.87371
EXTREME TENSILE STRESS (BOTTOM) =        53.62341
YC =          97.85001     ALFA =        .225
MOMENT OF RESISTANCE IF FAILING =        2.127128E+07
EXTREME COMPRESSIVE STRESS(TOP) =        49.06362
EXTREME TENSILE STRESS (BOTTOM) =        54.2282
YC =          103          ALFA =        .3500001
MOMENT OF RESISTANCE IF FAILING =        2.431879E+07
EXTREME COMPRESSIVE STRESS(TOP) =        54.90943
EXTREME TENSILE STRESS (BOTTOM) =        54.90941
YC =          108.15       ALFA =        .5250001
MOMENT OF RESISTANCE IF FAILING =        2.918278E+07
EXTREME COMPRESSIVE STRESS(TOP) =        61.54385
EXTREME TENSILE STRESS (BOTTOM) =        55.63253
YC =          113.3        ALFA =        .7249999
MOMENT OF RESISTANCE IF FAILING =        3.256404E+07
EXTREME COMPRESSIVE STRESS(TOP) =        69.13903
EXTREME TENSILE STRESS (BOTTOM) =        56.56749
YC =          118.45       ALFA =        .9499996
MOMENT OF RESISTANCE IF FAILING =        3.754133E+07
EXTREME COMPRESSIVE STRESS(TOP) =        77.9165
EXTREME TENSILE STRESS (BOTTOM) =        57.59046
YC =          123.6        ALFA =        1.249999
Break in 190

Ok

FINAL INTERPOLATION     ALFA =0.200 AND YC =96.4

RUN
TRANSFORMED SECTIONS
BREADTH,DEPTH.WALL THICKNESSES
? 98,206,20.1,16.6,14.9,14.1,17.1,15.9,30.6,31.2
NEUTRAL AXIS, ALFA
? 96.4,0.200
READ IN STEEL AREA,STEEL DEPTH,STEEL STRESS AND MODULAR RATIO
? 170.88,184.5,557,12.82
 FOR ALFA =    .2
 FOR YC   =    96.4
 DEPTH    =    206
 BREADTH  =    98
 STEEL AREA=   170.88
 STEEL DEPTH=  184.5
 TRANSFORMED SECOND MOMENT OF AREA=       4.052757E+07
 EXTREME COMPRESSIVE STRESS(TOP) =        47.541
 EXTREME TENSILE STRESS (BOTTOM) =        54.05076
 MOMENT OF RESISTANCE IF FAILING =        2.050278E+07
Break in 230

Ok
```

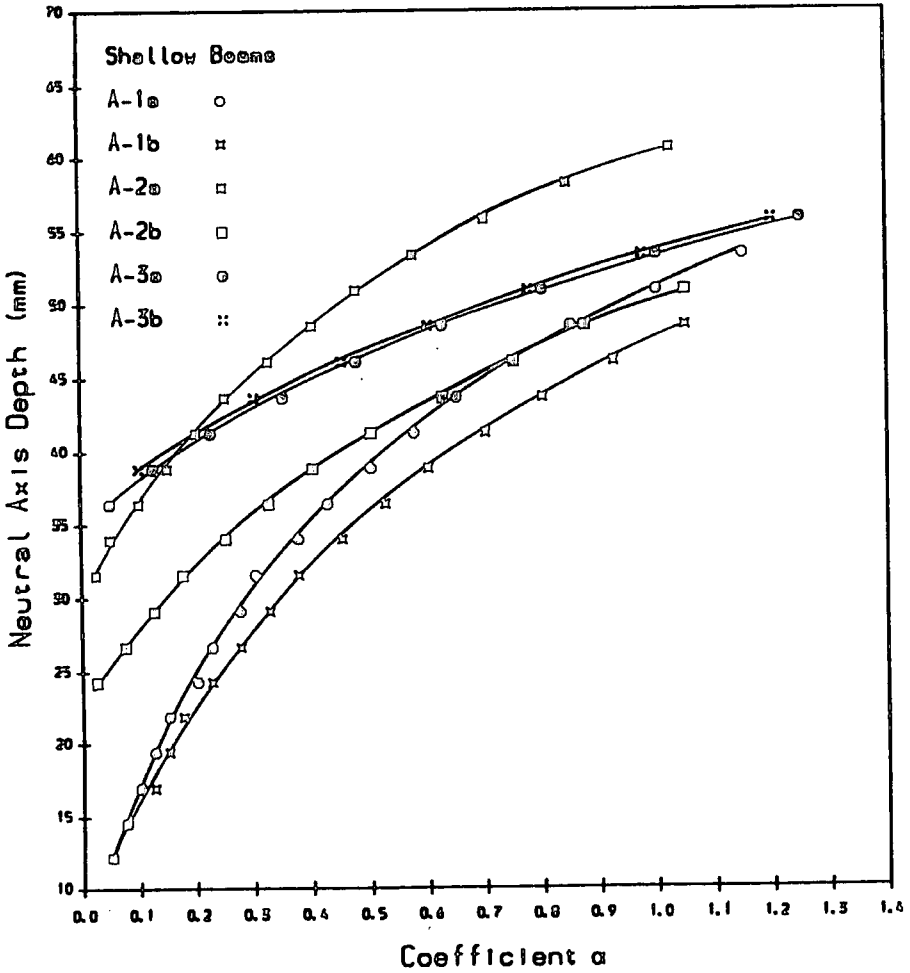

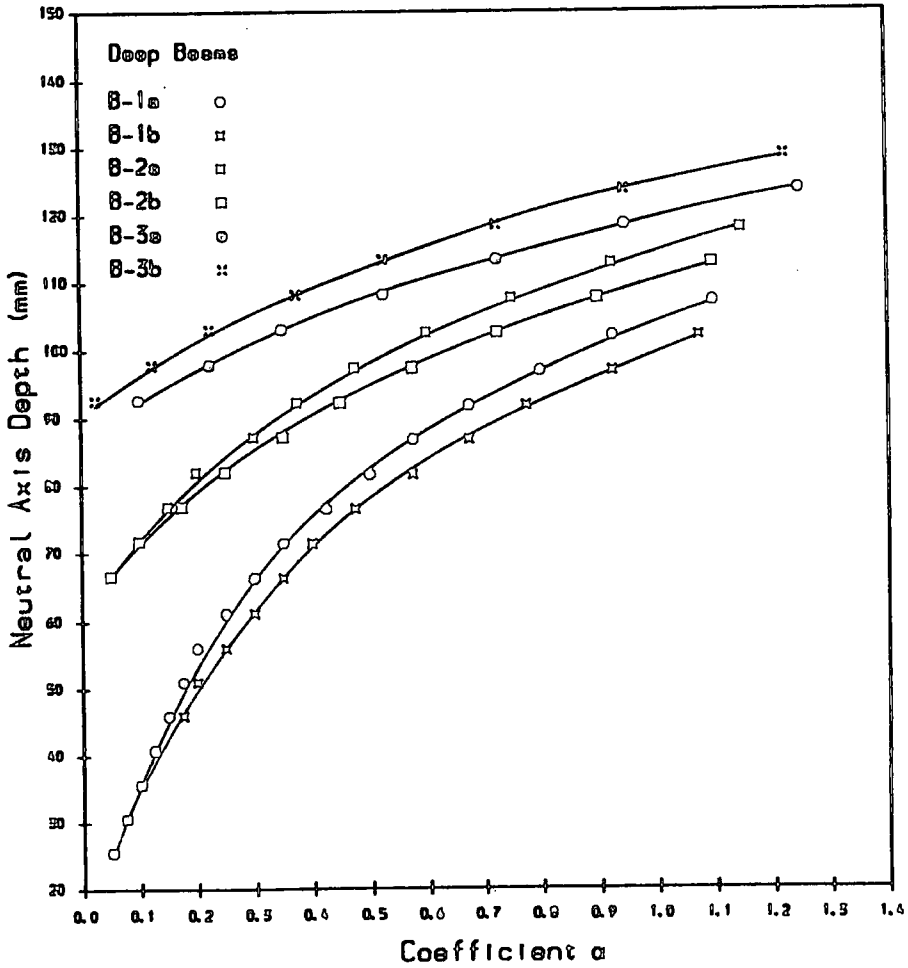

Figure A2.6 Variation of Neutral Axis Depth with Tension Zone Coefficient α

Table A2.1 (Theoretical and Experimental Moments at failure.)

Reference Beams						
Beam	Fibre Glass Ult. Tensile Strength					Sustained Ult. Moment at Failure M_U $N.mm$
	Tension Zone Coefficient α	Neutral Axis Depth Y (mm)	Extreme Face Stresses		Moment of Resistance M_{UR} $N.mm$	
			Tension F_{T1} $N.mm^{-2}$	Compression F_{C1} $N.mm^{-2}$		
A-1a	0.1000	17.0	130.0	27.58	3830545	3971625
A-1b	0.1125	16.5	130.0	26.65	3922439	3914888
B-1a	0.1125	37.8	130.0	29.57	7377156	7035450
B-1b	0.1375	41.7	130.0	33.40	8843711	8510625

Internally Reinforced Beams											
Beam	Steel Yield Stress					Steel Ult. Tensile Strength					Sustained Ult. Moment at Failure M_U $N.mm$
	Tension Zone Coefficient α	Neutral Axis Depth Y (mm)	Extreme Face Stresses		Moment of Resistance M_{UR} $N.mm$	Tension Zone Coefficient α	Neutral Axis Depth Y (mm)	Extreme Face Stresses		Moment of Resistance M_{UR} $N.mm$	
			Tension F_{T1} $N.mm^{-2}$	Compression F_{C1} $N.mm^{-2}$				Tension F_{T1} $N.mm^{-2}$	Compression F_{C1} $N.mm^{-2}$		
A-2a	0.2125	41.80	62.24	47.13	6770905	0.1500	38.80	71.70	47.80	6695080	6695025
A-2b	0.1500	30.35	75.24	34.26	5737881	0.1125	28.25	86.46	35.53	5759326	5730488
A-3a	0.1125	38.50	69.64	45.83	8467879	0.0625	36.85	77.36	47.39	8535044	8567363
A-3b	0.1125	40.20	61.55	41.74	8518042	0.0500	37.10	68.51	42.43	8504116	8510625
B-2a	0.1500	76.88	58.39	35.03	11340840	0.0875	71.50	67.68	36.25	11153250	11347500
B-2b	0.2250	80.60	59.86	38.78	13525200	0.1500	76.60	69.43	41.42	13543090	13617000
B-3a	0.2000	96.40	54.05	47.54	20582780	0.0875	92.40	60.52	49.22	20437650	20425500
B-3b	0.1375	98.60	52.22	48.12	19443700	0.0625	95.00	58.56	50.12	19820380	19858125

Table A2.2a. (Theoretical and Experimental Deflection of Beam A-1a.)

Load	Observed N.A. Depth	Transformed Section		Moment-Curvature Relationship				Theoretical Deflection		Experimental Deflection		
		Tension Zone Coefficient	2nd Moment of Area	Moment M	Curvature ϕ	Flexural Rigidity	Deflection Ctr. Pt.	Ctr. pt.	Ldg. Pts.	Ctr. Pt.	Ldg. Pt.1	Ldg. Pt.2
(lb)	Y (mm)	α	$I_c \times 10^{-4}$ (m^4)	$\times 10^2$ (N.m)	$\times 10^{-3}$ (m^{-1})	$E_eI_e \times 10^5$ ($N.m^2$)	y_c (mm)	y_c (mm)	y_l (mm)	y_c (mm)	y_{l1} (mm)	y_{l2} (mm)
0	.....	.....	.....	0.00	....	....	0.00	0.00	0.00	0.00	0.00	0.00
100	51.00	1.000	0.1089462	1.14	0.98	3.12	0.07	0.15	0.14	0.11	0.13	0.12
200	51.00	1.000	0.1089462	2.27	2.15	1.94	0.22	0.31	0.29	0.22	0.26	0.24
300	51.00	1.000	0.1089462	3.40	2.62	1.75	0.36	0.46	0.43	0.35	0.39	0.36
400	51.00	1.000	0.1089462	4.54	3.39	1.56	0.54	0.62	0.57	0.53	0.53	0.50
500	51.00	1.000	0.1089462	5.67	3.70	1.51	0.69	0.77	0.72	0.70	0.65	0.68
600	50.50	0.975	0.1076694	4.81	4.70	1.37	0.92	0.94	0.87	0.86	0.85	0.87
700	50.50	0.975	0.1076694	7.94	5.03	1.34	1.09	1.09	1.01	1.05	1.04	1.07
800	50.50	0.975	0.1076694	9.08	5.68	1.28	1.30	1.25	1.16	1.26	1.26	1.25
900	50.50	0.975	0.1076694	10.21	6.93	1.20	1.57	1.41	1.31	1.46	1.43	1.47
1000	49.50	0.875	0.1022347	11.35	8.59	1.13	1.86	1.65	1.52	1.67	1.65	1.67
1100	49.50	0.875	0.1022347	12.48	9.32	1.10	2.10	1.81	1.67	1.83	1.81	1.83
1200	48.00	0.825	0.0992815	13.62	10.24	1.07	2.36	2.03	1.89	2.09	2.01	2.05
1300	47.50	0.800	0.0977517	14.75	11.47	1.03	2.64	2.24	2.07	2.29	2.26	2.30
1500	47.00	0.775	0.0961873	17.02	12.70	1.00	3.14	2.63	2.43	2.68	2.63	2.64
1700	44.50	0.675	0.0894555	19.29	13.90	0.97	3.66	3.20	2.96	3.16	3.10	3.24
2000	27.00	0.225	0.0444655	22.70	50.30	0.45	9.35	7.48	7.02	7.33	7.75	8.02
2200	22.60	0.175	0.0369435	24.96	64.90	0.38	11.97	10.03	9.29	10.55	10.70	10.97
2500	19.50	0.125	0.0282954	28.37	107.00	0.24	19.74	14.88	13.78	16.76	15.60	16.02
3000	.....	.....	.....	34.04	.....	.....	.....	.....	.....	31.26	30.00	30.50

Notes :

Ctr. Pt.= Centre Point of the beam.

Ldg. Pt.= Loading Point on the beam.

Theoretical N.A. Depth(Y_{uc})=51.28 (mm)

Theoretical S.M. of A.(I_{uc})=0.1089399$\times 10^{-4}$ (m^4)

To calculate theoretical deflection values, the observed N.A. Depth values and corresponding Tension Zone Coefficients have been used.

Table A2.2b. (Theoretical and Experimental Deflection of Beam A-1b.)

Load	Observed N.A. Depth	Transformed Section		Moment-Curvature Relationship				Theoretical Deflection		Experimental Deflection		
		Tension Zone Coefficient	2nd Moment of Area	Moment	Curvature	Flexural Rigidity	Deflection Ctr. Pt.	Ctr. pt.	Ldg. Pts.	Ctr. Pt.	Ldg. Pt.1	Ldg. Pt.2
	Y	α	$I_c \times 10^{-4}$	M $\times 10^2$	ϕ $\times 10^{-3}$	$E_eI_e \times 10^5$	y_c	y_c	y_l	y_c	y_{l1}	y_{l2}
(lb)	(mm)		(m^4)	(N.m)	(m^{-1})	($N.m^2$)	(mm)	(mm)	(mm)	(mm)	(mm)	(mm)
0	.....	.....	.....	0.00	.....	....	0.00	0.00	0.00	0.00	0.00	0.00
100	47.00	0.975	0.1091374	1.14	0.83	3.51	0.06	0.15	0.14	0.12	0.14	0.14
200	47.00	0.975	0.1091374	2.27	2.12	1.95	0.21	0.30	0.28	0.35	0.34	0.38
300	47.00	0.975	0.1091374	3.40	2.58	1.77	0.36	0.47	0.43	0.53	0.52	0.55
400	47.00	0.975	0.1091374	4.54	3.25	1.59	0.53	0.62	0.57	0.73	0.71	0.73
500	47.00	0.975	0.1091374	5.67	3.65	1.52	0.69	0.77	0.72	0.99	0.92	0.96
600	46.00	0.925	0.1062094	6.81	4.36	1.41	0.89	0.95	0.88	1.17	1.12	1.15
700	46.00	0.925	0.1062094	7.94	5.38	1.31	1.12	1.11	1.03	1.39	1.32	1.35
800	37.50	0.550	0.0788894	9.08	6.31	1.24	1.35	1.71	1.58	1.60	1.52	1.57
900	37.00	0.550	0.0789252	10.21	7.82	1.16	1.63	1.92	1.78	1.85	1.73	1.71
1000	36.00	0.525	0.0766968	11.35	9.57	1.09	1.92	2.19	2.03	2.10	1.97	2.02
1100	36.00	0.525	0.0766968	12.48	10.21	1.07	2.16	2.42	2.23	....	....	....
1200	35.50	0.500	0.0743357	13.62	11.81	1.02	2.46	2.72	2.51	2.74	2.53	2.65
1300	32.00	0.400	0.0642147	14.75	12.65	1.00	2.72	3.41	3.15	....	....	....
1400	29.50	0.350	0.0586513	15.89	16.20	0.92	3.17	4.02	3.72	3.88	3.55	3.70
1600	23.50	0.200	0.0386921	18.16	26.32	0.77	4.35	6.76	6.11	....	....	....
2000	20.50	0.150	0.0307578	22.70	59.30	0.38	10.94	10.95	10.14	10.40	10.25	10.33
2500	17.50	0.125	0.0265205	28.37	99.66	0.28	18.38	15.87	14.70	15.85	15.01	15.25
3000	.....	.....	.....	34.04	.....	....	.....	....	....	30.85	30.01	30.25

Notes :

Ctr. Pt.= Centre Point of the beam.

Ldg. Pt.= Loading Point on the beam.

Theoretical N.A. Depth(Y_{uc})=47.87 (mm)

Theoretical S.M. of A.(I_{uc})=0.1105414$\times 10^{-4}$ (m^4)

To calculate theoretical deflection values, the observed N.A. Depth values and corresponding Tension Zone Coefficients have been used.

Table A2.2c. (Theoretical and Experimental Deflection of Beam A-2a.)

Load	Observed N.A. Depth	Transformed Section		Moment-Curvature Relationship				Theoretical Deflection		Experimental Deflection		
		Tension Zone Coefficient	2nd Moment of Area	Moment M	Curvature ϕ	Flexural Rigidity	Deflection Ctr. Pt.	Ctr. pt.	Ldg. Pts.	Ctr. Pt.	Ldg. Pt.1	Ldg. Pt.2
(lb)	Y (mm)	α	$I_c \times 10^{-4}$ (m^4)	$\times 10^2$ (N.m)	$\times 10^{-3}$ (m^{-1})	$E_eI_e \times 10^5$ $(N.m^2)$	y_c (mm)	y_c (mm)	y_l (mm)	y_c (mm)	y_{l1} (mm)	y_{l2} (mm)
0	.....	.....	.....	0.00	.....	.....	0.00	0.00	0.00	0.00	0.00	0.00
100	.....	.....	.....	1.14	.....	.....	.....	0.09	0.07	0.04	0.08	0.06
200	61.50	1.100	0.10249550	2.27	1.48	2.45	0.17	0.25	0.23	0.17	0.26	0.25
300	61.50	1.100	0.10249550	3.40	2.48	2.03	0.31	0.41	0.37	0.44	0.48	0.47
400	61.50	1.100	0.10249550	4.54	3.65	1.81	0.46	0.58	0.53	0.66	0.68	0.67
500	61.50	1.100	0.10249550	5.67	4.92	1.69	0.62	0.74	0.68	0.86	0.87	0.84
600	61.50	1.100	0.10249550	6.81	6.19	1.60	0.78	0.91	0.84	1.05	1.06	1.03
700	61.50	1.100	0.10249550	7.94	7.35	1.55	0.95	1.07	0.99	1.28	1.27	1.25
800	61.50	1.100	0.10249550	9.08	8.56	1.50	1.12	1.23	1.13	1.50	1.48	1.47
900	61.50	1.100	0.10249550	10.21	9.83	1.45	1.30	1.40	1.29	1.71	1.65	1.65
1000	61.50	1.100	0.10249550	11.35	10.63	1.43	1.46	1.57	1.44	1.93	1.88	1.86
1100	.....	.....	.....	12.48	.....	.....	.....	1.73	1.60	2.14	2.07	2.08
1200	61.50	1.100	0.10249550	13.62	13.07	1.37	1.84	1.89	1.75	2.37	2.30	2.29
1300	.....	.....	.....	14.75	.....	.....	.....	2.06	1.90	2.59	2.50	2.48
1400	61.00	1.050	0.10109960	15.89	15.14	1.32	2.23	2.25	2.08	2.81	2.70	2.70
1500	61.00	1.050	0.10109960	17.02	16.61	1.29	2.44	2.50	2.32	3.06	2.92	2.93
1600	60.50	1.025	0.10041471	18.16	17.18	1.28	2.63	2.69	2.49	3.28	3.13	3.13
1700	.....	.....	.....	19.29	.....	.....	.....	2.85	2.64	3.51	3.35	3.35
1800	60.50	1.025	0.10041471	20.43	19.87	1.22	3.08	3.02	2.80	3.74	3.55	3.56
1900	.....	.....	.....	21.56	.....	.....	.....	3.19	2.95	3.97	3.78	3.80
2000	60.50	1.025	0.10041471	22.70	22.52	1.18	3.56	3.35	3.11	4.24	4.04	4.05
2200	60.33	1.000	0.09965701	24.96	25.54	1.13	4.09	3.72	3.44	4.97	4.70	4.72
2500	58.67	0.875	0.09568603	28.37	31.50	1.04	5.04	4.40	4.07	5.63	5.44	5.45
2800	52.00	0.525	0.08097633	31.77	41.06	0.91	6.42	5.82	5.39	6.84	6.61	6.66
3000	.....	.....	.....	34.04	.....	.....	.....	.....	.....	7.41	7.33	7.38
3200	48.39	0.400	0.07375778	36.31	52.56	0.79	8.50	7.31	6.77	8.60	8.09	8.17
3500	.....	.....	.....	39.72	.....	.....	.....	.....	.....	.....	.....	.....
3600	47.00	0.350	0.07042600	40.85	65.09	0.68	11.08	8.61	7.97	9.90	9.36	9.42
4000	45.06	0.300	0.06679638	45.39	77.21	0.60	13.95	10.08	9.34	11.38	10.71	11.41
4400	43.39	0.250	0.06280810	49.93	94.99	0.53	17.41	11.80	10.93	13.06	12.38	12.41
4800	36.17	0.100	0.04796874	54.47	115.99	0.51	19.66	16.85	15.61	18.63	17.05	17.15
5200	32.56	0.025	0.03839706	59.01	142.16	0.41	26.48	22.80	21.12	.....	.....	.....

Notes :

Ctr. Pt.= Centre Point of the beam.

Ldg. Pt.= Loading Point on the beam.

Theoretical N.A. Depth(Y_{uc})=60.36 (mm)

Theoretical S.M. of A.(I_{uc})=0.0997412×10^{-4} (m^4)

To calculate theoretical deflection values, the observed N.A. Depth values and corresponding Tension Zone Coefficients have been used.

Table A2.2d. (Theoretical and Experimental Deflection of Beam A-2b.)

Load	Observed N.A. Depth	Transformed Section		Moment-Curvature Relationship				Theoretical Deflection		Experimental Deflection		
		Tension Zone Coefficient	2nd Moment of Area	Moment	Curvature	Flexural Rigidity	Deflection Ctr. Pt.	Ctr. pt.	Ldg. Pts.	Ctr. Pt.	Ldg. Pt.1	Ldg. Pt.2
		α	$I_c \times 10^{-4}$	M	ϕ	$E_eI_e \times 10^5$	y_c	y_c	y_l	y_c	y_{l1}	y_{l2}
(lb)	Y (mm)		(m^4)	$\times 10^2$ (N.m)	$\times 10^{-3}$ (m^{-1})	$(N.m^2)$	(mm)	(mm)	(mm)	(mm)	(mm)	(mm)
0	.....	.....	.....	0.00	.....	.....	0.00	0.00	0.00	0.00	0.00	0.00
100	49.00	0.925	0.11498500	1.14	0.01	150.73	0.00	0.00	0.00	0.00	0.00	0.00
200	49.00	0.925	0.11498500	2.27	0.85	3.21	0.13	0.15	0.13	0.05	0.09	0.09
300	49.00	0.925	0.11498500	3.40	1.68	2.33	0.27	0.29	0.27	0.20	0.24	0.23
400	49.00	0.925	0.11498500	4.54	2.10	2.14	0.39	0.45	0.40	0.40	0.40	0.40
500	49.00	0.925	0.11498500	5.67	2.38	2.05	0.51	0.59	0.54	0.58	0.57	0.57
600	49.00	0.925	0.11498500	6.81	3.14	1.89	0.67	0.74	0.68	0.72	0.72	0.71
700	49.00	0.925	0.11498500	7.94	4.15	1.76	0.83	0.88	0.82	0.92	0.87	0.89
800	49.00	0.925	0.11498500	9.08	5.14	1.67	1.00	1.03	0.95	1.08	1.03	1.03
900	49.00	0.925	0.11498500	10.21	5.71	1.63	1.16	1.17	1.09	1.23	1.19	1.18
1000	49.00	0.925	0.11498500	11.35	6.69	1.58	1.33	1.32	1.22	1.38	1.34	1.33
1100	49.00	0.925	0.11498500	12.48	7.57	1.54	1.50	1.47	1.36	1.56	1.49	1.48
1200	48.75	0.900	0.11358920	13.62	8.31	1.51	1.67	1.64	1.51	1.78	1.67	1.66
1300	48.75	0.900	0.11358920	14.75	9.05	1.48	1.84	1.78	1.65	1.93	1.82	1.81
1400	48.50	0.875	0.11216730	15.89	9.98	1.45	2.02	1.95	1.81	2.11	1.98	1.98
1500	48.50	0.875	0.11216730	17.02	11.55	1.40	2.24	2.10	1.94	2.32	2.19	2.17
1600	48.50	0.875	0.11216730	18.16	12.67	1.38	2.44	2.40	2.23	2.49	2.35	2.33
1700	48.50	0.875	0.11216730	19.29	13.18	1.36	2.61	2.55	2.37	2.71	2.56	2.63
1800	43.40	0.600	0.09433328	20.43	14.13	1.34	2.81	3.21	2.98	3.51	3.32	3.20
2000	38.50	0.400	0.07774137	22.70	17.10	1.28	3.28	4.33	4.01	4.62	4.35	4.34
2500	32.50	0.200	0.05641195	28.37	24.49	1.14	4.57	7.46	6.91	7.78	7.38	6.42
3000	29.50	0.125	0.04660659	34.04	36.75	0.97	6.49	10.84	10.04	11.10	10.40	10.38
3500	28.50	0.100	0.04306998	39.71	50.89	0.81	9.10	13.68	12.67	14.08	13.01	13.04
4000	26.75	0.075	0.03923901	45.39	87.90	0.55	16.72	17.17	15.90	17.58	16.34	16.25
4800	22.00	0.000	0.02674570	54.47	110.00	0.51	19.74	30.22	28.00	.....	.....	.....

Notes :

Ctr. Pt.= Centre Point of the beam.

Ldg. Pt.= Loading Point on the beam.

Theoretical N.A. Depth(Y_{uc})=50.40 (mm)

Theoretical S.M. of A.(I_{uc})=0.1189193$\times 10^{-4}$ (m^4)

To calculate theoretical deflection values, the observed N.A. Depth values and corresponding Tension Zone Coefficients have been used.

Table A2.2e. (Theoretical and Experimental Deflection of Beam A-3a.)

Load	Observed N.A. Depth	Transformed Section		Moment-Curvature Relationship				Theoretical Deflection		Experimental Deflection		
		Tension Zone Coefficient	2nd Moment of Area	Moment	Curvature	Flexural Rigidity	Deflection Ctr. Pt.	Ctr. pt.	Ldg. Pts.	Ctr. Pt.	Ldg. Pt.1	Ldg. Pt.2
	Y	α	$I_c \times 10^{-4}$	M $\times 10^2$	ϕ $\times 10^{-3}$	$E_c I_c \times 10^5$	y_c	y_c	y_l	y_c	y_{l1}	y_{l2}
(lb)	(mm)		(m^4)	(N.m)	(m^{-1})	($N.m^2$)	(mm)	(mm)	(mm)	(mm)	(mm)	(mm)
0	.....	.....	.....	0.00	0.00	0.00	0.00	0.00	0.00	0.00	0.00	0.00
300	52.50	0.925	0.12316760	3.40	1.43	2.83	0.22	0.21	0.18	0.12	0.12	0.12
400	52.50	0.925	0.12316760	4.54	1.57	2.72	0.31	0.34	0.31	0.23	0.22	0.23
500	52.50	0.925	0.12316760	5.67	2.13	2.44	0.43	0.48	0.44	0.36	0.34	0.35
600	52.50	0.925	0.12316760	6.80	3.12	2.18	0.58	0.62	0.56	0.50	0.47	0.48
700	52.50	0.925	0.12316760	7.94	3.83	2.07	0.71	0.75	0.69	0.63	0.59	0.60
800	52.50	0.925	0.12316760	9.08	4.54	1.99	0.84	0.89	0.82	0.75	0.72	0.73
900	52.50	0.925	0.12316760	10.21	5.53	1.91	0.99	1.03	0.94	0.94	0.84	0.85
1000	52.50	0.925	0.12316760	11.35	6.02	1.88	1.12	1.16	1.07	1.05	0.96	0.96
1100	52.50	0.925	0.12316760	12.48	6.30	1.86	1.24	1.30	1.20	1.22	1.11	1.11
1500	50.27	0.825	0.11853030	17.02	9.98	1.70	1.85	2.13	1.97	1.79	1.67	1.68
2000	46.10	0.475	0.09828492	22.70	14.23	1.58	2.65	3.43	3.17	3.07	2.86	2.87
2500	44.15	0.375	0.09129621	28.37	20.19	1.45	3.62	4.61	4.27	4.23	3.94	3.96
3000	42.44	0.300	0.08556978	34.04	27.04	1.32	4.75	5.90	5.47	5.79	5.44	5.45
4000	41.92	0.250	0.08157432	45.38	41.25	1.11	7.53	8.26	7.65	8.68	8.12	8.17
5000	41.15	0.225	0.07942861	56.73	58.12	0.92	11.39	10.60	9.81	11.66	10.94	10.94
6000	38.80	0.125	0.07035926	68.08	81.08	0.74	16.95	14.36	13.30	.....	.....	.....

Notes :

Ctr. Pt.= Centre Point of the beam.

Ldg. Pt.= Loading Point on the beam.

Theoretical N.A. Depth(Y_{uc})=53.29 (mm)

Theoretical S.M. of A.(I_{uc})=0.1265452$\times 10^{-4}$ (m^4)

To calculate theoretical deflection values, the observed N.A. Depth values and corresponding Tension Zone Coefficients have been used.

Table A2.2f. (Theoretical and Experimental Deflection of Beam A-3b.)

Load	Observed N.A. Depth	Transformed Section		Moment-Curvature Relationship				Theoretical Deflection		Experimental Deflection		
		Tension Zone Coefficient	2nd Moment of Area	Moment	Curvature	Flexural Rigidity	Deflection Ctr. Pt.	Ctr. pt.	Ldg. Pts.	Ctr. Pt.	Ldg. Pt.1	Ldg. Pt.2
	Y	α	$I_c \times 10^{-4}$	M $\times 10^2$	ϕ $\times 10^{-3}$	$E_eI_e \times 10^5$	y_c	y_c	y_l	y_c	y_{l1}	y_{l2}
(lb)	(mm)		(m^4)	(N.m)	(m^{-1})	$(N.m^2)$	(mm)	(mm)	(mm)	(mm)	(mm)	(mm)
0	.....	.....	.....	0.00	0.00	0.00	0.00	0.00	0.00	0.00	0.00	0.00
300	54.94	1.125	0.13702410	3.40	0.90	3.51	0.18	0.18	0.16	0.15	0.15	0.13
400	54.94	1.125	0.13702410	4.54	2.06	2.47	0.34	0.31	0.28	0.27	0.27	0.25
500	54.94	1.125	0.13702410	5.67	2.58	2.30	0.46	0.43	0.40	0.39	0.39	0.38
600	54.94	1.125	0.13702410	6.80	2.97	2.21	0.57	0.55	0.51	0.52	0.51	0.50
700	54.94	1.125	0.13702410	7.94	4.13	2.04	0.72	0.68	0.62	0.64	0.63	0.62
800	54.94	1.125	0.13702410	9.08	4.65	1.98	0.85	0.80	0.73	0.78	0.77	0.76
900	54.94	1.125	0.13702410	10.21	5.04	1.95	0.97	0.92	0.85	0.95	0.89	0.89
1000	54.94	1.125	0.13702410	11.35	5.56	1.91	1.10	1.04	1.00	1.08	1.02	1.02
1500	53.93	1.025	0.13302380	17.02	8.85	1.74	1.80	1.71	1.58	1.87	1.75	1.75
2000	49.80	0.700	0.11794391	22.70	13.99	1.54	2.64	2.73	2.52	3.09	2.92	2.91
2500	43.33	0.300	0.09294062	28.37	19.57	1.42	3.58	4.38	4.06	4.32	4.06	4.11
3000	36.79	0.025	0.06883900	34.04	26.75	1.26	4.73	6.16	5.63	5.95	5.48	5.52
4000	31.52	0.000	0.06658404	45.38	43.31	1.03	7.72	9.12	8.37	9.08	8.25	8.19
5000	28.90	0.000	0.06788596	56.73	63.30	0.82	12.01	12.40	11.48	12.04	11.11	11.08
6000	26.50	0.000	0.06976686	68.08	107.15	0.65	19.32	14.49	13.42	14.42	13.19	13.15

Notes :

Ctr. Pt.= Centre Point of the beam.

Ldg. Pt.= Loading Point on the beam.

Theoretical N.A. Depth(Y_{uc})=53.83 (mm)

Theoretical S.M. of A.(I_{uc})=0.1319631$\times 10^{-4}$ (m^4)

To calculate theoretical deflection values, the observed N.A. Depth values and corresponding Tension Zone Coefficients have been used.

Table A2.2g. (Theoretical and Experimental Deflection of Beam B-1a.)

Load	Observed N.A. Depth	Transformed Section		Moment-Curvature Relationship				Theoretical Deflection		Experimental Deflection		
		Tension Zone Coefficient	2nd Moment of Area	Moment M	Curvature ϕ	Flexural Rigidity	Deflection Ctr. Pt.	Ctr. pt.	Ldg. Pts.	Ctr. Pt.	Ldg. Pt.1	Ldg. Pt.2
(lb)	Y (mm)	α	$I_c \times 10^{-4}$ (m^4)	$\times 10^2$ (N.m)	$\times 10^{-3}$ (m^{-1})	$E_eI_e \times 10^5$ ($N.m^2$)	y_c (mm)	y_c (mm)	y_l (mm)	y_c (mm)	y_{l1} (mm)	y_{l2} (mm)
0	.....	.....	.....	0.00	.....	....	0.00	0.00	0.00	0.00	0.00	0.00
100	105.50	1.050	0.3921409	1.13	0.37	0.99	0.02	0.04	0.04	0.02	0.04	0.03
200	105.50	1.050	0.3921409	2.27	0.61	7.98	0.05	0.09	0.08	0.08	0.09	0.08
300	105.50	1.050	0.3921409	3.40	0.98	6.21	0.10	0.13	0.12	0.13	0.14	0.14
400	105.50	1.050	0.3921409	4.54	1.08	5.94	0.14	0.18	0.16	0.21	0.21	0.21
500	105.50	1.050	0.3921409	5.67	1.40	5.32	0.20	0.21	0.20	0.28	0.27	0.28
600	105.50	1.050	0.3921409	6.81	1.94	4.72	0.27	0.25	0.23	0.35	0.33	0.34
700	105.50	1.050	0.3921409	7.94	2.37	4.42	0.33	0.30	0.28	0.41	0.39	0.40
800	105.50	1.050	0.3921409	9.08	2.48	4.36	0.38	0.34	0.32	0.46	0.45	0.45
900	105.50	1.050	0.3921409	10.21	2.97	4.14	0.46	0.39	0.36	0.53	0.51	0.52
1000	105.50	1.050	0.3921409	11.35	3.33	4.01	0.52	0.43	0.40	0.59	0.57	0.57
1200	105.50	1.050	0.3921409	13.62	3.67	3.91	0.64	0.52	0.48	0.70	0.69	0.69
1500	105.50	1.050	0.3921409	17.02	4.23	3.77	0.83	0.64	0.60	0.89	0.85	0.87
2000	103.35	0.950	0.3733615	22.69	6.13	3.43	1.22	0.90	0.83	1.25	1.17	1.19
2500	101.50	0.900	0.3633889	28.37	7.60	3.24	1.62	1.16	1.07	1.60	1.49	1.54
3000	85.00	0.550	0.2784077	34.04	12.58	2.78	2.26	1.82	1.68	2.43	2.22	2.30
3500	71.42	0.350	0.2112798	39.72	20.79	2.23	3.29	2.79	2.59	3.33	3.00	3.13
4000	65.50	0.300	0.1912469	45.39	24.31	2.03	4.12	3.52	3.26	4.10	3.94	4.00
4500	52.40	0.200	0.1450077	51.06	37.62	1.46	6.46	5.23	4.84	5.90	5.57	5.62
5000	47.85	0.175	0.1319998	56.74	49.63	1.13	9.23	6.38	5.91	7.14	6.88	6.89
5500	45.00	0.150	0.1174455	62.41	58.58	1.00	11.47	7.89	7.30	8.61	8.23	8.26
6000	41.50	0.125	0.1020231	68.08	74.04	1.00	12.58	9.90	9.17	10.70	10.33	10.36

Notes :

Ctr. Pt.= Centre Point of the beam.

Ldg. Pt.= Loading Point on the beam.

Theoretical N.A. Depth(Y_{uc})=104.78 (mm)

Theoretical S.M. of A.(I_{uc})=0.3829132$\times 10^{-4}$ (m^4)

To calculate theoretical deflection values, the observed N.A. Depth values and corresponding Tension Zone Coefficients have been used.

Table A2.2h. (Theoretical and Experimental Deflection of Beam B-1b.)

Load	Observed N.A. Depth	Transformed Section		Moment-Curvature Relationship				Theoretical Deflection		Experimental Deflection		
		Tension Zone Coefficient	2nd Moment of Area	Moment	Curvature	Flexural Rigidity	Deflection Ctr. Pt.	Ctr. pt.	Ldg. Pts.	Ctr. Pt.	Ldg. Pt.1	Ldg. Pt.2
	Y	α	$I_c \times 10^{-4}$	M $\times 10^2$	ϕ $\times 10^{-3}$	$E_c I_c \times 10^5$	y_c	y_c	y_l	y_c	y_{l1}	y_{l2}
(lb)	(mm)		(m^4)	(N.m)	(m^{-1})	$(N.m^2)$	(mm)	(mm)	(mm)	(mm)	(mm)	(mm)
0	.....	.....	.....	0.00	.....	.....	0.00	0.00	0.00	0.00	0.00	0.00
100	103.00	1.100	0.4225728	1.13	0.12	26.85	0.01	0.03	0.03	0.01	0.02	0.01
200	103.00	1.100	0.4225728	2.27	0.37	10.99	0.04	0.09	0.07	0.07	0.03	0.08
300	103.00	1.100	0.4225728	3.40	1.10	5.89	0.11	0.11	0.10	0.13	0.12	0.15
400	103.00	1.100	0.4225728	4.54	1.74	4.90	0.17	0.15	0.13	0.18	0.20	0.20
500	103.00	1.100	0.4225728	5.67	2.10	4.59	0.23	0.19	0.17	0.25	0.26	0.26
600	103.00	1.100	0.4225728	6.81	2.47	4.37	0.29	0.23	0.21	0.31	0.31	0.32
700	103.00	1.100	0.4225728	7.94	2.90	4.17	0.35	0.27	0.25	0.37	0.37	0.38
800	103.00	1.100	0.4225728	9.08	3.01	4.12	0.41	0.31	0.29	0.43	0.43	0.44
900	103.00	1.100	0.4225728	10.21	3.27	4.03	0.47	0.35	0.32	0.50	0.49	0.49
1000	103.00	1.100	0.4225728	11.35	3.32	4.01	0.52	0.39	0.36	0.56	0.54	0.55
1200	103.00	1.100	0.4225728	13.62	3.75	3.89	0.65	0.47	0.43	.....	.....	.....
1500	103.00	1.100	0.4225728	17.02	4.68	3.67	0.86	0.59	0.54	0.86	0.79	0.85
2000	102.00	1.075	0.4177919	22.69	5.78	3.48	1.20	0.78	0.74	1.20	1.11	1.17
2500	97.50	0.925	0.3870247	28.37	7.43	3.26	1.61	1.09	1.01	1.60	1.47	1.56
3000	77.25	0.475	0.2646074	34.04	13.25	2.73	2.30	1.91	1.77	2.46	2.29	2.35
3500	69.00	0.375	0.2276042	39.72	17.71	2.41	3.04	2.59	2.40	3.28	2.99	3.13
4000	61.50	0.300	0.1961221	45.39	24.47	2.02	4.14	3.44	3.18	4.11	3.87	3.99
4500	52.00	0.200	0.1467606	51.06	36.51	1.50	6.29	5.16	4.78	5.73	5.57	5.60
5000	49.00	0.175	0.1327932	56.74	45.59	1.22	8.55	6.34	5.87	7.05	6.88	6.92
5500	45.00	0.150	0.1180208	62.41	57.32	1.02	11.32	7.85	7.27	8.48	8.31	8.36
6000	40.10	0.125	0.1023426	68.08	72.98	0.99	12.69	9.87	9.14	10.58	10.41	10.36

Notes :

Ctr. Pt.= Centre Point of the beam.

Ldg. Pt.= Loading Point on the beam.

Theoretical N.A. Depth(Y_{uc})=100.00 (mm)

Theoretical S.M. of A.(I_{uc})=0.4028642×10^{-4} (m^4)

To calculate theoretical deflection values, the observed N.A. Depth values and corresponding Tension Zone Coefficients have been used.

Table A2.2i. (Theoretical and Experimental Deflection of Beam B-2a.)

Load	Observed N.A. Depth Y	Transformed Section		Moment-Curvature Relationship				Theoretical Deflection		Experimental Deflection		
		Tension Zone Coefficient	2nd Moment of Area	Moment M	Curvature ϕ	Flexural Rigidity	Deflection Ctr. Pt.	Ctr. pt.	Ldg. Pts.	Ctr. Pt.	Ldg. Pt.1	Ldg. Pt.2
(lb)	(mm)	α	$I_c \times 10^{-4}$ (m^4)	$\times 10^2$ (N.m)	$\times 10^{-3}$ (m^{-1})	$E_e I_e \times 10^5$ ($N.m^2$)	y_c (mm)	y_c (mm)	y_l (mm)	y_c (mm)	y_{l1} (mm)	y_{l2} (mm)
0	.....	.....	.....	0.00	.....	.....	0.00	0.00	0.00	0.00	0.00	0.00
100	110.00	0.825	0.4420435	1.14	.....	.....	.....	0.02	0.01	0.00	0.01	0.00
200	110.00	0.825	0.4420435	2.27	0.22	19.84	0.02	0.05	0.05	0.05	0.03	0.03
300	110.00	0.825	0.4420435	3.40	.....	.....	.....	0.09	0.08	0.10	0.09	0.07
400	110.00	0.825	0.4420435	4.54	0.49	12.59	0.07	0.13	0.12	0.13	0.13	0.12
500	110.00	0.825	0.4420435	5.67	.....	.....	.....	0.17	0.16	0.16	0.15	0.14
600	110.00	0.825	0.4420435	6.81	1.03	9.43	0.13	0.21	0.19	0.20	0.18	0.18
700	110.00	0.825	0.4420435	7.94	.....	.....	.....	0.25	0.23	0.24	0.22	0.23
800	110.00	0.825	0.4420435	9.08	1.36	8.70	0.19	0.28	0.26	0.28	0.26	0.27
900	110.00	0.825	0.4420435	10.21	1.58	8.37	0.23	0.32	0.30	0.33	0.31	0.30
1000	110.00	0.825	0.4420435	11.35	1.69	8.23	0.25	0.36	0.33	0.37	0.35	0.33
1500	110.00	0.825	0.4420435	17.02	2.67	7.44	0.42	0.55	0.51	0.55	0.52	0.53
2000	110.00	0.825	0.4420435	22.70	3.53	7.04	0.59	0.75	0.68	0.72	0.70	0.69
2500	107.50	0.750	0.4263859	28.37	4.63	6.67	0.78	0.99	0.91	0.99	0.95	0.97
3000	107.50	0.750	0.4263859	34.04	6.39	6.23	1.01	1.18	1.10	1.18	1.11	1.12
3500	94.00	0.400	0.3360995	39.72	8.17	5.87	1.25	1.76	1.62	1.70	1.61	1.62
4000	83.50	0.225	0.2745988	45.39	9.81	5.57	1.50	2.45	2.27	2.43	2.34	2.33
4500	81.00	0.200	0.2642823	51.06	11.71	5.26	1.79	2.86	2.66	2.91	2.88	2.90
5000	78.00	0.175	0.2535156	56.74	13.70	4.96	2.11	3.32	3.07	3.34	3.35	3.32
5500	77.00	0.150	0.2425658	62.41	16.04	4.64	2.48	3.86	3.53	3.92	3.87	3.89
6000	75.00	0.125	0.2309882	68.09	18.54	4.32	2.91	4.38	4.05	4.27	4.12	4.15
6500	74.00	0.125	0.2307943	73.76	21.40	3.98	3.42	4.75	4.39	4.64	4.50	4.56
7000	72.50	0.100	0.2187494	79.43	23.87	3.71	3.95	5.39	4.99	5.28	5.19	5.15
7500	72.00	0.100	0.2186392	85.11	26.73	3.43	4.58	5.78	5.35	5.96	5.90	5.88
8000	68.00	0.075	0.2055469	90.78	30.96	3.06	5.47	6.55	6.07	6.70	6.52	6.58
8500	64.00	0.000	0.1638356	96.45	37.32	2.62	6.80	8.74	8.09	7.50	7.41	7.36
9000	61.00	0.000	0.1625481	102.13	44.51	2.27	8.31	9.32	8.63	8.40	8.26	8.28
9500	36.10	0.000	0.1746605	107.80	54.25	2.05	9.71	9.16	8.49	.....	.....	.....

Notes :

Ctr. Pt.= Centre Point of the beam.

Ldg. Pt.= Loading Point on the beam.

Theoretical N.A. Depth(Y_{uc})=114.30 (mm)

Theoretical S.M. of A.(I_{uc})=0.4750926$\times 10^{-4}$ (m^4)

To calculate theoretical deflection values, the observed N.A. Depth values and corresponding Tension Zone Coefficients have been used.

Table A2.2j. (Theoretical and Experimental Deflection of Beam B-2b.)

Load	Observed N.A. Depth	Transformed Section		Moment-Curvature Relationship				Theoretical Deflection		Experimental Deflection		
		Tension Zone Coefficient	2nd Moment of Area	Moment	Curvature	Flexural Rigidity	Deflection Ctr. Pt.	Ctr. pt.	Ldg. Pts.	Ctr. Pt.	Ldg. Pt.1	Ldg. Pt.2
	Y	α	$I_c \times 10^{-4}$	M	ϕ	E_eI_e	y_c	y_c	y_l	y_c	y_{l1}	y_{l2}
(lb)	(mm)		(m^4)	$\times 10^2$ (N.m)	$\times 10^{-3}$ (m^{-1})	$\times 10^5$ $(N.m^2)$	(mm)	(mm)	(mm)	(mm)	(mm)	(mm)
0	.....	.....	.....	0.00	.....	....	0.00	0.00	0.00	0.00	0.00	0.00
100	110.65	1.050	0.4920236	1.14	.....	.....	.....	0.02	0.01	0.00	0.00	0.00
200	110.65	1.050	0.4920236	2.27	0.39	14.12	0.03	0.05	0.05	0.02	0.02	0.02
300	110.65	1.050	0.4920236	3.40	.....	.....	.....	0.09	0.08	0.07	0.06	0.07
400	110.65	1.050	0.4920236	4.54	0.62	11.34	0.07	0.12	0.12	0.11	0.11	0.11
500	110.65	1.050	0.4920236	5.67	.....	.....	.....	0.16	0.14	0.14	0.16	0.15
600	110.65	1.050	0.4920236	6.81	0.90	9.85	0.13	0.18	0.17	0.18	0.20	0.19
700	110.65	1.050	0.4920236	7.94	.....	.....	.....	0.22	0.20	0.22	0.24	0.23
800	110.65	1.050	0.4920236	9.08	1.34	8.73	0.19	0.25	0.23	0.27	0.28	0.27
900	110.65	1.050	0.4920236	10.21	1.54	8.42	0.22	0.29	0.26	0.31	0.32	0.31
1000	110.65	1.050	0.4920236	11.35	1.65	8.28	0.25	0.32	0.30	0.35	0.35	0.35
1500	110.65	1.050	0.4920236	17.02	2.45	7.58	0.41	0.50	0.46	0.54	0.53	0.53
2000	110.65	1.050	0.4920236	22.70	3.35	7.12	0.59	0.66	0.61	0.74	0.70	0.72
2500	110.65	1.050	0.4920236	28.37	4.30	6.77	0.77	0.86	0.80	0.97	0.91	0.91
3000	110.65	1.050	0.4920236	34.04	5.14	6.53	0.96	1.03	0.95	1.24	1.13	1.12
3500	109.25	0.975	0.4781269	39.72	5.71	6.39	1.15	1.23	1.14	1.43	1.32	1.29
4000	90.24	0.400	0.3383063	45.39	7.41	6.02	1.39	1.99	1.85	1.91	1.75	1.74
4500	89.00	0.375	0.3301857	51.06	8.87	5.74	1.64	2.29	2.13	2.21	2.02	2.02
5000	87.50	0.350	0.3217627	56.74	10.75	5.42	1.93	2.61	2.43	2.47	2.27	2.27
5500	84.75	0.300	0.3041766	62.41	12.40	5.16	2.23	3.22	2.82	3.01	2.81	2.79
6000	83.00	0.275	0.2948588	68.09	14.57	4.84	2.60	5.10	4.72	3.41	3.20	3.18
6500	80.10	0.225	0.2754106	73.76	17.13	4.50	3.03	5.71	5.28	4.01	4.00	3.96
7000	77.00	0.175	0.2544974	79.43	19.68	4.18	3.51	6.34	5.87	4.66	4.50	4.44
7500	76.40	0.162	0.2488951	85.11	22.65	3.84	4.09	6.83	6.33	5.12	5.02	4.98
8000	76.00	0.150	0.2437150	90.78	25.55	3.54	4.73	7.31	6.77	5.85	5.60	5.52
8500	70.60	0.075	0.2076497	96.45	30.27	3.12	5.71	8.12	7.52	6.42	6.20	6.11
9000	66.50	0.050	0.1932330	102.13	40.51	2.44	7.72	8.81	8.16	7.20	6.96	6.91
9500	60.50	0.000	0.1636306	107.80	54.25	2.05	9.71	9.53	8.83	.....	.....	.....

Notes :

Ctr. Pt.= Centre Point of the beam.

Ldg. Pt.= Loading Point on the beam.

Theoretical N.A. Depth(Y_{uc})=110.20 (mm)

Theoretical S.M. of A.(I_{uc})=0.4827139$\times 10^{-4}$ (m^4)

To calculate theoretical deflection values, the observed N.A. Depth values and corresponding Tension Zone Coefficients have been used.

Table A2.2k. (Theoretical and Experimental Deflection of Beam B-3a.)

Load	Observed N.A. Depth	Transformed Section		Moment-Curvature Relationship				Theoretical Deflection		Experimental Deflection		
		Tension Zone Coefficient	2nd Moment of Area	Moment	Curvature	Flexural Rigidity	Deflection Ctr. Pt.	Ctr. pt.	Ldg. Pts.	Ctr. Pt.	Ldg. Pt.1	Ldg. Pt.2
(lb)	Y (mm)	α	$I_c \times 10^{-4}$ (m^4)	M $\times 10^2$ (N.m)	ϕ $\times 10^{-3}$ (m^{-1})	$E_eI_e \times 10^5$ ($N.m^2$)	y_c (mm)	y_c (mm)	y_l (mm)	y_c (mm)	y_{l1} (mm)	y_{l2} (mm)
0	.....	.....	.....	0.00	.....	.....	0.00	0.00	0.00	0.00	0.00	0.00
200	123.70	1.250	0.6118152	2.27	0.14	26.67	0.02	0.03	0.03	0.01	0.03	0.02
300	.....	.....	.....	3.40	.....	.....	....	0.06	0.05	0.05	0.06	0.05
400	123.70	1.250	0.6118152	4.54	0.33	15.30	0.06	0.08	0.08	0.09	0.10	0.09
500	.....	.....	.....	5.67	.....	.....	....	0.11	0.11	....	....	....
600	123.70	1.250	0.6118152	6.81	0.66	11.08	0.11	0.14	0.13	0.14	0.14	0.13
700	.....	.....	.....	7.94	.....	.....	....	0.17	0.16	....	....	....
800	123.70	1.250	0.6118152	9.08	0.98	9.68	0.17	0.20	0.19	0.20	0.19	0.18
900	.....	.....	.....	10.21	.....	.....	....	0.22	0.21	0.24	0.23	0.22
1000	123.70	1.250	0.6118152	11.35	1.30	8.95	0.23	0.24	0.23	0.28	0.28	0.26
1500	123.70	1.250	0.6118152	17.02	1.96	8.17	0.38	0.38	0.36	0.33	0.32	0.31
2000	123.70	1.250	0.6118152	22.69	2.84	7.64	0.55	0.52	0.49	0.37	0.36	0.35
2500	123.00	1.225	0.6085075	28.37	3.49	7.39	0.71	0.66	0.62	0.53	0.52	0.52
3000	123.00	1.225	0.6085075	34.04	4.24	7.18	0.88	0.83	0.77	0.71	0.69	0.70
4000	123.00	1.225	0.6085075	45.39	6.15	6.78	1.23	1.11	1.02	0.89	0.87	0.87
5000	120.10	1.050	0.5832519	56.74	8.52	6.43	1.63	1.45	1.33	1.09	1.07	1.07
6000	116.20	0.850	0.5509564	68.08	10.36	6.20	2.08	1.83	1.70	1.55	1.49	1.49
7000	112.65	0.700	0.5237755	79.43	12.89	5.91	2.48	2.25	2.09	2.09	1.99	2.02
8000	109.50	0.575	0.4987273	90.78	14.92	5.71	2.93	2.70	2.50	2.67	2.53	2.54
9000	108.70	0.525	0.4880642	102.13	18.16	5.40	3.49	3.11	2.88	3.12	2.96	2.97
10000	108.10	0.500	0.4825664	113.47	20.99	5.16	4.06	3.49	3.23	3.71	3.49	3.53
11000	106.70	0.475	0.4768367	124.82	24.50	4.87	4.72	3.88	3.60	5.50	5.10	5.17
12000	106.10	0.450	0.4710897	136.17	28.88	4.55	5.52	4.29	3.97	6.01	5.62	5.70
13000	105.20	0.425	0.4651838	147.52	32.79	4.29	6.34	4.70	4.36	6.62	6.11	6.19
15000	86.90	0.000	0.3382137	170.21	56.88	3.22	9.75	7.47	6.91	....	....	....

Notes :

Ctr. Pt.= Centre Point of the beam.

Ldg. Pt.= Loading Point on the beam.

Theoretical N.A. Depth(Y_{uc})=119.56 (mm)

Theoretical S.M. of A.(I_{uc})=0.5754929$\times 10^{-4}$ (m^4)

To calculate theoretical deflection values, the observed N.A. Depth values and corresponding Tension Zone Coefficients have been used.

Table A2.2*l*. (Theoretical amd Experimemtal Deflection of Beam B-3b.)

Load	Observed N.A. Depth	Transformed Section		Moment-Curvature Relationship				Theoretical Deflection		Experimental Deflection		
		Tension Zone Coefficient	2nd Moment of Area	Moment	Curvature	Flexural Rigidity	Deflection Ctr. Pt.	Ctr. pt.	Ldg. Pts.	Ctr. Pt.	Ldg. Pt.1	Ldg. Pt.2
		α	$I_c \times 10^{-4}$	$M \times 10^2$	$\phi \times 10^{-3}$	$E_cI_c \times 10^5$	y_c	y_c	y_l	y_c	y_{l1}	y_{l2}
(lb)	Y (mm)		(m^4)	(N.m)	(m^{-1})	$(N.m^2)$	(mm)	(mm)	(mm)	(mm)	(mm)	(mm)
0	.....	.....	.....	0.00	.....	.....	0.00	0.00	0.00	0.00	0.00	0.00
200	123.35	0.950	0.5638793	2.27	0.19	21.47	0.02	0.03	0.04	0.00	0.00	0.01
300	.....	.....	.....	3.40	.....	.....	.....	0.06	0.06	0.06	0.08	0.07
400	123.35	0.950	0.5638793	4.54	0.50	12.44	0.07	0.09	0.09	0.07	0.09	0.09
500	.....	.....	.....	5.67	.....	.....	.....	0.12	0.12	0.10	0.13	0.14
600	123.35	0.950	0.5638793	6.81	0.73	10.67	0.12	0.15	0.15	0.16	0.18	0.18
700	.....	.....	.....	7.94	.....	.....	.....	0.18	0.17	0.21	0.23	0.25
800	123.35	0.950	0.5638793	9.08	1.05	9.49	0.18	0.21	0.20	0.25	0.27	0.30
900	.....	.....	.....	10.21	.....	.....	.....	0.24	0.23	0.31	0.32	0.36
1000	123.35	0.950	0.5638793	11.35	1.50	8.65	0.24	0.27	0.26	0.33	0.36	0.40
1500	123.35	0.950	0.5638793	17.02	2.05	8.10	0.39	0.42	0.39	0.47	0.50	0.53
2000	123.35	0.950	0.5638793	22.69	2.74	7.69	0.55	0.57	0.53	0.72	0.70	0.76
2500	123.35	0.950	0.5638793	28.37	3.64	7.35	0.71	0.71	0.67	0.96	0.92	1.00
3000	123.35	0.950	0.5638793	34.04	4.55	7.10	0.88	0.89	0.83	1.16	1.11	1.21
4000	123.30	0.950	0.5638793	45.39	6.31	6.76	1.24	1.19	1.10	1.57	1.50	1.59
5000	117.68	0.700	0.5220568	56.74	8.83	6.39	1.64	1.61	1.50	2.12	2.02	2.13
6000	111.71	0.475	0.4766047	68.08	11.50	6.07	2.07	2.12	1.96	2.69	2.56	2.64
7000	108.97	0.400	0.4593074	79.43	14.23	5.78	2.54	2.57	2.38	3.25	3.09	3.19
8000	106.98	0.325	0.4407300	90.78	16.83	5.52	3.03	3.06	2.83	3.84	3.62	3.75
9000	105.49	0.300	0.4341311	102.13	19.60	5.28	3.57	3.49	3.23	4.11	3.77	3.81
10000	103.99	0.250	0.4205691	113.47	22.83	5.01	4.18	4.00	3.71	4.42	4.15	4.30
11000	103.00	0.225	0.4134771	124.82	25.87	4.77	4.71	4.48	4.15	5.08	4.77	4.93
12000	102.58	0.200	0.4063456	136.17	30.85	4.42	5.68	4.97	4.60	5.53	5.14	5.22
14000	100.26	0.175	0.3985163	158.86	40.48	3.86	7.60	5.92	5.48	6.69	6.11	6.18
16000	85.75	0.000	0.3379523	181.56	57.52	3.20	10.45	7.97	7.38	.....	.....	.....

Notes :

Ctr. Pt.= Centre Point of the beam.

Ldg. Pt.= Loading Point on the beam.

Theoretical N.A. Depth(Y_{uc})=124.94 (mm)

Theoretical S.M. of A.(I_{uc})=0.5712551×10^{-4} (m^4)

To calculate theoretical deflection values, the observed N.A. Depth values and corresponding Tension Zone Coefficients have been used.

Appendix (A3)

A3. Theoretical Analysis of the Bridge Deck Panels

A3.1. Introduction

The bridge-deck panels tested in this work were considered as structural members which are subjected to loads acting transversely to the longitudinal axis. In the theoretical analysis, the stresses and strains associated with the bending moments are considered. Since the panels were subjected to pure bending, hence longitudinally the panel fibres were in uniaxial stress (i.e. tension or compression).

The stresses σ_x acting normal to the cross-section of the panels can therefore be obtained from the normal strains ϵ_x. As the material of the panels is linear elastic (as explained in Chapter 5), hence Hooke's law for uniaxial stress is valid, so that $\sigma = E\epsilon$.

In the analysis of the bridge-deck panels, using the elastic theory, the geometrical properties, normal stresses and strains of the equivalent transformed sections were determined with respect to steel reinforcement.

From the tests it was determined that the Phenolic Concrete/steel bond remains viable up to steel either yielding in the lightly reinforced sections or slipping in the heavily reinforced sections and at the same time the Phenolic Concrete/fibre glass mat remained intact throughout the test. Therefore, the equivalent transformed section method can be used on the basis of an uncracked composite section in calculating the appropriate normal stresses and strains. This, however, indicates a difference between Polymer Concrete in general from ordinary reinforced concrete sections, since in the reinforced concrete section the equivalent transformed section

method can not be used in the same manner as for Polymer Concrete because of earlier cracking of concrete in tension.

The theoretical analysis of the bridge-deck panels is based on the following general assumptions:

1. The panels are subject to pure bending and that they are longitudinally in uniaxial stress.
2. The cross-sections that are plane before bending remain plane after bending.
3. Full composite action exists between the Phenolic Concrete and the laminated fibre glass mat throughout.
4. The bond between the Phenolic Concrete and the steel bars remains viable up to steel yielding.
5. The section properties assume an uncracked section.
6. The material of the composite section is linear elastic so that Hooke's law is valid such that $\sigma = E\epsilon$.
7. In the internally reinforced sections, the tension and compression elastic moduli are the same for Phenolic Concrete and also for the steel, but with $E_s > E_p$, the steel modulus remaining throughout such that $E_s = m \times E_p$.

A3.2. Normal Stresses

From the bending theory, when a beam is subjected to pure bending, the bending deflections occur in the plane of bending. Thus, the deflection curve of the beam is a plane curve lying in the plane of bending. As defined in calculus and analytic geometry, the curvature k is the reciprocal of the radius of curvature R. From deformation of a beam in pure bending produced by couples M_o as a result of positive bending moment, (as in the case of the tested panels), it is given that;

$$\epsilon_x = \frac{-Y}{R} = -kY \tag{3.1}$$

This equation shows that longitudinal strains in the element are propotional to the curvature and that they vary linearly with the distance Y from the neutral surface. We can use Hooke's law for uniaxial stress and obtain,

$$\sigma_x = E\epsilon_x = -EkY \tag{3.2}$$

This suggests that the normal stresses acting on the cross-section vary linearly with distance Y from the neutral surface. This type of stress distribution is shown in Figure A3.1a, where the stresses are negative (compression) above the neutral surface and positive (tension) below the surface when positive bending moment is introduced.

In the case of the internally reinforced tested panels, the sections are considered as composite sections and therefore the transformed-section method is used in determining the normal stresses. The Phenolic Concrete of the section is transformed into the equivalent steel area, using the elastic theory;

$$m = \frac{E_s}{E_p}$$

In the transformed panel sections, the normal stresses σ_x at any distance Y from the neutral surface are given by the following equations:

$$\sigma_{x_s} = -E_s kY \tag{3.3}$$

$$\sigma_{x_p} = -E_p kY = -E_s \times \frac{1}{m} \times kY \tag{3.4}$$

The position of the neutral axis can be found by using the condition that the resultant axial force acting on the cross-section is zero; therefore

$$\int_s \sigma_{x_s} dA + \int_p \sigma_{x_p} dA = 0 \tag{3.5}$$

where,

dA is element of area.

σ_{x_s} is the normal stresses relating to the steel bars.

σ_{x_p} is the normal stresses relating to the Phenolic Concrete matrix.

Substituting Equations 3.3 and 3.4 into Equation 3.5, we get

$$E_s \int_s Y dA + E_p \int_p Y dA = 0 \tag{3.6}$$

We can rewrite Equation 3.6 for the transformed section in the form of:

$$\int_s Y dA + \frac{1}{m} \int_p Y dA = 0 \tag{3.7}$$

This equation shows that from the first moment of area the resultant centroid or neutral axis position of the transformed panel section may be found in terms of steel modulus.

The only resultant of the normal stresses σ_x acting over the cross-section is the couple M_o which is equal the bending moment M. Therefore, from the equation of statics we can write;

$$M = \int \sigma_x Y dA \tag{3.8}$$

Considering the internally reinforced composite panel section and the corresponding normal stresses, the bending moment capacity of the transformed section can therefore be obtained as follows;

$$M = \int_s \sigma_{x_s} Y dA + \int_p \sigma_{x_p} Y dA \tag{3.9}$$

Substituting Equations 3.3 and 3.4 into above equation,

$$M = -kE_s \int_s Y^2 dA - kE_s \frac{1}{m} \int_p Y^2 dA \tag{3.10}$$

or,

$$M = -k(E_s I_s + E_p I_p) \tag{3.11}$$

This shows that the bending capacity of the transformed section remains unchanged from that of the composite section, as $(E_s I_s + E_p I_p)$ is the flexural rigidity of the internally reinforced composite panel section.

The Equation 3.11 can be expressed as,

$$M = -kE_s(I_s + \frac{1}{m} I_p) \tag{3.12a}$$

in which

$$I_t = I_s + \frac{1}{m} I_p \tag{3.12b}$$

is the second moment of area about the neutral axis of the transformed section.

Equation 3.12a can be rearranged as;

$$k = \frac{-M}{E_s(I_s + \frac{1}{m} I_p)} \tag{3.12c}$$

Substituting Equation 3.3 into above equation will give the normal stresses in the steel over the cross-section of the transformed section as;

$$\sigma_{x_s} = \frac{MY}{(I_s + \frac{1}{m} I_p)} = \frac{MY}{I_t} \tag{3.13}$$

which is the well-known flexure formula for stresses in the transformed section. This equation can be rewritten as;

$$\sigma_{x_s} = \frac{MYE_s}{(E_sI_s + E_pI_p)} \tag{3.14}$$

in which the denominator can be considered to be the flexural rigidity of the reinforced composite panel.

To obtain the normal stresses in the Phenolic Concrete of the panel section, the stresses in the steel of the transformed section (i.e. Equation 3.14) should be divided by the modular ratio m so that,

$$\sigma_{x_p} = \frac{MYE_s}{m(E_sI_s + E_pI_p)} = \frac{MY}{mI_t} \tag{3.15}$$

This again is the flexure formula for the stresses in the Phenolic Concrete of the transformed section.

A3.3. Geometrical Properties of the Panels

Considering Figure A3.1, the Equation 3.7 can be solved over the transformed cross-section area in order to obtain the neutral axis position of the transformed section with respect to steel area. However, the following expression is derived in order to calculate the neutral axis position from the first moment of area of the transformed section about the bottom face of the panel section (see Figure A3.1b), such that;

$$\bar{Y} = \frac{\frac{A_p}{m}\bar{Y}_p + A_s\bar{Y}_s}{\frac{A_p}{m} + A_s} \tag{3.16}$$

in which;

A_p is the effective cross-sectional area of the Phenolic Concrete matrix.

$\bar{Y}_p$ is the distance from the centroid of the Phenolic Concrete matrix to bottom face of the panel section.

A_s is the total steel bars area.

$\bar{Y}_s$ is the distance from the centroid of the steel bars to bottom face of the panel section.

$\bar{Y}$ is the distance of the neutral axis of the panel section from its bottom face.

It should be noted that the neutral axis position obtained for the transformed equivalent panel section would in fact be in the same location as of the original composite panel section.

The Equation 3.12b, is rearranged in order to obtain the second moment of area of the transformed section about the neutral axis with respect to steel modulus; using the parallel-axis theorem from the following expression,

$$I_t = \frac{I_{tp} + (m-1)I_s}{m} \tag{3.17}$$

where

$$I_{tp} = (I_p + I_s)$$

in which,

I_{tp} is the second moment of area of the whole panel section.

I_p is the second moment of effective area of the Phenolic Concrete matrix of the panel section.

I_s is the second moment of area of the steel bars.

To obtain the normal stresses in the steel and in the Phenolic Concrete of the transformed section, Equations 3.13 and 3.14 can be used respectively. These equations (flexure formula for transformed sections) show that the stresses are propotional to the bending moment M and inversely propotional to the amount of I_t of the transformed equivalent section. Also the stresses vary linearly with the distance Y from the neutral axis.

The maximum tensile and compressive stresses in the steel and in the Phenolic Concrete of the panels occur at points located furthest from the neutral axis. Therefore, the maximum normal stresses (see Figure A3.1b) will be as follows:

for steel bars in;

$$tension \qquad \sigma_{bs} = \frac{MY_{bs}}{I_t} \tag{3.18a}$$

$$compression \qquad \sigma_{ts} = \frac{MY_{ts}}{I_t} \tag{3.18b}$$

and for Phenolic Concrete in;

$$tension \qquad \sigma_{bp} = \frac{MY_{bp}}{m.I_t} \tag{3.19a}$$

$$compression \qquad \sigma_{tp} = \frac{MY_{tp}}{m.I_t} \tag{3.19b}$$

in which, for steel bars

$$Z_{bs} = \frac{I_t}{Y_{bs}} \qquad Z_{ts} = \frac{I_t}{Y_{ts}}$$

and for Phenolic Concrete

$$Z_{bp} = \frac{m.I_t}{Y_{bp}} \qquad Z_{tp} = \frac{m.I_t}{Y_{tp}}$$

are the section moduli of the cross-sectional area.

For all the panel sections from their corresponding measured geometrical dimensions, using the B/DECK program (by G.M.Parton) based on the preceding expressions and modular ratio $m = 30$, the neutral axis position $\bar{Y}$, the second moment of area I_t about the neutral axis and the relevant section moduli values were computed and are given in the output of B/DECK in this Appendix (see Table A3.1).

A3.4. Flexural Rigidity (EI) and Modulus (E) values

The panels were tested subject to four point flexural loading in a similar manner to the Box Beams of Chapter 5. Therefore the deflection formula derived in Appendix A2 from bending theory are also used in determinig the flexural rigidity of the tested bridge-deck panels, such that

$$EI = \frac{W}{y_l} \times \frac{L^3}{12}[3(\frac{a}{L})^2 - 4(\frac{a}{L})^3]$$

$$= \frac{W}{y_l} \times C_l$$

and

$$EI = \frac{W}{y_c} \times \frac{L^3}{12}[\frac{3a}{4L} - (\frac{a}{L})^3]$$

$$= \frac{W}{y_c} \times C_c$$

which are based on the deflection at loading points and at mid-span of the panels respectively. Considering Figure 6.3 in Chapter 6, the loading arrangement of the bridge-deck panels, the deflection equation constants are found to be;

$$C_l = 39583333.4 \quad (mm^3)$$

$$C_c = 42395833.3 \quad (mm^3)$$

For all the panels the flexural rigidity EI values were calculated from the deflection equation relating to deflection at loading points and the deduced slopes $\frac{W}{y_l}$ from the corresponding load-deflection graphs. The second moments of area I_e of the tested panels were then evaluted from the relevent EI valuse with respect to steel modulus (see Table 6.6 of Chapter 6). In order to obtain an effective modular ratio, theoretical second moments of area I_t of the transformed equivalent panel sections were computed (i.e. from Equation 3.17) using B/DECK program for a range of

modular ratio values between 10 to 40. A graph of I_t against modular ratio m was plotted (see Figure A3.2), from which, using the deduced I_e values of the relevant panel section, the effective modular ratios were extrapolated. A modulus value E for each panel was calculated from the deflection formula, based on its corresponding theoretical second moment of area I_t, modular ratio $m = 30$ and its relevant slope value $\frac{W}{y_l}$ (see Table 6.6 of Chapter 6).

A3.5. Load at First Cracking and Ultimate Failure Load

To predict the load to cause the first crack in the Phenolic Concrete matrix of the panels subject to flexure, it was assumed that a uniform tensile stress distribution existed across the bottom face of the flat slab (flange) of the panels (i.e. at extreme tension face). From bending theory and Equation 3.19a the bending capacity to cause the first crack in the Phenolic Concrete matrix of the panels was obtained; such that

$$M_{cracking} = \frac{\sigma_{bp}.m.I_t}{Y_{bp}}$$

with

$$\sigma_{bp} = f_{ct} \qquad \frac{I_t}{Y_{bp}} = Z_{bp}$$

therefore

$$M_{cracking} = f_{ct}.m.Z_{bp}$$

where,

$M_{cracking}$ is the bending capacity to cause the first crack.

f_{ct} is the Phenolic Concrete tensile strength obtained from Brazilian Disc tests.

Z_{bp} is the uncracked section modulus.

The load (W_{C1}) at first cracking was then calculated from the respective bending

capacity as follows,

$$W_{C1} = \frac{2 \times M_{cracking}}{a}$$

where,

W_{C1} is the load at first cracking of the Phenolic Concrete matrix of the composite section.

a is the maximum moment lever arm.

The theoretical load at first cracking of the test panels are tabulated in Table 6.5 of Chapter 6. These values were in close agreement when compared with the corresponding experimental values (see Table 6.4 of Chapter 6).

The mode of failure of the internally reinforced panels was of two types. In lightly reinforced panels, steel bars yielded as failure approached, whereas in the heavily reinforced panels at higher loads the steel bars slipped causing the failure to occur with extensive cracking of the matrix in tension before full steel strengths were utilized.

From Figure A3.1b, it can be seen that the maximum steel stresses would develope in the steel of compression zone as the couple M_o which is the result of the positive bending moment would have greater moment lever arm from compression steel. Therefore, prediction of the ultimate failure moment of the lightly reinforced panels could be based on their compression steels reaching their yield stresses at failure. Using the Equation 3.18b the failure moments and hence the failure loads of these panels were calculated and tabulated in Table 6.5.

The strains in the compression steel bars of the internally reinforced panels were calculated at load levels indicating the onset of the steel bars yielding and/or slipping

and also at the relevant ultimate sustained loads at failure from the expressions;

$$\epsilon_s = \frac{M}{E_s Z_{ts}}$$

$$\epsilon_p = \frac{m.M}{E_s Z_{bp}}$$

which are derived by substituting $\sigma_s = E_s \epsilon_s$ for the steel stress, $\sigma_p = \frac{E_s}{m} \epsilon_p$ for the Phenolic Concrete stress and the corresponding section moduli in Equations 3.18b and 3.19b respectively. The compression steel strains and the corresponding Phenolic Concrete strains at the extreme tension face of the internally reinforced panels are compared with the steel yield strain and the Phenolic Concrete tensile fracture strains respectively and tabulated in Table A3.2.

From the experimental failure moments of the reference bridge-deck panels, the tensile stresses at their extreme tension faces were deduced using the expression;

$$\sigma_{bp} = \frac{MY_{tp}}{I_{tp}}$$

which defines the maximum normal tensile stresses develop on the extreme tension face of the unreinforced panel section as a result of applied positive bending moment. These stresses indicated that the reference panels on their extreme tension faces at failure developed stresses equal to the tensile fracture strengths obtained from flexural testing of the corresponding control coupon specimens without laminated fibre glass. This therefore suggested that in calculating the ultimate failure loads of the unreinforced panel sections, the tensile fracture strengths of the plain control coupon specimens should be used rather than those of the coupons with laminated fibre glass mat.

For those test panels which were not "over-reinforced" the predicted ultimate failure loads calculated from the preceding expressions are tabulated in Table 6.5.

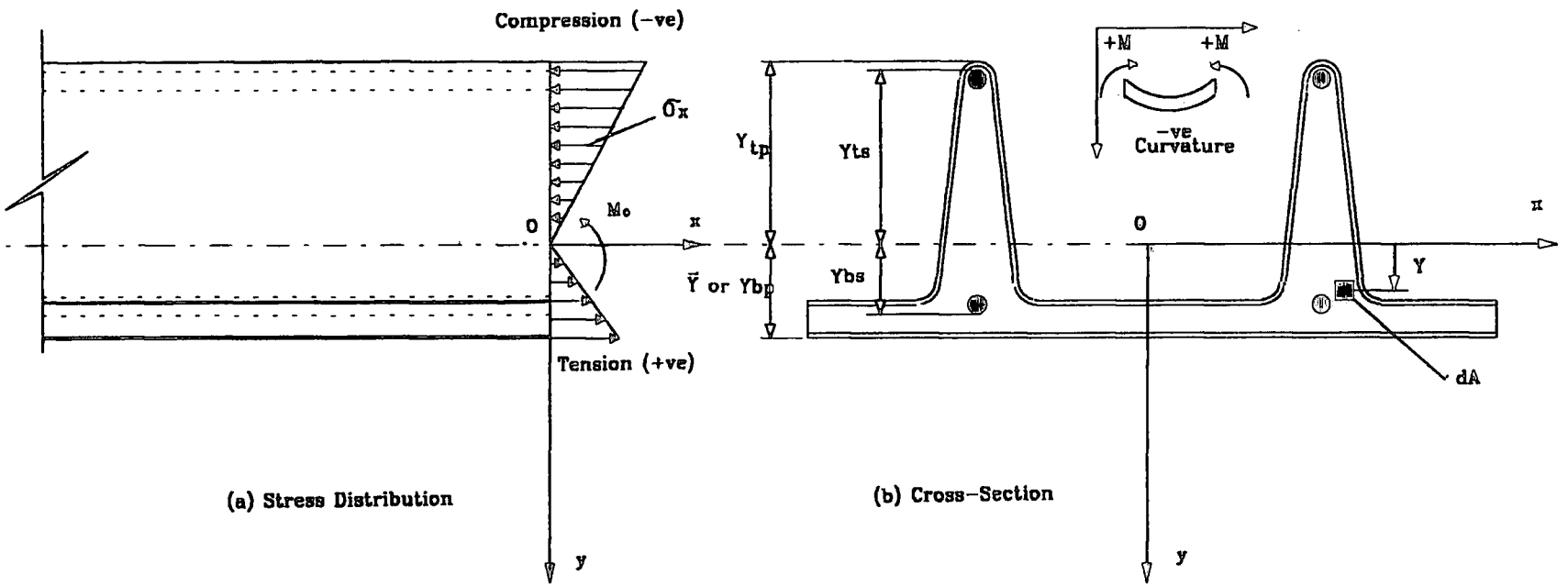

Figure A3.1 Distribution of normal stresses in bridge−deck panel
(Note: The bending moment $M=M_o$)

Table A3.1 OUTPUT FROM B/DECK PROGRAMME (MODULAR RATIO=30.0)

PANEL DIMENSIONS

NUM	SHT THS	SHT WTH	RIBS	TOP THS	BOT THS	DEPTH	BARS	TYPE	DIAMETER	DEPTHS	LEV1	LEV2
A1a	7.87	300.	2	16.24	27.85	65.50	0	0	0.00	0.0	0.00	0.00
A1b	7.74	300.	2	16.27	27.78	65.92	0	0	0.00	0.0	0.00	0.00
A2a	8.95	300.	2	16.17	27.77	65.95	2	0	6.39	0.0	16.80	61.55
A2b	8.82	300.	2	16.09	27.96	65.92	2	0	6.39	0.0	14.51	61.13
A3a	8.98	300.	2	16.05	27.89	65.63	2	0	10.43	0.0	12.68	57.18
A3b	8.91	300.	2	16.07	27.74	65.94	2	0	10.43	0.0	10.67	58.67
B1a	8.22	300.	2	16.10	28.07	58.40	0	0	0.00	0.0	0.00	0.00
B1b	8.55	300.	2	16.09	28.39	58.62	0	0	0.00	0.0	0.00	0.00
B2a	8.80	300.	2	16.08	28.45	58.88	2	0	6.39	0.0	17.66	59.91
B2b	8.48	300.	2	16.01	28.01	58.82	2	0	6.39	0.0	17.74	58.29
B3a	9.73	300.	2	16.14	28.91	58.85	2	0	10.43	0.0	12.50	50.25
B3b	9.31	300.	2	16.06	28.90	58.82	2	0	10.43	0.0	15.18	51.93
C1a	7.35	300.	2	16.01	28.20	46.35	0	0	0.00	0.0	0.00	0.00
C1b	7.66	300.	2	16.03	28.70	46.84	0	0	0.00	0.0	0.00	0.00
C2a	8.52	300.	2	16.01	28.79	46.83	2	0	6.39	0.0	17.64	41.39
C2b	8.64	300.	2	16.10	28.28	46.88	2	0	6.39	0.0	17.57	41.64
C3a	8.79	300.	2	16.17	28.89	46.78	2	0	10.43	0.0	12.89	35.51
C3b	8.76	300.	2	16.16	28.84	46.80	2	0	10.43	0.0	13.01	36.01
D1a	7.36	300.	2	16.01	28.05	34.79	0	0	0.00	0.0	0.00	0.00
D1b	7.73	300.	2	16.09	28.43	34.90	0	0	0.00	0.0	0.00	0.00

GEOMETRICAL PROPERTIES

NUM	AM	MATRIX AREA	STL AREA	YBAR	2ND MOI	ZTS	ZBS	ZTP	ZBP
A1a	0.	5248.89	0.00	22.54	2505742.	0.	0.	49294.	-111183.
A1b	0.	5225.77	0.00	22.74	2527131.	0.	0.	49629.	-111132.
A2a	30.	5582.84	128.28	29.25	173568.	5963.	-18755.	114063.	-178022.
A2b	30.	5549.77	128.28	28.72	174733.	5981.	-15860.	113912.	-182506.
A3a	30.	5577.78	341.76	30.46	273998.	12743.	-21801.	186197.	-269830.
A3b	30.	5561.83	341.76	30.35	300229.	12991.	-20762.	202380.	-296813.
B1a	0.	5045.53	0.00	19.79	1915165.	0.	0.	40897.	-96769.
B1b	0.	5172.41	0.00	19.84	1976498.	0.	0.	41763.	-99606.
B2a	30.	5261.92	128.28	27.88	149177.	5173.	-21237.	112443.	-160524.
B2b	30.	5133.25	128.28	27.64	140803.	5129.	-20994.	106513.	-152815.
B3a	30.	5570.19	341.76	27.32	207273.	11702.	-21575.	150715.	-227588.
B3b	30.	5437.54	341.76	28.81	205403.	11471.	-24411.	156713.	-213893.
C1a	0.	4254.13	0.00	15.58	1016509.	0.	0.	26668.	-65236.
C1b	0.	4393.15	0.00	15.77	1071141.	0.	0.	27658.	-67917.
C2a	30.	4653.98	128.28	21.97	68721.	4236.	-60522.	61763.	-93837.
C2b	30.	4672.53	128.28	21.99	69743.	4239.	-56740.	62408.	-95129.
C3a	30.	4744.90	341.76	21.53	90724.	10351.	-26489.	79956.	-126415.
C3b	30.	4734.00	341.76	21.75	92652.	10239.	-26312.	82202.	-127818.
D1a	0.	3740.85	0.00	11.67	504420.	0.	0.	16547.	-43237.
D1b	0.	3872.75	0.00	11.77	526388.	0.	0.	17057.	-44724.

Table A3.2 (Calculated strain values in the steel bars and Phenolic Concrete of the bridge-deck panels)

Panel		Recorded		Calculated (*modular ratio* = 30)							
		Sustained moments		Section moduli		Steel Strains $\times 10^{-3}$			Phenolic Concrete strains $\times 10^{-3}$		
Group	Set	M_{C2} $(kN.mm)$	M_U $(kN.mm)$	Z_{ts} (mm^3)	Z_{bp} (mm^3)	ϵ_{ys}	ϵ_{2ts}	ϵ_{Uts}	ϵ_{Fp}	ϵ_{2bp}	ϵ_{Ubp}
A	2a	3250.00	3746.25	5963	178022	3.0500	2.7251	3.1413	3.8775	2.7384	3.1566
A	2b	3614.75	3988.25	5981	182506	3.0500	3.0219	3.3341	3.9135	2.9709	3.2779
A	3a	4850.50	5374.25	12743	269830	2.6908	1.8388	2.0374	3.7575	2.6964	2.9876
A	3b	4577.50	5315.25	12991	296813	2.6908	1.7022	1.9766	3.6615	2.3133	2.6862
B	2a	3142.50	3572.50	5173	160524	3.0500	3.0374	3.4530	3.9930	2.9365	3.3383
B	2b	3131.50	3714.25	5129	152815	3.0500	3.0527	3.6208	3.7950	3.0738	3.6458
B	3a	3806.25	4384.50	11702	227588	2.6908	1.5713	1.8101	3.6600	2.5086	2.8898
B	3b	3880.25	4437.25	11471	213893	2.6908	1.6341	1.8687	3.8355	2.7212	3.1118
C	2a	2524.25	2637.25	4236	93837	3.0500	2.9795	3.1129	4.1910	4.0351	4.2157
C	2b	2534.00	2736.75	4239	95129	3.0500	2.9889	3.2281	4.1940	3.9956	4.3153
C	3a	2618.75	2880.75	10351	126415	2.6908	1.2222	1.3445	3.8925	3.1073	3.4182
C	3b	2637.25	2926.25	10239	127818	2.6908	1.2443	1.3806	3.9645	3.0949	3.4341

Note:

M_{C2} is the sustained moment at the end of the elastic range of the bridge-deck panels.

M_U is the sustained failure moment of the bridge-deck panels.

ϵ_{ys} is the steel yield strain (i.e. proof stress/ elastic modulus).

ϵ_{Fp} is the Phenolic Concrete strain at fracture of the coupon specimens.

Z_{ts} is the section modulus refering to top steel (compression) of the bridge-deck panels.

Z_{bp} is the section modulus refering to bottom Phenolic Concrete face (tension) of the bridge-deck panels.

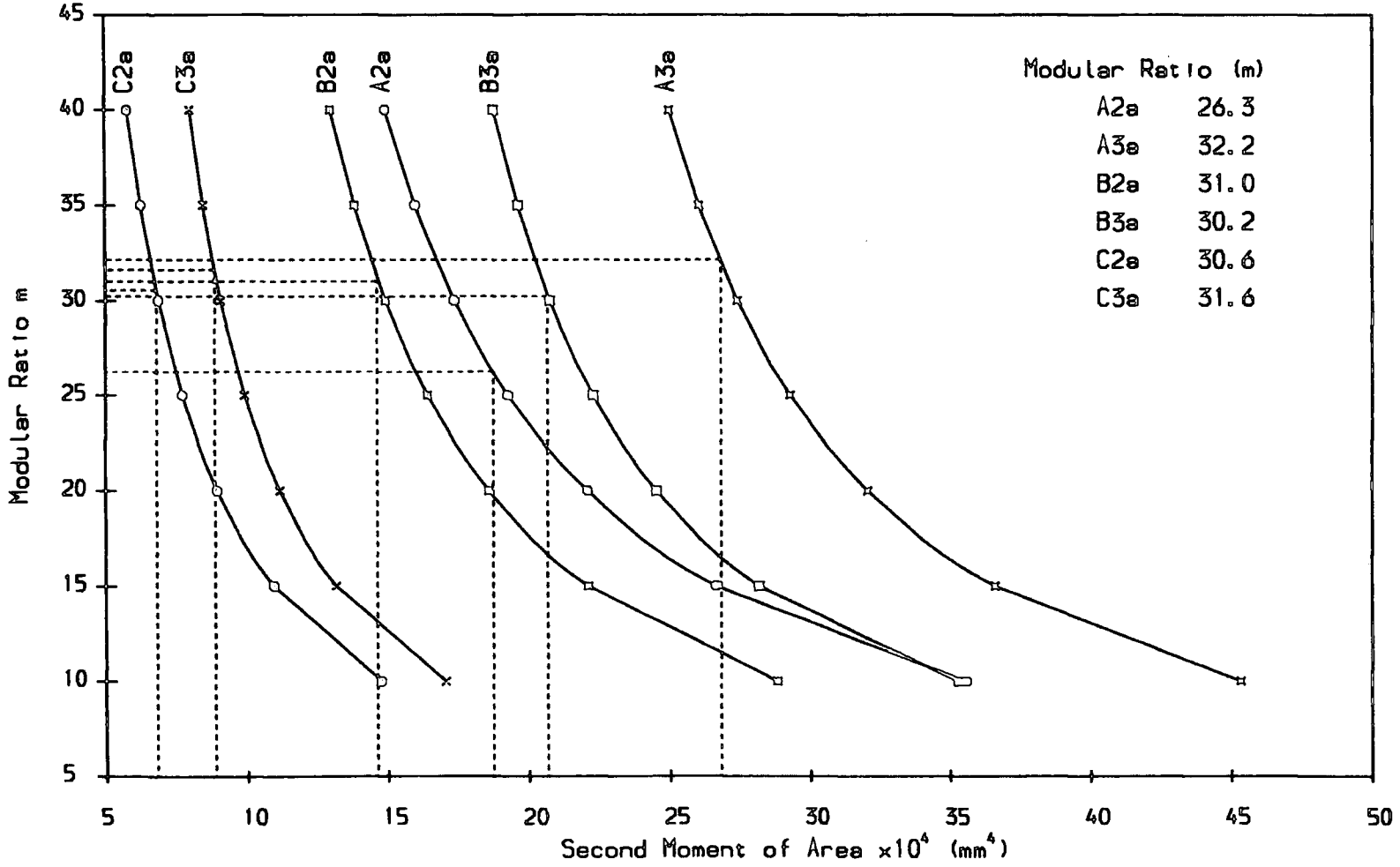

Figure A3.2 Graph of Modular Ratio against Second Moment of Area for Internally reinforced Phenolic Concrete Bridge-Deck Panels.

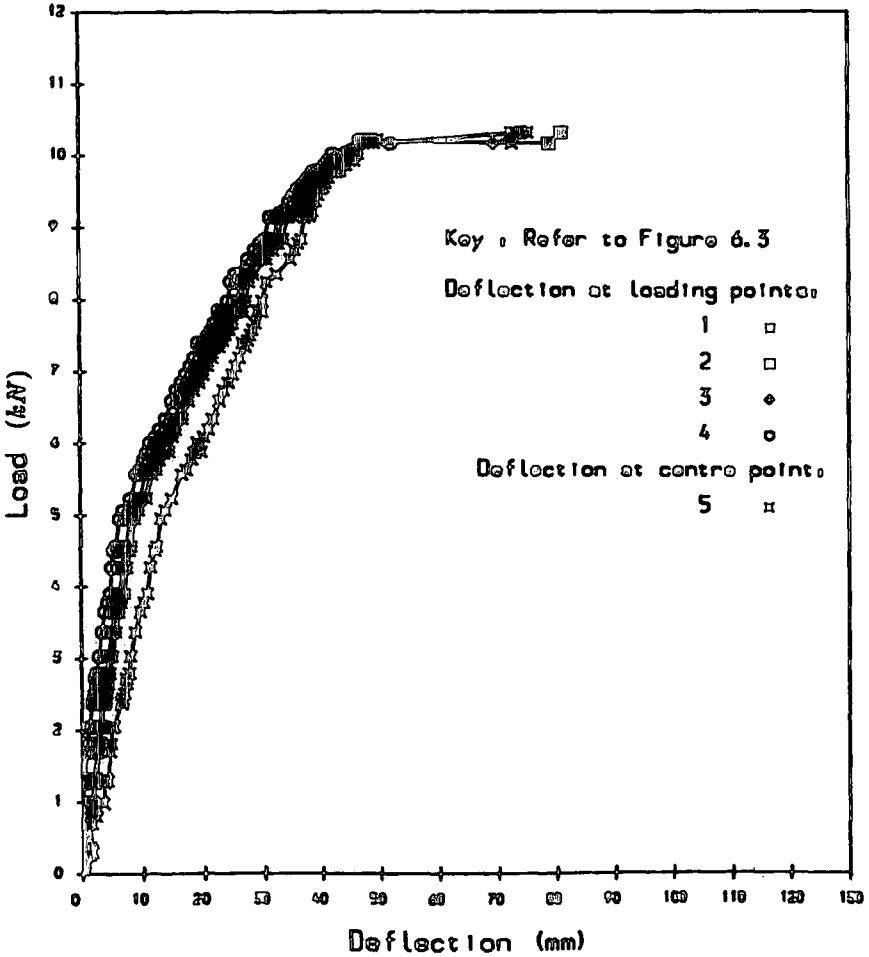

(a) Load v Deflections

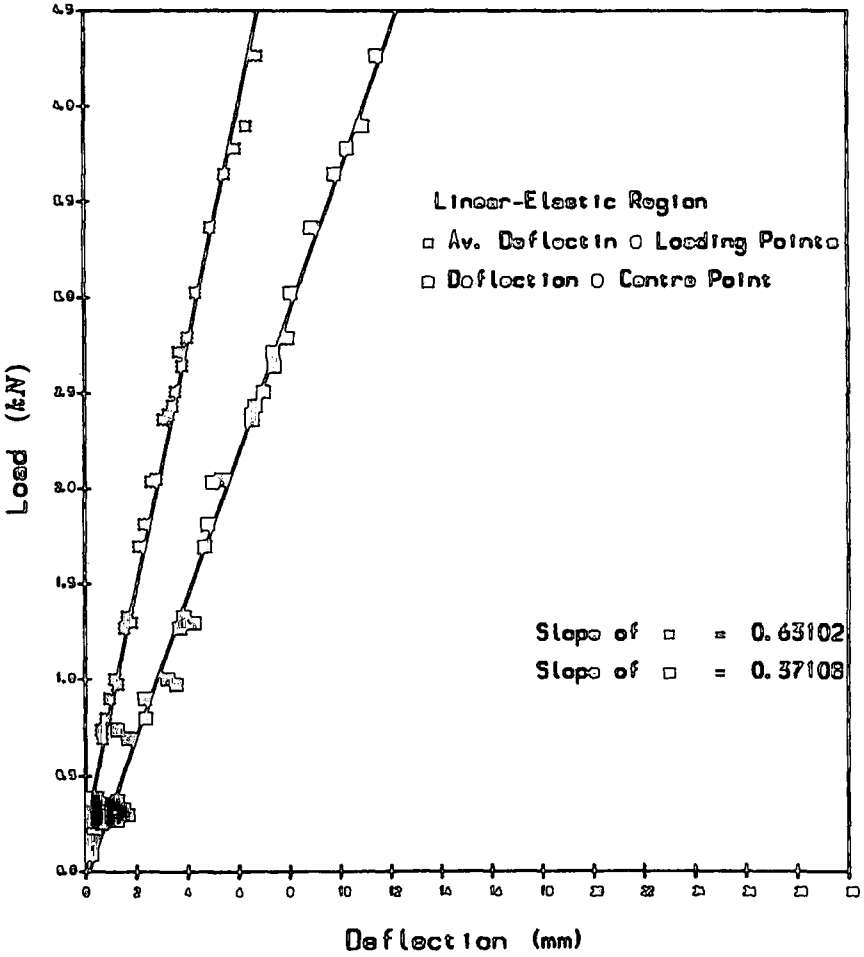

(b) Evaluation of Slopes

Figure A3.3 Recorded Load-Deflection values for Phenolic Concrete Bridge Deck Panel A1a.

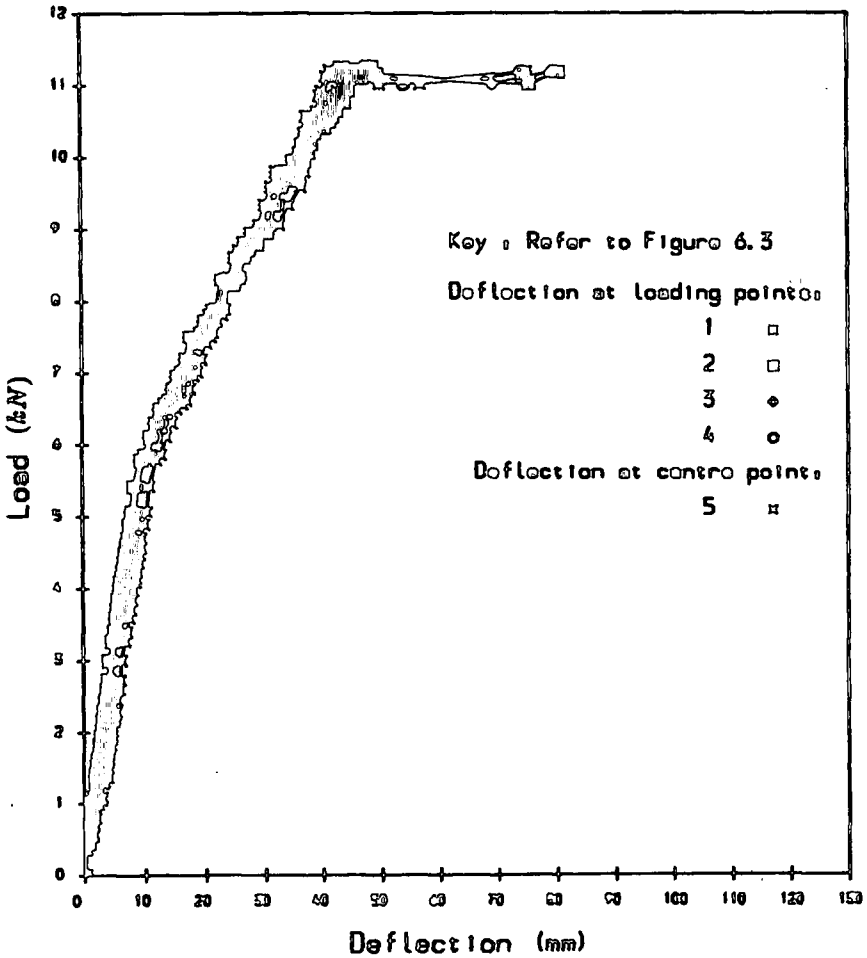

(a) Load v Deflections

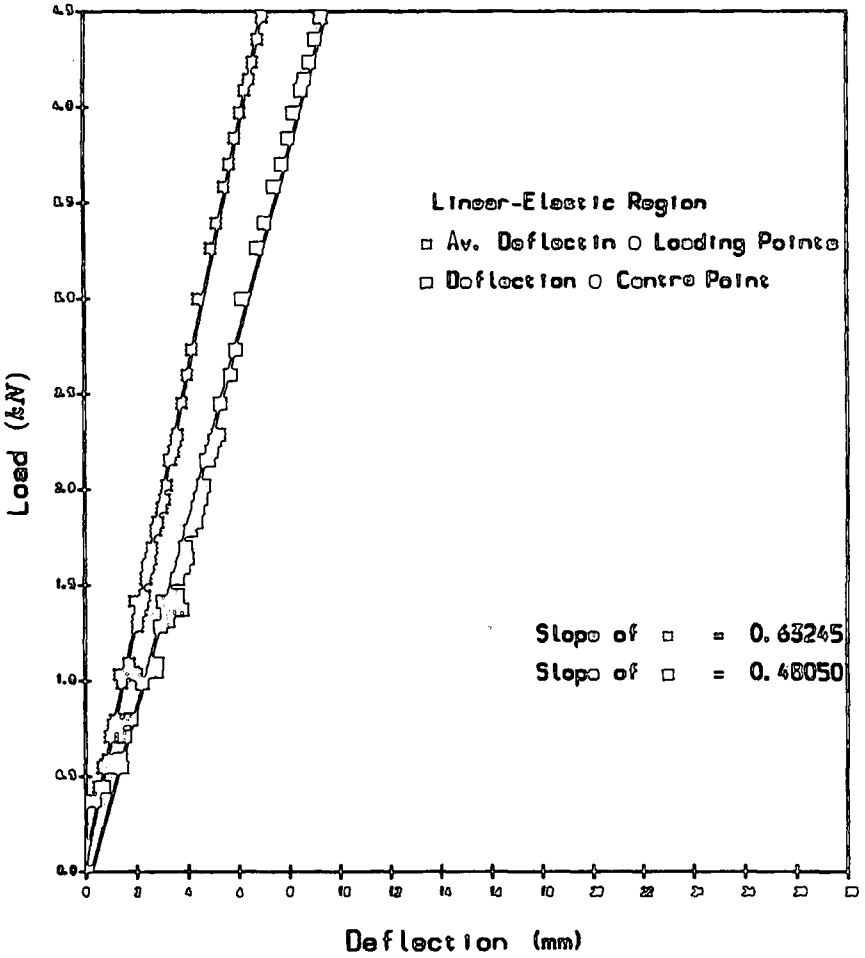

(b) Evaluation of Slopes

Figure A3.4 Recorded Load-Deflection values for Phenolic Concrete Bridge Deck Panel A1b.

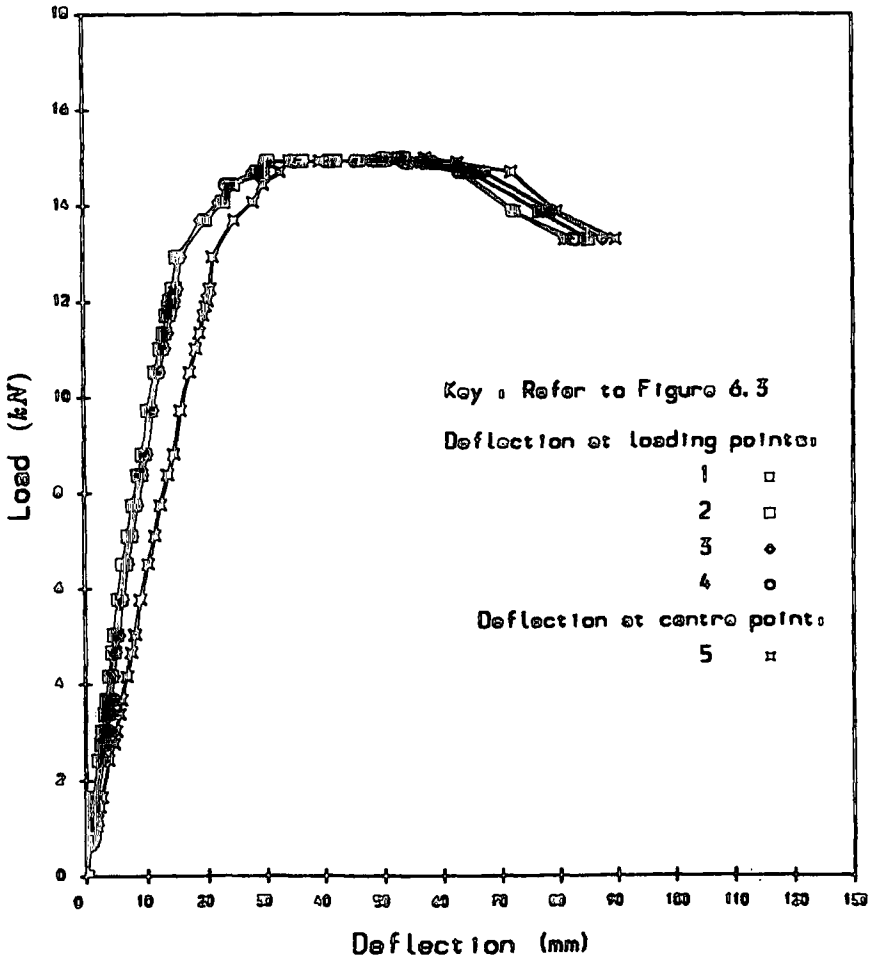

(a) Load v Deflections

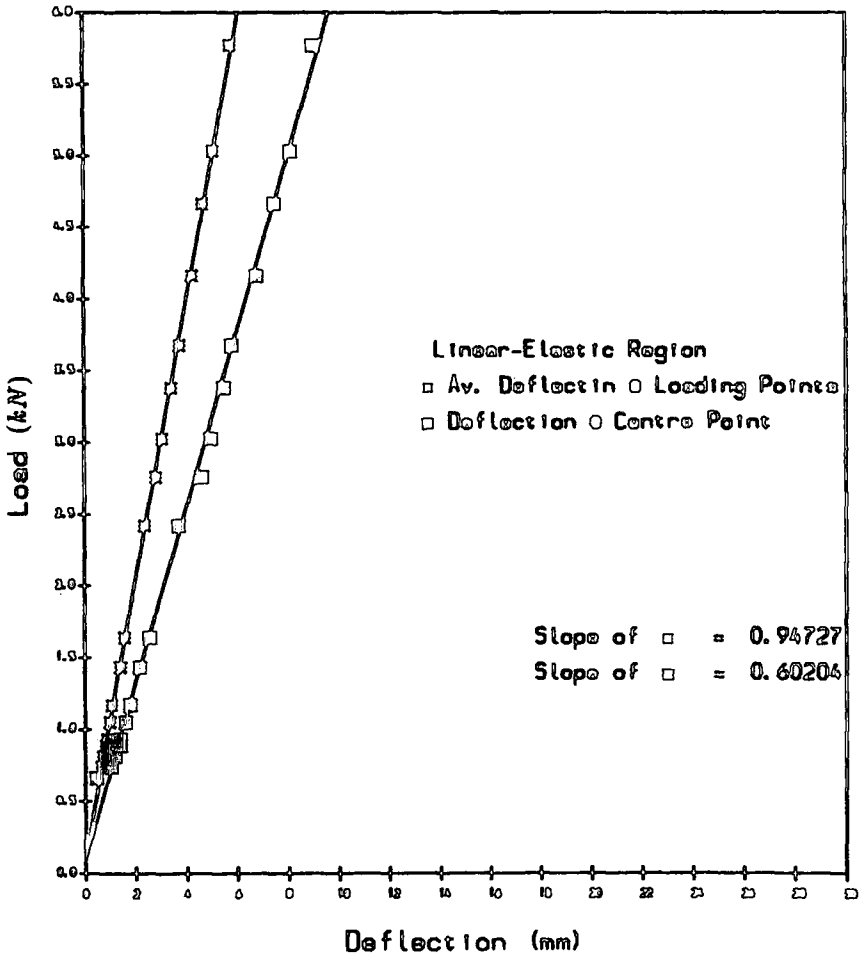

(b) Evaluation of Slopes

Figure A3.5 Recorded Load-Deflection values for Phenolic Concrete Bridge Deck Panel A2a.

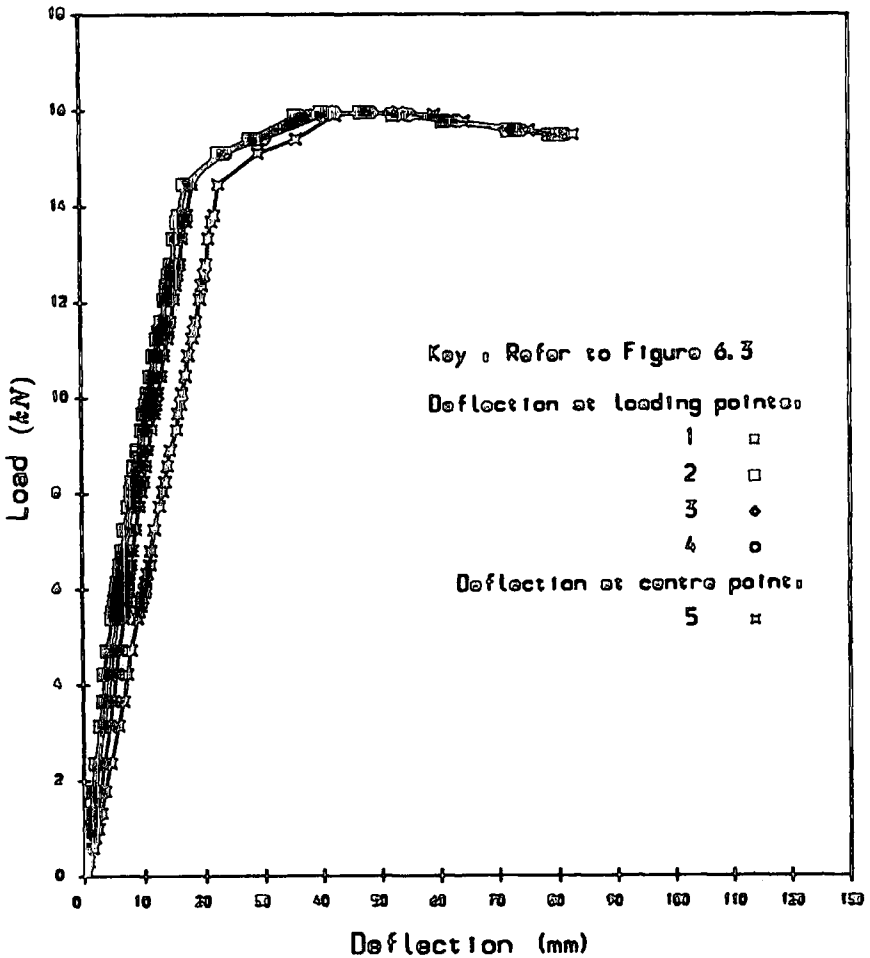

(a) Load v Deflections

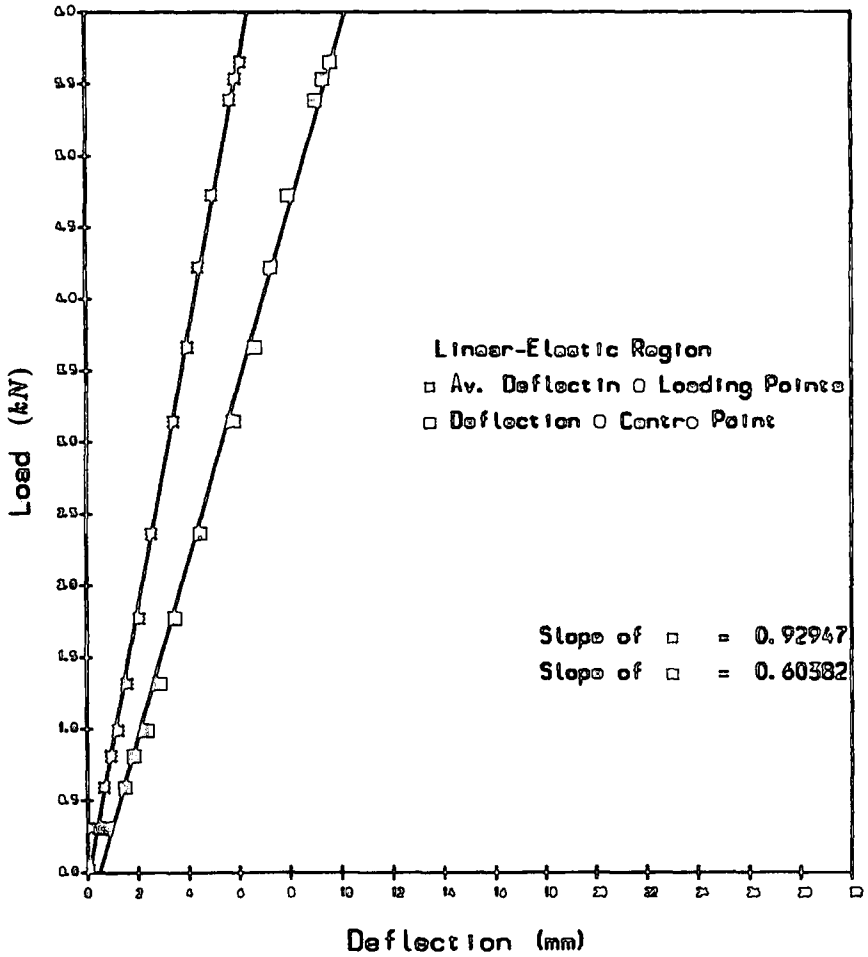

(b) Evaluation of Slopes

Figure A3.6 Recorded Load-Deflection values for Phenolic Concrete Bridge Deck Panel A2b.

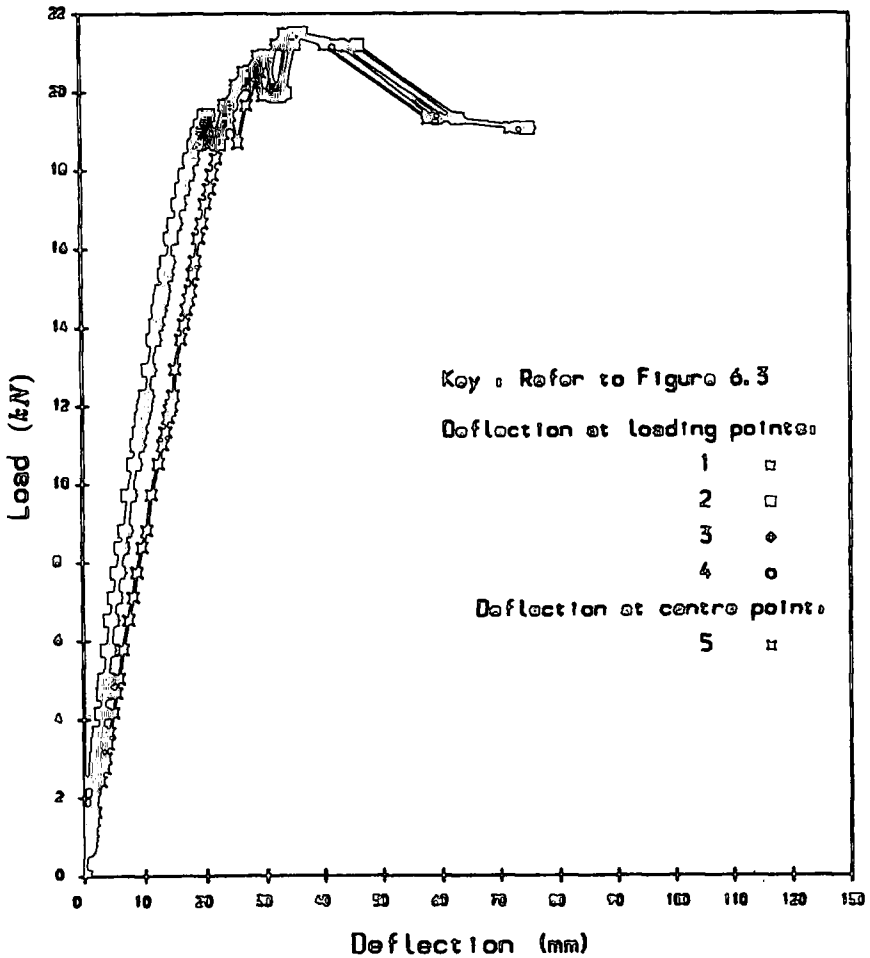

(a) Load v Deflections

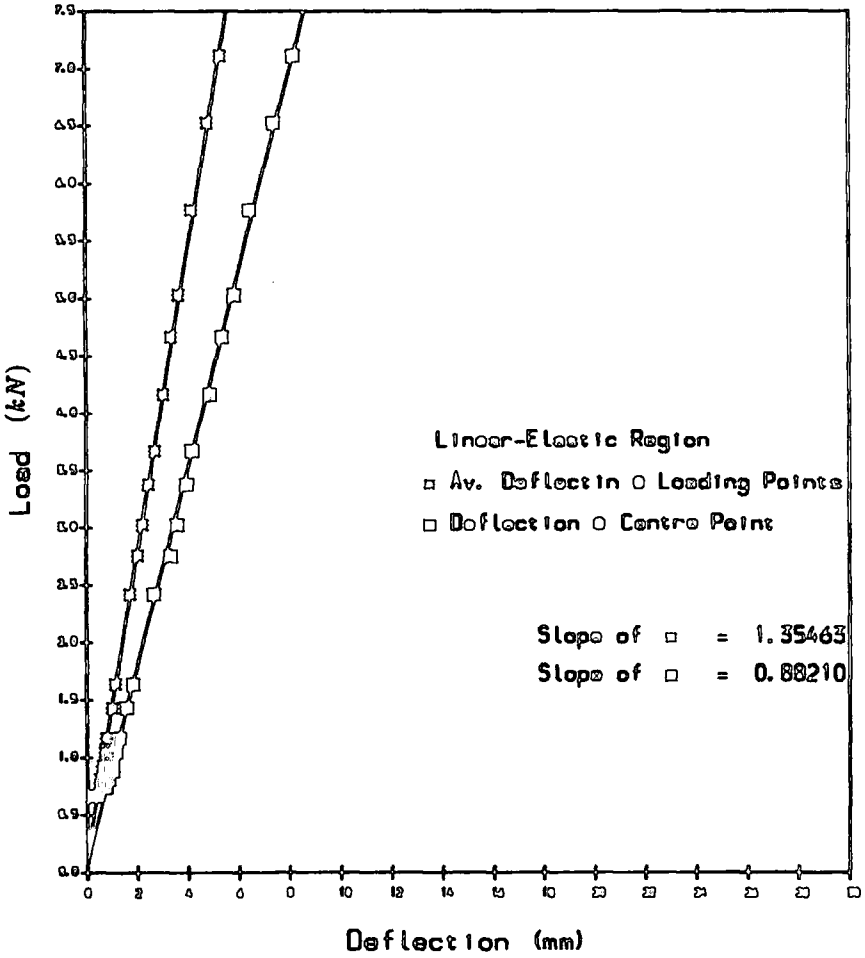

(b) Evaluation of Slopes

Figure A3.7 Recorded Load-Deflection values for Phenolic Concrete Bridge Deck Panel A3a.

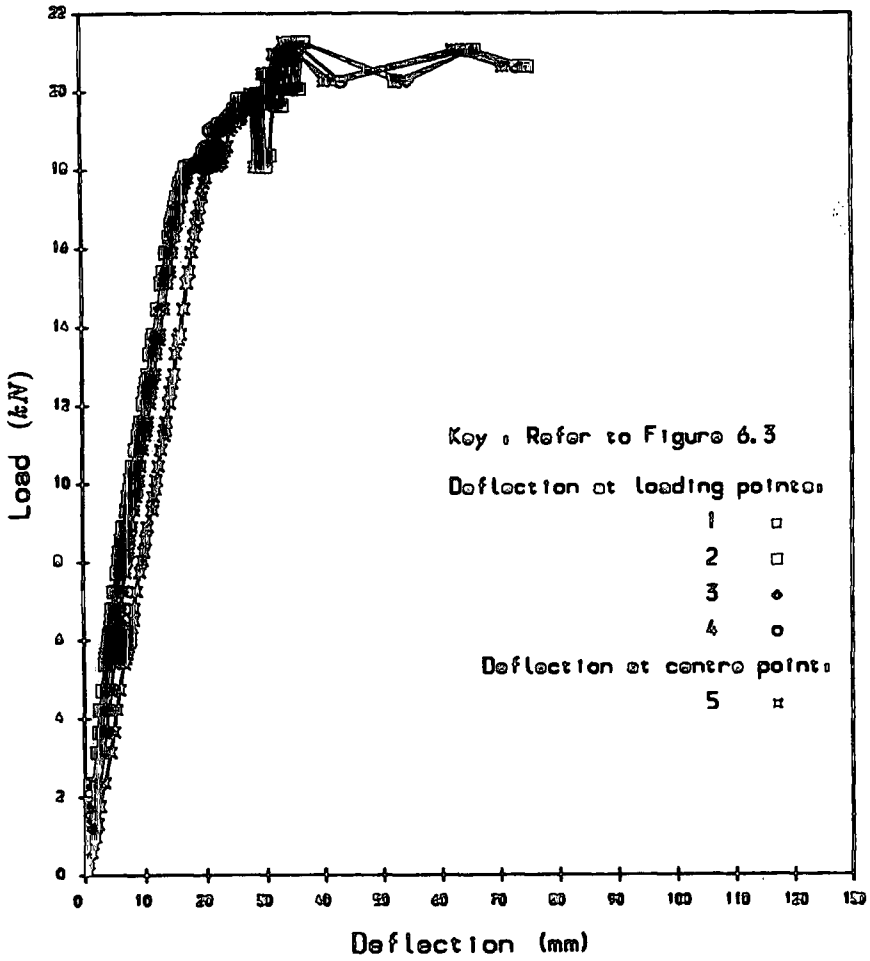

(a) Load v Deflections

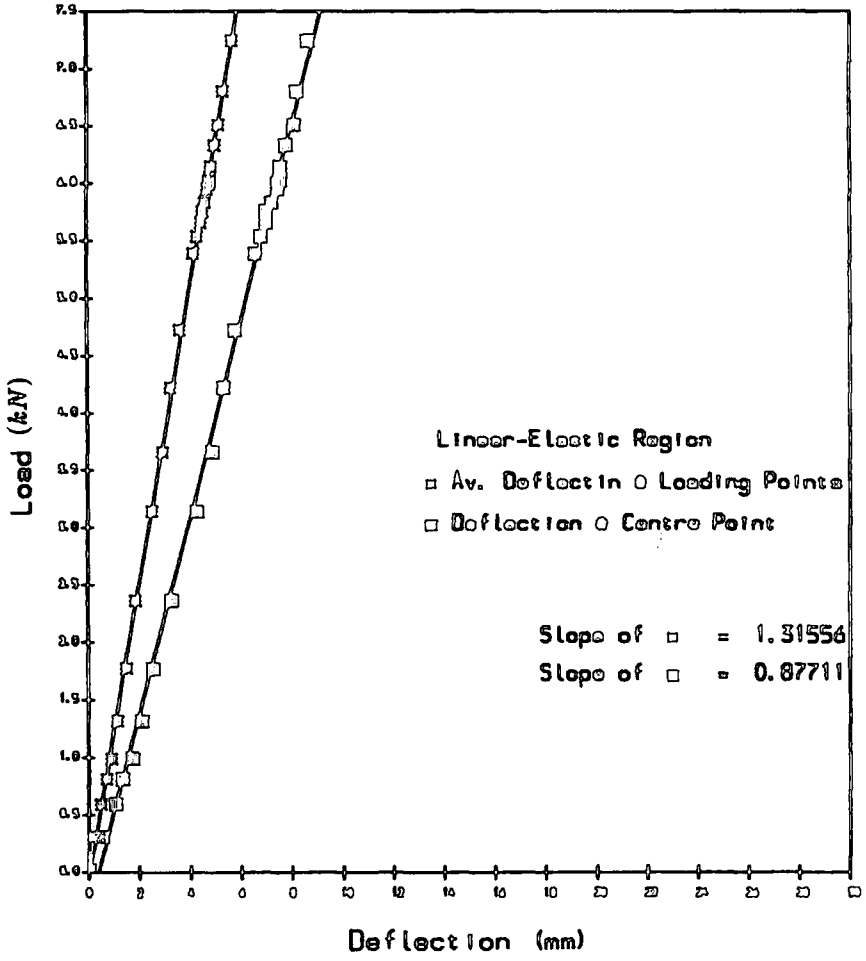

(b) Evaluation of Slopes

Figure A3.8 Recorded Load-Deflection values for Phenolic Concrete Bridge Deck Panel A3b.

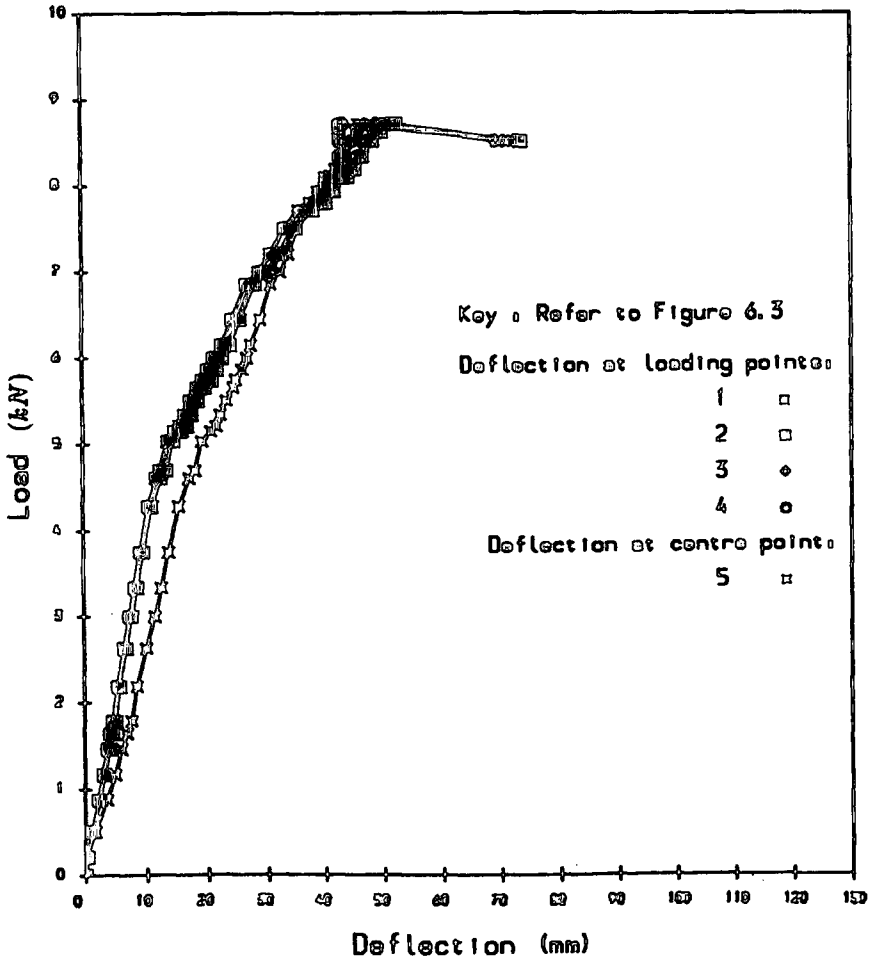

(a) Load v Deflections

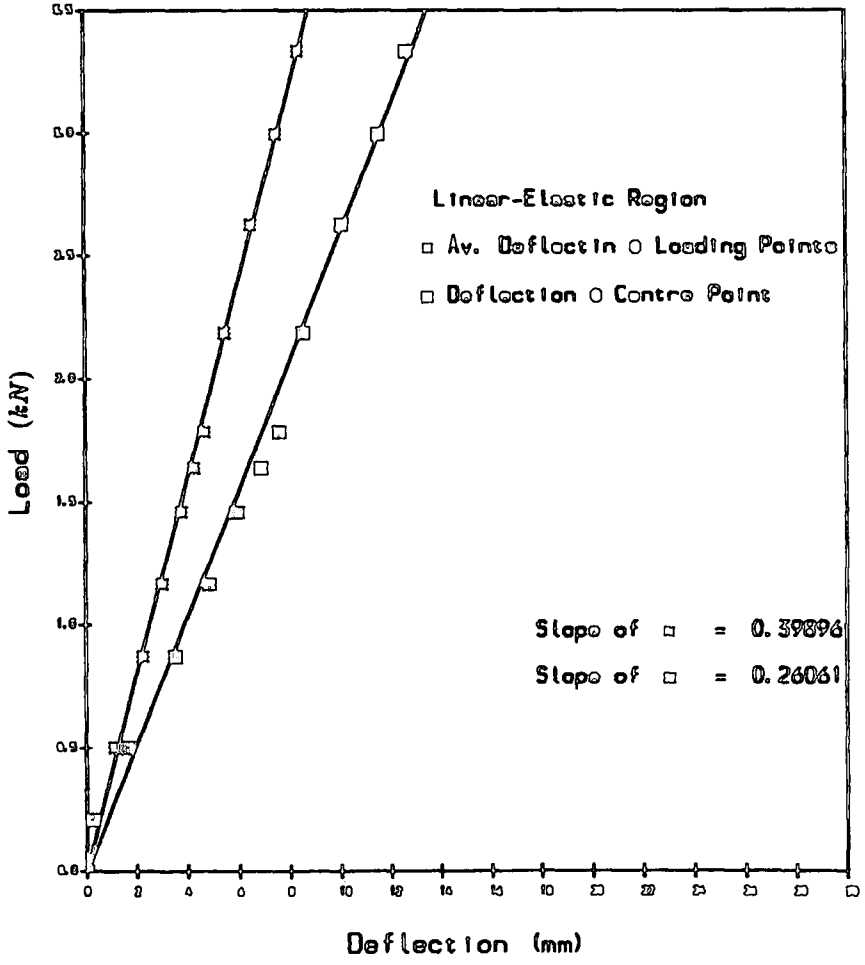

(b) Evaluation of Slopes

Figure A3.9 Recorded Load-Deflection values for Phenolic Concrete Bridge Deck Panel B1a.

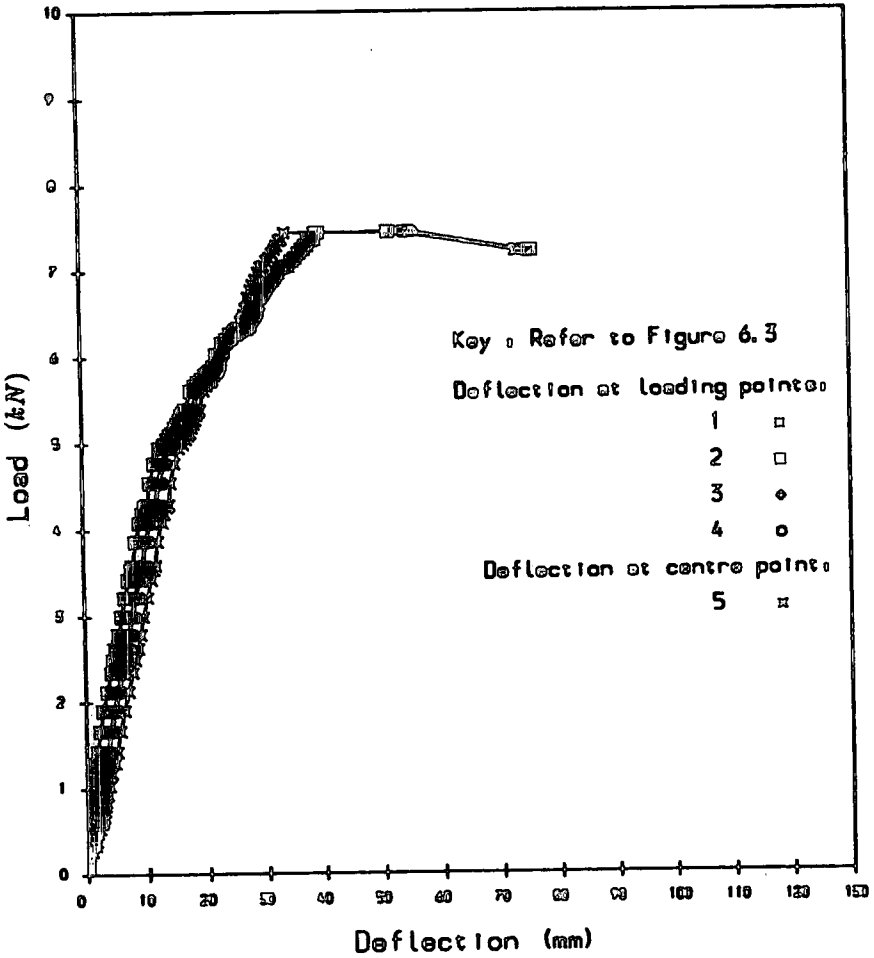

(a) Load v Deflections

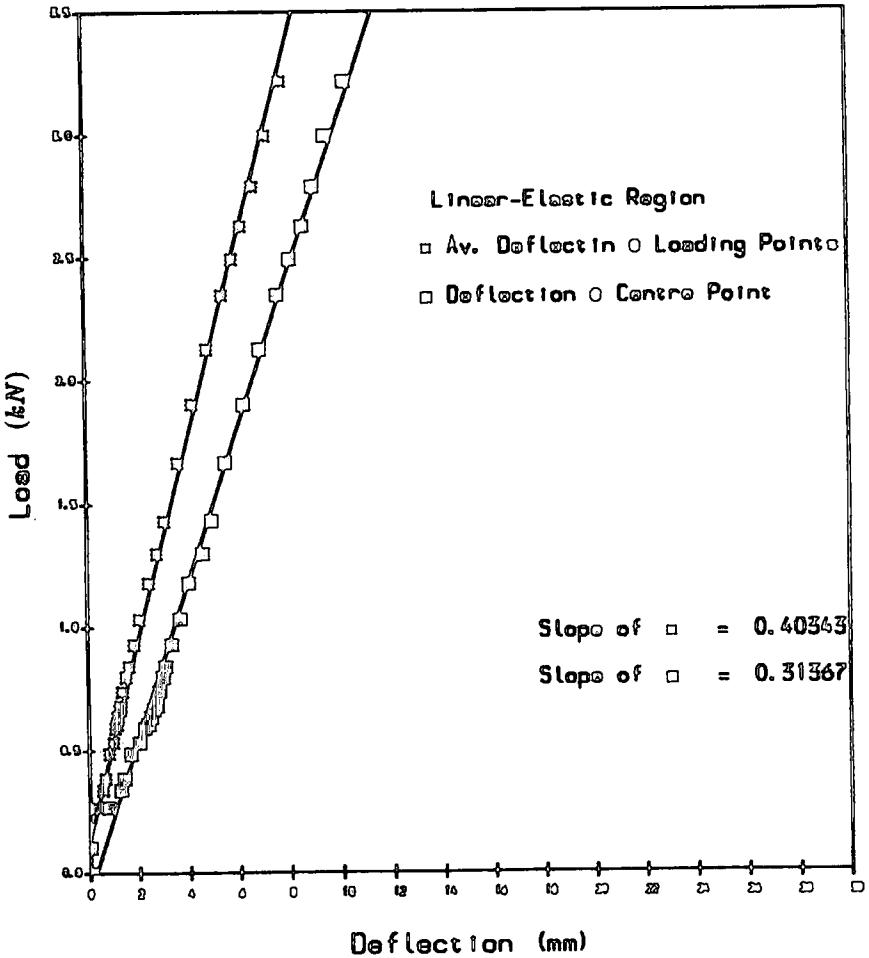

(b) Evaluation of Slopes

Figure A3.10 Recorded Load-Deflection values for Phenolic Concrete Bridge Deck Panel B1b.

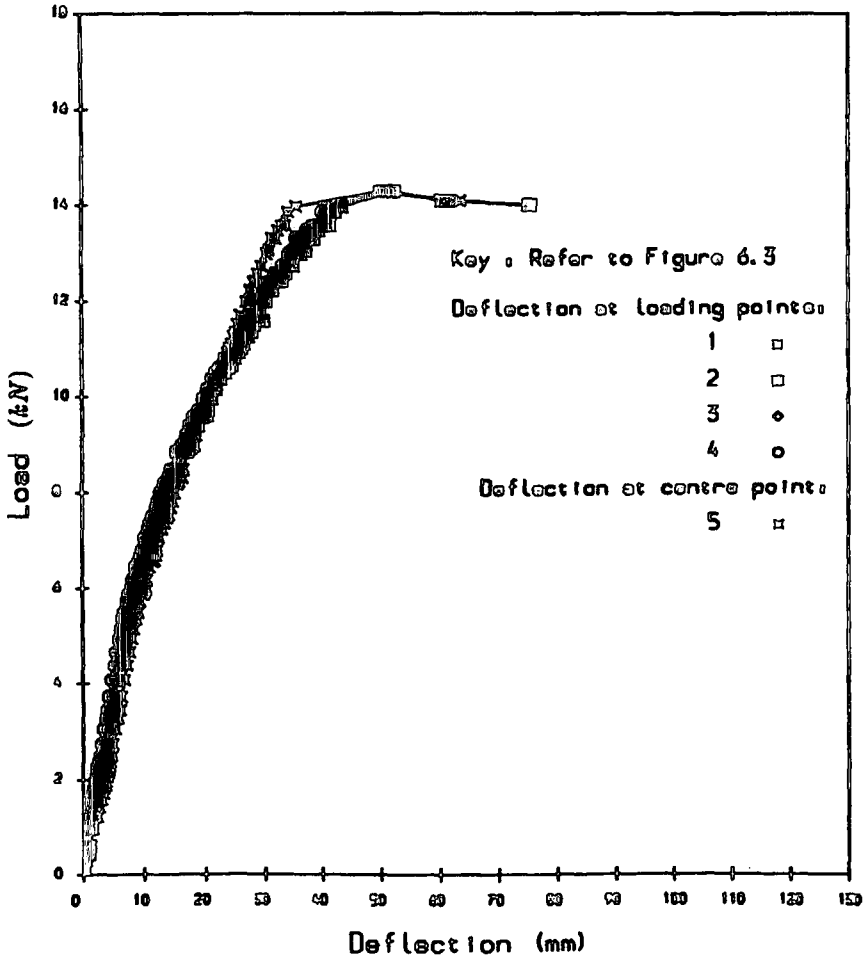

(a) Load v Deflections

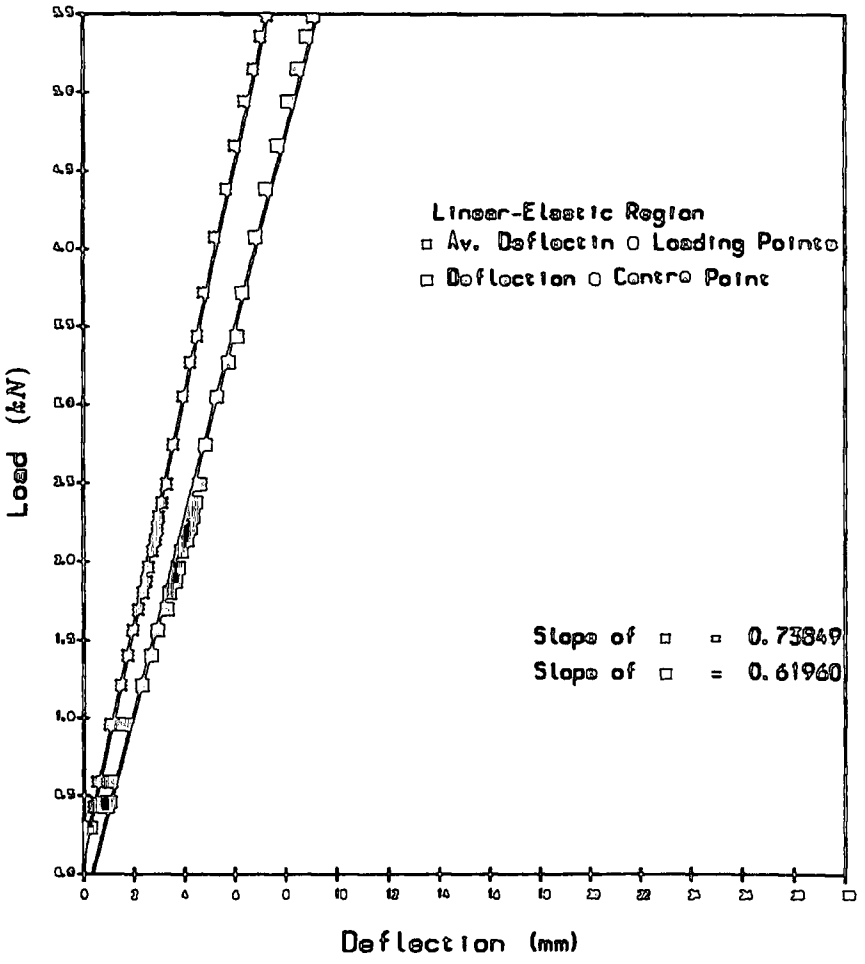

(b) Evaluation of Slopes

Figure A3.11 Recorded Load-Deflection values for Phenolic Concrete Bridge Deck Panel B2a.

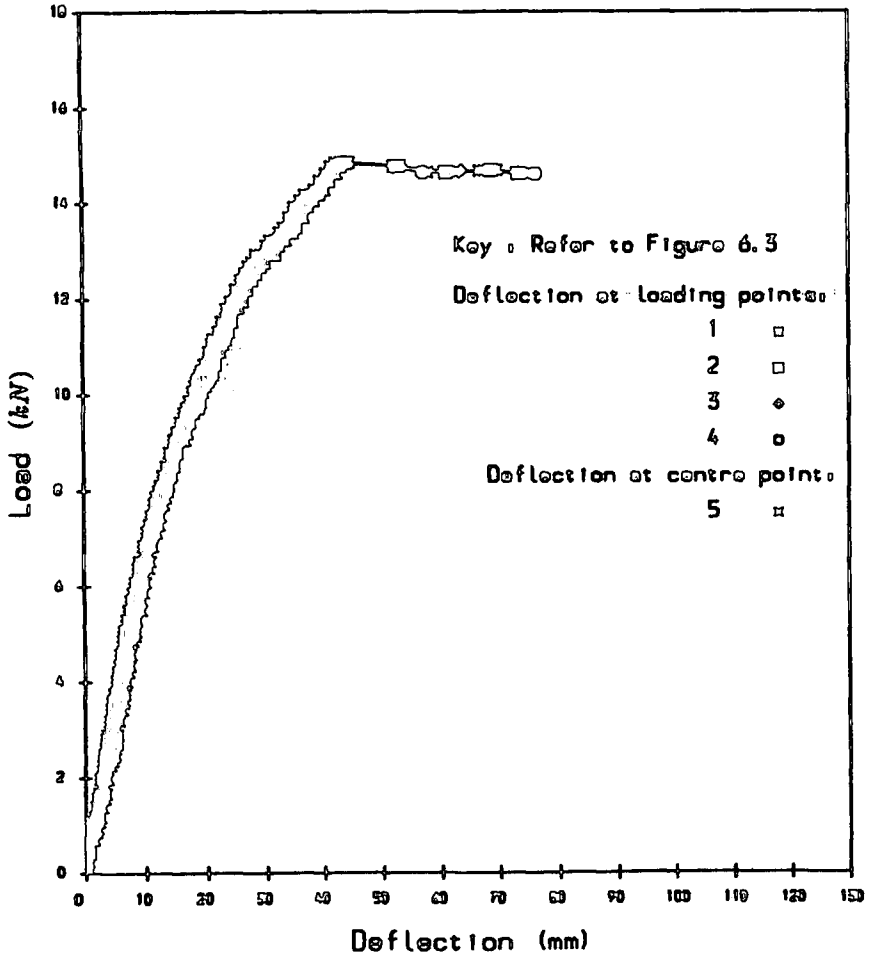

(a) Load v Deflections

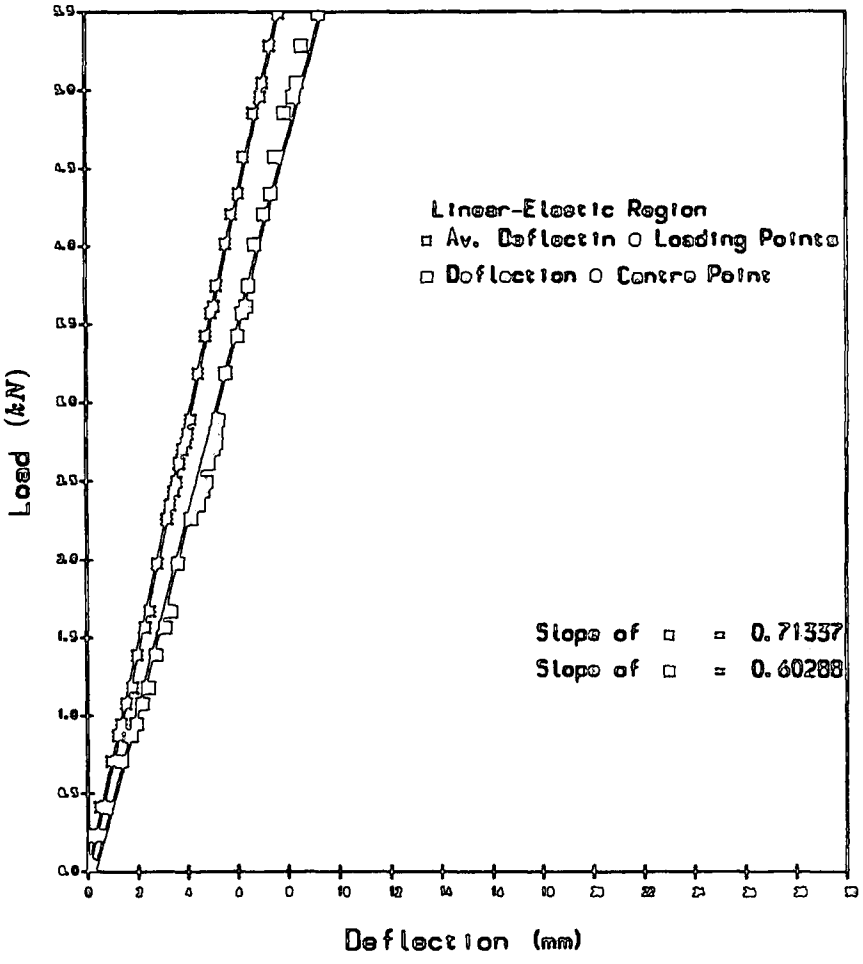

(b) Evaluation of Slopes

Figure A3.12 Recorded Load-Deflection values for Phenolic Concrete Bridge Deck Panel B2b.

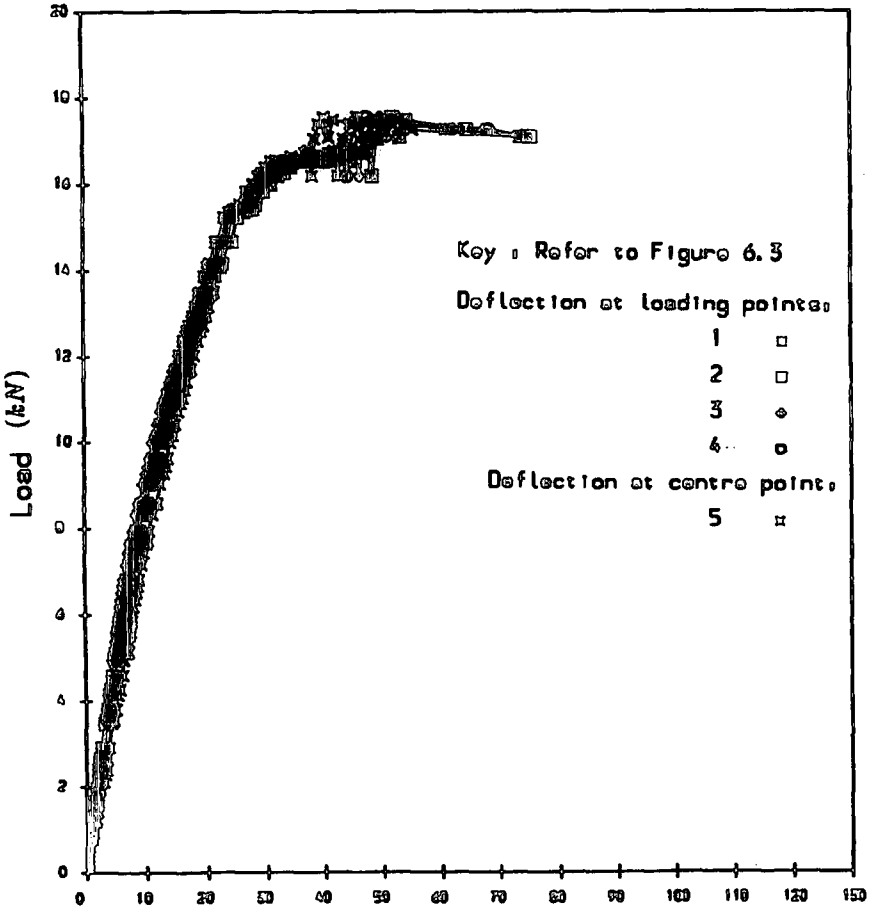

(a) Load v Deflections

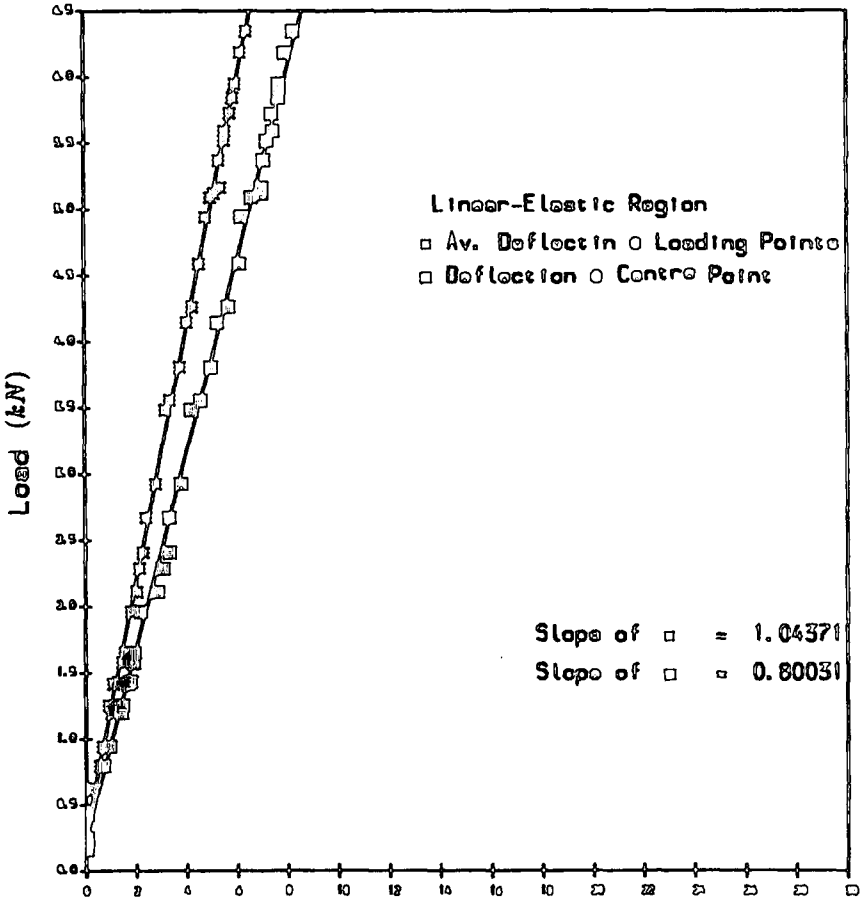

(b) Evaluation of Slopes

Figure A3.13 Recorded Load-Deflection values for Phenolic Concrete Bridge Deck Panel B3a.

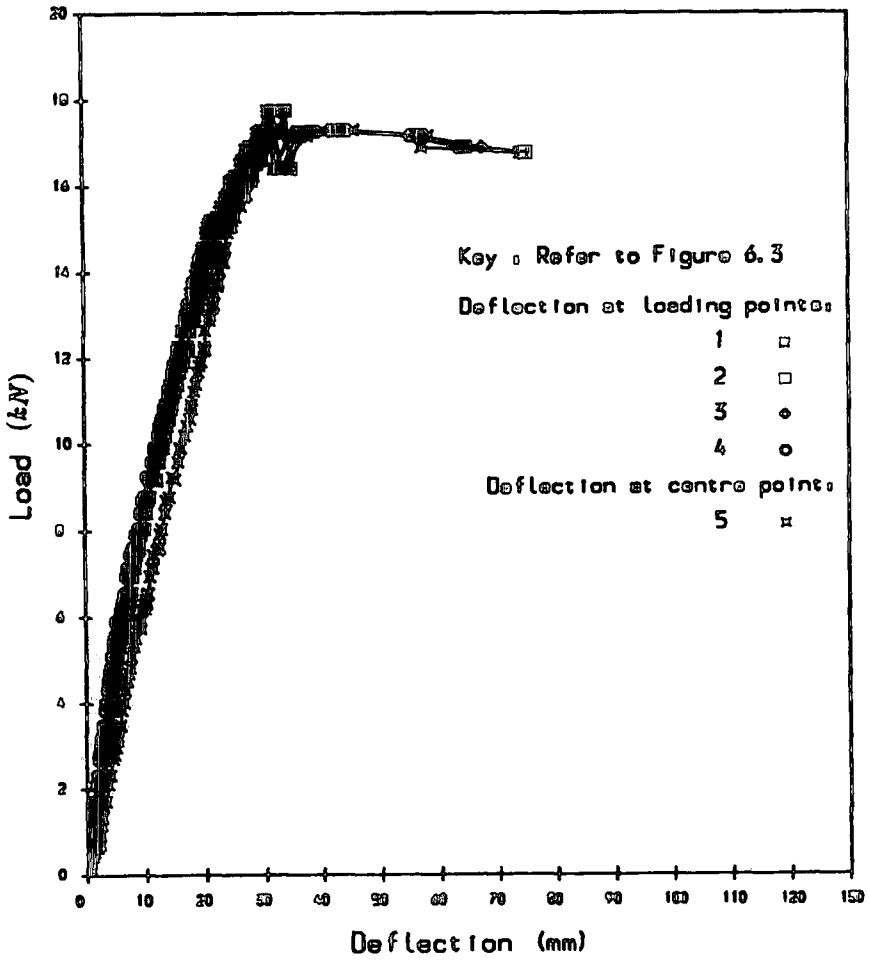

(a) Load v Deflections

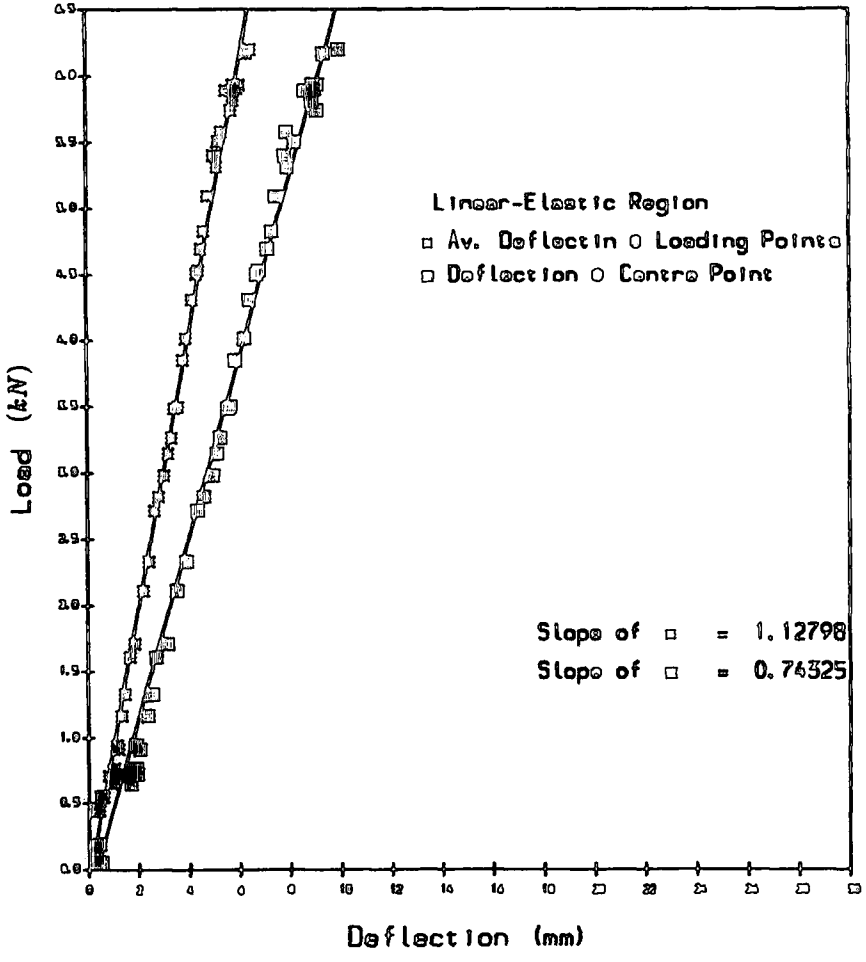

(b) Evaluation of Slopes

Figure A3.14 Recorded Load-Deflection values for Phenolic Concrete Bridge Deck Panel B3b.

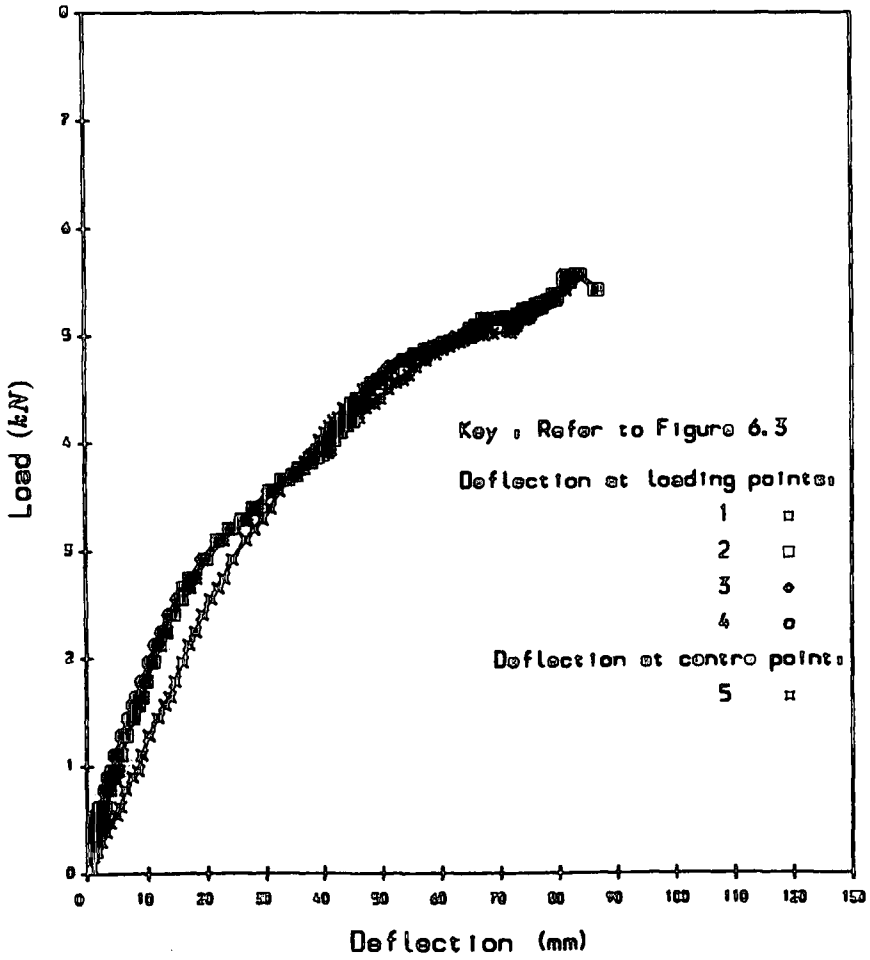

(a) Load v Deflections

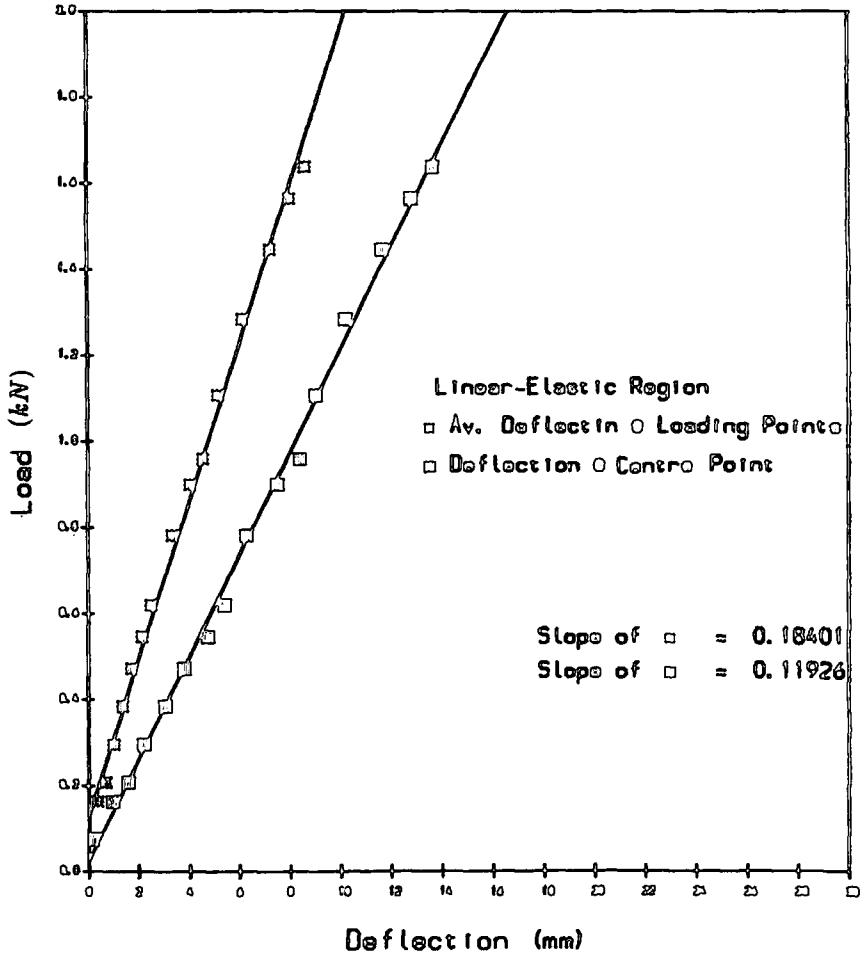

(b) Evaluation of Slopes

Figure A3.15 Recorded Load-Deflection values for Phenolic Concrete Bridge Deck Panel C1a.

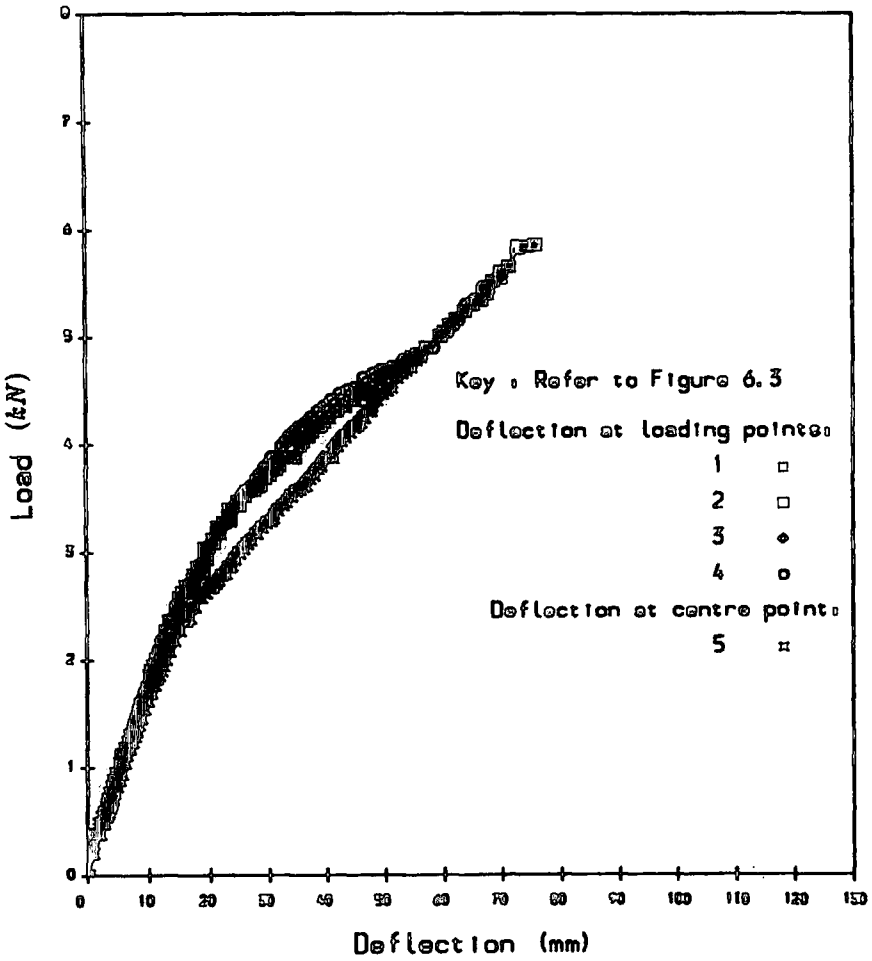

(a) Load v Deflections

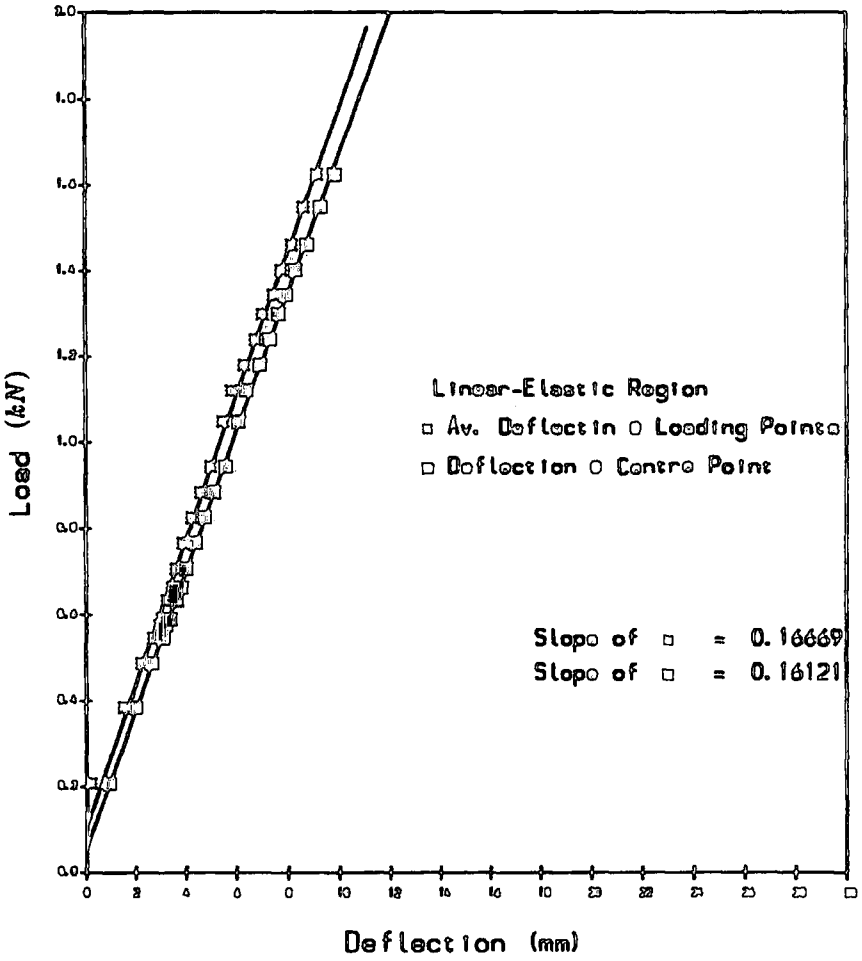

(b) Evaluation of Slopes

Figure A3.16 Recorded Load-Deflection values for Phenolic Concrete Bridge Deck Panel C1b.

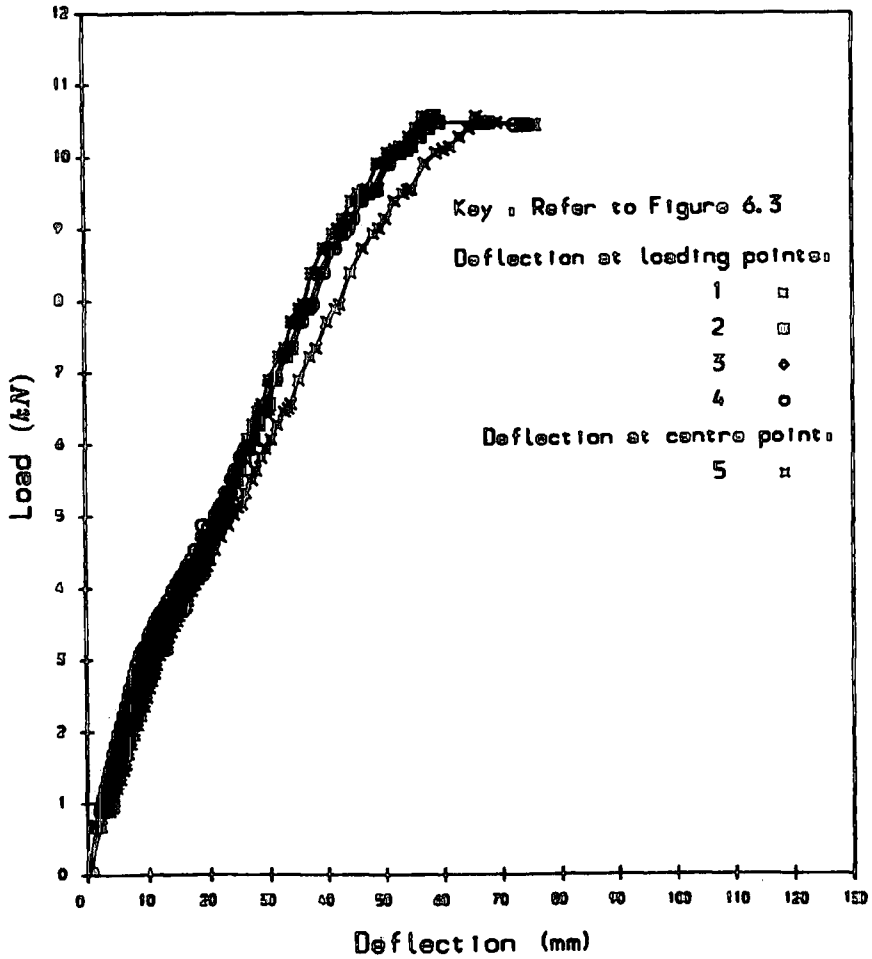

(a) Load v Deflections

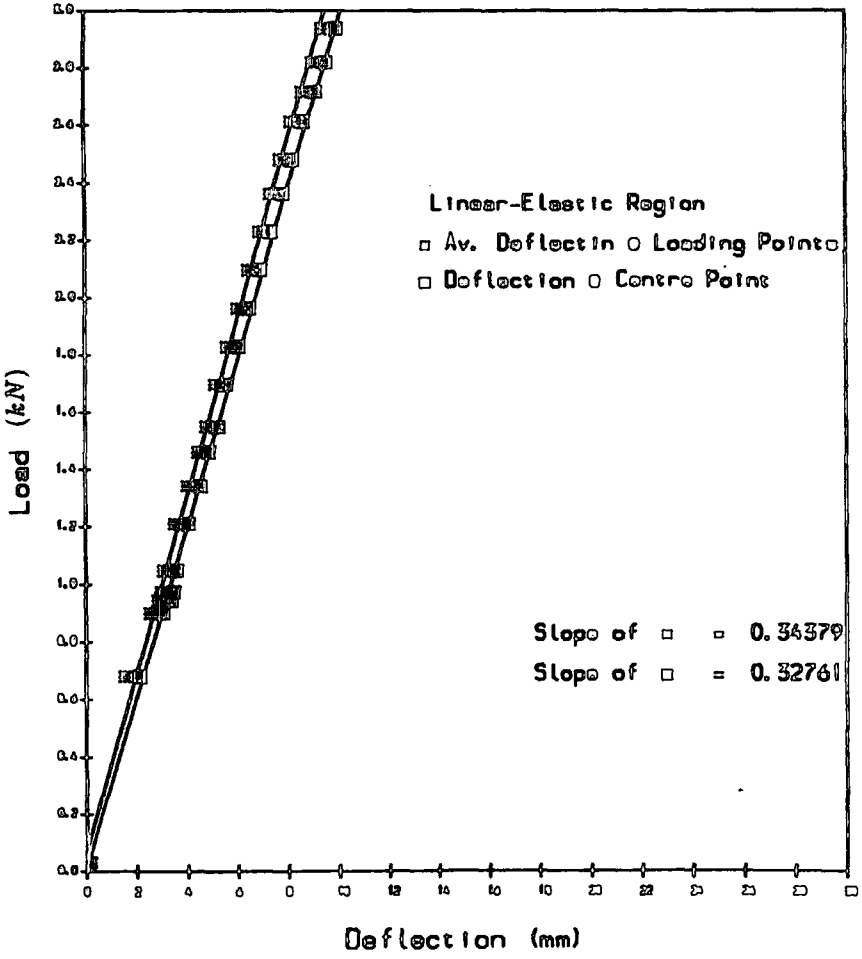

(b) Evaluation of Slopes

Figure A3.17 Recorded Load-Deflection values for Phenolic Concrete Bridge Deck Panel C2a.

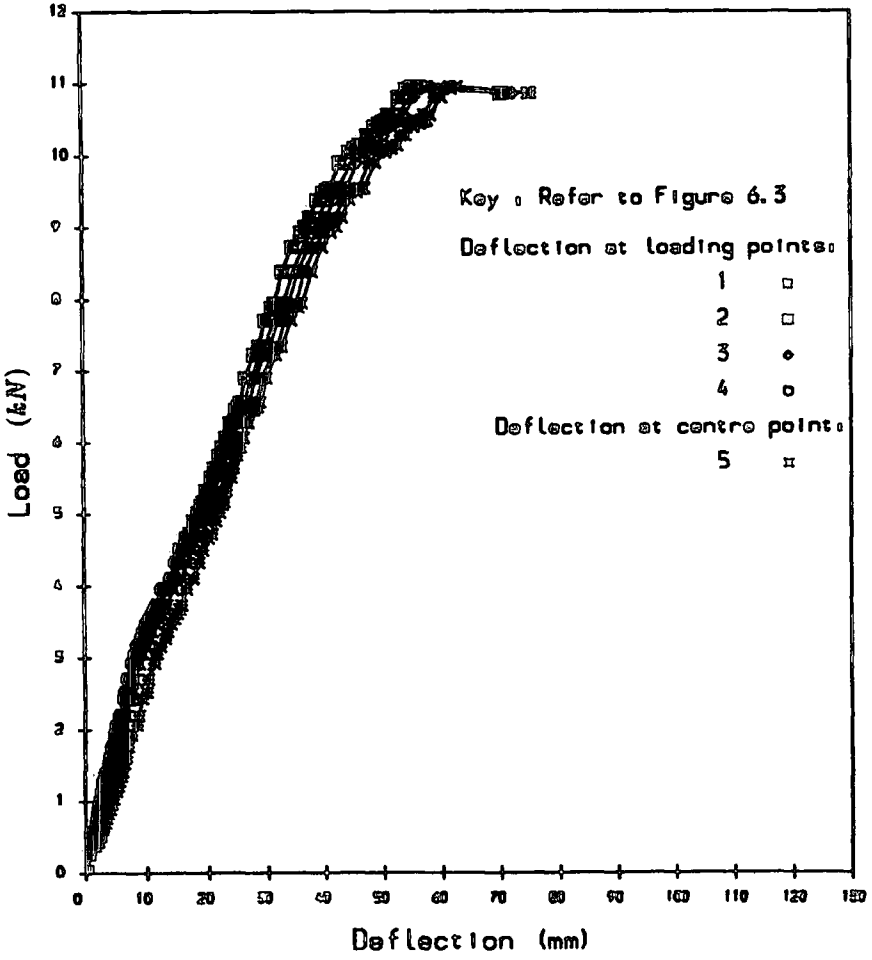

(a) Load v Deflections

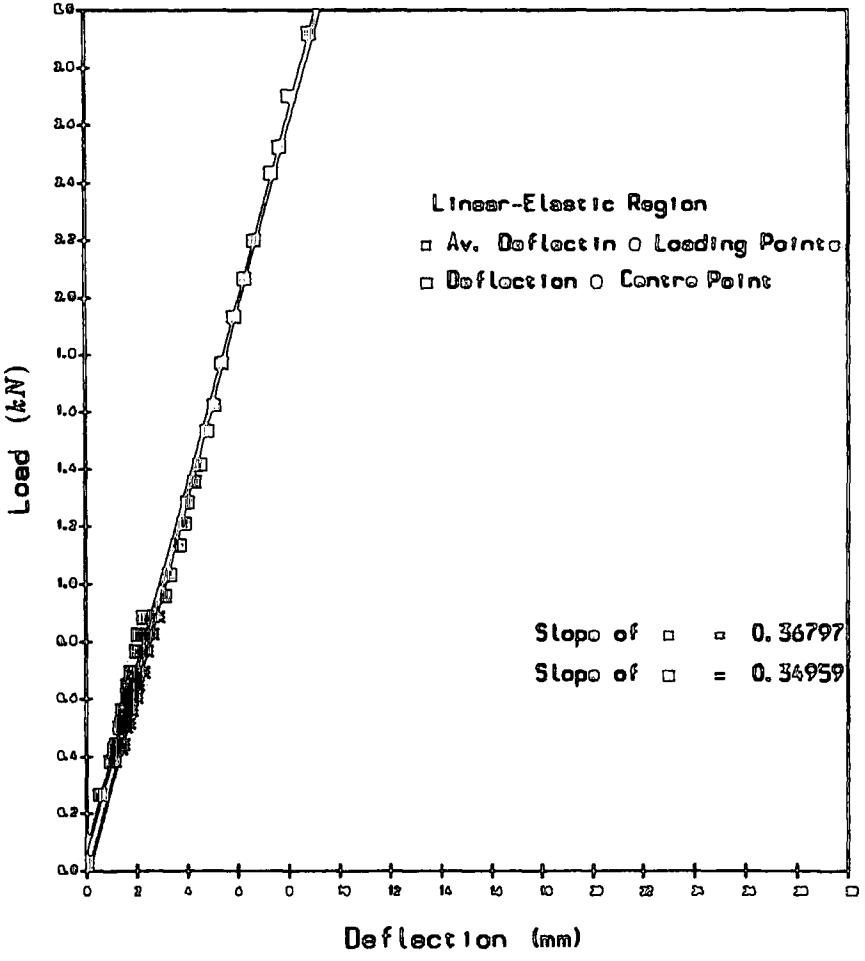

(b) Evaluation of Slopes

Figure A3.18 Recorded Load-Deflection values for Phenolic Concrete Bridge Deck Panel C2b.

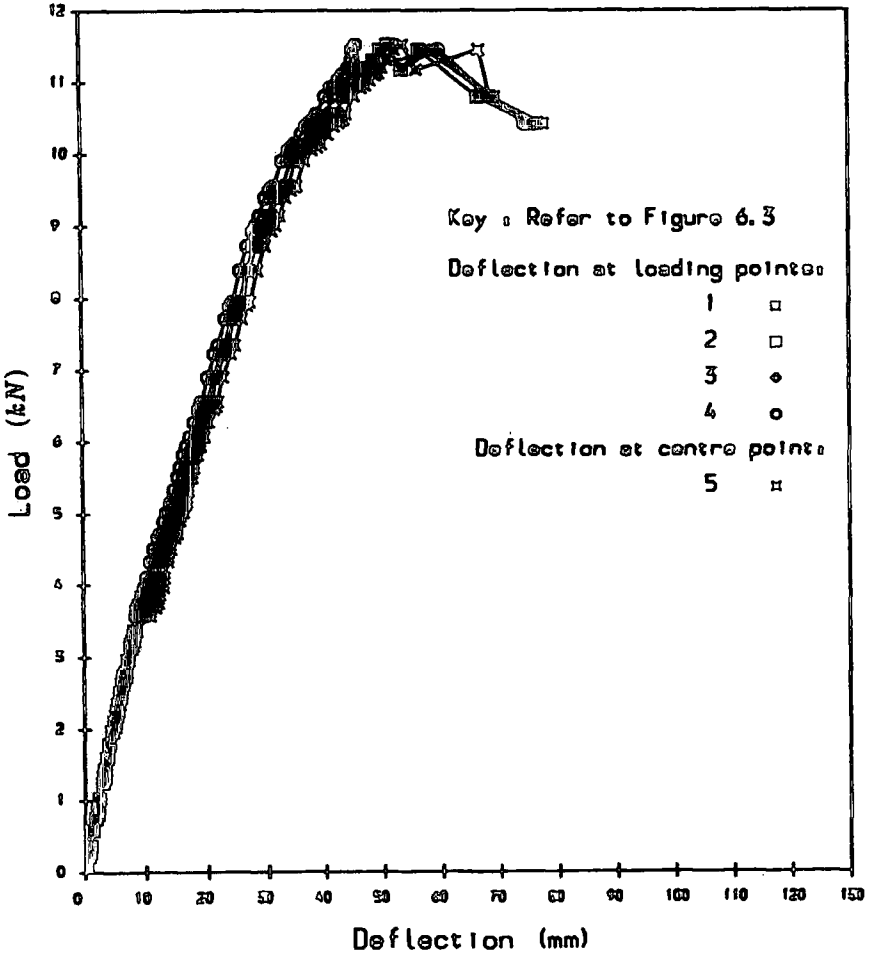

(a) Load v Deflections

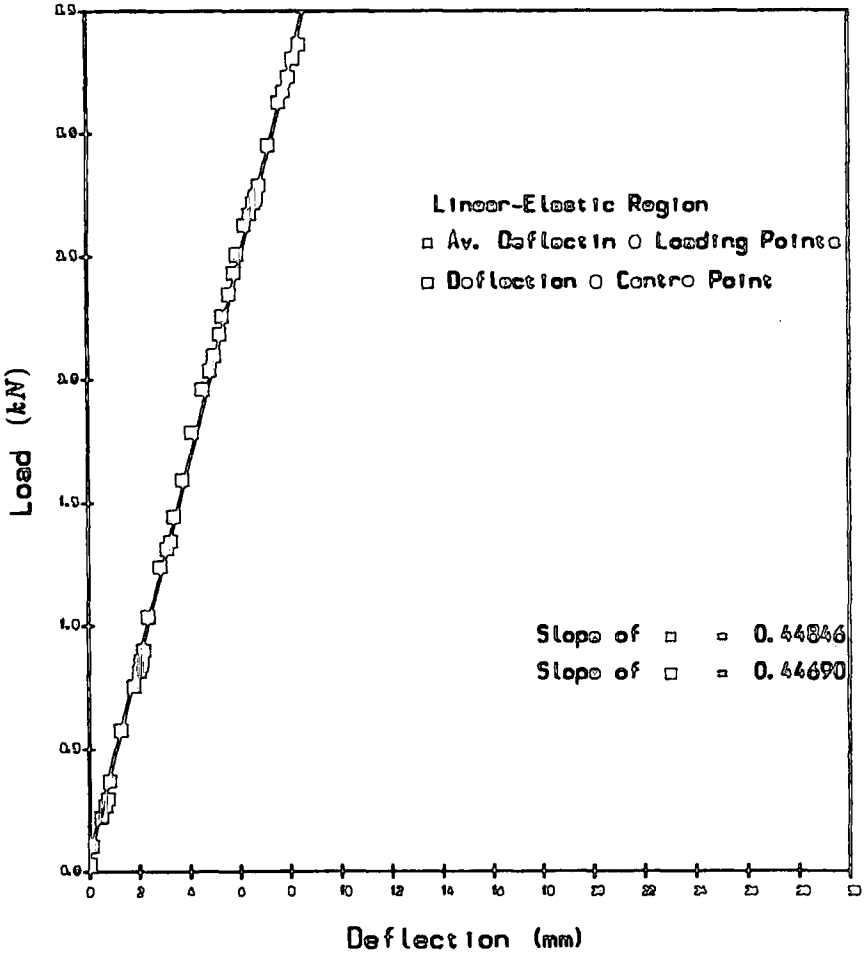

(b) Evaluation of Slopes

Figure A3.19 Recorded Load-Deflection values for Phenolic Concrete Bridge Deck Panel C3a.

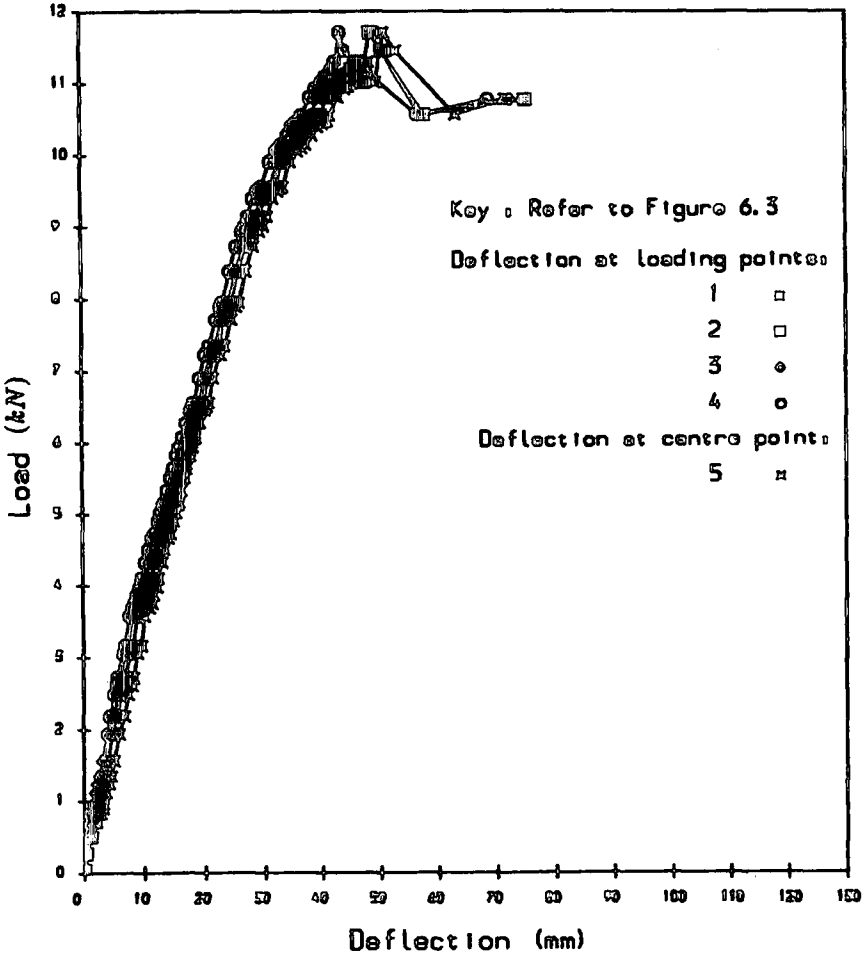

(a) Load v Deflections

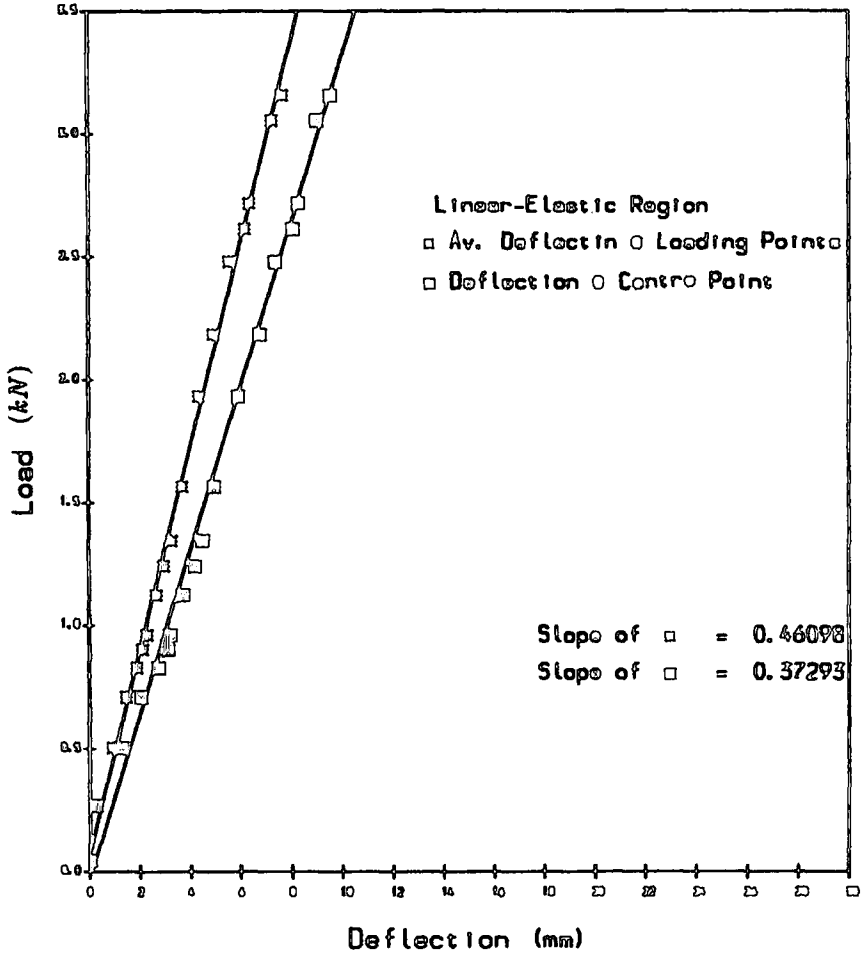

(b) Evaluation of Slopes

Figure A3.20 Recorded Load-Deflection values for Phenolic Concrete Bridge Deck Panel C3b.

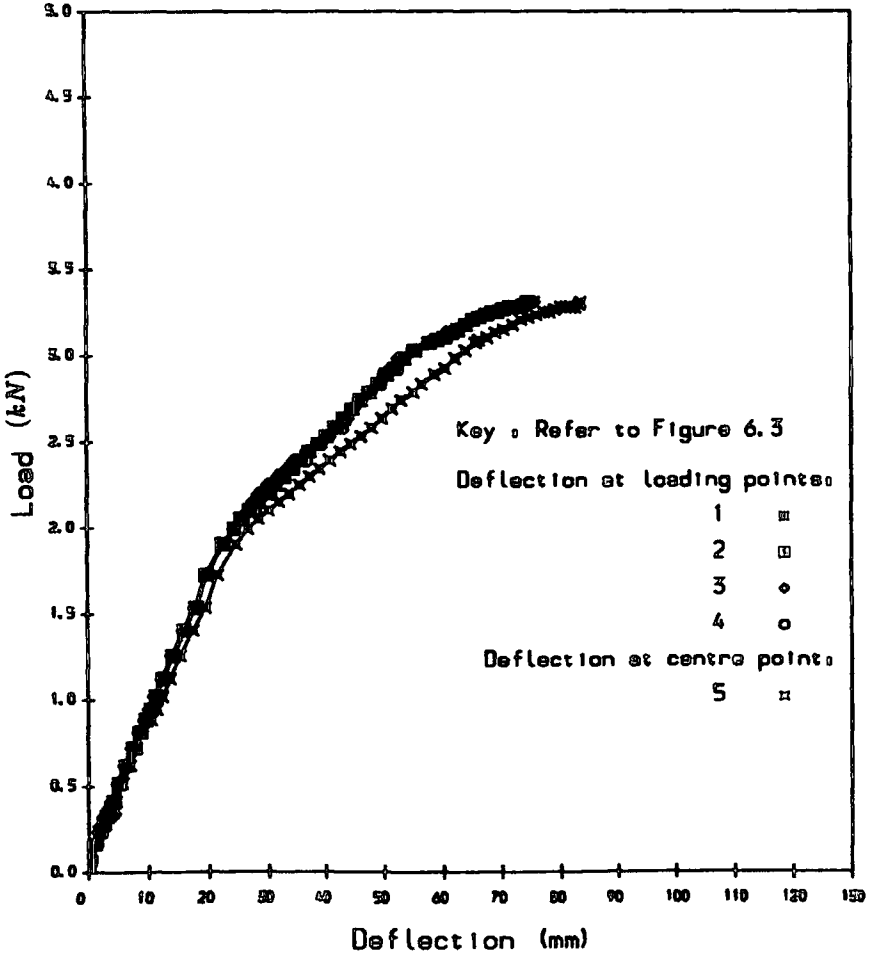

(a) Load v Deflections

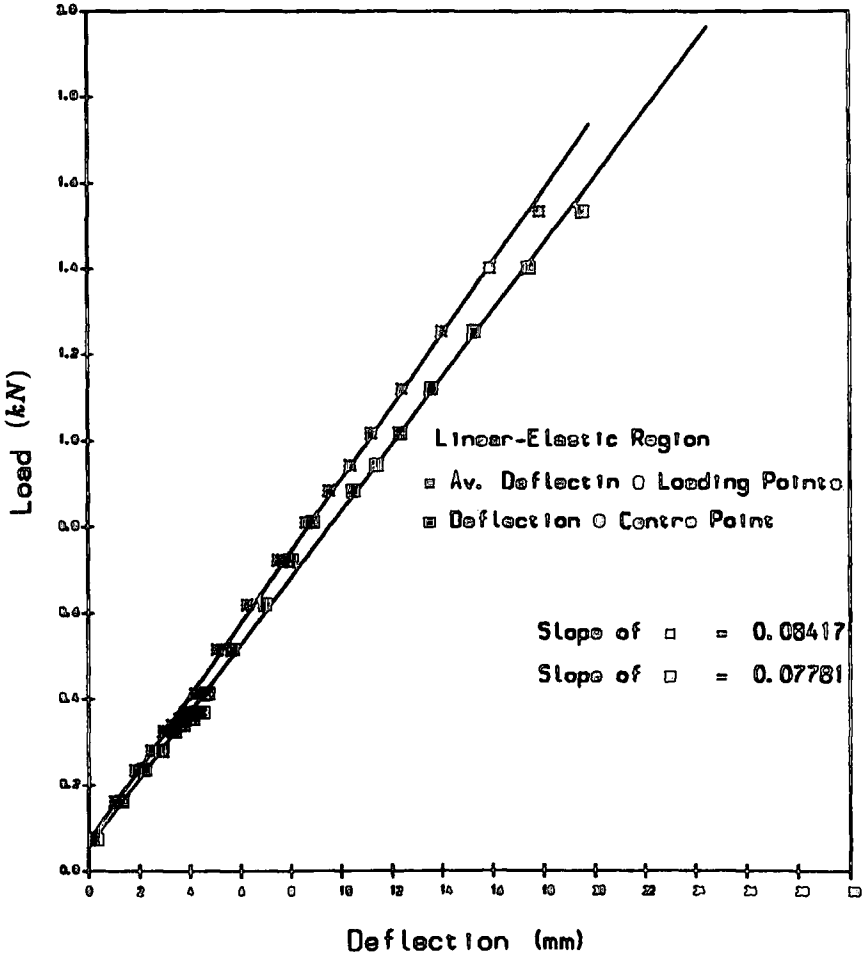

(b) Evaluation of Slopes

Figure A3.21 Recorded Load-Deflection values for Phenolic Concrete Bridge Deck Panel D1a.

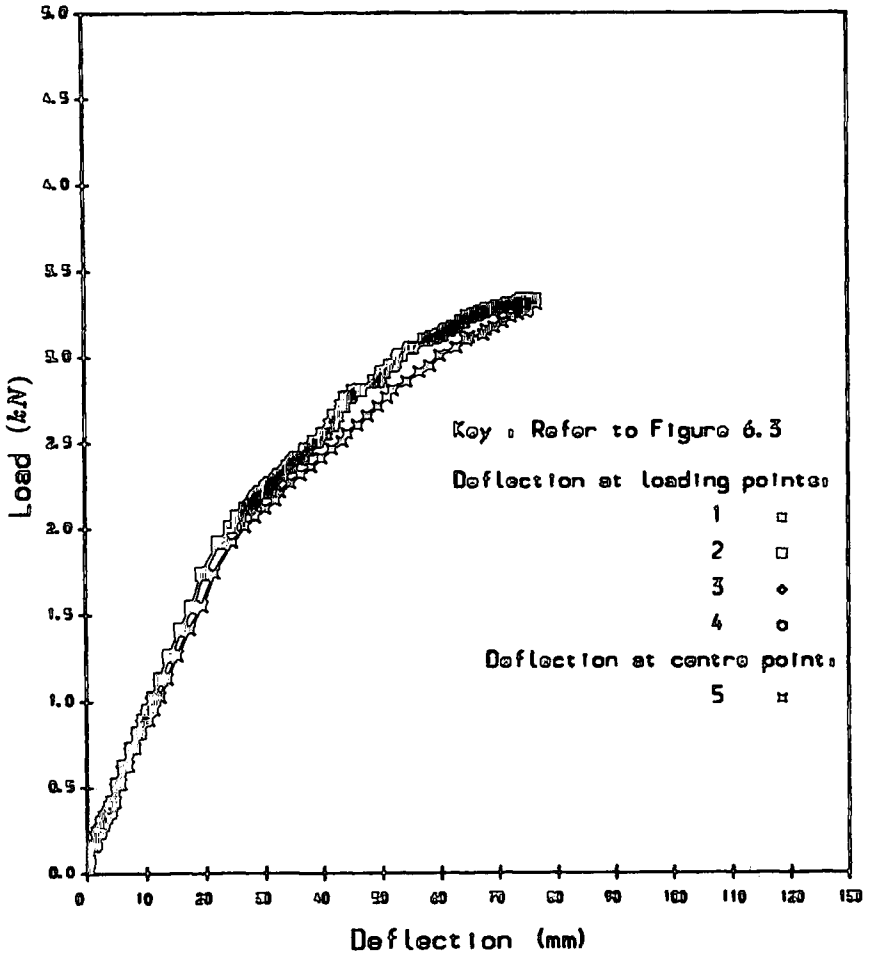

(a) Load v Deflections

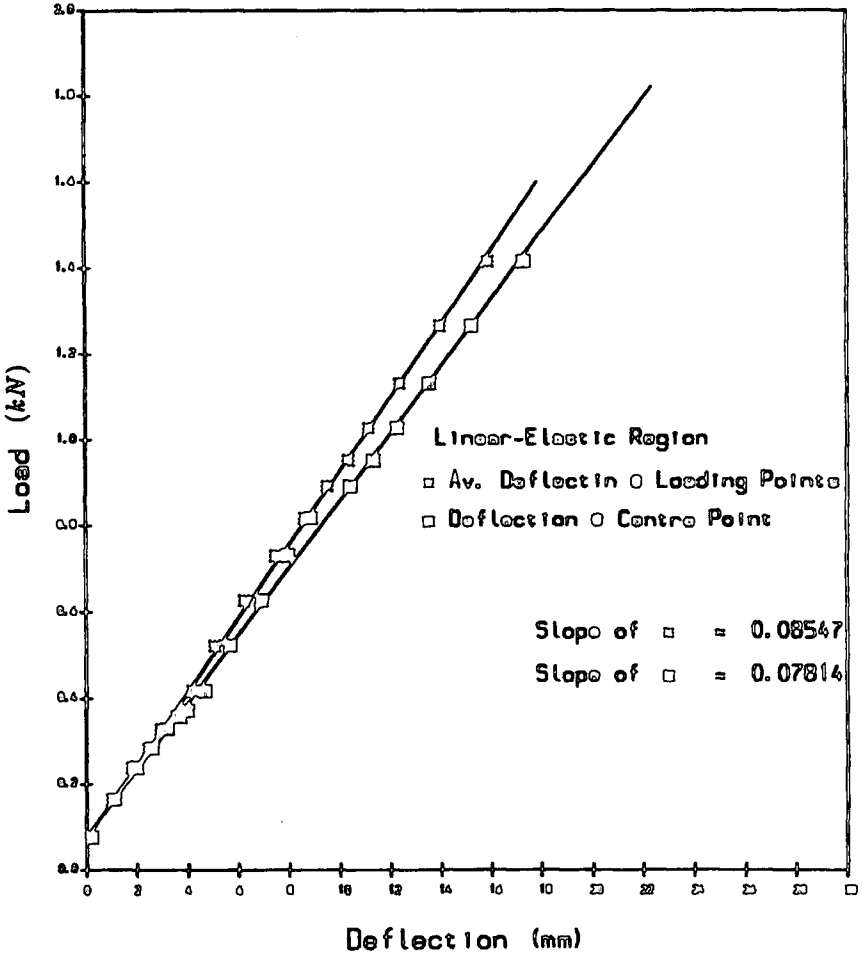

(b) Evaluation of Slopes

Figure A3.22 Recorded Load-Deflection values for Phenolic Concrete Bridge Deck Panel D1b.

References

1. Fowler, D.W., "*Polymers in Concrete*", handbook of structural concrete, Edited by Kong, F.K., Evans, R.H., Cohen, E., and Roll, F., Pitman advanced publishing program, London, 1983.
2. "*Synthetic Resins in Building Construction*", Experimental research on new developments brought by synthetic resins to building techniques, International Symposium, Paris, Vol. 1 and 2, Sept. 1967.
3. ACI Committee 548, "*Polymers in Concrete*", American Concrete Institute, Detriot, 1977, 92pp.
4. "*Polymers in Concrete*", International Symposium, Publication SP-58, American Concrete Society, 1978.
5. "*Polymers in Concrete*", The Concrete Society (London), Papers presented at International Symposium on Polymer Concrete, 1st, London, 1975, Construction Press Ltd., London 1976.
6. "*Polymers in Concrete*", 2nd International Congress on Polymers in Concrete, Proceedings, American Concrete Institute, Texas, Austin, November, 1978.
7. "*Polymers in Concrete*", 3rd International Congress on Polymers in Concrete, American Concrete Institute, Vol. 1 and 2, May, 1981.
8. "*Polymers in Concrete*", 4th International Congress on Polymers in Concrete, Institut fur Spanende Technologic und Werkzengmachinen, Darmstadt, Sep., 1984.
9. "*Polymers in Concrete*", 5th International Congress on Polymers in Concrete, "*The Production, Performance and Potential of Polymers in Concrete*", Brighton, England, 22-24 Sep., 1987.
10. "*Polymers in Concrete*", 6th International Congress on Polymers in Concrete, Proceedings, International Academic Publishers, A Pergamon - CNPIEC joint venture, Tongji University, Shanghai, China, 24-27 Sep., 1990.
11. Manson, J.A., "*Over review of current research on polymer concrete: Materials*

and future needs", Application of polymer concrete, American Concrete Institute, Publication SP-69, Detriot, 1981, pp. 1-20.

12. Kukacka, L.E., "*Concrete-Polymer Composites, Current Status and Future Research needs*", Proceedings of ICP, Rilem, IBK International Symposium held in Prague 1981, Elsevier Scientific Publishing Co., 1982, pp. 815-826.
13. Dietz, A.G.H., "*Plastics in Building: Past, Present and Future*", Proceedings of ICP, Rilem, IBK International Symposium held in Prague 1981, Elsevier Scientific Publishing Co., 1982, pp. 689-702.
14. Polymer Concrete, "*Uses, Materials, and Properties*", Symposium on Polymers in Concrete, American Concrete Institute, Committee 548, SP-89, Kansas City, 1983.
15. Polymers, "*Estimation and Correlation of Polymer Properties*", Symposium, ACS, Division of Polymer Chemistry, Chicago, IL., Vol. 26, No. 2, 1985.
16. Polymers, "*Deformation, Yield and Fracture of Polymers*", 6th International Conference, Plastic and Rubber Institute, Cambridge, April, 1985.
17. "*Polymer Modified Concrete*", American Concrete Institute, SP-99, 1987.
18. "*Polymers in Concrete*", "Advances and Applications", Annual Convention, American Concrete Institute, Orlando, FL., 1988.
19. Sabnis, G.M., Harris, H.G., White, R.N., and Mirza, S.M., "*Structural Modeling and Experimental Techniques*", Prentice Hall, Eaglewood Cliffs, NJ, 1982, pp. 63-103.
20. Prusinski, R.C., "*Study of Commercial Development in Precast Polymer Concrete*", Polymers in Concrete, International Symposium, ACI, Publication SP-58, 1978, pp. 75-102.
21. Bares, R., and Navratil, J., "*Some Physical Properties of Resin Concrete*", Synthetic Resins in Building Construction, Experimental research on new developments brought by synthetic resins to building techniques, International Symposium, Paris, Vol. 2, Sept. 1967.
22. Bares, R.A., "*Furane Resin Concrete and its Application to Large Diameter*

Sewer Pipes", Polymers in Concrete, International Symposium, ACI, Publication SP-58, 1978, pp. 41-74.

23. Elshin, I.M., "*Experience in Using Plastic Concrete with Furane Resins in different structures*", Synthetic Resins in Building Construction, Experimental research on new developments brought by synthetic resins to building techniques, International Symposium, Paris, Vol. 2, Sept. 1967.
24. Burleson, J.D., Long Jr., Ch.G., Armeniades, C.D., and Krahl, N.W., "*An Investigation of the Properties of Polymer Concrete*", Polymers in Concrete, International Symposium, ACI, Publication SP-58, 1978, pp. 1-20.
25. Scanlon Jr., J.M., "*Application of Polymer Concrete Materials in Hydrotechnical Construction*", Application of Polymer Concrete, ACI, Publication SP-69, Detroit, Michigan, 1981, pp. 45-62.
26. Ionescu, I., and Enculescu, M., "*Betons Base De Resins Synthetiques Sans Liants Mineraux*", English Translation, Synthetic Resins in Building Construction, Experimental research on new developments brought by synthetic resins to building techniques, International Symposium, Paris, Vol. 2, Sept. 1967.
27. Fontana, J.J., and Bartholomew, J., "*Use of Concrete Polymer Materials in the Transportation Industry*", Application of Polymer Concrete, ACI, Publication SP-69, Detroit, Michigan 1981, pp. 21-44.
28. McNerney, M.T., "*Research in progress: Rapid All-Weather Pavement Repair with Polymer Concrete*", Application of Polymer Concrete, ACI, Publication SP-69, Detroit, Michigan, 1981, pp. 93-106.
29. Fowler, D.W., Meyer, A.H., and Paul, D.R., "*Techniques to Improve Strength of Polymer Concrete made with Wet Aggregate*", Application of Polymer Concrete, ACI, Publication SP-69, Detroit, Michigan, 1981, pp. 107-122.
30. Perry, E.R., "*Polymer Concrete and the Electric Power Industry*", Application of Polymer Concrete, ACI, Publication SP-69, Detroit, Michigan, 1981, pp. 63-72.
31. Gunasekaran, M., and Perry, E.R., "*Polymer Concrete for high voltage electri-*

cal insulation", Proceeding, 2nd International Congress, Polymers in Concrete, University of Texas at Austin, 1978, pp. 187-191.

32. Becerra, R.T., "*Polymer Concrete for Electrical Application*", Application of Polymer Concrete, ACI, Publication SP-69, Detroit, Michigan, 1981, pp. 145-154.
33. Zeldia, A.N., Kukacka, L.E., and Carciello, N., "*New Novel Well- Cementing Polymer Concrete Composite*", Application of Polymer Concrete, ACI, Publication SP-69, Detroit, Michigan, 1981, pp. 73-92.
34. Eagorn, C., "*Organosilicon Compounds*", Butterworths, Publications Ltd., London, 1960.
35. Kukacka, L.E., "*Polymer Concrete Materials for use in Geothermal Energy Processes*", Proceedings 2nd International Congress, Polymers in Concrete, University of Texas at Austin, 1978, pp. 157-172.
36. Imamura, K., Toyokawa, K., and Murai, N., "*Precast Polymer Concrete for Utilities Applications*", Proceedings 2nd International Congress, Polymers in Concrete, University of Texas at Austin, 1978, pp. 173-186.
37. Koblischek, P., "*Acryl-Concrete*", Proceedings 2nd International Congress, Polymers in Concrete, University of Texas at Austin, 1978, pp. 413-430.
38. Kreis, R., "*World-Wide Application and Industrial Manufacturing of Polymer Concrete*", Proceedings 2nd International Congress, Polymers in Concrete, University of Texas at Austin, 1978, pp. 519-575.
39. Kubase Construction Co. Ltd., "*Fypol Polyester Resin Concrete*", Kestrel Communications Ltd., London, Northallerton, 1989.
40. Shohada Fadaie, M., "*Polyester Resin Concrete and its Application*", Ph.D. student, University of Durham, S.E.A.S., Personal Communication, 1987.
41. Rolinson, E.A., "*Building Component*", UK Patent, GB, 2097314-A, Application No. 8112819, Nov., 1982.
42. Hansom, R.G., and Primarolo, C.A., "*A method of, and apparatus for, continuously forming sheeting and the manufacture of building panels from such*

sheeting", UK Patent, GB, 2159066-B, Application No. 8413486, Oct., 1987.

43. Knop, A., and Scheib, W., "*Chemistry and Application of Phenolic Resins*", Berlin, Heidelberg, New York, Springe-Verlag, 1979.
44. Knop, A., and Pilato, L.A., "*Phenolic Resins: Chemistry, Application, Performance and Future Directions*", Berlin, Heidelberg, New York, Tokyo, Springer-Verlag, 1985, 313 pp.
45. BP Chemicals Ltd., "*Information on Developed Phenolic Resins*", Applied Phenolic Resin Division Library, Sully, South Glamorgan, 1988.
46. Forsdyke, K.L., "*What's in it for me?-Phenolic Resins for PRIM*", Plastic and Rubber Institute Conference, Reinforced Reaction Injection Moulding (RRIM), Solihull, Feb., 1981.
47. Forsdyke, K.L., "*Developments in the Applications Technology of Phenolic GRP*", B.P.F. 13th Reinforced Plastic Congress, Brighton, 1982.
48. Forsdyke, K.L., Lawrence, G., Mayer, R.M., and Patterson, I., "*Use of Phenolic Resins for Load Bearing Structures*", Engineering with Composites, Paper 9, SAMPE Conference, London,1983.
49. Forsdyke, K.L., "*Phenolic Resin Composites for Fire and High Temperature Application*", Fibre Reinforced Composites, 1984.
50. Aveston, J., Greenwood, W.J., and Sillwood, J.M., "*Long term strength of glass fibre/phenolic resin composites*", National Physical Laboratory, Division of Materials Application, NPL report DMA(A) 98, Feb., 1985.
51. BP Cellobond, "*Phenolic Resins for Fibre Reinforced Plastics: J2018L and J2027L phenolic resol resins*", Technical Information Data, BP Chemicals Ltd., Sully, 1985.
52. Little, G.E., "*The Chemistry of the Acid-Catalysed setting of Phenol-Formaldehyde resins*", Journal of Applied Chemistry, Vol. 12, Part 4, April, 1962, pp. 196-200.
53. Marley, J.G., "*The Chemistry of Foundary Resin Binder Systems*", Report 1528 BCRIA Journal, Vol. 31, No. 3, May 1973.
54. Hunter, J., and Forsdyke, K.L., "*Developed Phenolic Resin BP*", Applied Pheno-

lic Resin Division, Personal Comunication, BP Chemicals Ltd., Sully, 1986-1989.

55. Fordath Ltd., "*Phenolic Resins*", British Industrial Sand Group (BIS), Applied Resin Division, West Bromwich, U.K., 1986-1989.

56. QO Chemicals Inc., "*Furfuryl Alcohol*", Technical Information Data, Sheffield, U.K., 1987.

57. British Standard Institution, "*Standard method for fine-grained soils (sieve method)*", Method of Test for soils for civil engineering purposes, BS 1377, Test 7(b), 1975, pp. 31-33.

58. British Standard Institution, "*Standard method for fine-grained soils (pipette method)*", Method of Test for soils for civil engineering purposes, BS 1377, Test 7(c), 1975, pp. 33-39.

59. Johnston, C.D., "*Steel Fibre Reinforced Concrete pavement*", Second Interim Performance Report, Neville, A.M., RILEM Symposium, Fibre Reinforced Cement and Concrete, 1975, pp. 409-418.

60. Tavakoli, S.M., Palfery, R.A., and Philips, M.G., "*Compatibility of commercial chopped-strand mats with a phenolic resin system for hand laminating*", Journal of Composites, Vol. 20, No. 2, March, 1989, pp. 159-165.

61. Ohama, Y., and Demura, K., "*Evaluation of Performance of Mold-releasing Agents for Polyester Resin Concrete (or Polymer Concrete)*", Application of Polymer Concrete, ACI, Publication SP-69, Detroit, Michigan, 1981, pp. 179-188.

62. Teychenne, D.C., Franklin, R.E., and Erntory, H.C., "*Design of normal concrete mixes*", Her Majesty's Stationary office, 1975, pp. 11-12.

63. Shacklock, B.W., "*Concrete constituents and mix proportions*", Palladian Publications Ltd., Publication 11.004, 1974, pp. 89-92.

64. "*Soil Mechanics for road engineers*", Her Majesty's Stationary office, Section 11.23, 1952, pp. 223-229.

65. Kapasny, L., "*Design of the optimum grading of aggregates for resin concrete*", Editted by Bares, R.A., Proceedings of the International Symposium on Plastics

in Materials and Structural Engineering, Prague, 1981, pp. 307-310.

66. Parton, G.M., Shariatmadari, A.A., and Hansom, R.G., "*Efficiency in aggregate mix design: a least-squares method*", The International Journal of Cement Composites and Lightweight Concrete, Edited by Swamy, R.N., Vol. 11, No. 3, Aug., 1989, pp. 167-174.
67. Tioxide Information, "*Titanium Pigments*", The Tioxide Group Plc., U.K., June, 1984.
68. Tioxide Central Laboratories, "*Selection of a Tioxide pigment for use in resin-bonded concrete*", Report C032, The Tioxide Group Plc., U.K., July, 1985.
69. Mellor, M., and Hawkes, I., "*Measurement of tensile strength by diametral compression of discs and annuli*", Engineering Geology, Vol. 5, 1971, pp. 173-225.
70. Bieniawski, Z.T., and Franklin, J.A., "*Suggested method for determining the universal compressive strength for rock materials*", Commission on Standardization of Laboratory and Field Tests, ISRM, 1972.
71. British Standard, "*Method of determination of density of hardened concrete*", Testing Concrete, BS 1881, Part 114, 1983.
72. British Standard, "*Method of determination of water absorption*", Testing Concrete, BS 1881, Part 122, 1983.
73. British Standard, "*Method of determination of water absorption*", Ceramic floor and wall tiles, BS 6431, Part 11, EN99, 1983.
74. Freiman, S.W., Fuller Jr., E.R., "*Fracture Mechanics for Ceramics, Rocks, and Concrete*", Symposium by American Society for Testing and Materials, ASTM special technical publication 745, Philadelphia, 1981.
75. Evans, A.G., Longdon, T.G., "*Structural Ceramics*", Progress in Material Science, Vol.21, No.3/4, 1976, pp 171-442.
76. Bradt, R.C., Hasselman, D.P.H., Lange, F.F., "*Fracture Mechanics of Ceramics*", Plenum Press, New York, London, Vol.1-2, 1974, Vol.3-4, 1978.
77. Kinloch, A.J., Shaw, S.J., "*Developments in Adhesives*", Vol.2, Edited by Kinloch, A.J., Applied Science, 1981, pp 83-124.

78. Parry, T.V., Igbinedion, S.G., and Wronski, A.S., "*Use of the Double-Torsion technique to evaluate Fracture Energy of Adhesive Cements in the temperature range 20-700° C*", Special Ceramics 8, Edited by Howlett, S.P., Taylor, D., British Ceramics Proceedings, 1986, pp 281-286.

79. Igbinedion, S.G., Parry, T.V., Wronski, A.S., "*Fracture Toughness of some adhessive cement systems measured in the temperature range 20-700° C*", International Journal of Adhesion and Adhesives, Vol. 7, No.4, Oct. 1987, pp 205-208.

80. British Standard Institution, "*Method of test for plane strain fracture toughness (K_{IC}) of metallic materials*", BS5447, BSI, 1977.

81. Gray, A., Mallinson, J.N., Price, J.B., "*Fracture behaviour of polyethylene pipes*", Vol.1, No.1, 1981.

82. Bochenek, A., Prokopski, G., "*The investigation of aggregate grain size effect on fracture toughness of ordinary concrete structures*", International Journal of Fracture 41, Netherlands, 1989, pp197-205.

83. Kennedy, E.P., Kennedy, C.R., "*Dependence of Strength on Particle Size in Graphite*", Proceedings of the Thirteen National Symposium of Fracture Mechanics, American Society for Testing and Materials, Philadelphia, June 1980, pp 303-315.

84. Annis, C.G., Cargill, J.S., "*Modified Double-Torsion method for measuring crack velocity in NC-132 (S_{i3} N_4)*", Fracture Mechanics of Ceramics, Vol.4, Edited by Bradt, R.C., Hasselman, D.P.H., Lange, F.F., Plenum Press, New York-London, 1978, pp 737-744.

85. Evans, A.G., "*A method for evaluating the time dependent failure characteristics of brittle materials and its application to polycrystalline alumina*", Journal of Materials Science, Vol.7, 1972 pp1137-1146.

86. Beaumont, P.W.R., Young, J.R., "*Failure of brittle polymers by slow crack growth*", Journal of Material Science, Vol.10, 1975 pp 1334-1342.

87. Michalske, T.A., Singh, M., Frechette, V.D., "*Experimental Observation of Crack Velocity and Crack Front Shape Effects in Double-Torsion Fracture Me-*

chanics Tests", Fracture Mechanics for Ceramics, Rocks, and Concrete, ASTM, Philadelphia, 1981, pp 3-12.

88. Lewis, M.H., Karunaratne, B.S.B., "*Determination of High-Temperature $K_I - V$ Data for $S_i - Al - O - N$ Ceramics*", Fracture Mechanics for Ceramics, Rocks, and Concrete, ASTM, Philadelphia, 1981, pp 13-32.
89. Stability of Cracks, "*Fracture Mechanics*", T353 Unit 6B, Open University Press, 1983, pp. 43-73.
90. Almond, E.A., Roebuck, B., "*Precracking of Fracture Toughness Specimens by Wedge Indentation*", Fracture Mechanics for Ceramics, Rocks, Concrete, ASTM, Philadelphia, 1981, pp 85-95.
91. Timoshenko, S.P., Goodier, J.N., "*Theory of Elasticity*", Third Edition, McGraw-Hill, 1984 p 312.
92. Kong, F.K. , Evans, R.H. , Cohen, E. , Roll, F., Handbook of Structural Concrete, "*Fibre Reinforced Concrete-Ch.-6 and Polymers in Concrete Ch.-8*", Pitman Publication, London, 1983.
93. Hannan, D.J. ,"*Fibre Cements and Fibre Concretes*", Wiley, New York, 1978, 219 pp.
94. Castro, J. and Naaman, A.E., "*Cement Mortar Reinforced with Natural Fibres*", J. Am. Concrete Inst., Proc., Vol.78, No. 2, Jan 1981, pp. 69-78.
95. ACI Comittee 544, "*Revision of State-of-Art Report (ACI 544 TR-73) on Fibre Reinforced Concrete*", J. Amr. Concrete Inst., Proce., Vol. 70 , No. 11, Nov., 1973, pp. 729-744.
96. RILEM Technical Committee 19-FRC, "*Fibre Concrete Materials*", Materials and Structures, Test Res., Vol. 10, No. 56, 1977, pp. 103-120.
97. Thorn, P.W. ,"*Feasibility Study of a Sandwich Material Composed of Glass Reinforced and Aerated Concrete*", Honours degree project report presented to the Department of Engineering, University of Durham, June 1971.
98. Saglam, B., "*The Properties of Fibre Reinforced Cement based Sandwich Beams*", M.Sc. thesis presented to the Department of Engineering, University of Durham,

June 1977.

99. Shendy-El-Barbary, M.E., "*The Properties of Concrete Sandwich Beams with Polystyrene Concrete Cores*", Ph.D. thesis presented to the Department of Engineering, University of Durham, 1981.

100. British Standard Institution, "*Method for Tensile Testing of Metals, Steel (general)*", BS18 : Part 2 : 1971.

101. B.P. Chemicals, "*Cellobond Phenolic Resin, Phenolic Foam, Slabstock Production*", Sully, 1980.

102. Crreira, D.J., and Chu, K.H., "*The Moment-Curvature Relationship of Reinforced members*", ACI Journal, No. 83-19, March-April 1986, pp. 191-198.

103. Duan, L., Wang, F.M., and Chen, W.F., "*Flexural Rigidity of Reinforced Concrete Members*", ACI Structural Journal, No. 86-S39, July-August 1989, pp. 419-427.

104. Park, R., Ruitong, D., "*Ductility of Doubly Reinforced Concrete Beam Sections*", ACI Structural Journal, No. 85-S24, March-April 1988, pp. 217-225.

105. Mullin, J.V., and Knoell, A.C., "*Basic Concepts in Composite Beam Testing*", Materials research and standards, Vol. 10, 1970, pp. 16-33.

106. Bullock, R.E., "*Strength Ratio of Composite Materials in Flexure and in Torsion*", Journal of composite materials, Vol. 8, 1974, pp. 200-206.

107. Zweben, C., Smith, W.S., and Wardle, M.W., "*Test methods for fibre tensile strength, Composite flexural modulus, and properties of fabric-reinforced laminates*", Composite materials: Testing and design, 5th Conference, American Society for Testing and Materials, ASTM SP-674, New Orleans, La., 20-22 March, 1978, pp. 228-262.

108. Megson, T.H.G., "*Linear Analysis of Thin-Walled Elastic Structures*", Surrey University Press, 1966.

109. Plantema, F.J., "*Sandwich Construction, The Bending and Buckling of Sandwich Beams, Plates, and Shells*" John Wiley and Sons, Inc, April 1966.

110. Allen, H.G., "*Analysis and Design of Structural Sandwich Panels*", Pergamon

Press, 1969.

111. Zbirohowski-Koscia, K., "*Thin Walled Beams from Theory to Practice*", Crosby Lockwood and Sons Ltd., 1967.

112. Timoshenko, S.P. ,and Gere, J.M., "*Mechanics of Materials*", Second SI Edition, Wadsworth International, 1985.